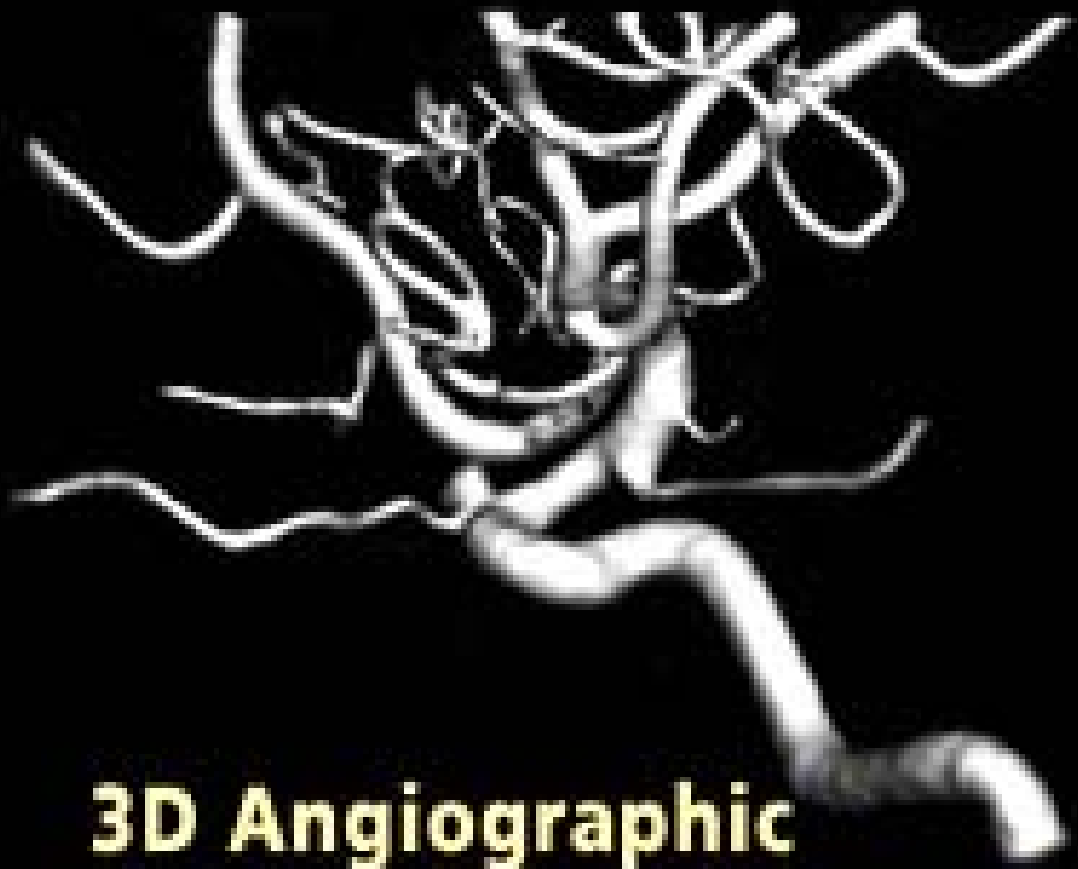

3D Angiographic Atlas of Neurovascular Anatomy and Pathology

NEIL M. BORDEN

With text contributions from Jay Costantino

CAMBRIDGE www.cambridge.org/9780521856843

This page intentionally left blank

3D ANGIOGRAPHIC ATLAS OF NEUROVASCULAR ANATOMY AND PATHOLOGY

The *3D Angiographic Atlas of Neurovascular Anatomy and Pathology* is the first atlas to present neurovascular information and images based on catheter three-dimensional (3D) rotational angiographic studies. The images in this book are the culmination of work done by Neil M. Borden over several years using one of the first 3D neurovascular angiographic suites in the United States. With the aid of this revolutionary technology, Dr. Borden has performed numerous diagnostic neurovascular angiographic studies as well as endovascular neurosurgical procedures. The spectacular 3D images he obtained are extensively labeled and juxtaposed with conventional 2D angiograms for orientation and comparison. Anatomical color drawings and concise descriptions of the major intracranial vascular territories further enhance understanding of the complex cerebral vasculature.

Neil M. Borden, MD, is a board-certified neuroradiologist who has been practicing for 20 years. He completed a neuroradiology fellowship at the Neurological Institute of New York at Columbia Presbyterian Medical Center and a two-year fellowship in endovascular neurosurgery at the Barrow Neurological Institute in Phoenix, Arizona. Dr. Borden is a senior member of the American Society of Neuroradiology and is currently practicing at the Cleveland Clinic Foundation in Cleveland, Ohio.

3D ANGIOGRAPHIC ATLAS OF NEUROVASCULAR ANATOMY AND PATHOLOGY

Neil M. Borden, MD

Division of Radiology
The Cleveland Clinic Foundation
Cleveland, Ohio

With text contributions from

Jay K. Costantini, MD

Division of Radiology
The Cleveland Clinic Foundation
Cleveland, Ohio

Foreword by Robert F. Spetzler, MD

CAMBRIDGE
UNIVERSITY PRESS

CAMBRIDGE UNIVERSITY PRESS
Cambridge, New York, Melbourne, Madrid, Cape Town, Singapore, São Paulo

Cambridge University Press
The Edinburgh Building, Cambridge CB2 8RU, UK
Published in the United States of America by Cambridge University Press, New York

www.cambridge.org
Information on this title: www.cambridge.org/9780521856843

© Neil M. Borden 2007 OK

This publication is in copyright. Subject to statutory exception and to the provision of relevant collective licensing agreements, no reproduction of any part may take place without the written permission of Cambridge University Press.

First published in print format 2006

ISBN-13 978-0-511-29447-1 eBook (EBL)
ISBN-10 0-511-29447-6 eBook (EBL)

ISBN-13 978-0-521-85684-3 hardback
ISBN-10 0-521-85684-1 hardback

Cambridge University Press has no responsibility for the persistence or accuracy of urls for external or third-party internet websites referred to in this publication, and does not guarantee that any content on such websites is, or will remain, accurate or appropriate.

This book is dedicated to my wife Nina, my daughter Rachel, and my son Jonathan, whose support and encouragement made this effort possible. They are my inspiration and guiding light.

NMB

CONTENTS

	Foreword by Robert F. Spetzler, MD	*page* ix
	Introduction	1
1	Technique of Three-Dimensional (3D) Rotational Angiography	5
2	Color Illustrations of Normal Neurovascular Anatomy	11
3	The Aortic Arch	31
4	Cervical Vasculature	41
5	Intracranial Carotid Circulation: Anterior Circulation	87
6	Intracranial Vertebral Basilar Circulation: Posterior Circulation	161
7	Intracranial Venous Circulation	217
8	The Circle of Willis	259
	Index	265

FOREWORD

We have all – patients and physicians alike – come to take the capabilities of diagnostic imaging technology for granted; indeed, our expectations of that technology continue to increase – higher resolution, faster acquisition times, less artifact – the list of demands goes on and on. However, it is scarcely within the span of a generation that lesions considered occult in one imaging modality can now be diagnosed based on features that are pathognomonic in another modality. Young clinicians embarking on their careers at this time may be unaware, for example, that cerebral cavernous malformations with their distinctive appearance on magnetic resonance images were not that long ago considered to be angiographically occult arteriovenous malformations.

I offer this brief historical detail because readers of this volume are about to embark on an amazing three-dimensional visual journey of the circulation of the brain and neck that very few years ago would have been impossible. From the perspective of a neurosurgeon, the appreciation of the vascular system afforded by these images is priceless. Not only does three-dimensional rotational angiography improve the accuracy of diagnosis, it considerably enhances our ability to optimize treatment for patients with challenging neurovascular disorders. Preoperative planning is immeasurably improved by the ability to rotate these images in space to view the posterior regions of vessels that can even be difficult to view intraoperatively. The neck of an aneurysm, for example, can be assessed to determine its suitability for clipping or the presence of other vessels whose inclusion in a clip could be catastrophic. The experience is the neurosurgical equivalent of viewing the dark side of the moon – and always somewhat miraculous to those of us who trained when little more than conventional radiography and angiography were available. To note merely that patient outcomes are concomitantly improved is an understatement that fails to do justice to the lives that can be saved and the devastating complications that can be avoided.

The technology and images showcased in this volume also offer a huge educational benefit. Students, neurosurgical trainees in particular, have always had to struggle with translating the two-dimensional images of neurovascular anatomy in textbooks into the pulsating three-dimensional wonder of the human brain. The hundreds of beautiful images in this text will offer great solace to those striving to master this complex task. The color anatomical illustrations in Chapter 2 and the three-dimensional reconstructions in the orientation insets on each page help readers to place the three-dimensional angiographic images of the vasculature in their anatomical context. The liberal use of conventional angiographic images also helps readers to appreciate the normal anatomy and its perturbation by pathology.

That this superb angiographic atlas was assembled by Dr. Neil Borden is no surprise. Even as a resident Neil gained the reputation of being a "walking radiology encyclopedia" and a "sponge" for knowledge. Between 1994 and 1996, Neil completed a fellowship in interventional neuroradiology with us at the Barrow Neurological Institute in Phoenix. He joined us as a seasoned neuroradiologist who left an established practice to pursue additional training, and I believe that his choice to do so reflects his undiminished love of learning and teaching.

Remarkably, Neil had little experience in research or publishing when he joined us. His commitment and dedication to medical education are now manifest in the volume before you. Having assembled a few neurosurgical atlases during my career, I can assure readers that the finished product is the culmination of hundreds and hundreds of hours spent acquiring and weeding through countless images to optimize the learning process. The technology provides the images, it is true. However, only Neil's keen intellectual competency could have created this thoughtfully formatted and beautiful atlas. It is my pleasure and honor to recommend *3D Angiographic Atlas of Neurovascular Anatomy and Pathology* to both students and masters of the neurosciences.

Robert F. Spetzler, MD
Phoenix, Arizona

INTRODUCTION

Over the last 8 years I have been archiving and cataloging angiographic images that I obtained using one of the first three-dimensional rotational angiographic systems. My career has allowed me to use angiographic cut film, two-dimensional digital subtraction angiography (2D DSA), and now three-dimensional rotational angiography (3DRA). This revolutionary angiographic technique maximizes diagnostic accuracy and provides an invaluable teaching tool for anyone interested in learning more about cerebral vascular anatomy.

The 3D representation of the human neurovascular system represents an enormous step forward in our ability to display this complex anatomy. Our goal in anatomical imaging is to try to recreate the in vivo status as close to its natural state as possible.

Until recently we have had to rely solely on 2D representation of this anatomy. Only recently have certain techniques emerged that can display the natural anatomic state in a 3D display. These techniques include 3D rotational catheter angiography, CT angiography (CTA), and magnetic resonance angiography.

There are three reasons why it is important to have the ability to view vascular anatomy in a 3D display. First, a 3D display is a more accurate representation of the pre-existing anatomy of the subject and can only improve our diagnostic accuracy. The evolution of imaging techniques over the last few decades has been aimed at achieving the most accurate reproduction of the anatomy and pathology possible.

The second reason for the importance of 3D display is a natural extension of the first reason. Only through analysis of the true/real anatomic composition of our subject can we make the most appropriate recommendations regarding prognosis and potential interventions (conservative management, traditional surgery, and/or endovascular surgery).

Any technique that converts and illustrates a 3D object as a 2D representation must involve the loss of certain data that can limit the

accuracy of this transformation. This limitation in the representation of vascular anatomy can result in diagnostic inaccuracies and errors in interpretation that can ultimately lead to errors of judgment in therapeutic decisions. Ultimately, patient care can be negatively impacted by traditional 2D imaging methods that do not provide a 3D display of the anatomy.

The third advantage of displaying anatomy in a 3D format involves the education of individuals interested in learning this complex anatomy. This is of great importance to the authors of this book.

Excellent edge resolution can be achieved with both cut film and 2D DSA. However, these techniques lack the ability to provide critical information regarding the dimension of depth. Why is the ability to render depth so important? The cerebral vascular tree is tortuous and inconstant. Vessels often overlap each other. The relationship of one vessel to another provides critical data for operative/endovascular planning and execution.

3DRA has become a valuable tool in assessing the morphology of intracranial aneurysms. The neck of an aneurysm can be more precisely assessed with this technique. In addition, the takeoff of vascular branches and their relationship to the neck and walls of the aneurysm are data that can mean the difference between an easily treatable aneurysm to one that carries a higher risk for the patient. This information is important to have prior to any intervention.

3DRA is unlike any other technique because it allows for an unobtrusive view of the posterior wall of the vessel. This ability improves diagnostic accuracy and ultimately will improve patient care. Pathology does not limit itself to the anterior or lateral regions of a blood vessel. It is the angiographic technique (prior to 3DRA) which has limited assessment of posterior wall abnormalities. With certain steep oblique radiographic projections it might be possible to see certain regions of the posterior/postero-lateral walls of the vessel with high-resolution DSA. In most cases, optimum assessment of the posterior regions is not achievable. This region is easily assessed with 3DRA. In most cases, even direct observation during operative procedures does not allow adequate visualization of the cerebral vasculature.

Interventional neuroradiology has advanced rapidly in a short time. Microcatheter technology allows us to navigate throughout much of the cerebral vascular tree. Vessel relationships and morphologic detail provided by 3DRA can be critical information to those entering the complexity of the human cerebral vascular system. This knowledge can make these procedures safer for the patient.

This technique also enhances preoperative surgical planning. In my practice, the vascular neurosurgeon investigates the 3D image with me in real time at a computer workstation prior to taking patients to the operating room. The ability to observe the vessels in 3D prior to an operative intervention reduces any unwanted surprises at the time of surgery.

One of the limitations of 3DRA is its inability to demonstrate the smaller branches of the vascular tree. The larger proximal vascular trunks and medium-sized vessels are routinely observed and included when possible in this atlas. In my practice, 3DRA has been primarily used in the assessment of the arterial circulation with the only exception being lesions with arterial-venous shunts. Routine utilization of this technique for examining the venous circulation has not been performed except in unusual cases. Another limitation of 3DRA is the lack of visibility of background anatomy that provide spatial references.

This atlas contains images that demonstrate both normal vascular anatomy as well as different pathological entities. The text describes in broad strokes the most commonly encountered patterns of the arterial vascular tree both in the neck and intracranially. We cover the most frequently encountered vessels but leave detailed discussions of the different variations and functional neuroanatomical considerations to other textbooks in this field. We also touch on the subject of the intracranial venous system in more limited fashion as we have used 3DRA only in rare instances to image the venous circulation. 3D examples are supplemented with 2D images where appropriate to further enhance the utility of the atlas.

This book is intended to be a reference atlas of neurovascular anatomy (cervical and intracranial) and pathology. It is not intended to be a primer on the technique of generating 3D images. We have

written this atlas with the intention of enhancing your ability to understand complex neurovascular anatomy. It is our expectation that the knowledge you take from this work will aid in your understanding of neurovascular anatomy in whatever imaging modality or clinical application you choose.

Neil M. Borden, MD

CHAPTER ONE

TECHNIQUE OF THREE-DIMENSIONAL (3D) ROTATIONAL ANGIOGRAPHY

Angiography is the study of blood vessels. Conventional catheter angiography is a technique that involves the injection of a positive contrast agent directly into the blood vessels through an indwelling vascular catheter (long thin hollow tube). These catheters are generally inserted percutaneously (via needles inserted through the skin).

Cerebral angiography using catheter technology involves accessing the arterial tree most often from the femoral artery (groin). Occasionally the brachial or axillary arteries may be used as the access point.

After the catheter is inserted into the desired arterial access point it is navigated into the vascular territory of interest. In cerebral angiography the catheters are most often placed into the cervical (neck) common carotid artery, internal carotid artery, external carotid artery, or vertebral artery. When nonselective injections are desired the catheters may be positioned in the innominate artery, subclavian artery, or even the aortic arch.

Once the catheter is in the desired position, a bolus injection of a positive contrast agent is performed during which X-rays are obtained for varying periods of time. This allows one to obtain images of the contrast agent as it progresses through the vascular tree from artery to capillary and then into the venous phase of circulation. Most often, the X-rays are obtained in fixed position. Different views of the blood vessels of interest can be obtained either by moving the patient relative to the X-ray tube or changing the position of the X-ray tube relative to a stationary subject. This is the basis for two-dimensional (2D) angiography.

The technique of three-dimensional rotational angiography (3DRA) occurs during the bolus injection of the positive contrast into the vascular tree when a movable X-ray tube rotates in an arc around the patient during acquisition of the X-rays. The X-ray data obtained from this series of exposures is sent to a computer workstation which then creates a 3D model of the vessels studied. This 3D model can then be manipulated

on the workstation in real-time to provide an infinite number of projections (views) of the vessels imaged.

The technique of 3DRA will vary depending upon the manufacturer of the X-ray hardware and software. The author's experience, and all of the 3D images included in this atlas, were acquired using General Electric (GE) LCN+ equipment with a Sun workstation.

The X-ray c-arm (floor mounted X-ray tube and image intensifier) rotates in an arc of approximately 220 degrees around the patient during the injection of a contrast agent bolus. The speed of rotation of the GE equipment was 40 degrees per second. The entire arc of rotation during which data acquisition occurred would take approximately 5 seconds. It acquires approximately 8.8 frames (X-rays) per second generating approximately 44 images in a 512×512 matrix over that 5-second timeframe.

During setup for the 3D data acquisition, the region of interest would be placed in the isocenter of the image under fluoroscopy. The blood vessels of interest need to be in the center of the X-ray image in the frontal (AP) and lateral (from the side) projections. This would ensure that X-ray data from all projections would be included in the final 3D model that is generated. If the region of interest were to be placed at the edge of the X-ray field and was not included in the entire rotation, then the final 3D image would not include this partially imaged segment.

The next step after placing the subject in the center of the X-ray image would be to perform a test rotation. This is critical to ensure that there would be no physical collisions between the large, rotating c-arm and any nearby structures. This is especially important when dealing with interventional neuroradiology procedures requiring anesthesia equipment, arterial and other lines, ventilator equipment, and sometimes a ventricular drainage catheter setup. If a test rotation is not done then inadvertent removal of life supporting lines and equipment might occur if there was a collision or if one of the lines were to become tangled with the rotating c-arm gantry.

The technique of 3DRA utilizes a single bolus injection of contrast. As opposed to standard 2D angiography where the contrast bolus is visualized as it progresses through the vascular tree, the goal of imaging with 3DRA is to obtain all of the X-ray images in the same phase of circula-

tion. Most often the arterial phase is desired, although this can be altered so that the venous phase can be the predominant portion of the vascular bed imaged. Since the image data is acquired over a 5-second time period during the arc of rotation, the goal of the injection is to opacify the desired vessels during the entire 5 seconds. Through experience we found that in most cases adequate opacification could be accomplished with approximately 15 cc total volume injected at a rate of 3 cc per second. These numbers could be modified depending on the size of the vessel where the catheter was residing, the cardiac output, and whether we were trying to image a high-flow state such as an arterial-venous malformation (AVM). We did not have a single complication related to these injection volumes over a 4-year period.

The operator/physician chooses a delay time to begin the rotational sequence after initiating the contrast injection. When the arterial circulation is the desired phase of circulation to be imaged, the delay is usually between 0.5 and 2 seconds depending upon the position of the catheter tip relative to the vessels of interest and the patient's cardiac output. The closer the catheter tip is to the area of interest the shorter the needed delay. When patients have impaired cardiac function, a longer time delay may be required to allow time for the injected contrast to reach the area of interest. Again, the goal is complete opacification of the vasculature of interest for the entire rotational sequence (about 5 seconds). Occasionally, when the venous circulation is the region of interest, much longer delay times are used. This can be estimated by evaluating the timing of the appearance of the veins on prior 2D angiographic sequences.

Once the rotational sequence is completed, the data is transferred to the Sun workstation where a 3D model is generated. With a 3D model available the operator/physician applies a threshold and utilizes other 3D tools to generate the final 3D image.

A variety of reconstruction algorithms are available which include shaded surface display (SSD), maximum intensity projection (MIP), volume rendering (VR), and a navigator view which allows for an endoluminal view of the vessels in the 3D volume set.

Most of the 3D images in this atlas are shaded surface display 3D images. This algorithm simulates a light source projected on the model, which generates varying shades of gray that enhance the 3D perspective.

After several software updates, a program was developed which allowed reconstruction of surgical clips and endovascular coils in the 3D image. When possible, I include some of these images in the atlas.

As stated in the "Introduction", there are certain limitations inherent with 3DRA technique. Visualization of small/distal vessels is limited. This limitation is partly related to the lower injection rate used compared with standard two-dimensional digital subtraction angiography (2D DSA). A second limitation is the lack of bony landmarks on the final 3D image. A third limitation is the lack of sequential visualization of angiographic images showing the progression of contrast through the various phases of circulation. For this reason 3DRA should not replace traditional high resolution 2D DSA, but should complement the angiographic examination.

CHAPTER TWO

COLOR ILLUSTRATIONS OF NORMAL NEUROVASCULAR ANATOMY

The illustrations in this chapter are intended to provide the reader with a reference point for the images that follow in subsequent chapters. These illustrations provide the reader with the necessary background anatomy and the most commonly encountered patterns of vascular branching.

Variability and inconstancy are the rule rather than the exception in how the vasculature tree branches within the neck and face, as well as how it branches intracranially. It is important to understand that vessels are named for the territory of tissue that they supply. We hope that your understanding of neurovascular anatomy is enhanced by the application of this concept in the atlas.

The illustrations that are presented are meant to provide the reader with a basic understanding of the relationship of the vascular tree with the tissues they nourish. During your journey through this three-dimensional (3D) atlas, refer back to these color illustrations when needed.

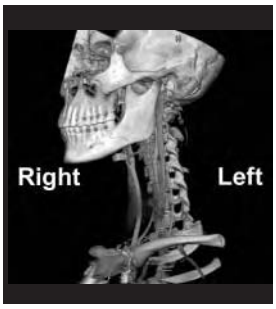

BLACK KEY

1 ascending thoracic aorta
2 descending thoracic aorta
3 innominate artery
4 right subclavian artery
5 stump of right common carotid artery
6 right vertebral artery
7 right thyrocervical trunk
8 right costocervical trunk
9 right internal mammary artery
10 left subclavian artery
11 left vertebral artery
12 left thyrocervical trunk
13 left costocervical trunk
14 left internal mammary artery
15 left common carotid artery

RED KEY

2 internal carotid artery
3 external carotid artery
4 ascending pharyngeal artery
5 occipital artery
6 posterior auricular artery
7 superior thyroid artery
9 lingual artery
10 facial artery
11 superficial temporal artery
12 internal maxillary artery
24 transverse facial artery

Fig. 2.1 Left anterior oblique view showing the great vessels arising from the aortic arch. The carotid vasculature is seen with numerous branches of the proximal external carotid artery visualized. Reprinted with permission of The Cleveland Clinic Foundation.

BLACK KEY

1 common carotid artery
2 internal carotid artery
3 external carotid artery
7 superior thyroid artery
9 lingual artery
10 facial artery
12 internal maxillary artery
13 middle meningeal artery
15 deep temporal artery
16 inferior alveolar artery
17 infraorbital artery
18 posterior superior alveolar artery
19 greater palatine artery
20 sphenopalatine artery
25 masseteric muscular branches
26 buccal muscular branches
da deep auricular artery
at anterior tympanic artery
fs foramen spinosum
PDB posterior directed branches of distal internal maxillary artery. These are 1. artery of foramen rotundum 2. artery of the pterygoid canal (vidian artery), and 3. pharyngeal artery (pterygovaginal artery)

RED KEY

3 innominate artery
4 right subclavian artery
6 right vertebral artery
7 right thyrocervical trunk
9 right internal mammary artery
10 left subclavian artery
11 left vertebral artery
12 left thyrocervical trunk
13 left costocervical trunk
14 left internal mammary artery

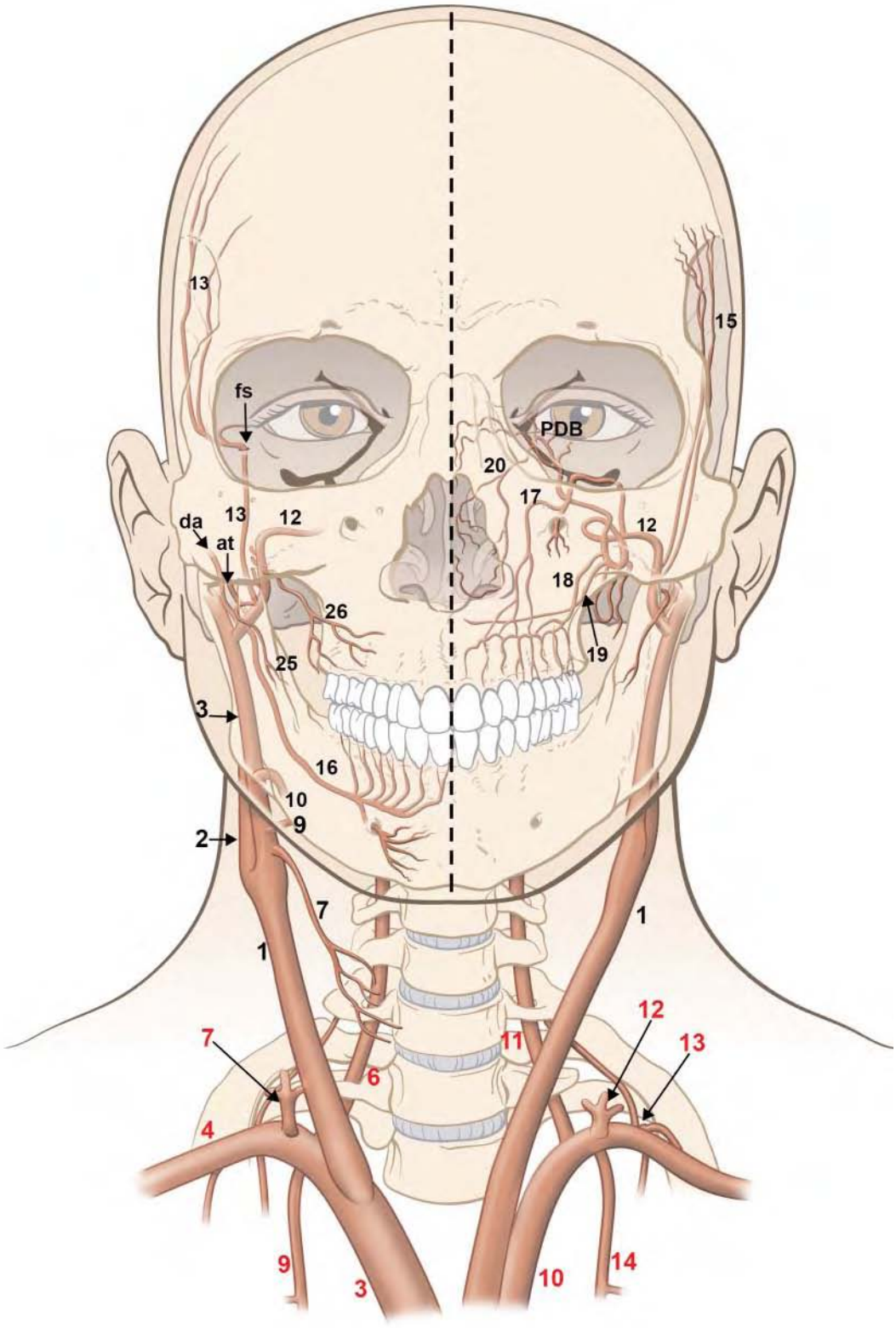

Fig. 2.2 Frontal view of the head, neck, and upper chest. The great vessels are seen in the lower portion of the image. The arteries of the face and neck are demonstrated. The arteries of the first (mandibular) portion of the internal maxillary artery are on the reader's left. The arteries of the second (pterygoid) and third (pterygopalatine) portions of the internal maxillary artery are on the reader's right. Reprinted with permission of The Cleveland Clinic Foundation.

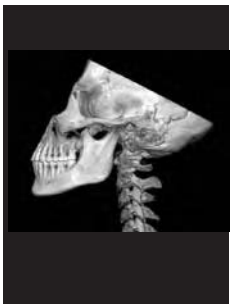

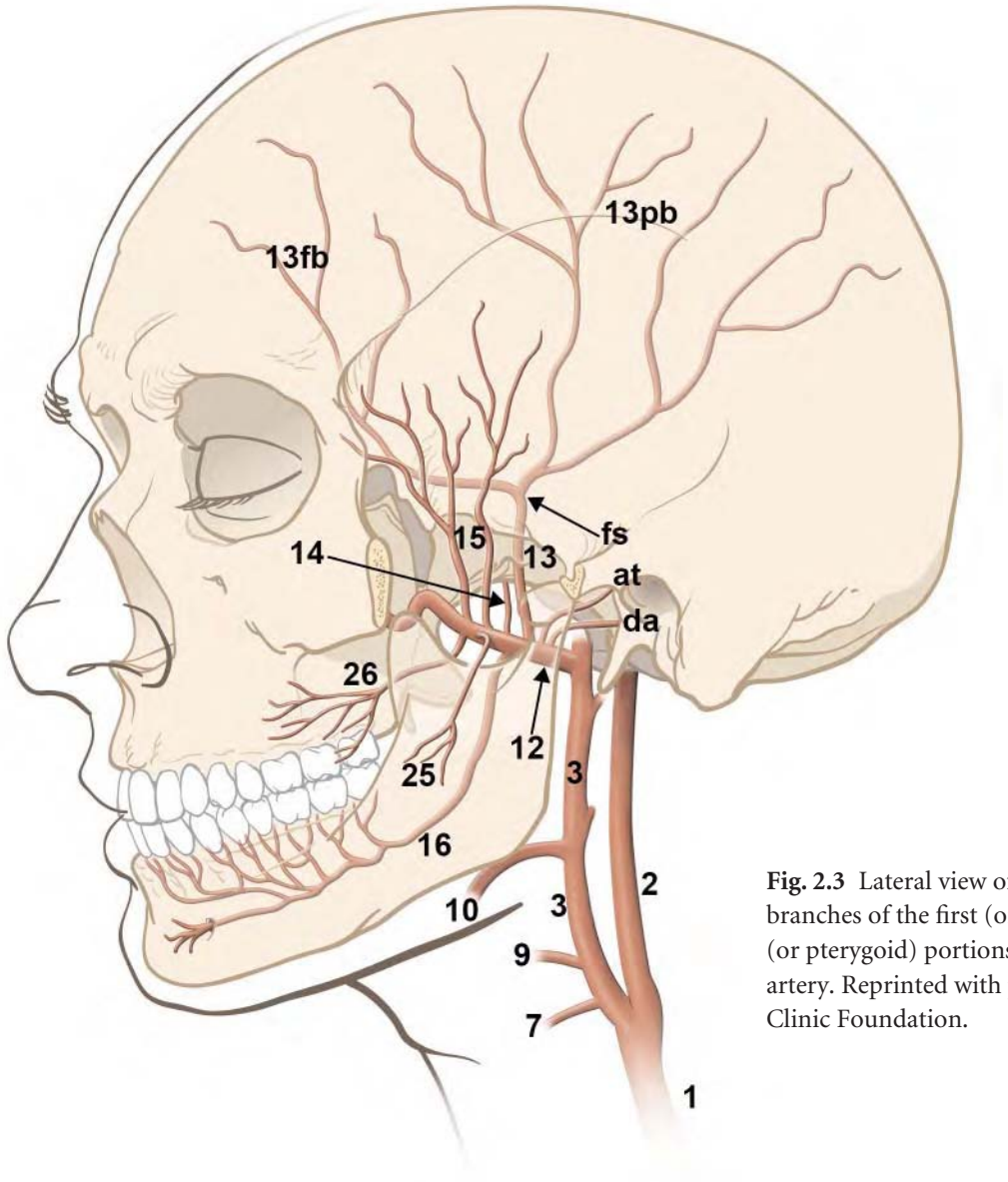

Fig. 2.3 Lateral view of the face showing the branches of the first (or mandibular) and the second (or pterygoid) portions of the internal maxillary artery. Reprinted with permission of The Cleveland Clinic Foundation.

FIGURE KEY

1 common carotid artery
2 internal carotid artery
3 external carotid artery
7 superior thyroid artery
9 lingual artery
10 facial artery
12 internal maxillary artery
13 middle meningeal artery
13fb frontal branch of middle meningeal artery
13pb parietal branch of middle meningeal artery
14 accessory meningeal artery
15 deep temporal artery
16 inferior alveolar artery
25 masseteric muscular branches
26 buccal muscular branches
at anterior tympanic artery
da deep auricular artery
fs foramen spinosum

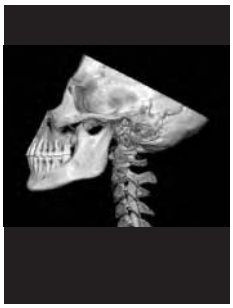

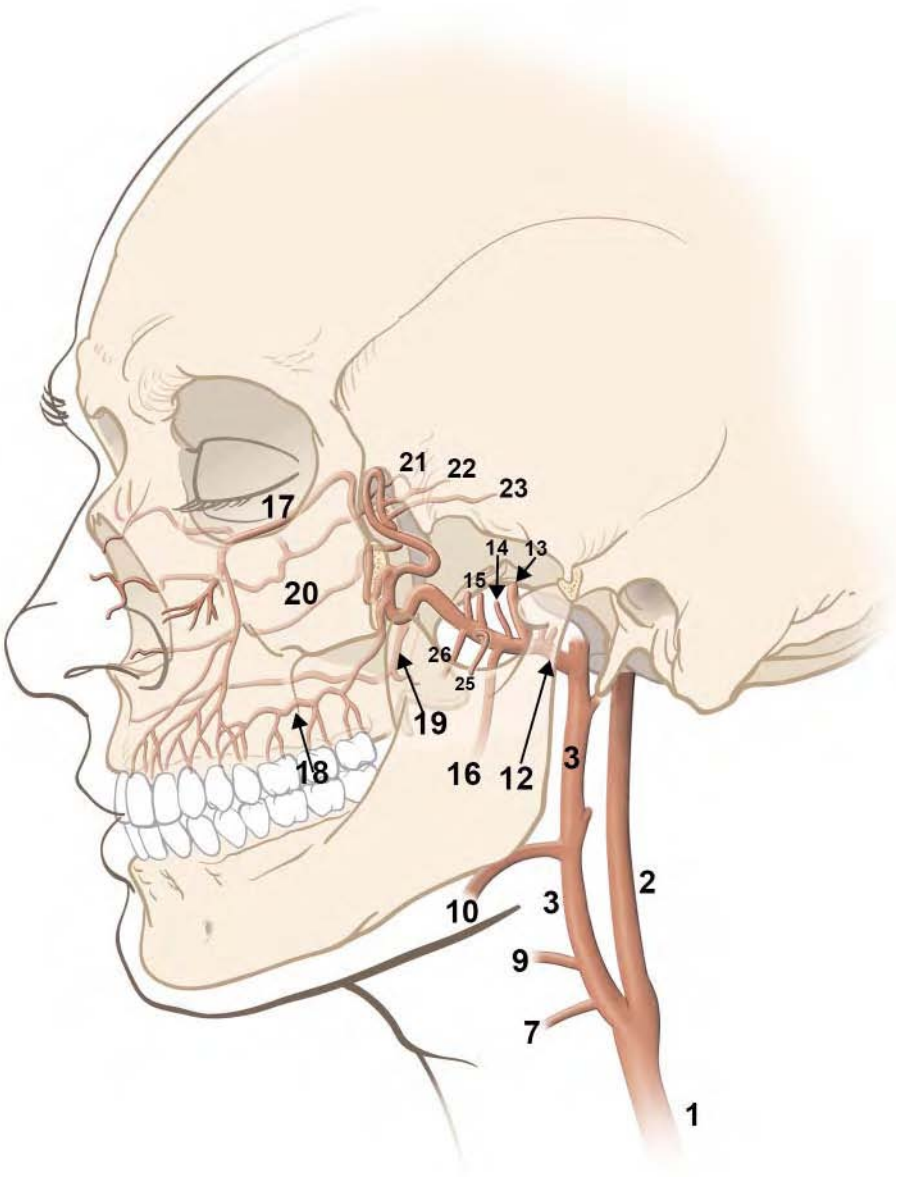

FIGURE KEY

1 common carotid artery
2 internal carotid artery
3 external carotid artery
7 superior thyroid artery
9 lingual artery
10 facial artery
12 internal maxillary artery
13 middle meningeal artery
14 accessory meningeal artery
15 deep temporal artery
16 inferior alveolar artery
17 infraorbital artery
18 posterior superior alveolar artery
19 greater palatine artery
20 sphenopalatine artery
21 artery of the foramen rotundum
22 artery of the pterygoid canal (vidian artery)
23 pharyngeal artery (pterygovaginal artery)
25 masseteric muscular branches
26 buccal muscular branches

Fig. 2.4 Lateral view of the face showing the branches of the third (or pterygopalatine) portion of the internal maxillary artery. Reprinted with permission of The Cleveland Clinic Foundation.

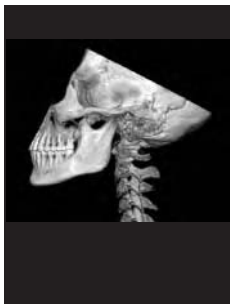

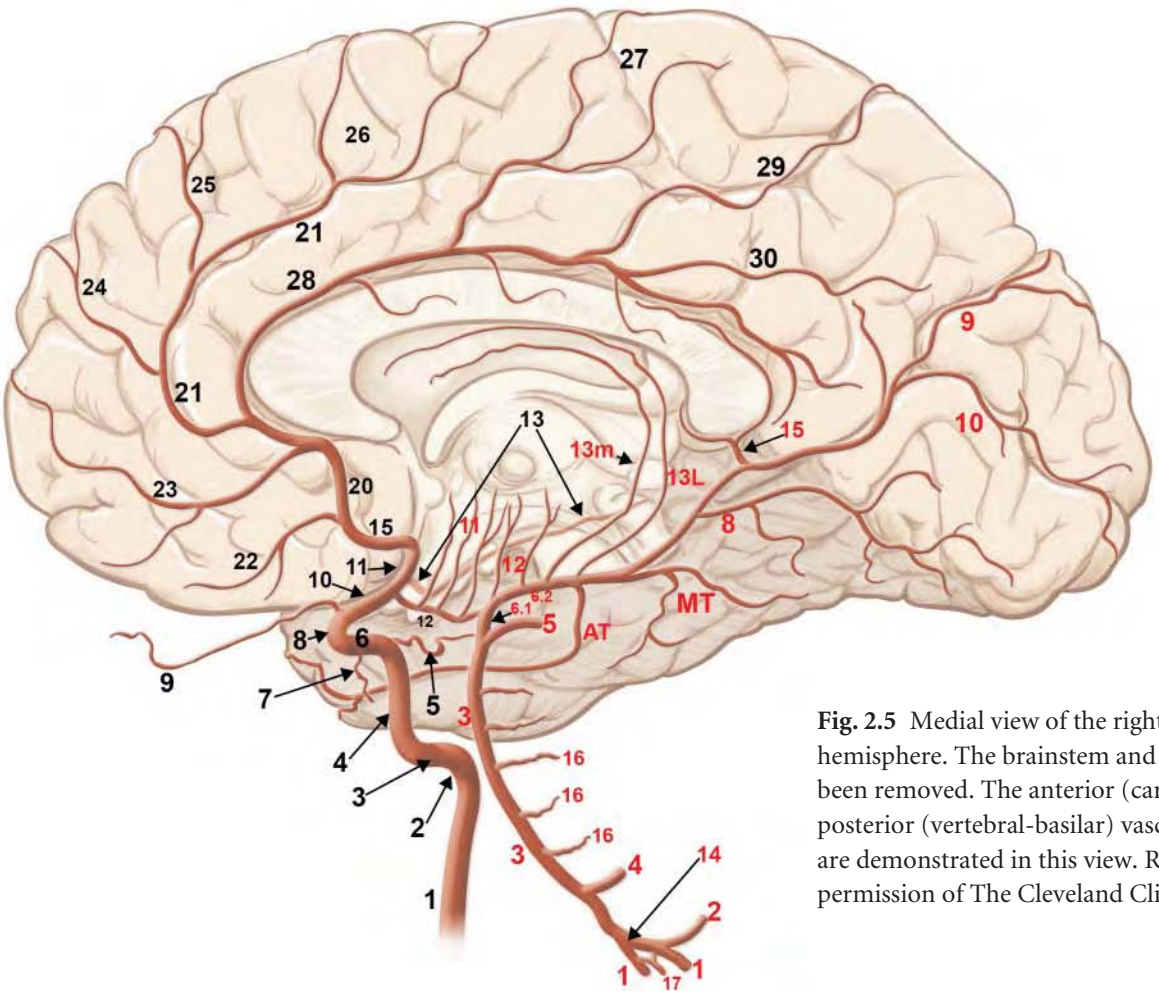

Fig. 2.5 Medial view of the right cerebral hemisphere. The brainstem and cerebellum have been removed. The anterior (carotid) and the posterior (vertebral-basilar) vascular circulations are demonstrated in this view. Reprinted with permission of The Cleveland Clinic Foundation.

BLACK KEY

1 internal carotid artery – cervical segment
2 internal carotid artery – vertical petrous segment
3 internal carotid artery – horizontal petrous segment
4 presellar segment (C5) internal carotid artery
5 meningohypophyseal trunk
6 horizontal (C4) intracavernous internal carotid artery
7 inferolateral trunk
8 anterior genu (C3) intracavernous internal carotid artery
9 ophthalmic artery
10 supraclinoid (C2) segment internal carotid artery
11 supraclinoid (C1) segment internal carotid artery
12 posterior communicating artery
13 anterior choroidal artery
15 A1 segment of anterior cerebral artery
20 proximal A2 segment anterior cerebral artery
21 callosomarginal branch of anterior cerebral artery
22 orbitofrontal branch of anterior cerebral artery
23 frontopolar branch of anterior cerebral artery
24 anterior internal frontal branch of anterior cerebral artery
25 middle internal frontal branch of anterior cerebral artery
26 posterior internal frontal branch of anterior cerebral artery
27 paracentral lobule artery branch of anterior cerebral artery
28 pericallosal branch of anterior cerebral artery
29 superior internal parietal branch of anterior cerebral artery
30 inferior internal parietal branch of anterior cerebral artery

RED KEY

1 vertebral artery
2 posterior inferior cerebellar artery
3 basilar artery
4 anterior inferior cerebellar artery
5 superior cerebellar artery
6.1 P1 segment of posterior cerebral artery
6.2 P2 segment of posterior cerebral artery
8 posterior temporal branch of posterior cerebral artery
9 parieto-occipital branch of posterior cerebral artery
10 calcarine branch of posterior cerebral artery
11 anterior thalamoperforators
12 posterior thalamoperforators
13m medial posterior choroidal artery
13L lateral posterior choroidal artery
14 vertebral-basilar junction
15 posterior pericallosal artery (splenial artery)
16 pontine perforator
17 anterior spinal artery
AT anterior temporal branches of posterior cerebral artery
MT mid-temporal branches of posterior cerebral artery

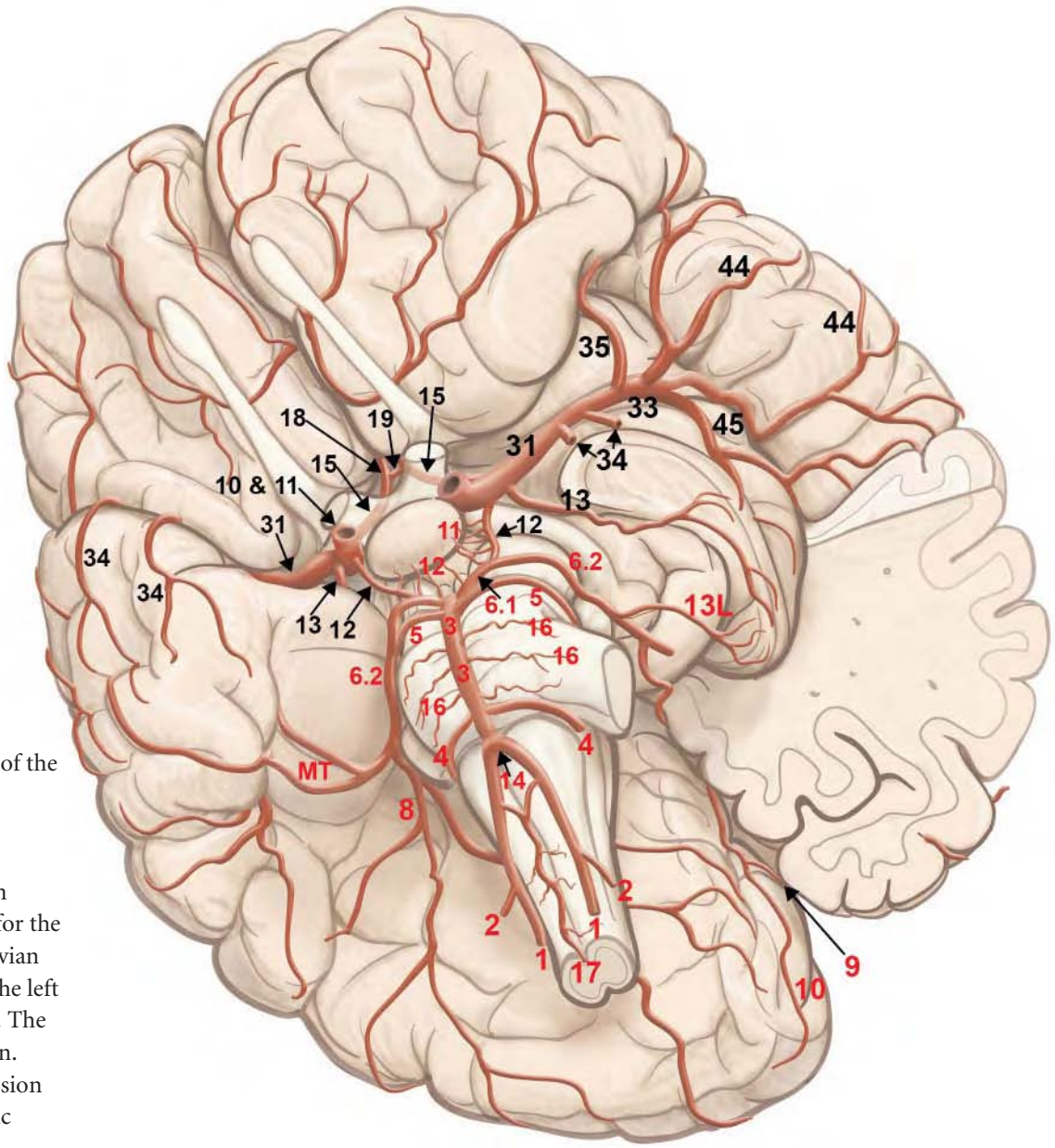

Fig. 2.6 Oblique view of the brain looking from an inferior to superior orientation. The left temporal lobe has been removed/cut to allow for the visualization of the sylvian (insular) branches of the left middle cerebral artery. The circle of Willis is shown. Reprinted with permission of The Cleveland Clinic Foundation.

BLACK KEY

10 supraclinoid (C2) segment internal carotid artery
11 supraclinoid (C1) segment internal carotid artery
12 posterior communicating artery
13 anterior choroidal artery
15 A1 segment of anterior cerebral artery
18 A1-A2 junction anterior cerebral artery
19 anterior communicating artery
31 M1 segment of middle cerebral artery
33 bifurcation/trifurcation of middle cerebral artery
34 anterior temporal lobe branches of middle cerebral artery
35 orbitofrontal branch of middle cerebral artery
44 opercular branches of middle cerebral artery
45 sylvian (insular) branches of middle cerebral artery

RED KEY

1 vertebral artery
2 posterior inferior cerebellar artery
3 basilar artery
4 anterior inferior cerebellar artery
5 superior cerebellar artery
6.1 P1 segment of posterior cerebral artery
6.2 P2 segment of posterior cerebral artery
8 posterior temporal branch of posterior cerebral artery
9 parieto-occipital branch of posterior cerebral artery
10 calcarine branch of posterior cerebral artery
11 anterior thalamoperforators
12 posterior thalamoperforators
13L lateral posterior choroidal arteries
14 vertebral-basilar junction
16 pontine perforator
17 anterior spinal artery
MT mid-temporal branches of posterior cerebral artery

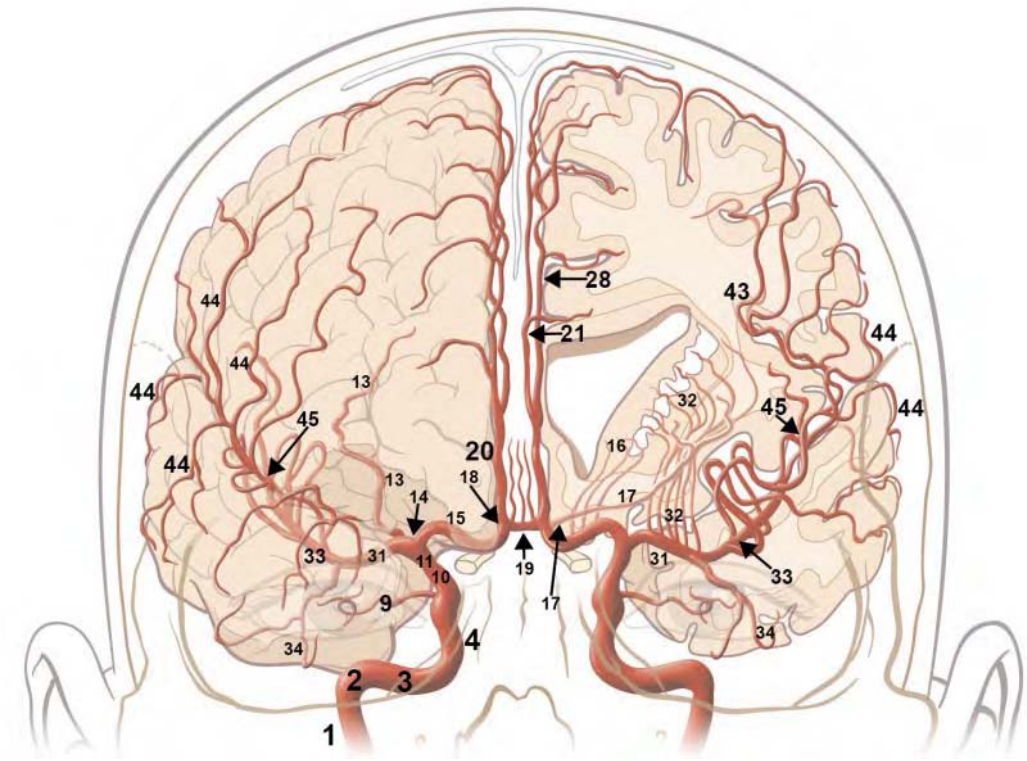

Fig. 2.7 Frontal view of the anterior (carotid) intracranial circulation. The anterior and middle cerebral arteries are shown. In this view many of the anterior and middle cerebral arteries are obscured because of the overlap in this projection. Reprinted with permission of The Cleveland Clinic Foundation.

FIGURE KEY

1 internal carotid artery - cervical segment
2 internal carotid artery - vertical petrous segment
3 internal carotid artery – horizontal petrous segment
4 presellar segment (C5) internal carotid artery
9 ophthalmic artery
10 and 11 supraclinoid segment internal carotid artery
13 anterior choroidal artery
14 internal carotid artery bifurcation
15 A1 segment of anterior cerebral artery
16 medial lenticulostriate arteries
17 recurrent artery of Heubner
18 A1-A2 junction anterior cerebral artery
19 anterior communicating artery
20 proximal A2 segment anterior cerebral artery
21 callosomarginal branch of anterior cerebral artery
28 pericallosal branch of anterior cerebral artery
31 M1 segment of middle cerebral artery
32 lateral lenticulostriate arteries
33 bifurcation/trifurcation of middle cerebral artery
34 anterior temporal lobe branches of middle cerebral artery
43 sylvian point
44 opercular branches of middle cerebral artery
45 sylvian(insular) branches of middle cerebral artery

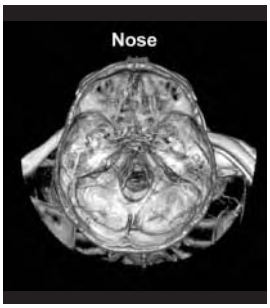

BLACK KEY

5 meningohypophyseal trunk
6 horizontal (C4) intracavernous internal carotid artery
7 inferolateral trunk
9 ophthalmic artery
12 posterior communicating artery
13 anterior choroidal artery
14 internal carotid artery bifurcation
15 A1 segment of anterior cerebral artery
19 anterior communicating artery
20 proximal A2 segment anterior cerebral artery
21 callosomarginal branch of anterior cerebral artery
28 pericallosal branch of anterior cerebral artery
31 M1 segment of middle cerebral artery
33 bifurcation/trifurcation of middle cerebral artery
34 anterior temporal lobe branches of middle cerebral artery
35 orbitofrontal branch of middle cerebral artery
45 sylvian(insular) branches of middle cerebral artery

RED KEY

1 vertebral artery
2 posterior inferior cerebellar artery
3 basilar artery
4 anterior inferior cerebellar artery
5 superior cerebellar artery
6.1 P1 segment posterior cerebral artery
6.2 P2 segment posterior cerebral artery
8 posterior temporal branch of posterior cerebral artery
9 parieto-occipital branch of posterior cerebral artery
10 calcarine branch of posterior cerebral artery
14 vertebral-basilar junction
16 pontine perforators
17 anterior spinal artery

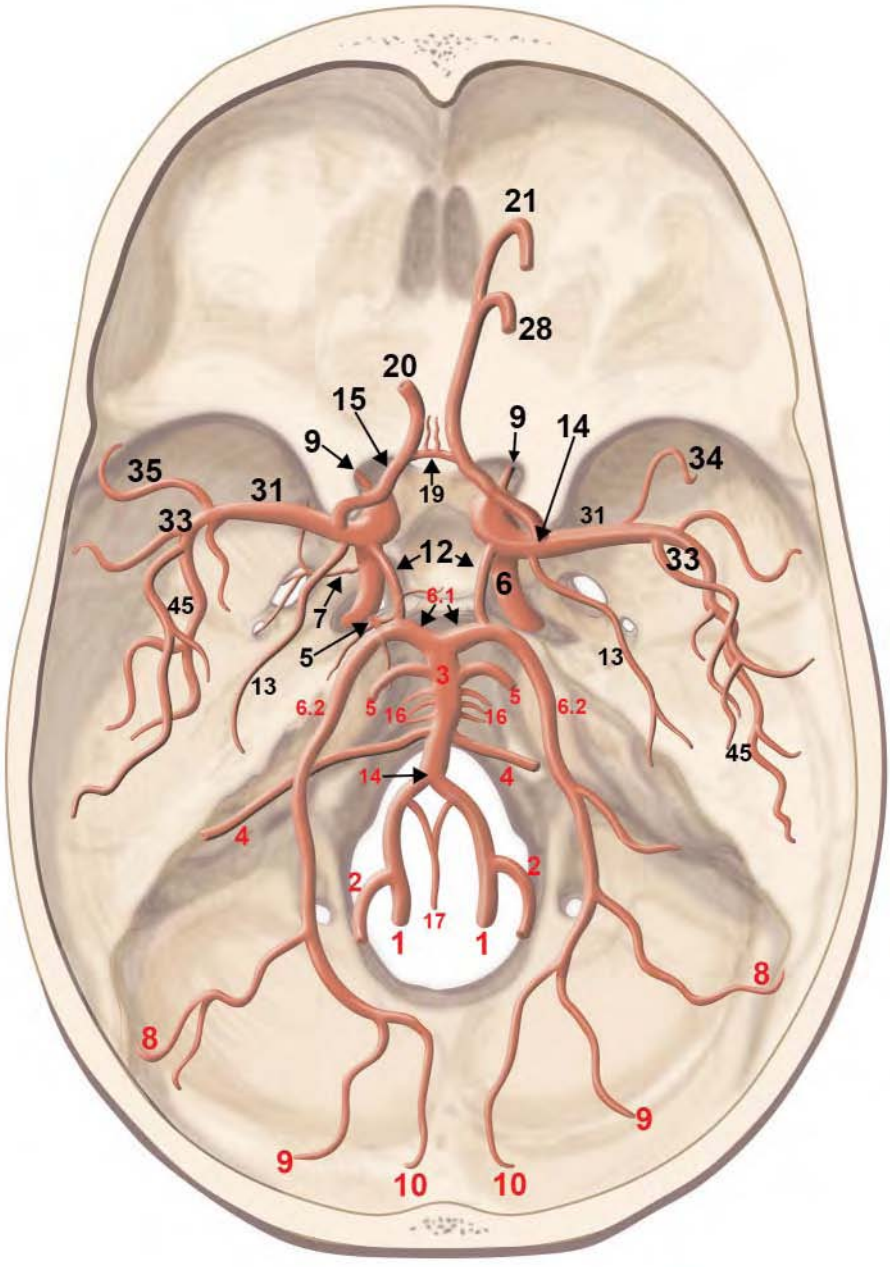

Fig. 2.8 Top down view (superior to inferior) of the skull base. The proximal arterial branches of the anterior (carotid) and the posterior (vertebral-basilar) circulations are demonstrated. The circle of Willis is clearly shown. Reprinted with permission of The Cleveland Clinic Foundation.

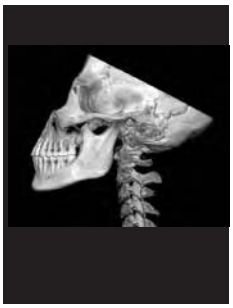

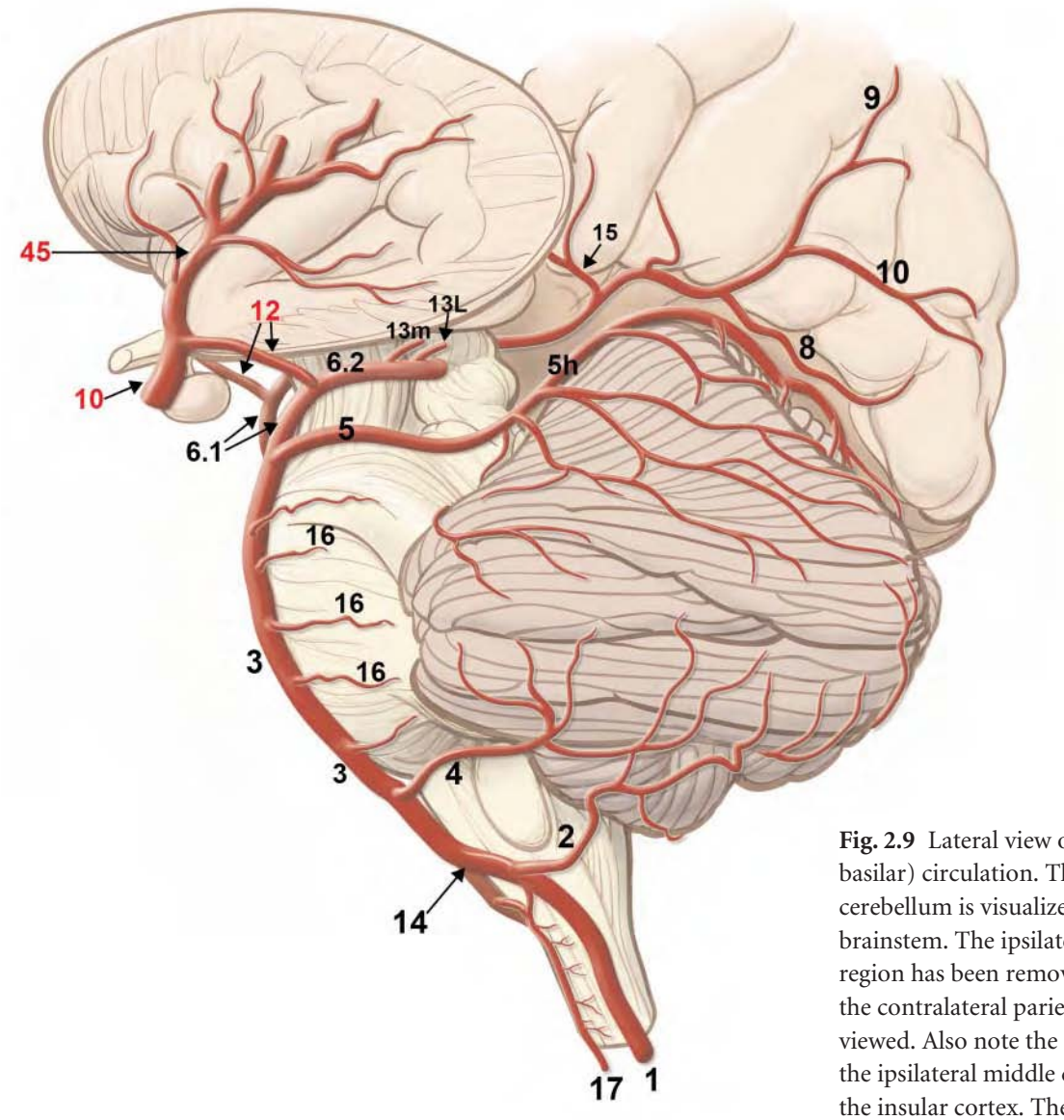

Fig. 2.9 Lateral view of the posterior (vertebral-basilar) circulation. The lateral surface of the cerebellum is visualized in addition to the brainstem. The ipsilateral parieto-occipital region has been removed. The medial surface of the contralateral parieto-occipital region is viewed. Also note the sylvian branches (45) of the ipsilateral middle cerebral artery overlying the insular cortex. The ipsilateral temporal lobe has been removed. Reprinted with permission of The Cleveland Clinic Foundation.

BLACK KEY

1 vertebral artery
2 posterior inferior cerebellar artery
3 basilar artery
4 anterior inferior cerebellar artery
5 superior cerebellar artery
5h hemispheric branch of superior cerebellar artery
6.1 P1 segment of posterior cerebral artery
6.2 P2 segment of posterior cerebral artery
8 posterior temporal branch of posterior cerebral artery
9 parieto-occipital branch of posterior cerebral artery
10 calcarine branch of posterior cerebral artery
13m medial posterior choroidal artery
13L lateral posterior choroidal artery
14 vertebral-basilar junction
15 posterior pericallosal artery (splenial artery)
16 pontine perforator
17 anterior spinal artery

RED KEY

10 supraclinoid (C2) segment internal carotid artery
12 posterior communicating artery
45 sylvian(insular) branches of middle cerebral artery

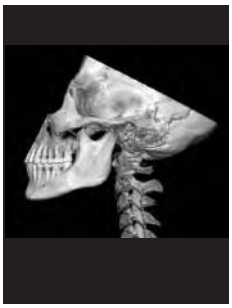

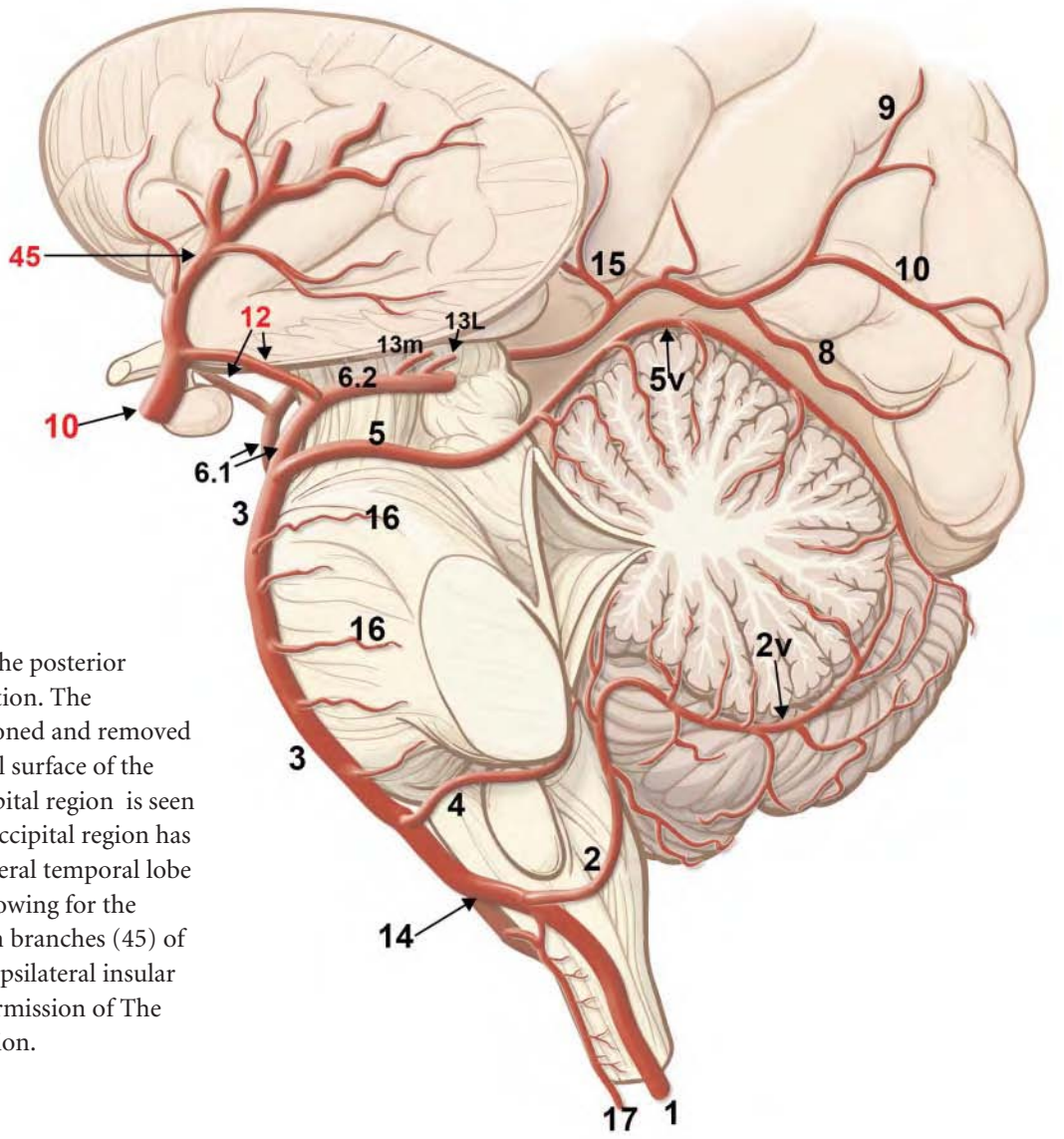

Fig. 2.10 Lateral view of the posterior (vertebral-basilar) circulation. The cerebellum has been sectioned and removed in the midline. The medial surface of the contralateral parieto-occipital region is seen as the ipsilateral parieto-occipital region has been removed. The ipsilateral temporal lobe has also been removed allowing for the visualization of the sylvian branches (45) of the MCA that overlie the ipsilateral insular cortex. Reprinted with permission of The Cleveland Clinic Foundation.

BLACK KEY

1 vertebral artery
2 posterior inferior cerebellar artery
2v vermian branch of PICA
3 basilar artery
4 anterior inferior cerebellar artery
5 superior cerebellar artery
5v vermian branch of superior cerebellar artery
6.1 P1 segment of posterior cerebral artery
6.2 P2 segment of posterior cerebral artery
8 posterior temporal branch of posterior cerebral artery
9 parieto-occipital branch of posterior cerebral artery
10 calcarine branch of posterior cerebral artery
13m medial posterior choroidal artery
13L lateral posterior choroidal artery
14 vertebral-basilar junction
15 posterior pericallosal artery (splenial artery)
16 pontine perforator
17 anterior spinal artery

RED KEY

10 supraclinoid (C2) segment internal carotid artery
12 posterior communicating artery
45 sylvian(insular) branches of middle cerebral artery

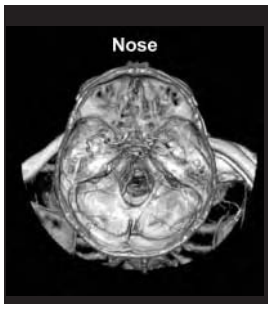

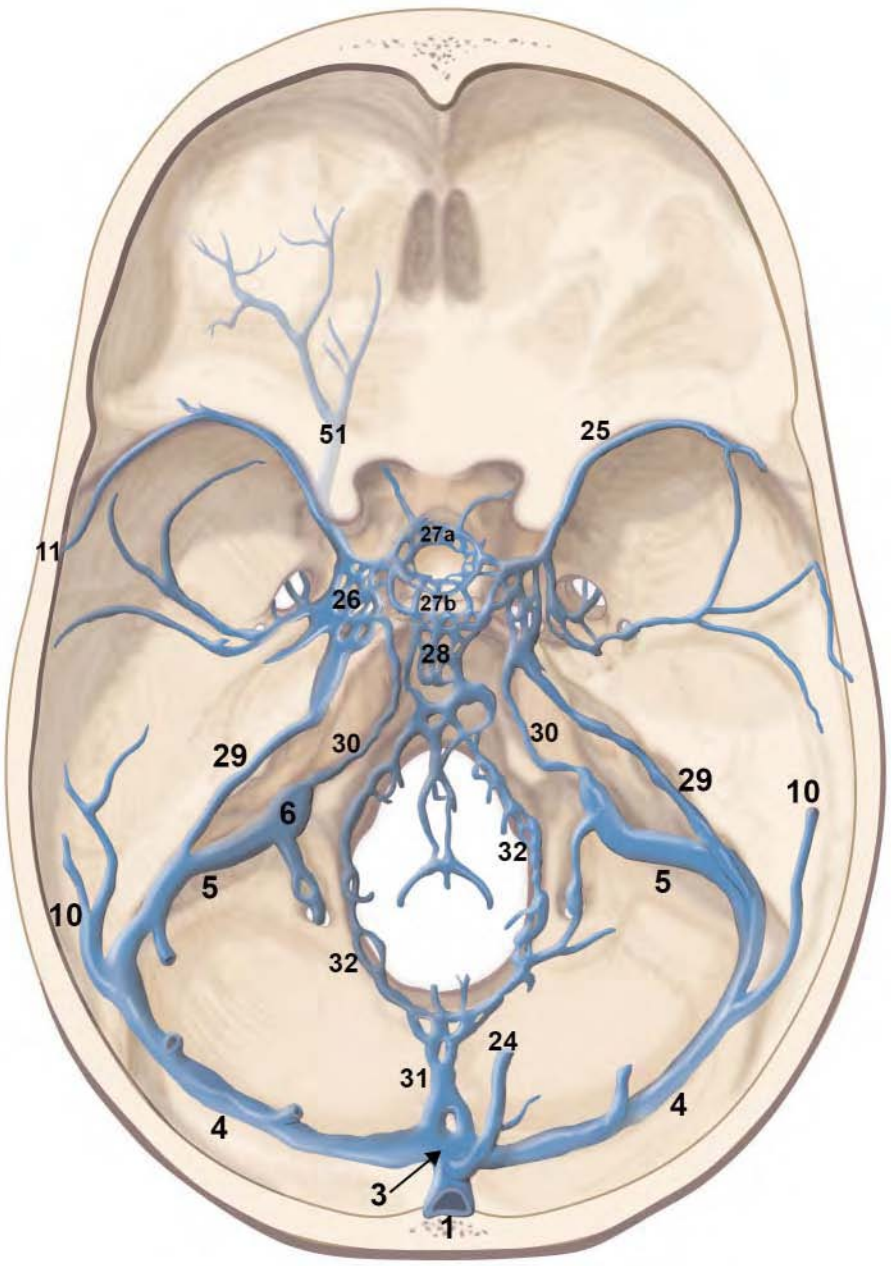

FIGURE KEY

1 superior sagittal sinus
3 torcular herophili
4 transverse sinus
5 sigmoid sinus
6 jugular bulb
10 vein of Labbé
11 superficial middle cerebral vein
24 straight sinus
25 sphenoparietal sinus
26 cavernous sinus
27a anterior intercavernous sinus
27b posterior intercavernous sinus
28 clival venous plexus
29 superior petrosal sinus
30 inferior petrosal sinus
31 occipital sinus
32 marginal sinus
51 superior ophthalmic vein

Fig. 2.11 A top down view (superior to inferior) of the skull base. The venous circulation in the skull base region is visualized. The numerous venous communications that exist around the skull base are also illustrated. Reprinted with permission of The Cleveland Clinic Foundation.

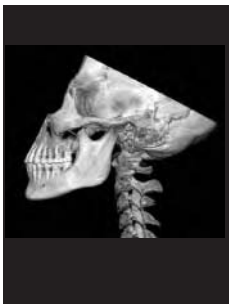

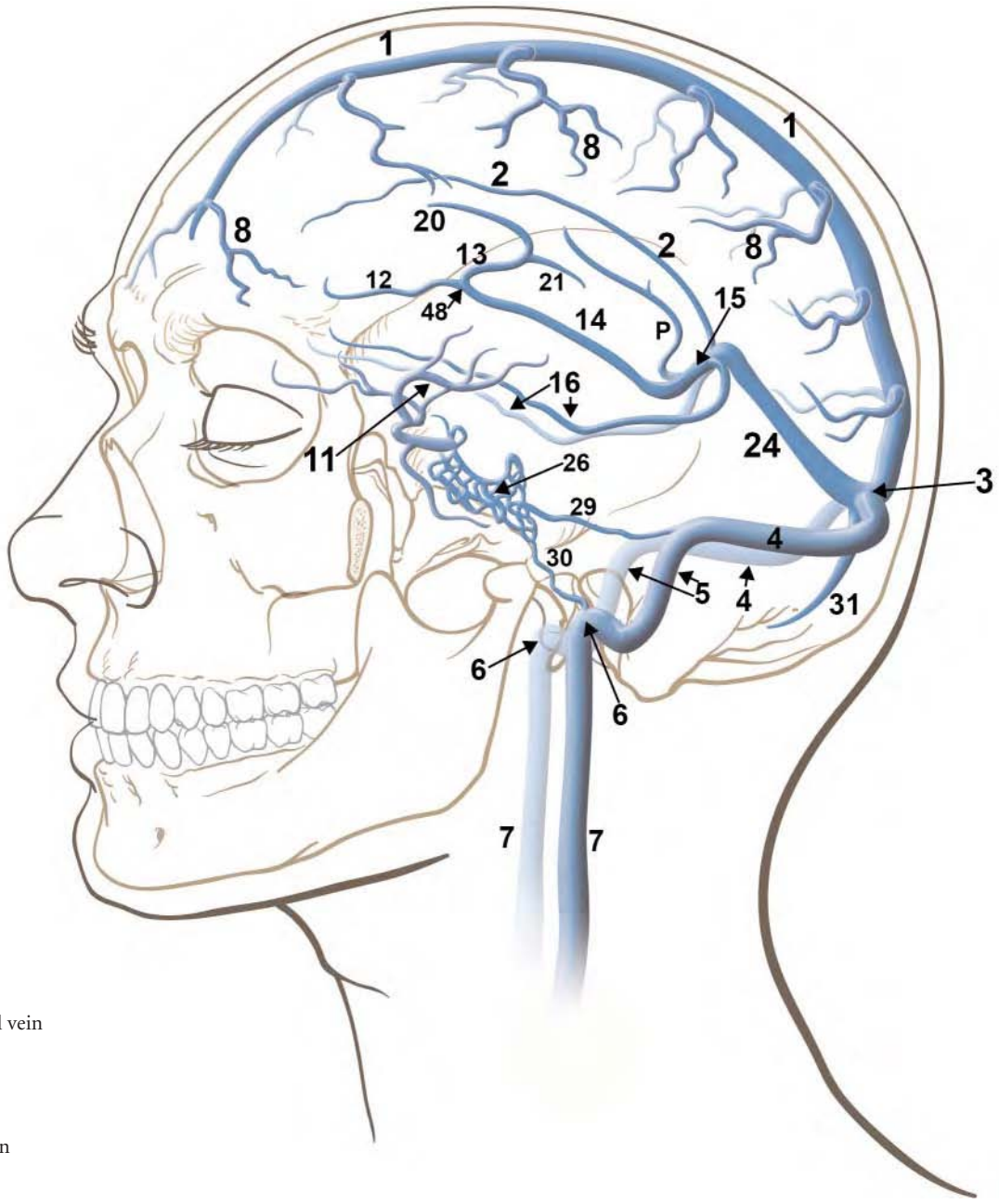

FIGURE KEY

1 superior sagittal sinus
2 inferior sagittal sinus
3 torcular herophili
4 transverse sinus
5 sigmoid sinus
6 jugular bulb
7 internal jugular vein
8 superficial cortical vein
11 superficial middle cerebral vein
12 septal vein
13 thalamostriate vein
14 internal cerebral vein
15 great cerebral vein of Galen
16 basal vein of Rosenthal
20 anterior caudate vein
21 terminal vein
26 cavernous sinus
29 superior petrosal sinus
30 inferior petrosal sinus
31 occipital sinus
48 true venous angle
P posterior pericallosal vein

Fig. 2.12 Near lateral (slight obliquity) view of the supratentorial superficial and deep venous systems. Reprinted with permission of The Cleveland Clinic Foundation.

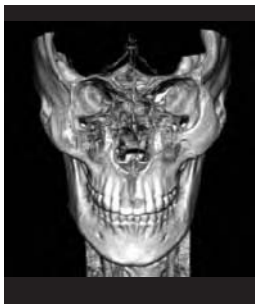

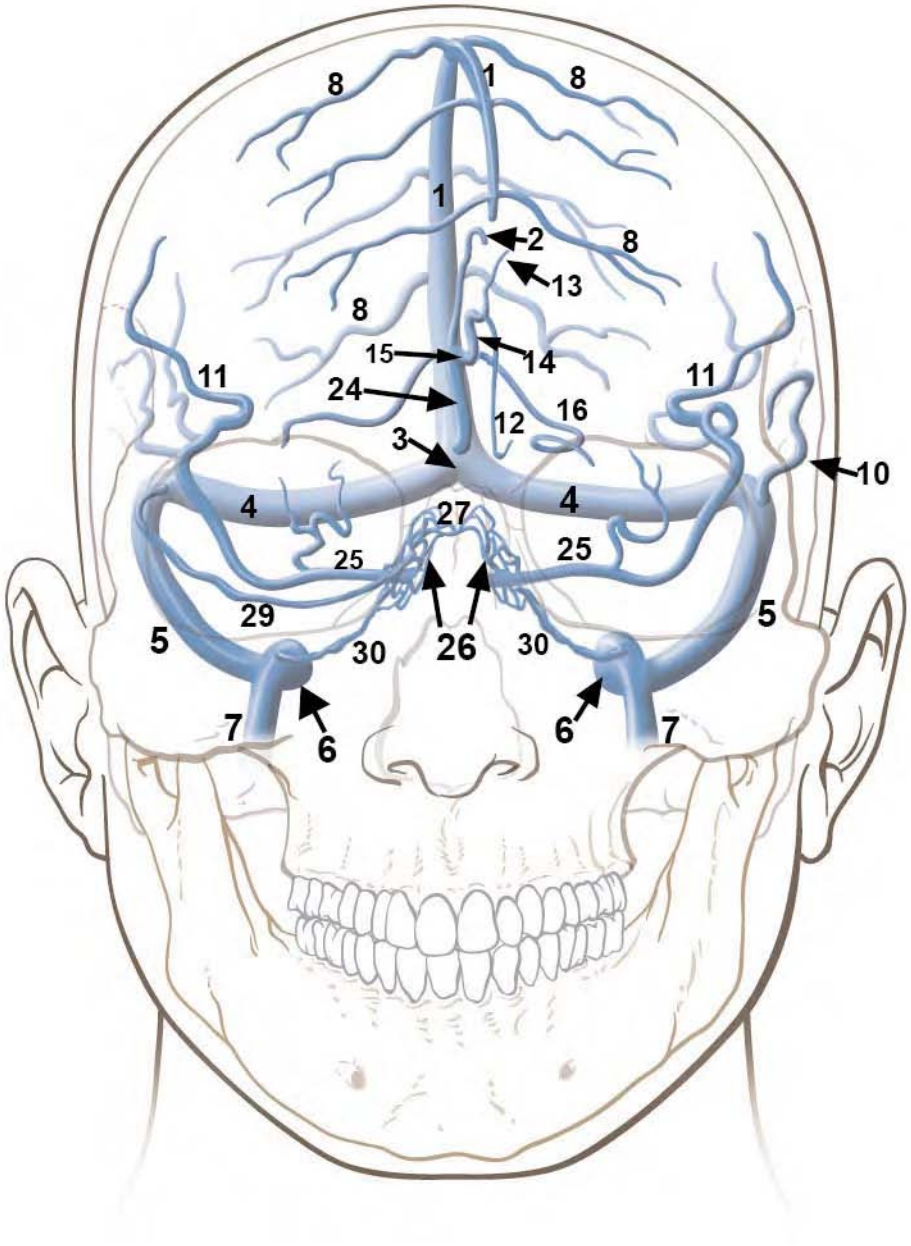

Fig. 2.13 Frontal view demonstrating the major cerebral veins and the dural sinuses. Reprinted with permission of The Cleveland Clinic Foundation.

FIGURE KEY

1 superior sagittal sinus
2 inferior sagittal sinus
3 torcular herophili
4 transverse sinus
5 sigmoid sinus
6 jugular bulb
7 internal jugular vein
8 superficial cortical vein
10 vein of Labbé
11 superficial middle cerebral vein
12 septal vein
13 thalamostriate vein
14 internal cerebral vein
15 great cerebral vein of Galen
16 basal vein of Rosenthal
24 straight sinus
25 sphenoparietal sinus
26 cavernous sinus
27 intercavernous sinus
29 superior petrosal sinus
30 inferior petrosal sinus

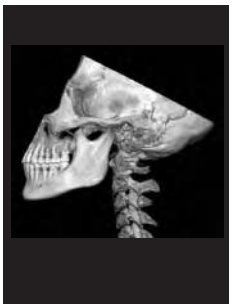

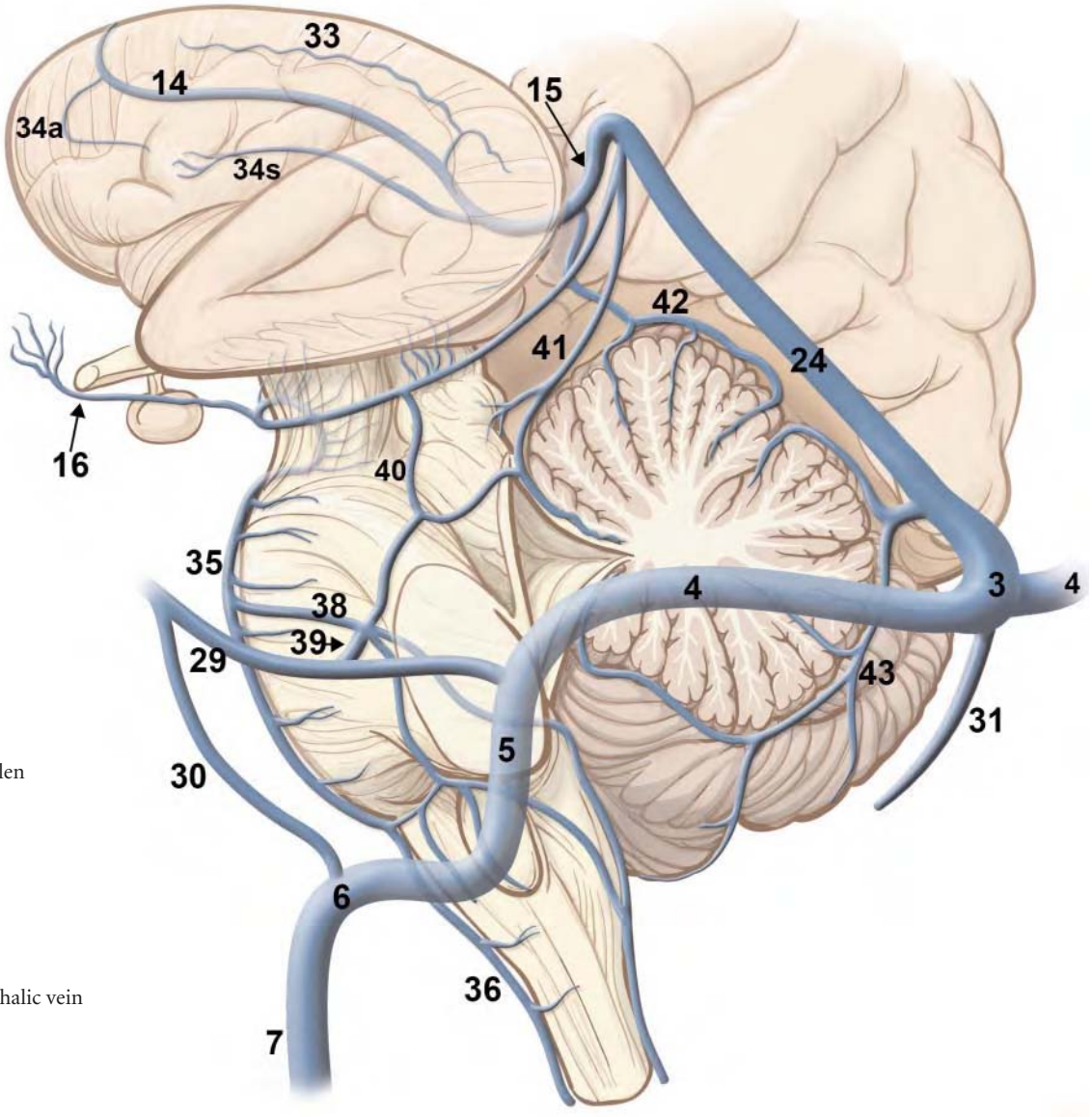

FIGURE KEY

3 torcular herophili
4 transverse sinus
5 sigmoid sinus
6 jugular bulb
7 internal jugular vein
14 internal cerebral vein
15 great cerebral vein of Galen
16 basal vein of Rosenthal
24 straight sinus
31 occipital sinus
33 superior choroid vein
34a anterior thalamic vein
34s superior thalamic vein
35 anterior pontomesencephalic vein
36 anterior medullary vein
38 transverse pontine vein
39 petrosal vein
40 lateral mesencephalic vein
41 precentral cerebellar vein
42 superior vermian vein
43 inferior vermian vein

Fig. 2.14 Lateral view of the posterior fossa veins. The cerebellum has been sectioned and removed in the midline. Reprinted with permission of The Cleveland Clinic Foundation.

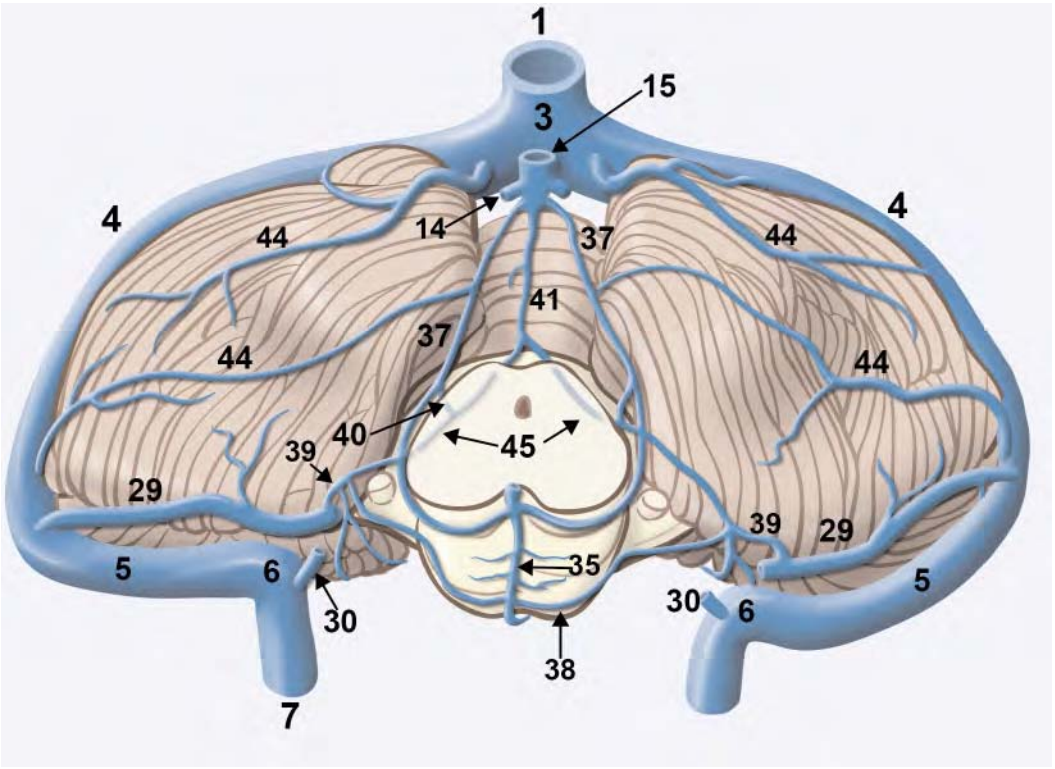

Fig. 2.15 Posterior fossa veins as seen from above looking posterioraly as well as inferiorly. Reprinted with permission of The Cleveland Clinic Foundation.

FIGURE KEY

1 superior sagittal sinus
3 torcular herophili
4 transverse sinus
5 sigmoid sinus
6 jugular bulb
7 internal jugular vein
14 internal cerebral vein
15 great cerebral vein of Galen
29 superior petrosal sinus
30 inferior petrosal sinus
35 anterior pontomesencephalic vein
37 posterior mesencephalic vein
38 transverse pontine vein
39 petrosal vein
40 lateral mesencephalic vein
41 precentral cerebellar vein
44 cerebellar hemispheric vein
45 brachial vein

FIGURE KEY

24 straight sinus
37 posterior mesencephalic vein
41 precentral cerebellar vein
43 inferior vermian vein
44 cerebellar hemispheric vein
* inferior retrotonsillar vein

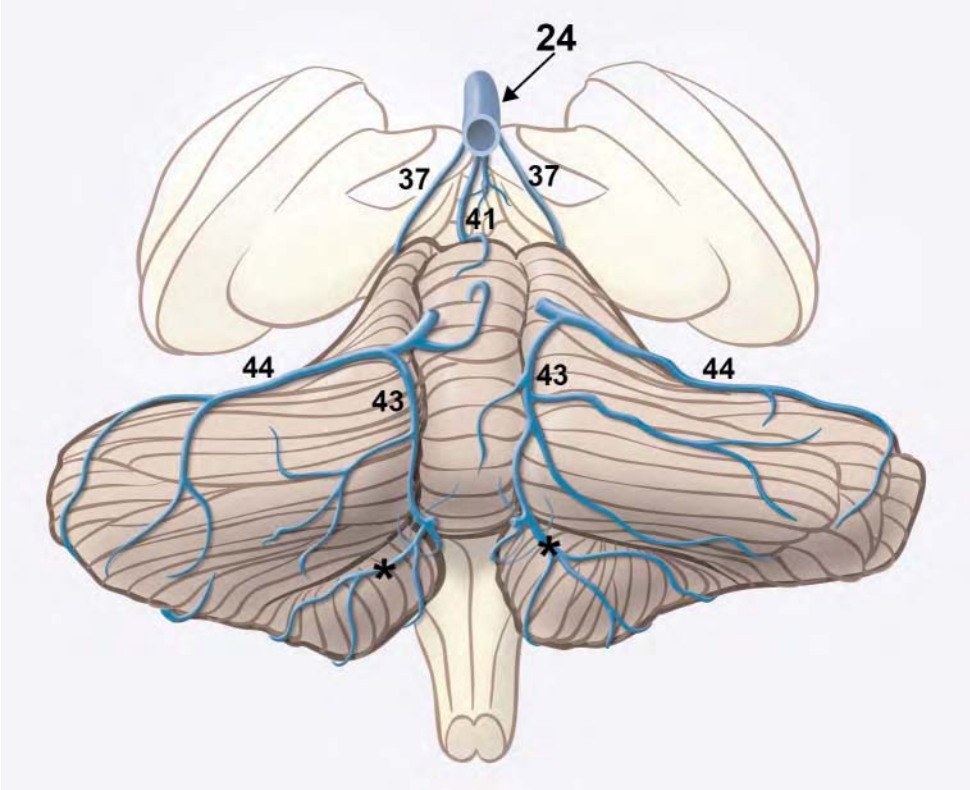

Fig. 2.16 Posterior fossa veins as seen from the dorsal (posterior) aspect looking anteriorly. Reprinted with permission of The Cleveland Clinic Foundation.

CHAPTER THREE

THE AORTIC ARCH

The aortic arch is the main conduit through which arterial blood pumped from the left ventricle of the heart is transmitted to the entire body. Blood passes through the aortic valve and enters the ascending thoracic aorta. This is a tubular structure, 4 to 5 cm in length, and usually of uniform caliber. The ascending aorta is continuous with the aortic arch at about the right second costal cartilage. Blood is then directed into the upper extremities and the head and neck through the innominate artery, the left common carotid artery, and the left subclavian artery. These vessels are collectively referred to as the great vessels. They arise in that order (in most instances) from the aortic arch. The aortic arch is semicircle in shape. Beyond the takeoff of the great vessels, the diameter of the aortic arch is approximately two-thirds that of the ascending aorta (1).

In a typical situation, the first branch of the aortic arch is the innominate artery. This vascular pedicle ascends toward the right and divides into the right common carotid artery and the right subclavian artery.

The innominate artery continues beyond the takeoff of the right common carotid artery as the right subclavian artery. Arising from the superior aspect of the right subclavian artery (in order) are the right vertebral artery, the right thyrocervical trunk, and the right costocervical trunk. The right internal mammary artery arises from the inferior aspect of the right subclavian artery usually opposite that of the right vertebral artery. The right vertebral artery courses superiorally and medially to enter the foramen transversarium of the cervical spine. Ninety-five percent of the time the artery then enters C6. In 5 percent of the cases, the artery enters a foramen transversarium at another variable level (2). Blood flowing through the right subclavian artery will eventually supply the right upper extremity more distally.

Beyond the innominate artery the next branch that is usually encountered is the left common carotid artery. In the majority of cases, the

common carotid artery arises from the aortic arch or the innominate artery. Seventy-five percent of the time it arises from the aortic arch (2). It is also not unusual that it arises in common origin with the innominate artery. It also may arise from the medial aspect of the innominate artery. This anatomic relationship can result in a technically more difficult catheterization.

The last branch and the most left-sided of the branches to arise from the aortic arch is the left subclavian artery. Typically, the first branch of the left subclavian artery is the left vertebral artery. In a similar fashion as the right side, it courses superiorally and medially towards the cervical spine. In 95 percent of the instances it ascends in the neck after entering the foramen transversarium of C6. Five percent of the time it enters the foramen transversarium at other variable levels (2). The left thyrocervical and costocervical trunks arise from the superior aspect of the left subclavian artery beyond the left vertebral artery. The internal mammary artery arises from the inferior aspect of the subclavian artery opposite the vertebral artery. In approximately 6 percent of the cases, the left vertebral artery arises directly from the aortic arch between the left common carotid artery and the left subclavian artery. When this happens the left vertebral artery will usually enter the foramen transversarium at C4 or C5 (2). As on the right side, blood flow through the left subclavian artery will eventually supply the left upper extremity more distally.

There are numerous congenital anomalies and developmental variations in the anatomy of the aortic arch and the branching of the great vessels. These are beyond the scope of this atlas.

There are factors that limit the utility of three-dimensional rotational angiography (3DRA) in the imaging of the aortic arch. In order to achieve adequate opacification of the aortic arch and its vessels, an unacceptably large volume of contrast would have to be injected. In addition to this, the degree of cardiac/aortic pulsation during the 5-second injection and the acquisition of the 3DRA would create a large amount of motion artifact that would degrade the diagnostic quality of the angiographic images. Despite these limitations a few 3D angiograms of the aortic arch were obtained during early experiences with this technique. In certain limited indications, the 3DRA technique was also utilized in the assessment of the great vessels.

REFERENCES

1. Abrams, H.L., and G. Jonsson. 1983. *The normal thoracic aorta.* In Abrams Angiography: Vascular and Interventional Radiology, Third Edition. H.L. Abrams, editor. Boston: Little, Brown and Company, pp. 360–362.
2. Haughton, V.M., and A.E. Rosenbaum. 1974. *The normal and anomalous aortic arch and brachiocephalic arteries.* In Radiology of the Skull and Brain: Angiography Volume 2. T.H. Newton and D.G. Potts, editors. St. Louis, Mo: C.V. Mosby Company, pp. 1155, 1157, 1160.

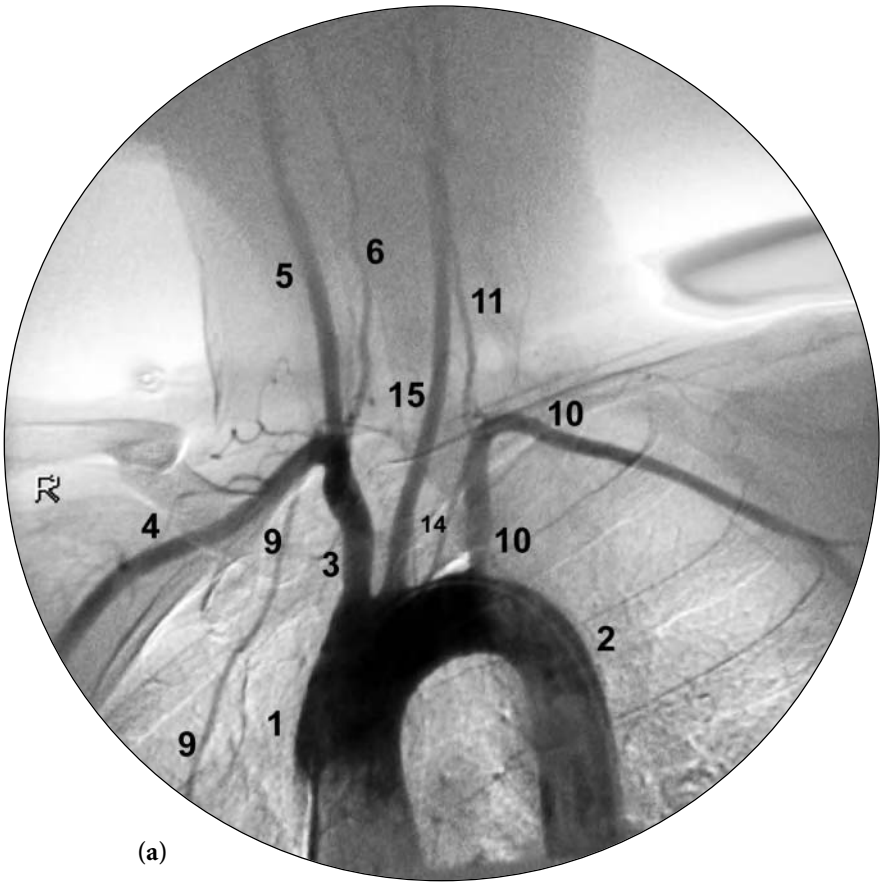

(**a**)

Fig. 3.1 (a,b) Left anterior oblique 2D (*a*) and 3D (*b*) aortic arch angiograms. The 2D angiogram shows a more complete visualization of the normal branches. The 3D angiogram is of limited quality and fails to adequately image the normal anatomy.

FIGURE KEY

1 ascending thoracic aorta
2 descending thoracic aorta
3 innominate artery
4 right subclavian artery
5 right common carotid artery
6 right vertebral artery
9 right internal mammary artery
10 left subclavian artery
11 left vertebral artery
12 left thyrocervical trunk
14 left internal mammary artery
15 left common carotid artery

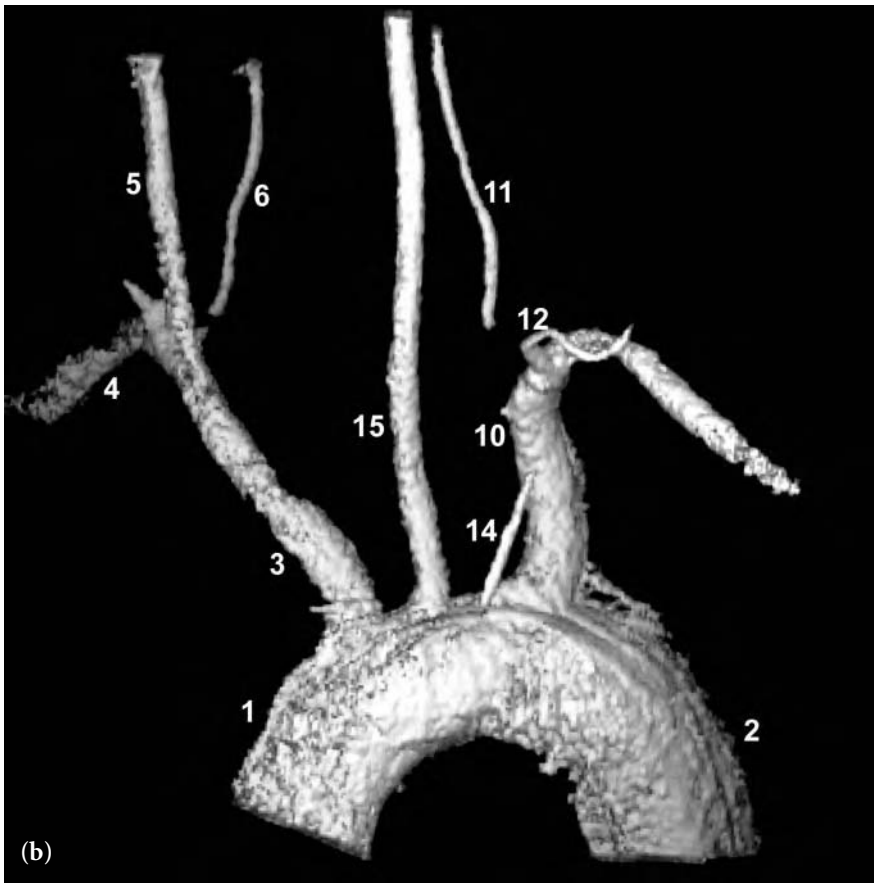
5
6
11
12
4
15
10
14
3
1
2
(b)

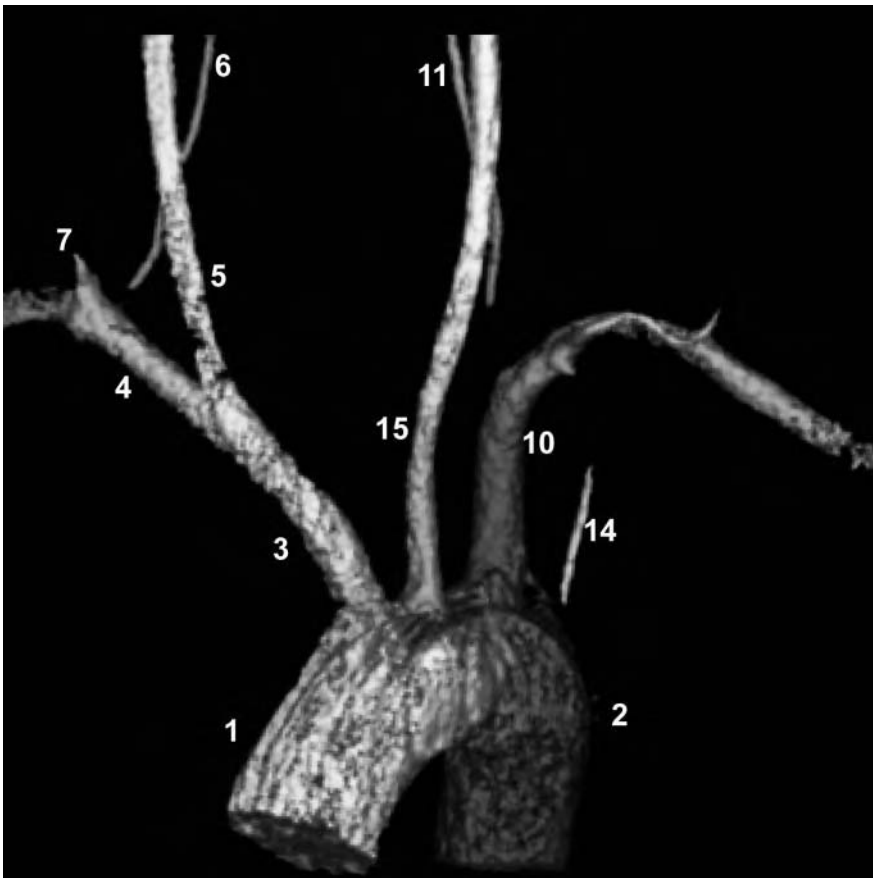

Fig. 3.2 Frontal 3D view aortic arch angiogram. There is an artifactual lack of visualization of the proximal vertebral arteries due to the limitations of this technique in imaging this region.

FIGURE KEY

1 ascending thoracic aorta
2 descending thoracic aorta
3 innominate artery
4 right subclavian artery
5 right common carotid artery
6 right vertebral artery
7 right thyrocervical trunk
10 left subclavian artery
11 left vertebral artery
14 left internal mammary artery
15 left common carotid artery

Fig. 3.3 Left anterior oblique 2D aortic arch angiogram. This view illustrates a marked elongation and tortuosity of the great vessels that arise from the aortic arch. These changes are often seen in people with a long-standing hypertension.

FIGURE KEY

1 ascending thoracic aorta
2 descending thoracic aorta
3 innominate artery
4 right subclavian artery
5 right common carotid artery
6 right vertebral artery
10 left subclavian artery
11 left vertebral artery
15 left common carotid artery

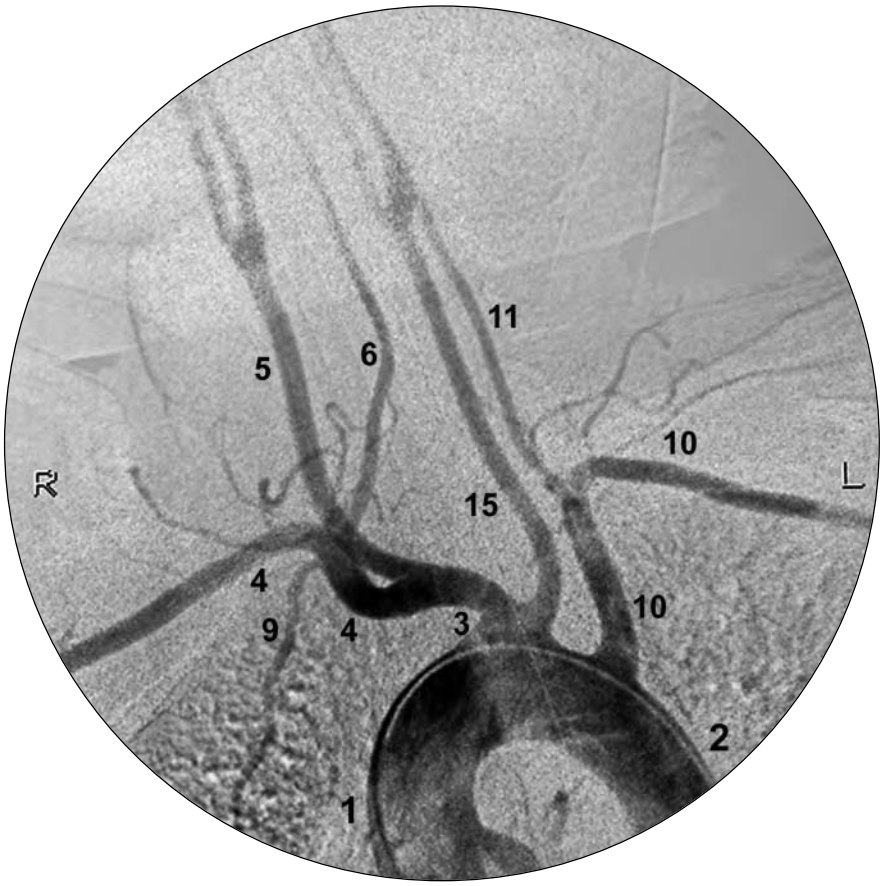

Fig. 3.4 Left anterior oblique 2D aortic arch angiogram shows a normal variation in branching where the left common carotid artery arises at the point where the innominate artery arises.

FIGURE KEY

1 ascending thoracic aorta
2 descending thoracic aorta
3 innominate artery
4 right subclavian artery
5 right common carotid artery
6 right vertebral artery
9 right internal mammary artery
10 left subclavian artery
11 left vertebral artery
15 left common carotid artery

CHAPTER FOUR

CERVICAL VASCULATURE

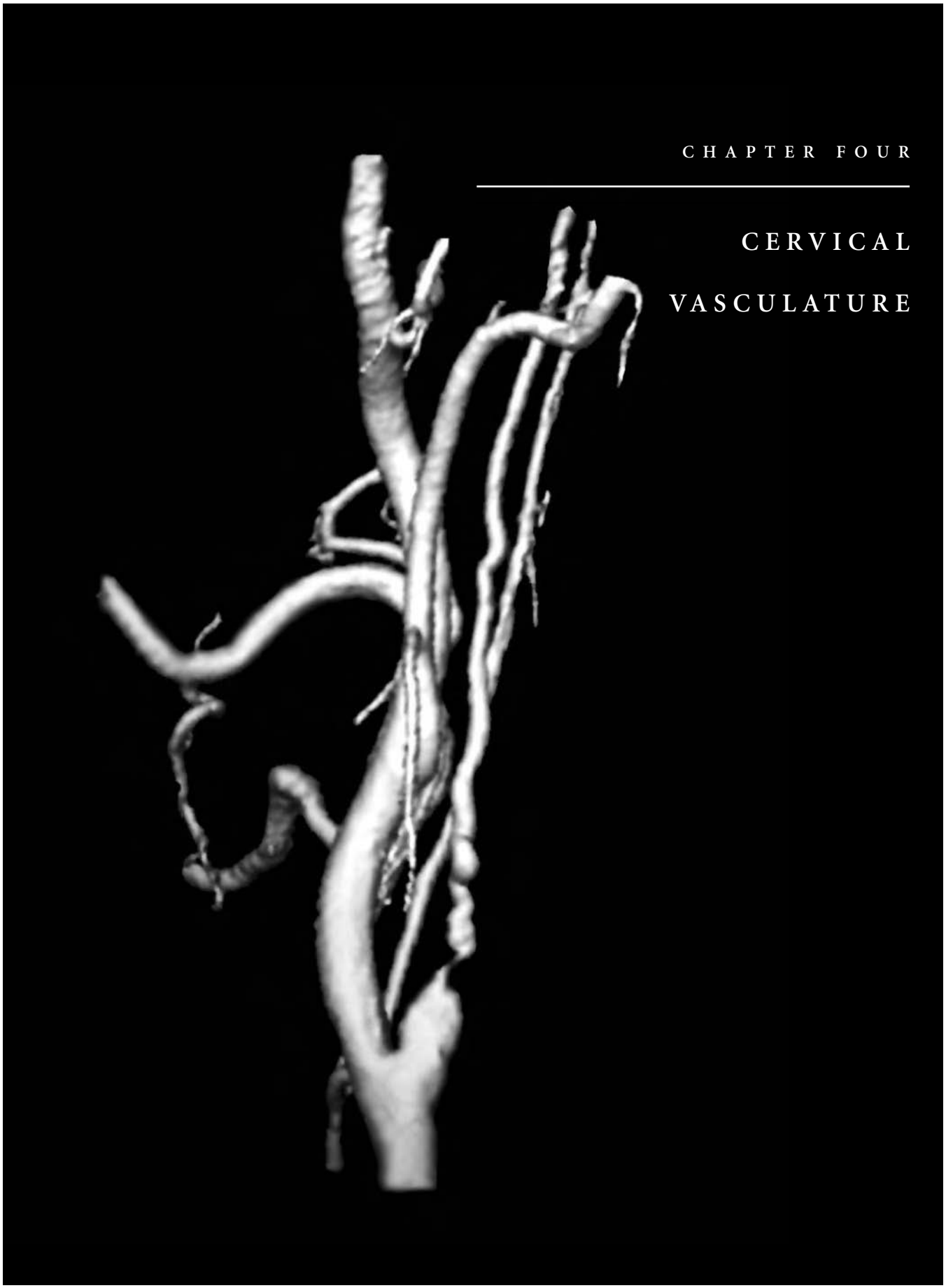

I. CAROTID CIRCULATION

The common carotid arteries ascend within both sides of the neck. They are invested by a condensation of the deep layer of the cervical fascia (carotid sheath) along with the internal jugular vein and vagus nerve (cranial nerve X). The carotid sheath structures are deep to the sternocleidomastoid muscle. The common carotid artery (CCA) lies medial to the internal jugular vein. At the C3-4 (34 %) or C4-5 (46 %) level the common carotid artery bifurcates into the external carotid artery (ECA) and the internal carotid artery (ICA) (1). The bifurcation can occur as high as C1 or as low as T2 (2). The proximal internal carotid artery most often lies postero-lateral to the proximal external carotid artery and medial to the internal jugular vein. The internal carotid artery ascends almost vertically in the neck and enters the skull base through an aperture within the petrous bone called the carotid canal. There are no major named branches of the ICA within the neck. Rarely one may encounter takeoff of an occipital or other normal branch of the ECA from an otherwise normal ICA.

After arising from the common carotid artery, the external carotid artery travels in a tortuous course within the deep spaces of the upper neck/face and gives rise to multiple branches that supply the face, scalp, major portions of the dura, and upper pole of the thyroid gland. These include the superior thyroid artery, ascending pharyngeal artery, lingual and facial arteries, occipital artery, posterior auricular and muscular branches that supply the masseter, the buccinator, and the pterygoid muscles. The two terminal branches of the primary external carotid artery are the superficial temporal artery (STA) and the internal maxillary artery (IMAX). These terminal branches arise near the superior ramus of the mandible. The STA arises within the parotid gland ascending deep to the temporalis muscle, crosses the zygomatic process giving off the transverse facial artery, and divides into terminal branches to supply the majority of the

scalp. The IMAX is typically the largest terminal branch of the ECA originating behind the neck of the mandible coursing medially towards the sphenopalatine fissure giving off numerous branches along its course. The three portions of the IMAX are the first or mandibular, second or pterygoid, and the third or pterygopalatine.

The mandibular portion arises within the parotid gland and then courses inferiorly along the lateral pterygoid muscle. Its branches are the middle meningeal, accessory meningeal, inferior alveolar, deep auricular, and anterior tympanic arteries. The pterygoid portion courses anteriorly, superiorly, and medially through the infratemporal fossa. Its branches include the buccal, masseteric, and deep temporal arteries. The pterygopalatine portion lies within the pterygopalatine fossa. Its branches are named for the foramen or fissures from which they exit the pterygopalatine fossa including four anterior and three posterior branches. The anterior branches include the posterior superior alveolar, infraorbital, greater (descending) palatine, and sphenopalatine arteries. The posterior branches include the arteries of the foramen rotundum, artery of the pterygoid canal (vidian artery), and the pterygovaginal (pharyngeal) artery which courses through the palatovaginal canal in the skull base (2,3).

The middle meningeal artery is the largest meningeal vessel and the largest branch of the internal maxillary artery (4). It has a short vertical segment then enters the cranium through the foramen spinosum and then abruptly courses ventrally (anteriorly) to run along the dura within the grooves of the inner table of the middle cranial fossa to the internal surface of the frontal and parietal bones. The middle meningeal artery commonly supplies convexity meningiomas. A small petrous branch of the middle meningeal artery can supply the vasa nervorum of the facial nerve (cranial nerve VII) in the middle ear. Facial paralysis, secondary to untoward occlusion, can occur during embolization through the middle meningeal artery if small particles or liquid embolic agents are used. Anastomosis between middle meningeal artery branches and lacrimal branches of the ophthalmic artery may provide collateral blood flow in the setting of internal carotid artery occlusion. This communication is demonstrated in Figures 4.9 and 4.10. This potential communication can also result in blindness during embolization through the middle meningeal artery.

Branches of the pterygopalatine portion of the internal maxillary artery include the infraorbital artery, sphenopalatine artery, and the artery of the foramen rotundum. The infraorbital artery courses through the infraorbital canal and infraorbital foramen supplying the cheek, lower eyelid, upper lip, lacrimal sac, and nose (4). It can also anastomose with terminal branches of the ophthalmic artery as well as provide potential collateral blood flow in the setting of internal carotid artery occlusion.

The sphenopalatine branch of the distal internal maxillary artery supplies the nasal cavity and is often the source of bleeding in posterior epistaxis. Particulate embolization of the distal internal maxillary artery is often directed towards the treatment of posterior epistaxis when bleeding from the sphenopalatine artery is believed to be the source.

Numerous small anastomotic channels exist between branches of the external carotid artery and the intracranial circulation. Branches of the middle meningeal artery, the accessory meningeal artery, and the artery of the foramen rotundum normally anastomose with the inferolateral trunk (artery of the inferior cavernous sinus). These anastomotic channels can provide collateral flow to the horizontal intracavernous segment of the intracranial internal carotid artery (5). They may also provide arterial supply to dural arterial venous fistulas around the cavernous sinus and skull base. In addition these various arterial branches often provide nutrient supply to the vasa nervorum of a number of cranial nerves. Careful attention to the presence of these extracranial to intracranial communications, as well as their importance in the integrity of multiple cranial nerves, is mandatory when embolization procedures are performed in the external carotid artery territory (6).

Another important extracranial to intracranial anastomotic channel is between the occipital artery and the upper cervical vertebral artery. This normal communication is not often readily visible on routine angiographic studies. Extreme caution must be exercised when embolization involving the occipital artery is undertaken to prevent potential inadvertent embolization of the vertebral basilar circulation.

Utilization of three-dimensional rotational angiography (3DRA) has significant benefits compared to traditional 2D-angiography in the evaluation of carotid artery disease in the neck. 3DRA provides an infinite number of

imaging projections of the common carotid artery bifurcation obtained through a single contrast injection. By providing these multiple views we can have confidence in the accuracy of our estimation of the degree of vascular stenosis (narrowing). In addition to enhancing our accuracy in evaluating stenosis, our ability to identify complicated atherosclerotic plaques with ulcerations is enhanced.

The acquisition of infinite projections from a single bolus injection of contrast is also beneficial. This reduces the overall volume of contrast needed to complete the angiographic exam, thereby reducing the potential for harmful effects of the radiographic contrast media.

As a result of the advantages of 3DRA compared with traditional 2D imaging, we have the potential to improve patient care through the more accurate assessment of atherosclerotic vascular changes. This might alter and improve treatment options for these patients.

In contrast to the added benefits of 3DRA in assessing the common carotid artery bifurcation, this technique was found to be of limited benefit in angiographic assessment during selective external carotid angiography for a variety of indications. The factors limiting the use of 3DRA in external carotid angiography include the small size of the various branches of the external carotid artery that limit their opacification, patient movement during these injections (which can be uncomfortable), and the propensity for the branches of the external carotid artery to undergo vasospasm from catheter manipulation.

II. VERTEBRAL ARTERIES

After arising from the subclavian arteries (or occasionally directly from the aortic arch on the left), initially the vertebral arteries course medially and superiorly and, in most cases, enter the foramen transversarium of C6. They then ascend vertically in the foramen transversaria C6 through C3 turning superolaterally to pass through the foramen transversarium of C2. They remain anterior to the ventral roots of the cervical spinal cord with the exception of the first cervical root where they are lateral to the roots. The verterbral arteries then course superiorly and slightly anteriorly pass-

ing through the transverse foramen of the atlas. Near the cranio-vertebral junction, the vertebral arteries course posteriorally around the atlanto-occipital joint (7) and lie over the posterior neural arch of C1. They then make a sharp turn to change their direction superiorly and anteriomedially to enter the cranial cavity through the foramen magnum. They pierce the dura to enter the subarachnoid space just above the bony posterior neural arch of C1. Often a mild change in caliber or mild ring-like constriction of these vessels is seen as they pierce the dura. The vertebral arteries unite to form the basilar artery near the inferior pons/ponto-medullary junction. The vertebral arteries are usually unequal in size. The left vertebral artery is often larger than the right artery. Hypoplasia of a vertebral artery is not unusual.

Within the neck, the vertebral arteries give rise to numerous small deep muscular branches as well as small segmental branches to the bony cervical spine and spinal cord (7). Inconstant, variable vascular supply to the cervical spinal cord via the radiculomedullary branches of the vertebral arteries is noted. Radiculomedullary refers to the segmental nature of the vascular supply to the spinal cord. Often a single dominant arterial branch to the brachial widening (brachial plexus C4-T1) of the cervical spinal cord arises from one or both vertebral arteries. At other times this important branch may arise from the thyrocervical trunk, costocervical trunk, or even from branches of the external carotid artery such as the superior thyroid artery.

REFERENCES

1. Huber, P. 1982. *Krayenbuhl/Yasargil Cerebral Angiography*. New York: Thieme Medical Publishers, p. 37.
2. Rael, R.R., and L.R. Casey. 2000. *Cerebral Angiography*. In Neuroimaging. W.W. Orrrison, ed. Philadelphia: W.B. Saunders, pp. 206–212.
3. Borden NB, D. Dungan, B.L. Dean, and R.A. Flom. 1996. Postraumatic epistaxis from injury to the pterygovaginal artery. *Am. J. Neuroradiol.* 17:1148–1150.
4. Haughton, V.M., and A.E. Rosenbaum. 1974. *The normal and anomalous aortic arch and brachiocephalic arteries.* In Radiology of the Skull and Brain: Angiography Volume 2. T.H. Newton and D.G. Potts, eds., St. Louis: C.V. Mosby, pp.1145–1163.

5. Berenstein A, and P. Lasjaunias. 1992. *Surgical Neuroangiography: Functional Anatomy of the Craniofacial Arteries, Volume 1.* New York: Springer-Verlag, 1992, pp. 239–244.
6. Berenstein and Lasjaunias, pp. 231–237.
7. Stephens, R.B., and D.L. Stillwell. 1969. *Arteries and Veins of the Human Brain.* Springfield, Ill: Charles C Thomas, pp. 71–73.

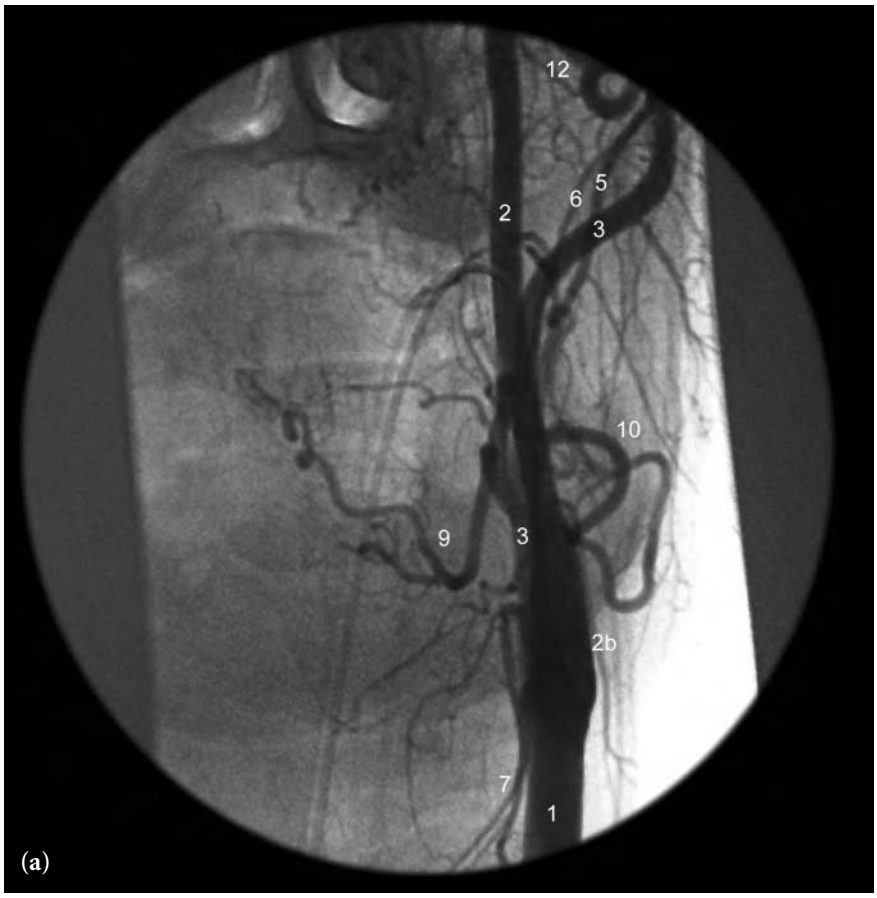

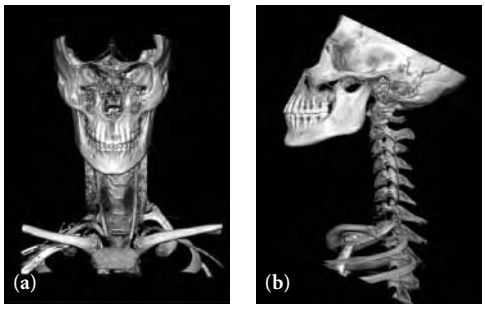

Fig. 4.1 (a, b) Frontal (*a*) and lateral (*b*) left common carotid artery injection. Normal 2D appearance of the left common carotid artery bifurcation region.

FIGURE KEY

1 common carotid artery
2 internal carotid artery
2b carotid bulb
3 external carotid artery
4 ascending pharyngeal artery
5 occipital artery
6 posterior auricular artery
7 superior thyroid artery
9 lingual artery
10 facial artery
11 superficial temporal artery
12 internal maxillary artery

Fig. 4.2 (a-d) Frontal (*a*), lateral (*b*), posterior (*c*), and right anterior oblique views (*d*) following left common carotid artery injection. There is a normal 3D appearance of the left common carotid artery bifurcation region. This is the same patient as in Figure 4.1.

FIGURE KEY

1 common carotid artery
2 internal carotid artery
2b carotid bulb
3 external carotid artery
5 occipital artery
6 posterior auricular artery
7 superior thyroid artery
9 lingual artery
10 facial artery

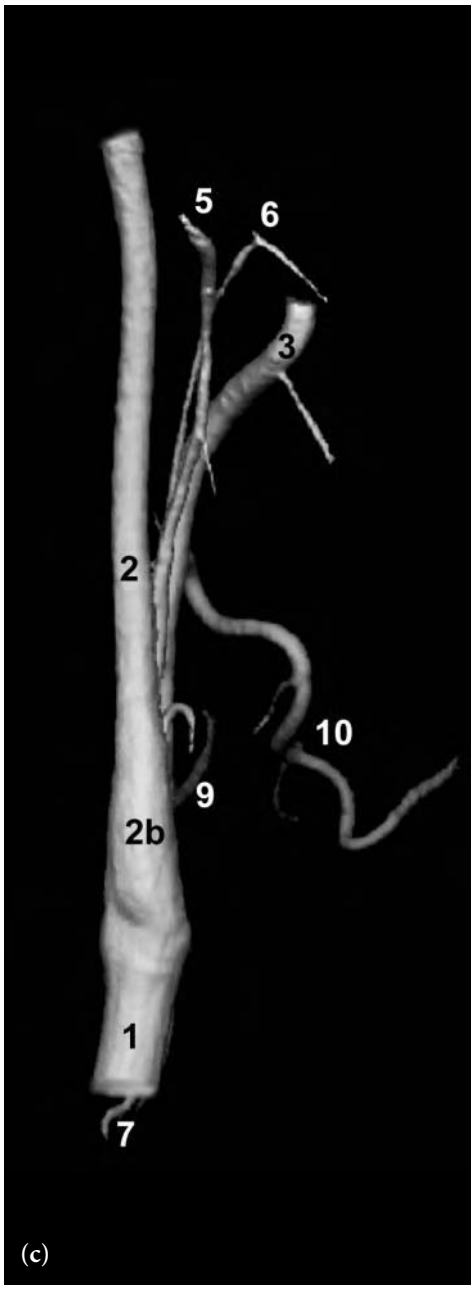
5
6
3
2
10
9
2b
1
7
(c)

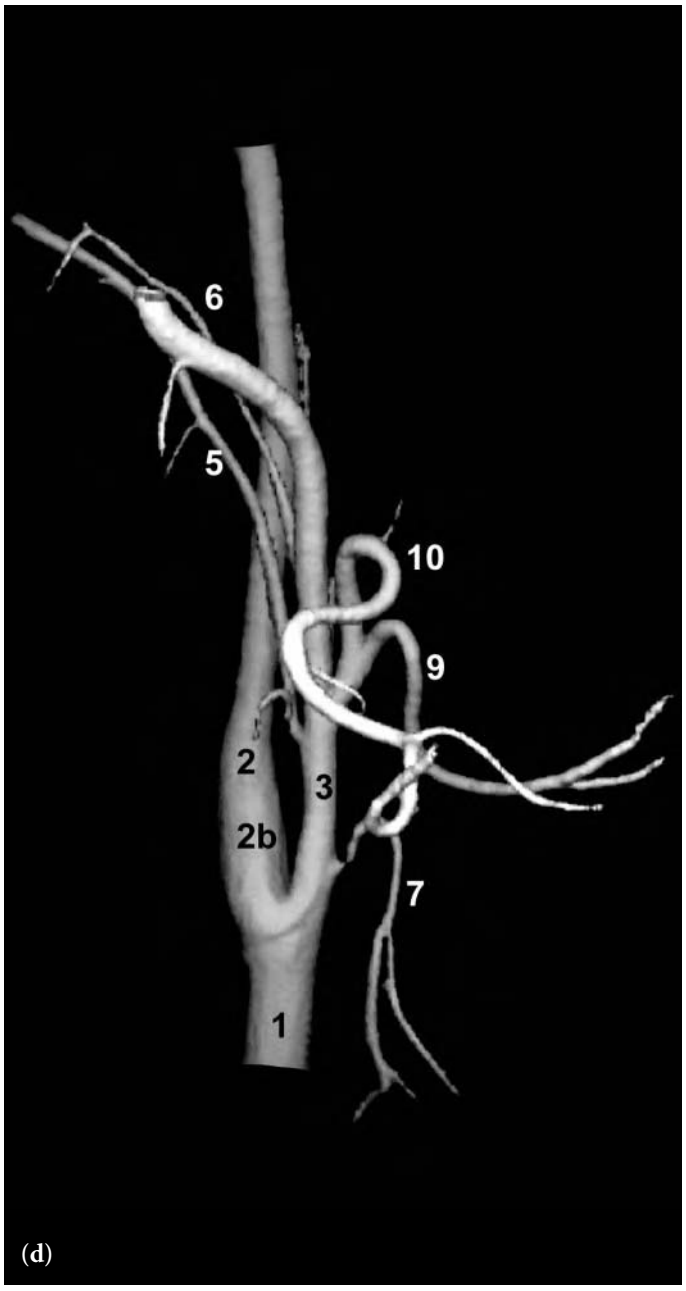
6
5
10
9
2
3
2b
7
1
(d)

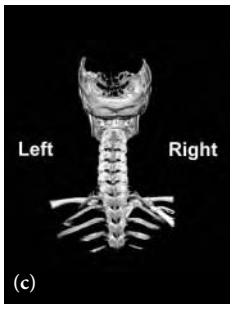
Left
Right
(c)

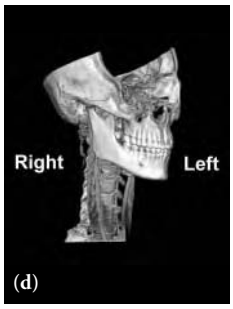
Right
Left
(d)

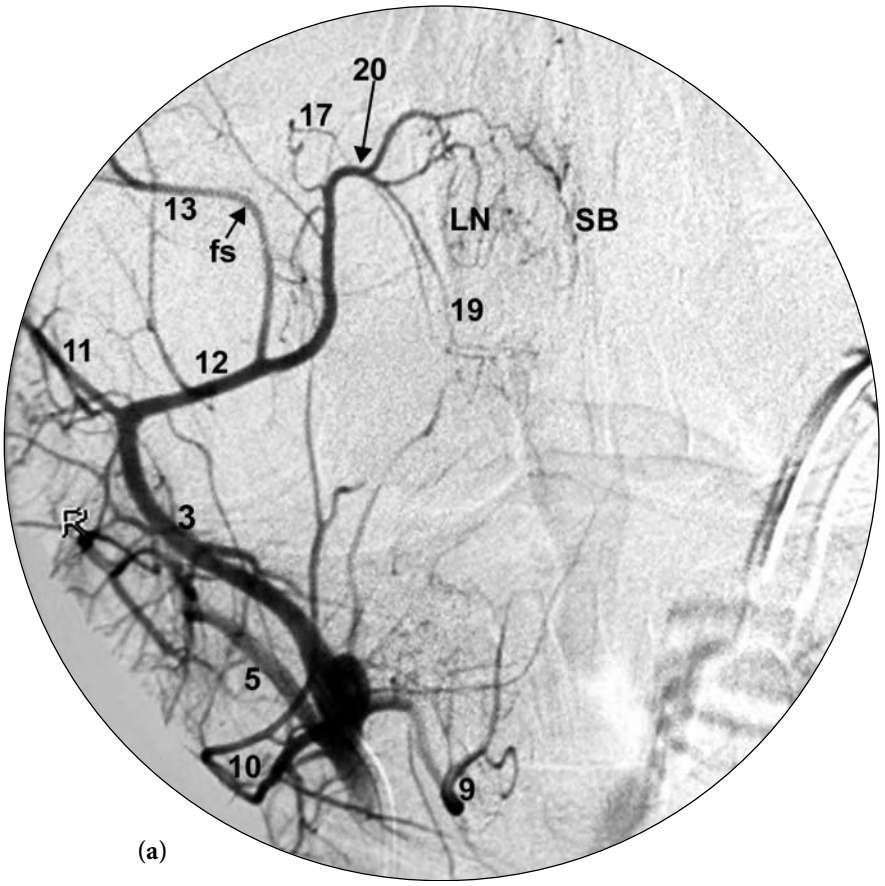

(**a**)

Fig. 4.3 (a-e) Frontal 2D (*a*), lateral 2D (*b*), coned down lateral 2D (*c*), frontal 2D early arterial (*d*), and later arterial phase (*e*) views following selective external carotid artery injections in different patients. There is a normal appearance of the external carotid artery branches.

FIGURE KEY

3 external carotid artery
5 occipital artery
6 posterior auricular artery
9 lingual artery
10 facial artery
11 superficial temporal artery
12 internal maxillary artery
13 middle meningeal artery
14 accessory meningeal artery
15 deep temporal artery
16 inferior alveolar artery
17 infraorbital artery
18 posterior superior alveolar artery
19 greater palatine artery
20 sphenopalatine artery
24 transverse facial artery
25 masseteric muscular branches
26 buccal muscular branches
fs foramen spinosum
m muscular branches
LN lateral nasal branches of sphenopalatine artery
SB septal branches of sphenopalatine artery

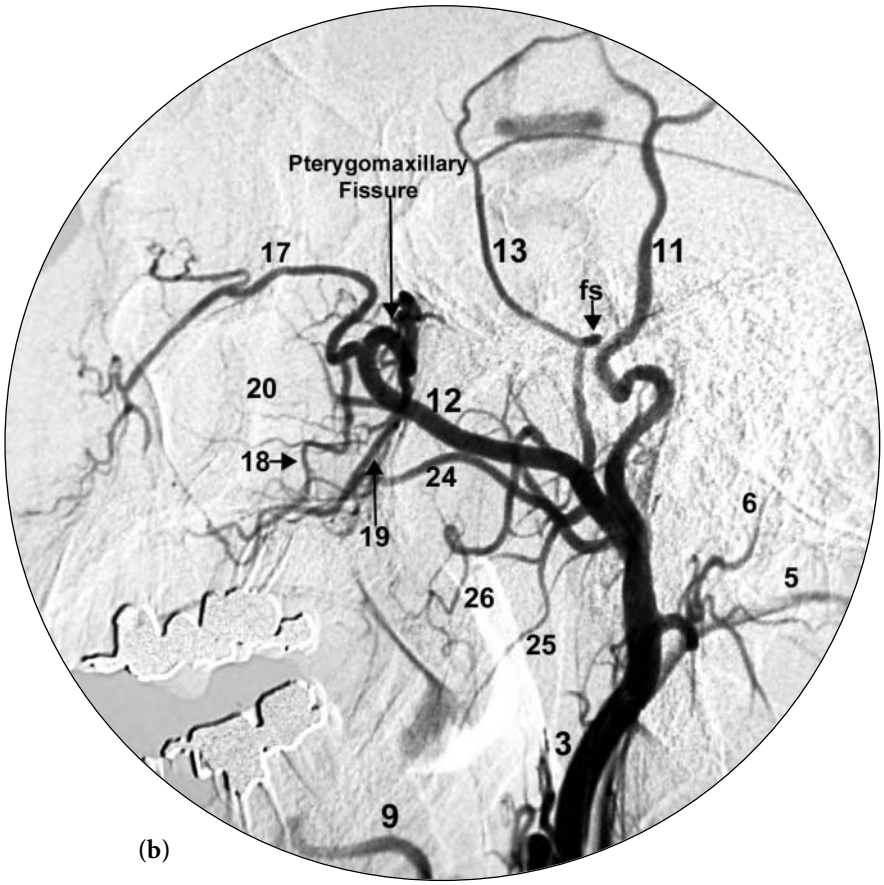
Pterygomaxillary
Fissure
17
13
11
fs
20
12
18
24
6
19
5
26
25
3
9

(b)

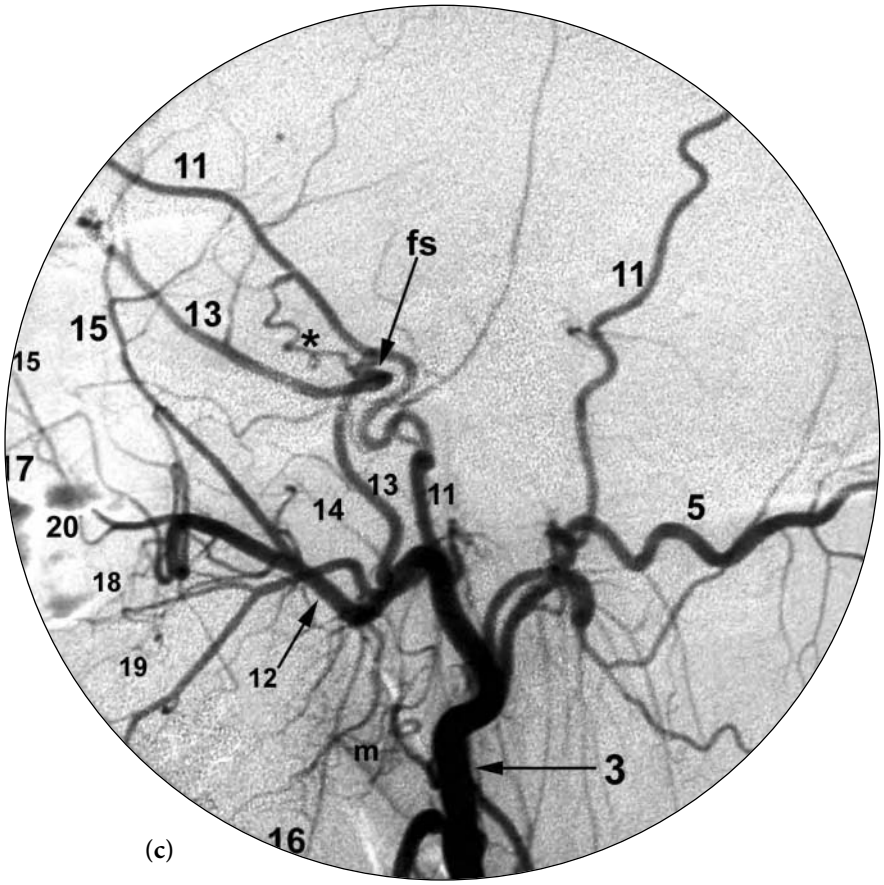
11
fs
11
15
13
*
15
17
13
11
14
5
20
18
19
12
m
3
16

(c)

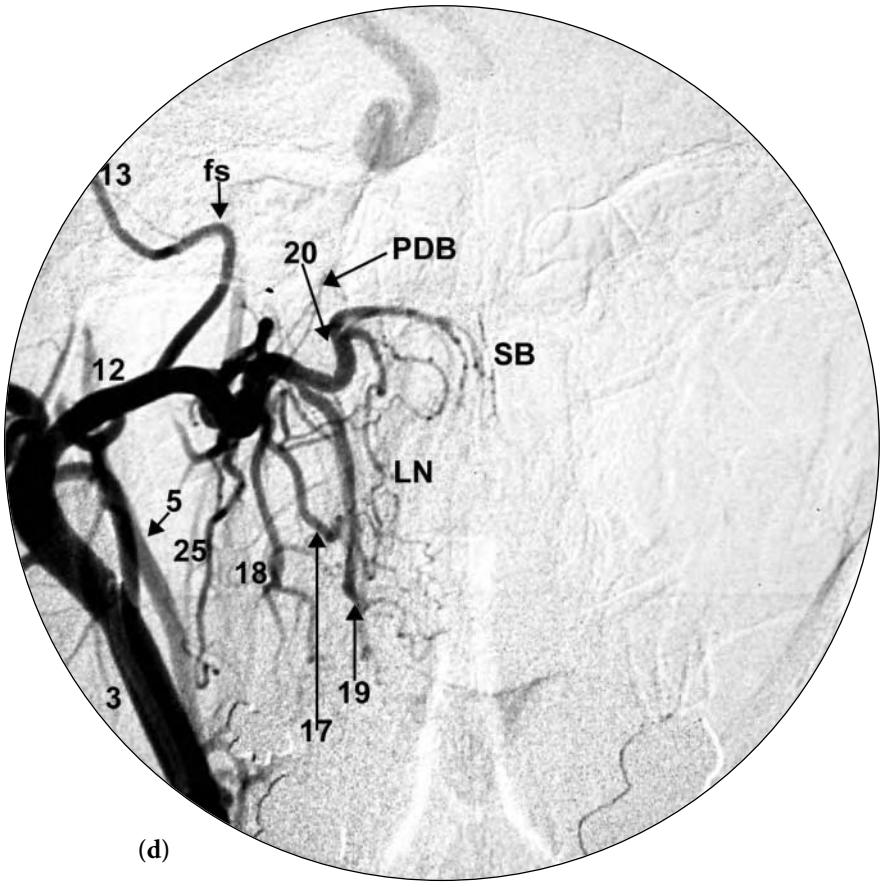

(**d**)

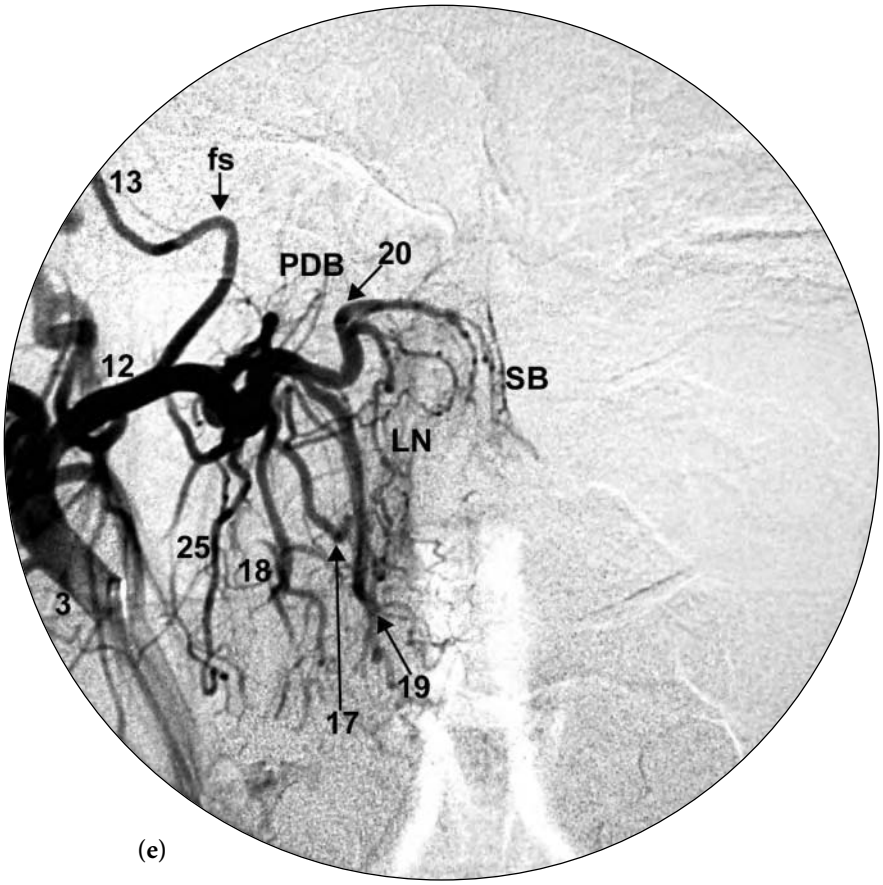

(**e**)

Fig. 4.3 (continued)

FIGURE KEY

3 external carotid artery
5 occipital artery
6 posterior auricular artery
9 lingual artery
10 facial artery
11 superficial temporal artery
12 internal maxillary artery
13 middle meningeal artery
14 accessory meningeal artery
15 deep temporal artery
16 inferior alveolar artery
17 infraorbital artery
18 posterior superior alveolar artery
19 greater palatine artery
20 sphenopalatine artery
24 transverse facial artery
25 masseteric muscular branches
26 buccal muscular branches
fs foramen spinosum
m muscular branches
LN lateral nasal branches of sphenopalatine artery
SB septal branches of sphenopalatine artery
PDB posterior directed branches of distal internal maxillary artery. These are 1. artery of foramen rotundum 2. artery of the pterygoid canal (vidian artery), and 3. pharyngeal artery (pterygovaginal artery)

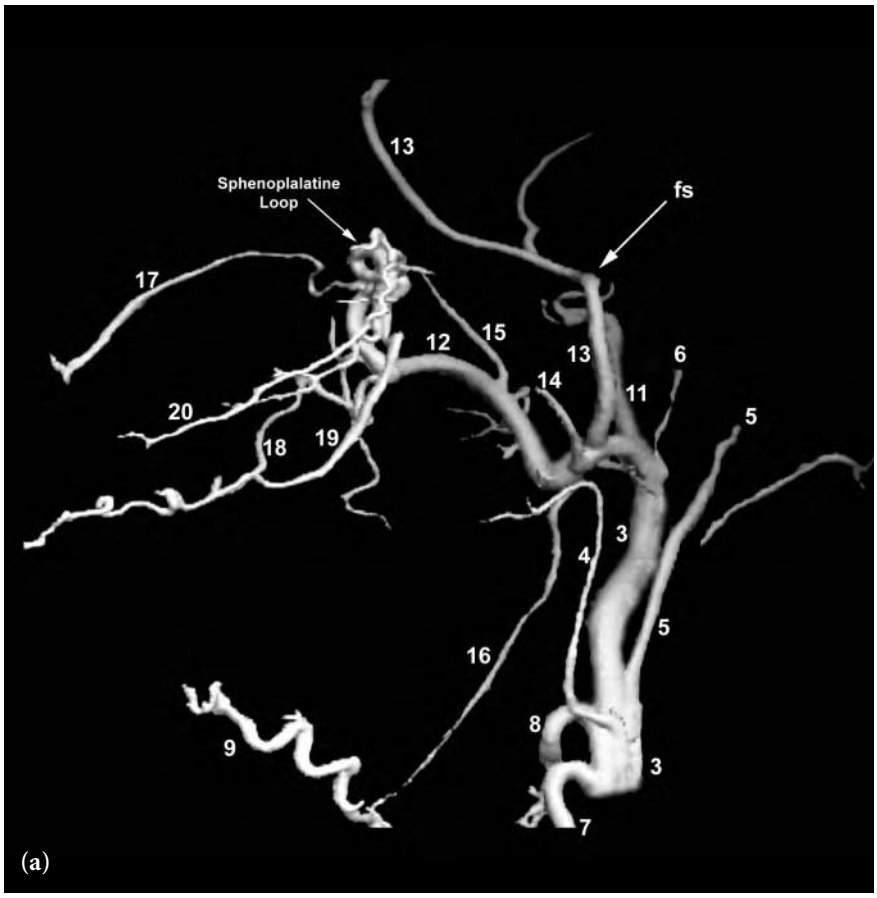

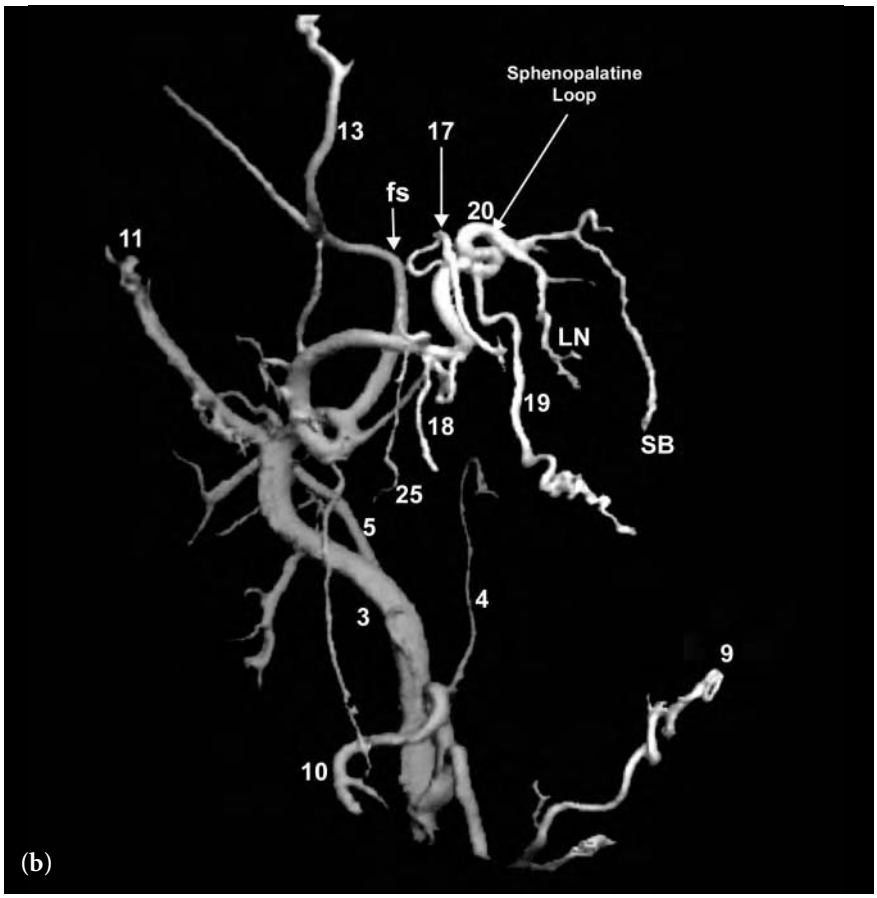

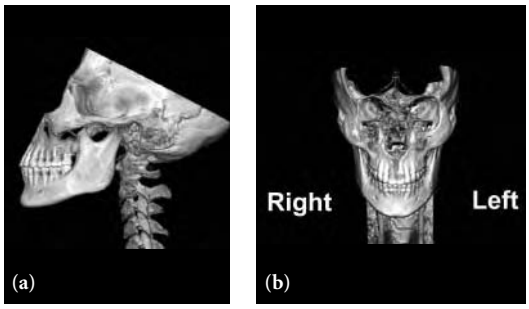

Fig. 4.4 (a, b) 3D lateral (*a*) and frontal (*b*) views following selective external carotid artery injection. There is a normal appearance of the external carotid artery branches.

FIGURE KEY

3 external carotid artery
4 ascending pharyngeal artery
5 occipital artery
6 posterior auricular artery
7 superior thyroid artery
8 lingual-facial artery trunk
9 lingual artery
10 facial artery
11 superficial temporal artery
12 internal maxillary artery
13 middle meningeal artery
14 accessory meningeal artery
15 deep temporal artery
16 inferior alveolar artery
17 infraorbital artery
18 posterior superior alveolar artery
19 greater palatine artery
20 sphenopalatine artery
25 masseteric muscular branches
fs foramen spinosum
LN lateral nasal branches of sphenopalatine artery
SB septal branches of sphenopalatine artery

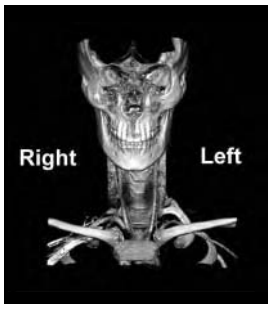

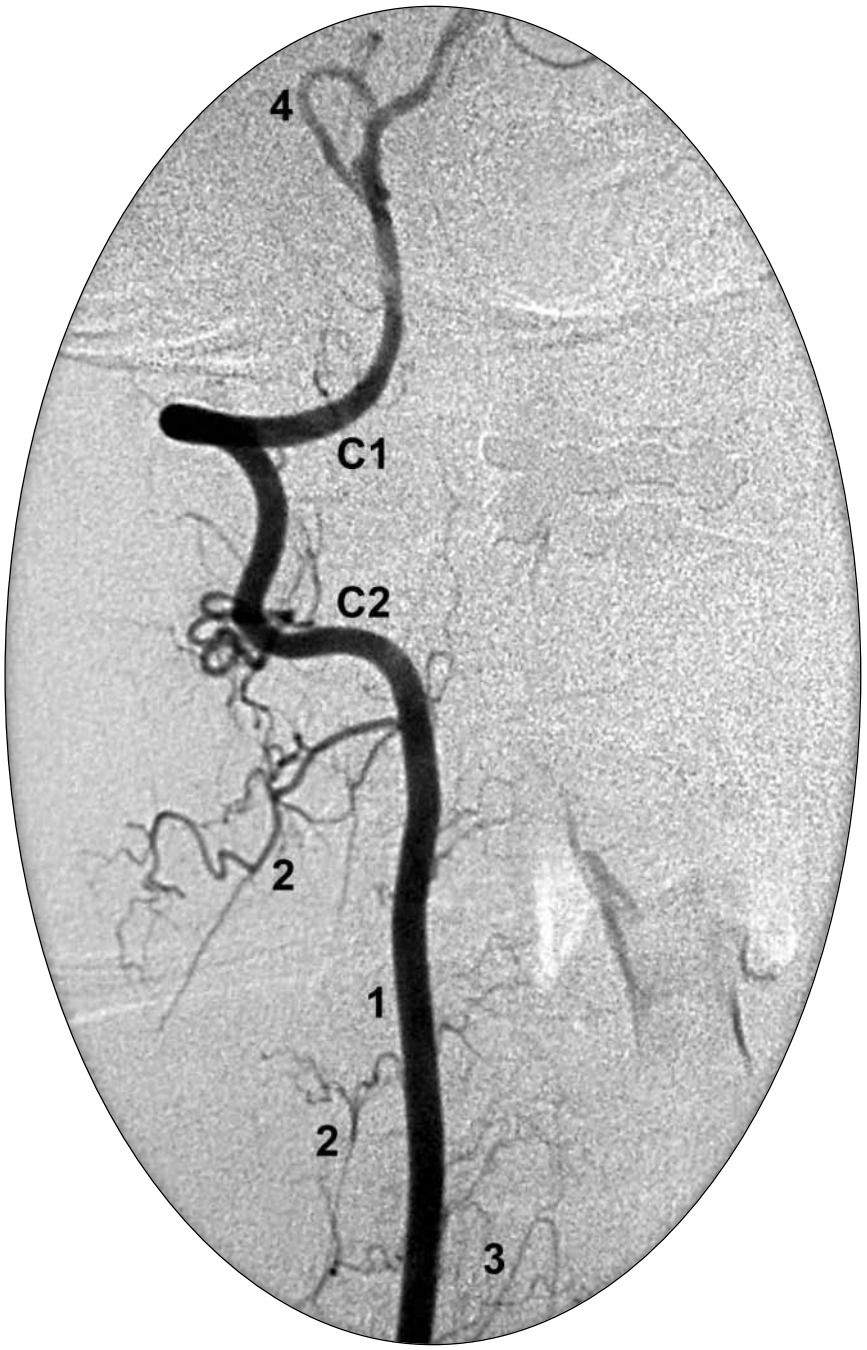

Fig. 4.5 Frontal 2D view following right vertebral artery injection. There is a normal appearance of the cervical vertebral artery extending approximately to the vertebral-basilar junction.

FIGURE KEY

1 vertebral artery
2 muscular branches
3 radiculomedullary feeder to anterior spinal artery
4 PICA
C1 first cervical vertebrae
C2 second cervical vertebrae

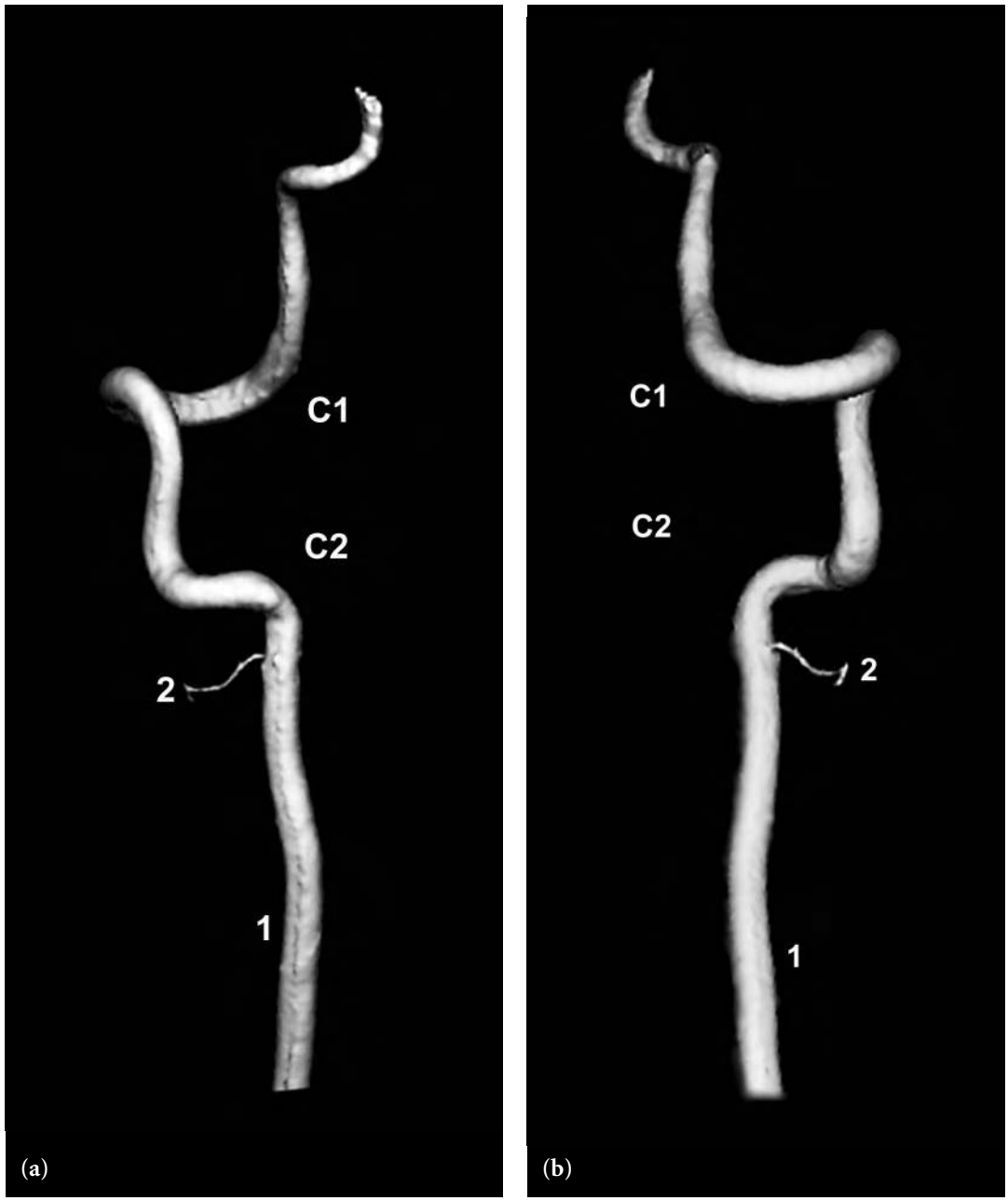

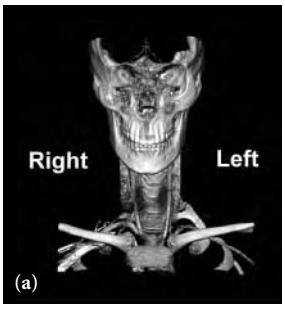

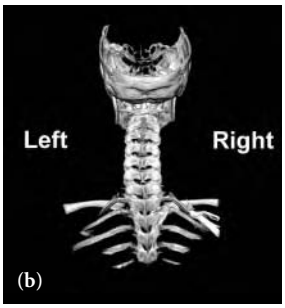

Fig 4.6 (a,b) Frontal (*a*) and posterior 3D (*b*) views following right vertebral artery injection. There is a normal appearance of the cervical vertebral artery extending approximately to the skull base.

FIGURE KEY

1 vertebral artery
2 muscular branches
C1 first cervical vertebrae
C2 second cervical vertebrae

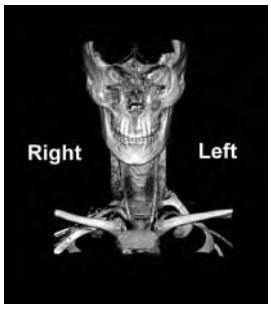

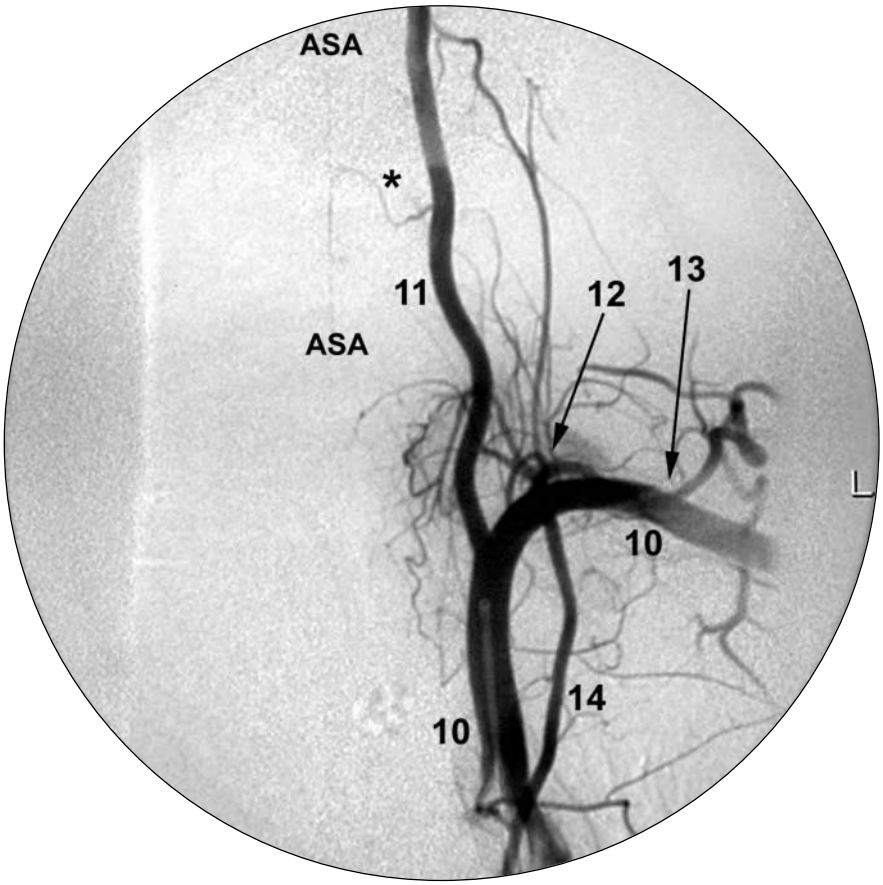

Fig. 4.7 Frontal 2D view following left subclavian artery injection. There is a normal appearance of the origin and the lower cervical segment of the left vertebral artery.

FIGURE KEY

10 left subclavian artery
11 left vertebral artery
12 left thyrocervical trunk
13 left costocervical trunk
14 left internal mammary artery
* radiculomedullary feeder to anterior spinal artery
ASA anterior spinal artery

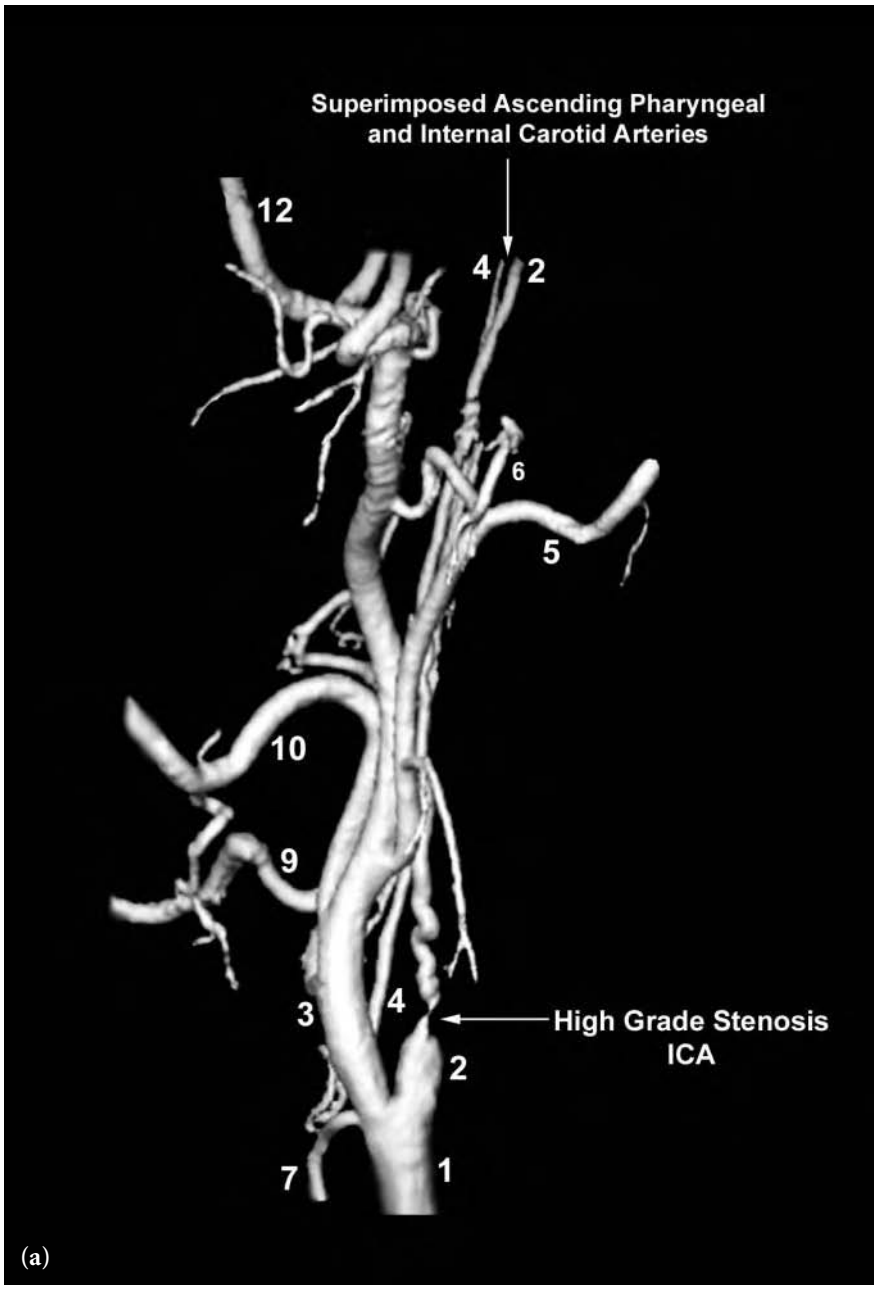

Fig. 4.8 (a-c) Lateral (*a*), left posterior oblique (*b*), and medial 3D (*c*) views following left common carotid artery injection. There is high grade (severe) stenosis of the proximal left internal carotid artery secondary to the atherosclerotic plaque. Note the normal branches of the external carotid artery.

FIGURE KEY

1 common carotid artery
2 internal carotid artery
3 external carotid artery
4 ascending pharyngeal artery
5 occipital artery
6 posterior auricular artery
7 superior thyroid artery
9 lingual artery
10 facial artery
12 internal maxillary artery
13 middle meningeal artery

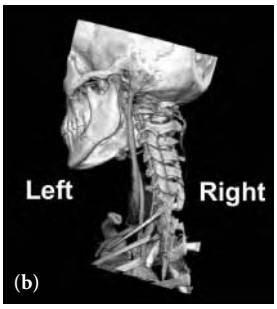

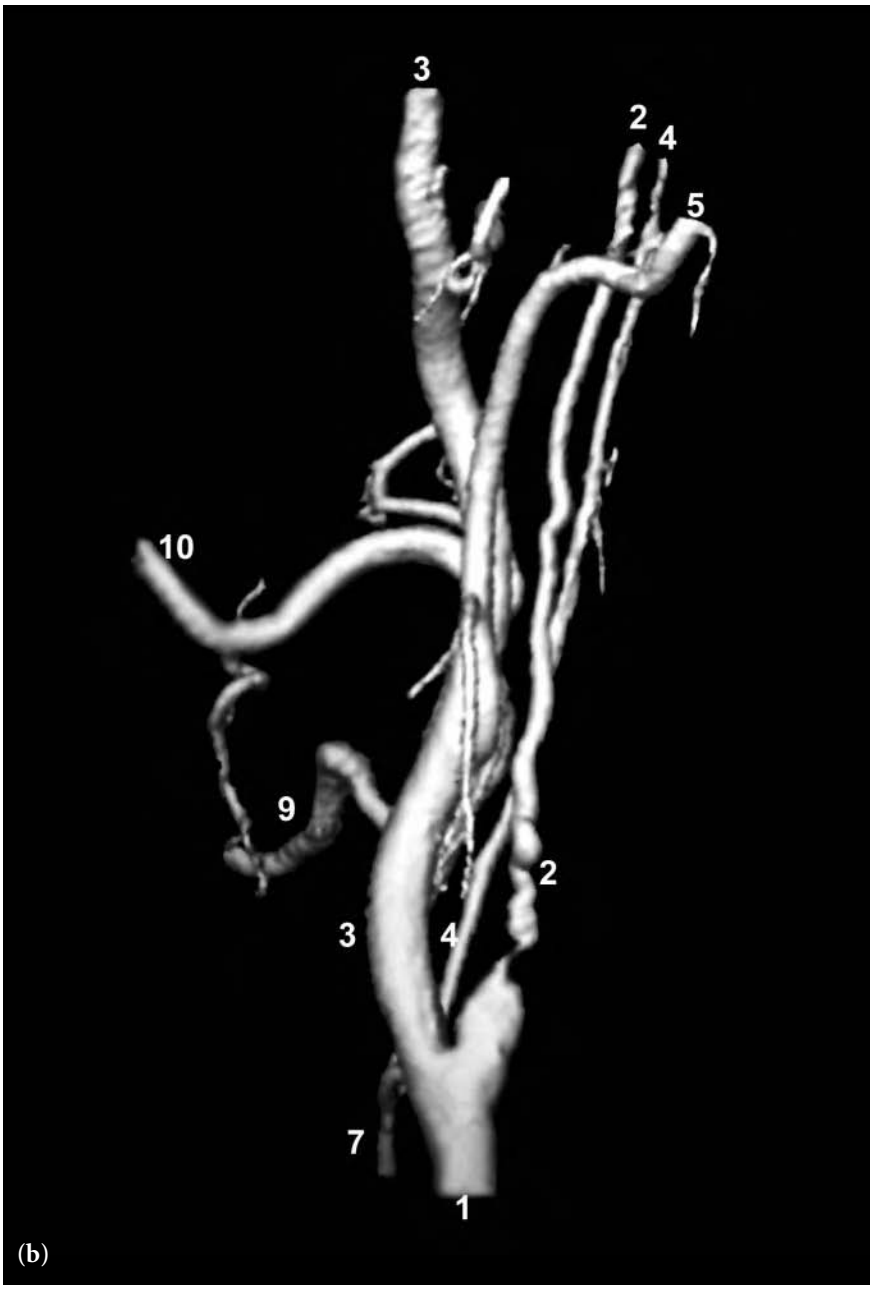

Fig. 4.8 (continued)

FIGURE KEY

1 common carotid artery
2 internal carotid artery
3 external carotid artery
4 ascending pharyngeal artery
5 occipital artery
6 posterior auricular artery
7 superior thyroid artery
9 lingual artery
10 facial artery
12 internal maxillary artery
13 middle meningeal artery

(c)

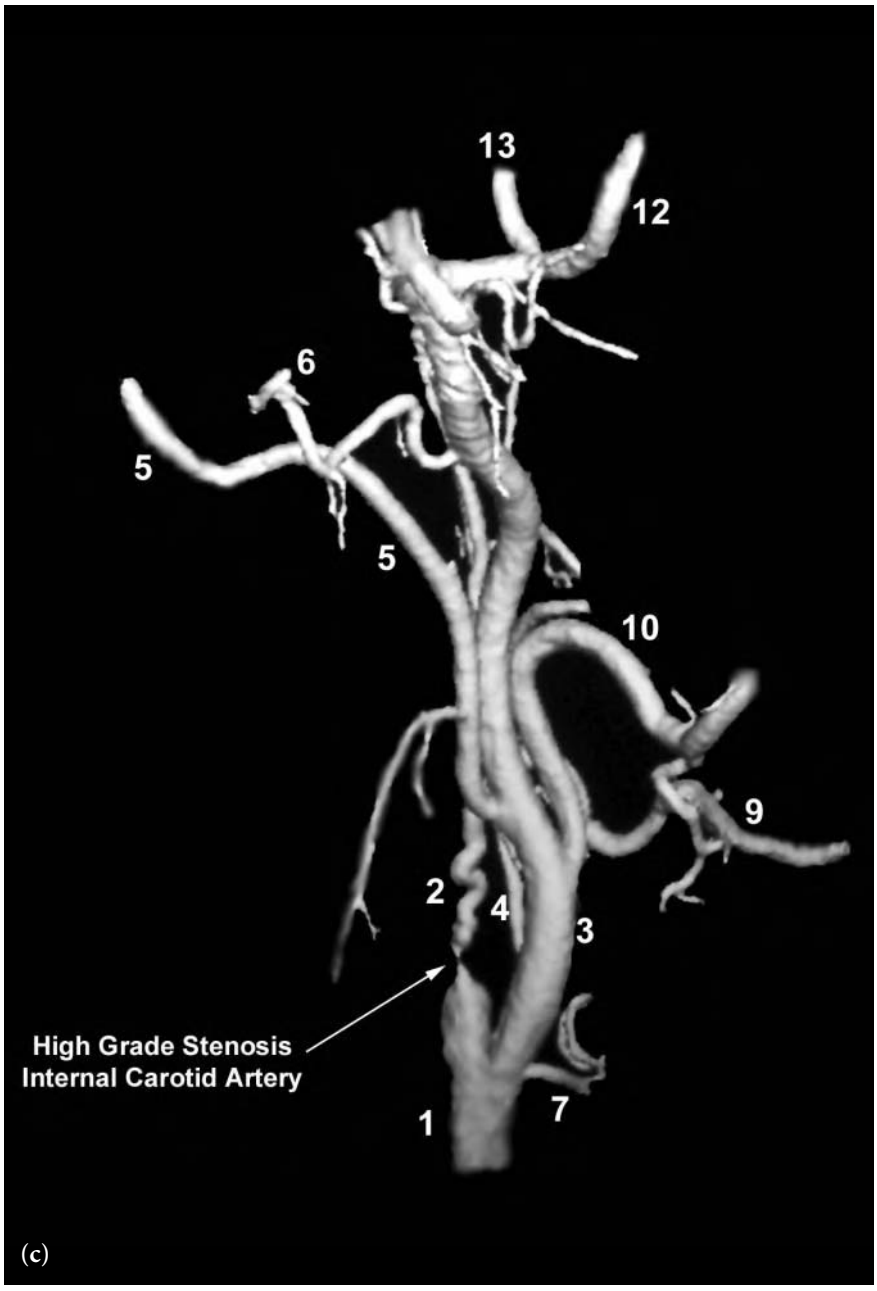
13
12
6
5
5
10
9
2
4
3
High Grade Stenosis
Internal Carotid Artery
1
7
(c)

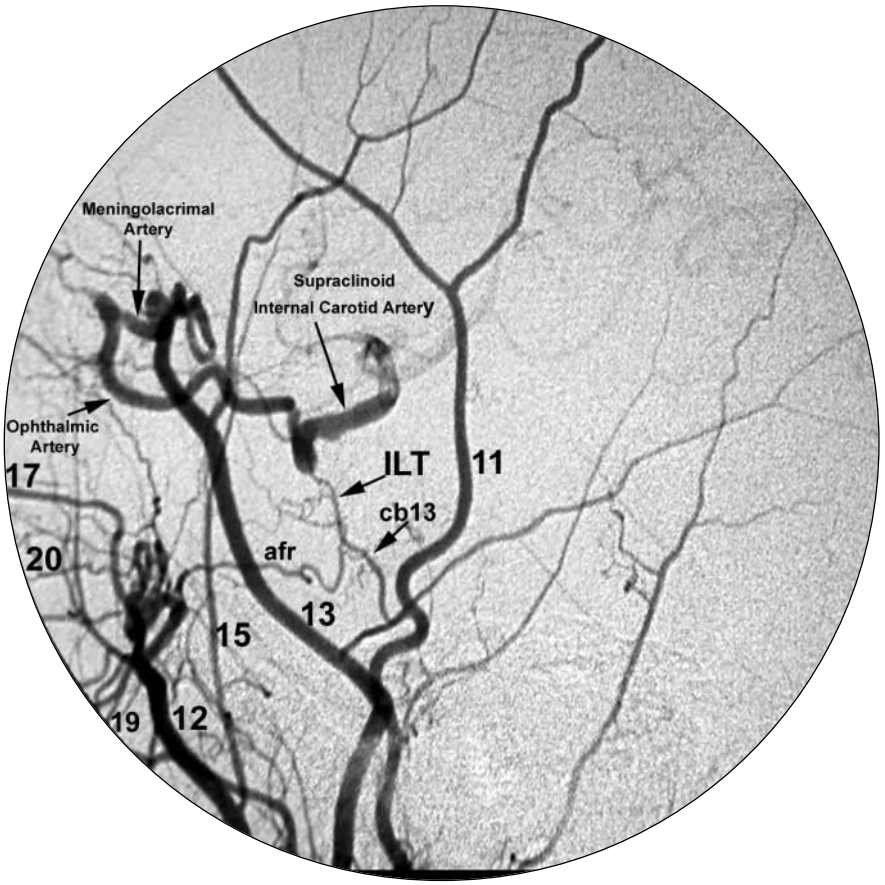

Fig. 4.9 Lateral 2D view following common carotid artery injection. There is complete occlusion of the internal carotid artery. The intracranial internal carotid artery is reconstituted by flow from the meningolacrimal branch of the middle meningeal artery to the ophthalmic artery with retrograde flow to the paraclinoid segment of the internal carotid artery.

FIGURE KEY

11 superficial temporal artery
12 internal maxillary artery
13 middle meningeal artery
15 deep temporal artery
17 infraorbital artery
19 greater palatine artery
20 sphenopalatine artery
afr artery of the foramen rotundum
cb13 cavernous branch of middle meningeal artery
ILT inferolateral trunk

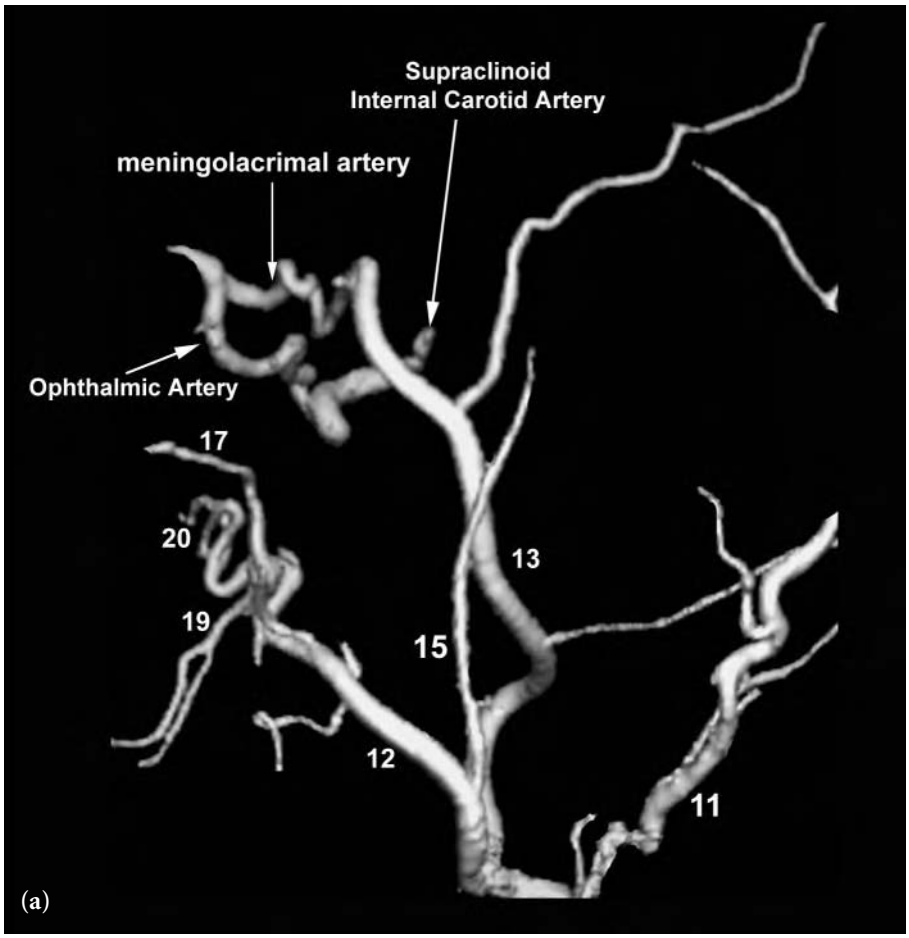

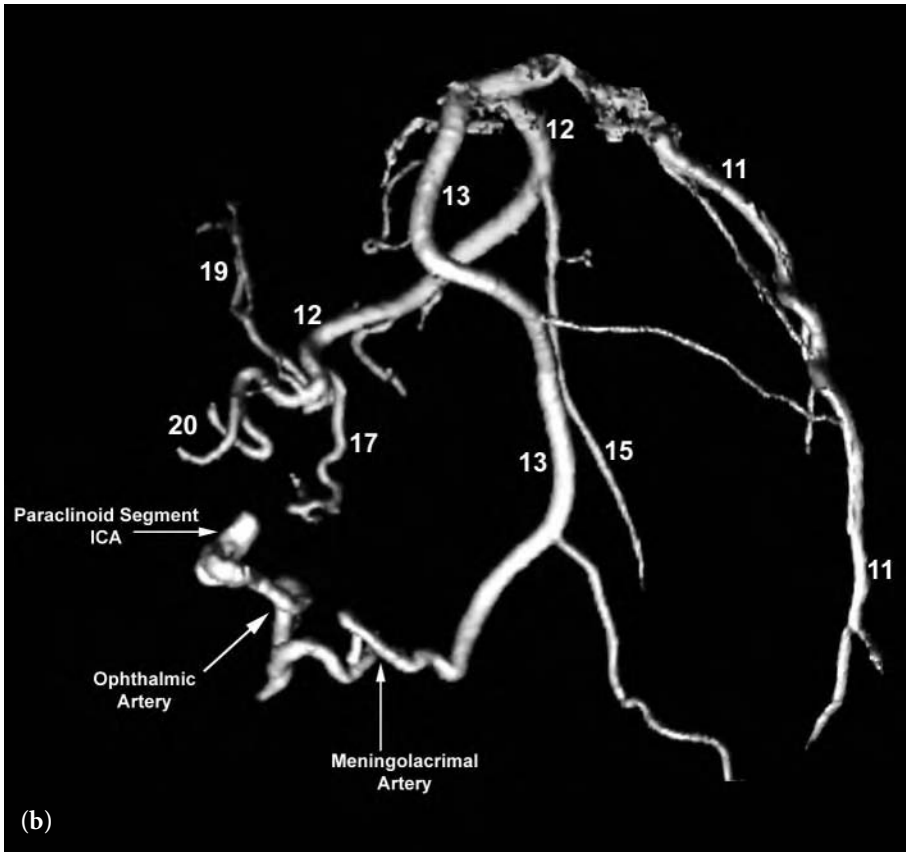

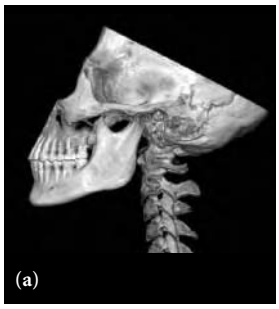

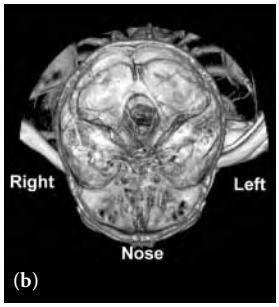

Fig. 4.10 (a,b) Lateral (*a*) and superior-inferior (*b*) 3D views following common carotid artery injection. Note the various branches of the external carotid artery and the meningolacrimal branch of the middle meningeal artery providing flow to the intracranial internal carotid artery via retrograde flow through the ophthalmic artery.

FIGURE KEY

11 superficial temporal artery
12 internal maxillary artery
13 middle meningeal artery
15 deep temporal artery
17 infraorbital artery
19 greater palatine artery
20 sphenopalatine artery

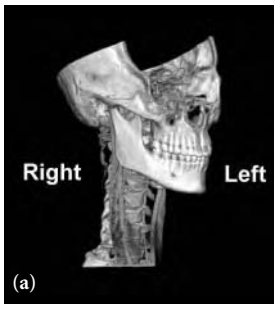

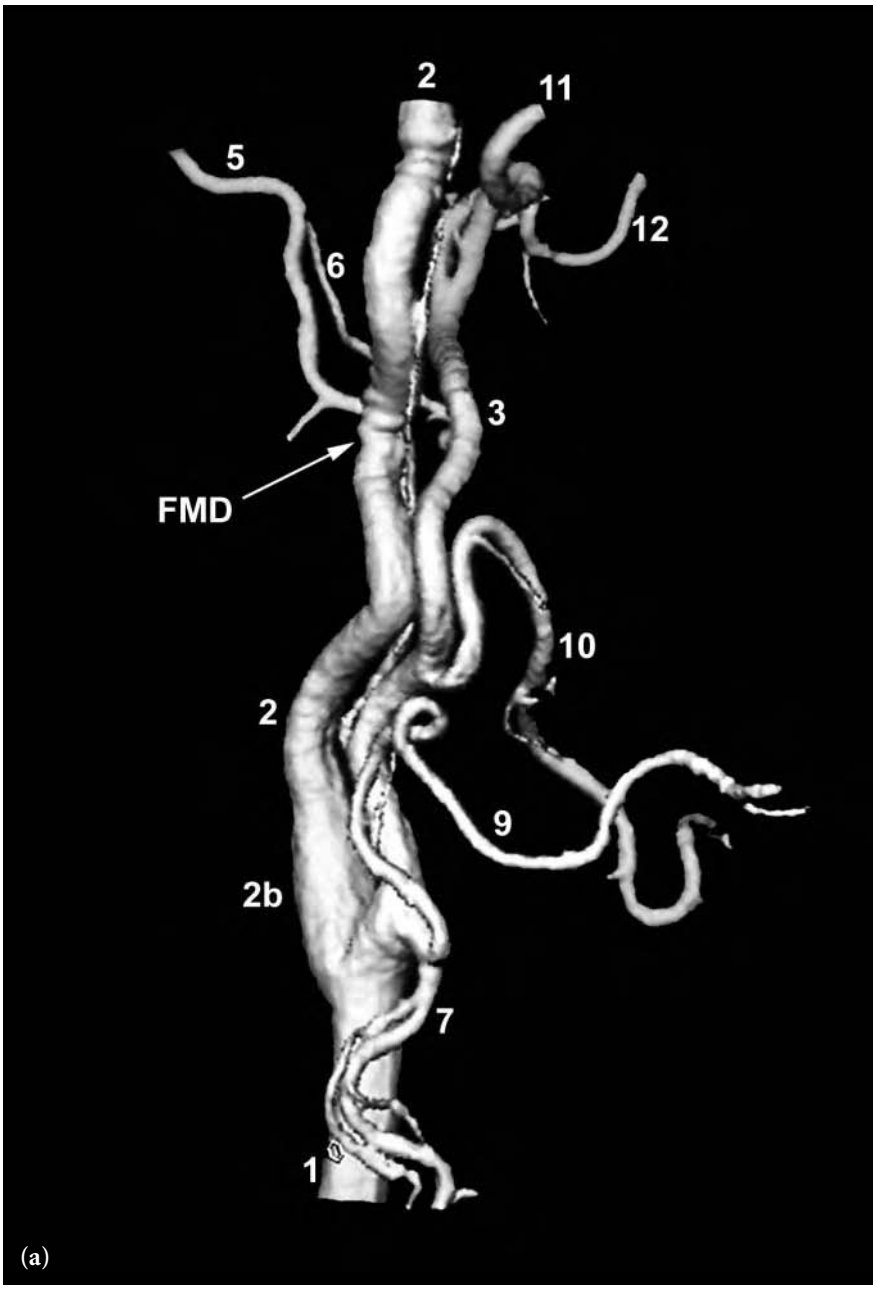

Fig. 4.11 (a,b) Right anterior oblique (*a*) and right lateral (*b*) 3D views following common carotid artery injection. Note the medial form of fibromuscular dysplasia (fmd) involving the midcervical segment of the internal carotid artery which is partially hidden by overlapping vessels on the lateral (*b*) view.

FIGURE KEY

1 common carotid artery
2 internal carotid artery
2b carotid bulb
3 external carotid artery
4 ascending pharyngeal artery
5 occipital artery
6 posterior auricular artery
7 superior thyroid artery
9 lingual artery
10 facial artery
11 superficial temporal artery
12 internal maxillary artery

(b)

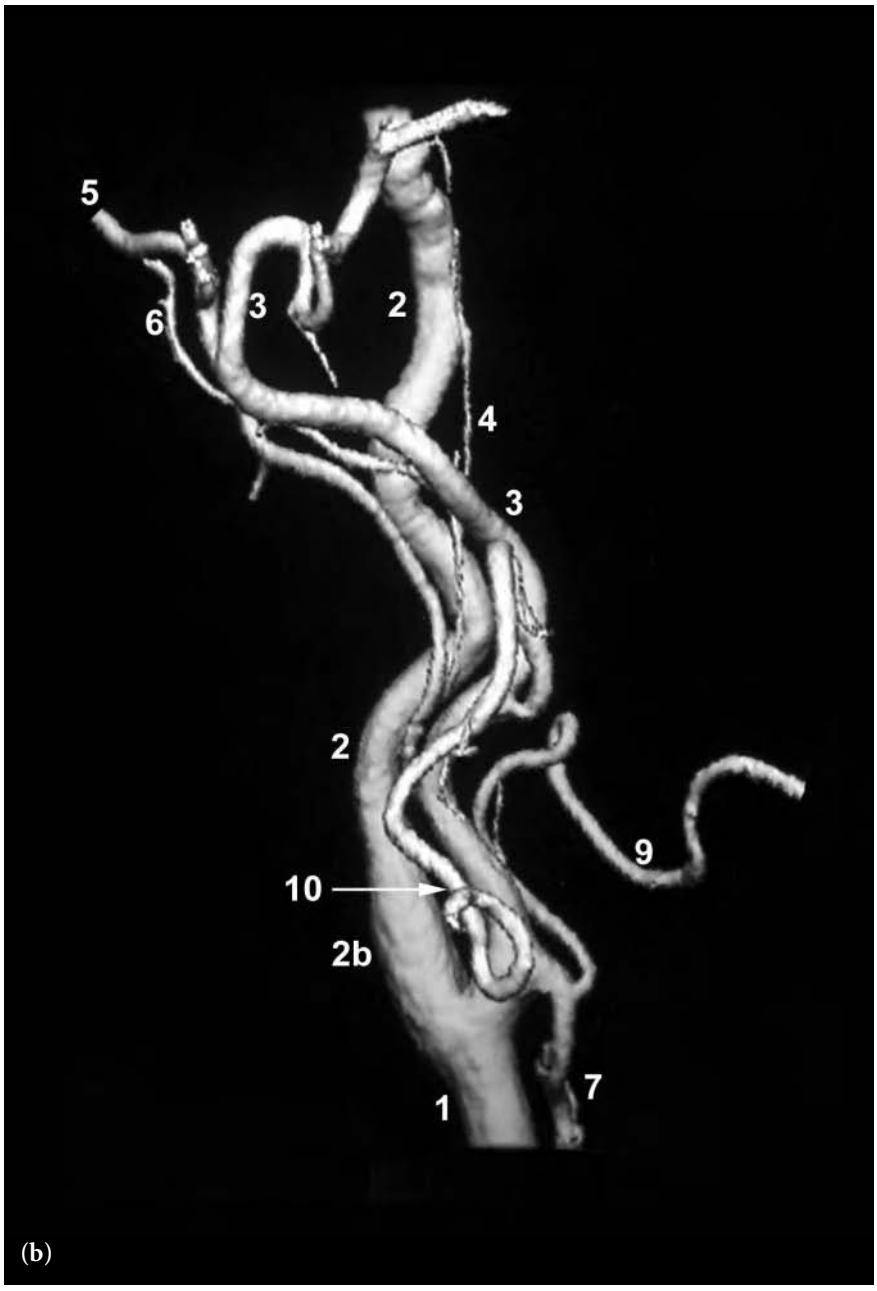
5
6
3
2
4
3
2
9
10
2b
1
7
(b)

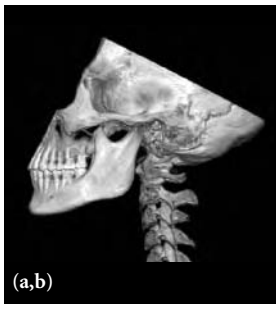

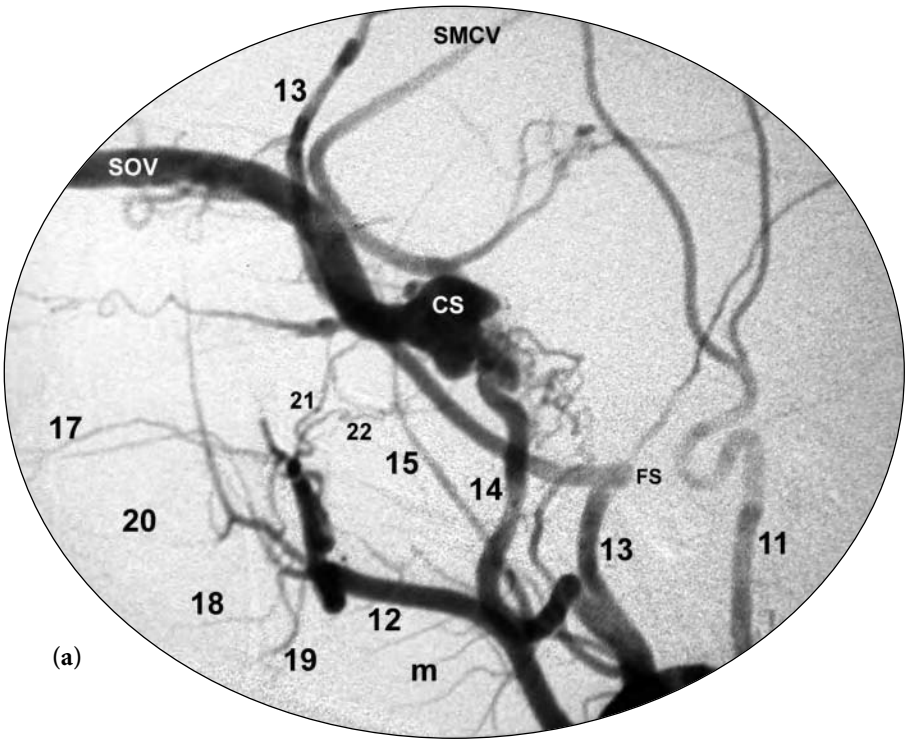

Fig. 4.12 (a,b) Lateral 2D (*a*) and 3D (*b*) views following selective external carotid artery injection. There is a direct hole fistula (arterial-venous fistula) between the accessory meningeal artery and the posterior aspect of the cavernous sinus.

FIGURE KEY

11 superficial temporal artery
12 internal maxillary artery
13 middle meningeal artery
14 accessory meningeal artery
15 deep temporal artery
17 infraorbital artery
18 posterior superior alveolar artery
19 greater palatine artery
20 sphenopalatine artery
21 artery of the foramen rotundum
22 artery of the pterygoid canal (vidian artery)
m muscular branches
CS cavernous sinus
SOV superior ophthalmic vein
SMCV superficial middle cerebral vein

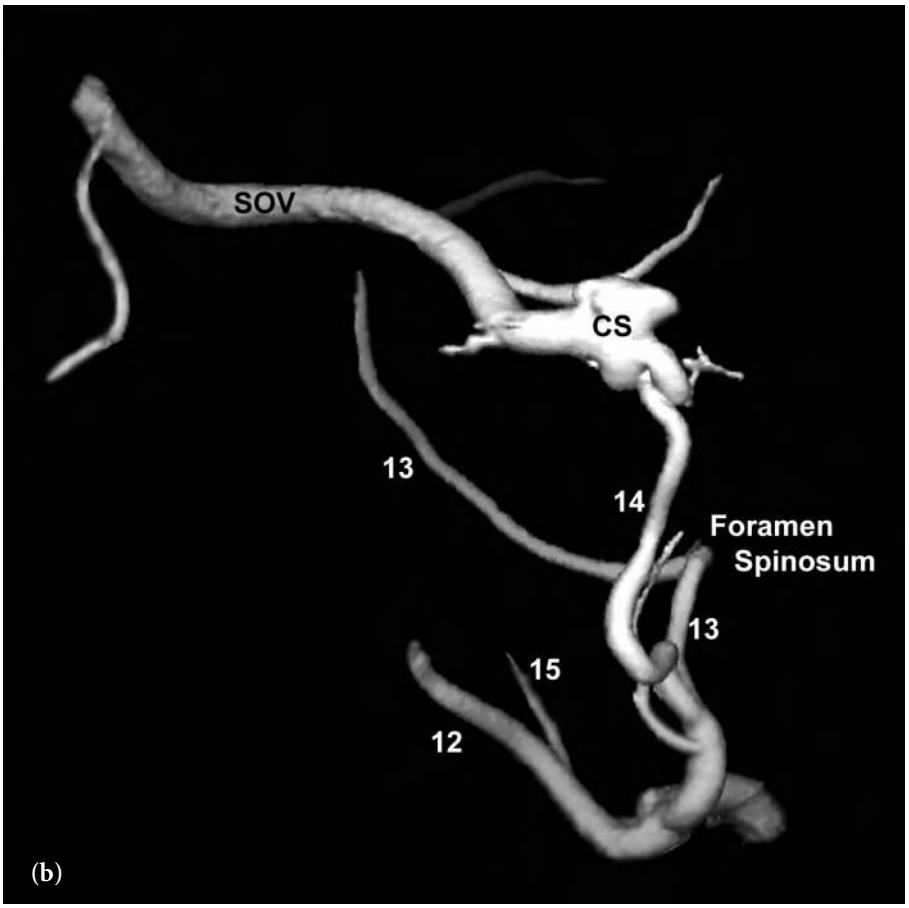

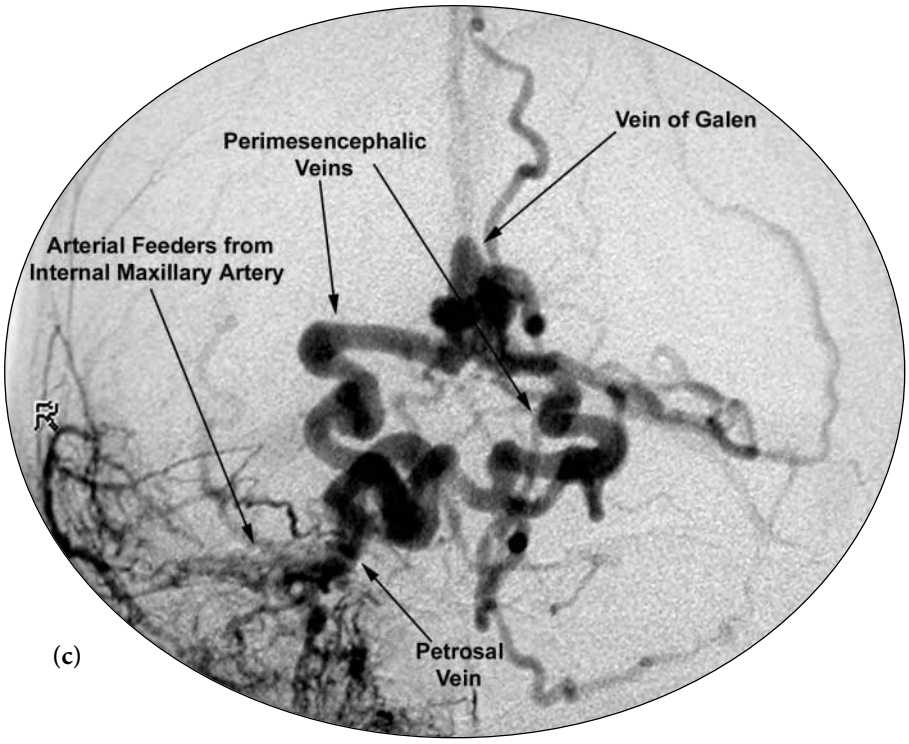

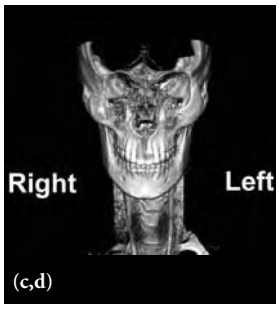

Fig. 4.12 (c, d) Frontal 2D (*c*) and 3D (*d*) views following right external carotid artery injection demonstrate a complex dural arterial-venous fistula supplied by multiple branches of the internal maxillary artery. Early venous drainage is directly into a dilated petrosal vein just posterior to the petrous ridge. This then drains through dilated perimesencephalic veins into the vein of Galen.

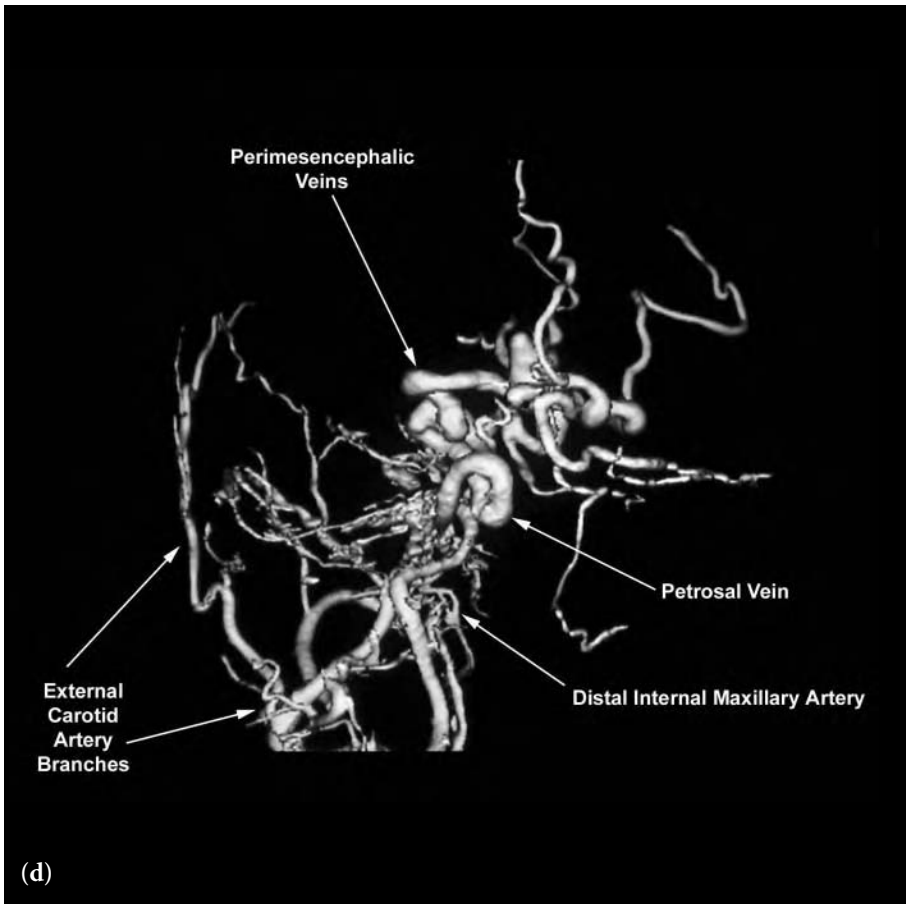

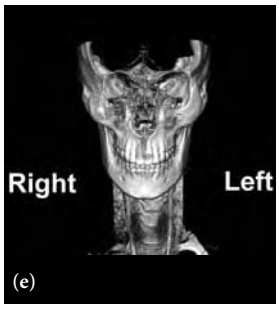

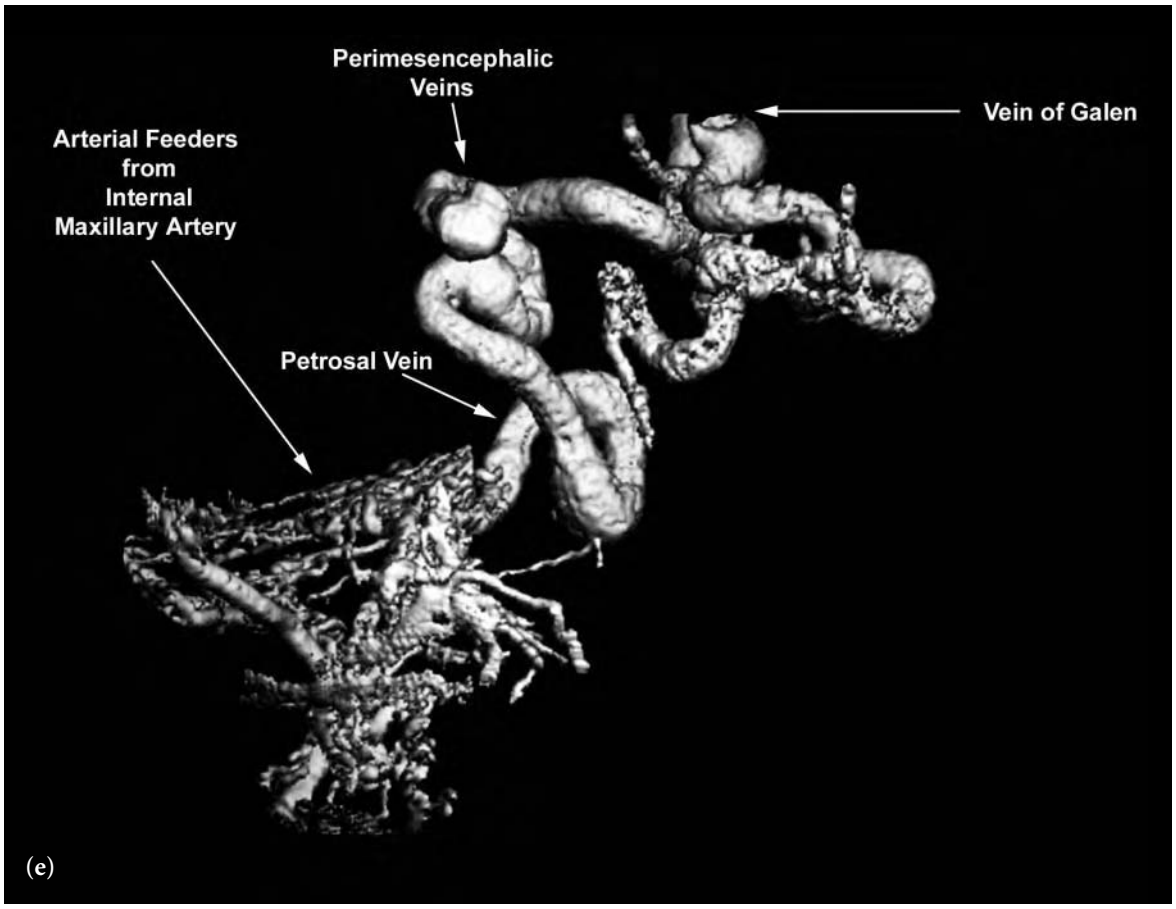

Fig. 4.12 (e) Frontal 3D view following a selective injection into the right internal maxillary artery showing more completely the massive number of small arterial feeders from the internal maxillary artery feeding this complex dural arterial-venous fistula.

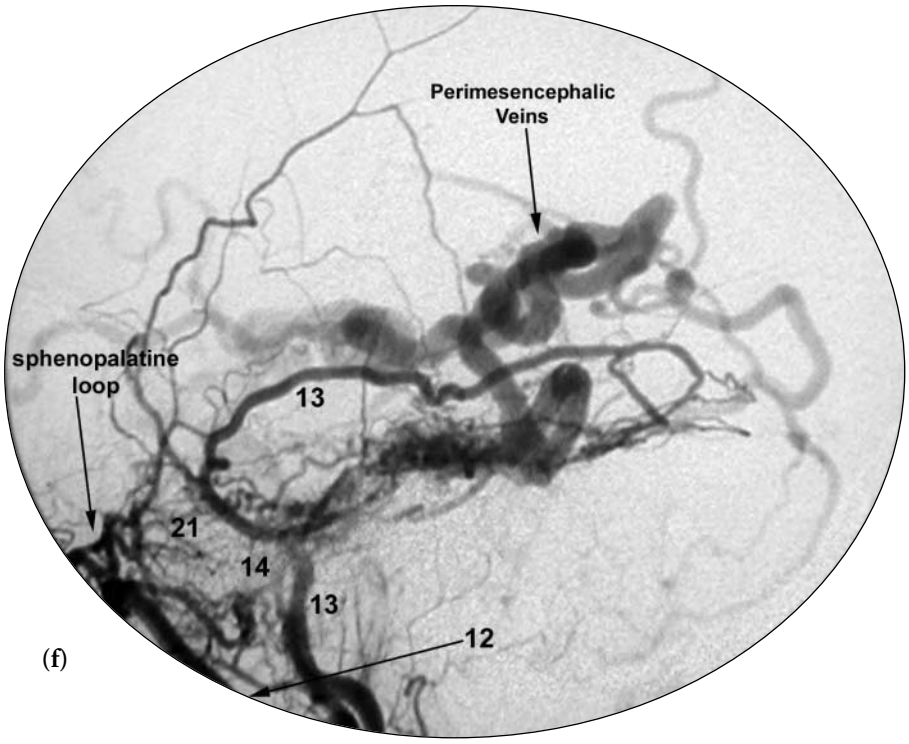

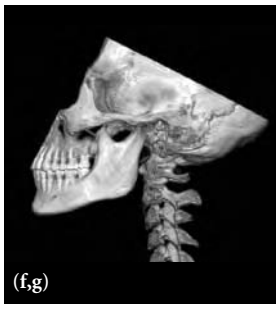

Fig. 4.12 (f, g) Lateral 2D (*f*) and 3D (*g*) views following right external carotid artery injection showing the complex dural arterial-venous fistula supplied by branches of the internal maxillary artery which drain directly into a dilated petrosal vein which then drains through dilated perimesencephalic veins into the vein of Galen.

FIGURE KEY

12 internal maxillary artery
13 middle meningeal artery
14 accessory meningeal artery
21 artery of the foramen rotundum

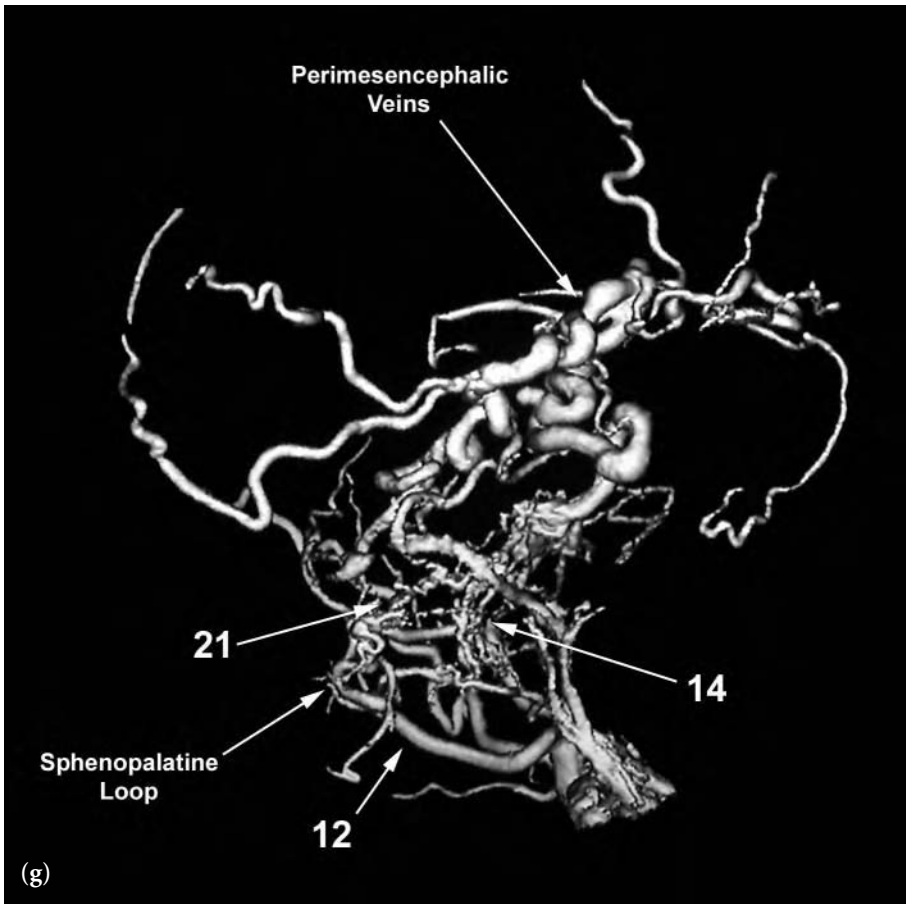

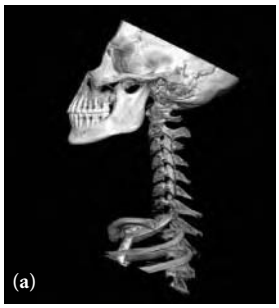

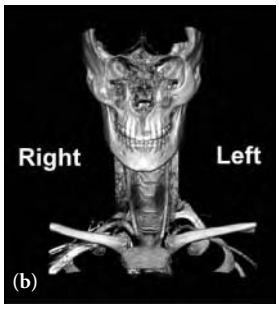

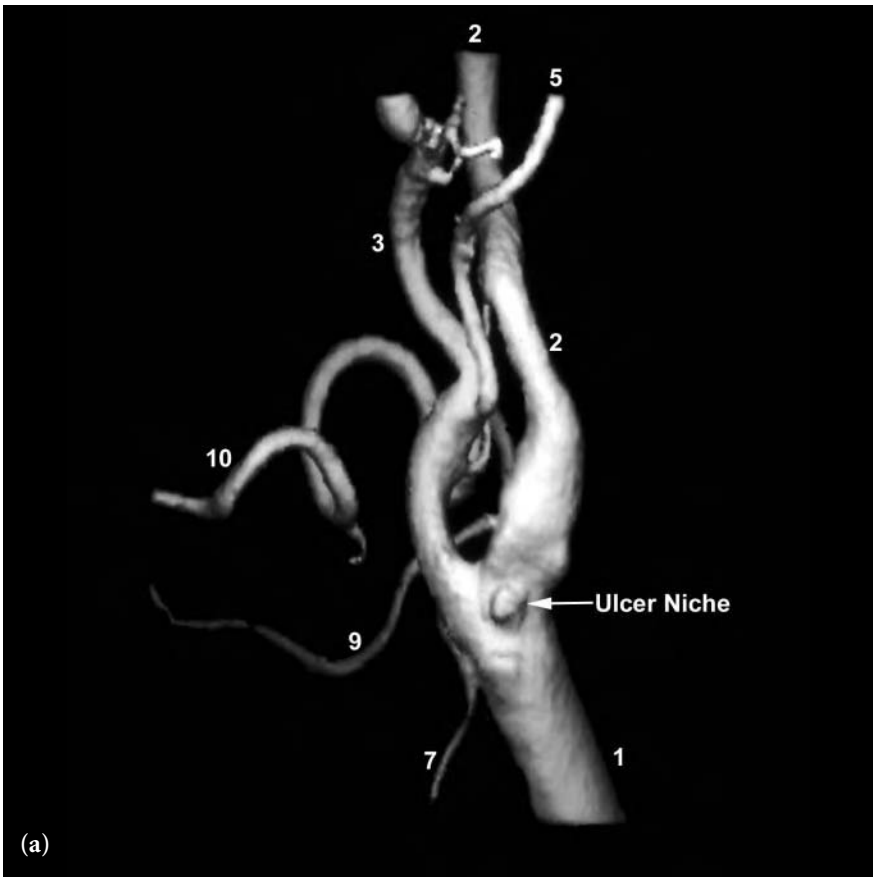

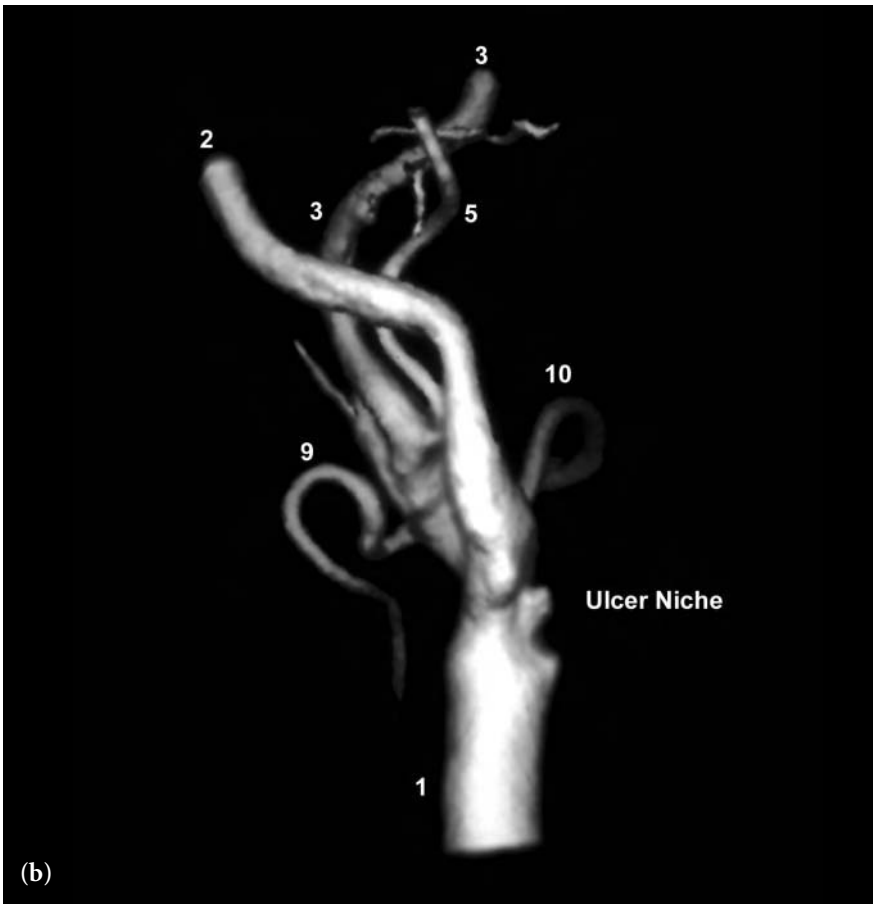

Fig. 4.13 (a,b) Lateral (*a*) and frontal (*b*) 3D views following left common carotid artery injection. Note the deep ulcer crater seen en face (*a*) and in profile (*b*) within the large atherosclerotic plaque at the common carotid artery bifurcation.

FIGURE KEY

1 common carotid artery
2 internal carotid artery
3 external carotid artery
5 occipital artery
7 superior thyroid artery
9 lingual artery
10 facial artery

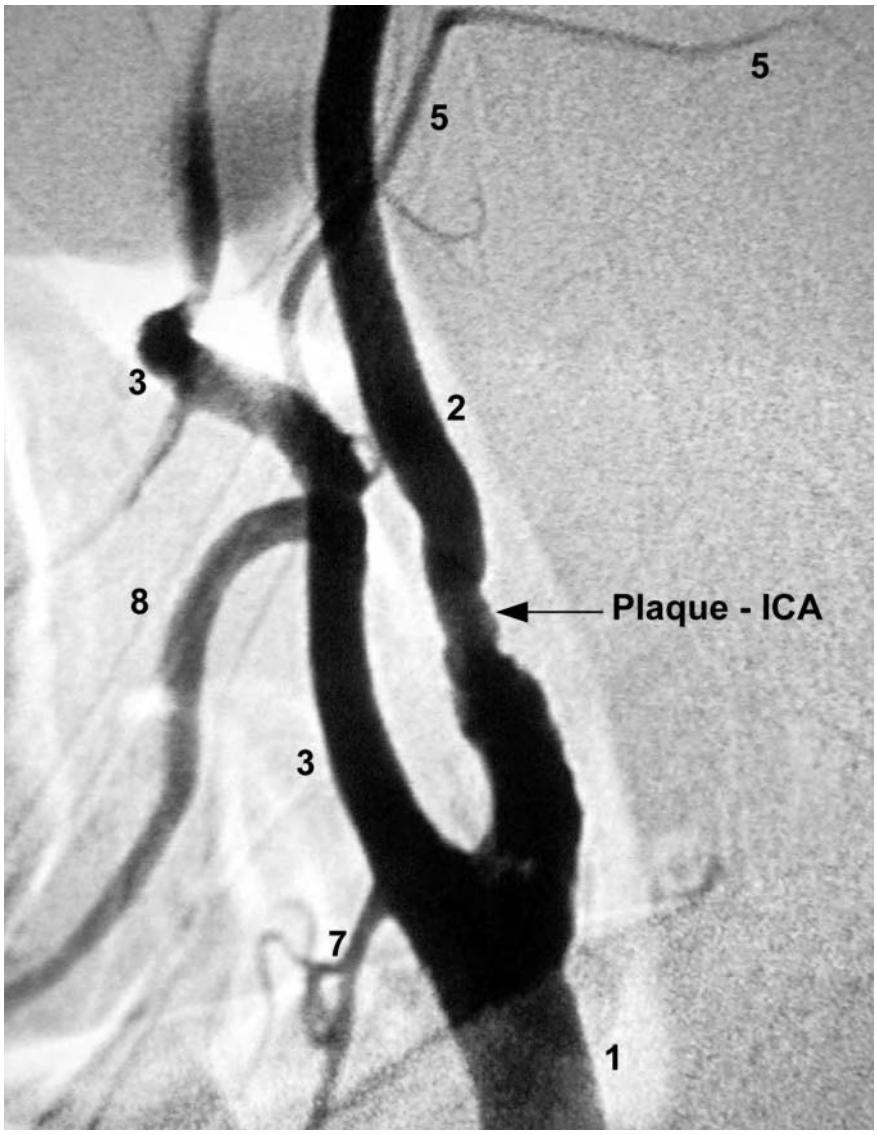

Fig. 4.14 Lateral 2D view following left common carotid artery injection. Note the atherosclerotic plaque involving the proximal internal carotid artery.

FIGURE KEY

1 common carotid artery
2 internal carotid artery
3 external carotid artery
5 occipital artery
7 superior thyroid artery
8 lingual-facial artery trunk

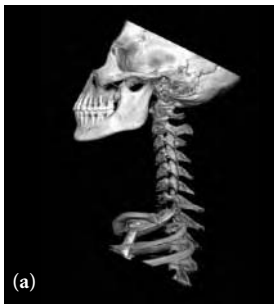

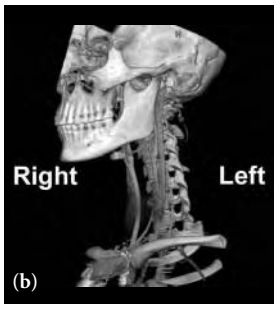

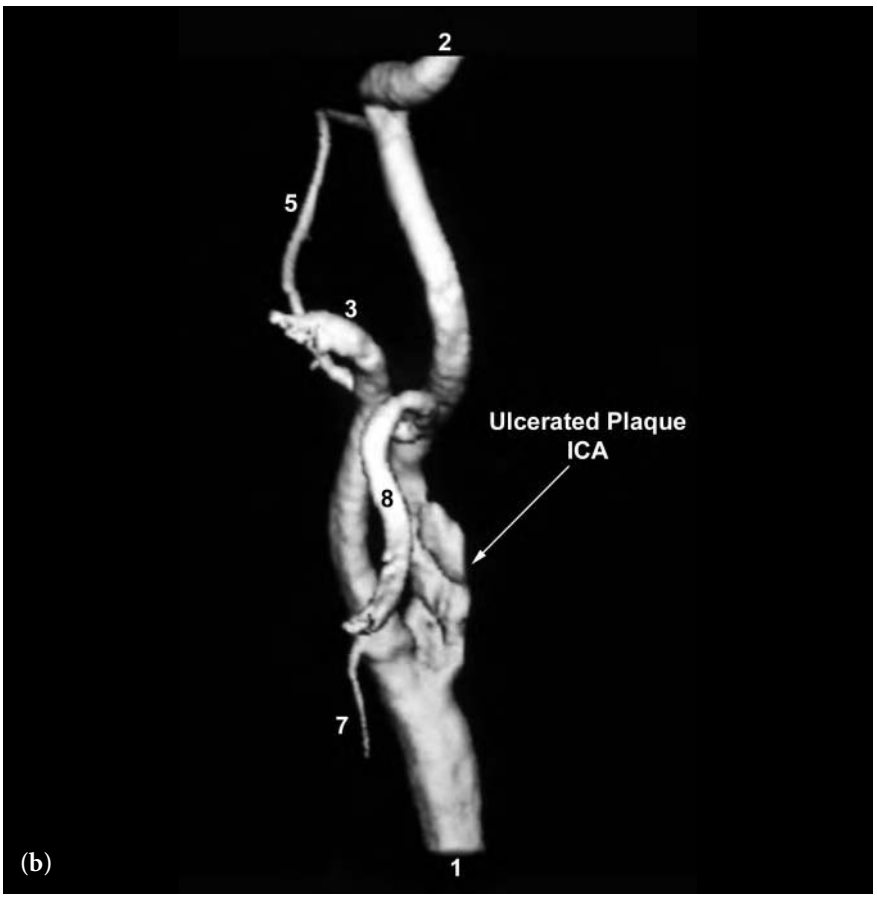

Fig. 4.15 (a, b) Lateral (*a*) and left anterior oblique (*b*) 3D views following left common carotid artery injection. Note the clear visualization of extensive ulceration within the atherosclerotic plaque involving the proximal internal carotid artery. Compare this with the 2D angiogram of the same vessel (Fig. 4.14).

FIGURE KEY

1 common carotid artery
2 internal carotid artery
3 external carotid artery
5 occipital artery
7 superior thyroid artery
8 lingual-facial artery trunk

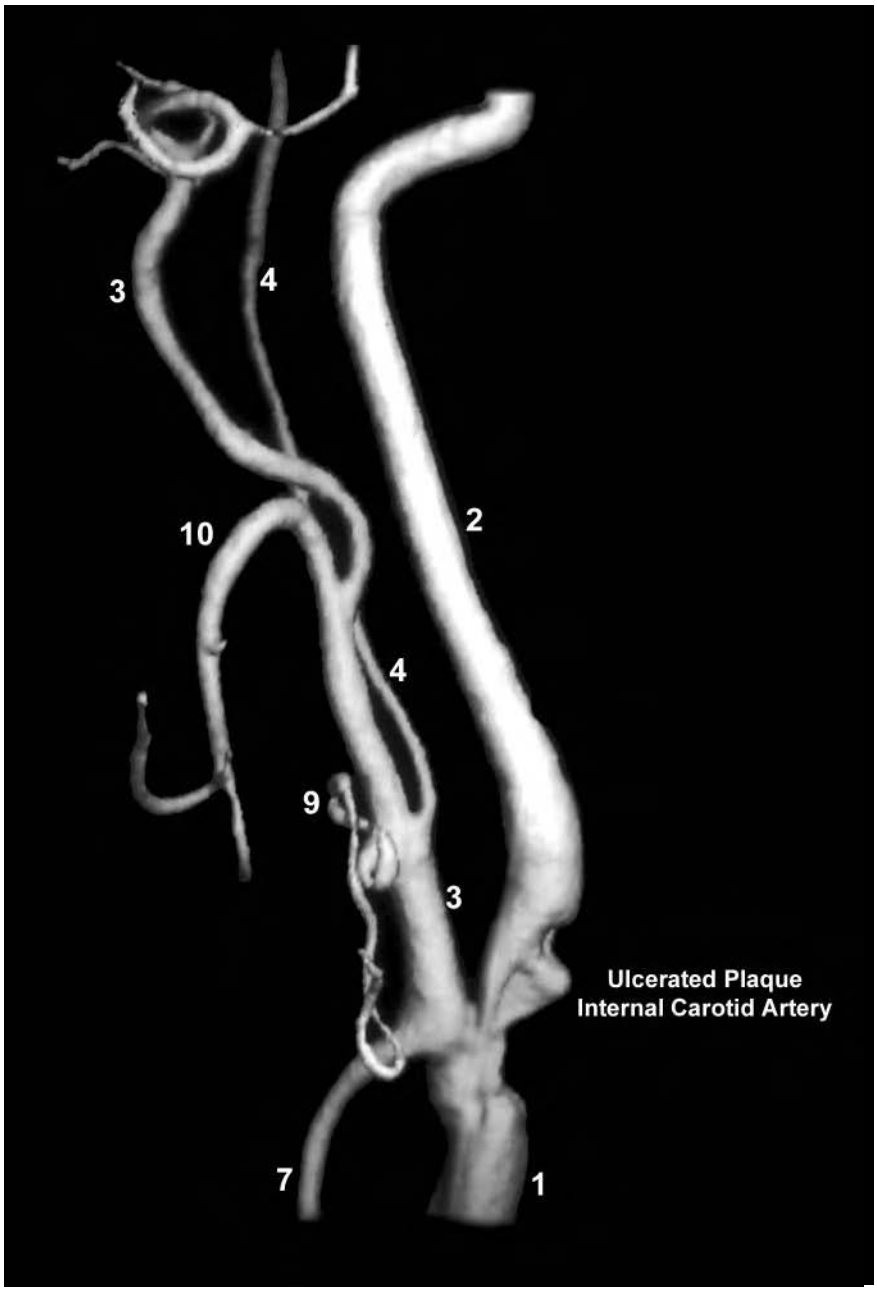

Fig. 4.16 Lateral 3D view of a left common carotid artery injection. Note the extensive atherosclerotic plaque with the deep ulceration involving the common carotid artery and proximal internal carotid artery.

FIGURE KEY

1 common carotid artery
2 internal carotid artery
3 external carotid artery
4 ascending pharyngeal artery
7 superior thyroid artery
9 lingual artery
10 facial artery

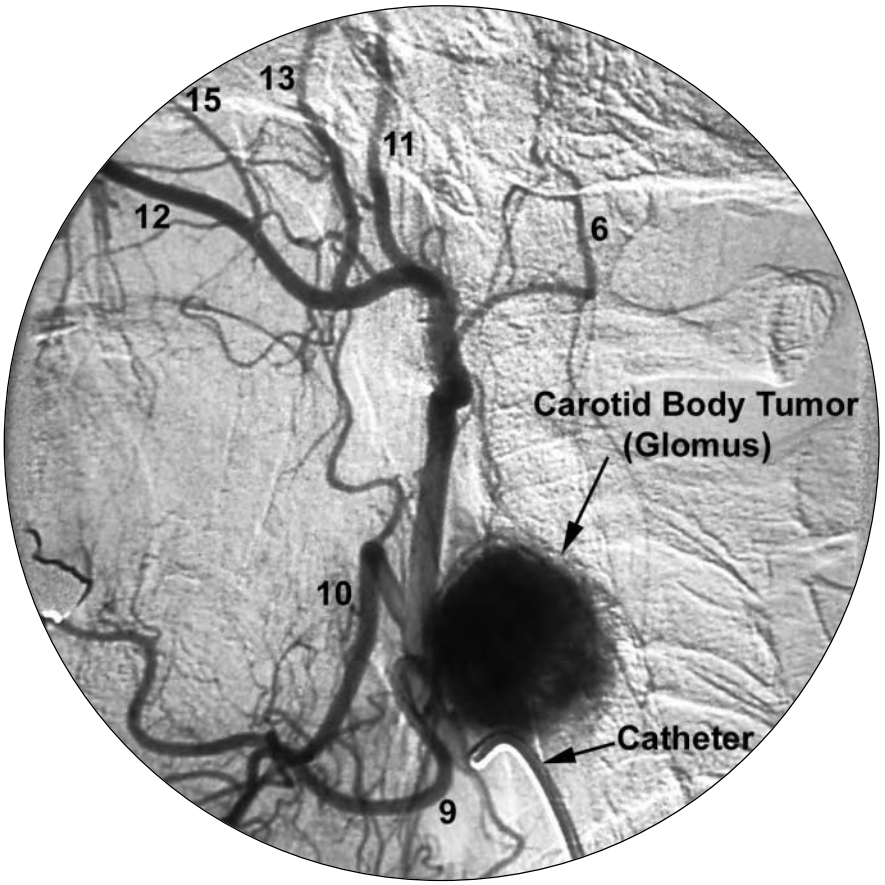

Fig. 4.17 Lateral 2D view following selective external carotid artery injection. There is a hypervascular mass adjacent to the proximal external carotid artery. This is the typical appearance of a carotid body tumor (glomus or paraganglioma). This is the same patient as in Figure 4.18.

FIGURE KEY

6 occipital artery
9 lingual artery
10 facial artery
11 superficial temporal artery
12 internal maxillary artery
13 middle meningeal artery
15 deep temporal artery

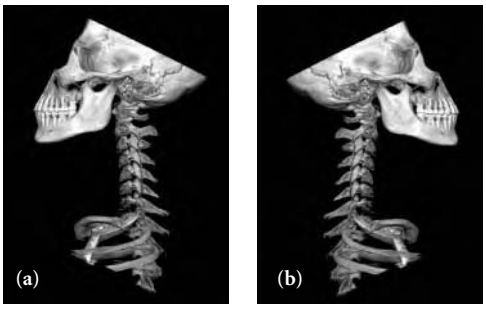

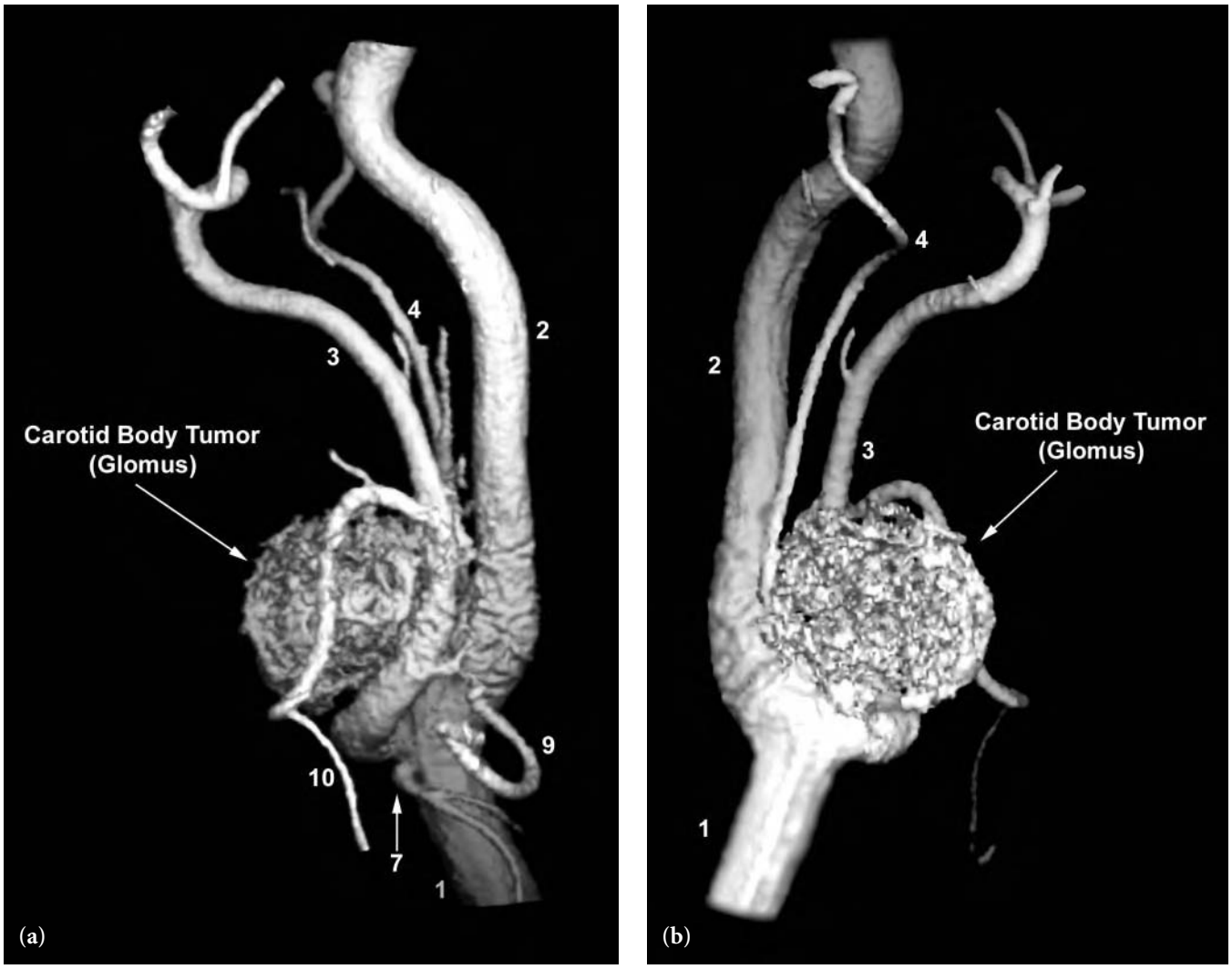

Fig. 4.18 (a, b) Lateral (*a*) and medial (*b*) 3D views following left common carotid artery injection. Note the hypervascular mass typical of a carotid body tumor (glomus or paraganglioma) situated between the proximal internal and external carotid arteries. This is the same patient as in Figure 4.17.

FIGURE KEY

1 common carotid artery
2 internal carotid artery
3 external carotid artery
4 ascending pharyngeal artery
7 superior thyroid artery
9 lingual artery
10 facial artery

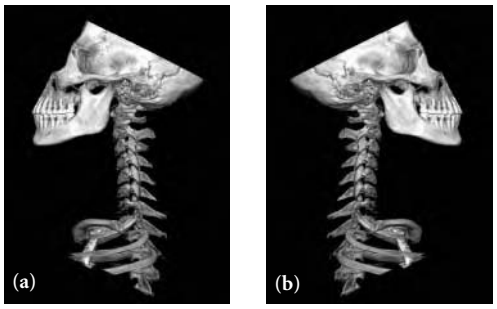

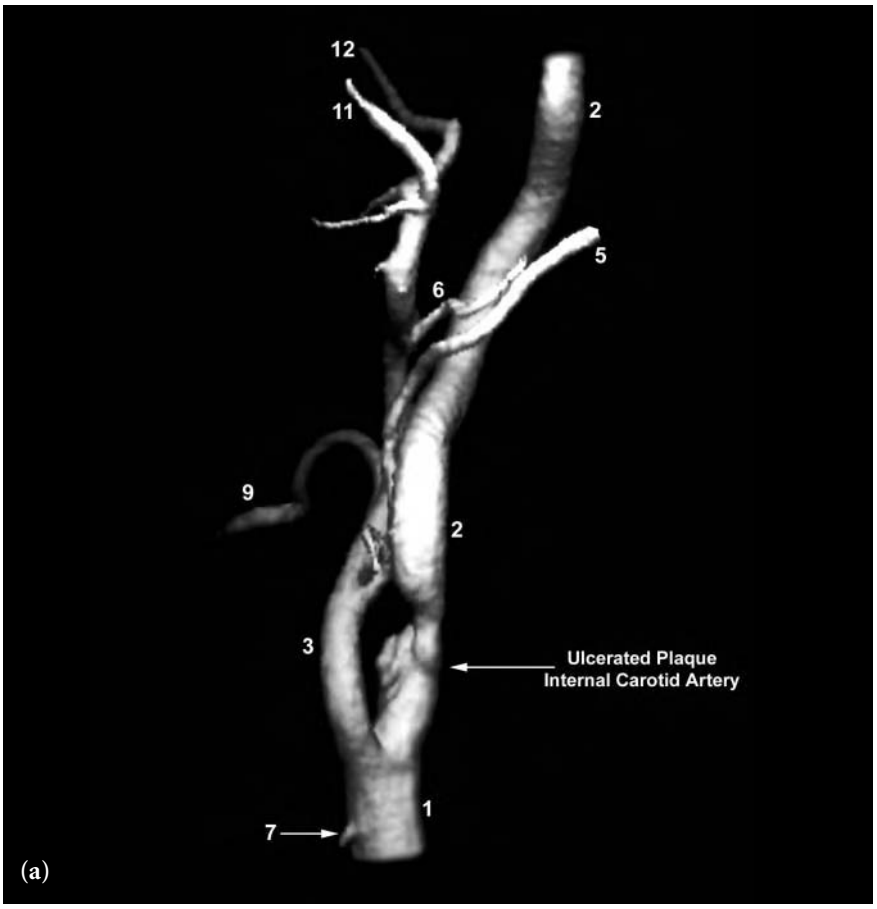

Fig. 4.19 (a, b) Lateral (*a*) and medial (*b*) 3D views following left common carotid artery injection. There is extensive atherosclerotic plaque involving the proximal internal carotid artery. Note the "terraced" appearance of deep ulceration on the lateral view which is not visible on the medial view.

FIGURE KEY

1 common carotid artery
2 internal carotid artery
3 external carotid artery
5 occipital artery
6 posterior auricular artery
7 superior thyroid artery
9 lingual artery
11 superficial temporal artery
12 internal maxillary artery

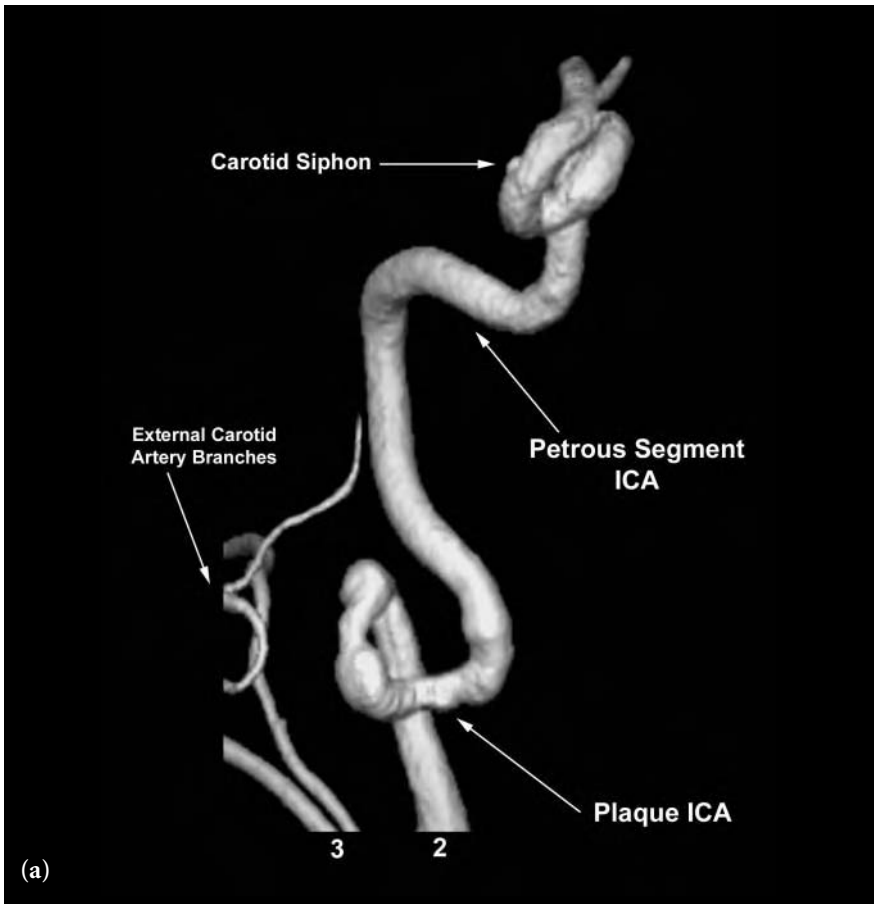

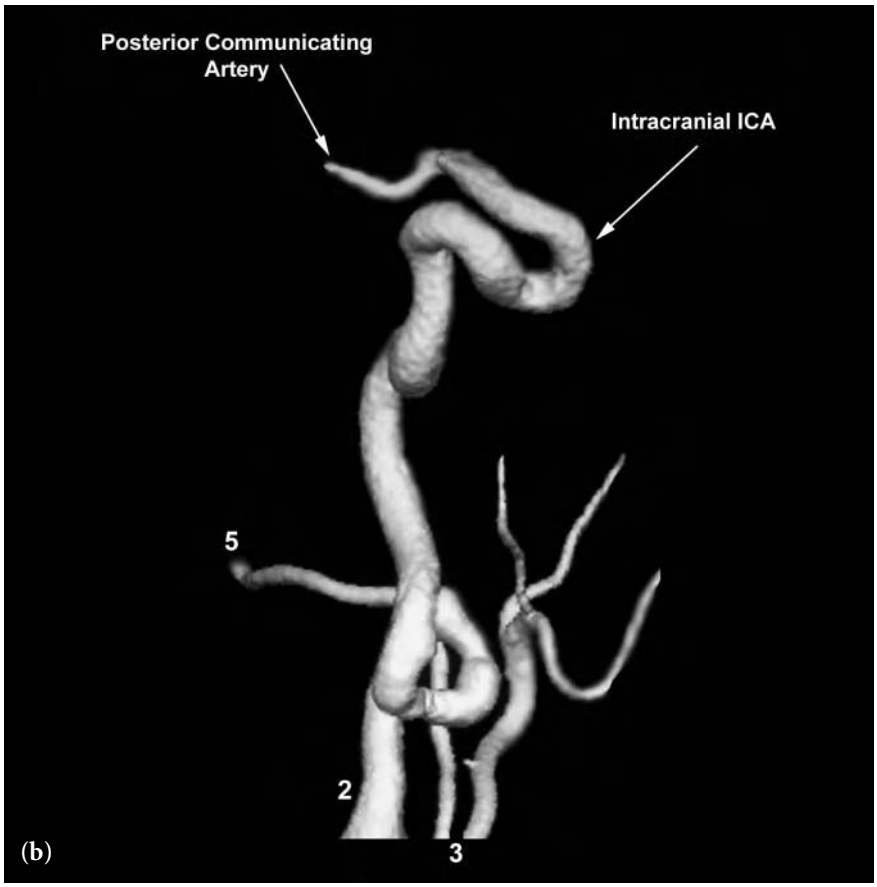

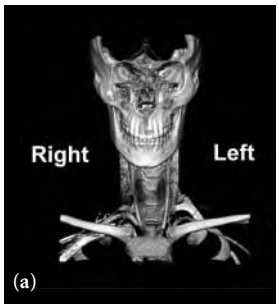

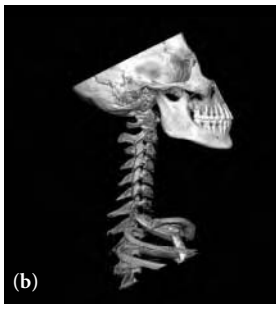

Fig. 4.20 (a-c) Frontal (*a*), lateral (*b*), and medial (*c*) 3D views following right common carotid artery injection. There is marked tortuosity of the cervical segment of the internal carotid artery. Note the atherosclerotic irregularity and narrowing of the tortuous segment. These changes are often seen in patients with long-standing hypertension. Also note the tiny aneurysms within the intracavernous segment of the internal carotid artery seen on the medial view.

FIGURE KEY

2 internal carotid artery
3 external carotid artery branches
5 occipital artery
ICA internal carotid artery

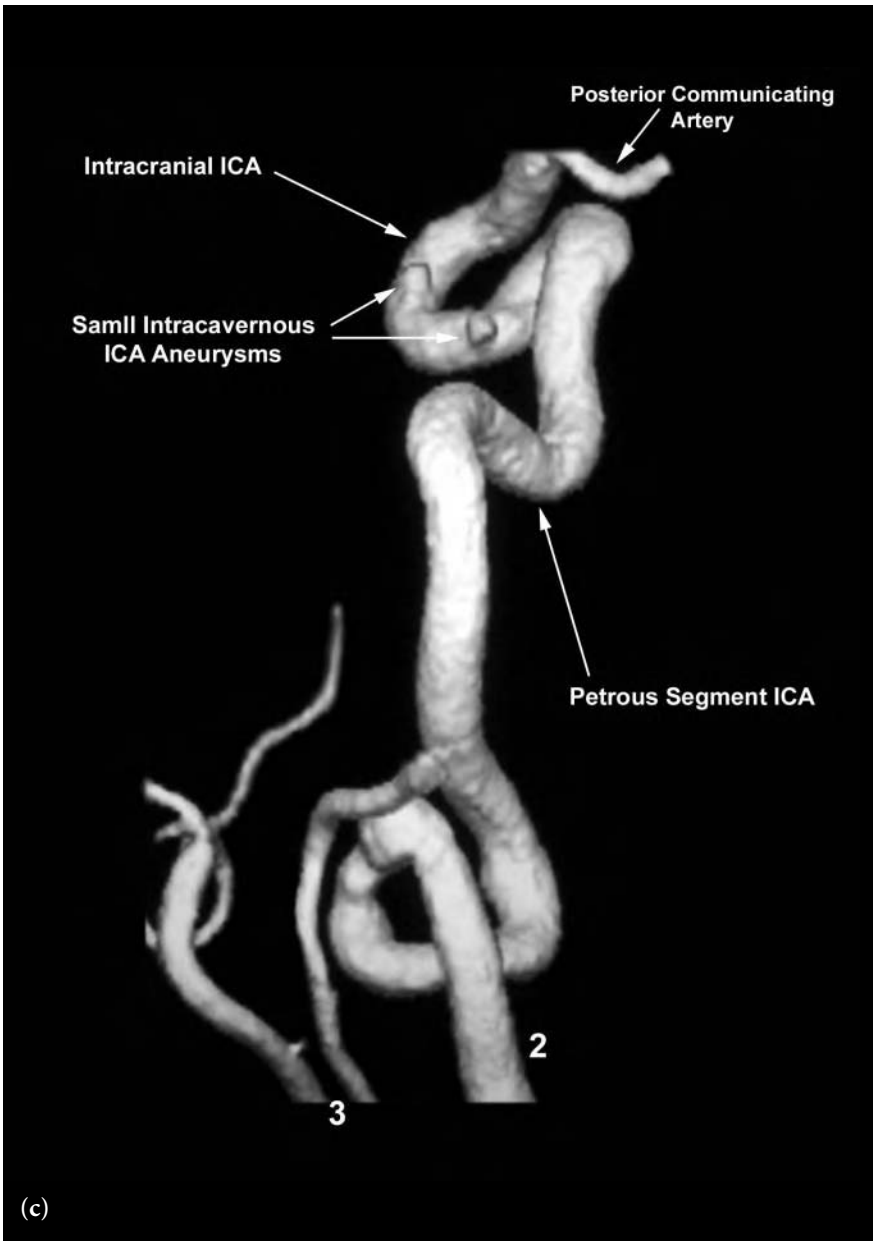

Fig. 4.20 (continued)

2 internal carotid artery
3 external carotid artery branches
5 occipital artery
ICA internal carotid artery

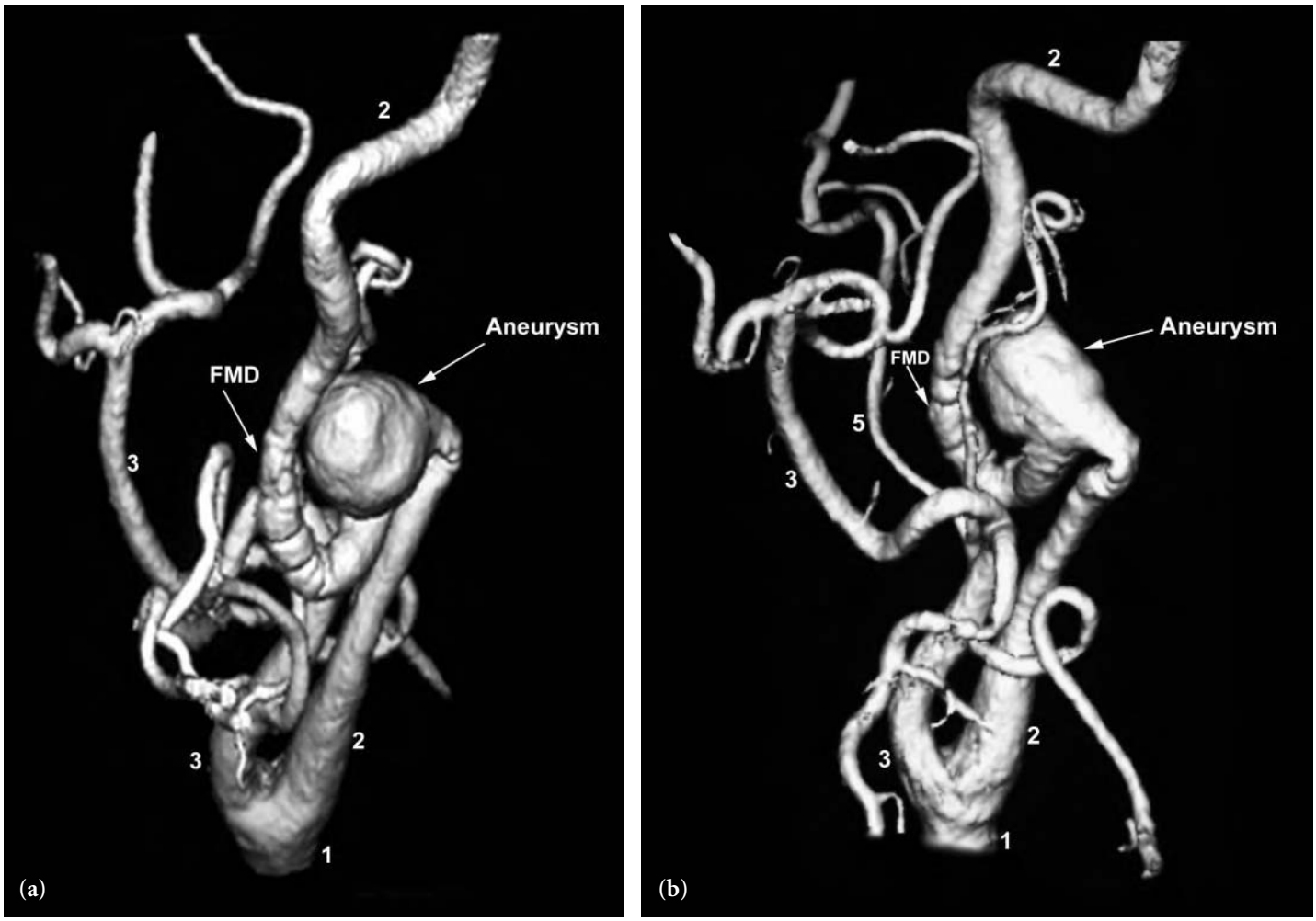

Fig. 4.21 (a, b) Two 3D views following common carotid artery injection. There is fibromuscular dysplasia (fmd) of the cervical segment of the internal carotid artery with a large associated aneurysm.

FIGURE KEY

1 common carotid artery
2 internal carotid artery
3 external carotid artery
5 occipital artery

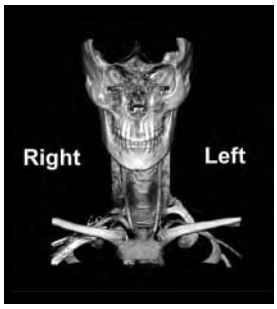

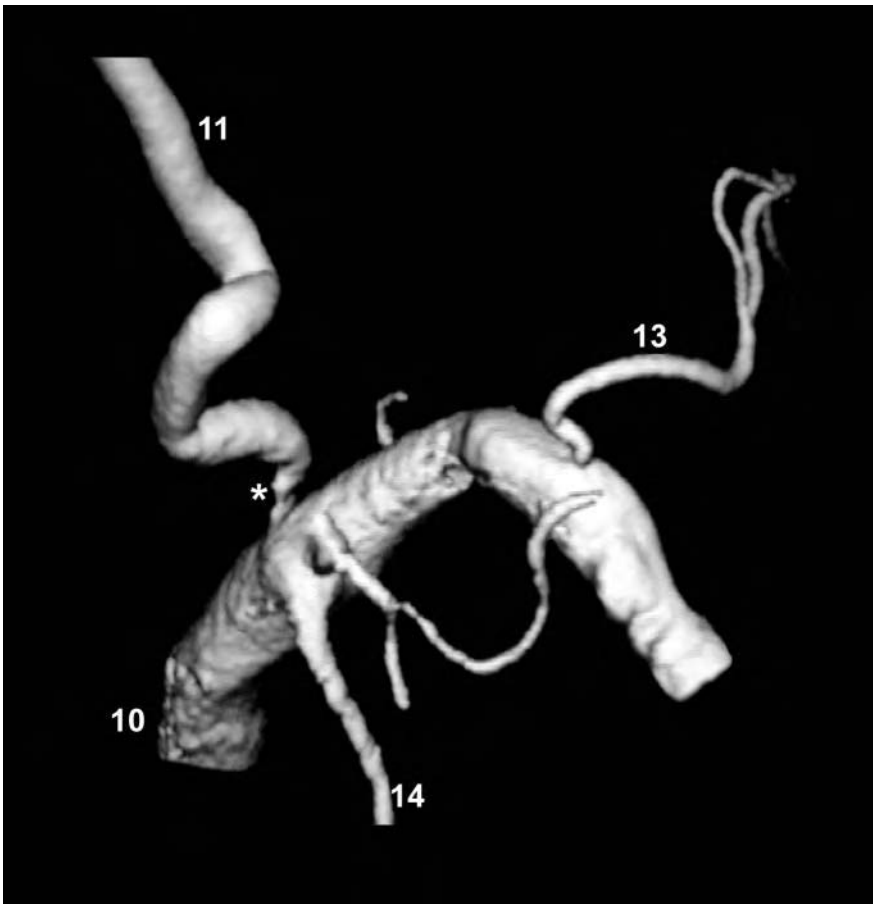

Fig. 4.22 Frontal 3D view following left subclavian artery injection. Note the high grade (severe) stenosis involving the origin of the left vertebral artery. This is the same patient as in Figure 4.23.

FIGURE KEY
10 left subclavian artery
11 left vertebral artery
13 left costocervical trunk
14 left internal mammary artery
*high grade stenosis origin left vertebral artery

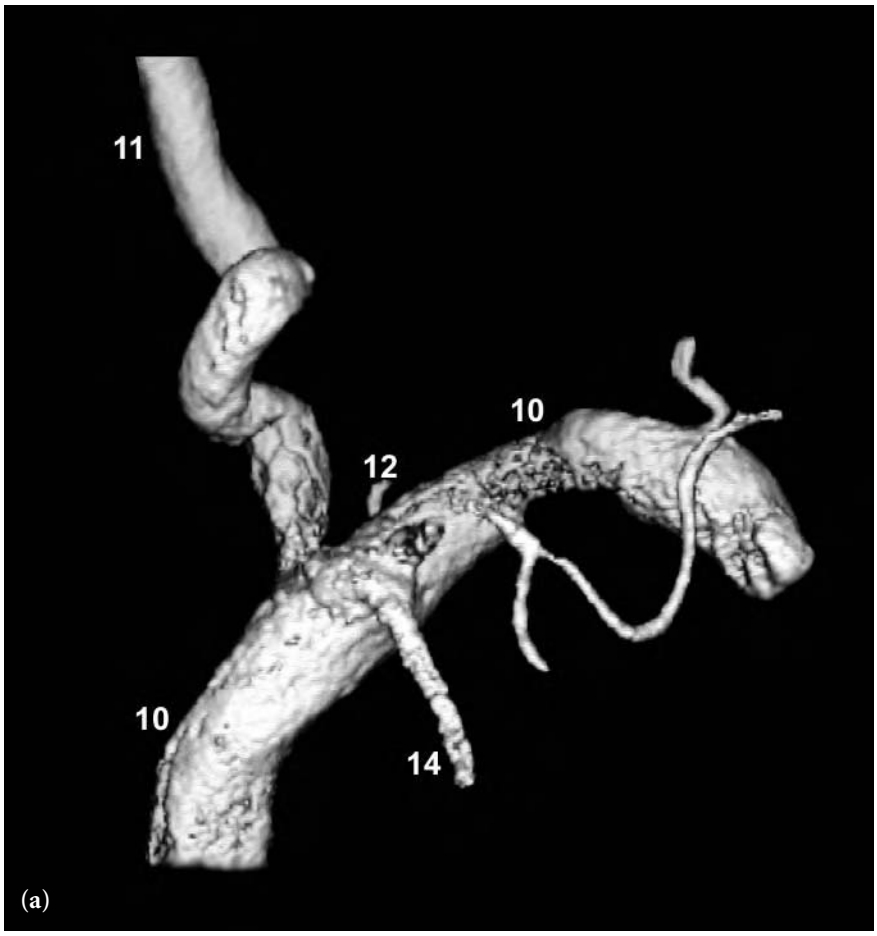

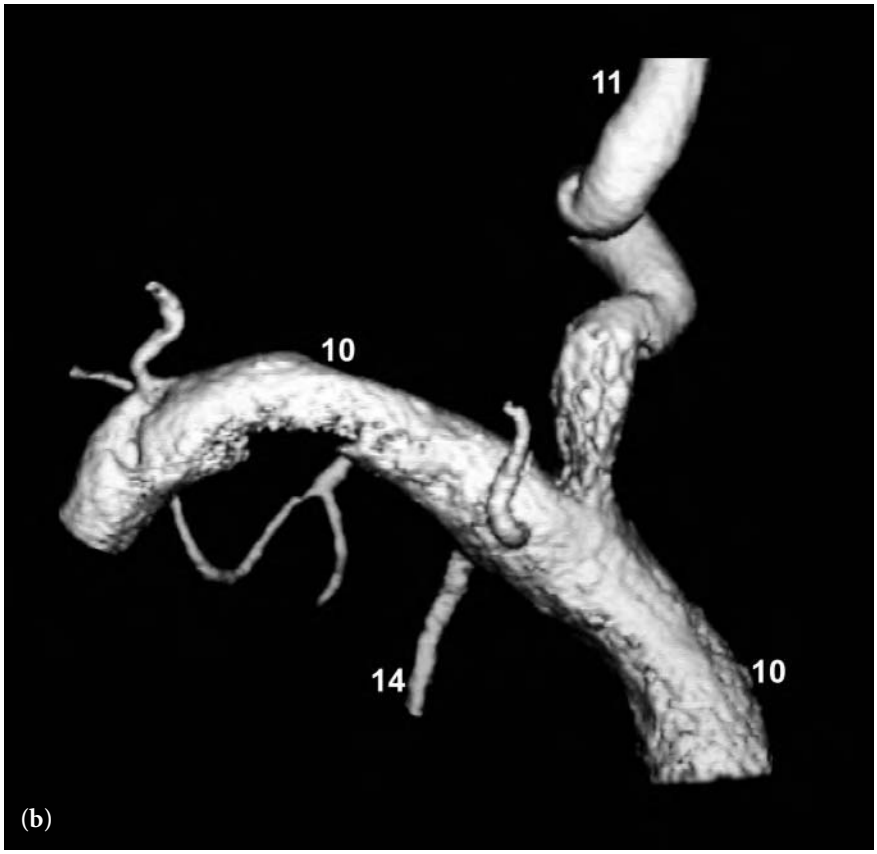

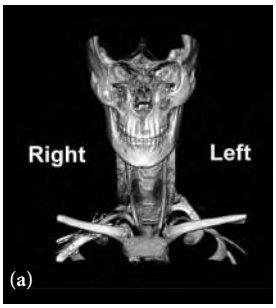

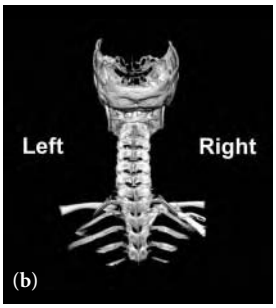

Fig. 4.23 (a, b) Frontal (*a*) and posterior (*b*) 3D views following left subclavian artery injection. These images were obtained after placement of a balloon expandible stent in the proximal left vertebral artery for treatment of the high grade stenosis (Fig. 4.22). Note the endoluminal impression of the struts of the stent on the surface of the left vertebral artery.

FIGURE KEY
10 left subclavian artery
11 left vertebral artery
12 left thyrocervical trunk
14 left internal mammary artery

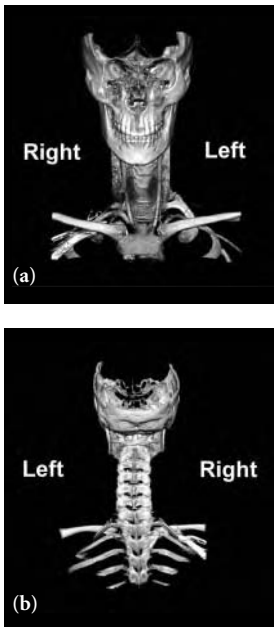

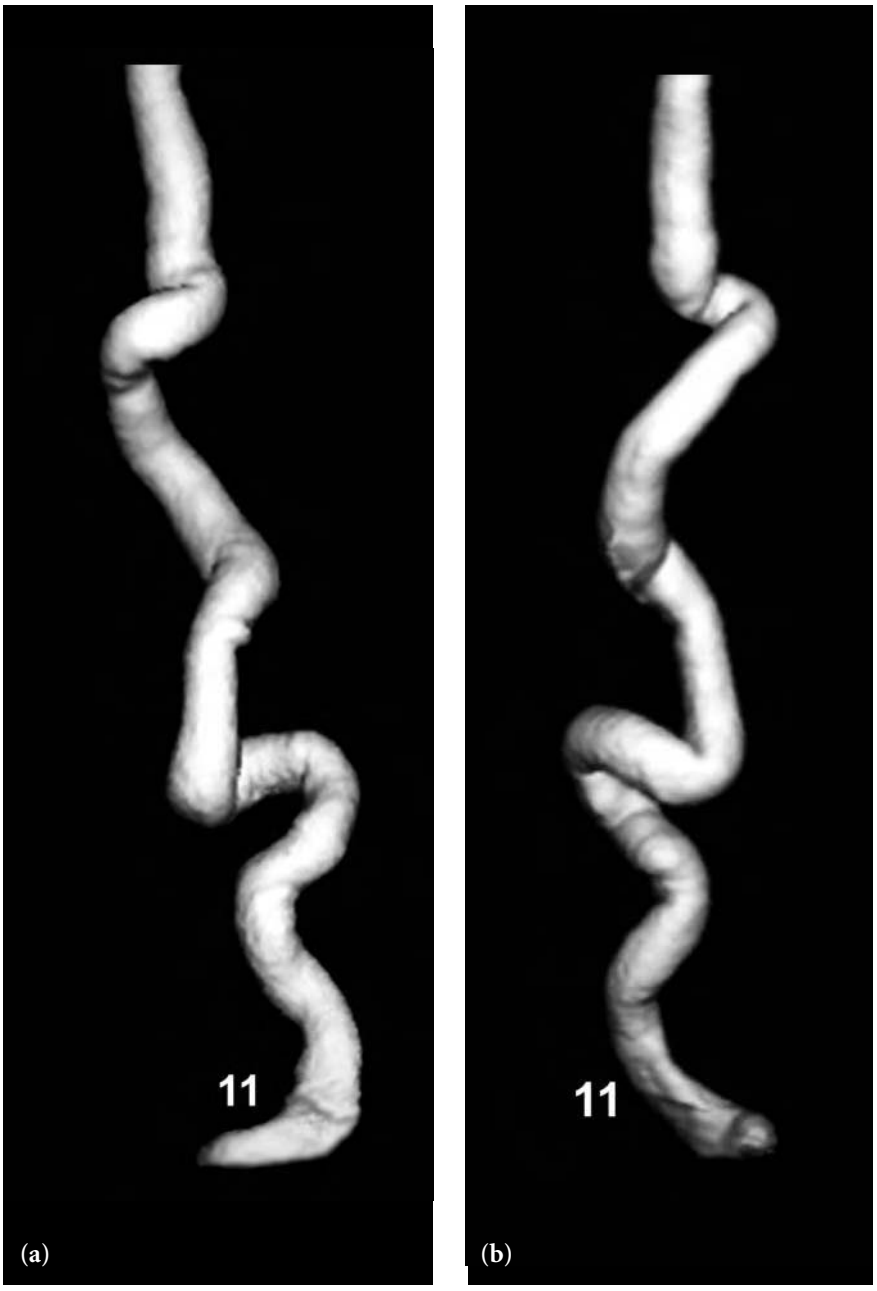

Fig. 4.24 (a, b) Frontal (*a*) and posterior (*b*) 3D views following left vertebral artery injection. There is elongation and tortuosity of the cervical segment of the left vertebral artery.

FIGURE KEY
11 vertebral artery

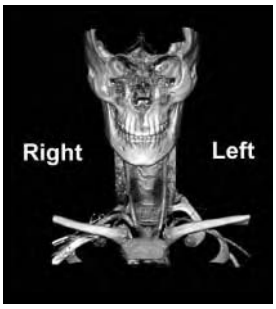

Fig. 4.25 Frontal 3D view following left vertebral artery injection. Note the fibromuscular dysplasia in the lower cervical segment of the left vertebral artery.

FIGURE KEY
11 vertebral artery

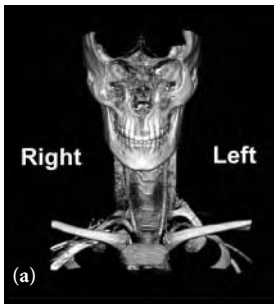

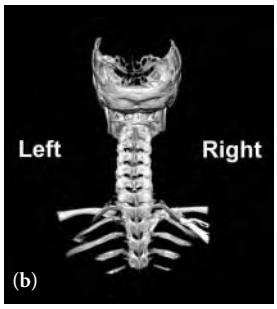

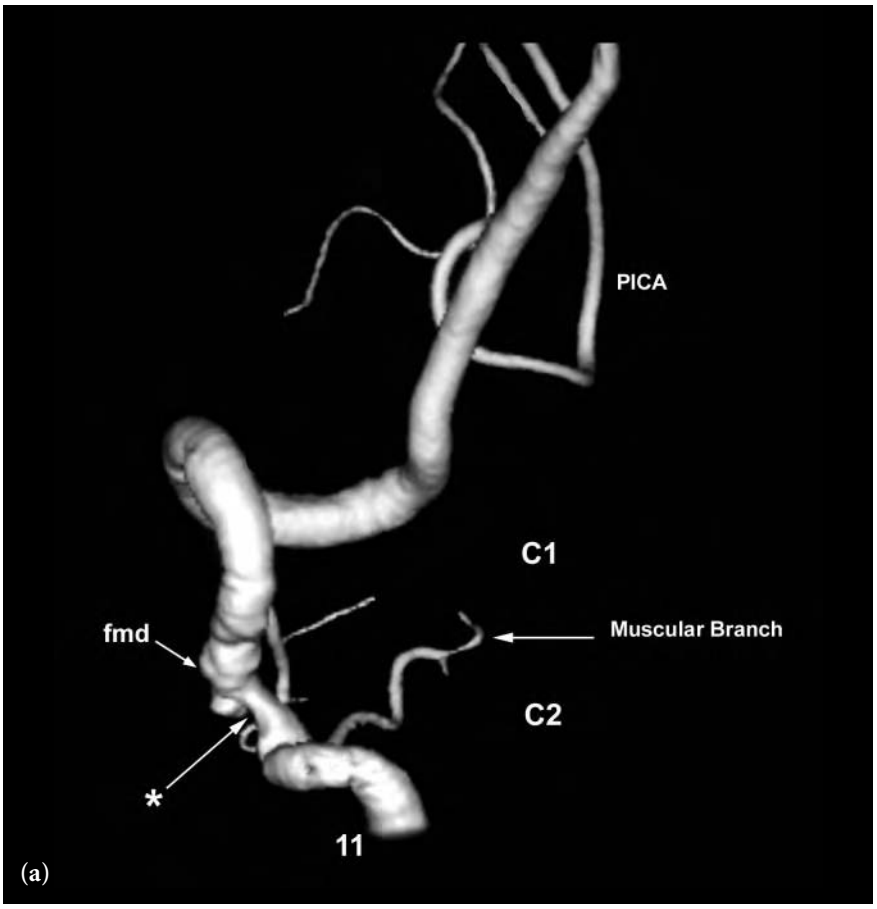

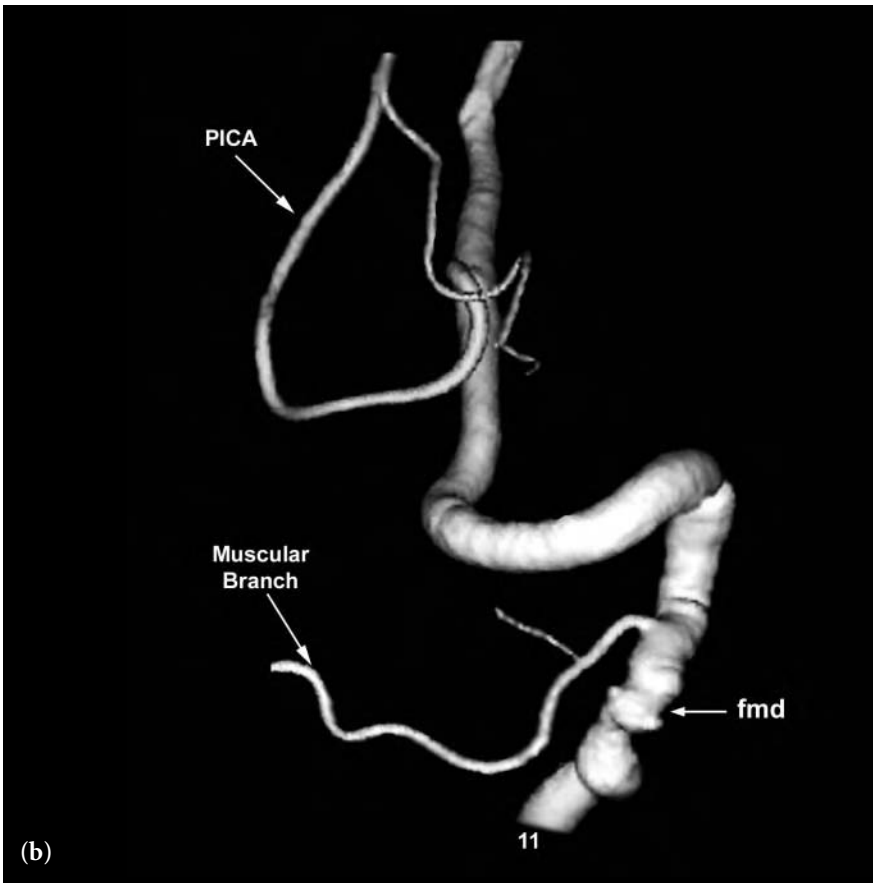

Fig. 4.26 (a, b) Frontal (*a*) and posterior (*b*) 3D views following right vertebral artery injection. There is severe fibromuscular dysplasia (fmd) involving the upper cervical segment (at the C2 level) of the vertebral artery. Note the stenosis related to the dysplastic segment on the anterior view (*a*).

FIGURE KEY
11 vertebral artery
C1 C1 vertebral segment
C2 C2 vertebral segment
PICA posterior inferior cerebellar artery
* stenosis
fmd fibromuscular dysplasia

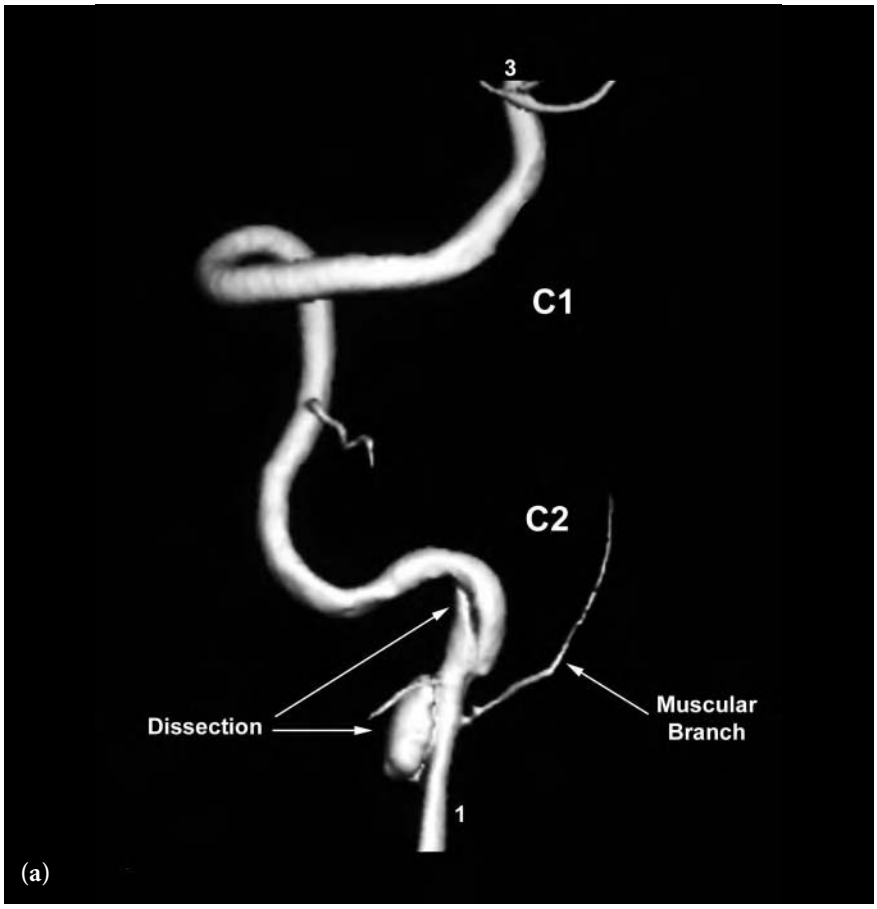

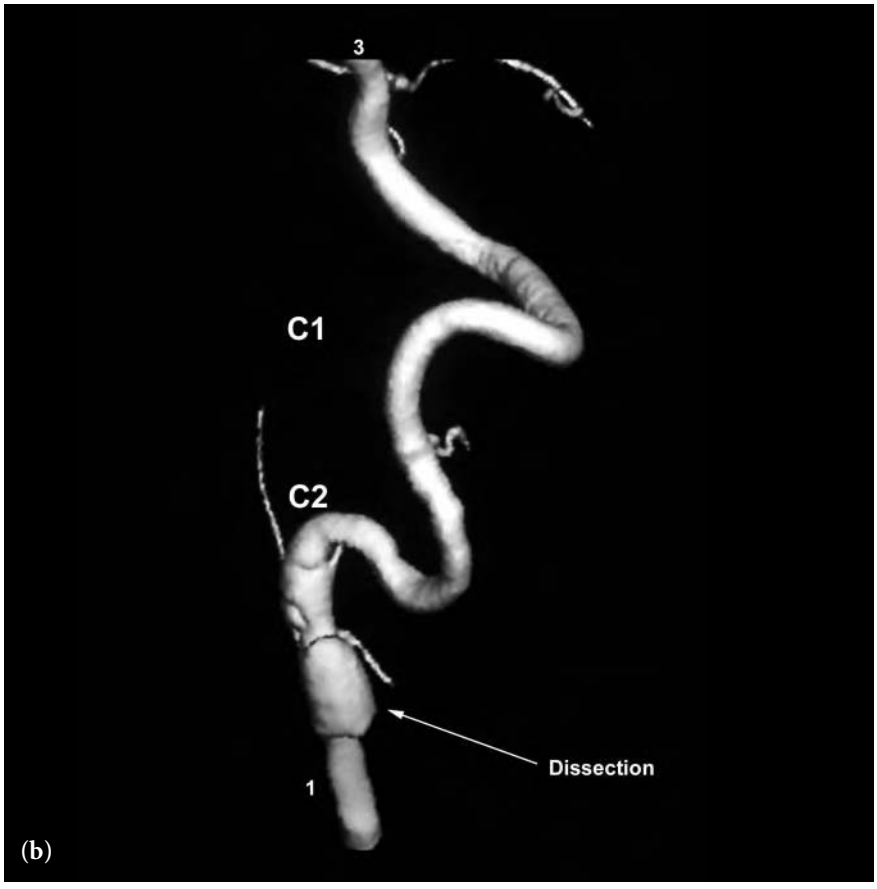

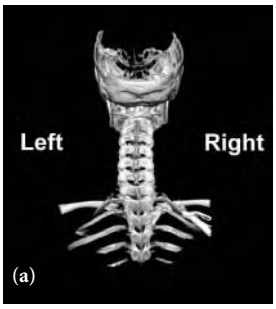

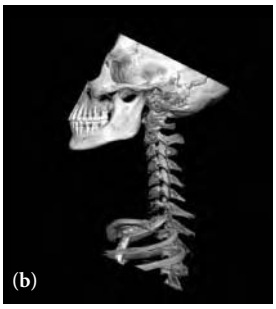

Fig. 4.27 (a, b) Posterior (*a*) and lateral (*b*) views following 3D left vertebral artery injection. There is a dissection of the upper cervical segment of the vertebral artery with aneurysm formation at the C2-C3 vertebral level.

FIGURE KEY
1 vertebral artery
3 basilar artery
C1 C1 vertebral segment
C2 C2 vertebral segment

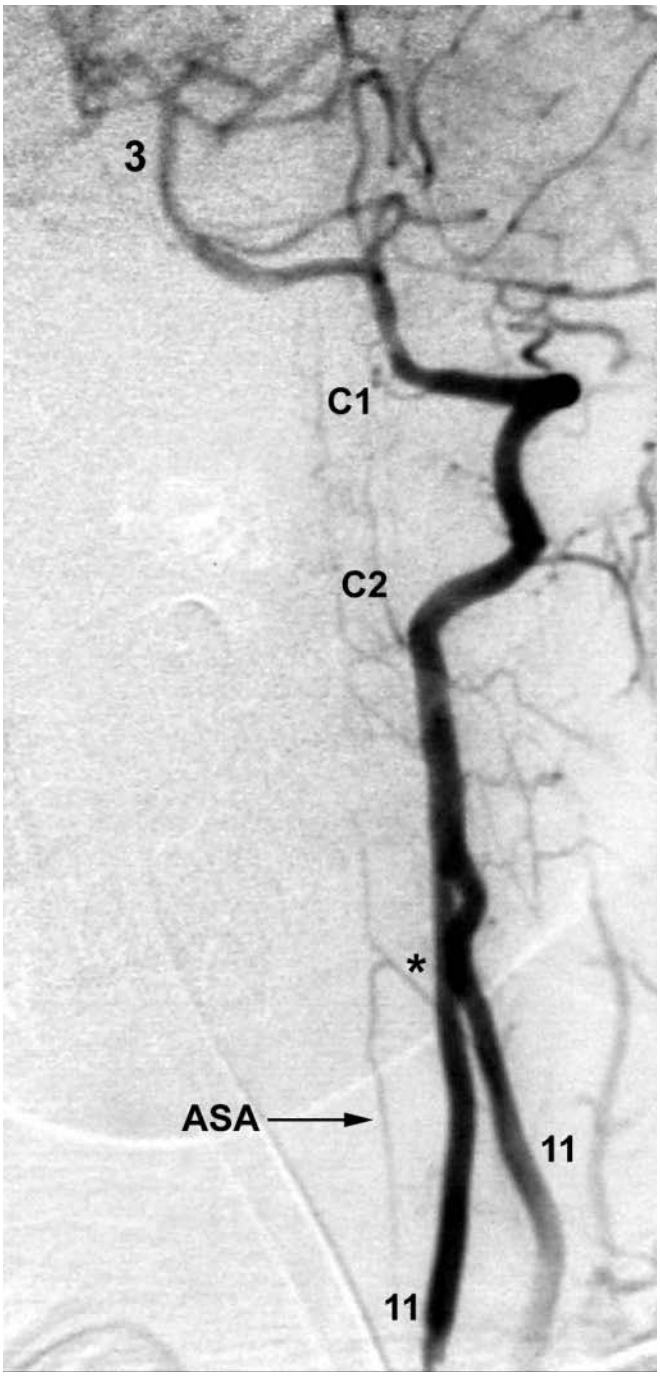

Fig. 4.28 Frontal 2D view following left vertebral artery injection. There is developmental duplication of the left vertebral artery. Note the radiculomedullary feeder (*) to the anterior spinal artery (ASA).

FIGURE KEY

3 basilar artery
11 vertebral artery
C1 C1 vertebral segment
C2 C2 vertebral segment
ASA anterior spinal artery
* radiculomedullary feeder to ASA

CHAPTER FIVE

INTRACRANIAL CAROTID ARTERY CIRCULATION/ANTERIOR CIRCULATION

The intracranial internal carotid artery (ICA) has petrous, presellar, intracavernous, and supraclinoid segments. In the illustrations and legend keys we further subdivide those segments into the vertical and horizontal petrous, presellar (Fischer C5), horizontal intracavernous (Fischer C4), anterior genu (Fischer C3), as well as the proximal and distal supraclinoid segments. This is the nomenclature we find most helpful in discussing the anatomy and the relevant pathology.

After entering the skull base the internal carotid artery travels within the vertical and horizontal segments of the petrous carotid canal before emerging near the petrous apex. It courses over the foramen lacerum in the distal horizontal segment and then assumes a vertical orientation to become the presellar or Fischer C5 segment. Near the posterior aspect of the sella turcica the ICA changes from a vertical to an anteriorly projecting horizontal path to become the Fischer C4 or horizontal intracavernous segment. The size and extent of the cavernous sinus is variable and therefore the level where the ICA pierces the dura is also variable. For the purposes of this atlas, we will consider that the ICA pierces the dura of the cavernous sinus near the Fischer C5-C4 junction.

The intracavernous ICA gives rise to several small branches. The meningohypophyseal artery (MHA) trunk most often arises from the posterior wall of the ICA at the Fischer C5-C4 junction. This normally small vessel can often be seen on high-resolution two-dimensional digital subtraction angiography (2D DSA). Visualization of the normal-sized proximal MHA trunk with 3DRA occurs to a variable degree. The inferolateral trunk or artery of the inferior cavernous sinus most often arises from the lateral aspect of the Fischer C4 segment. Occasionally seen on routine 2D DSA, this vessel is usually not seen on routine 3DRA unless it is pathologically enlarged. Variably arising medially from the Fischer C4 segment are normally tiny capsular branches (McConnell's capsular arteries). These

branches course medially along the sellar floor in an extradural position. They anastomose with their counterparts on the opposite side.

The intracavernous ICA has a sinuous course from posterior to anterior. The most posterior aspect is usually the most medial segment. We will also call the Fischer C5-C4 junction the first (posterior) genu of the intracavernous ICA. In the anterior cavernous sinus a second (anterior) genu occurs where the ICA becomes the Fischer C3 segment. It turns superiorly and posteriorly as it courses just inferior and medial to the anterior clinoid process. It is still within the cavernous sinus but will soon pierce the dura of the cavernous sinus a second time before it becomes subarachnoid in the supraclinoid segment.

The origin of the ophthalmic artery varies, arising near the junction of the anterior genu and supraclinoid segments. It is typically depicted as the last Fischer C3 vessel (1) and infraclinoid (2,3). The ophthalmic artery most often arises from the medial margin of the paraclinoidal segment of the ICA. In approximately 90% of all individuals, the origin of the ophthalmic artery is intradural in location (4). In other words, it most often arises just above where the intracavernous ICA pierces the dura for a second time (the dural ring).

We divide the supraclinoid segment into the proximal and distal supraclinoid segments. The portion between the anterior genu/Fischer C3 segment and the posterior communicating artery (PCoA) will be called the proximal supraclinoid segment and the distal supraclinoid segment will include the PCoA and anterior choroidal artery ending at the ICA bifurcation. We use the terms proximal and distal supraclinoid instead of Fischer C1 and C2 as we find them to be more descriptive, universal, and simplistic.

A very small branch to the pituitary gland arises from the superior-medial margin of the proximal supraclinoid segment of the ICA. This is called the superior hypophyseal artery. This is generally not seen on 3DRA unless pathologically enlarged.

Arising from the posterior wall of the supraclinoid segment of the ICA distal to the superior hypophyseal artery are the PCoA and the anterior choroidal arteries (from inferior to superior). The proximal portion of these vessels is frequently seen on 3DRA. A junctional dilatation or infundibulum is also seen and can be easily differentiated from small aneurysms on 3DRA because of the infinite number of views available.

This, however, can often be a source of diagnostic uncertainty on routine 2D DSA. The ability to differentiate between a nonpathologic infundibulum and an aneurysm on 2D DSA is limited because of the limited number of views this technique offers.

The distal supraclinoid segment of the intracranial ICA beyond the anterior choroidal artery ends at the ICA bifurcation. The two major divisions of the ICA bifurcation are the A1 and M1 segments of the anterior (ACA) and middle cerebral arteries (MCA). The medial and lateral lenticulostriate arteries arise from the A1 and M1 segments, respectively. When these vessels are pathologically enlarged or arise from a larger trunk that subsequently divides into individual perforating arteries the larger proximal trunks are often visualized on 3DRA.

The nature of the intracranial circulation is one of variability and inconstancy. General schemas on the naming of individual intracranial branches are often based on the distal cerebral territory supplied. For instance, one would name a specific branch to the pre-central/pre-rolandic gyrus (motor strip) as the pre-central or pre-rolandic branch. This is a useful scheme as it more clearly defines the parenchymal vascular territory. One can then infer (within certain limitations) the functional importance of a particular vascular branch. To aid in the naming of the cortical branches, Salamon et al. devised a clear plastic disc to be used as a template that could be placed over the lateral carotid angiogram to provide a convenient means to identify the cortical branches (5).

The A1 segment of the ACA extends from the ICA bifurcation to the A1-A2 junction. The A1 segment courses slightly anterior in a medial direction towards the midline. When it reaches the A1-anterior communicating artery (ACoA) junction it changes course. It then runs superiorly as the A2 segment. The first branch of the A2 ACA is the orbitofrontal artery and the second branch is the frontopolar artery. Variable branching of the A2 into the pericallosal and callosomarginal branches follows. The pericallosal artery runs in the pericallosal cistern while the callosomarginal branch runs in the cingulate sulcus, just above the cingulate gyrus. A single pericallosal artery is seen supplying both cerebral hemispheres in 10% of the cases (6). Branches of the pericallosal and callosomarginal arteries divide into the branches that supply the medial surface of the frontal and parietal lobes and the medial one-third of the cerebral hemisphere in the

frontal and parietal regions. The callosomarginal artery is usually the smaller of the two giving rise to the anterior, middle, and posterior internal frontal arteries, usually wandering off the midline. The pericallosal artery gives rise to three major branches: the paracentral, the superior internal parietal (precuneal), and the inferior internal parietal branches. The distal aspect of the callosomarginal artery runs in the callosomarginal fissure which lies just posterior to the mesial continuation of the central sulcus. The distal pericallosal artery courses under the splenium of the corpus callosum into the transverse fissure anastomosing with the splenial or posterior pericallosal artery, a small branch of the posterior cerebral artery. In cases of ACA or PCA occlusion this can provide anastomotic collateral flow to the occluded vascular territory. It is also necessary to discuss the Recurrent Artery of Heubner. This important perforating artery arises most often from the distal A1 or proximal A2 segment. It courses laterally, running parallel to the A1 ACA and M1 MCA axis and then enters the anterior perforated substance to supply the caudate head, lateral putamen, and the anterior limb of the internal capsule.

The M1 segment of the middle cerebral artery courses laterally in the horizontal sylvian cistern. Frequently, an early cortical branch to the anterior temporal lobe arises from the M1 segment of the MCA. This branch courses inferiorly around the tip of the anterior temporal lobe. Coursing laterally within the sylvian fissure, the MCA bifurcates (75%) or trifurcates (25%) (7). There is variability in the location of the middle cerebral artery bifurcation/trifurcation. In the majority of cases the location is where the sylvian fissure changes from a horizontal to an anterior to posterior axis, the genu or knee of the MCA. The MCA branches within the sylvian fissure posterior to the bifurcation/trifurcation overlie the insular cortex. These are referred to as the M2 branches. The different divisions of the middle cerebral artery continue to divide into cortical branches supplying the lateral convexity surfaces of the frontal, temporal, and parietal lobes. The branches coursing over the various opercular are designated as the M3 branches. The distal cortical ramifications of the MCA designated M4 branches supply the lateral two-thirds of the cerebral hemisphere.

The distal cortical branches of the MCA are named for their vascular territories. In the most common branching pattern, an MCA bifurcation, the anterior-superior division gives rise to the orbitofrontal branch sup-

plying the inferolateral frontal lobe and the operculofrontal branches (candelabra group) supplying the middle and inferior frontal gyri including Broca's region. Arising posteriorly to these branches, the pre-central and central rolandic branches ascend to supply the motor and sensory gyri, respectively. The posterior-inferior division of the middle cerebral artery include the anterior and posterior parietal branches supplying the ventral parietal lobe, the angular artery running parallel to the sylvian fissure and then posteriorly and superiorly to supply the inferior parietal lobule, the lateral occipital lobe and the superior temporal lobe, as well as the middle and posterior temporal branches that course laterally around the convexity surface of the temporal lobe to supply the remainder of the temporal lobe.

Mention should also be made of the sylvian point. The sylvian point corresponds to the most superior and the most medial point where the last sylvian MCA branch turns inferolateraly to exit the posterior and superior aspect of the sylvian fissure. In the pre-crossectional neuroimaging era, when angiography was the usual procedure for diagnosing intracranial lesions, multiple points of reference including the sylvian triangle were necessary tools for diagnosis. The sylvian triangle represents the geometric representation of the middle cerebral arteries overlying the insular cortex. Distortions of this triangle help in the localization of intracranial lesions.

REFERENCES

1. Huber, P., 1982. *Krayenenbuhl/Yasargil Cerebral Angiography*. New York: Thieme Medical Publishers, pp. 50–55.
2. Osborn, A. 1980. *Introduction to Cerebral Angiography*. Philadelphia: Harper & Row Publishers, p. 114.
3. Grossman, R., D. and Yousem. 2004. Neuroradiology: The Requisites, Second Edition. St. Louis: C.V. Mosby, p. 84.
4. Hayreh, S. 1974. *The ophthalmic artery*. In Radiology of the Skull and Brain: Angiography Volume 2. T.H. Newton and D.G. Potts, eds., St.Louis: C.V. Mosby, p. 1334.
5. Pierre, M., N. Moscow, and G. Salamon.1974. *Anatomy of the cortical branches of the middle cerebral artery*. In Radiology of the Skull and Brain: Angiography Volume 2, T.H. Newton and D.G. Potts, eds., St.Louis: C.V. Mosby Company, pp. 1477–1478.

6. Rael, J., and L. Casey. 2000. *Cerebral angiography*. In Neuroimaging. W.W. Orrison, ed. Philadelphia: W. B. Saunders Company, p. 228.
7. Ring B. A. 1974. *The middle cerebral artery*. In Radiology of the Skull and Brain: Angiography Volume 2. T.H. Newton and D.G. Potts, eds., St. Louis: C.V. Mosby, pp. 1447.

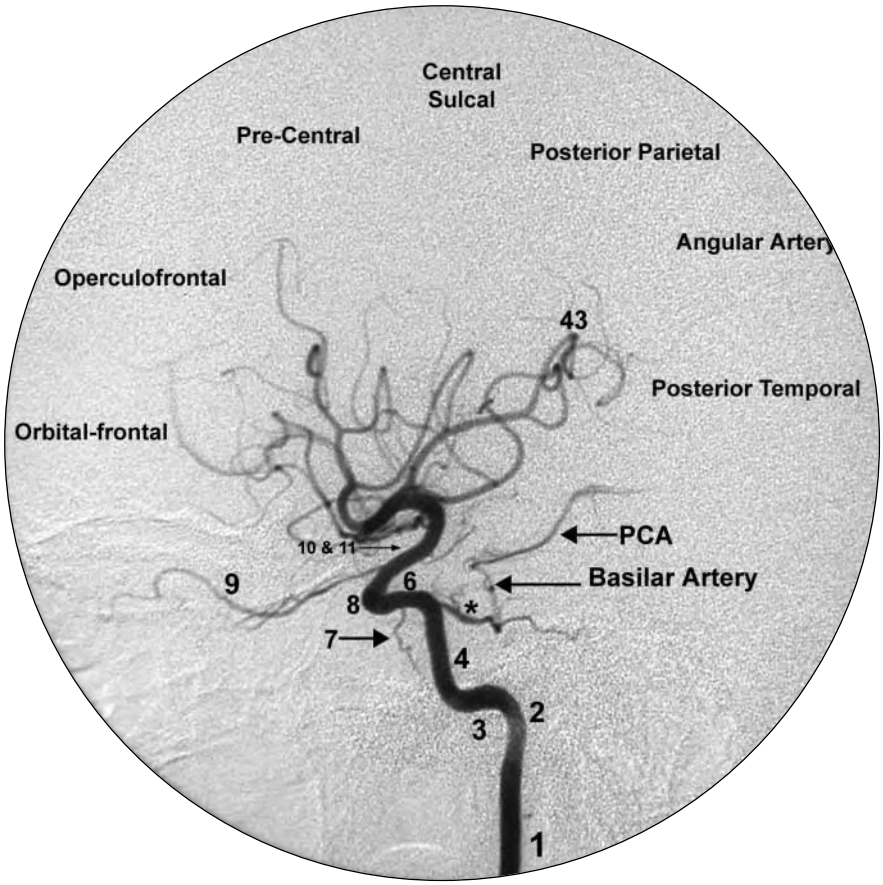

Fig. 5.1a Lateral 2D view following internal carotid artery injection early arterial phase. Non-filling of the anterior cerebral artery allows for an unobtrusive view of the proximal middle cerebral artery (mca) branches. Note the filling of the embryonic persistent trigeminal artery (*) providing communication between the carotid and vertebral-basilar circulation. The names of the distal branches of the mca have been placed in a template fashion. This allows for greater variability of the proximal branching pattern of the middle cerebral artery vessels.

FIGURE KEY

1 internal carotid artery – cervical segment
2 internal carotid artery – vertical petrous segment
3 internal carotid artery – horizontal petrous segment
4 presellar segment (Fischer C5) internal carotid artery
6 horizontal (Fischer C4) intracavernous segment internal carotid artery
7 inferolateral trunk
8 anterior genu (Fischer C3) intracavernous segment internal carotid artery
9 ophthalmic artery
10 proximal supraclinoid segment internal carotid artery (from ophthalmic to posterior communicating artery)
11 distal supraclinoid segment internal carotid artery (from posterior communicating artery to internal carotid artery bifurcation)
43 sylvian point
* persistent trigeminal artery

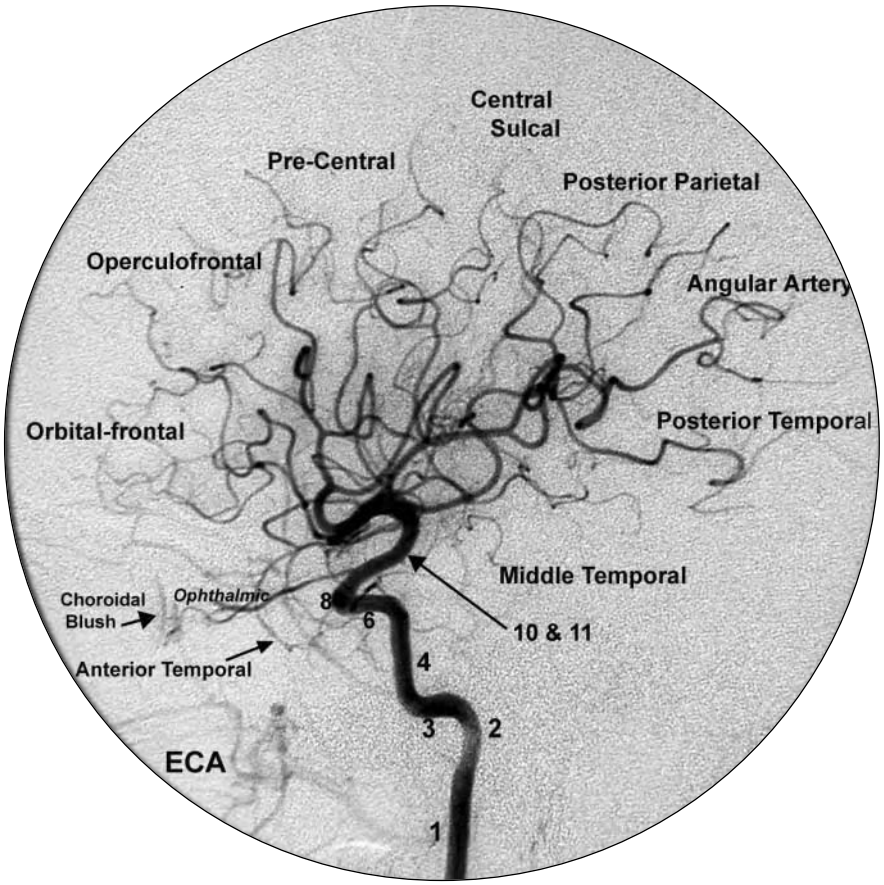

Fig. 5.1b Lateral 2D view following internal carotid artery injection mid arterial phase. Non-filling of the anterior cerebral artery allows for an unobtrusive view of the more distal middle cerebral artery (mca) branches. A template type labeling of the distal middle cerebral artery branches allows for greater variability in the proximal branching pattern of the mca vessels. Note the choroidal blush along the posterior margin of the globe (eye).

FIGURE KEY

1 internal carotid artery – cervical segment
2 internal carotid artery – vertical petrous segment
3 internal carotid artery – horizontal petrous segment
4 presellar (Fischer C5) segment internal carotid artery
6 horizontal (Fischer C4) intracavernous segment internal carotid artery
8 anterior genu (Fischer C3) intracavernous segment internal carotid artery
10 & 11 proximal and distal supraclinoid segments internal carotid artery

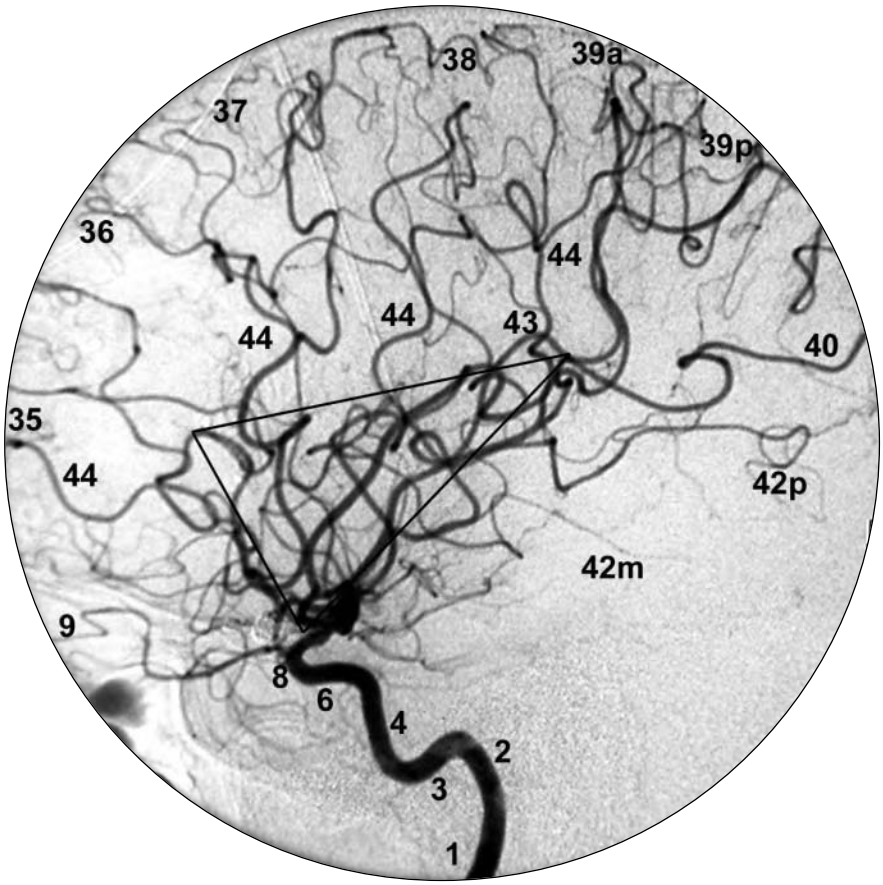

Fig. 5.1c Lateral 2D view following internal carotid artery injection in the late arterial phase. The triangle placed on the image is called the sylvian triangle. This represents the geometric representation of the middle cerebral arteries overlying the insular cortex. Alteration in the shape of this triangle can indicate mass displacements of the middle cerebral artery (mca) branches. The template pattern for the naming of the distal mca branches is used to simplify the identification of the individual branches due to the marked variability in the proximal pattern.

FIGURE KEY

1 internal carotid artery – cervical segment
2 internal carotid artery – vertical petrous segment
3 internal carotid artery – horizontal petrous segment
4 presellar (Fischer C5) segment internal carotid artery
6 horizontal (Fischer C4) intracavernous internal carotid artery
8 anterior genu (Fischer C3) intracavernous internal carotid artery
9 ophthalmic artery
35 orbitofrontal branch of middle cerebral artery
36 operculofrontal branches of middle cerebral artery
37 pre-central branch(es) of middle cerebral artery
38 central rolandic branches of middle cerebral artery
39a anterior parietal branch of middle cerebral artery
39p posterior parietal branch of middle cerebral artery
40 angular artery
42m middle temporal branches of middle cerebral artery
42p posterior temporal branches of middle cerebral artery
43 sylvian point
44 opercular branches of MCA

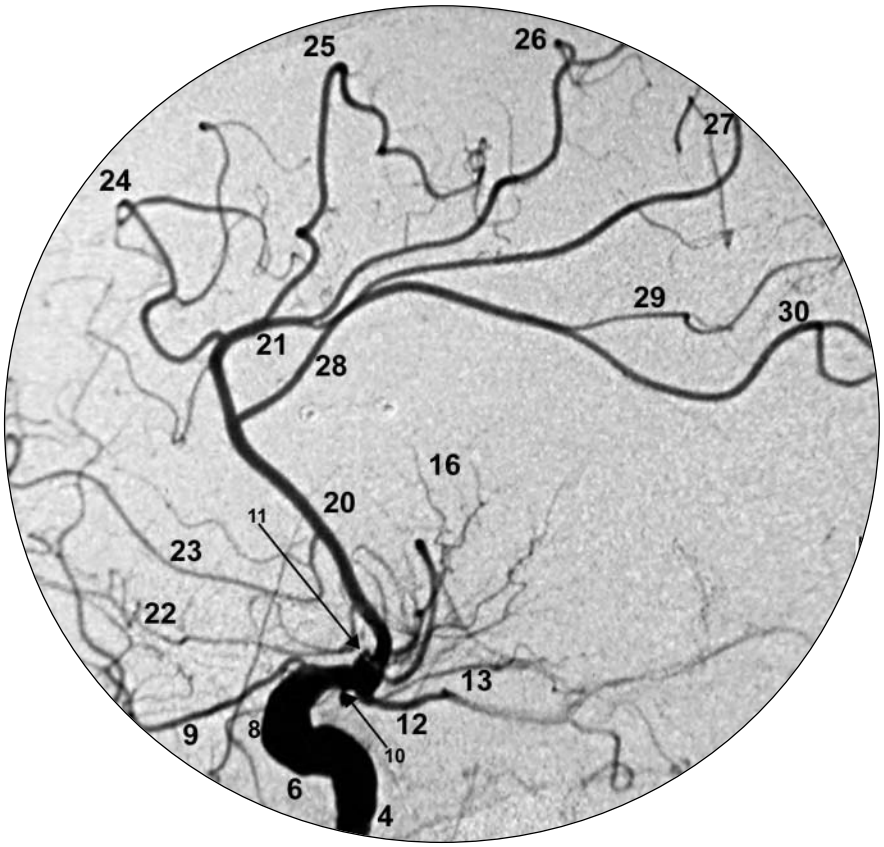

Fig. 5.2 Lateral view following common carotid artery injection. Non-filling of the middle cerebral artery from atherosclerotic occlusion allows unobtrusive view of the anterior cerebral artery territory.

FIGURE KEY

4 presellar (Fischer C5) segment internal carotid artery
6 horizontal (Fischer C4) intracavernous internal carotid artery
8 anterior genu (Fischer C3) intracavernous internal carotid artery
9 ophthalmic artery
10 & 11 proximal and distal supraclinoid segment internal carotid artery
12 posterior communicating artery
13 anterior choroidal artery
16 medial lenticulostriate arteries
21 callosomarginal branch of anterior cerebral artery
22 orbitofrontal branch of anterior cerebral artery
23 frontopolar branch of anterior cerebral artery
24 anterior internal frontal branch of anterior cerebral artery
25 middle internal frontal branch of anterior cerebral artery
26 posterior internal frontal branch of anterior cerebral artery
27 paracentral lobule artery branch of anterior cerebral artery
28 pericallosal branch of anterior cerebral artery
29 superior internal parietal branch of anterior cerebral artery
30 inferior internal parietal branch of anterior cerebral artery

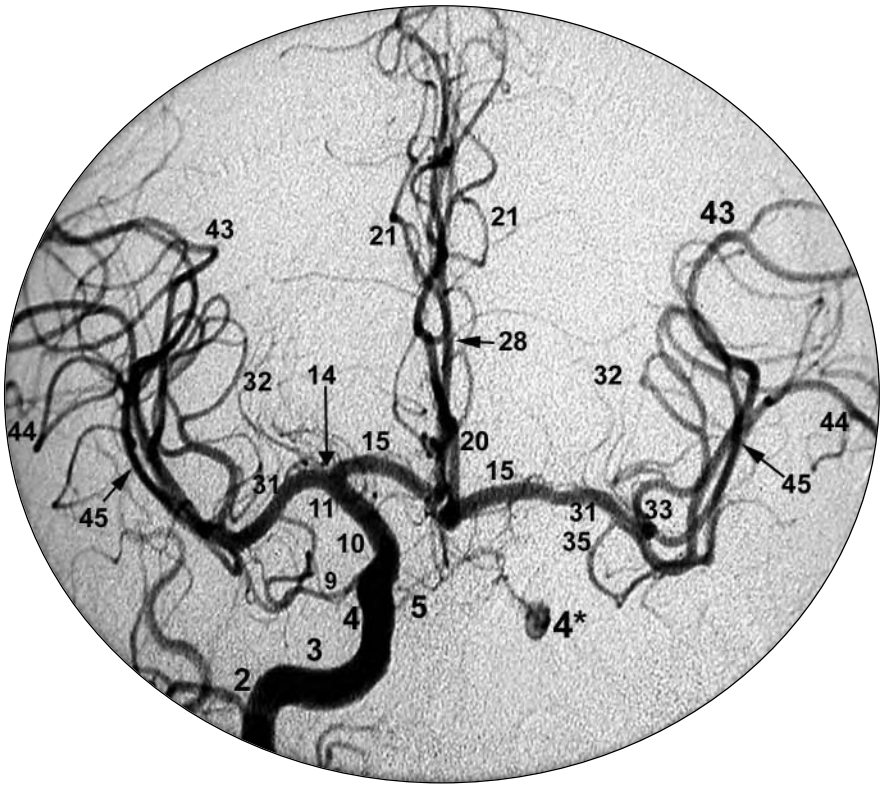

Fig. 5.3 A 2D frontal view following right common carotid artery injection. This view shows the normal appearance of the intracranial internal carotid artery circulation with filling of the anterior and middle cerebral artery branches. There is filling of both sides from a patent anterior communicating artery. There is also a small clival branch of the meningohypophyseal trunk providing flow to the left intracranial internal carotid artery (4). Note the prominent superimposition of the different ACA and MCA branches on this projection limiting identification of individual named branches.

FIGURE KEY

2 internal carotid artery – vertical petrous segment
3 internal carotid artery – horizontal petrous segment
4 presellar (Fischer C5) segment internal carotid artery
5 meningohypophyseal trunk
9 ophthalmic artery
10 & 11 proximal and distal supraclinoid segment internal carotid artery
14 internal carotid artery bifurcation
15 A1 segment anterior cerebral artery
20 proximal A2 segment anterior cerebral artery
21 callosomarginal branch of anterior cerebral artery
28 pericallosal branch of anterior cerebral artery
31 M1 segment of middle cerebral artery
32 lateral lenticulostriate arteries
33 bifurcation/trifurcation of middle cerebral artery
35 orbitofrontal branch of middle cerebral artery
43 sylvian point
44 opercular branches of middle cerebral artery
45 sylvian (insular) branches of middle cerebral artery

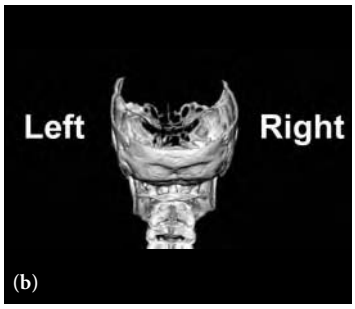

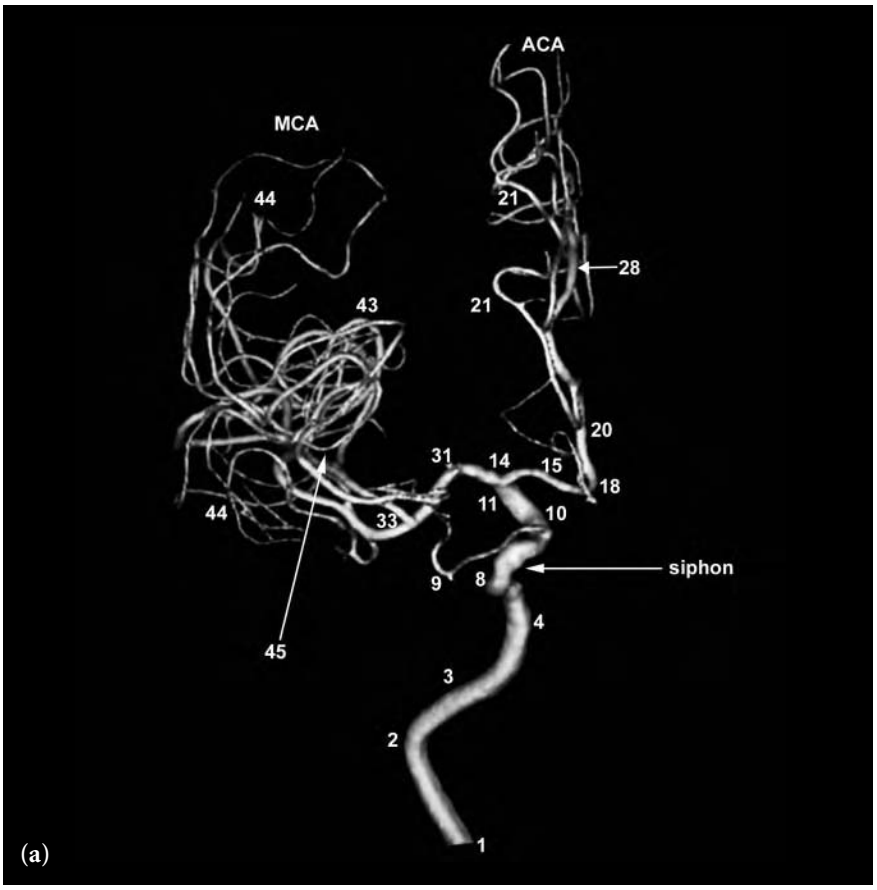

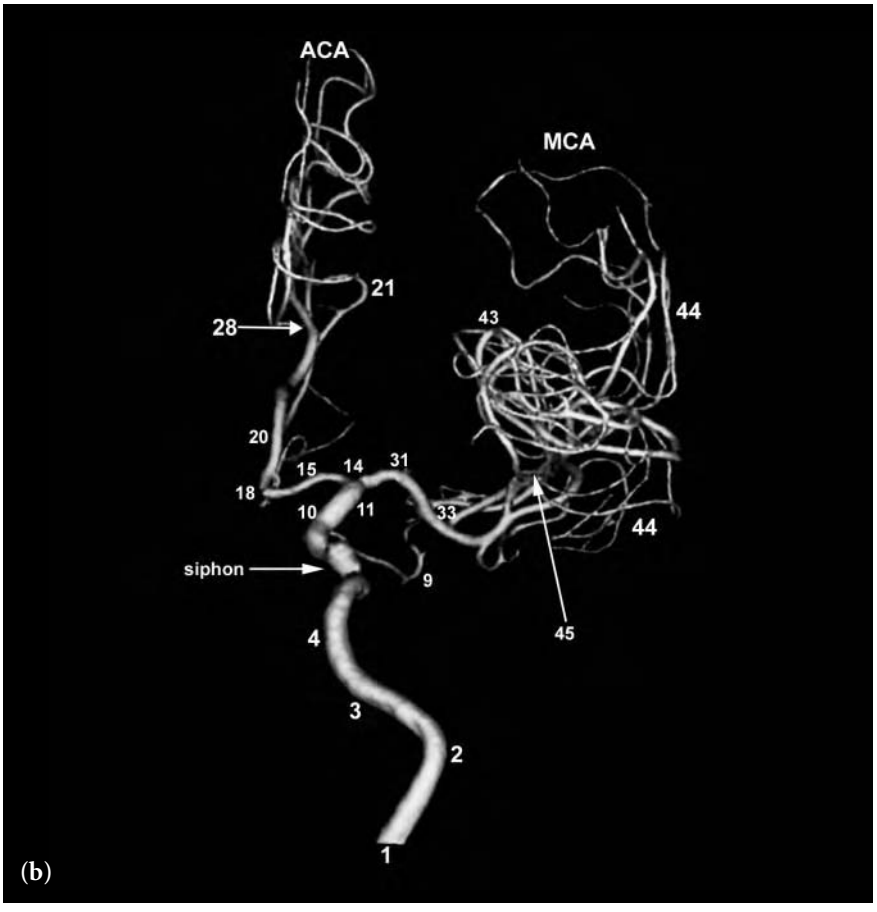

Fig. 5.4 (a,b) 3D frontal (*a*) and posterior (*b*) views following right internal carotid artery injection. This image is normal except for an atherosclerotic irregularity of the intracranial branches. The position and branching pattern is also normal.

FIGURE KEY

1 internal carotid artery – cervical segment
2 internal carotid artery – vertical petrous segment
3 internal carotid artery – horizontal petrous segment
4 presellar (Fischer C5) segment internal carotid artery
8 anterior genu (Fischer C3) intracavernous internal carotid artery
9 ophthalmic artery
10 & 11 proximal and distal supraclinoid segment internal carotid artery
14 internal carotid artery bifurcation
15 A1 segment of anterior cerebral artery
18 A1-A2 junction anterior cerebral artery
20 proximal A2 segment anterior cerebral artery
21 callosomarginal branch of anterior cerebral artery
28 pericallosal branch of anterior cerebral artery
31 M1 segment of middle cerebral artery
33 bifurcation/trifurcation of middle cerebral artery
43 sylvian point
44 opercular branches of middle cerebral artery
45 sylvian (insular) branches of middle cerebral artery

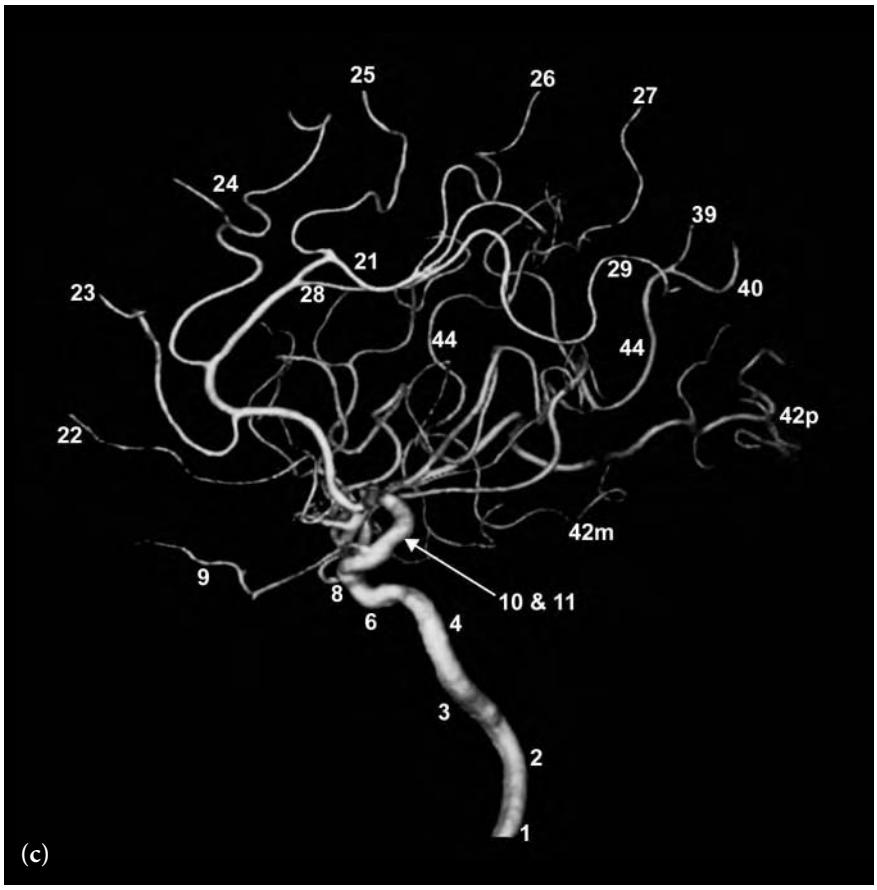

Fig. 5.4c A 3D medial view following right internal carotid artery injection. This is the same patient as in Figures 5.4*a* and *b*. There is atherosclerotic irregularity of the intracranial internal carotid artery (carotid siphon).

FIGURE KEY

1 internal carotid artery – cervical segment
2 internal carotid artery - vertical petrous segment
3 internal carotid artery – horizontal petrous segment
4 presellar (Fischer C5) segment internal carotid artery
6 horizontal (Fischer C4) intracavernous internal carotid artery
8 anterior genu (Fischer C3) intracavernous internal carotid artery
9 ophthalmic artery
10 & 11 proximal and distal supraclinoid segment internal carotid artery
21 callosomarginal branch of anterior cerebral artery
22 orbitofrontal branch of anterior cerebral artery
23 frontopolar branch of anterior cerebral artery
24 anterior internal frontal branch of anterior cerebral artery
25 middle internal frontal branch of anterior cerebral artery
26 posterior internal frontal branch of anterior cerebral artery
27 paracentral lobule artery branch of anterior cerebral artery
28 pericallosal branch of anterior cerebral artery
29 superior internal parietal branch of anterior cerebral artery
39 parietal branch of middle cerebral artery
40 angular artery
42m middle temporal branch of middle cerebral artery
42p posterior temporal branch of middle cerebral artery
44 opercular branches of middle cerebral artery

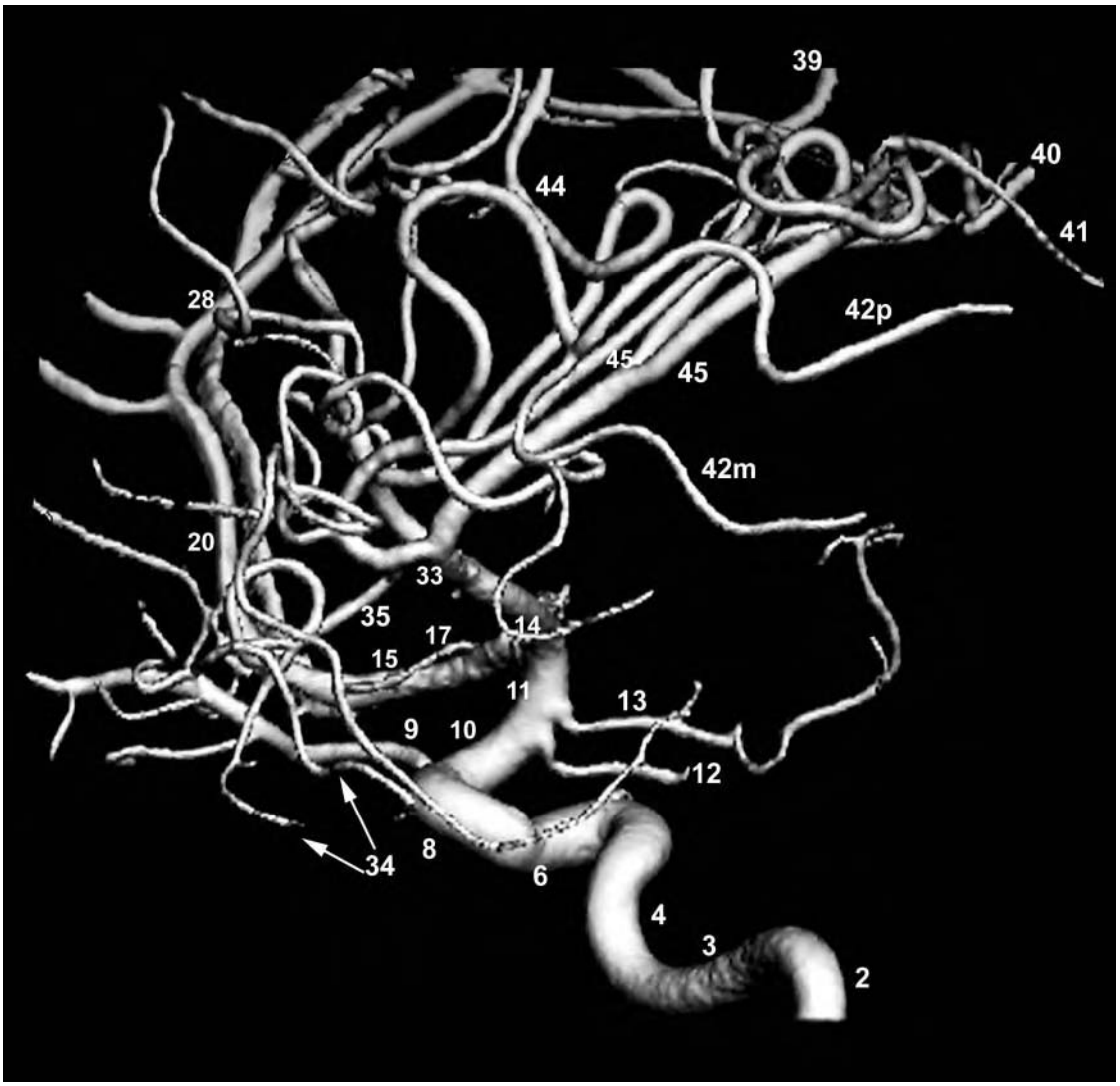

Fig. 5.5a 3D lateral view following left internal carotid artery injection. In this projection there is a marked overlap of the middle and anterior cerebral artery branches which can result in difficulty identifying the individual branches.

FIGURE KEY

2 internal carotid artery – vertical petrous segment
3 internal carotid artery – horizontal petrous segment
4 presellar (Fischer C5) segment internal carotid artery
6 horizontal (Fischer C4) intracavernous internal carotid artery
8 anterior genu (Fischer C3) intracavernous internal carotid artery
9 ophthalmic artery
10 & 11 proximal and distal supraclinoid segment internal carotid artery
12 posterior communicating artery
13 anterior choroidal artery
14 internal carotid artery bifurcation
15 A1 segment of anterior cerebral artery
17 recurrent artery of Heubner
20 proximal A2 segment anterior cerebral artery
28 pericallosal branch of anterior cerebral artery
33 bifurcation/trifurcation of middle cerebral artery
34 anterior temporal lobe branches of middle cerebral artery
35 orbitofrontal branch of middle cerebral artery
39 parietal branch of middle cerebral artery
40 angular artery
41 temporo-occipital branch of middle cerebral artery
42m middle temporal branches of middle cerebral artery
42p posterior temporal branches of middle cerebral artery
44 opercular branches of middle cerebral artery
45 sylvian (insular) branches of middle cerebral artery

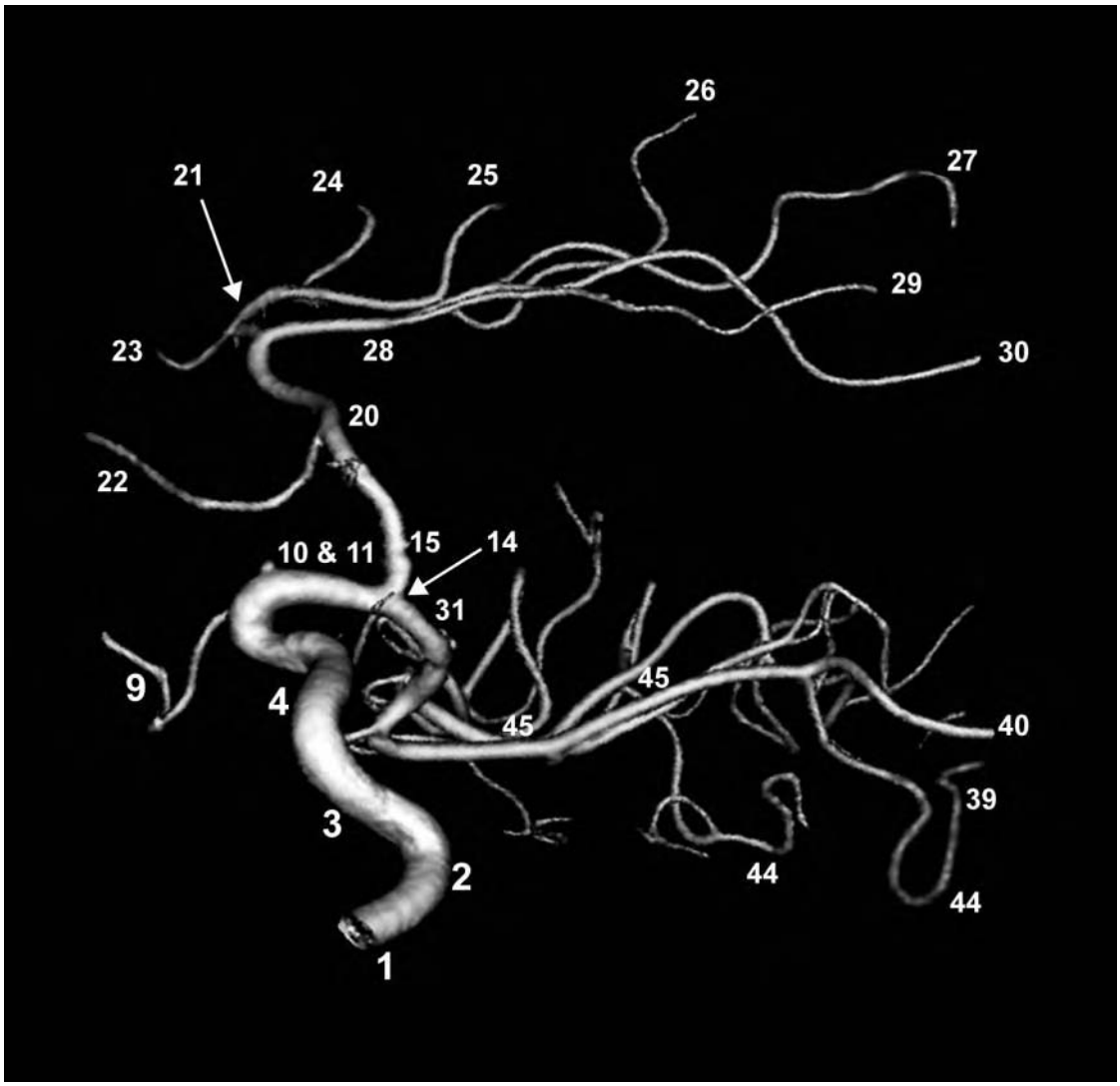

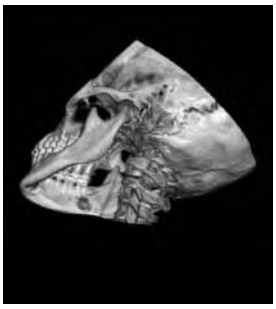

Fig. 5.5b 3D complex view (looking up at the vessels from below and from the midline) following right internal carotid artery injection. This view allows for the separation of the anterior and the middle cerebral artery branches. This view is better for naming the specific branches (as opposed to the view in Figure 5.5*a*).

FIGURE KEY

1 internal carotid artery – cervical segment
2 internal carotid artery – vertical petrous segment
3 internal carotid artery – horizontal petrous segment
4 presellar (Fischer C5) segment internal carotid artery
9 ophthalmic artery
10 & 11 proximal and distal supraclinoid segment internal carotid artery
14 internal carotid artery bifurcation
15 A1 segment of anterior cerebral artery
20 proximal A2 segment anterior cerebral artery
21 callosomarginal branch of anterior cerebral artery
22 orbitofrontal branch of anterior cerebral artery
23 frontopolar branch of anterior cerebral artery
24 anterior internal frontal branch of anterior cerebral artery
25 middle internal frontal branch of anterior cerebral artery
26 posterior internal frontal branch of anterior cerebral artery
27 paracentral lobule artery branch of anterior cerebral artery
28 pericallosal branch of anterior cerebral artery
29 superior internal parietal branch of anterior cerebral artery
30 inferior internal parietal branch of anterior cerebral artery
31 M1 segment of middle cerebral artery
39 parietal branch of middle cerebral artery
40 angular artery
44 opercular branches of middle cerebral artery
45 sylvian (insular) branches of middle cerebral artery

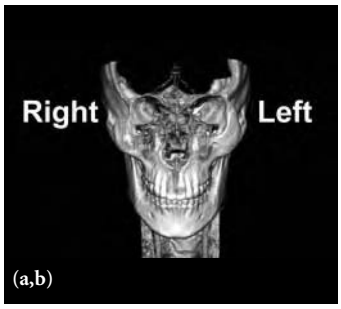

Fig. 5.6 (a–d) 2D frontal (*a*), 3D frontal (*b*), 3D lateral (*c*), and 3D medial (*d*) views following left internal carotid artery injection. There is severe developmental hypoplasia (a normal variant) of the A1 segment of the anterior cerebral artery allowing for the visualization of only the middle cerebral artery territory.

FIGURE KEY

1 internal carotid artery – cervical segment
2 internal carotid artery – vertical petrous segment
3 internal carotid artery – horizontal petrous segment
4 presellar (Fischer C5) segment internal carotid artery
6 horizontal (Fischer C4) intracavernous internal carotid artery
8 anterior genu (Fischer C3) intracavernous internal carotid artery
9 ophthalmic artery
10 & 11 proximal and distal supraclinoid segment internal carotid artery
13 anterior choroidal artery
31 M1 segment of middle cerebral artery
32 lateral lenticulostriate arteries
33 bifurcation/trifurcation of middle cerebral artery
35 orbitofrontal branch of middle cerebral artery
39 parietal branch of middle cerebral artery
40 angular artery
41 temporo-occipital branch of middle cerebral artery
43 sylvian point
44 opercular branches of middle cerebral artery
45 sylvian (insular) branches of middle cerebral artery
* truncated lateral lenticulostriate arteries

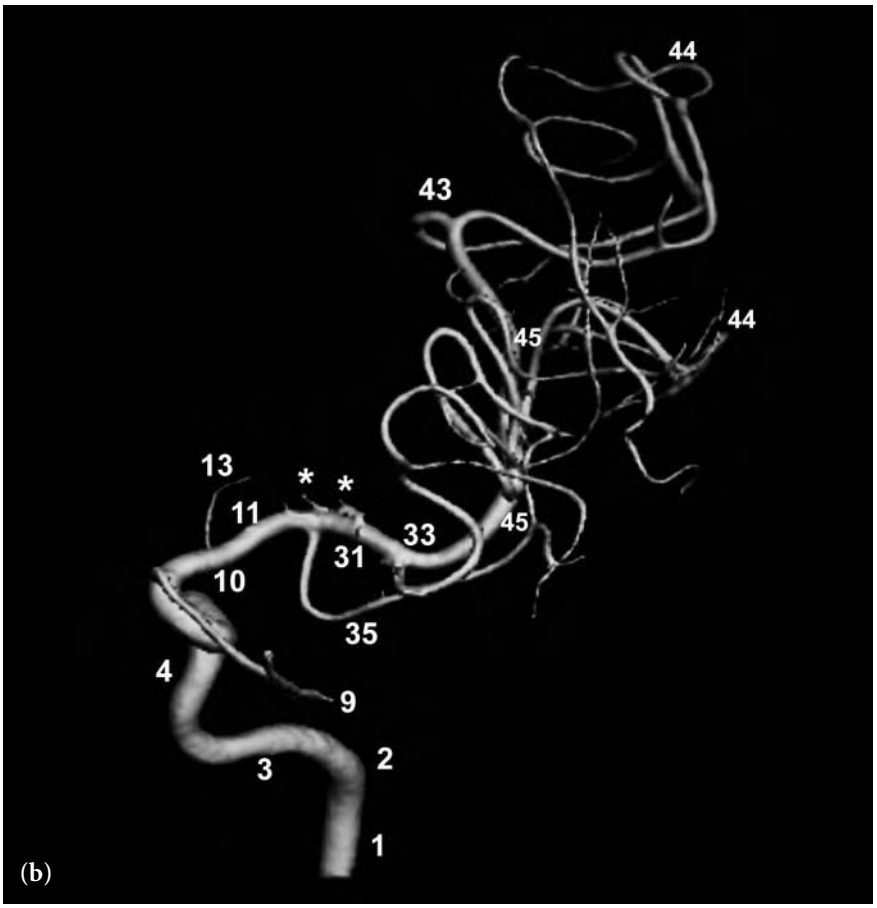

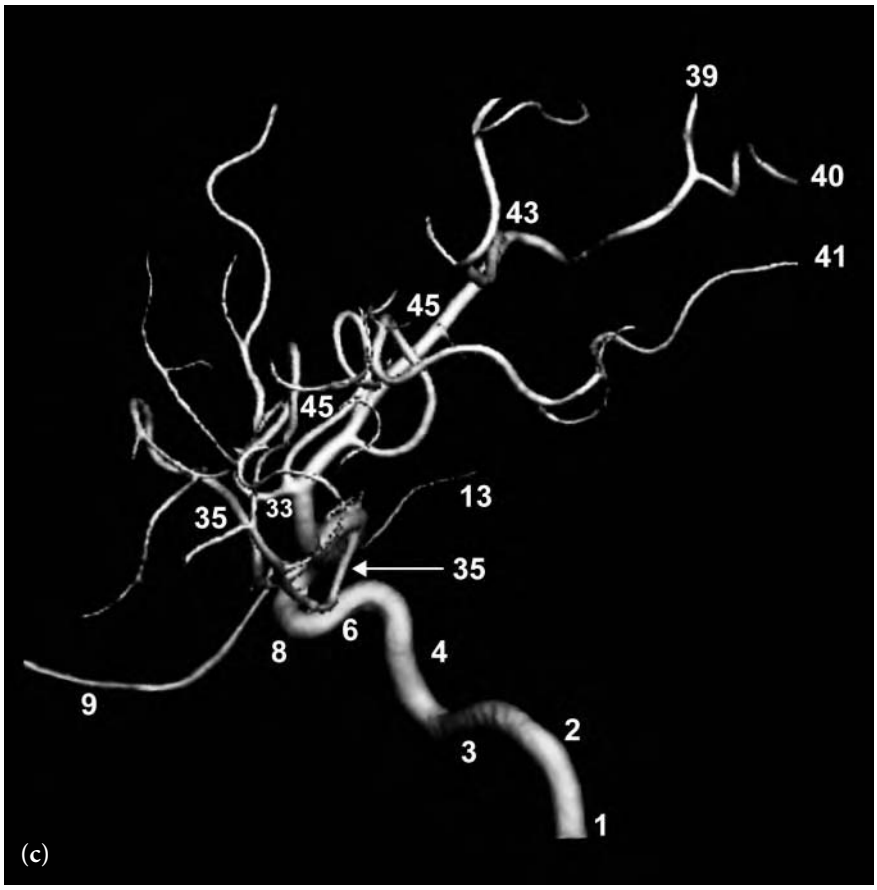
39
40
43
41
45
45
35
33
13
35
8
6
4
9
2
3
1
(c)

(c)

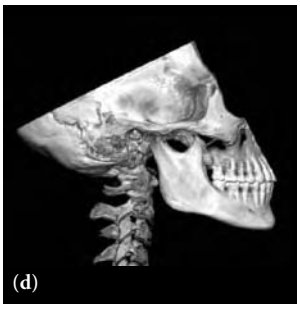
(d)

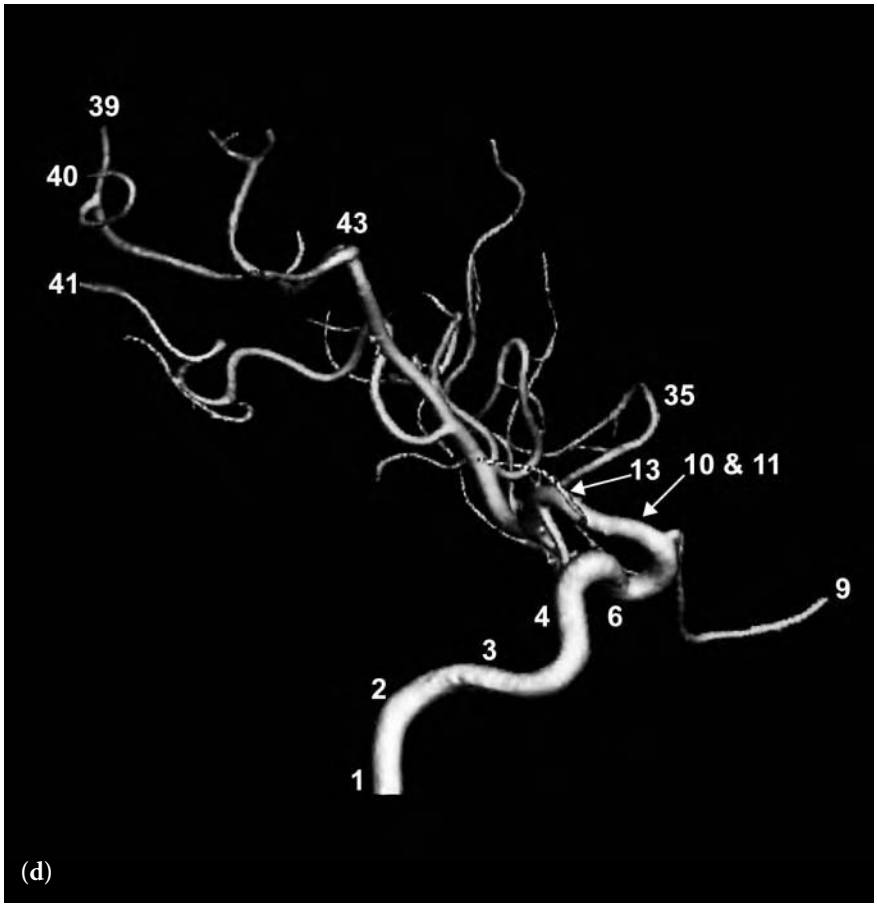
39
40
43
41
35
13
10 & 11
9
4
6
3
2
1
(d)

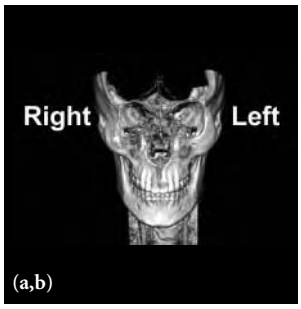

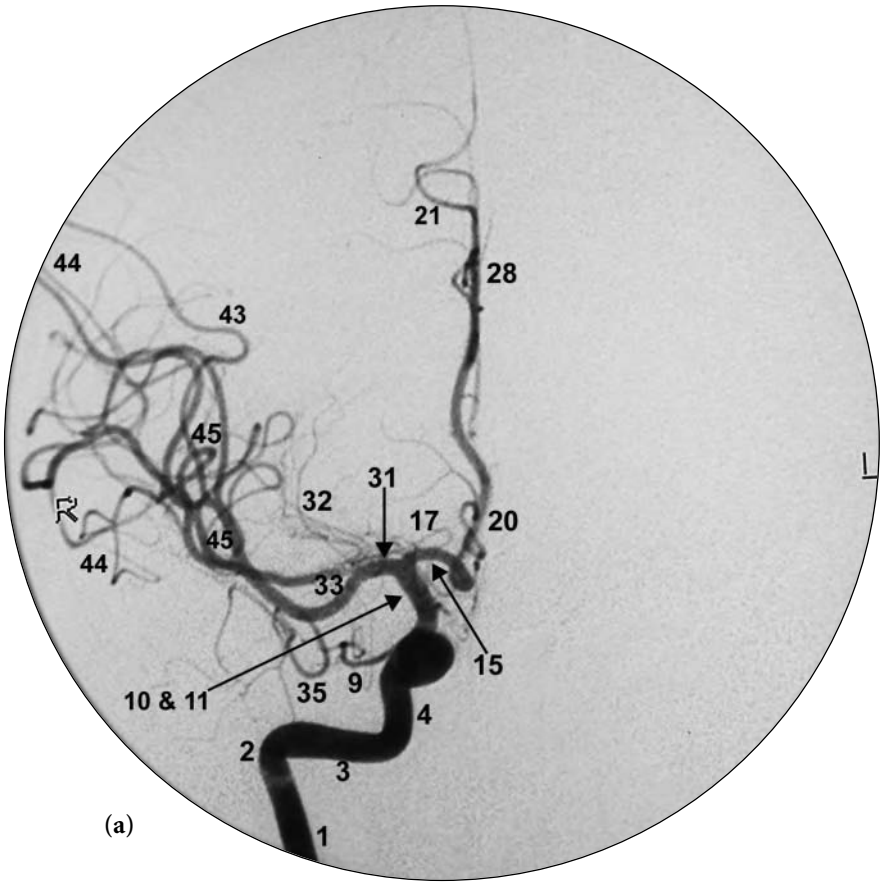

Fig. 5.7 (a–d) 2D frontal (*a*), 3D frontal (*b*), 3D inferior to superior (*c*), and 3D superior to inferior (*d*) views following right internal carotid artery injection. The appearance of the carotid circulation is normal. The A2 segment of the anterior cerebral artery and its branches were intentionally removed on the 3D views. Note the early bifurcation of the middle cerebral artery (normal variant).

FIGURE KEY

1 internal carotid artery – cervical segment
2 internal carotid artery – vertical petrous segment
3 internal carotid artery – horizontal petrous segment
4 presellar (Fischer C5) segment internal carotid artery
6 horizontal (Fischer C4) intracavernous internal carotid artery
9 ophthalmic artery
10 & 11 proximal and distal supraclinoid segment internal carotid artery
12 posterior communicating artery
13 anterior choroidal artery
14 internal carotid artery bifurcation
15 A1 segment of anterior cerebral artery
17 recurrent artery of Heubner
20 proximal A2 segment anterior cerebral artery
21 callosomarginal branch of anterior cerebral artery
28 pericallosal branch of anterior cerebral artery
31 M1 segment of middle cerebral artery
32 lateral lenticulostriate arteries
33 bifurcation/trifurcation of middle cerebral artery
34 anterior temporal lobe branches of middle cerebral artery
35 orbitofrontal branch of middle cerebral artery
43 sylvian point
44 opercular branches of middle cerebral artery
45 sylvian (insular) branches of middle cerebral artery

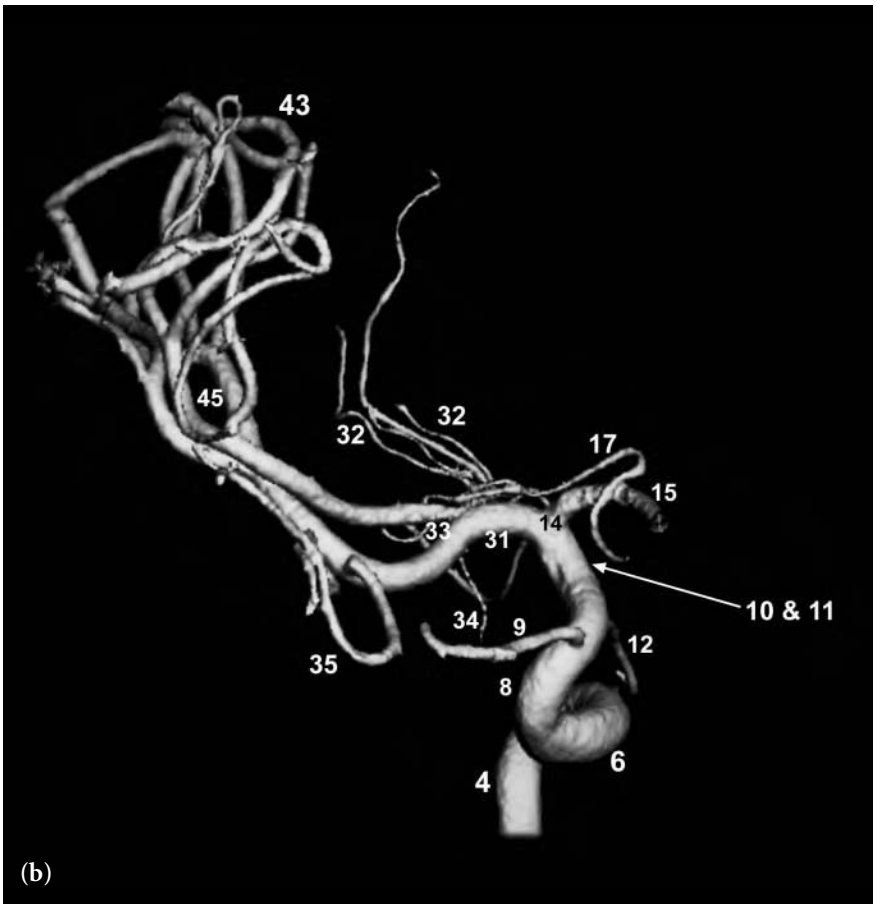

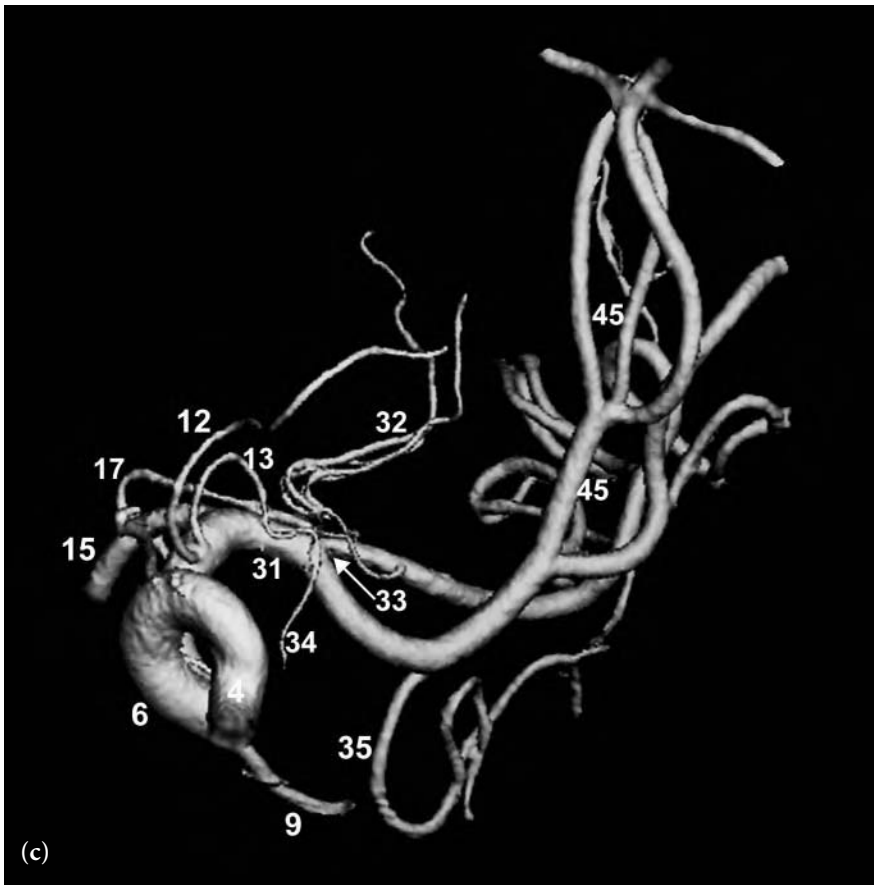
45
12
32
13
17
45
15
31
33
34
4
6
35
9
(c)

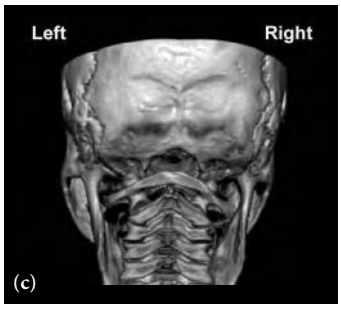
Left
Right
(c)

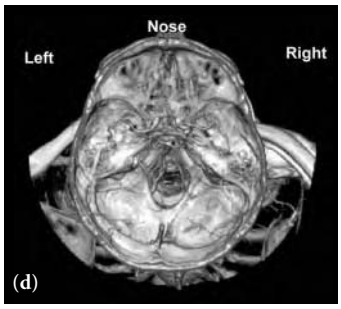
Nose
Left
Right
(d)

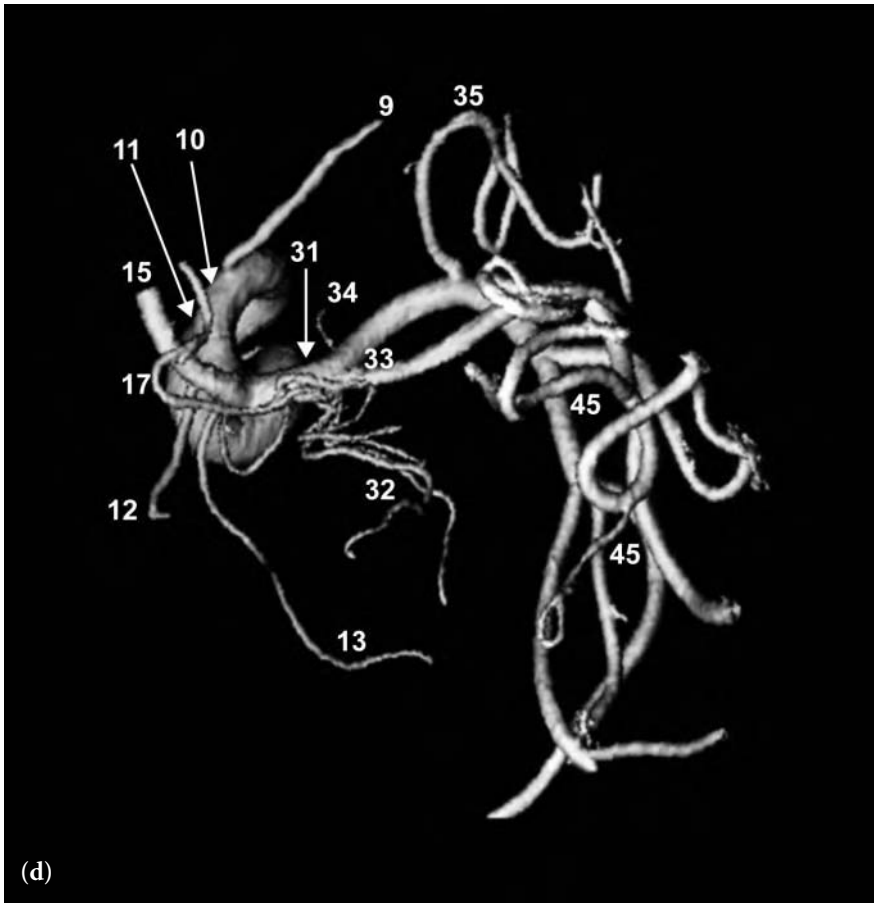
9
35
11
10
31
15
34
33
17
45
32
12
45
13
(d)

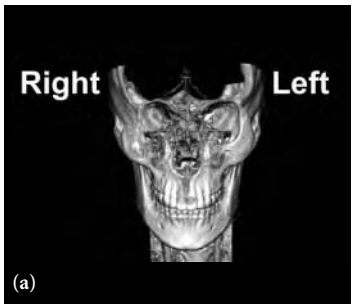

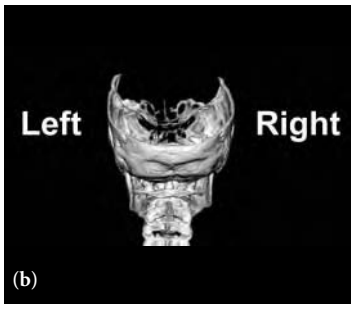

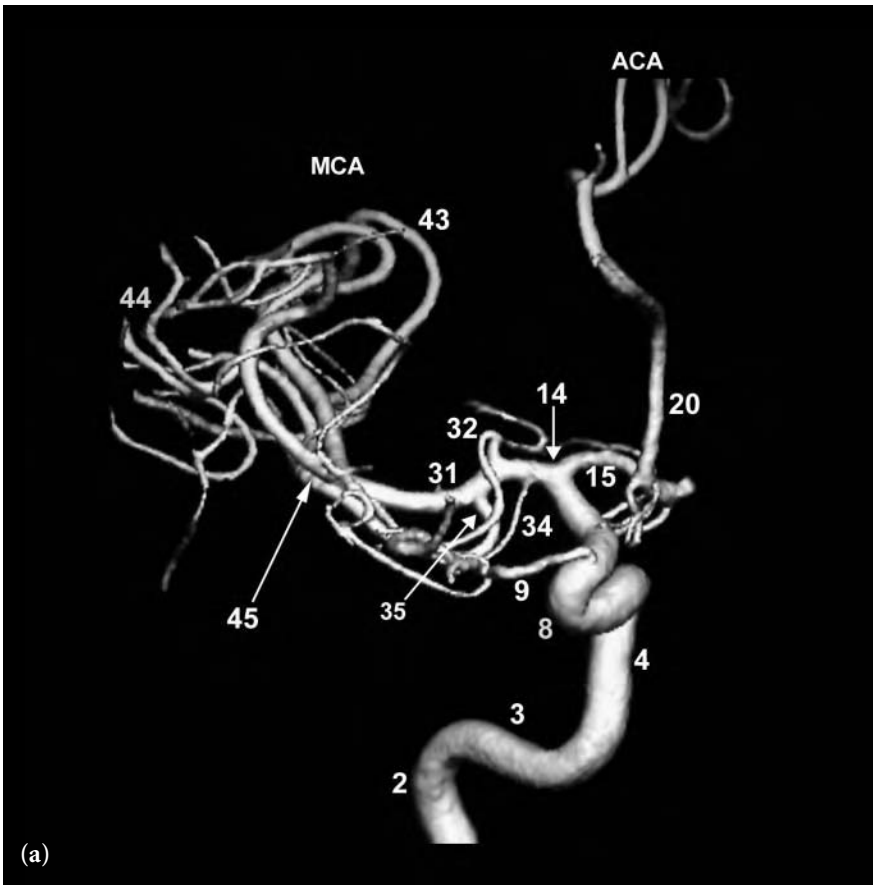

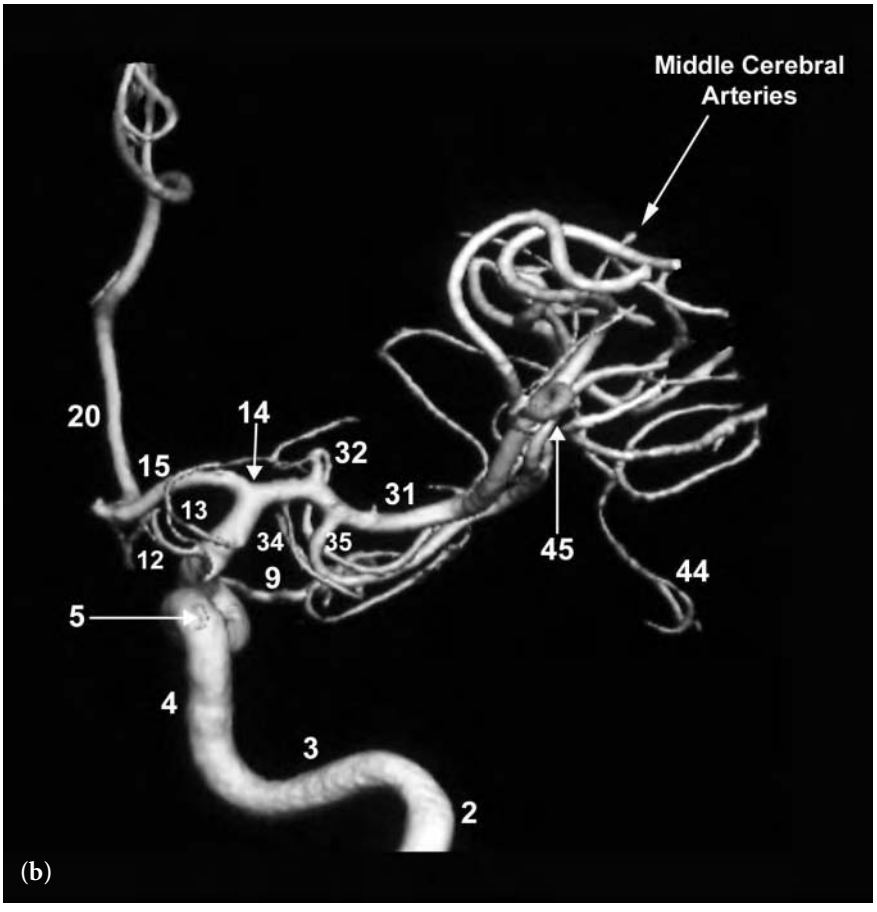

Fig. 5.8 (a–d) 3D frontal (*a*), posterior (*b*), shallow right posterior oblique (RPO) (*c*), and steeper RPO (*d*) views following a right internal carotid artery injection shows a normal appearance of the intracranial internal carotid artery circulation. Note the infindibular widening at the origins of the posterior communicating and anterior choroidal arteries.

FIGURE KEY

2 internal carotid artery – vertical petrous segment
3 internal carotid artery – horizontal petrous segment
4 presellar (Fischer C5) segment internal carotid artery
5 proximal meningohypophyseal trunk
6 horizontal (Fischer C4) intracavernous internal carotid artery
8 anterior genu (Fisher C3) intracavernous internal carotid artery
9 ophthalmic artery
10 & 11 proximal and distal supraclinoid segment internal carotid artery
12 posterior communicating artery
13 anterior choroidal artery
14 internal carotid artery bifurcation
15 A1 segment of anterior cerebral artery
20 proximal A2 segment anterior cerebral artery
31 M1 segment of middle cerebral artery
32 trunk of lateral lenticulostriate arteries
34 anterior temporal lobe branche of middle cerebral artery
35 orbitofrontal branch of middle cerebral artery
43 sylvian point
44 opercular branches of middle cerebral artery
45 sylvian (insular) branches of middle cerebral artery

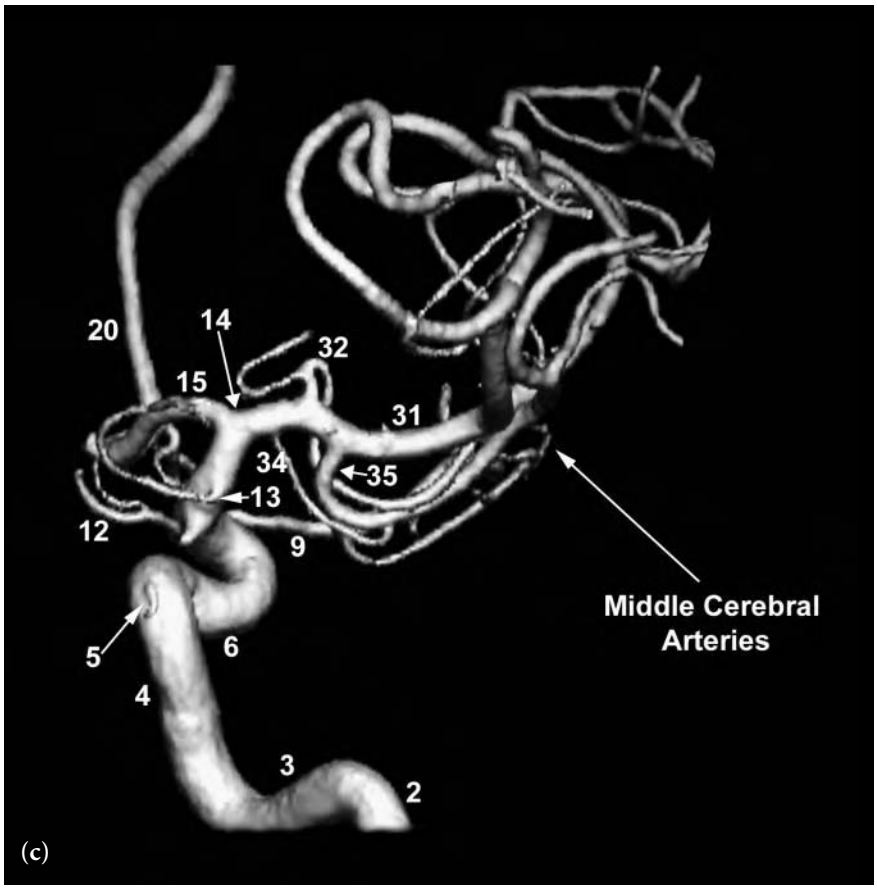
20
14
32
15
31
34
35
13
12
9
Middle Cerebral
Arteries
5
6
4
3
2
(c)

Left
Right
(c)

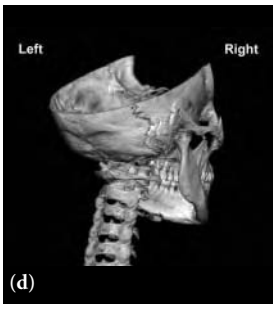
Left
Right
(d)

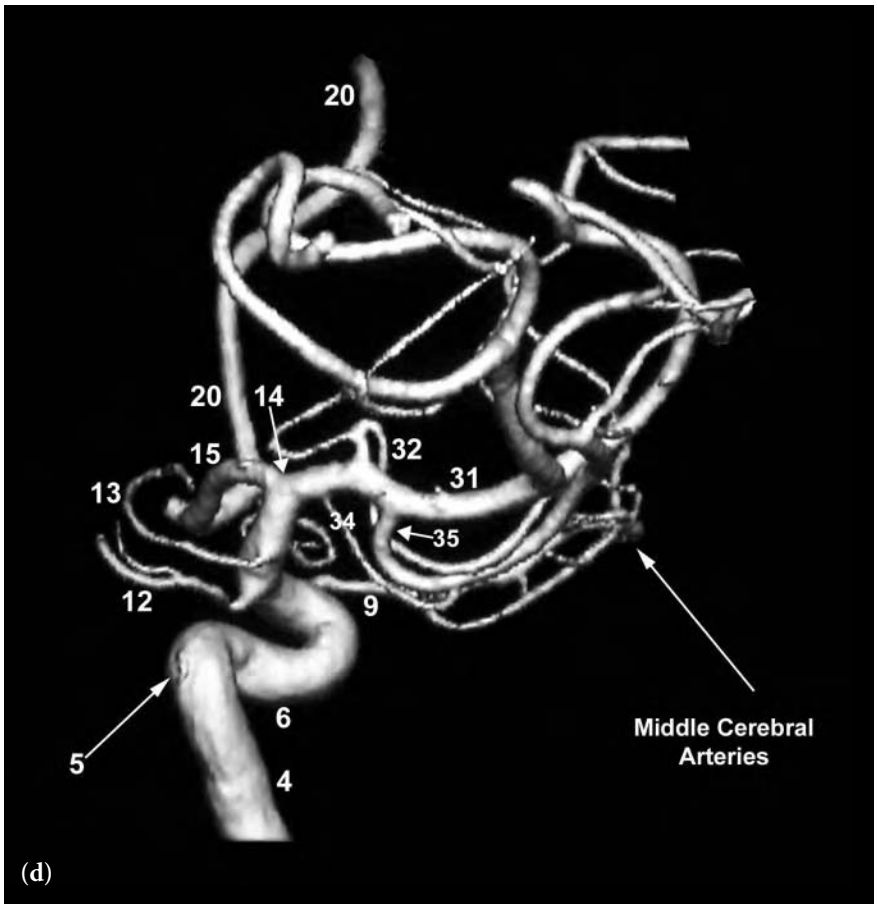
20
20
14
15
32
13
31
34
35
12
9
Middle Cerebral
Arteries
6
5
4
(d)

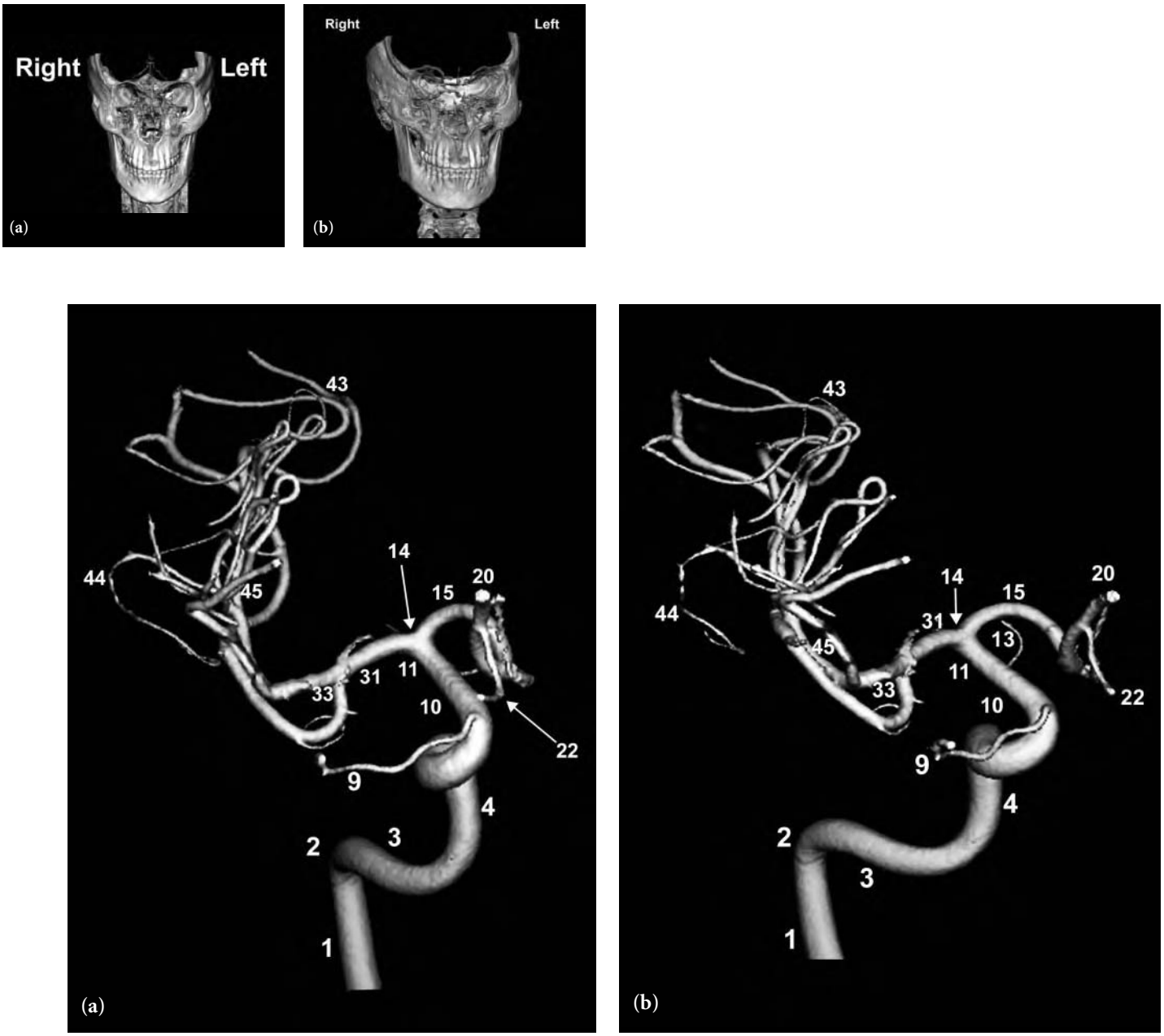

Fig. 5.9 (a–d) 3D frontal (*a*), right anterior oblique (RAO) (*b*), lateral (*c*), and medial (*d*) views following right internal carotid artery injection. These views show the normal appearance of the intracranial internal carotid artery circulation. The proximal A2 segments of the anterior cerebral arteries have been intentionally removed from the images.

FIGURE KEY

1 internal carotid artery – cervical segment
2 internal carotid artery – vertical petrous segment
3 internal carotid artery – horizontal petrous segment
4 presellar (Fischer C5) segment internal carotid artery
6 horizontal (Fischer C4) intracavernous internal carotid artery
8 anterior genu (Fischer C3) intracavernous internal carotid artery
9 ophthalmic artery
10 & 11 proximal and distal supraclinoid segment internal carotid artery
13 anterior choroidal artery
14 internal carotid artery bifurcation
15 A1 segment of anterior cerebral artery
20 proximal A2 segment anterior cerebral artery
22 orbitofrontal branch of anterior cerebral artery
31 M1 segment of middle cerebral artery
33 bifurcation/trifurcation of middle cerebral artery
43 sylvian point
44 opercular branches of middle cerebral artery
45 sylvian (insular) branches of middle cerebral artery

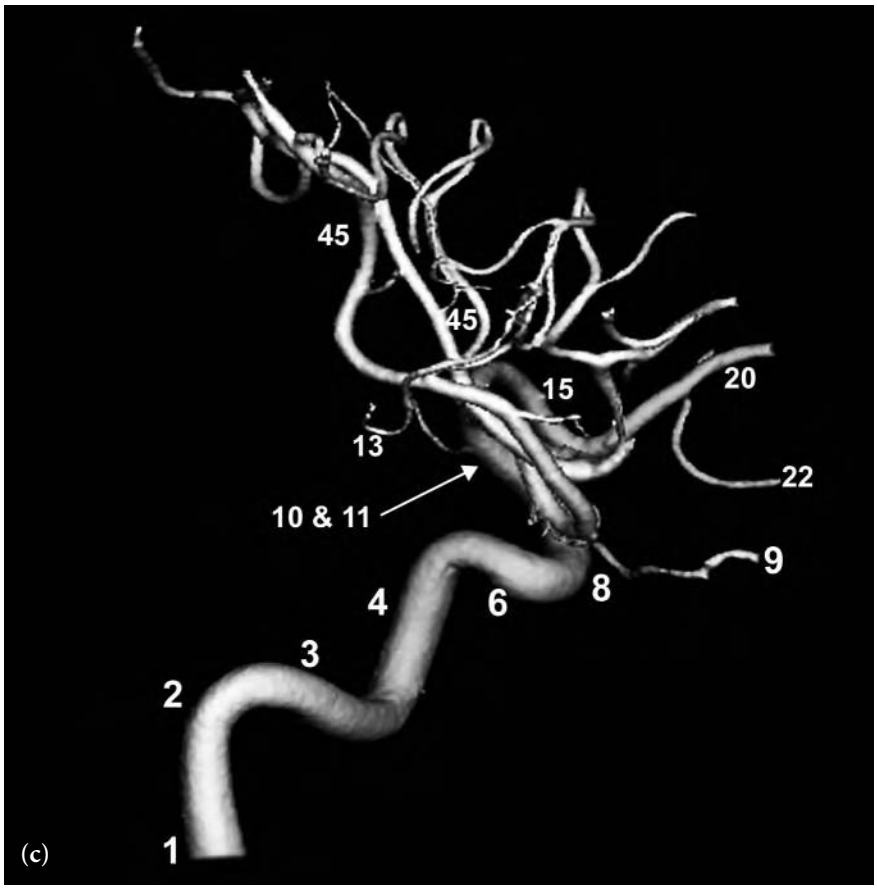
45
45
15
20
13
22
10 & 11
9
4
6
8
3
2
1
(c)

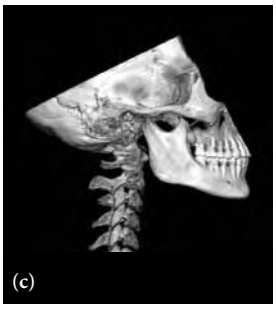
(c)

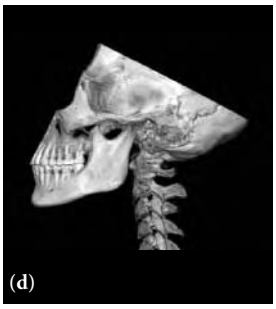
(d)

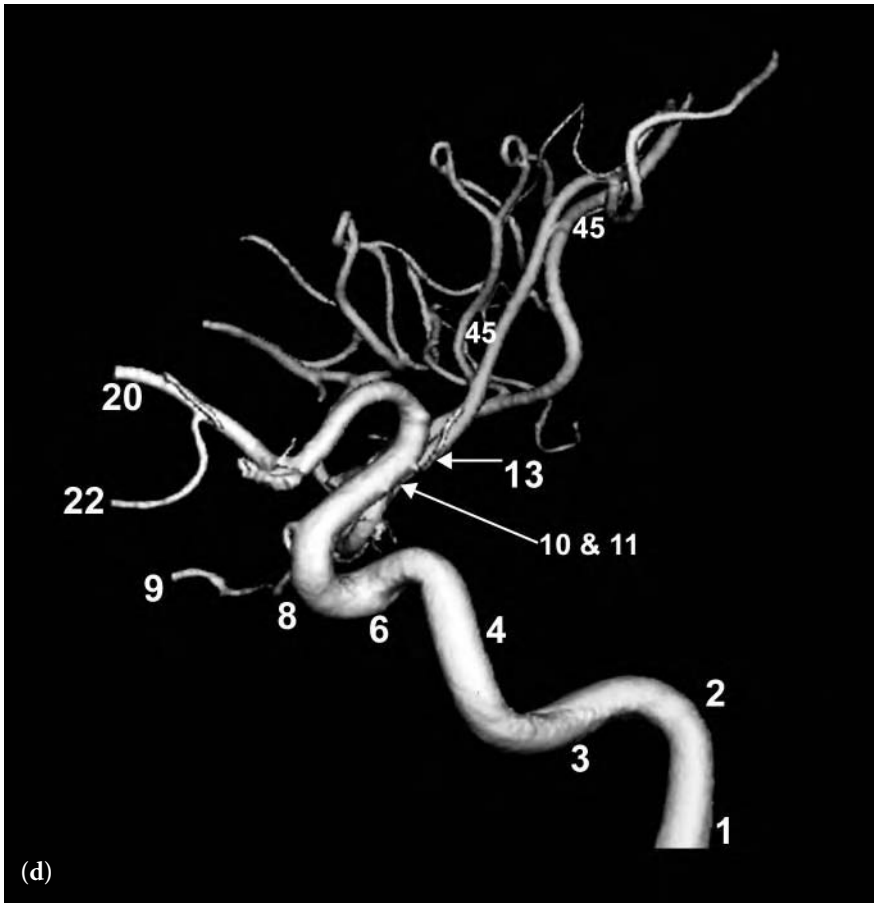
45
45
20
13
22
10 & 11
9
8
6
4
2
3
1
(d)

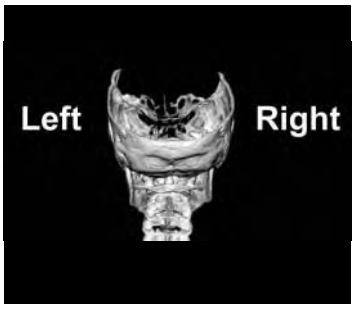

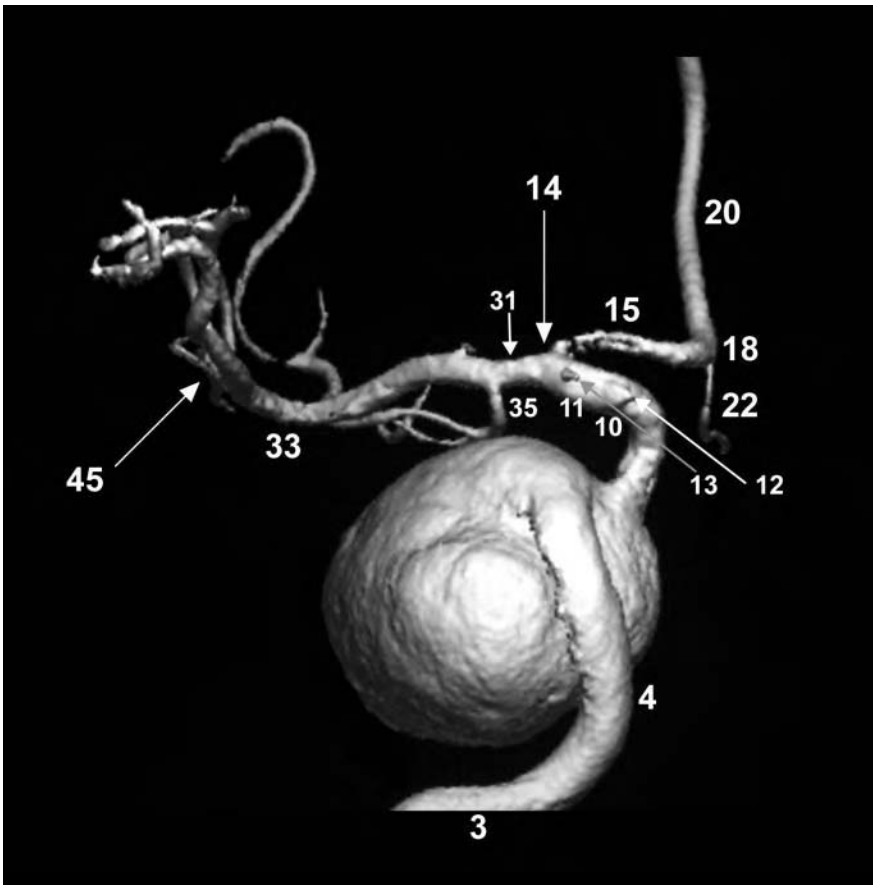

Fig. 5.10 3D posterior view following left internal carotid artery injection. This view demonstrates a giant (more than 2.5 cm) aneurysm of the intracavernous segment of the internal carotid artery.

FIGURE KEY

3 internal carotid artery – horizontal petrous segment
4 presellar (Fischer C5) segment internal carotid artery
10 & 11 proximal and distal supraclinoid segment internal carotid artery
12 stump of the posterior communicating artery
13 stump of the anterior choroidal artery
14 internal carotid artery bifurcation
15 A1 segment of anterior cerebral artery
18 A1-A2 junction anterior cerebral artery
20 proximal A2 segment anterior cerebral artery
22 orbitofrontal branch of anterior cerebral artery
31 M1 segment of middle cerebral artery
33 bifurcation/trifurcation of middle cerebral artery
35 orbitofrontal branch of middle cerebral artery
45 sylvian (insular) branches of middle cerebral artery

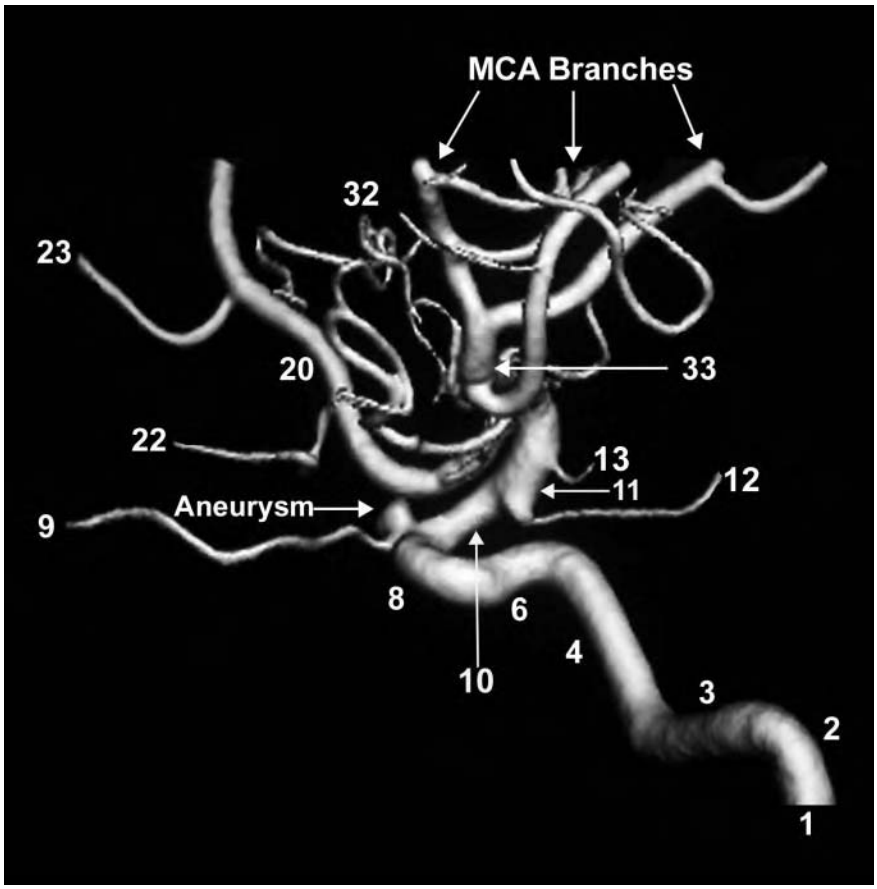

Fig. 5.11 3D lateral view following left internal carotid artery injection. This view shows a small aneurysm of the internal carotid artery at the level of the ophthalmic artery origin. Note the infundibular widening at the origin of the posterior communicating artery.

FIGURE KEY

1 internal carotid artery – cervical segment
2 internal carotid artery – vertical petrous segment
3 internal carotid artery – horizontal petrous segment
4 presellar (Fischer C5) segment internal carotid artery
6 horizontal (Fischer C4) intracavernous internal carotid artery
8 anterior genu (Fischer C3) intracavernous internal carotid artery
9 ophthalmic artery
10 & 11 proximal and distal supraclinoid segment internal carotid artery
12 posterior communicating artery
13 anterior choroidal artery
20 proximal A2 segment anterior cerebral artery
22 orbitofrontal branch of anterior cerebral artery
23 frontopolar branch of anterior cerebral artery
32 lateral lenticulostriate arteries
33 bifurcation/trifurcation of middle cerebral artery

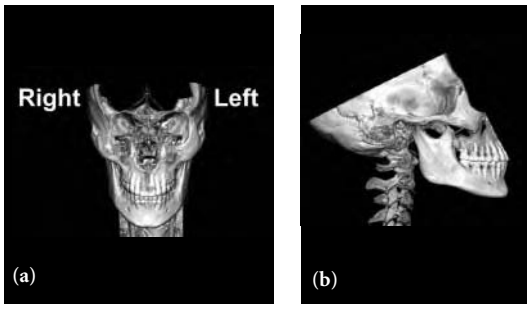

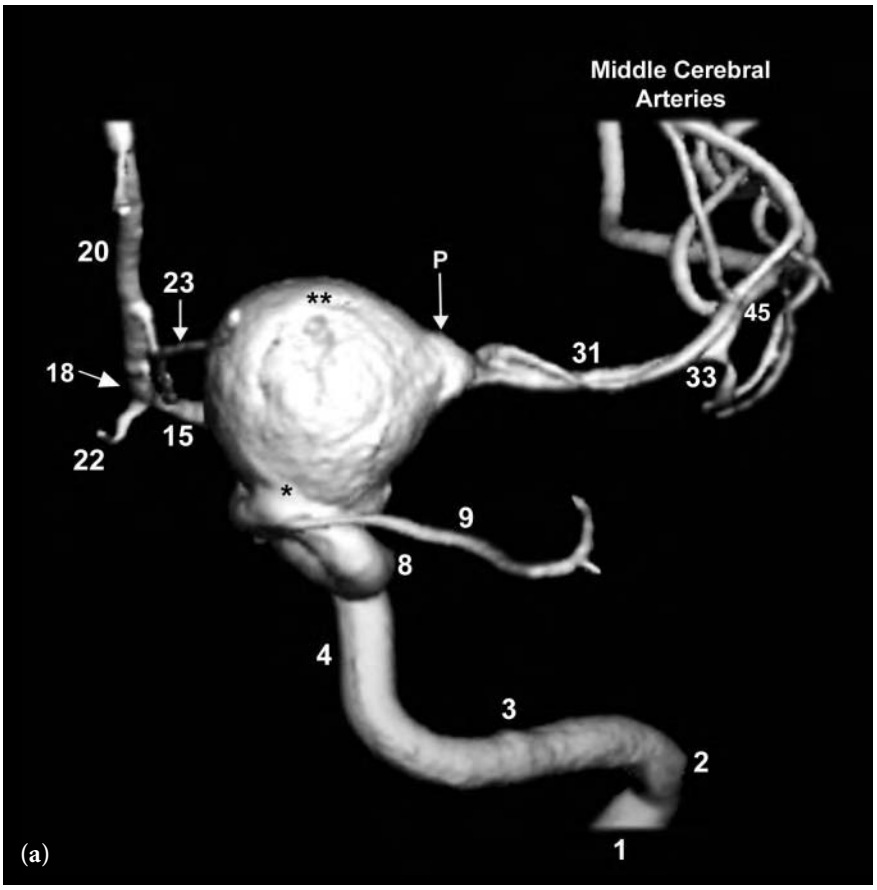

Fig. 5.12 (a–c) 3D frontal (*a*), medial (*b*), and superior to inferior (*c*) views following left internal carotid artery injection show a large aneurysm of the internal carotid artery at the level of the ophthalmic artery origin. Note the focal protrusion of the aneurysm along the lateral margin that represents a focal area of wall weakening and a potential site for rupture.

FIGURE KEY

1 internal carotid artery – cervical segment
2 internal carotid artery – vertical petrous segment
3 internal carotid artery – horizontal petrous segment
4 presellar (Fischer C5) segment internal carotid artery
5 truncated origin of meningohypophyseal trunk
6 horizontal (Fischer C4) intracavernous internal carotid artery
8 anterior genu (Fischer C3) intracavernous internal carotid artery
9 ophthalmic artery
10 & 11 proximal and distal supraclinoid segment internal carotid artery
14 internal carotid artery bifurcation
15 A1 segment of anterior cerebral artery
18 A1-A2 junction anterior cerebral artery
20 proximal A2 segment anterior cerebral artery
22 orbitofrontal branch of anterior cerebral artery
23 frontopolar branch of anterior cerebral artery
31 M1 segment of middle cerebral artery
33 bifurcation/trifurcation of middle cerebral artery
35 orbitofrontal branch of middle cerebral artery
45 sylvian (insular) branches of middle cerebral artery
* neck of aneurysm
** dome of aneurysm
P focal protrusion of aneurysm wall

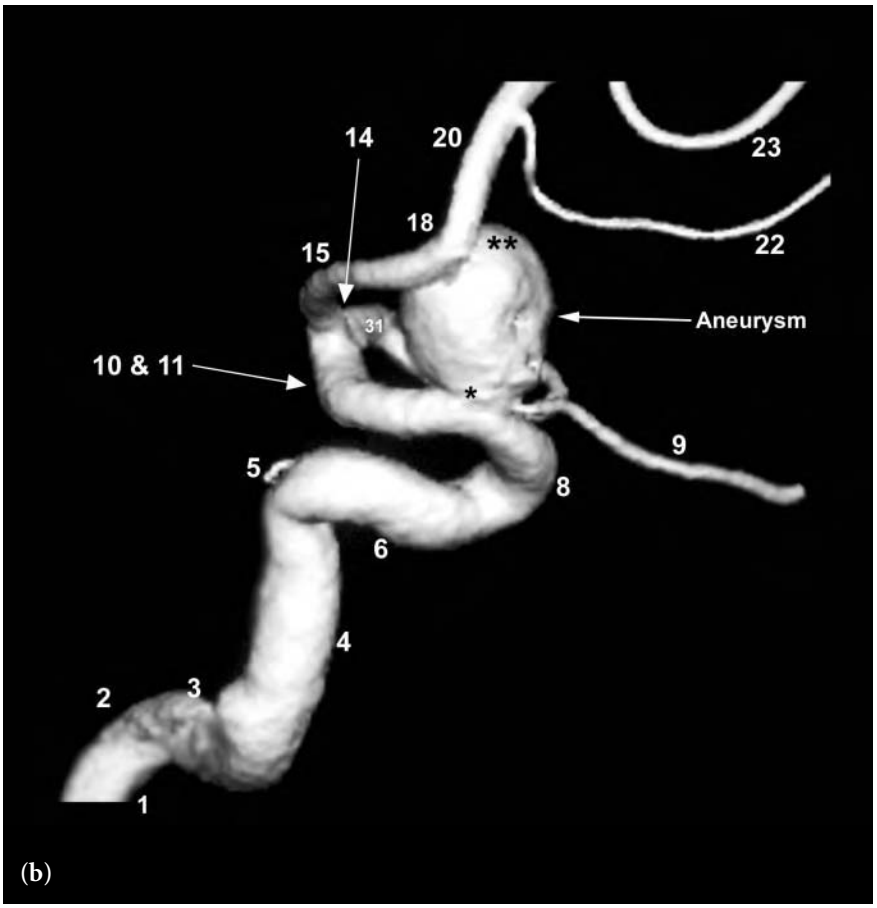

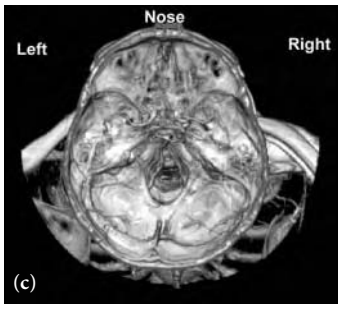
Nose
Left
Right
(c)

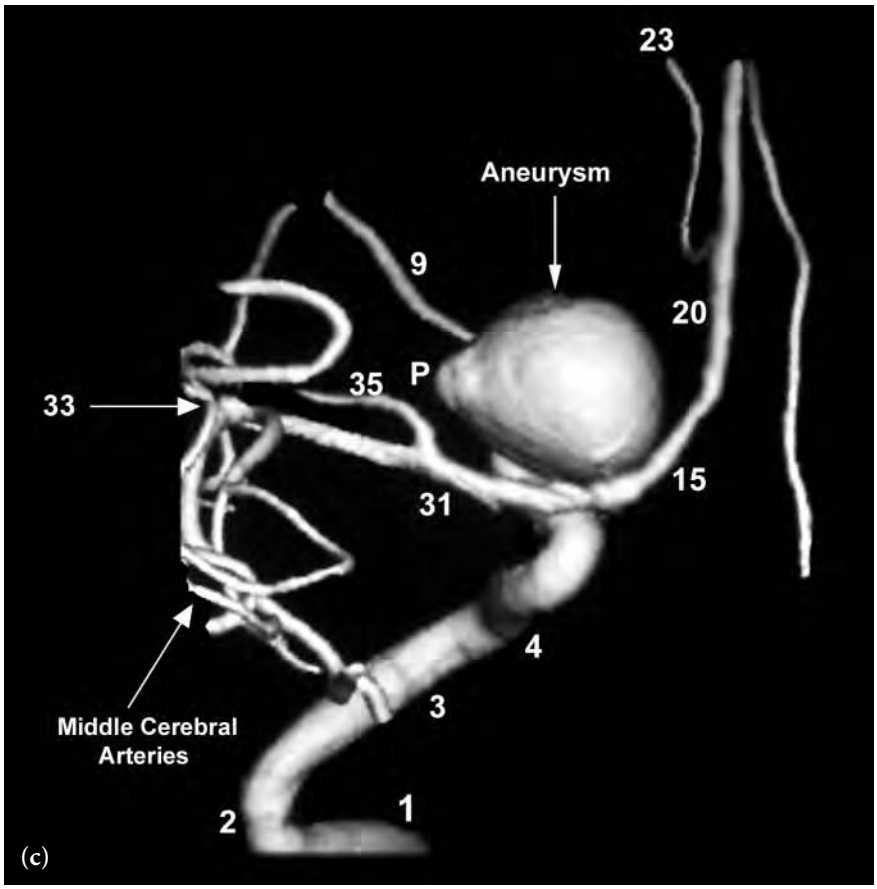
23
Aneurysm
9
20
33
35
P
15
31
4
3
Middle Cerebral
Arteries
2
1
(c)

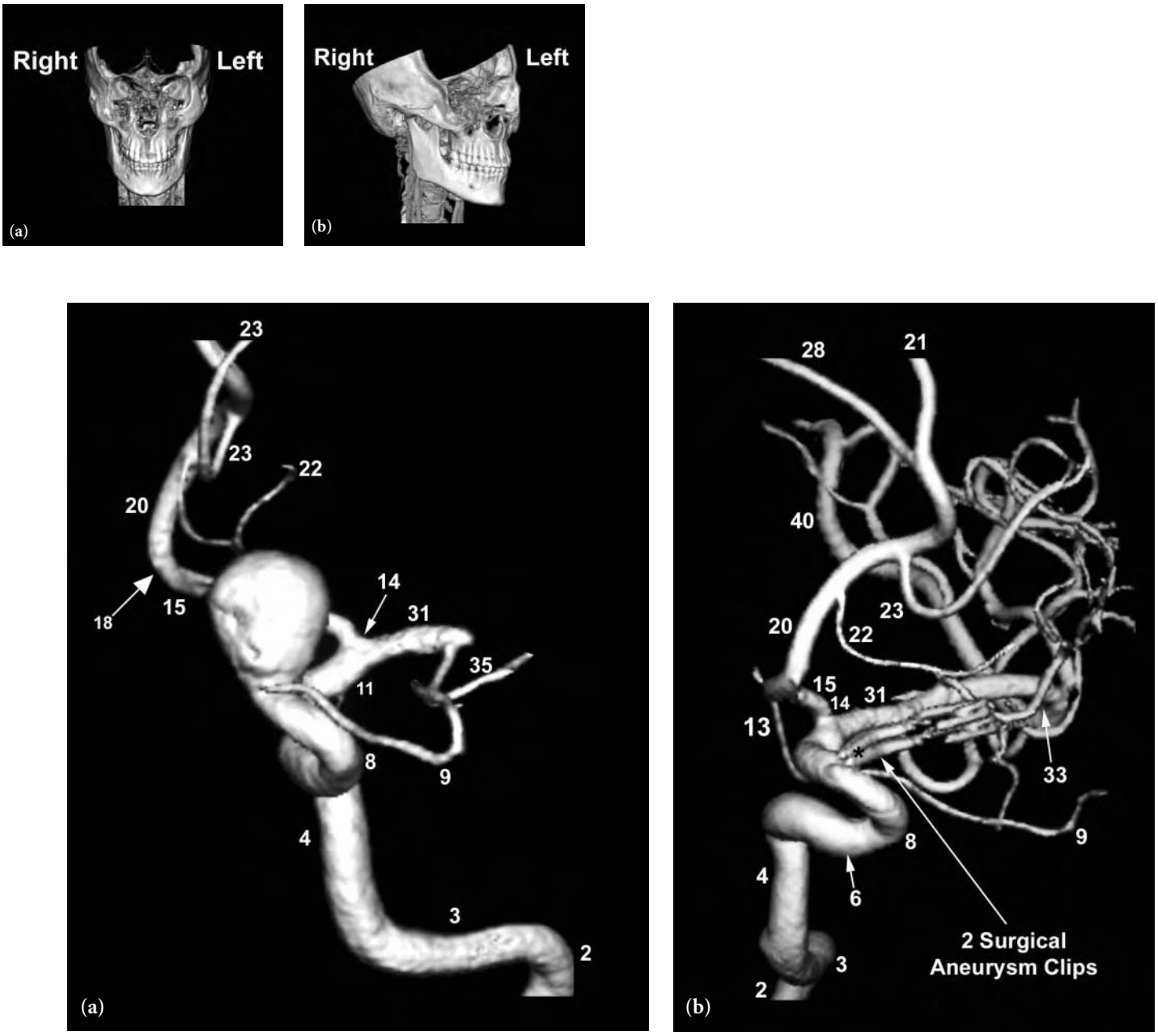

Fig. 5.13 (a,b) 3D frontal (*a*) and right anterior oblique (RAO) (*b*) views following left internal carotid artery injection. A large internal carotid artery aneurysm at the level of the ophthalmic artery is seen in image (*a*). Image (*b*) was obtained following a neurosurgical clipping. Two aneurysm clips completely occlude the aneurysm at its neck. Software technology allowed for the 3D reconstruction of the metallic clips and coils.

FIGURE KEY

2 internal carotid artery – vertical petrous segment
3 internal carotid artery – horizontal petrous segment
4 presellar (Fischer C5) segment internal carotid artery
6 horizontal (Fischer C4) intracavernous internal carotid artery
8 anterior genu (Fischer C3) intracavernous internal carotid artery
9 ophthalmic artery
11 distal supraclinoid segment internal carotid artery
13 anterior choroidal artery
14 internal carotid artery bifurcation
15 A1 segment of anterior cerebral artery
20 proximal A2 segment anterior cerebral artery
21 callosomarginal branch of anterior cerebral artery
22 orbitofrontal branch of anterior cerebral artery
23 frontopolar branch of anterior cerebral artery
28 pericallosal branch of anterior cerebral artery
31 M1 segment of middle cerebral artery
33 bifurcation/trifurcation of middle cerebral artery
35 orbitofrontal branch of middle cerebral artery
* surgical aneurysm clips

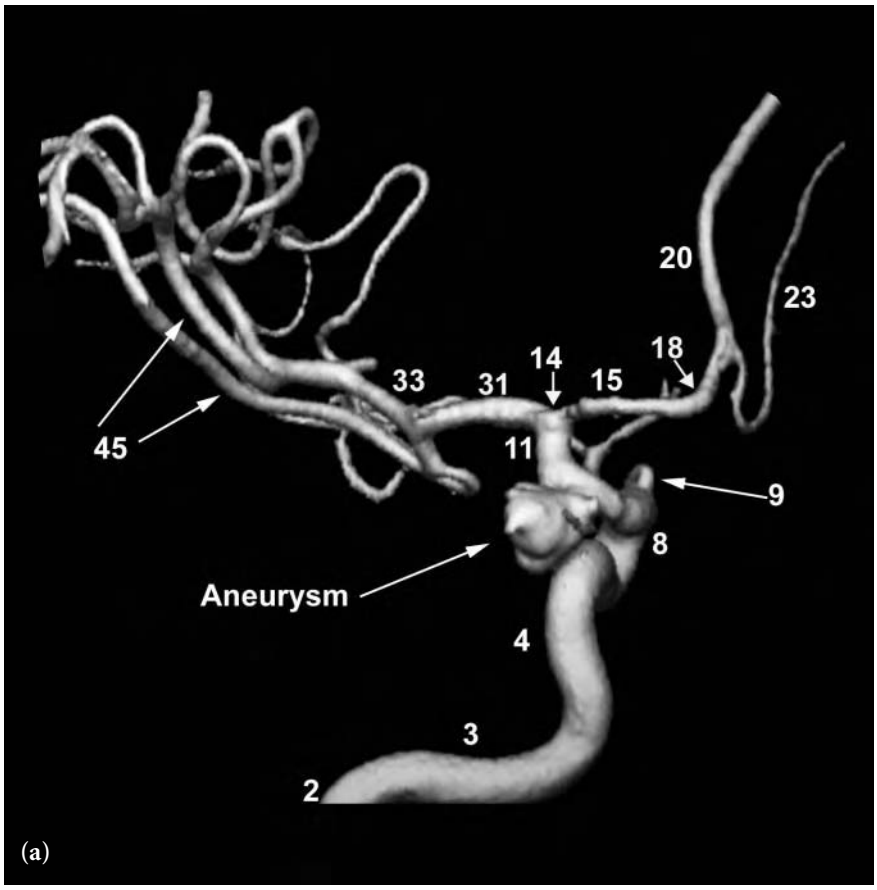

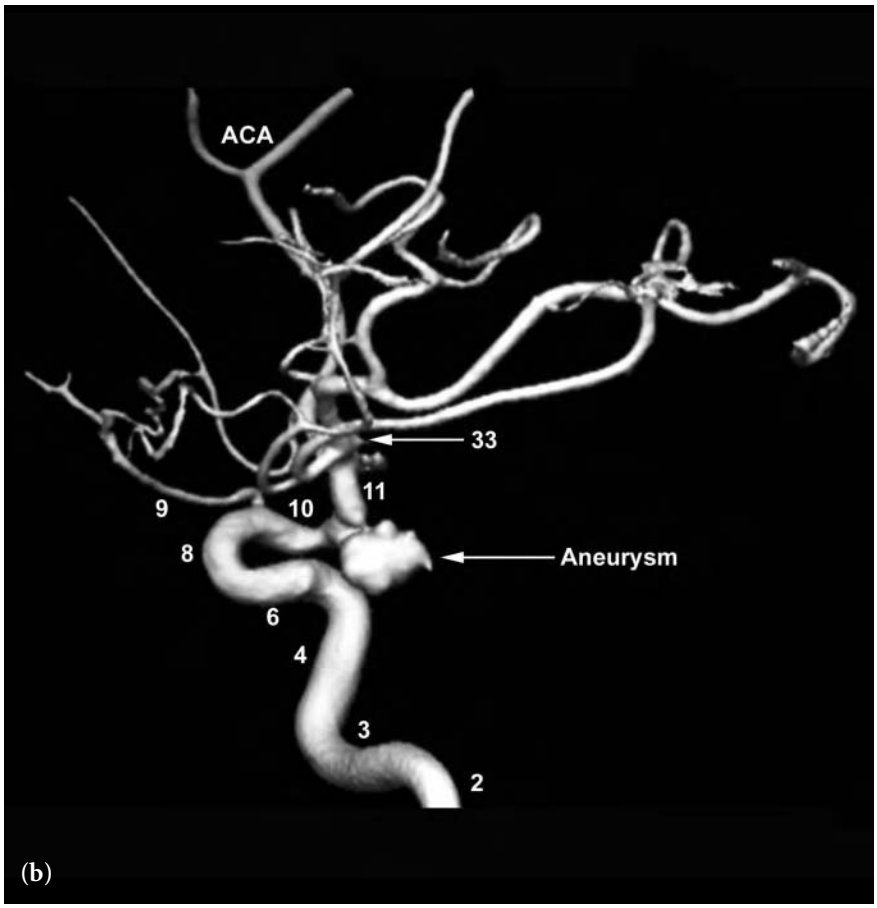

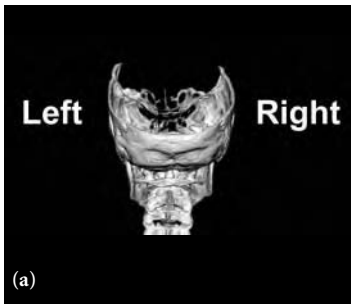

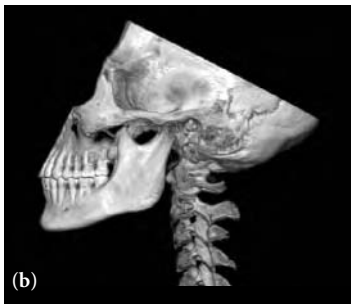

Fig. 5.14 (a–e) 3D posterior (*a*), lateral (*b*), left anterior oblique (LAO) (*c*), magnified LAO (*d*), and superior to inferior (*e*) views following left internal carotid artery injection. The views show an aneurysm with multiple lobulations arising from the posterior wall of the supraclinoid segment of the internal carotid artery. The lobulations represent areas of focal weakness of the aneurysm wall and potential sites for rupture.

FIGURE KEY

- 2 internal carotid artery – vertical petrous segment
- 3 internal carotid artery – horizontal petrous segment
- 4 presellar (Fischer C5) segment internal carotid artery
- 6 horizontal (Fischer C4) intracavernous internal carotid artery
- 8 anterior genu (Fischer C3) intracavernous internal carotid artery
- 9 ophthalmic artery
- 10 & 11 proximal and distal supraclinoid segment internal carotid artery
- 14 internal carotid artery bifurcation
- 15 A1 segment of anterior cerebral artery
- 18 A1-A2 junction anterior cerebral artery
- 20 proximal A2 segment anterior cerebral artery
- 23 frontopolar branch of anterior cerebral artery
- 31 M1 segment of middle cerebral artery
- 33 bifurcation/trifurcation of middle cerebral artery
- 45 sylvian (insular) branches of middle cerebral artery
- * neck of aneurysm

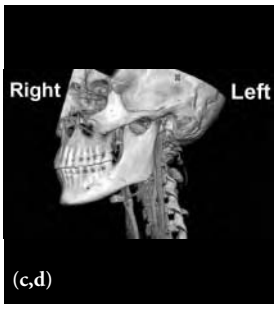

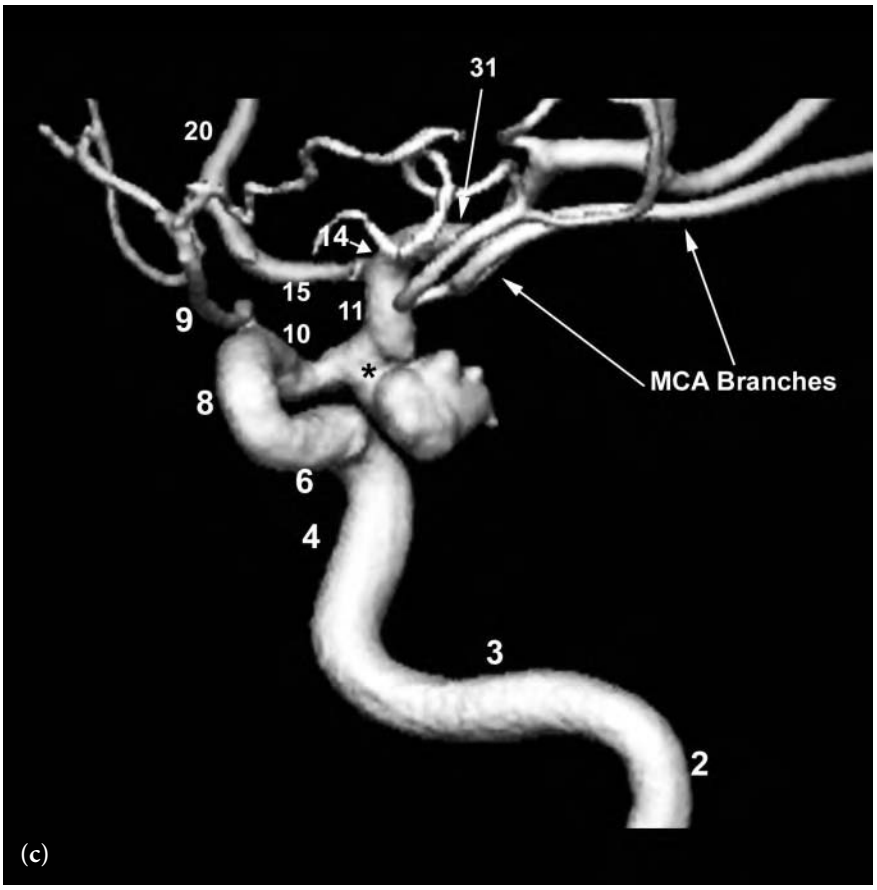

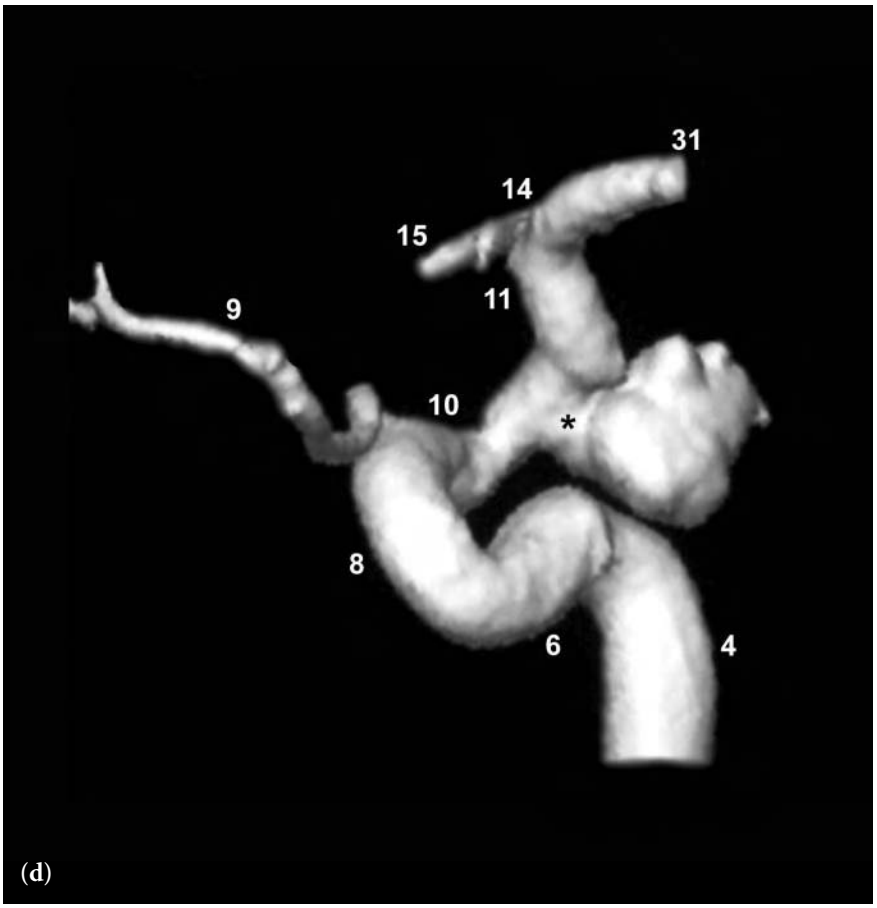

Fig. 5.14 (continued)

FIGURE KEY

2 internal carotid artery – vertical petrous segment
3 internal carotid artery – horizontal petrous segment
4 presellar (Fischer C5) segment internal carotid artery
6 horizontal (Fischer C4) intracavernous internal carotid artery
8 anterior genu (Fischer C3) intracavernous internal carotid artery
9 ophthalmic artery
10 & 11 proximal and distal supraclinoid segment internal carotid artery
14 internal carotid artery bifurcation
15 A1 segment of anterior cerebral artery
18 A1-A2 junction anterior cerebral artery
20 proximal A2 segment anterior cerebral artery
23 frontopolar branch of anterior cerebral artery
31 M1 segment of middle cerebral artery
33 bifurcation/trifurcation of middle cerebral artery
45 sylvian (insular) branches of middle cerebral artery
* neck of aneurysm

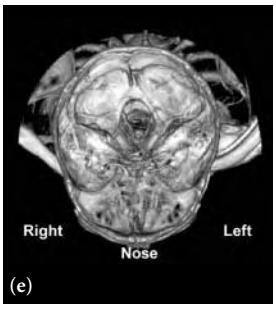
Right
Left
Nose
(e)

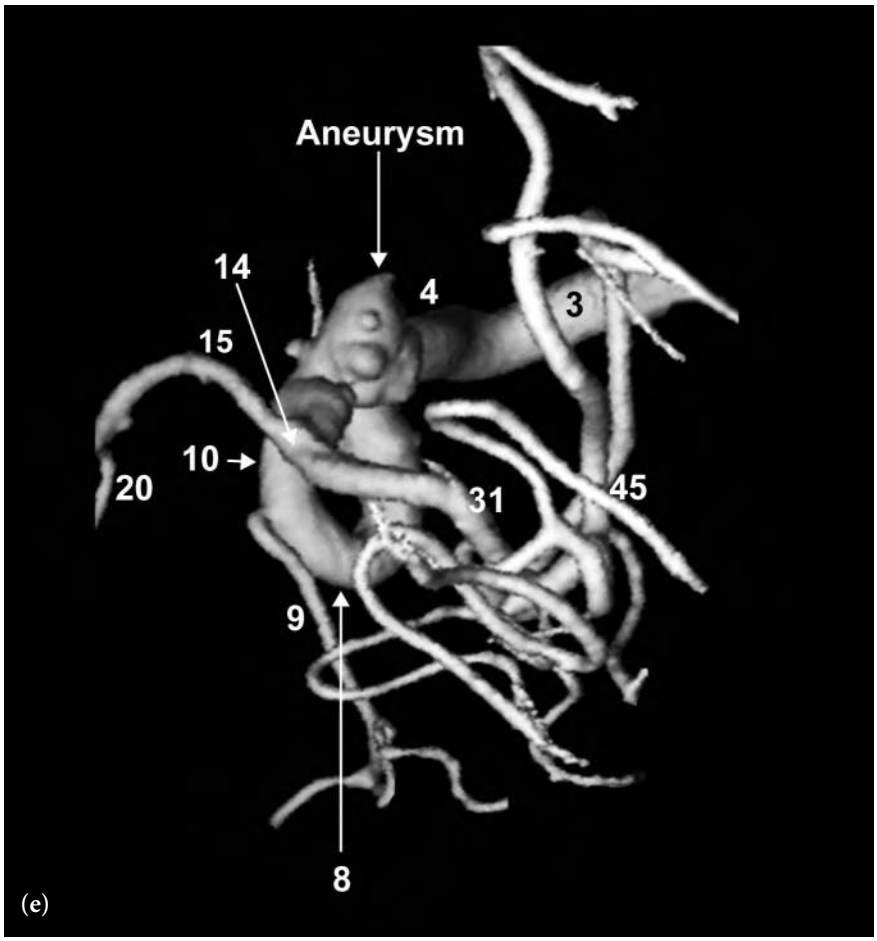
Aneurysm
14
4
3
15
10
20
31
45
9
8
(e)

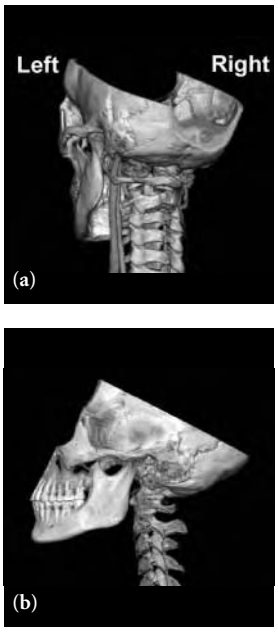

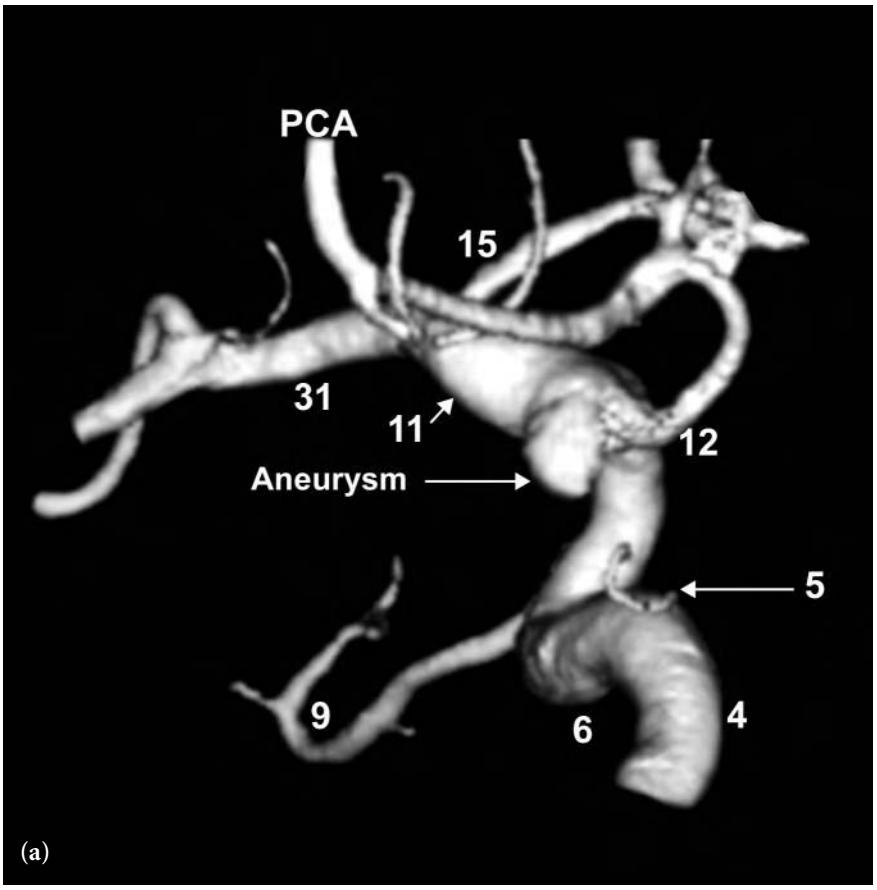

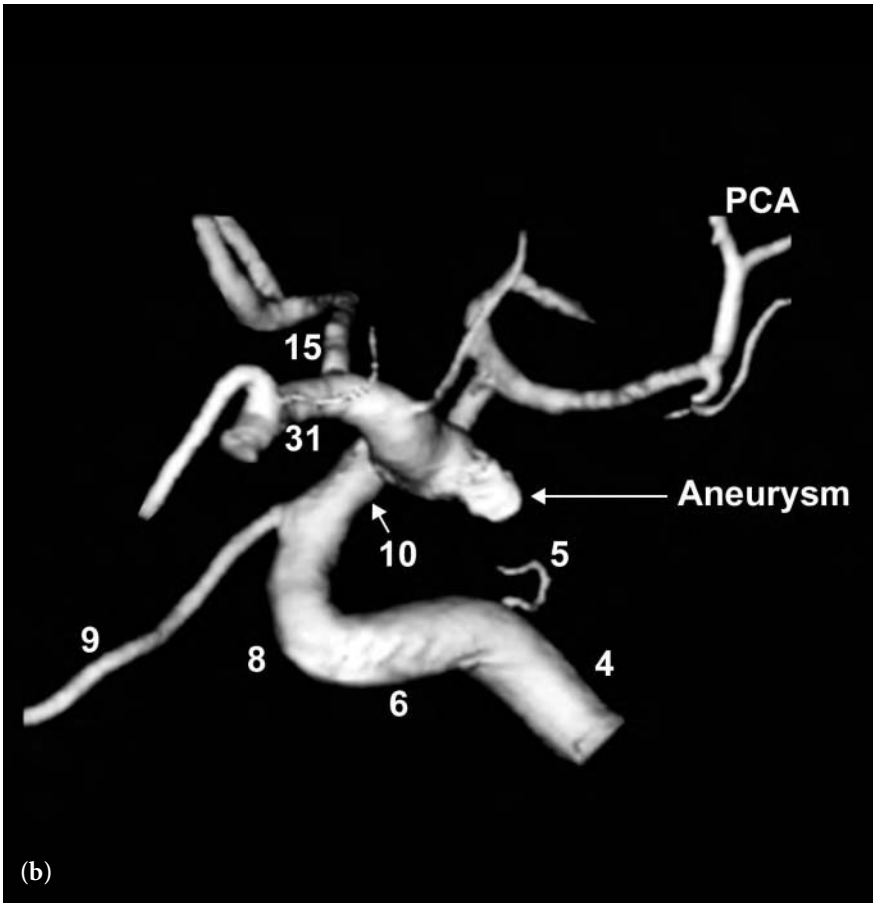

Fig. 5.15 (a,b) 3D shallow left posterior oblique (LPO) (*a*) and lateral (*b*) views following left internal carotid artery injection. There is a small aneurysm arising at the origin of a large posterior communicating artery/fetal posterior cerebral artery from the posterior wall of the supraclinoid segment of the internal carotid artery. The field of view on these images has been limited intentionally.

FIGURE KEY

4 presellar (Fischer C5) segment internal carotid artery
5 meningohypophyseal trunk
6 horizontal (Fischer C4) intracavernous internal carotid artery
8 anterior genu (Fischer C3) intracavernous internal carotid artery
9 ophthalmic artery
10 & 11 proximal and distal supraclinoid segment internal carotid artery
12 posterior communicating artery/fetal origin posterior cerebral artery
15 A1 segment of anterior cerebral artery
31 M1 segment of middle cerebral artery
PCA posterior cerebral artery

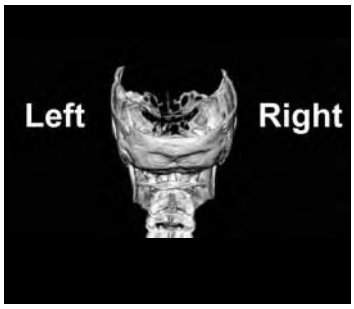

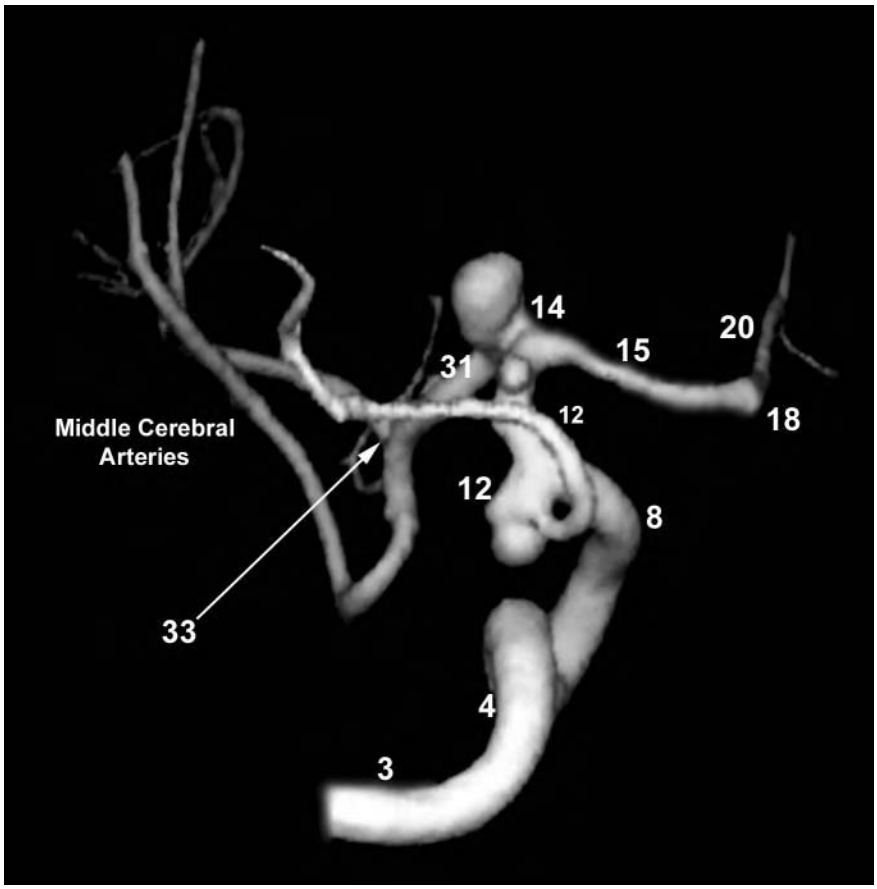

Fig. 5.16 A 3D posterior view following left internal carotid artery injection. Three separate aneurysms are identified. One aneurysm arises from the posterior wall of the supraclinoid segment of the internal carotid artery at the level of the posterior communicating artery. The second, smaller aneurysm arises from the posterior wall of the supraclinoid internal carotid artery just inferior to the internal carotid artery bifurcation. The third and largest aneurysm arises from the internal carotid artery bifurcation and projects superiorly.

FIGURE KEY

3 internal carotid artery – horizontal petrous segment
4 presellar (Fischer C5) segment internal carotid artery
8 anterior genu (Fischer C3) intracavernous internal carotid artery
12 posterior communicating artery
14 internal carotid artery bifurcation
15 A1 segment of anterior cerebral artery
18 A1-A2 junction anterior cerebral artery
20 proximal A2 segment anterior cerebral artery
31 M1 segment of middle cerebral artery
33 bifurcation/trifurcation of middle cerebral artery

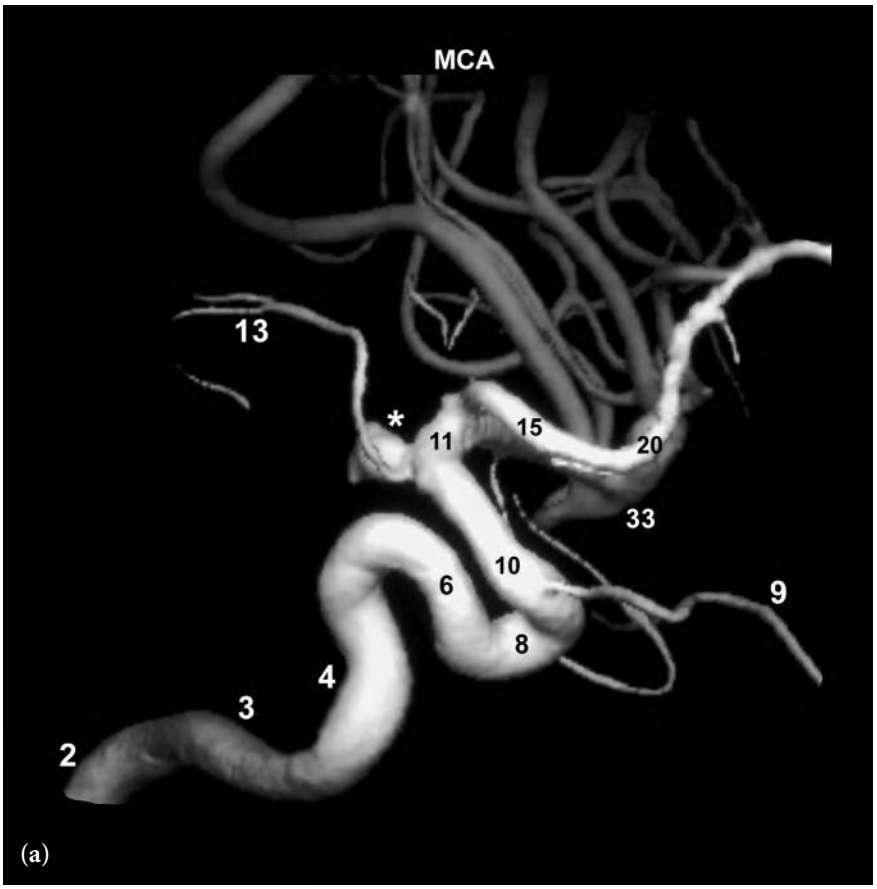

Fig. 5.17 (a–c) 3D medial (*a*), inferior to superior left posterior oblique (LPO) complex angle (*b*), and inferior to superior right posterior oblique (RPO) (*c*) views following left internal carotid artery injection. There is an aneurysm rising from the posterior wall of the supraclinoid segment of the internal carotid artery at the takeoff of the anterior choroidal artery. Note the small focal lobulation along the posterior-inferior aspect of the aneurysm in (*c*) which is a focal area of weakness/thinning of the aneurysm wall and a potential site for rupture.

FIGURE KEY

2 internal carotid artery – vertical petrous segment
3 internal carotid artery – horizontal petrous segment
4 presellar (Fischer C5) segment internal carotid artery
6 horizontal (Fischer C4) intracavernous internal carotid artery
8 anterior genu (Fischer C3) segment internal carotid artery
9 ophthalmic artery
10 & 11 proximal and distal supraclinoid segment internal carotid artery
13 anterior choroidal artery
14 internal carotid artery bifurcation
15 A1 segment of anterior cerebral artery
20 proximal A2 segment anterior cerebral artery
31 M1 segment of middle cerebral artery
33 bifurcation/trifurcation of middle cerebral artery
34 anterior temporal lobe branches of middle cerebral artery
45 sylvian (insular) branches of middle cerebral artery
* aneurysm

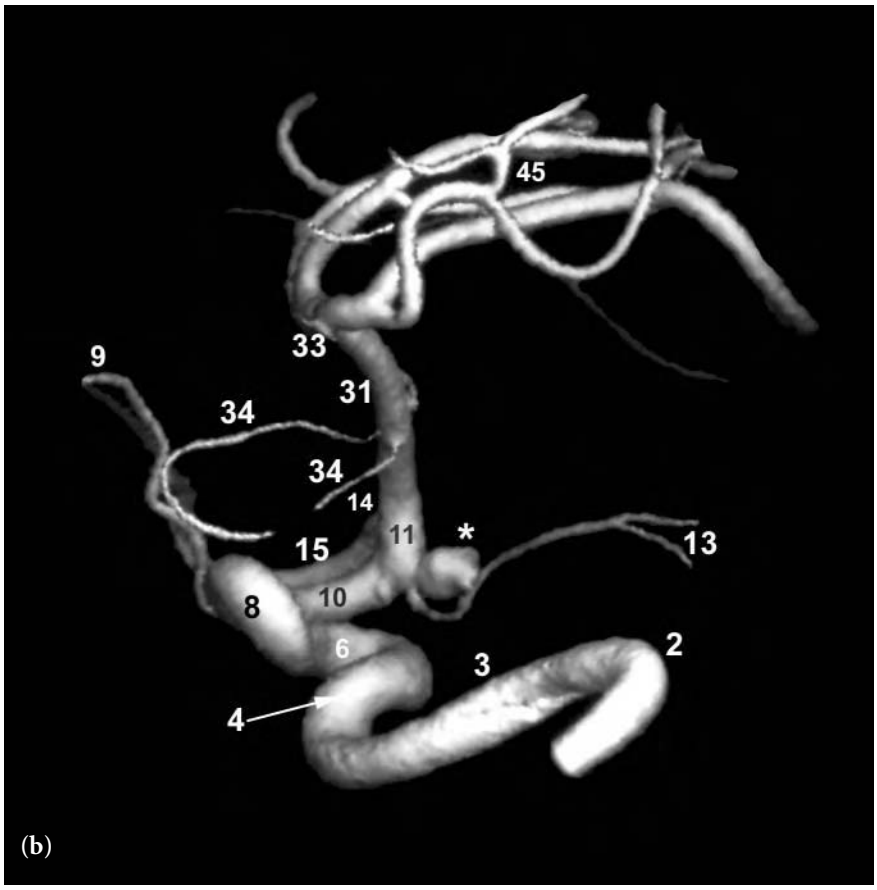
45
9
33
31
34
34
14
11
*
13
15
8
10
6
3
2
4
(b)

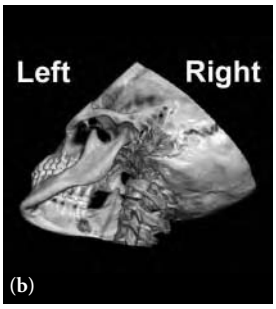
Left
Right
(b)

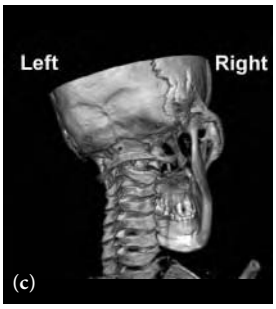
Left
Right
(c)

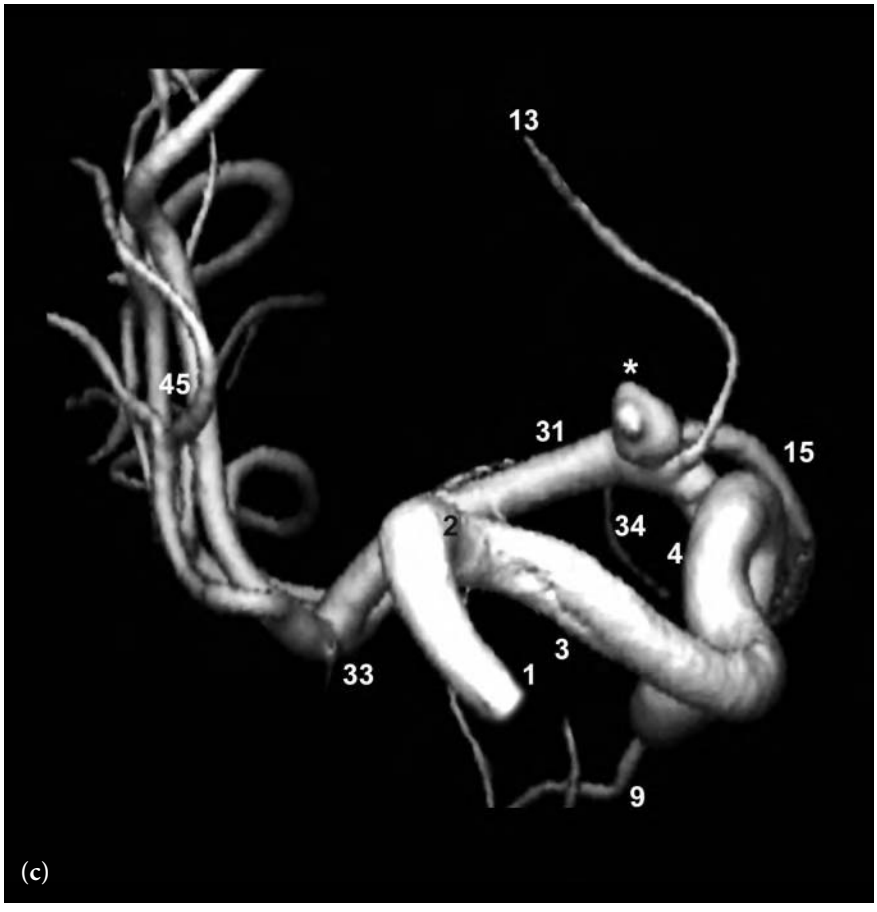
13
45
*
31
15
2
34
4
3
33
1
9
(c)

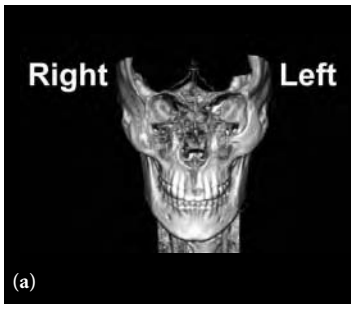

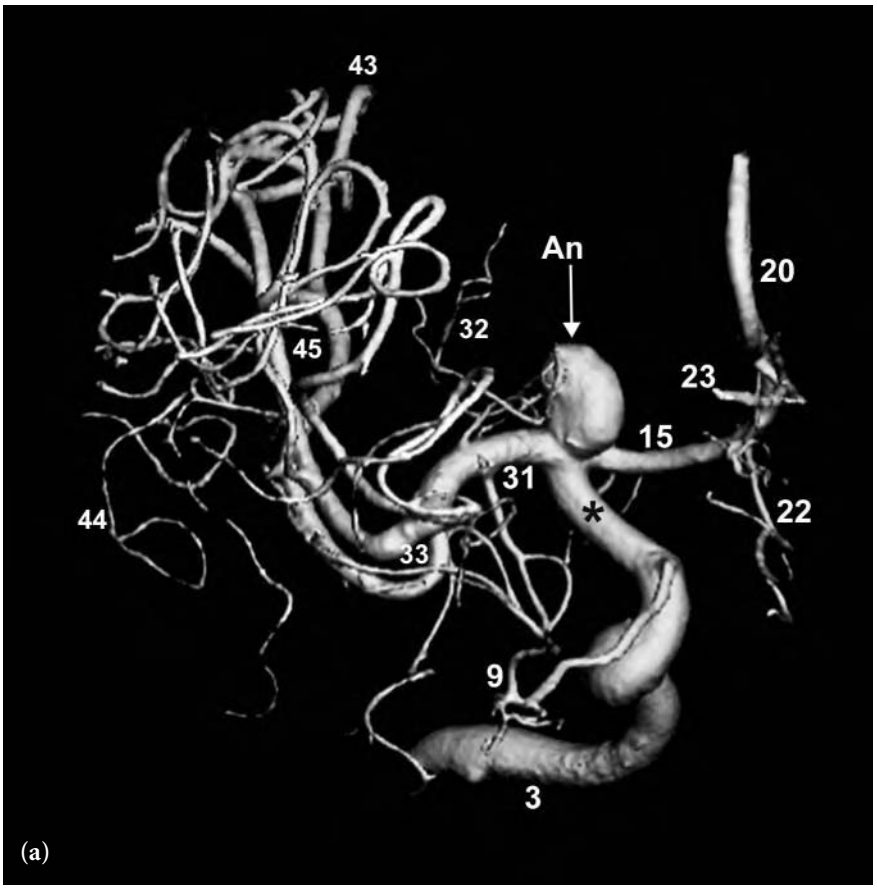

Fig. 5.18 (a–e) 3D frontal (*a*), shallow left posterior oblique (LPO) (*b*), steeper LPO (*c*), right posterior oblique (RPO) (*d*), and superior to inferior (*e*) views following right internal carotid injection. These images demonstrate an aneurysm rising at the internal carotid artery bifurcation. Note the otherwise normal appearance of the vasculature.

FIGURE KEY

3 internal carotid artery – horizontal petrous segment
4 presellar (Fischer C5) segment internal carotid artery
5 meningohypophyseal trunk
6 horizontal (Fischer C4) intracavernous internal carotid artery
8 anterior genu (Fischer C3) segment internal carotid artery
9 ophthalmic artery
12 posterior communicating artery
13 anterior choroidal artery
15 A1 segment of anterior cerebral artery
20 proximal A2 segment anterior cerebral artery
22 orbitofrontal branch of anterior cerebral artery
23 frontopolar branch of anterior cerebral artery
28 pericallosal branch of anterior cerebral artery
31 M1 segment of middle cerebral artery
32 lateral lenticulostriate arteries
33 bifurcation/trifurcation of middle cerebral artery
34 anterior temporal lobe branches of middle cerebral artery
40 angular artery
43 sylvian point
44 opercular branches of middle cerebral artery
45 sylvian (insular) branches of middle cerebral artery
* supraclinoid segment of internal carotid artery
An aneurysm
D dome of aneurysm

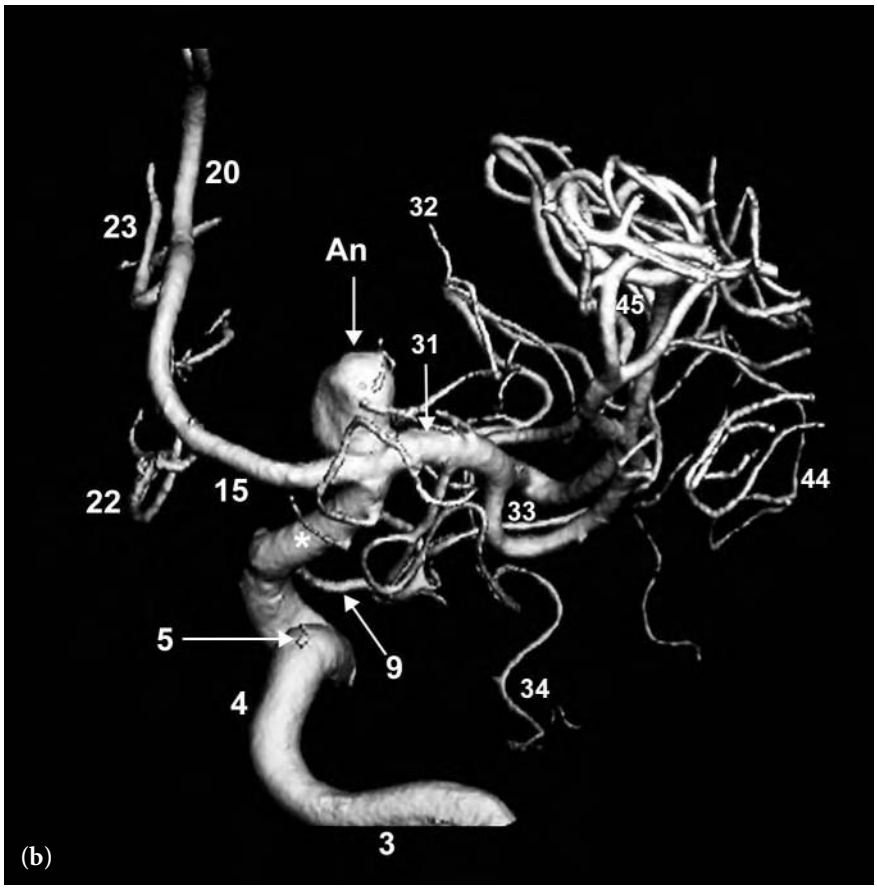
20
23
32
An
45
31
22
15
44
33
*
5
9
34
4
3
(b)

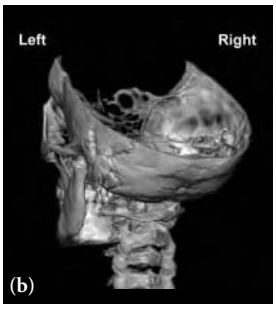
Left
Right
(b)

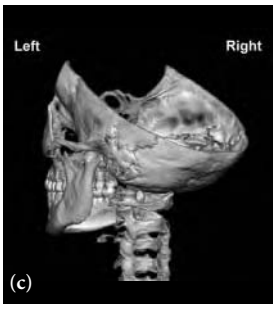
Left
Right
(c)

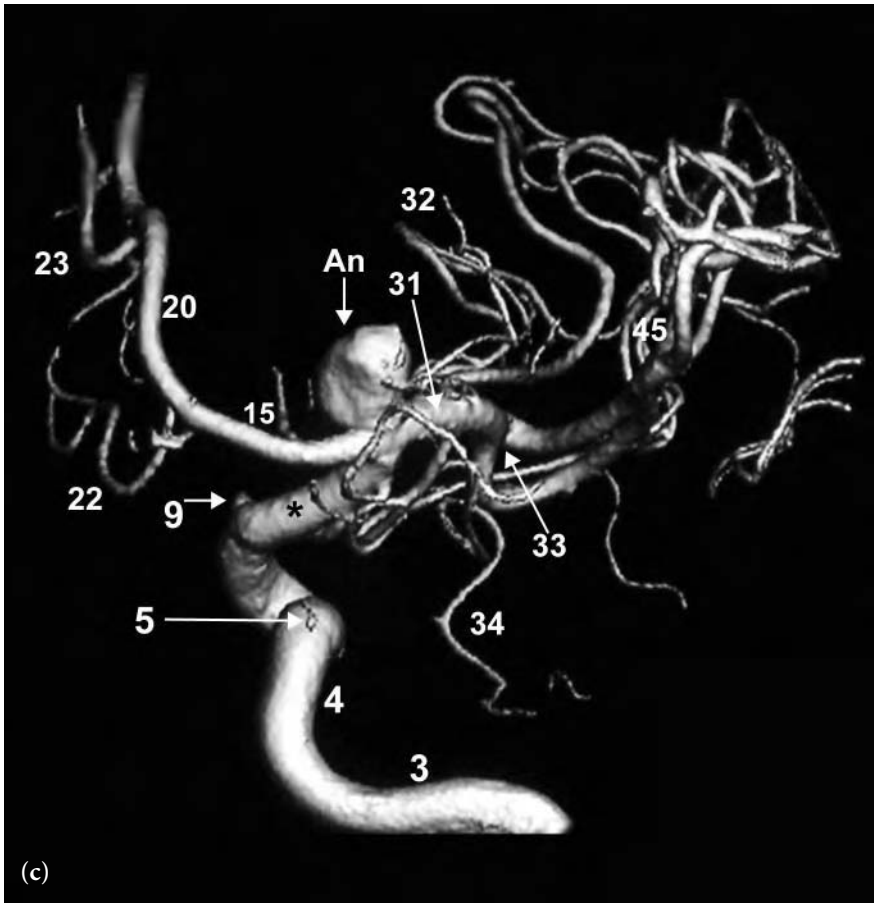
32
23
An
31
20
45
15
22
9
*
33
5
34
4
3
(c)

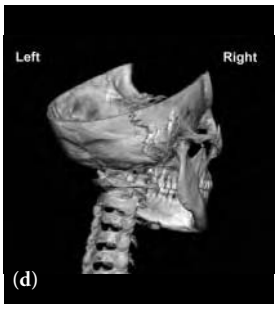

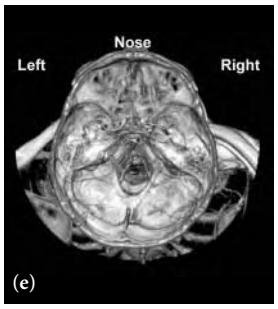

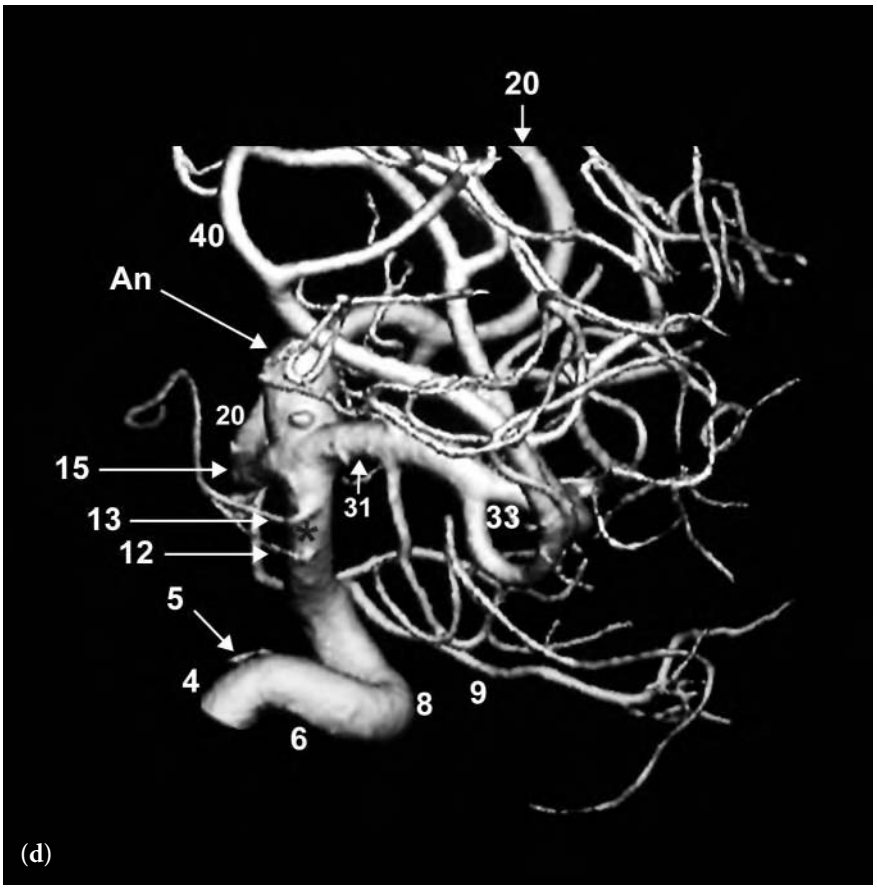

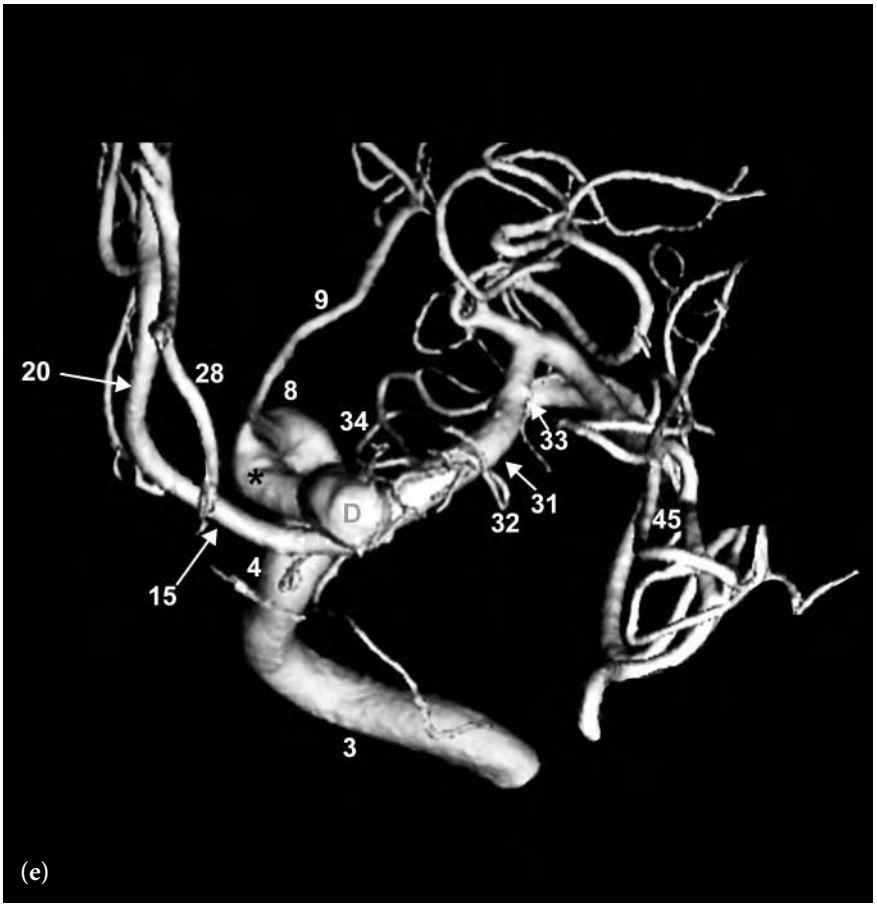

Fig. 5.18 (continued)

FIGURE KEY

3 internal carotid artery – horizontal petrous segment
4 presellar (Fischer C5) segment internal carotid artery
5 meningohypophyseal trunk
6 horizontal (Fischer C4) intracavernous internal carotid artery
8 anterior genu (Fischer C3) segment internal carotid artery
9 ophthalmic artery
12 posterior communicating artery
13 anterior choroidal artery
15 A1 segment of anterior cerebral artery
20 proximal A2 segment anterior cerebral artery
22 orbitofrontal branch of anterior cerebral artery
23 frontopolar branch of anterior cerebral artery
28 pericallosal branch of anterior cerebral artery
31 M1 segment of middle cerebral artery
32 lateral lenticulostriate arteries
33 bifurcation/trifurcation of middle cerebral artery
34 anterior temporal lobe branches of middle cerebral artery
40 angular artery
43 sylvian point
44 opercular branches of middle cerebral artery
45 sylvian (insular) branches of middle cerebral artery
* supraclinoid segment of internal carotid artery
An aneurysm
D dome of aneurysm

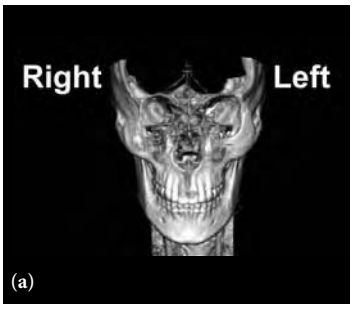

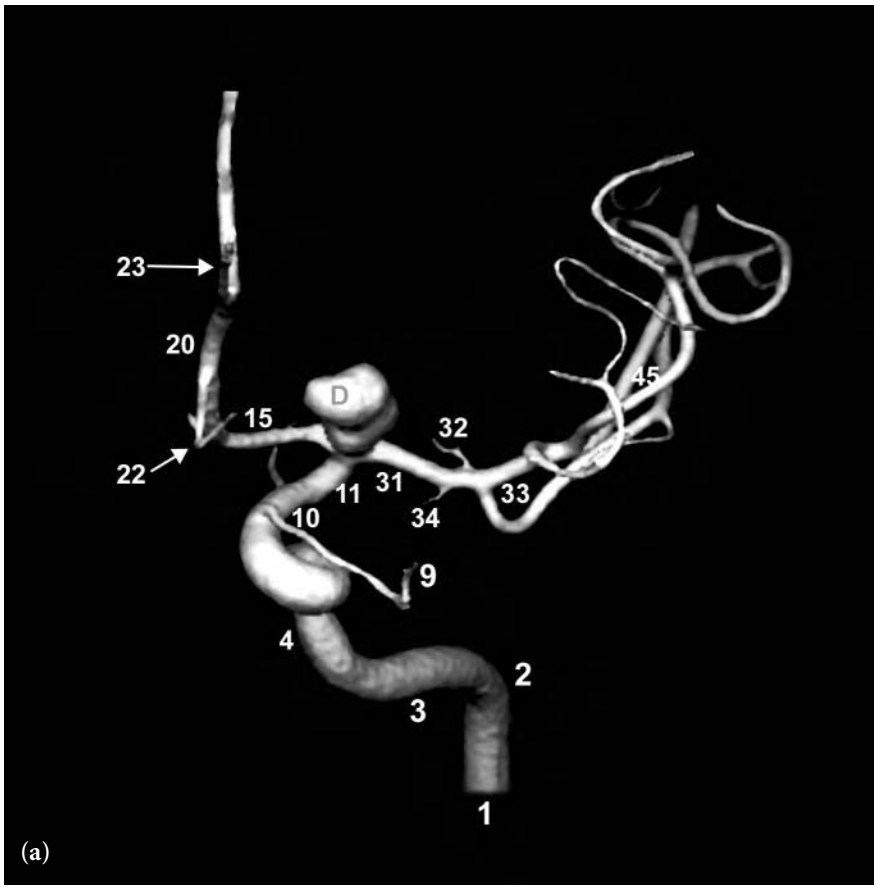

Fig. 5.19 (a–e) 3D frontal (*a*), frontal with inferior to superior angulation (*b*), posterior (*c*), left posterior oblique (LPO) (*d*), and superior to inferior (*e*) views following left internal carotid artery injection. There is a large internal carotid artery bifurcation aneurysm projecting anteriorly and slightly superiorly.

FIGURE KEY

1 internal carotid artery – cervical segment
2 internal carotid artery – vertical petrous segment
3 internal carotid artery – horizontal petrous segment
4 presellar (Fischer C5) segment internal carotid artery
6 horizontal (Fischer C4) intracavernous internal carotid artery
8 anterior genu (Fischer C3) intracavernous internal carotid artery
9 ophthalmic artery
10 & 11 proximal and distal supraclinoid segment internal carotid artery
12 posterior communicating artery
13 origin of anterior choroidal artery
15 A1 segment of anterior cerebral artery
18 A1-A2 junction anterior cerebral artery
19 anterior communicating artery
20 proximal A2 segment anterior cerebral artery
22 orbitofrontal branch of anterior cerebral artery
23 frontopolar branch of anterior cerebral artery
28 pericallosal branch of anterior cerebral artery
31 M1 segment of middle cerebral artery
32 lateral lenticulostriate arteries
33 bifurcation/trifurcation of middle cerebral artery
34 anterior temporal lobe branches of middle cerebral artery
35 orbitofrontal branch of middle cerebral artery
40 angular artery
43 sylvian point
45 sylvian (insular) branches of middle cerebral artery
D dome of the aneurysm
* neck of the aneurysm at the internal carotid artery bifurcation

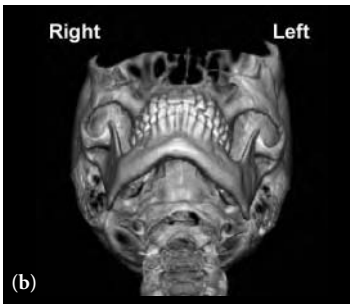

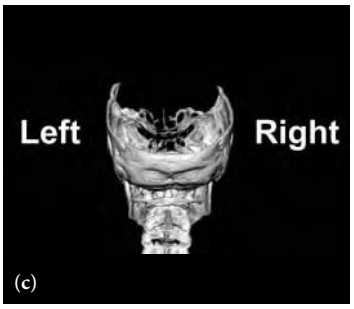

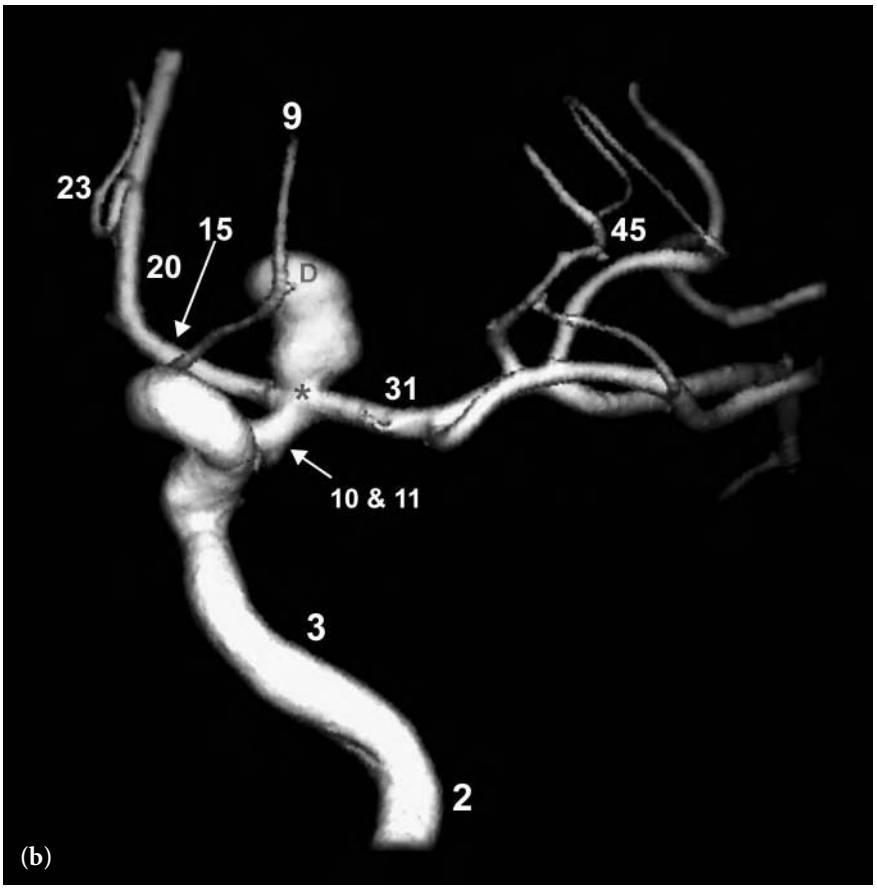

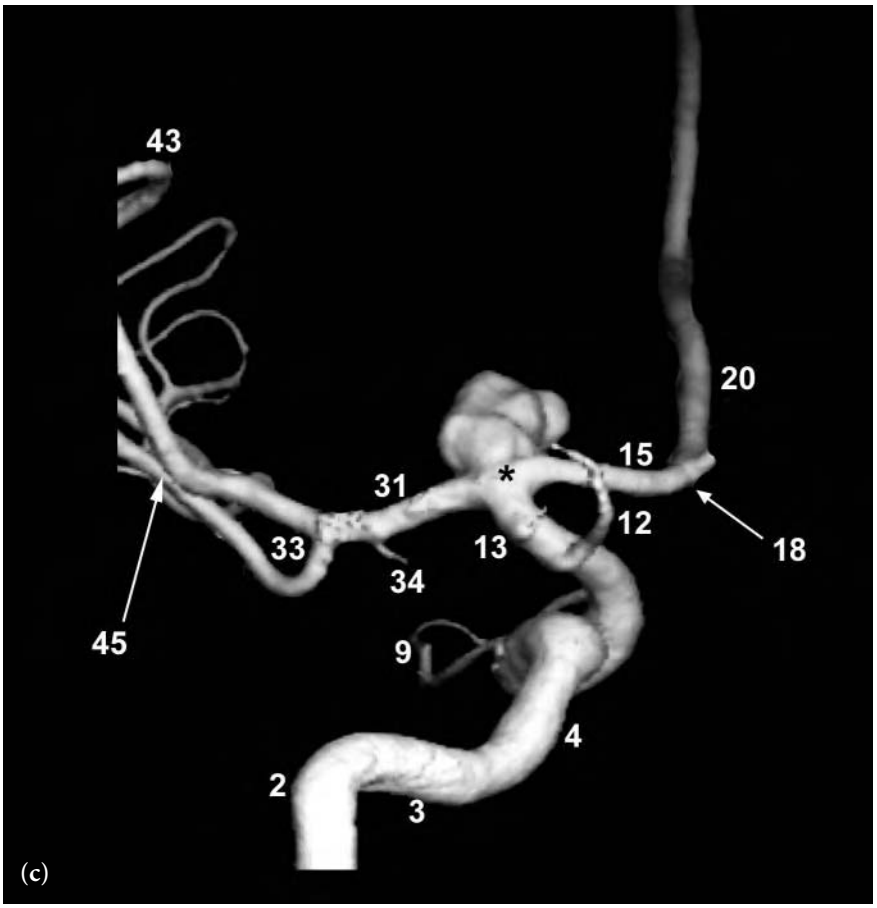

Fig. 5.19 (continued)

FIGURE KEY

1 internal carotid artery – cervical segment
2 internal carotid artery – vertical petrous segment
3 internal carotid artery – horizontal petrous segment
4 presellar (Fischer C5) segment internal carotid artery
6 horizontal (Fischer C4) intracavernous internal carotid artery
8 anterior genu (Fischer C3) intracavernous internal carotid artery
9 ophthalmic artery
10 & 11 proximal and distal supraclinoid segment internal carotid artery
12 posterior communicating artery
13 origin of anterior choroidal artery
15 A1 segment of anterior cerebral artery
18 A1-A2 junction anterior cerebral artery
19 anterior communicating artery
20 proximal A2 segment anterior cerebral artery
22 orbitofrontal branch of anterior cerebral artery
23 frontopolar branch of anterior cerebral artery
28 pericallosal branch of anterior cerebral artery
31 M1 segment of middle cerebral artery
32 lateral lenticulostriate arteries
33 bifurcation/trifurcation of middle cerebral artery
34 anterior temporal lobe branches of middle cerebral artery
35 orbitofrontal branch of middle cerebral artery
40 angular artery
43 sylvian point
45 sylvian (insular) branches of middle cerebral artery
D dome of the aneurysm
* neck of the aneurysm at the internal carotid artery bifurcation

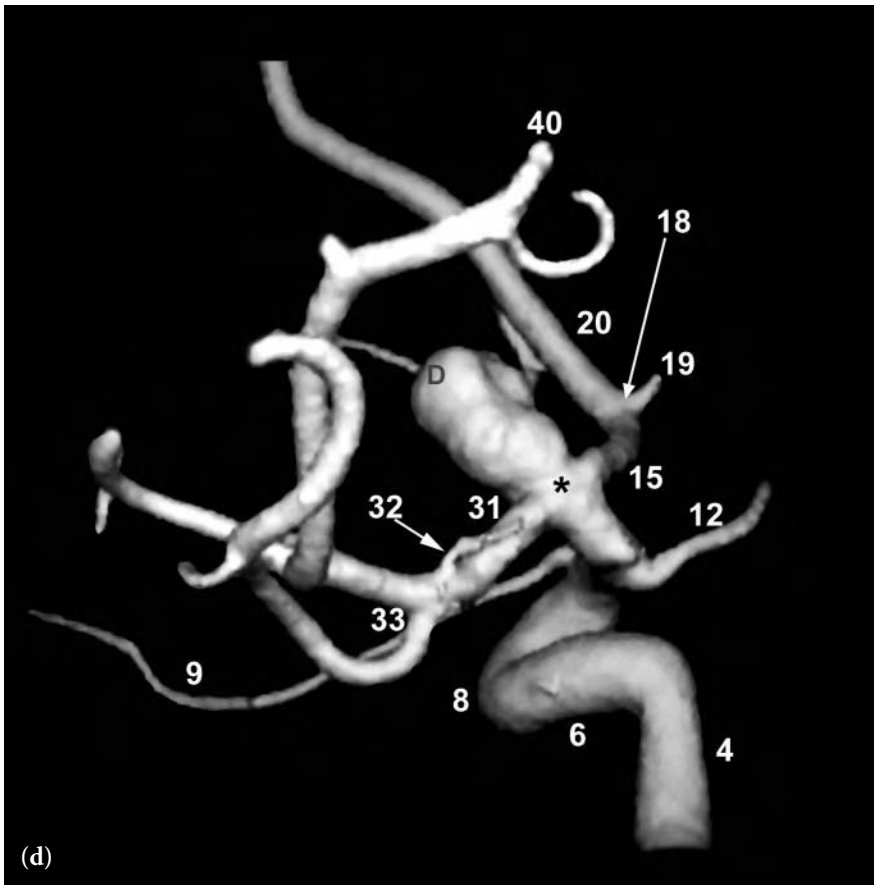
40
18
20
19
D
*
15
32
31
12
33
9
8
6
4
(d)

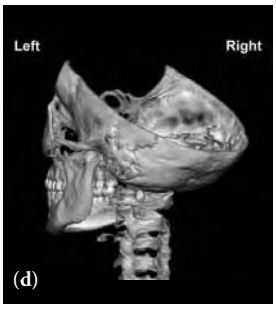
Left
Right
(d)

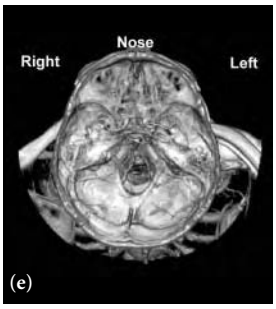
Nose
Right
Left
(e)

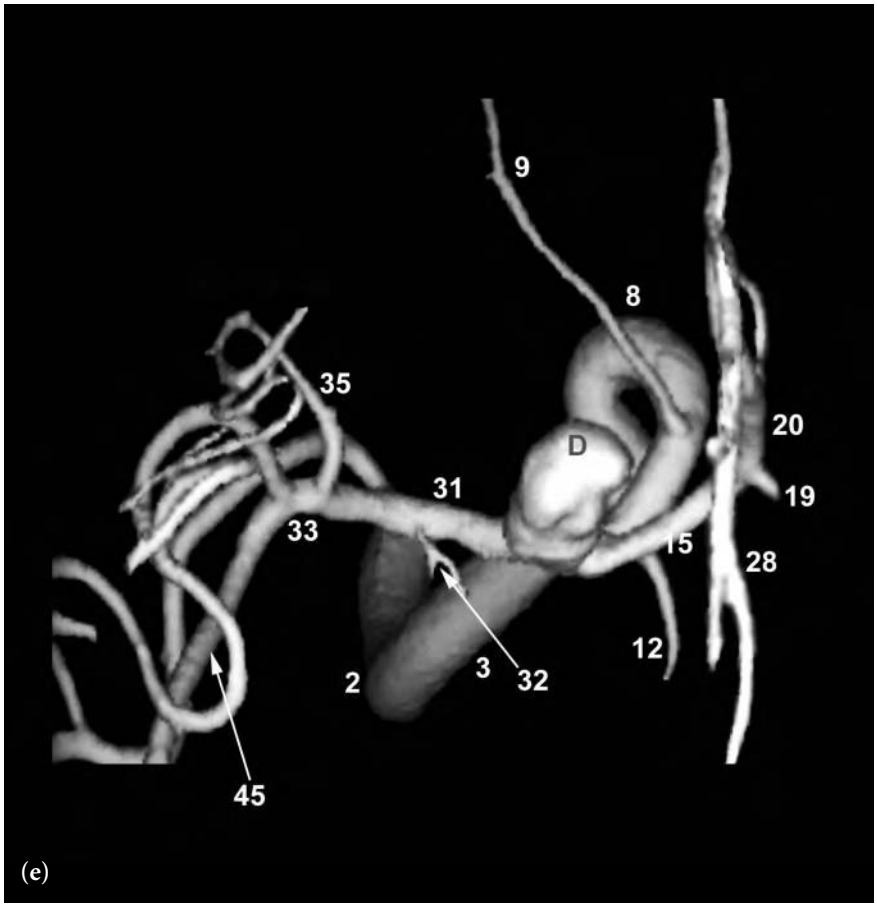
9
8
35
20
D
31
19
33
15
28
12
2
3
32
45
(e)

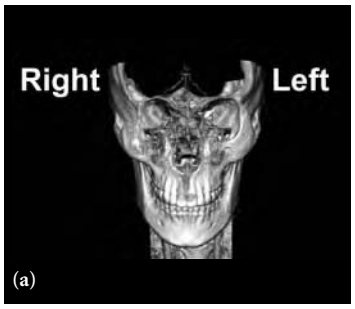

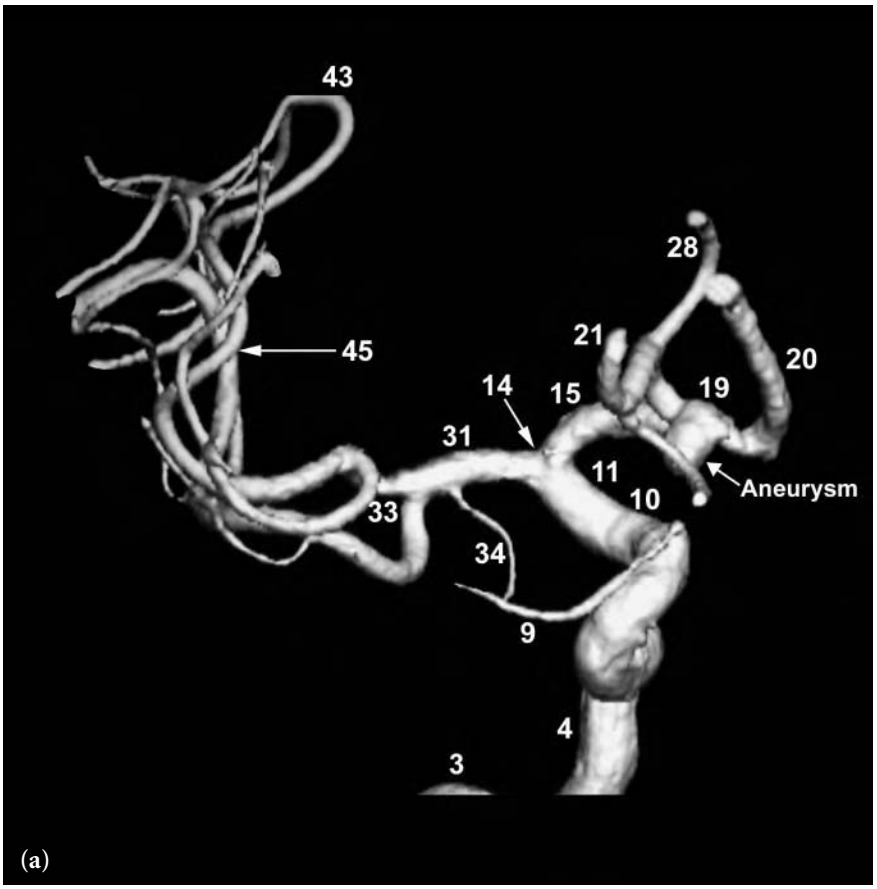

Fig. 5.20 (a–c) 3D frontal (*a*), posterior (*b*), and medial (*c*) views following right internal carotid artery injection. These images show an aneurysm arising in the region of the anterior communicating artery. There is a small focal lobulation along the medial surface of the aneurysm that represents an area of weakness of the aneurysm wall and a potential site for rupture. Note the additional tiny aneurysms within the intracavernous segment of the internal carotid artery.

FIGURE KEY

2 internal carotid artery – vertical petrous segment
3 internal carotid artery – horizontal petrous segment
4 presellar (Fischer C5) segment internal carotid artery
6 horizontal (Fischer C4) intracavernous internal carotid artery
8 anterior genu (Fischer C3) intracavernous internal carotid artery
9 ophthalmic artery
10 & 11 proximal and distal supraclinoid segment internal carotid artery
14 internal carotid artery bifurcation
15 A1 segment of anterior cerebral artery
19 anterior communicating artery
20 proximal A2 segment anterior cerebral artery
31 M1 segment of middle cerebral artery
33 bifurcation/trifurcation of middle cerebral artery
34 anterior temporal lobe branches of middle cerebral artery
43 sylvian point
45 sylvian (insular) branches of middle cerebral artery
* origin of the posterior communicating artery
** origin of the anterior choroidal artery

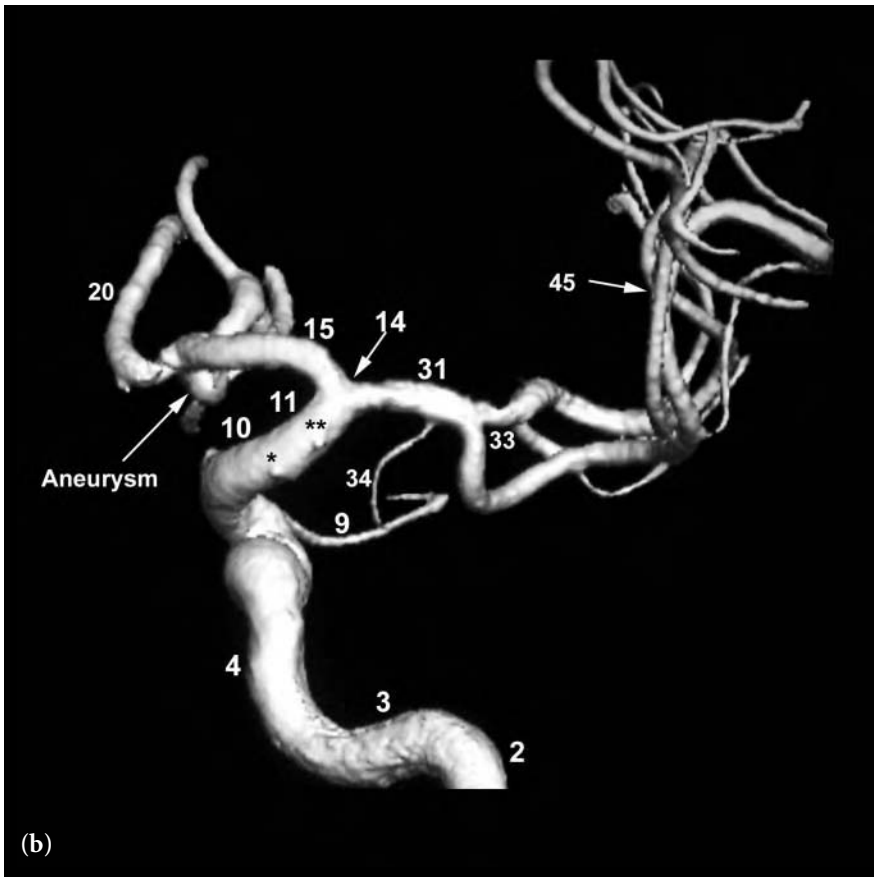
20
15
14
45
31
11
10
**
*
Aneurysm
33
34
9
4
3
2
(b)

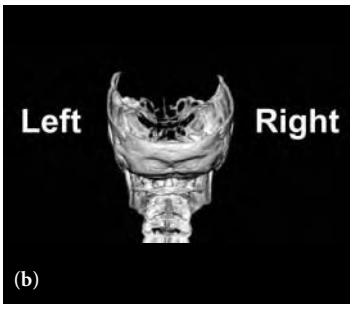
Left
Right
(b)

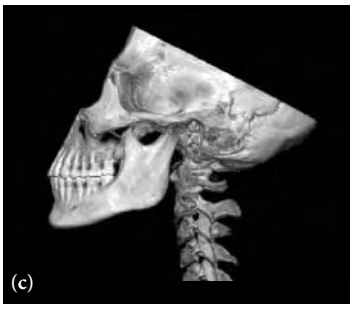
(c)

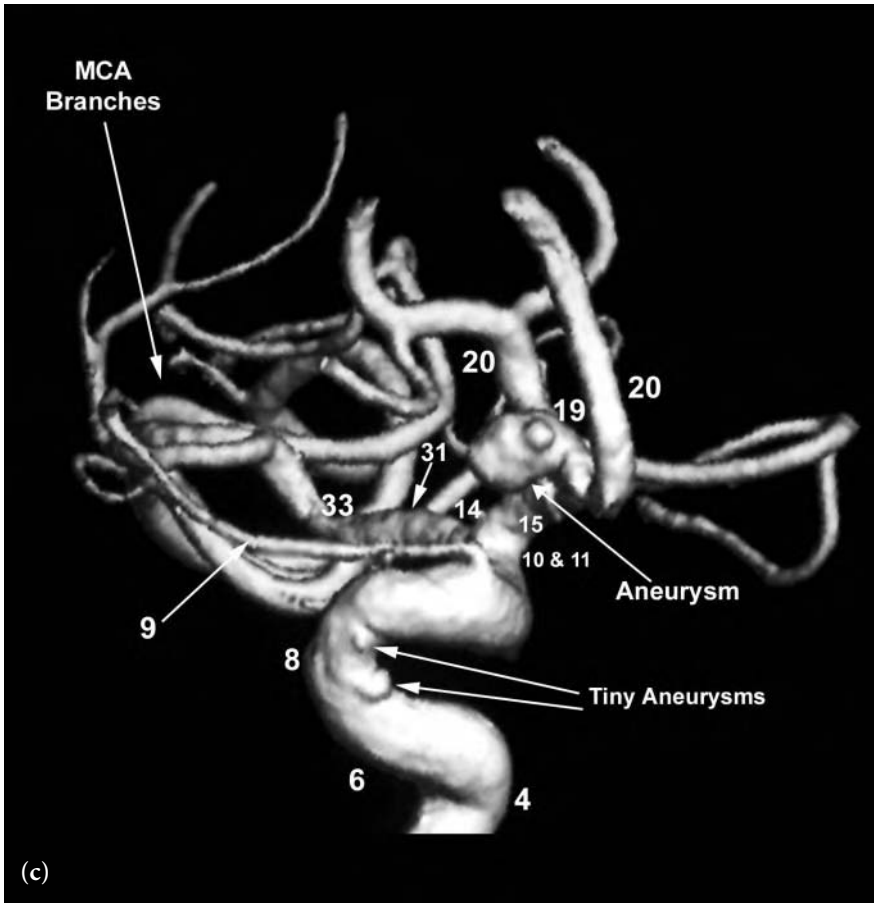
MCA
Branches
20
19
20
31
33
14
15
10 & 11
Aneurysm
9
8
Tiny Aneurysms
6
4
(c)

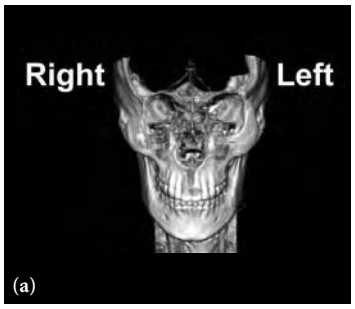

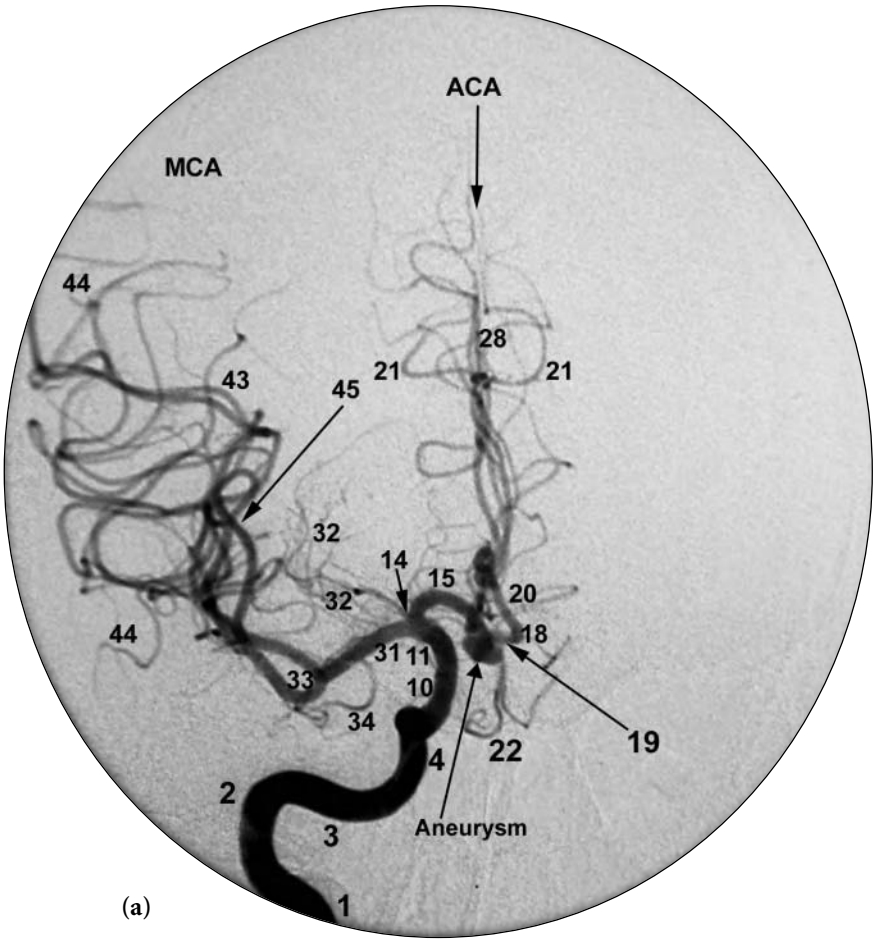

Fig. 5.21 (a–c) 2D frontal (*a*), 3D frontal (*b*), and 3D left posterior oblique (LPO) (*c*) views following right internal carotid artery injection. There is an aneurysm in the region of the anterior communicating artery.

FIGURE KEY

1 internal carotid artery – cervical segment
2 internal carotid artery – vertical petrous segment
3 internal carotid artery – horizontal petrous segment
4 presellar (Fischer C5) segment internal carotid artery
6 horizontal (Fischer C4) intracavernous internal carotid artery
10 & 11 proximal and distal supraclinoid segment internal carotid artery
14 internal carotid artery bifurcation
15 A1 segment of anterior cerebral artery
18 A1-A2 junction anterior cerebral artery
19 anterior communicating artery
20 proximal A2 segment anterior cerebral artery
21 callosomarginal branch of anterior cerebral artery
22 orbitofrontal branch of anterior cerebral artery
28 pericallosal branch of anterior cerebral artery
32 lateral lenticulostriate arteries
33 bifurcation/trifurcation of middle cerebral artery
34 anterior temporal lobe branches of middle cerebral artery
43 sylvian point
44 opercular branches of middle cerebral artery
45 sylvian (insular) branches of middle cerebral artery

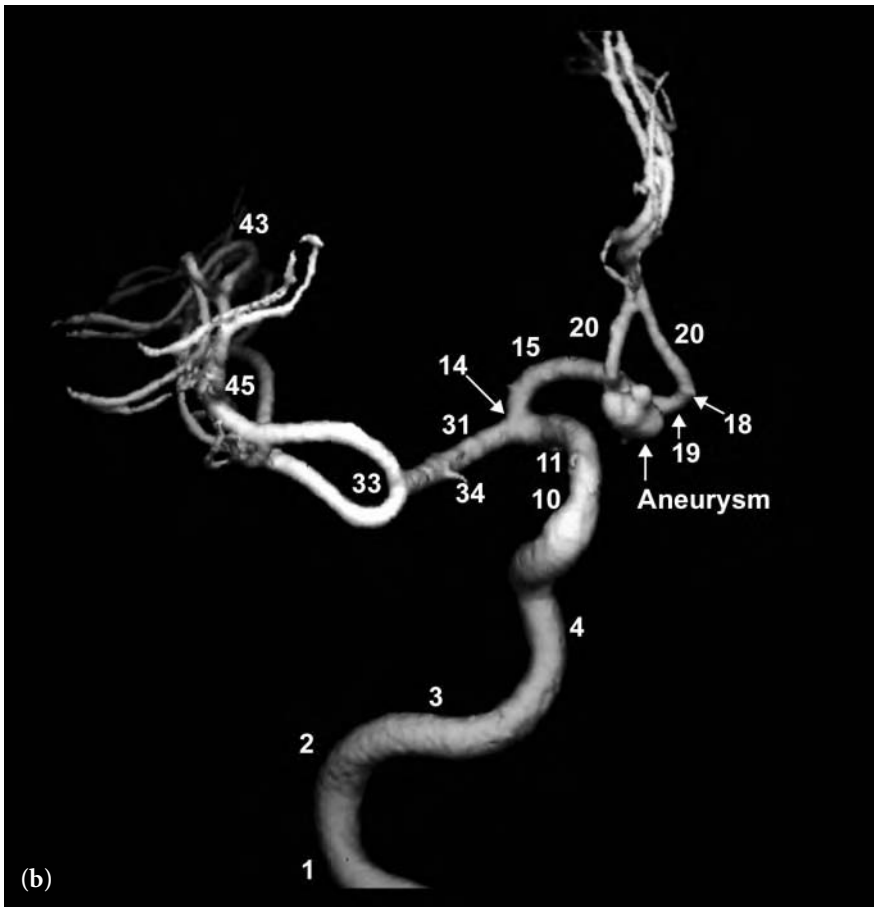
43
45
14
15
20
20
31
18
19
11
33
34
10
Aneurysm
4
3
2
1
(b)

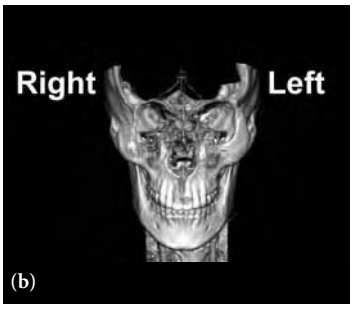
Right
Left
(b)

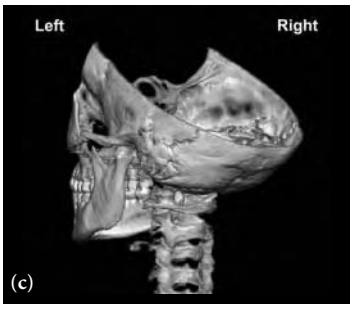
Left
Right
(c)

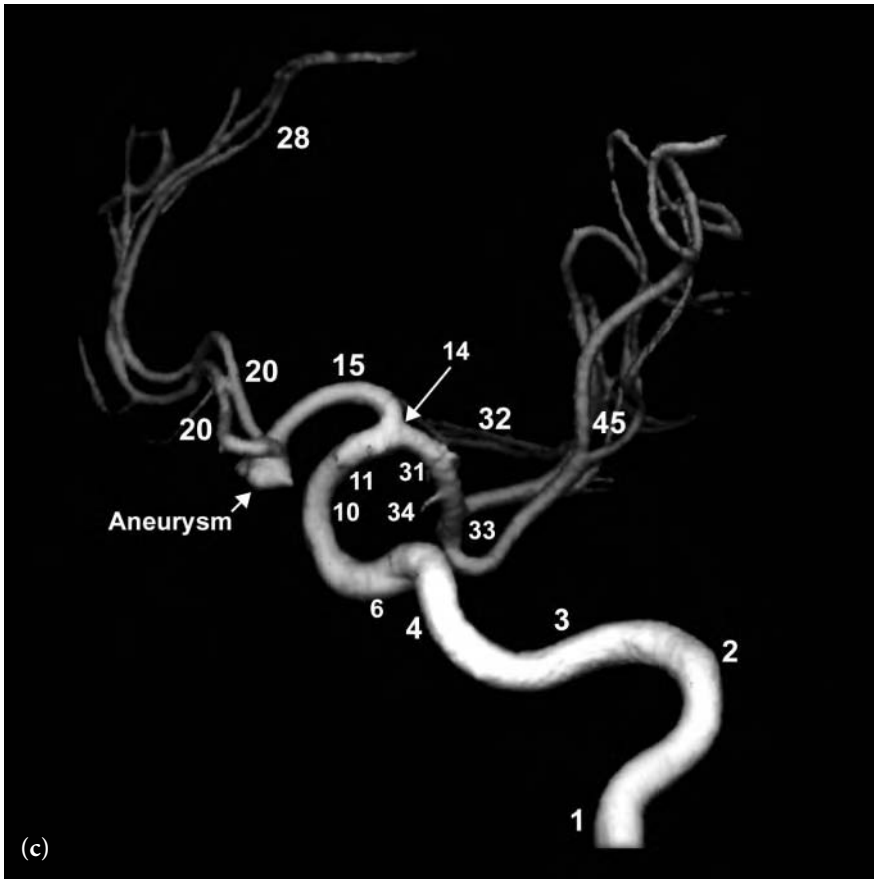
28
20
15
14
20
32
45
11
31
Aneurysm
10
34
33
6
4
3
2
1
(c)

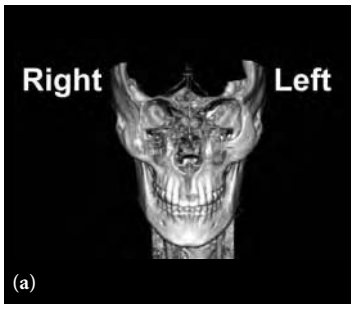

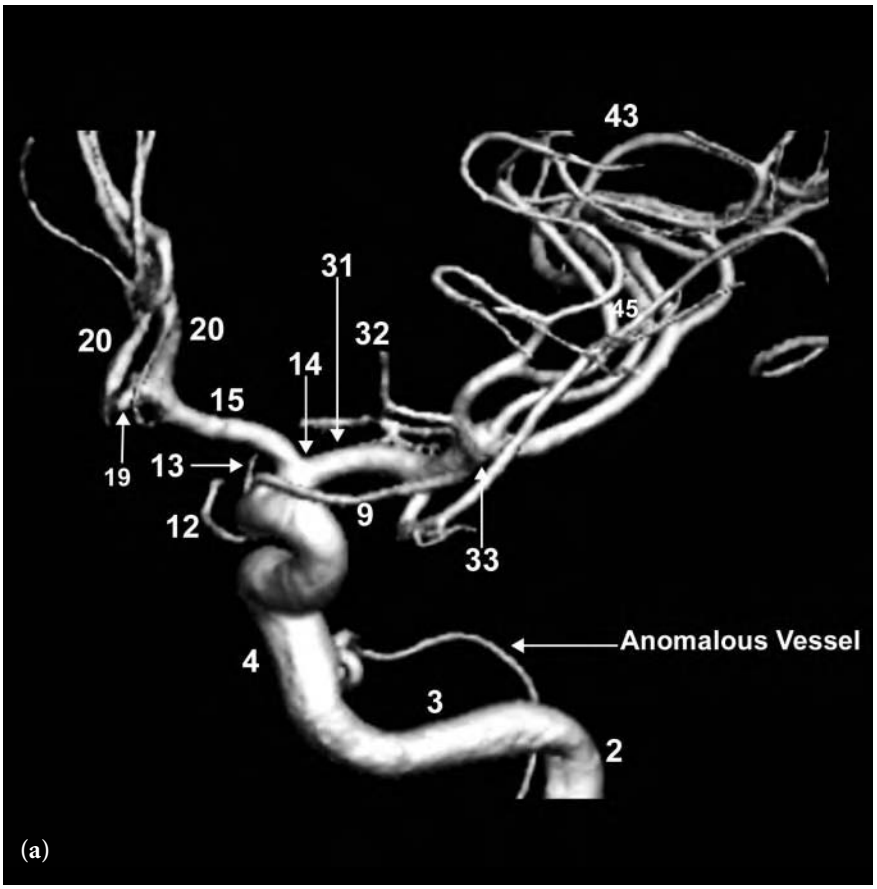

Fig. 5.22 (a–c) 3D frontal (*a*), posterior (*b*), and superior to inferior (*c*) views following left internal carotid artery injection. These images show an anomalous vessel between the presellar segment of the internal carotid artery and the cerebellum. Also note a tiny aneurysm (approximately 2 mm) along the posterior wall at the junction of the A1 and A2 segments of the left anterior cerebral artery.

FIGURE KEY

2 internal carotid artery – vertical petrous segment
3 internal carotid artery – horizontal petrous segment
4 presellar (Fischer C5) segment internal carotid artery
8 anterior genu (Fischer C3) intracavernous internal carotid artery
9 ophthalmic artery
10 & 11 proximal and distal supraclinoid segments internal carotid artery
12 posterior communicating artery
13 anterior choroidal artery
14 internal carotid artery bifurcation
15 A1 segment of anterior cerebral artery
18 A1-A2 junction anterior cerebral artery
19 anterior communicating artery
20 proximal A2 segment anterior cerebral artery
21 callosomarginal branch of anterior cerebral artery
28 pericallosal branch of anterior cerebral artery
31 M1 segment of middle cerebral artery
32 lateral lenticulostriate arteries
33 bifurcation/trifurcation of middle cerebral artery
43 sylvian point
45 sylvian (insular) branches of middle cerebral artery
An Aneurysm

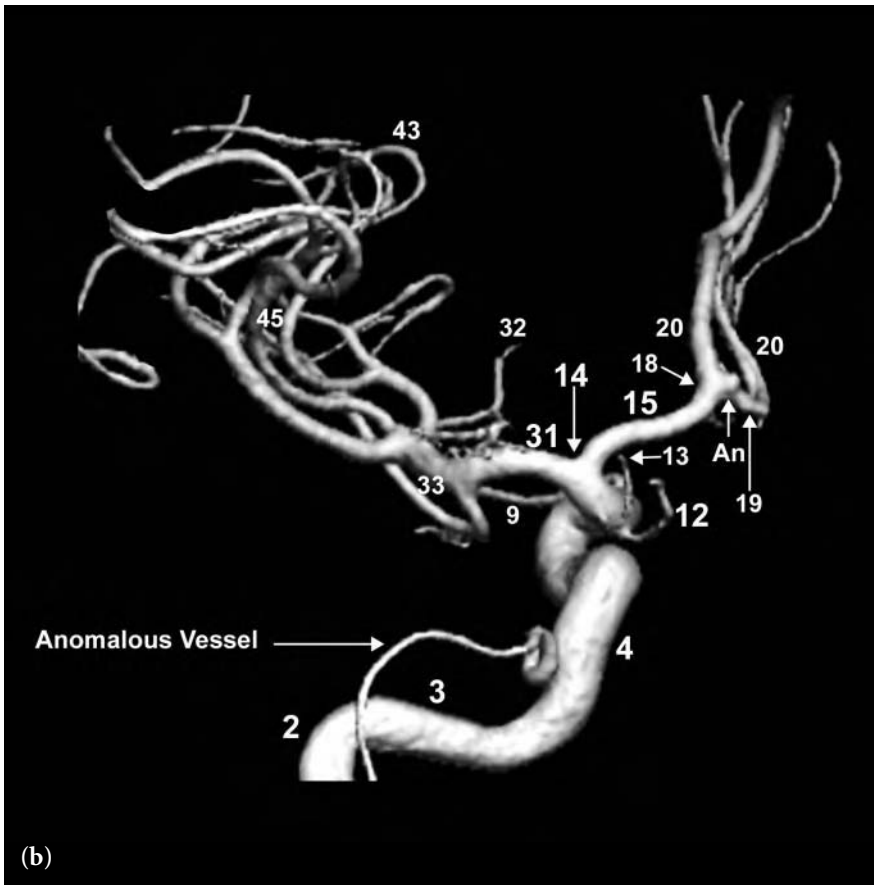
43
45
32
20
18
20
14
15
31
13
An
33
9
12
19
Anomalous Vessel
4
3
2
(b)

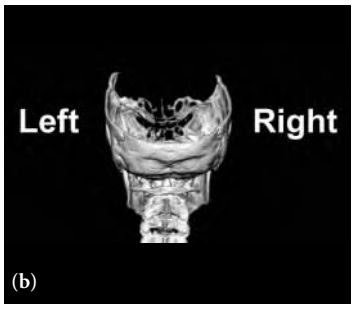
Left
Right
(b)

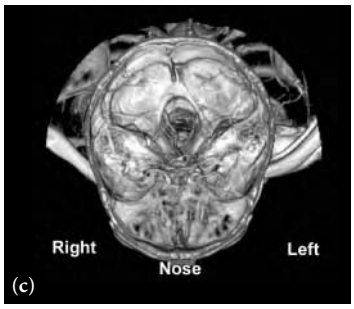
Right
Nose
Left
(c)

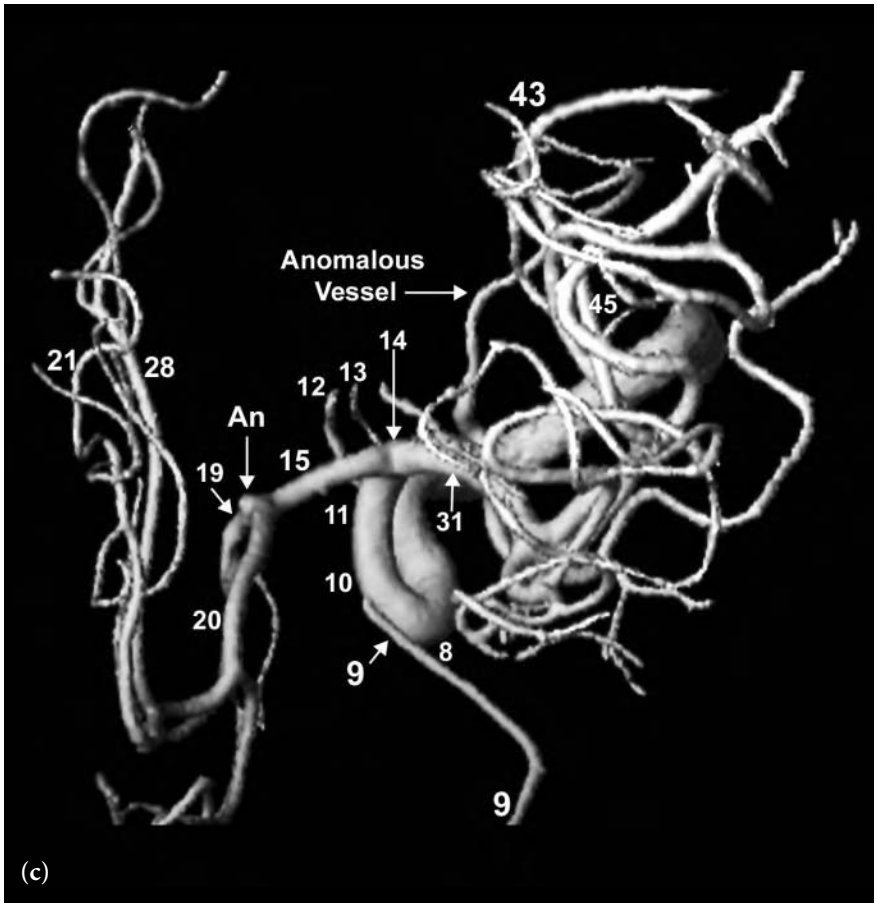
43
Anomalous
Vessel
45
14
21
28
12
13
An
19
15
11
31
10
20
9
8
9
(c)

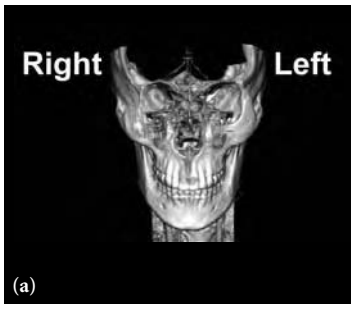

Fig. 5.23 (a–c) 3D frontal (*a*), left anterior oblique (LAO) (*b*), and posterior (*c*) views following left internal carotid artery injection. There is a "boot" shaped aneurysm rising in the region of the left middle cerebral artery bifurcation/trifurcation.

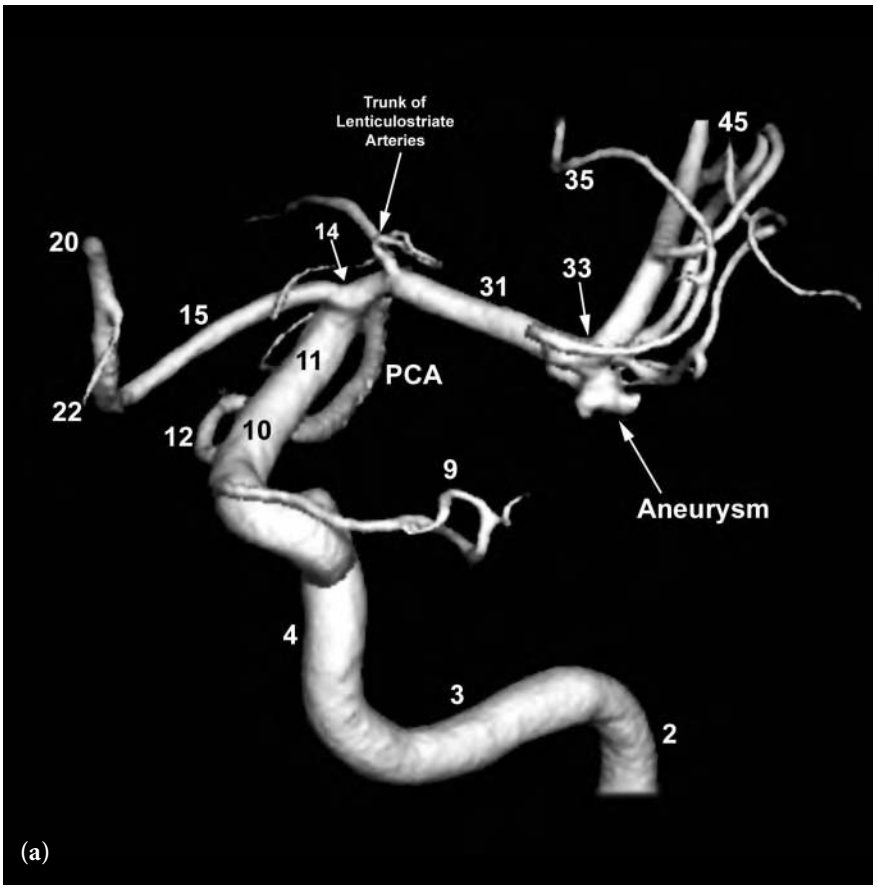

FIGURE KEY

2 internal carotid artery – vertical petrous segment
3 internal carotid artery – horizontal petrous segment
4 presellar (Fischer C5) segment internal carotid artery
6 horizontal (Fischer C4) intracavernous internal carotid artery
8 anterior genu (Fischer C3) intracavernous internal carotid artery
9 ophthalmic artery
10 & 11 proximal and distal supraclinoid segments internal carotid artery
12 posterior communicating artery
13 anterior choroidal artery
14 internal carotid artery bifurcation
15 A1 segment of anterior cerebral artery
16 medial lenticulostriate artery
18 A1-A2 junction anterior cerebral artery
20 proximal A2 segment anterior cerebral artery
22 orbitofrontal branch of anterior cerebral artery
31 M1 segment of middle cerebral artery
33 bifurcation/trifurcation of middle cerebral artery
35 orbitofrontal branch of middle cerebral artery
45 sylvian (insular) branches of middle cerebral artery
PCA posterior cerebral artery

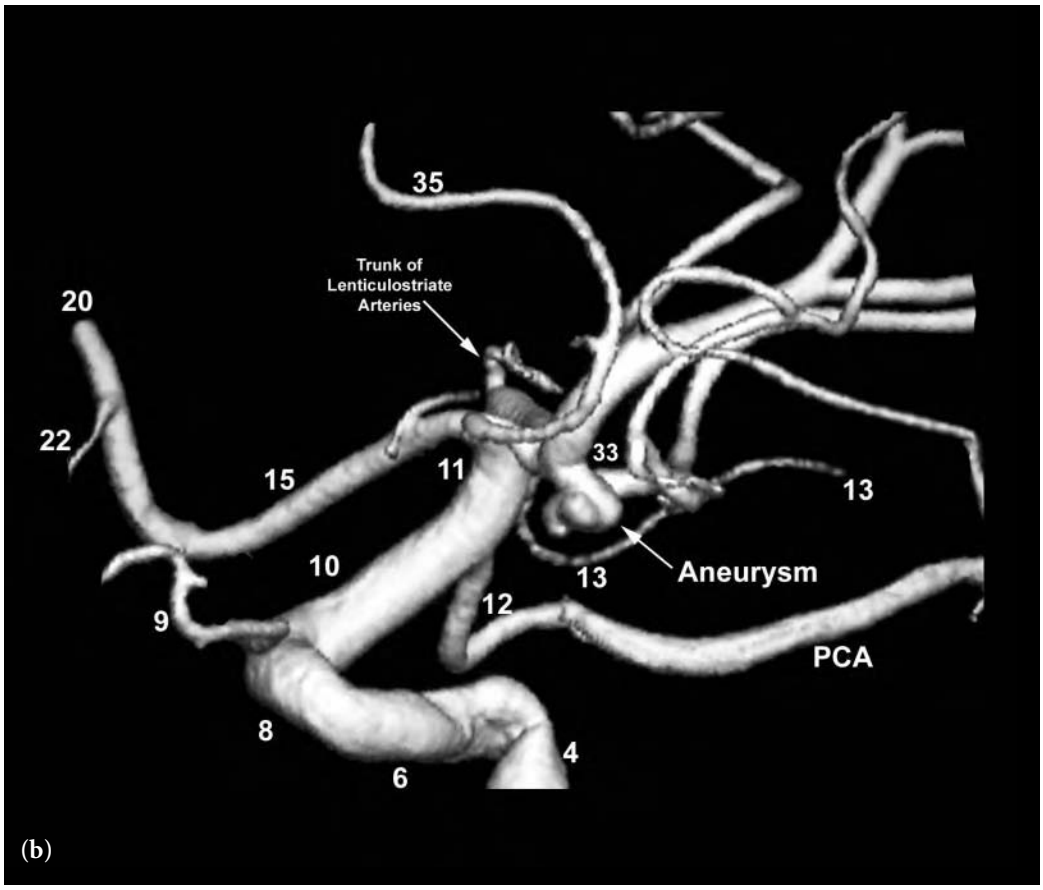
35
Trunk of
Lenticulostriate
Arteries
20
22
15
11
33
13
10
13
Aneurysm
12
9
PCA
8
4
6
(b)

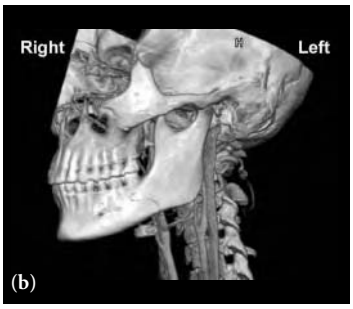
Right
Left
(b)

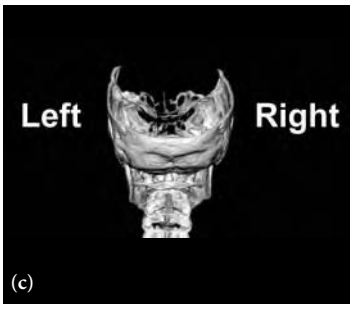
Left
Right
(c)

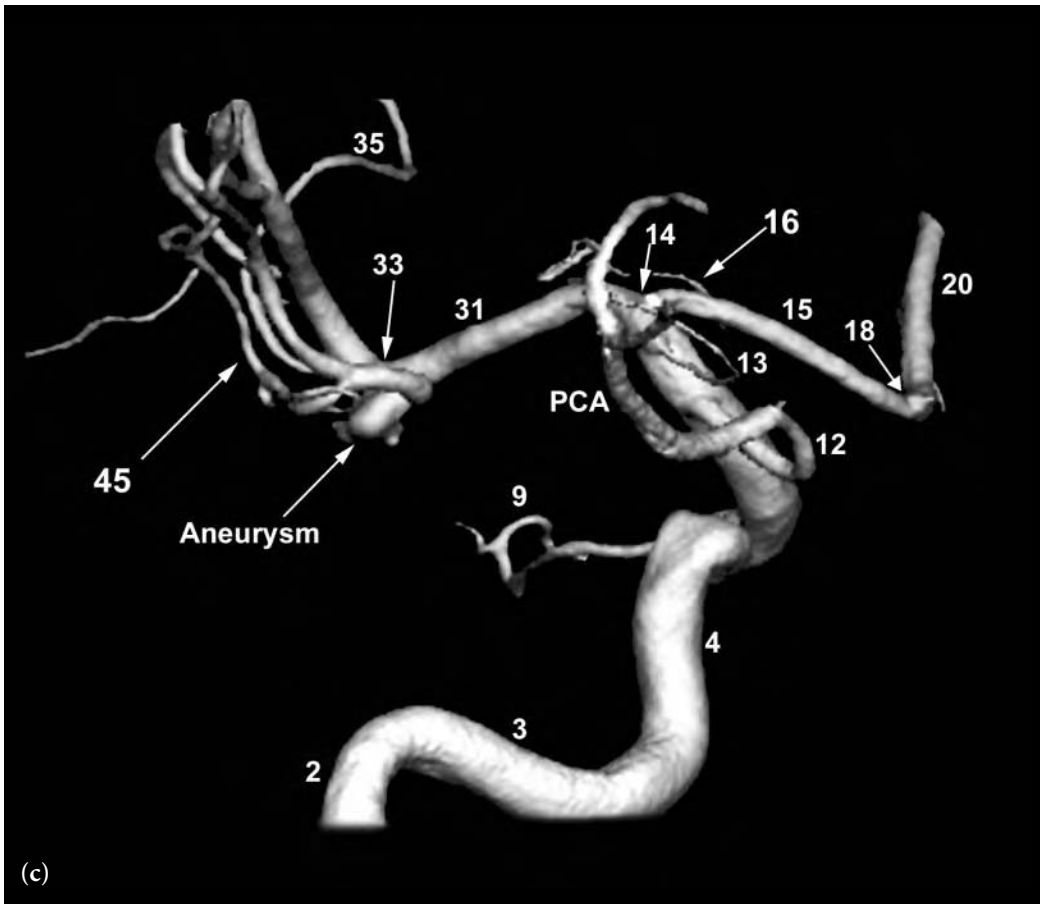
35
14
16
33
31
20
15
18
13
PCA
12
45
9
Aneurysm
4
3
2
(c)

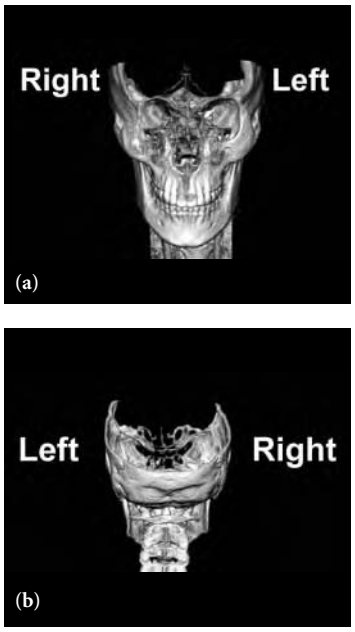

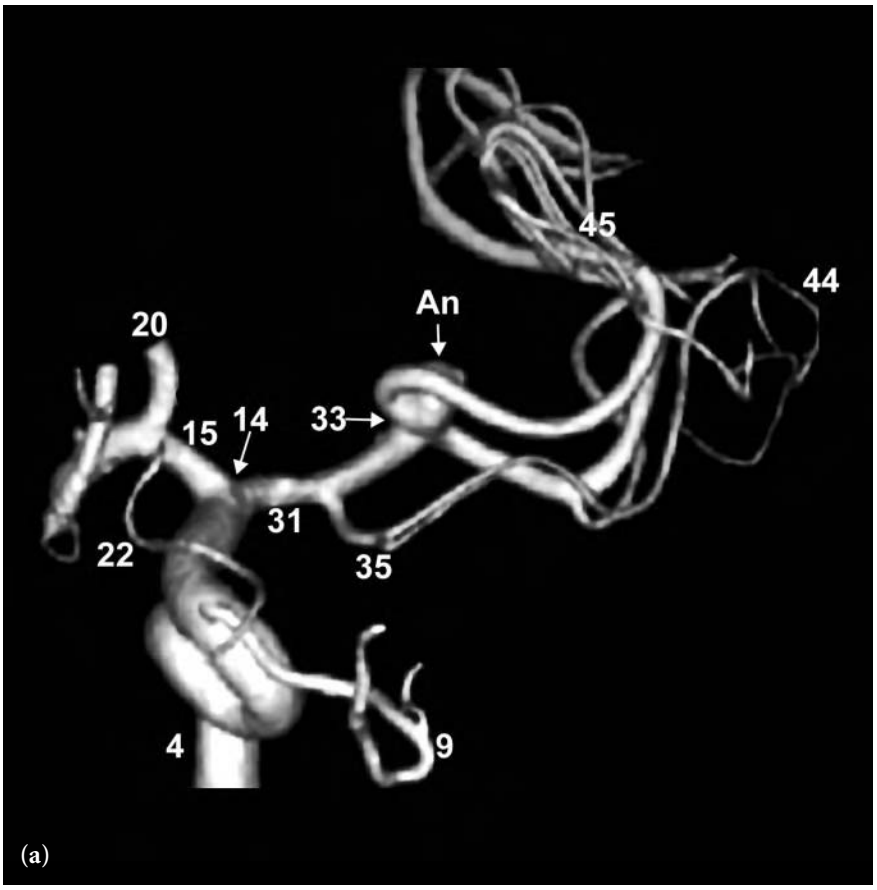

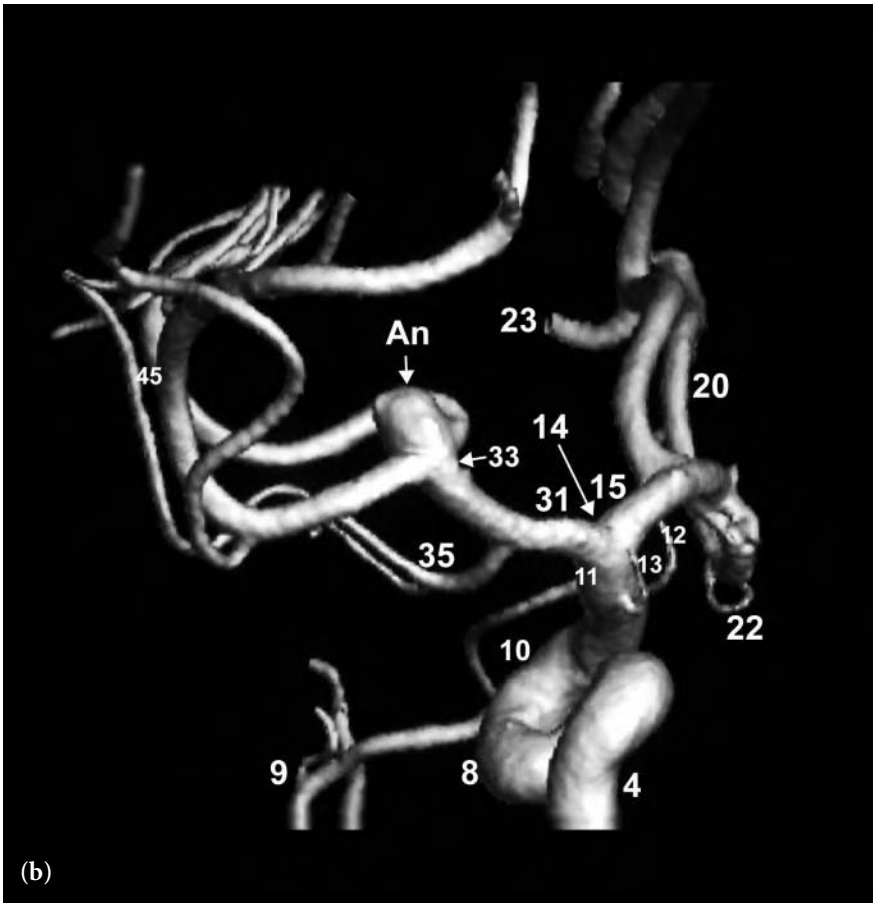

Fig. 5.24 (a–d) 3D frontal (*a*), posterior (*b*), left posterior oblique (LPO) with tilt (*c*), and lateral (*d*) views following left internal carotid artery injection. There is an aneurysm arising in the region of the middle cerebral artery bifurcation.

FIGURE KEY

1 internal carotid artery – cervical segment
2 internal carotid artery – vertical petrous segment
3 internal carotid artery – horizontal petrous segment
4 presellar (Fischer C5) segment internal carotid artery
6 horizontal (Fischer C4) intracavernous internal carotid artery
8 anterior genu (Fischer C3) intracavernous internal carotid artery
9 ophthalmic artery
10 & 11 proximal and distal supraclinoid segments internal carotid artery
12 posterior communicating artery
13 anterior choroidal artery
14 internal carotid artery bifurcation
15 A1 segment of anterior cerebral artery
18 A1-A2 junction anterior cerebral artery
19 anterior communicating artery
20 proximal A2 segment anterior cerebral artery
22 orbitofrontal branch of anterior cerebral artery
23 frontopolar branch of anterior cerebral artery
31 M1 segment of middle cerebral artery
33 bifurcation of middle cerebral artery
35 orbitofrontal branch of middle cerebral artery
D dome of aneurysm
An aneurysm

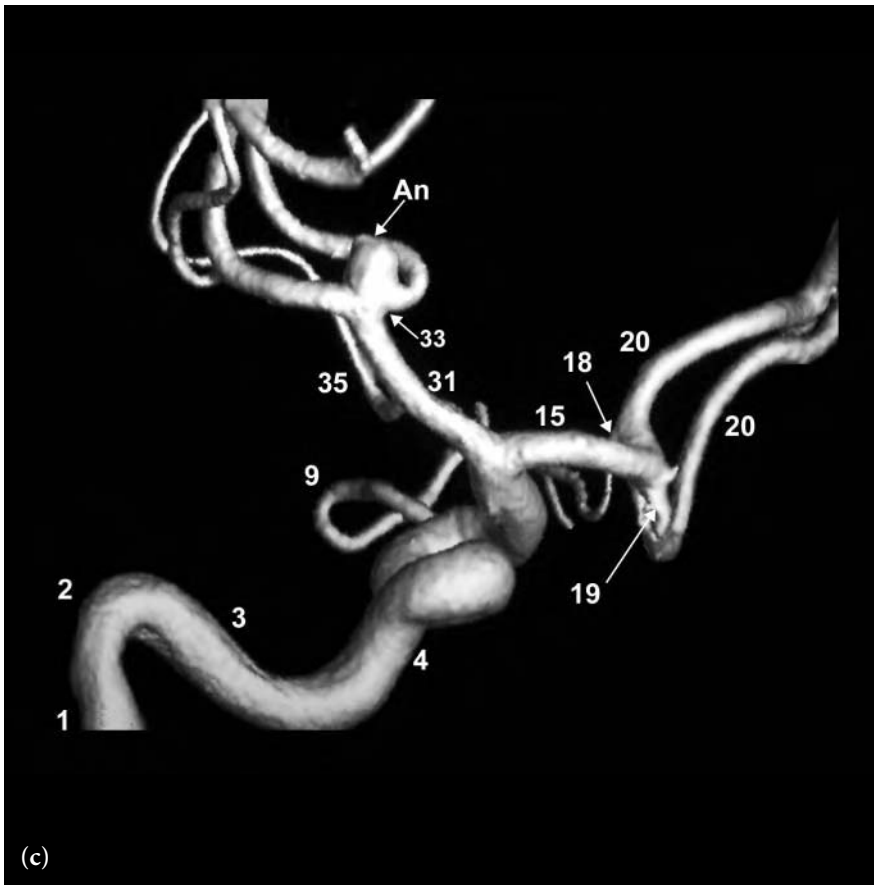
An
33
35
31
18
20
15
20
9
19
2
3
4
1
(c)

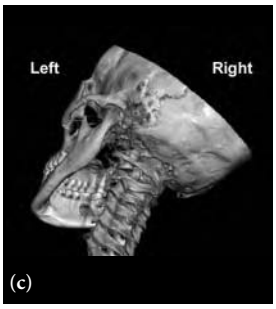
Left
Right
(c)

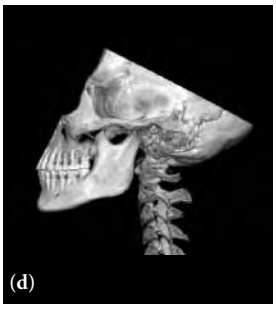
(d)

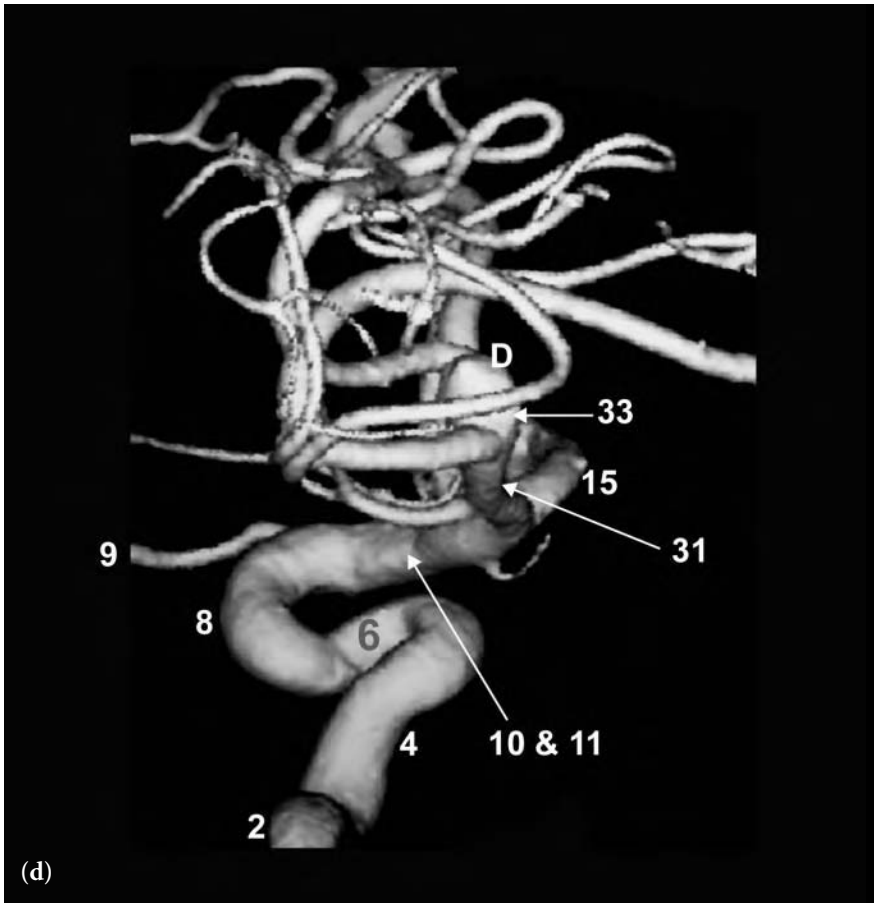
D
33
15
31
9
8
6
4
10 & 11
2
(d)

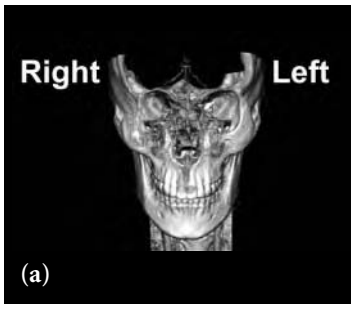

Fig. 5.25 (a–e) 2D frontal (*a*), 2D frontal magnified (*b*), 3D frontal (*c*), 3D posterior (*d*), and 3D inferior to superior (*e*) views following left internal carotid artery injections. These images show an aneurysm in the region of the left middle cerebral artery bifurcation/trifurcation. In image (*b*) you can see a microcatheter and coils within the aneurysm during endovascular occlusion.

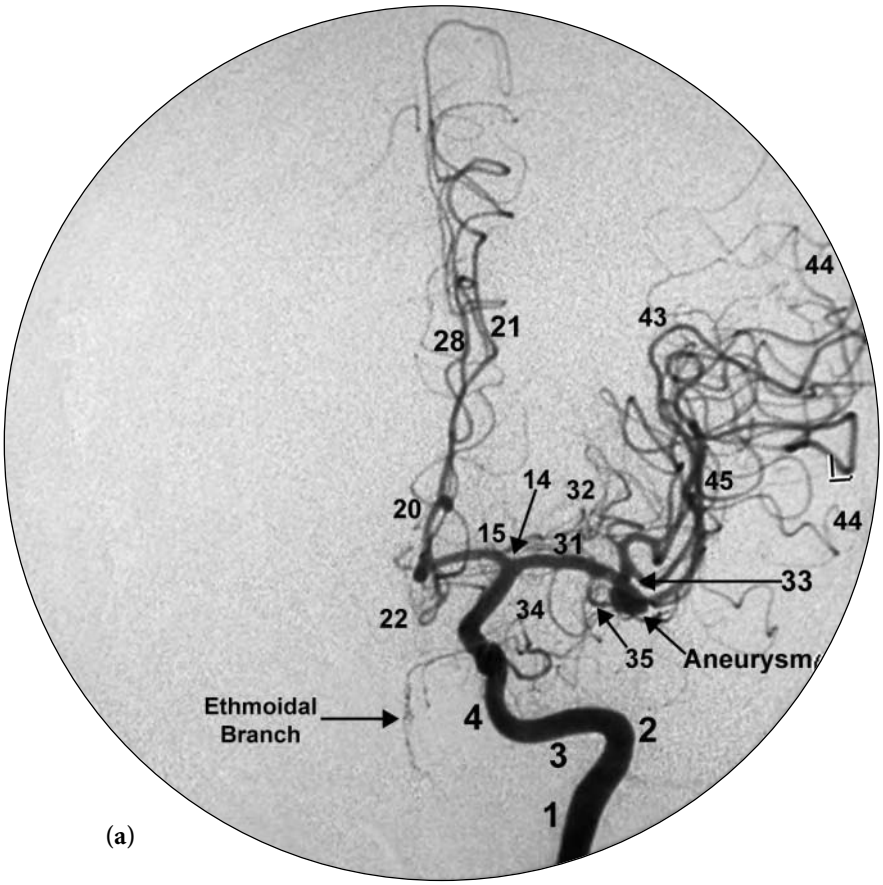

FIGURE KEY

2 internal carotid artery – vertical petrous segment
3 internal carotid artery – horizontal petrous segment
4 presellar (Fischer C5) segment internal carotid artery
6 horizontal (Fischer C4) intracavernous internal carotid artery
8 anterior genu (Fischer C3) intracavernous internal carotid artery
9 ophthalmic artery
10 & 11 proximal and distal supraclinoid segments internal carotid artery
12 posterior communicating artery
13 anterior choroidal artery
14 internal carotid artery bifurcation
15 A1 segment of anterior cerebral artery
18 A1-A2 junction anterior cerebral artery
20 proximal A2 segment anterior cerebral artery
21 callosomarginal branch of anterior cerebral artery
22 orbitofrontal branch of anterior cerebral artery
28 pericallosal branch of anterior cerebral artery
31 M1 segment of middle cerebral artery
32 lateral lenticulostriate arteries
33 bifurcation/trifurcation of middle cerebral artery
34 anterior temporal lobe branches of middle cerebral artery
35 orbitofrontal branch of middle cerebral artery
43 sylvian point
44 opercular branches of middle cerebral artery
45 sylvian (insular) branches of middle cerebral artery
* GDC coils in aneurysm sac (b)

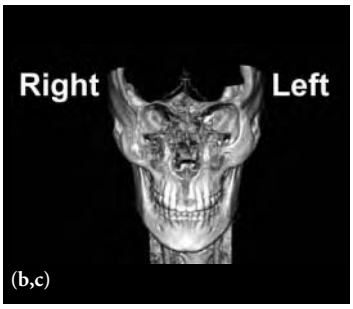
Right
Left
(b,c)

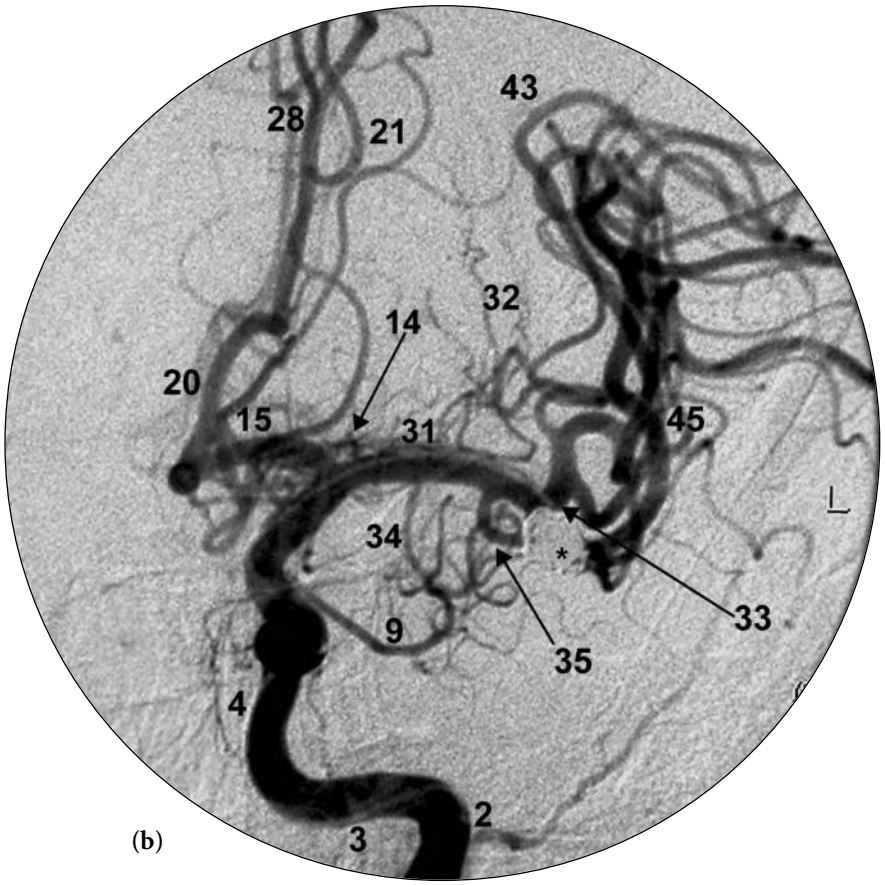
43
28
21
32
14
20
15
31
45
34
*
33
9
35
4
2
3

(**b**)

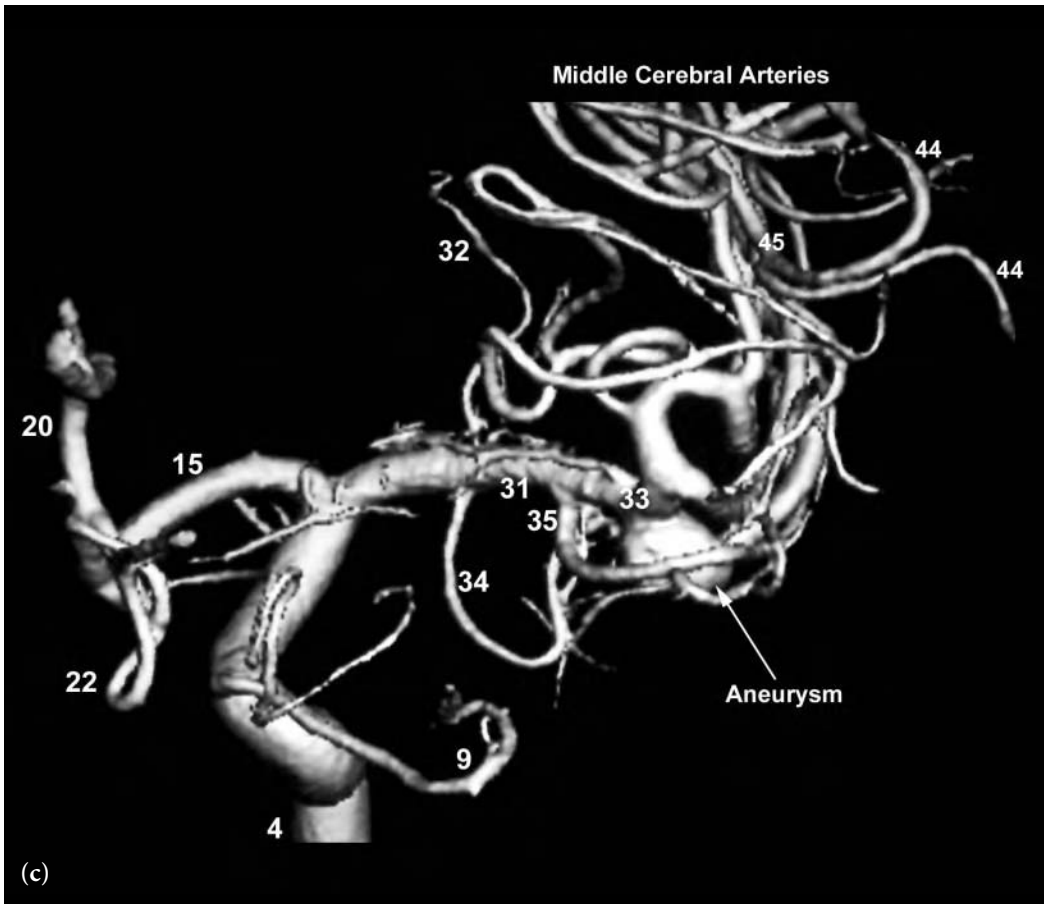
Middle Cerebral Arteries
44
32
45
44
20
15
31
33
35
34
22
Aneurysm
9
4

(**c**)

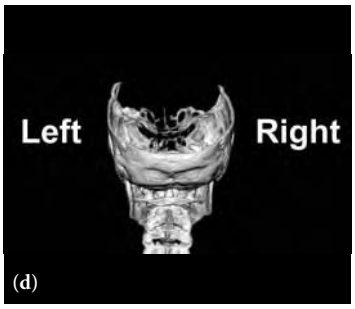

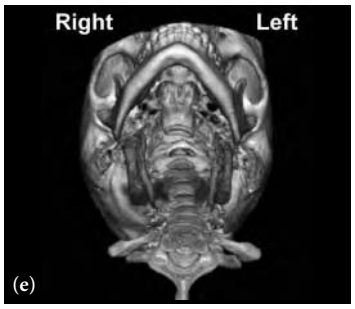

Fig. 5.25 (continued)

FIGURE KEY

2 internal carotid artery – vertical petrous segment
3 internal carotid artery – horizontal petrous segment
4 presellar (Fischer C5) segment internal carotid artery
6 horizontal (Fischer C4) intracavernous internal carotid artery
8 anterior genu (Fischer C3) intracavernous internal carotid artery
9 ophthalmic artery
10 & 11 proximal and distal supraclinoid segments internal carotid artery
12 posterior communicating artery
13 anterior choroidal artery
14 internal carotid artery bifurcation
15 A1 segment of anterior cerebral artery
18 A1-A2 junction anterior cerebral artery
20 proximal A2 segment anterior cerebral artery
21 callosomarginal branch of anterior cerebral artery
22 orbitofrontal branch of anterior cerebral artery
28 pericallosal branch of anterior cerebral artery
31 M1 segment of middle cerebral artery
32 lateral lenticulostriate arteries
33 bifurcation/trifurcation of middle cerebral artery
34 anterior temporal lobe branches of middle cerebral artery
35 orbitofrontal branch of middle cerebral artery
43 sylvian point
44 opercular branches of middle cerebral artery
45 sylvian (insular) branches of middle cerebral artery
* GDC coils in aneurysm sac (b)

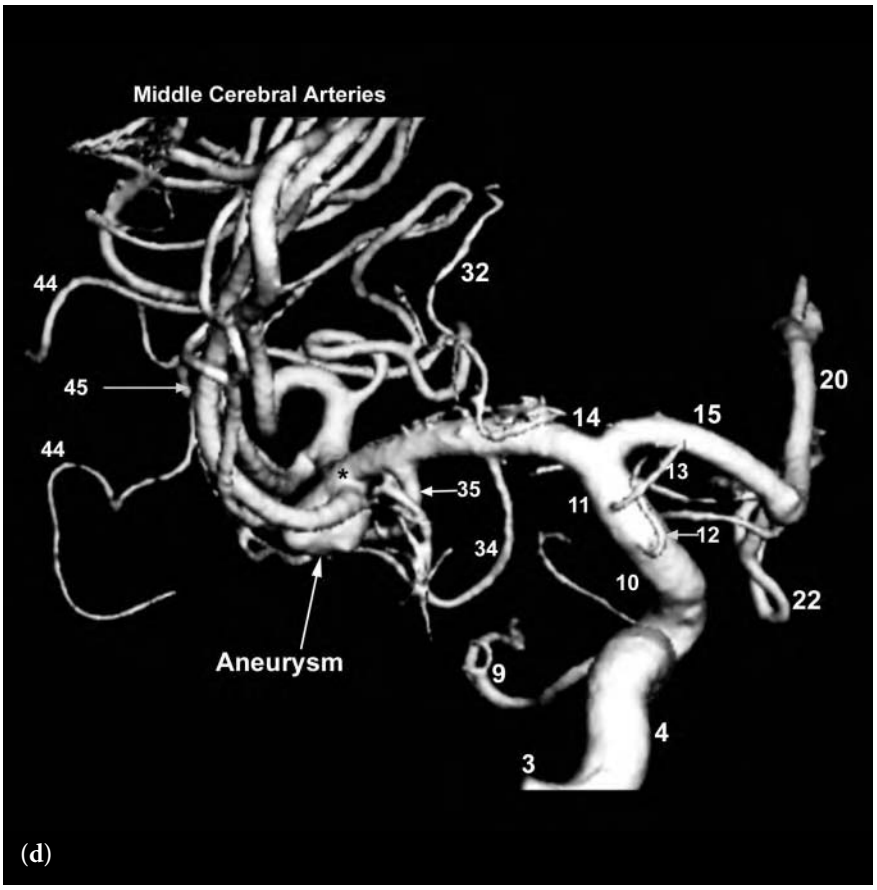

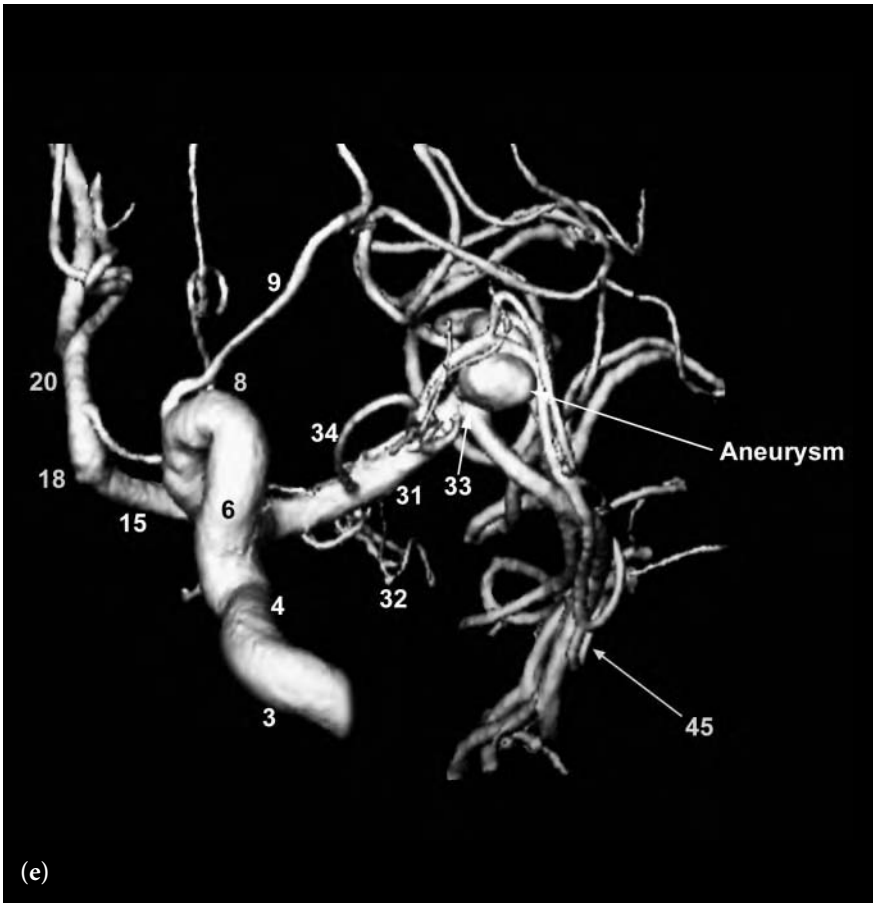

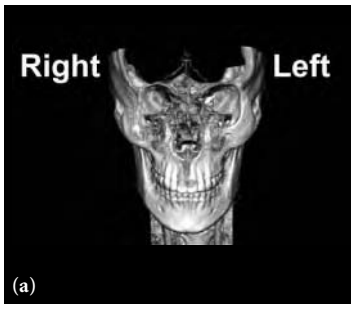

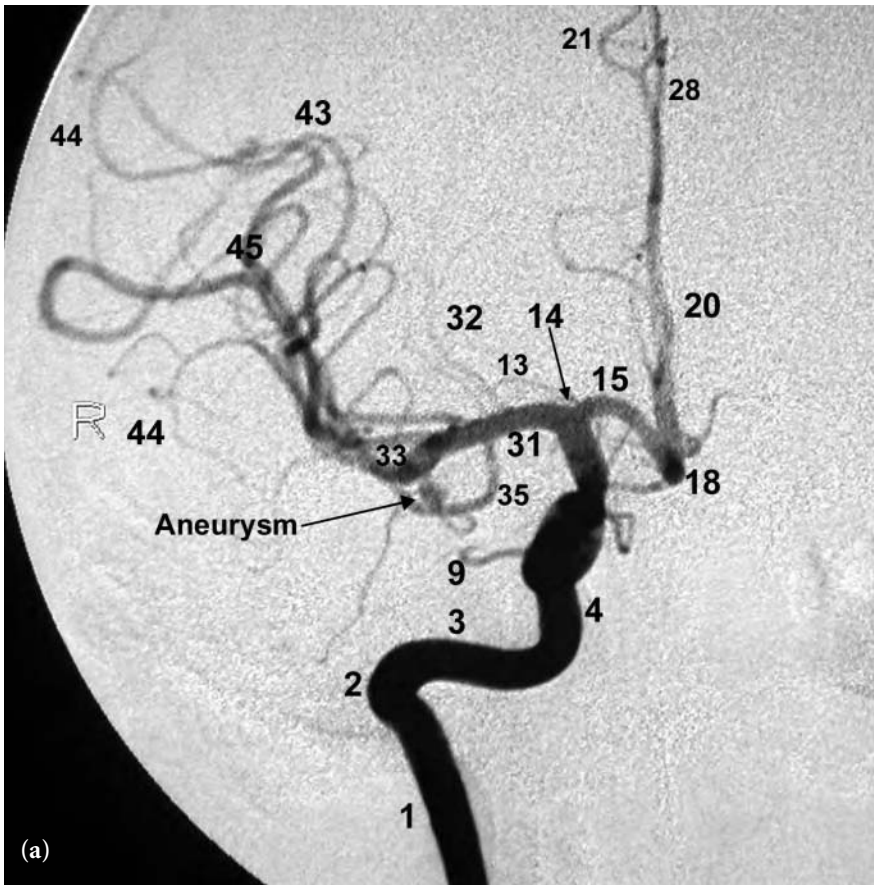

Fig. 5.26 (a–c) 2D frontal (*a*), 3D frontal (*b*), and 3D right anterior oblique (RAO) with tilt (*c*) views following right internal carotid artery injection. These views show a small aneurysm projecting inferiorly in the region of the right middle cerebral artery bifurcation.

FIGURE KEY

1 internal carotid artery – cervical segment
2 internal carotid artery – vertical petrous segment
3 internal carotid artery – horizontal petrous segment
4 presellar (Fischer C5) segment internal carotid artery
8 anterior genu (Fischer C3) intracavernous internal carotid artery
9 ophthalmic artery
10 & 11 proximal and distal supraclinoid segments internal carotid artery
13 anterior choroidal artery
14 internal carotid artery bifurcation
15 A1 segment of anterior cerebral artery
18 A1-A2 junction anterior cerebral artery
20 proximal A2 segment anterior cerebral artery
21 callosomarginal branch of anterior cerebral artery
22 orbitofrontal branch of anterior cerebral artery
23 frontopolar branch of anterior cerebral artery
28 pericallosal branch of anterior cerebral artery
31 M1 segment of middle cerebral artery
32 lateral lenticulostriate arteries
33 bifurcation/trifurcation of middle cerebral artery
35 orbitofrontal branch of middle cerebral artery
43 sylvian point
44 opercular branches of middle cerebral artery
45 sylvian (insular) branches of middle cerebral artery
An aneurysm

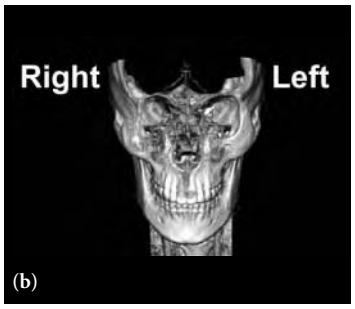

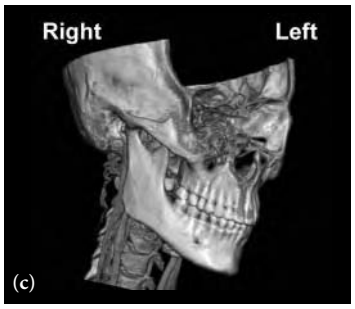

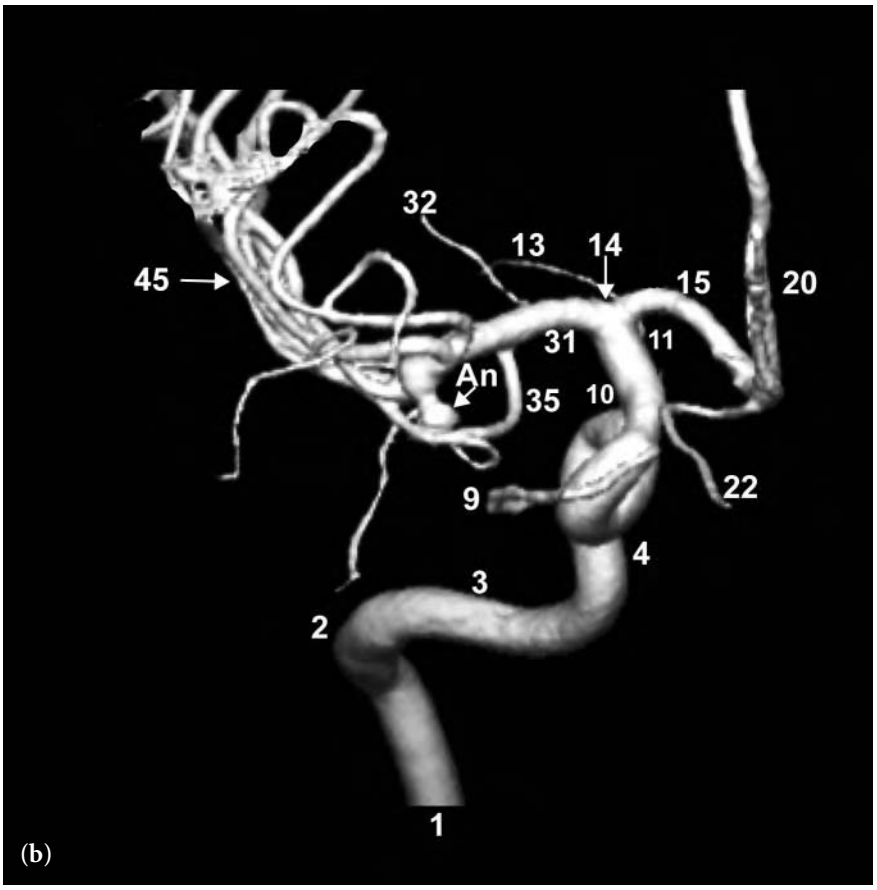

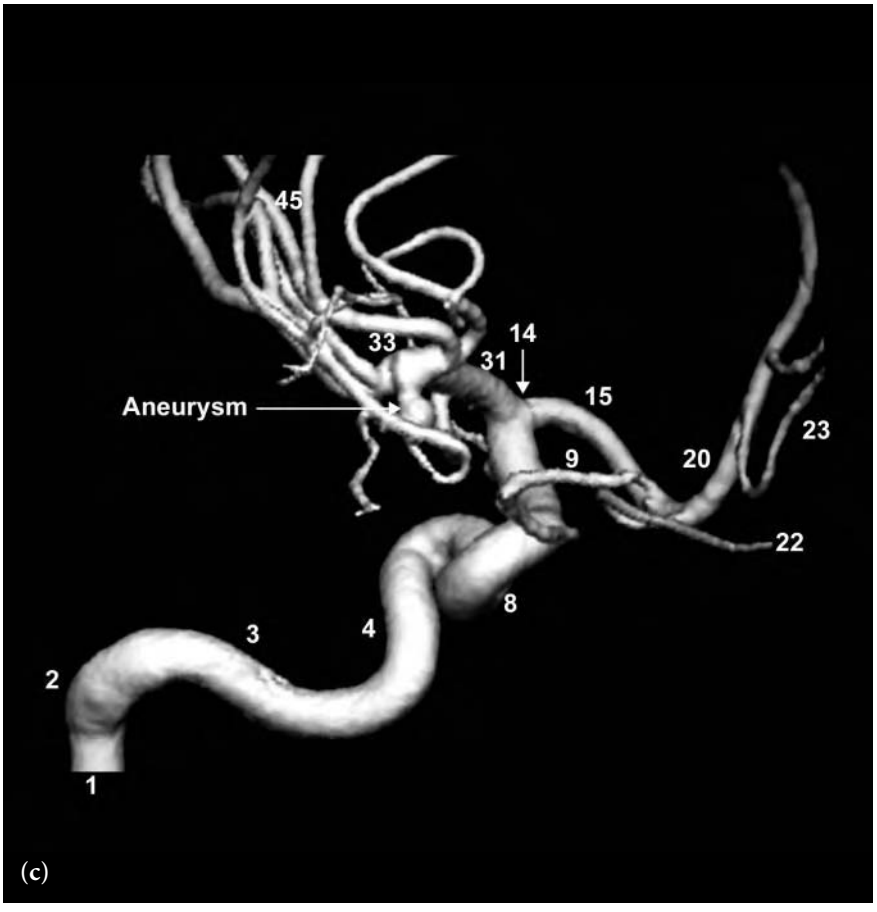

Fig. 5.26 (continued)

FIGURE KEY

1 internal carotid artery – cervical segment
2 internal carotid artery – vertical petrous segment
3 internal carotid artery – horizontal petrous segment
4 presellar (Fischer C5) segment internal carotid artery
8 anterior genu (Fischer C3) intracavernous internal carotid artery
9 ophthalmic artery
10 & 11 proximal and distal supraclinoid segments internal carotid artery
13 anterior choroidal artery
14 internal carotid artery bifurcation
15 A1 segment of anterior cerebral artery
18 A1-A2 junction anterior cerebral artery
20 proximal A2 segment anterior cerebral artery
21 callosomarginal branch of anterior cerebral artery
22 orbitofrontal branch of anterior cerebral artery
23 frontopolar branch of anterior cerebral artery
28 pericallosal branch of anterior cerebral artery
31 M1 segment of middle cerebral artery
32 lateral lenticulostriate arteries
33 bifurcation/trifurcation of middle cerebral artery
35 orbitofrontal branch of middle cerebral artery
43 sylvian point
44 opercular branches of middle cerebral artery
45 sylvian (insular) branches of middle cerebral artery
An aneurysm

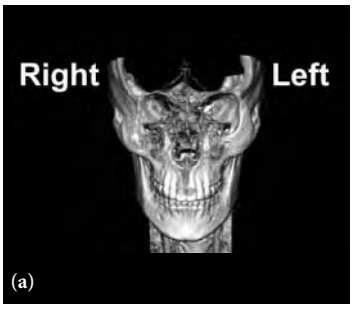

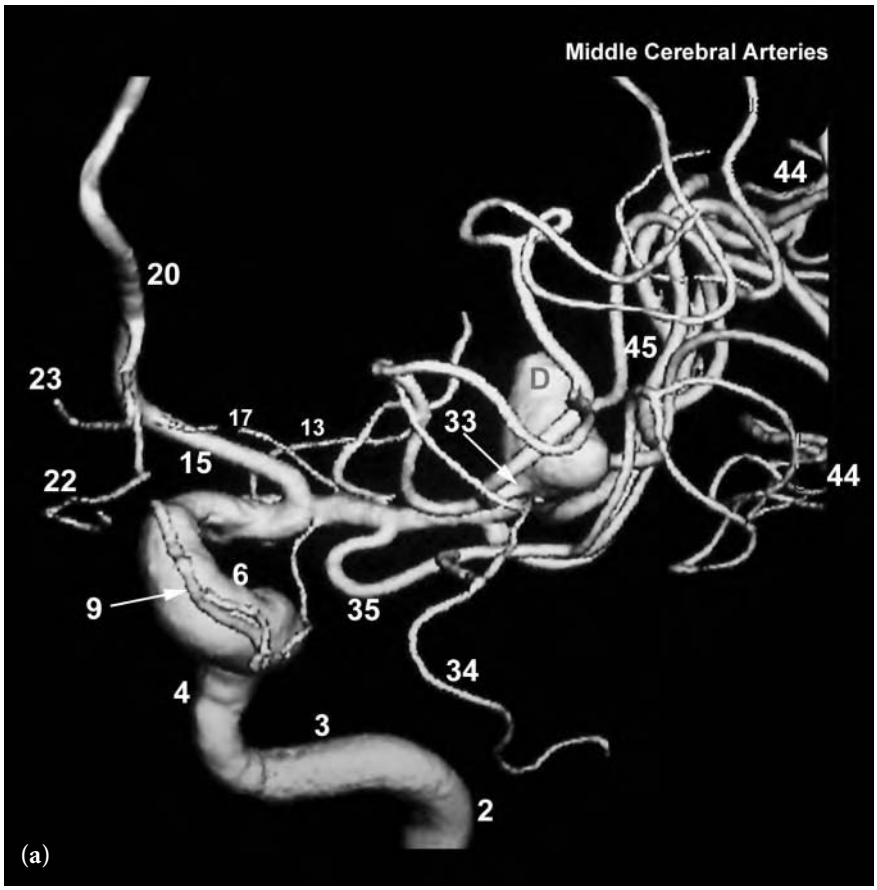

Fig. 5.27 (a–h) 3D frontal (*a*), 3D posterior (*b*), 3D right posterior oblique (*c*), 3D lateral (*d*), 3D oblique superior to inferior (*e*), 3D superior to inferior (*f*), and segmented 3D images (*g, h*)of an aneurysm and the surrounding middle cerebral artery branches. Left internal carotid artery injection was used. There is a large aneurysm in the region of the left middle cerebral artery bifurcation/trifurcation projecting superiorly which was imbedded in the temporal lobe.

FIGURE KEY

2 internal carotid artery – vertical petrous segment
3 internal carotid artery – horizontal petrous segment
4 presellar (Fischer C5) segment internal carotid artery
6 horizontal (Fischer C4) intracavernous internal carotid artery
8 anterior genu (Fischer C3) intracavernous internal carotid artery
9 ophthalmic artery
10 & 11 proximal and distal supraclinoid segments internal carotid artery
12 posterior communicating artery
13 anterior choroidal artery
14 internal carotid artery bifurcation
15 A1 segment of anterior cerebral artery
17 recurrent artery of Heubner
18 A1-A1 junction anterior cerebral artery
20 proximal A2 segment anterior cerebral artery
21 callosomarginal branch of anterior cerebral artery
22 orbitofrontal branch of anterior cerebral artery
23 frontopolar branch of anterior cerebral artery
28 pericallosal branch of anterior cerebral artery
31 M1 segment middle cerebral artery
32 lateral lenticulostriate arteries
33 bifurcation/trifurcation of middle cerebral artery
34 anterior temporal lobe branches of middle cerebral artery
35 orbitofrontal branch of middle cerebral artery
40 angular artery
44 opercular branches of middle cerebral artery
45 sylvian (insular) branches of middle cerebral artery
D dome of aneurysm

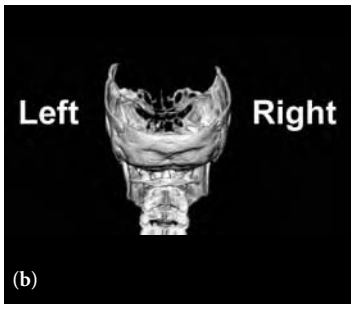

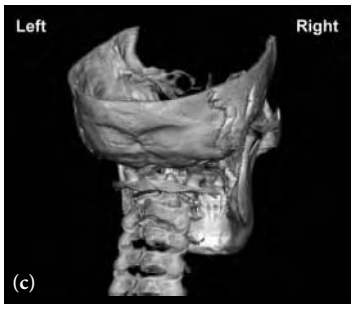

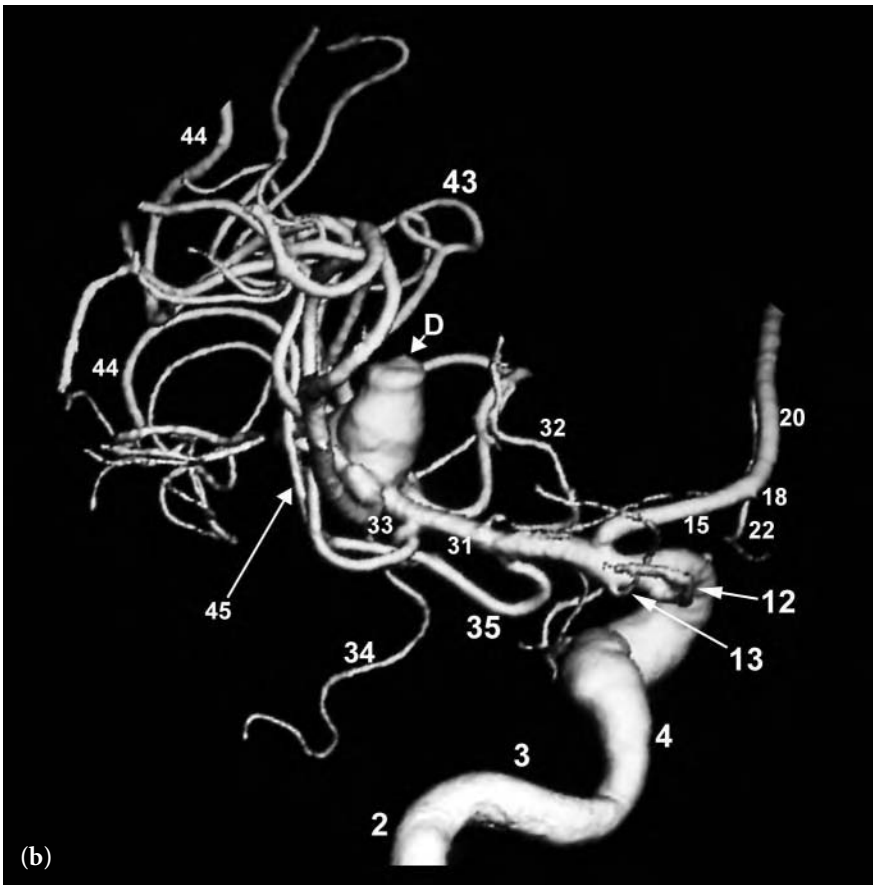

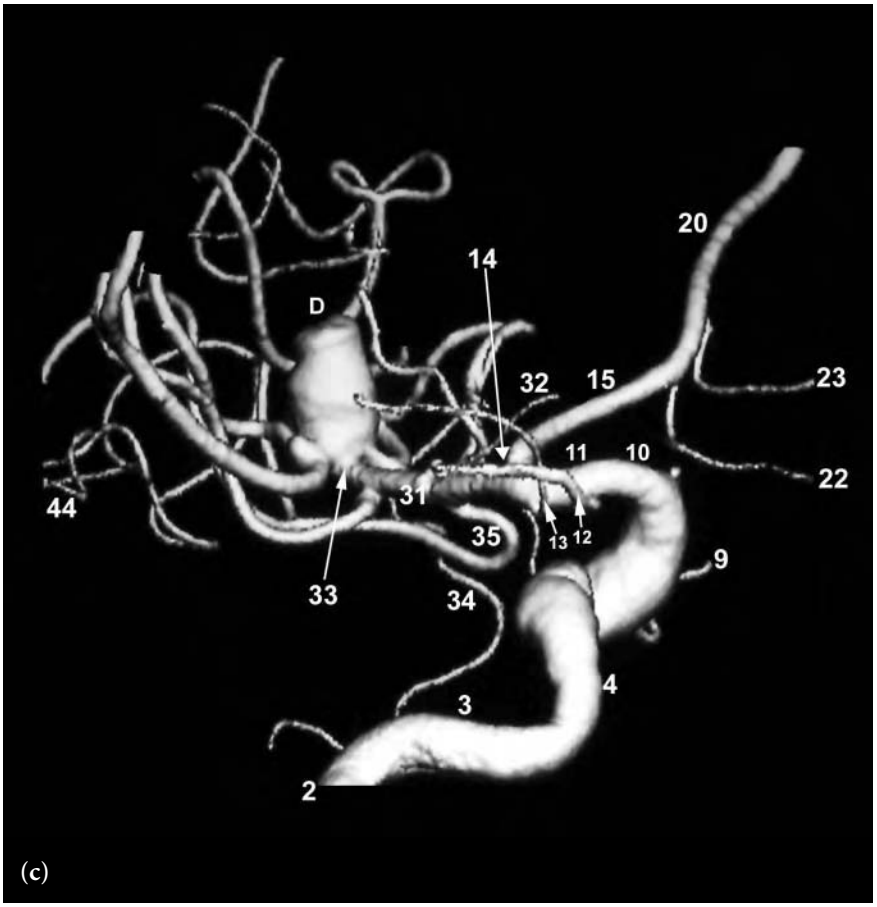

Fig. 5.27 (continued)

FIGURE KEY

2 internal carotid artery – vertical petrous segment
3 internal carotid artery – horizontal petrous segment
4 presellar (Fischer C5) segment internal carotid artery
6 horizontal (Fischer C4) intracavernous internal carotid artery
8 anterior genu (Fischer C3) intracavernous internal carotid artery
9 ophthalmic artery
10 & 11 proximal and distal supraclinoid segments internal carotid artery
12 posterior communicating artery
13 anterior choroidal artery
14 internal carotid artery bifurcation
15 A1 segment of anterior cerebral artery
18 A1-A1 junction anterior cerebral artery
20 proximal A2 segment anterior cerebral artery
21 callosomarginal branch of anterior cerebral artery
22 orbitofrontal branch of anterior cerebral artery
23 frontopolar branch of anterior cerebral artery
28 pericallosal branch of anterior cerebral artery
31 M1 segment middle cerebral artery
32 lateral lenticulostriate arteries
33 bifurcation/trifurcation of middle cerebral artery
34 anterior temporal lobe branches of middle cerebral artery
35 orbitofrontal branch of middle cerebral artery
40 angular artery
44 opercular branches of middle cerebral artery
45 sylvian (insular) branches of middle cerebral artery
D dome of aneurysm

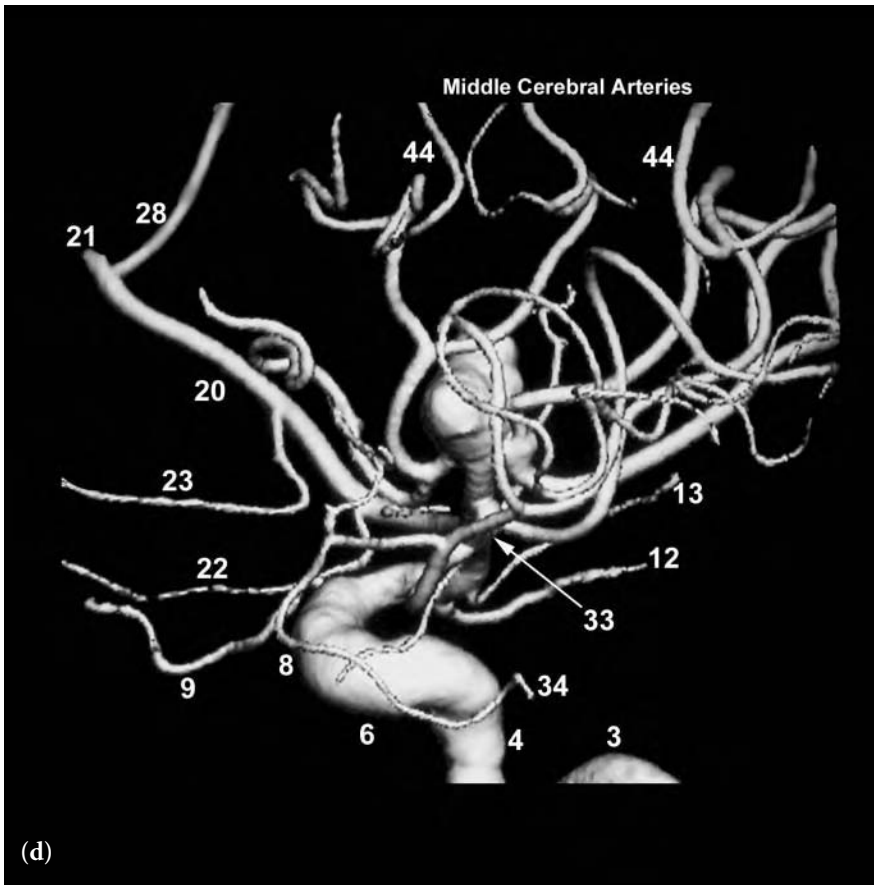
Middle Cerebral Arteries
44
44
28
21
20
23
13
22
12
33
9
8
34
6
4
3
(d)

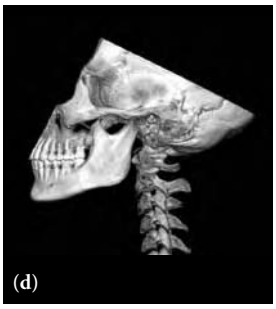
(d)

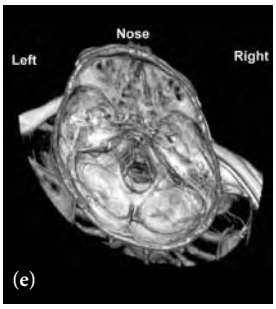
Nose
Left
Right
(e)

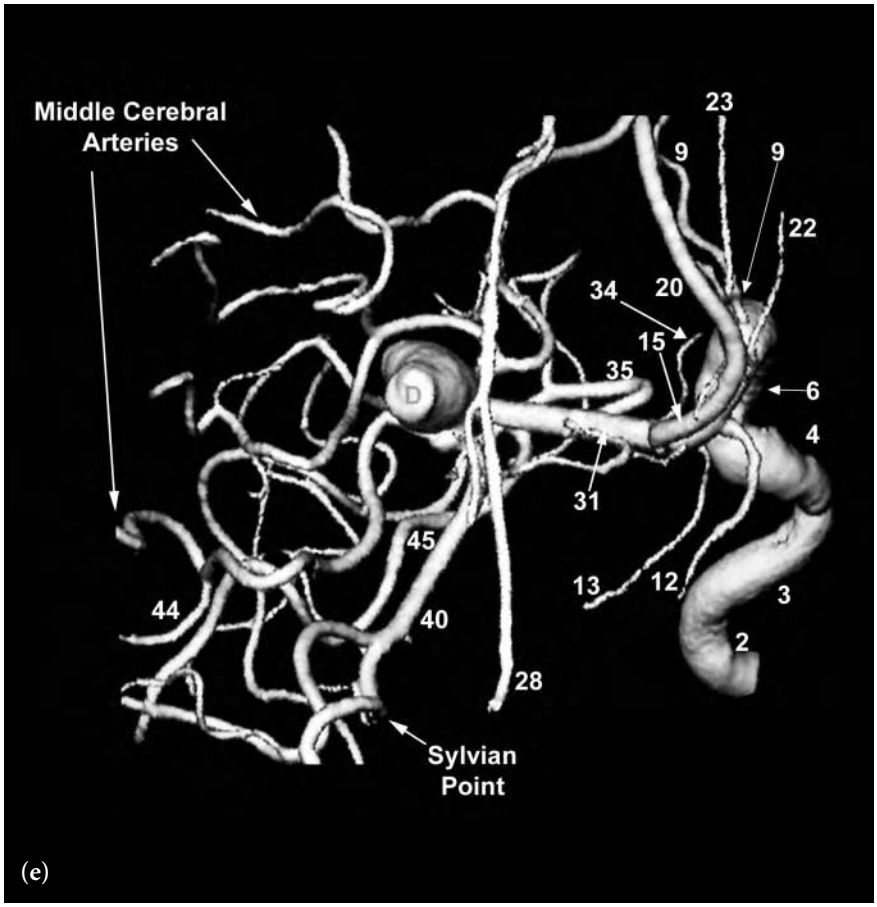
Middle Cerebral Arteries
23
9
9
22
34
20
15
35
6
4
31
45
13
12
3
44
40
2
28
Sylvian Point
(e)

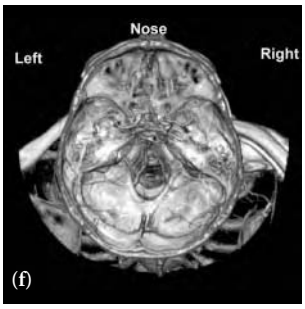

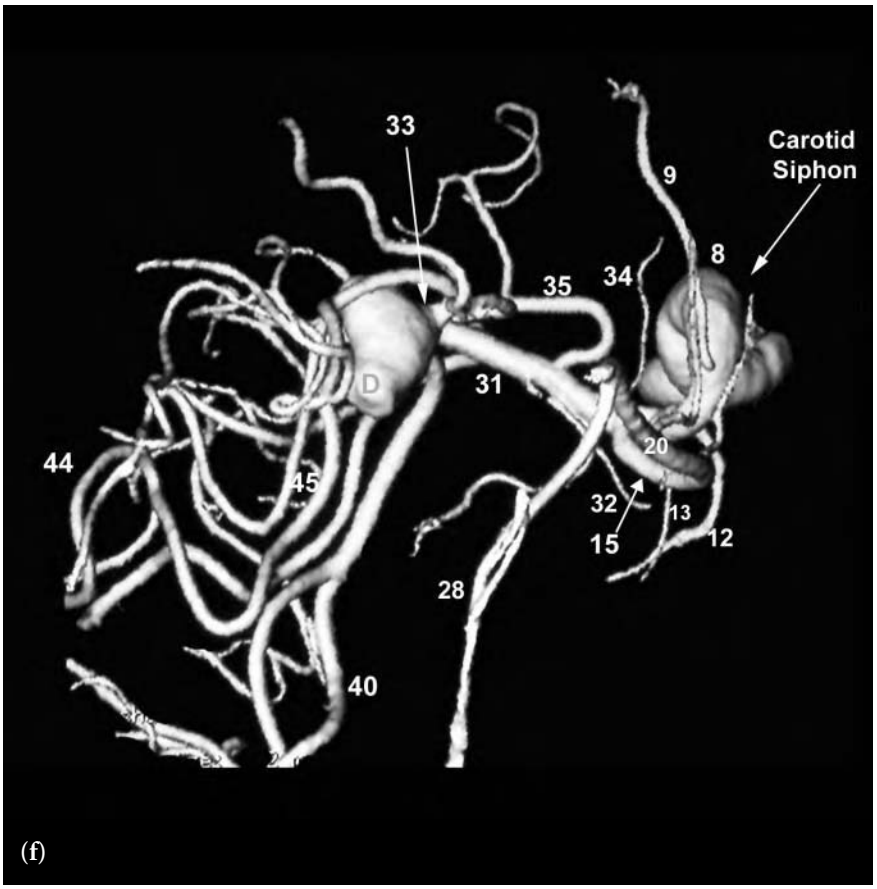

Fig. 5.27 (continued)

FIGURE KEY

2 internal carotid artery – vertical petrous segment
3 internal carotid artery – horizontal petrous segment
4 presellar (Fischer C5) segment internal carotid artery
6 horizontal (Fischer C4) intracavernous internal carotid artery
8 anterior genu (Fischer C3) intracavernous internal carotid artery
9 ophthalmic artery
10 & 11 proximal and distal supraclinoid segments internal carotid artery
12 posterior communicating artery
13 anterior choroidal artery
14 internal carotid artery bifurcation
15 A1 segment of anterior cerebral artery
18 A1-A1 junction anterior cerebral artery
20 proximal A2 segment anterior cerebral artery
21 callosomarginal branch of anterior cerebral artery
22 orbitofrontal branch of anterior cerebral artery
23 frontopolar branch of anterior cerebral artery
28 pericallosal branch of anterior cerebral artery
31 M1 segment middle cerebral artery
32 lateral lenticulostriate arteries
33 bifurcation/trifurcation of middle cerebral artery
34 anterior temporal lobe branches of middle cerebral artery
35 orbitofrontal branch of middle cerebral artery
40 angular artery
44 opercular branches of middle cerebral artery
45 sylvian (insular) branches of middle cerebral artery
D dome of aneurysm

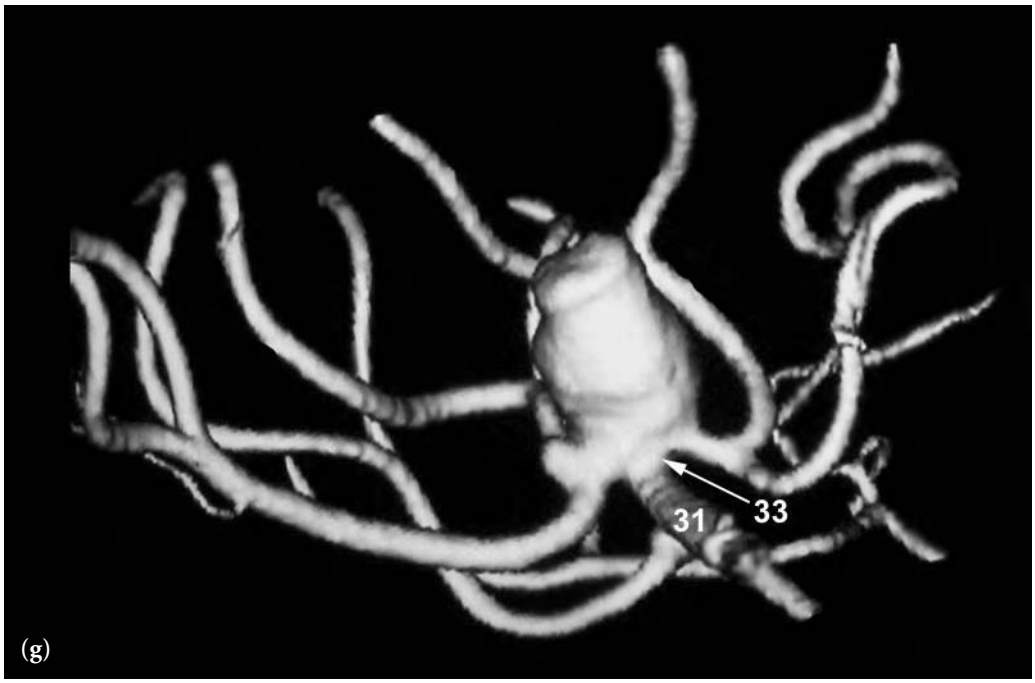

(g)

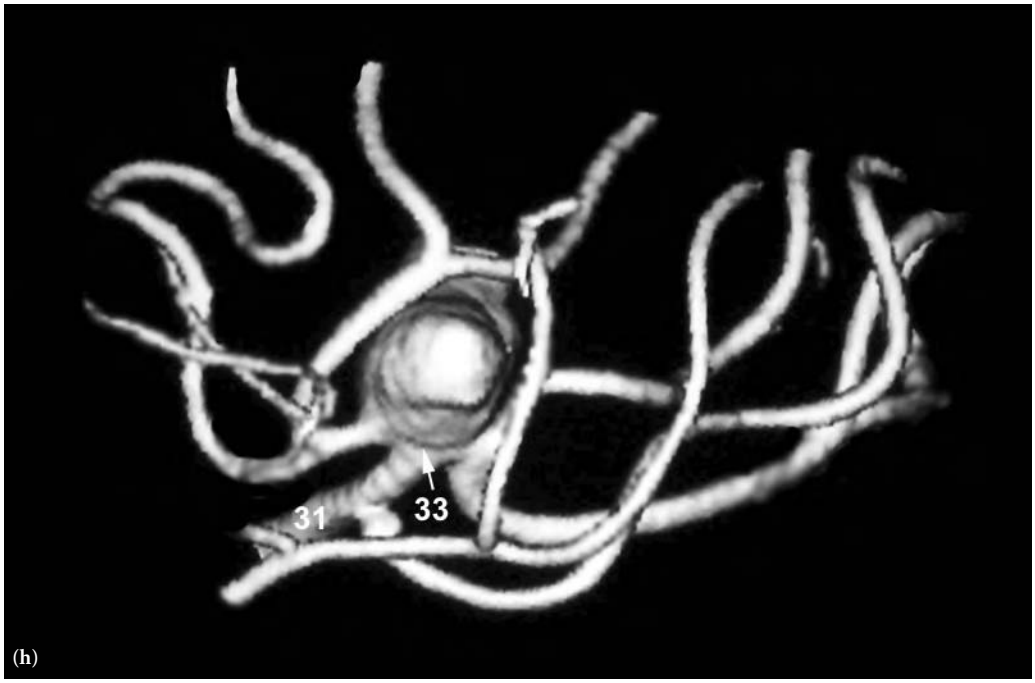

(h)

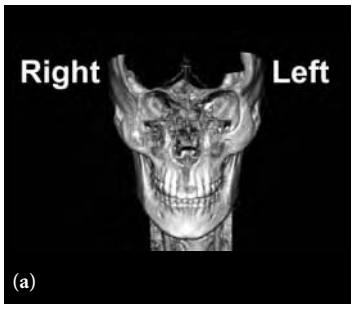

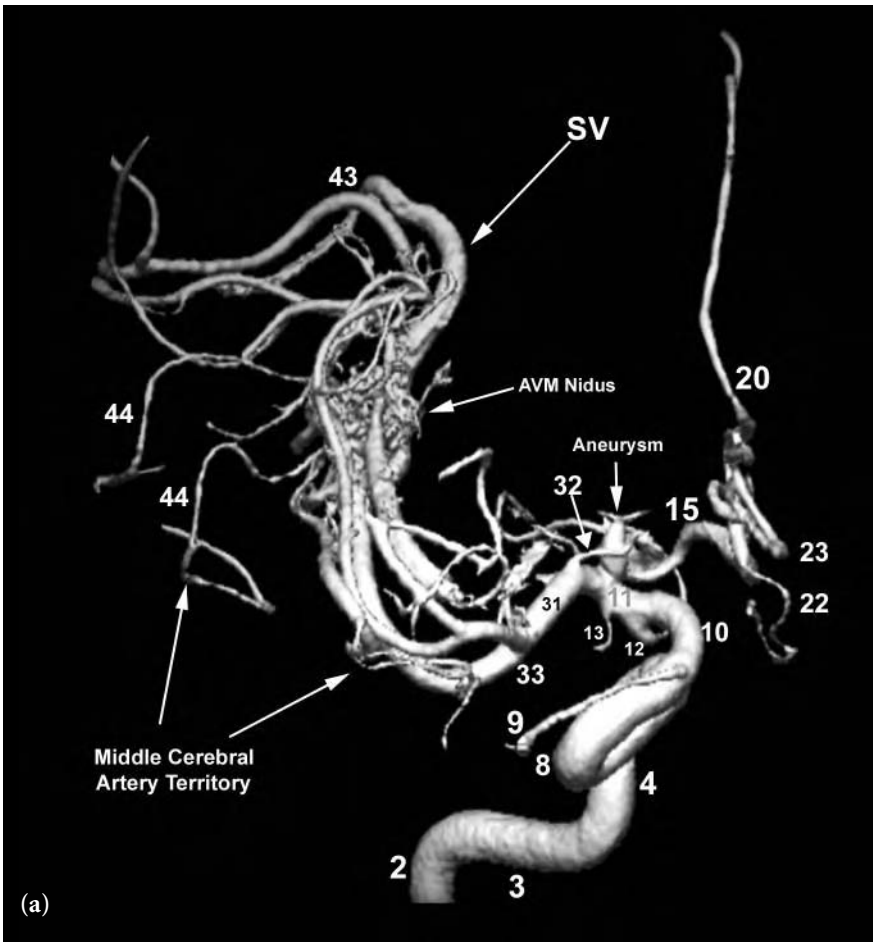

Fig. 5.28 (a–c) 3D frontal (*a*), 3D superior to inferior (*b*), and frontal post treatment (*c*) views following right internal carotid artery injection. Images (*a*) and (*b*) demonstrate an arterial-venous malformation (avm) in the right sylvian fissure. Partial arterial supply is from the sylvian (insular) branches (45) of the middle cerebral artery. Early venous drainage into a large sylvian vein (SV) can also be seen. Note a small associated aneurysm arising from the proximal A1 segment of the anterior cerebral artery and a lateral lenticulostriate artery draped along the anterior surface of the aneurysm. Following embolization and surgery, image (*c*) shows the obliteration of the AVM and the successful surgical clipping of the A1 segment aneurysm with the preservation of the adjacent lenticulostriate artery.

FIGURE KEY

2 internal carotid artery – vertical petrous segment
3 internal carotid artery – horizontal petrous segment
4 presellar (Fischer C5) segment internal carotid artery
6 horizontal (Fischer C4) intracavernous internal carotid artery
8 anterior genu (Fischer C3) intracavernous internal carotid artery
9 ophthalmic artery
10 & 11 proximal and distal supraclinoid segment internal carotid artery
12 infindibular widening at origin of posterior communicating artery
13 anterior choroidal artery
15 A1 segment of anterior cerebral artery
16 medial lenticulostriate arteries
20 proximal A2 segment anterior cerebral artery
22 orbitofrontal branch of anterior cerebral artery
23 frontopolar branch of anterior cerebral artery
31 M1 segment of middle cerebral artery
32 lateral lenticulostriate artery
33 bifurcation/trifurcation of middle cerebral artery
43 sylvian point
44 opercular branches of middle cerebral artery
45 sylvian (insular) branches of middle cerebral artery
SV early draining sylvian vein

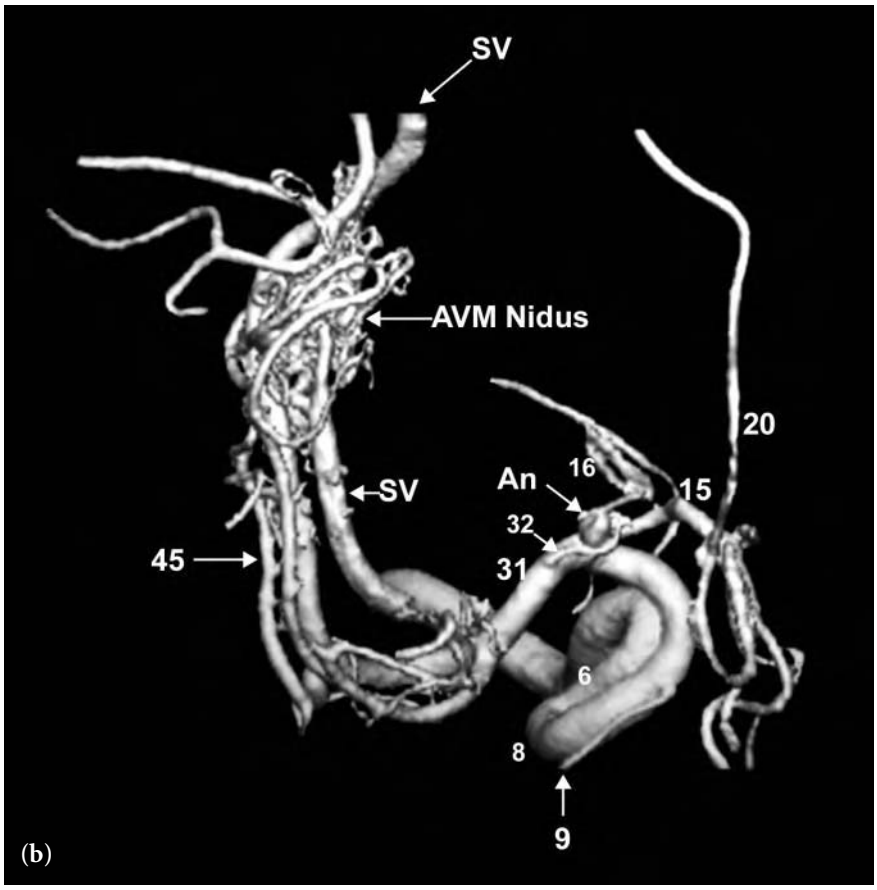
SV
AVM Nidus
20
SV
An
16
15
32
45
31
6
8
9
(b)

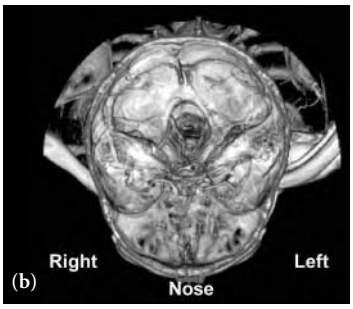
Right
Left
Nose
(b)

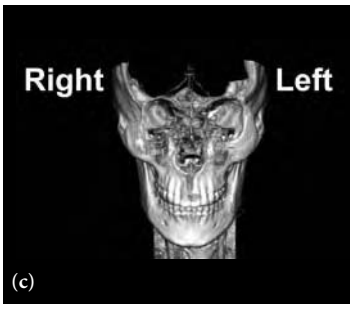
Right
Left
(c)

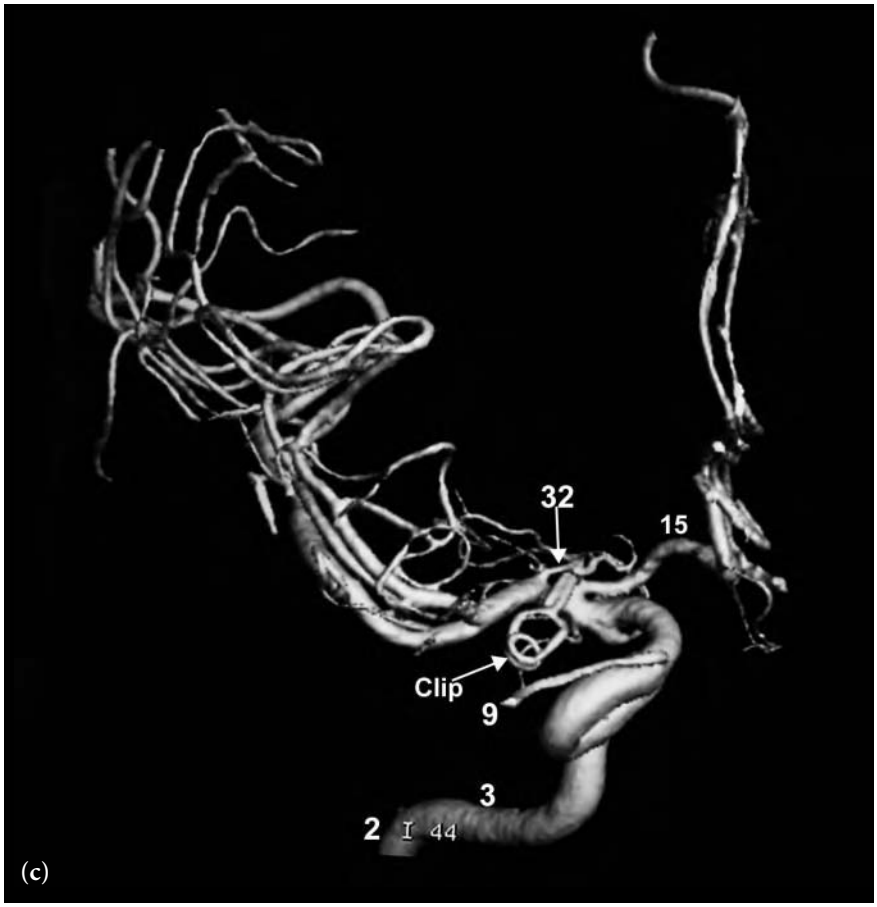
32
15
Clip
9
3
2
(c)

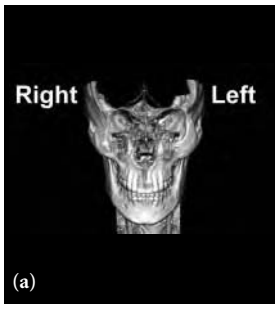

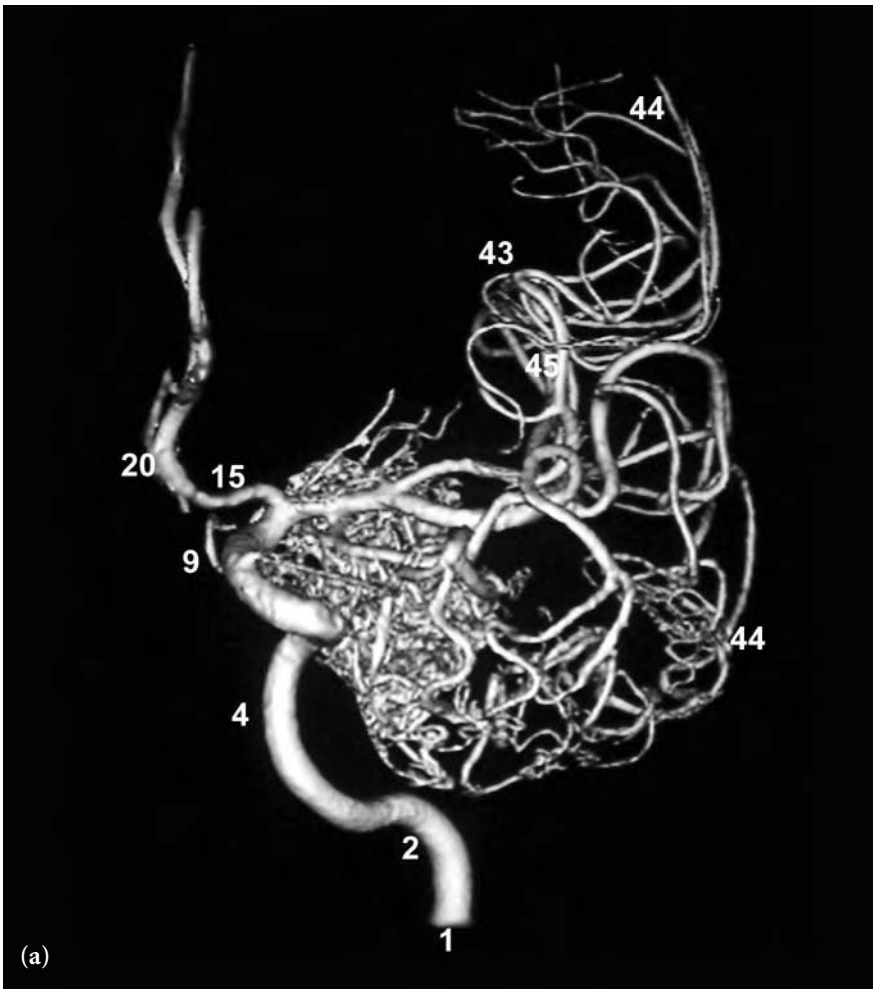

Fig. 5.29 (a–c) 3D frontal (*a*), 3D lateral (*b*), and 3D right anterior oblique (RAO) (*c*) views following left internal carotid artery injection. There is a large arterial-venous malformation (avm) in the left temporal lobe. Arterial supply is from multiple anterior and middle temporal lobe branches of the left middle cerebral artery. Note the proximal segment of an early draining vein (*) along the posterior-superior margin of the AVM nidus. The flat obliquely oriented surface along the inferior surface of the AVM is related to the superior surface of the tentorium cerebelli.

FIGURE KEY

1 internal carotid artery – cervical segment
2 internal carotid artery – vertical petrous segment
3 internal carotid artery – horizontal petrous segment
4 presellar (Fischer C5) segment internal carotid artery
9 ophthalmic artery
15 A1 segment of anterior cerebral artery
20 proximal A2 segment anterior cerebral artery
21 callosomarginal branch of anterior cerebral artery
23 frontopolar branch of anterior cerebral artery
28 pericallosal branch of anterior cerebral artery
34 anterior temporal lobe branches of middle cerebral artery
43 sylvian point
44 opercular branches of middle cerebral artery
45 sylvian (insular) branches of middle cerebral artery
* proximal segment of an early draining vein of avm

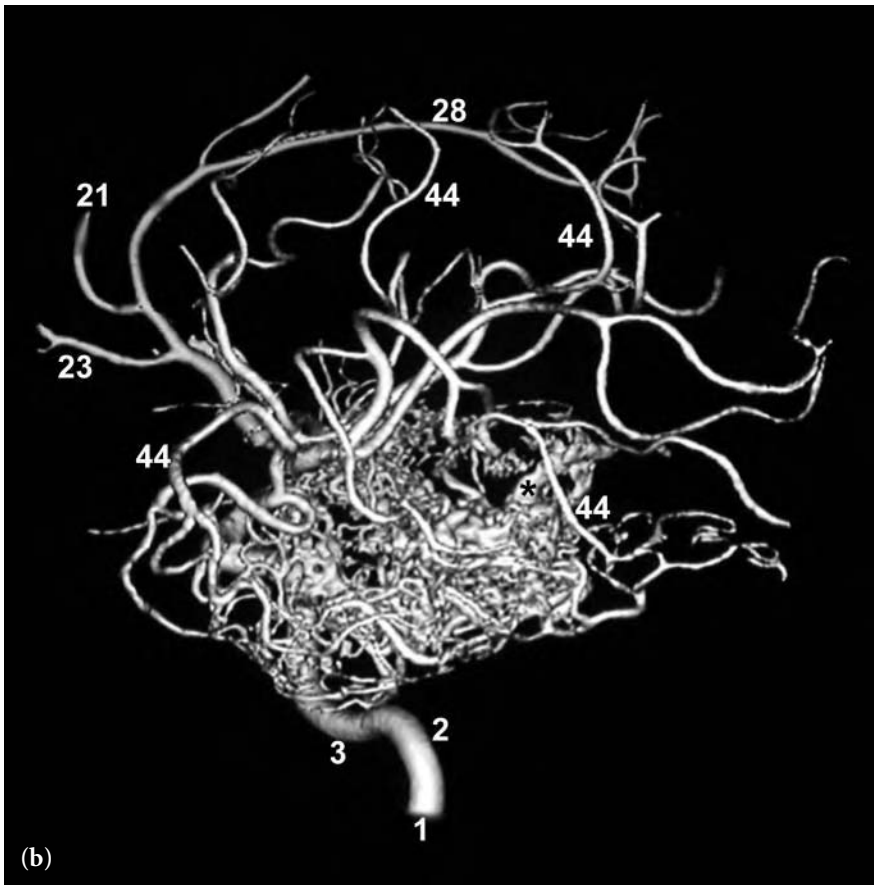
28
21
44
44
23
44
*
44
3
2
1
(b)

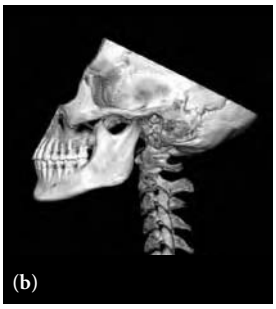
(b)

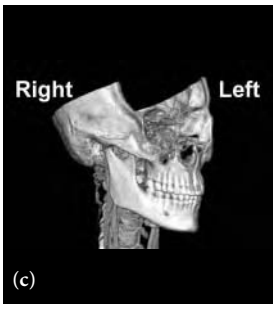
Right
Left
(c)

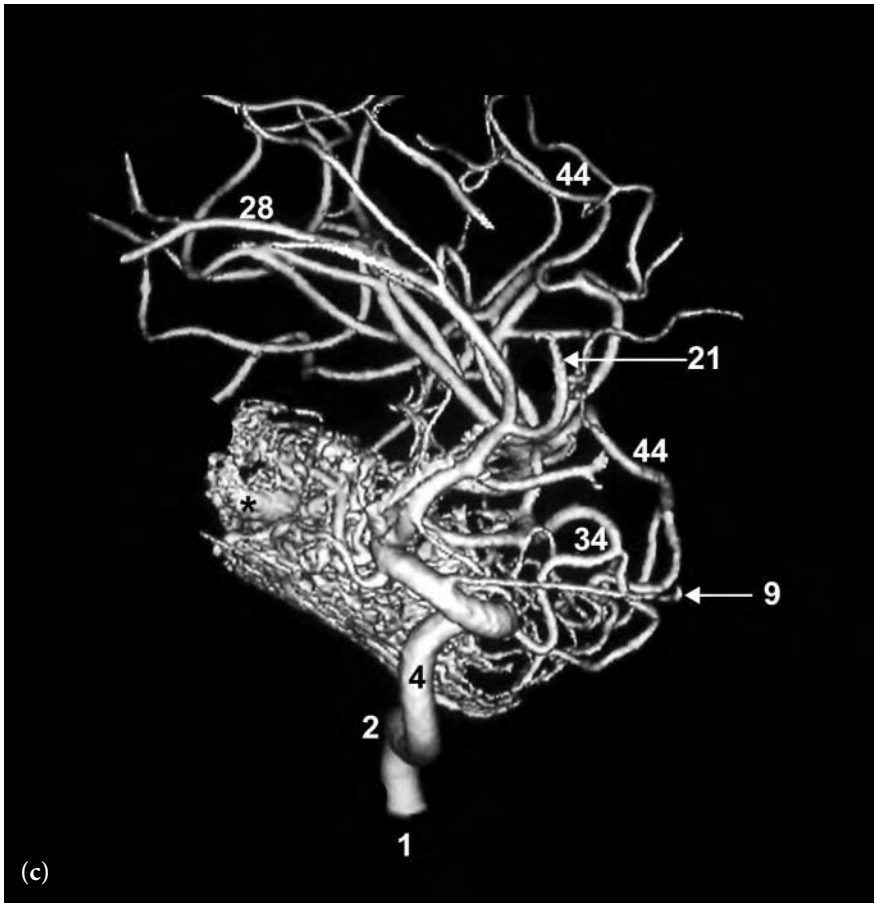
44
28
21
44
*
34
9
4
2
1
(c)

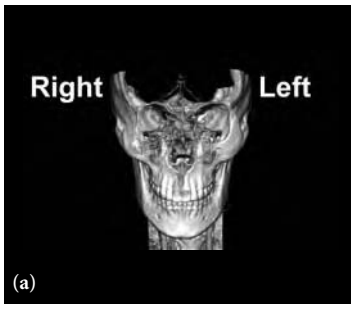

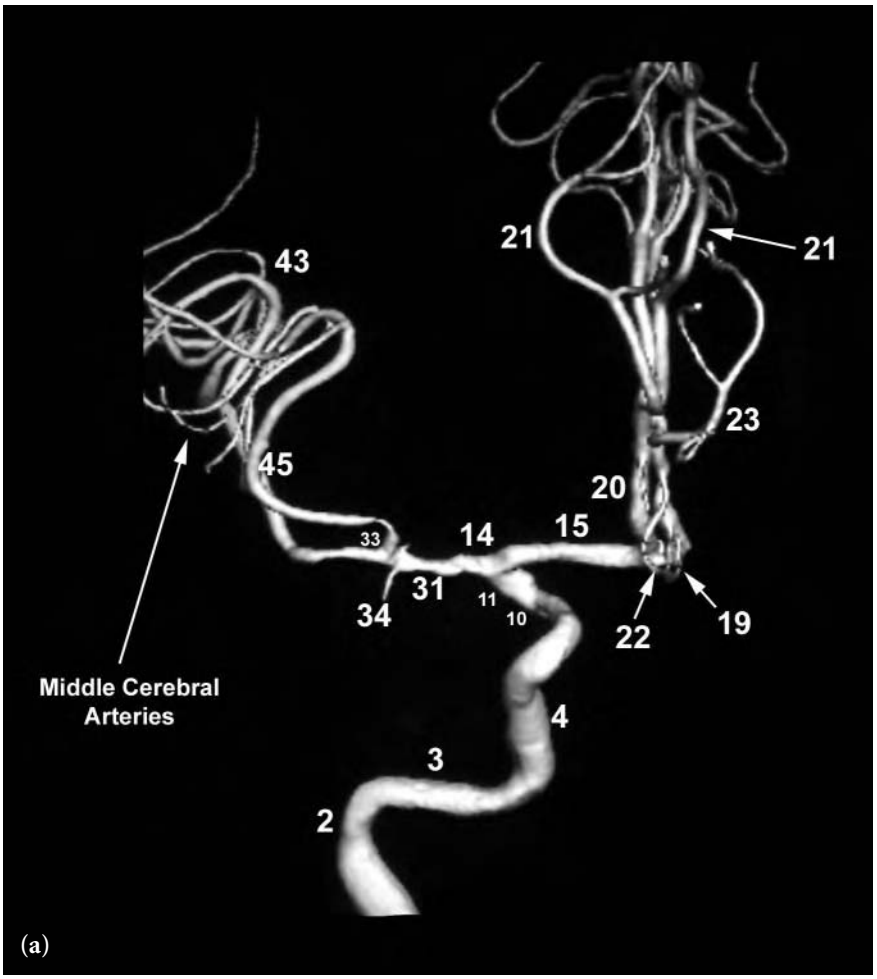

Fig. 5.30 (a–e) 3D frontal right carotid artery injection (*a*) and 3D complex angle (*b-e*) views following left carotid injection. These images demonstrate severe atherosclerotic irregularity of the intracranial vessels. Note the severe hypoplasia of the A1 segment of the left anterior cerebral artery which is not visualized. Both A2 segments fill from the right carotid circulation.

FIGURE KEY

2 internal carotid artery – vertical petrous segment
3 internal carotid artery – horizontal petrous segment
4 presellar (Fischer C5) segment internal carotid artery
6 horizontal (Fischer C4) intracavernous internal carotid artery
10 & 11 proximal and distal supraclinoid segments internal carotid artery
14 internal carotid artery bifurcation
15 A1 segment anterior cerebral artery
19 anterior communicating artery
20 proximal A2 segment anterior cerebral artery
21 callosomarginal branch of anterior cerebral artery
22 orbitofrontal branch of anterior cerebral artery
23 frontopolar branch of anterior cerebral artery
31 M1 segment of middle cerebral artery
33 bifurcation/trifurcation of middle cerebral artery
34 origin of anterior temporal lobe branch of middle cerebral artery
43 sylvian point
45 sylvian (insular) branches of middle cerebral artery

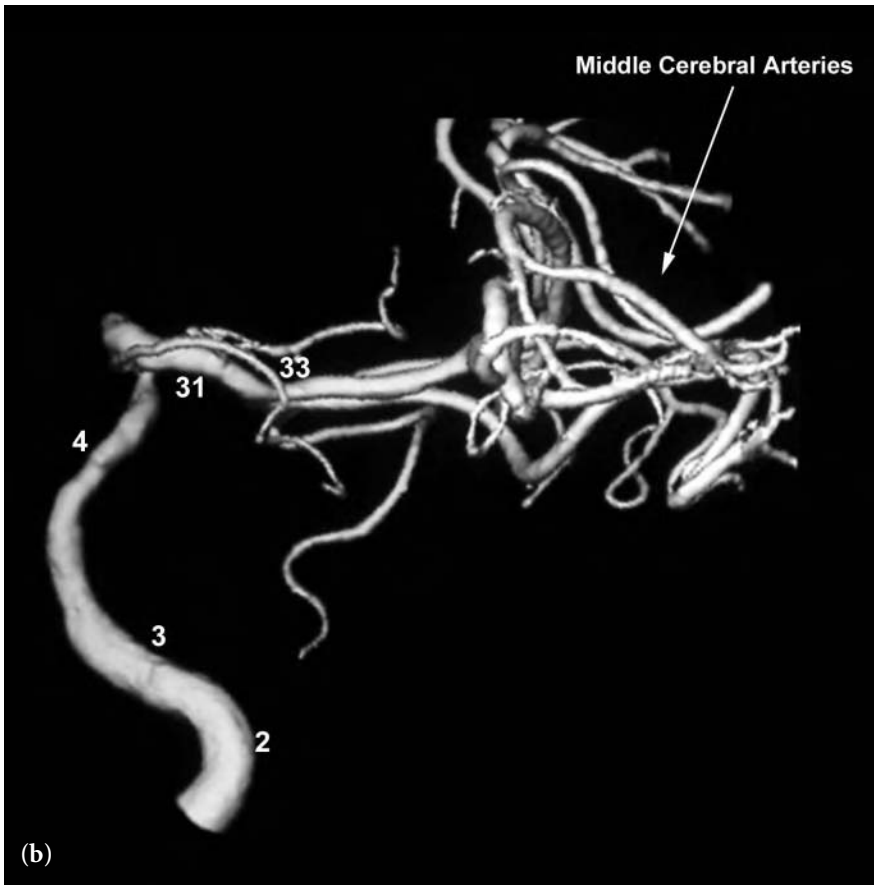
Middle Cerebral Arteries
33
31
4
3
2

(b)

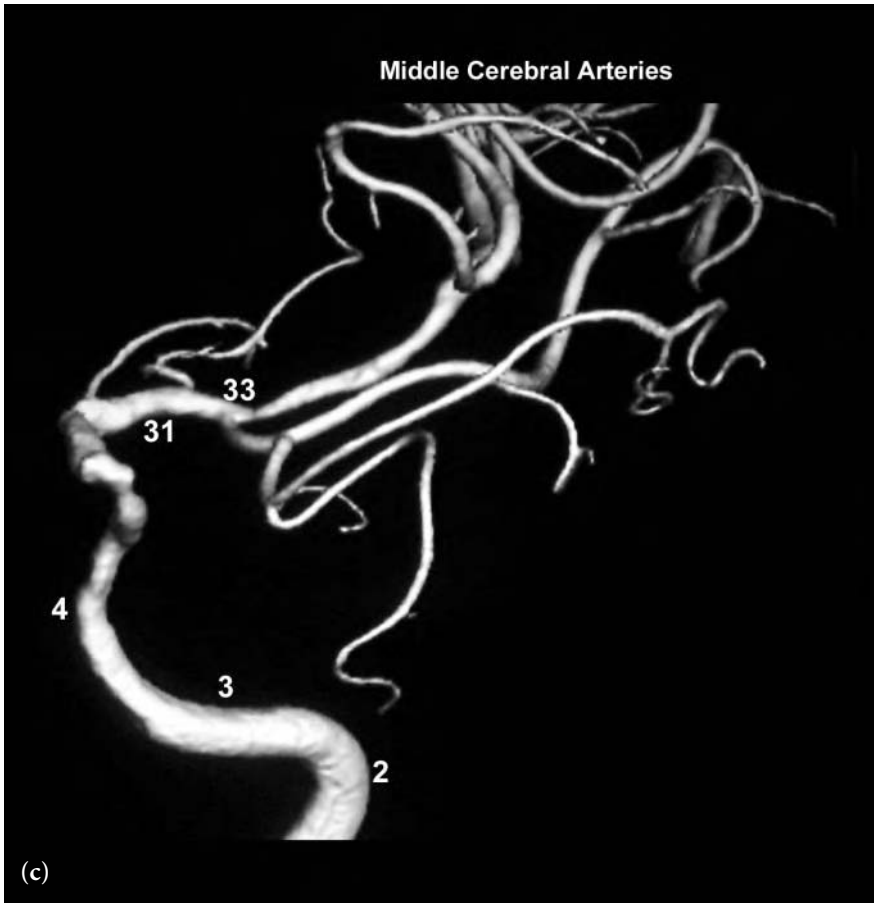
Middle Cerebral Arteries
33
31
4
3
2

(c)

Fig. 5.30 (continued)

FIGURE KEY

2 internal carotid artery – vertical petrous segment
3 internal carotid artery – horizontal petrous segment
4 presellar (Fischer C5) segment internal carotid artery
6 horizontal (Fischer C4) intracavernous internal carotid artery
10 & 11 proximal and distal supraclinoid segments internal carotid artery
14 internal carotid artery bifurcation
15 A1 segment anterior cerebral artery
19 anterior communicating artery
20 proximal A2 segment anterior cerebral artery
21 callosomarginal branch of anterior cerebral artery
22 orbitofrontal branch of anterior cerebral artery
23 frontopolar branch of anterior cerebral artery
31 M1 segment of middle cerebral artery
33 bifurcation/trifurcation of middle cerebral artery
34 origin of anterior temporal lobe branch of middle cerebral artery
43 sylvian point
45 sylvian (insular) branches of middle cerebral artery

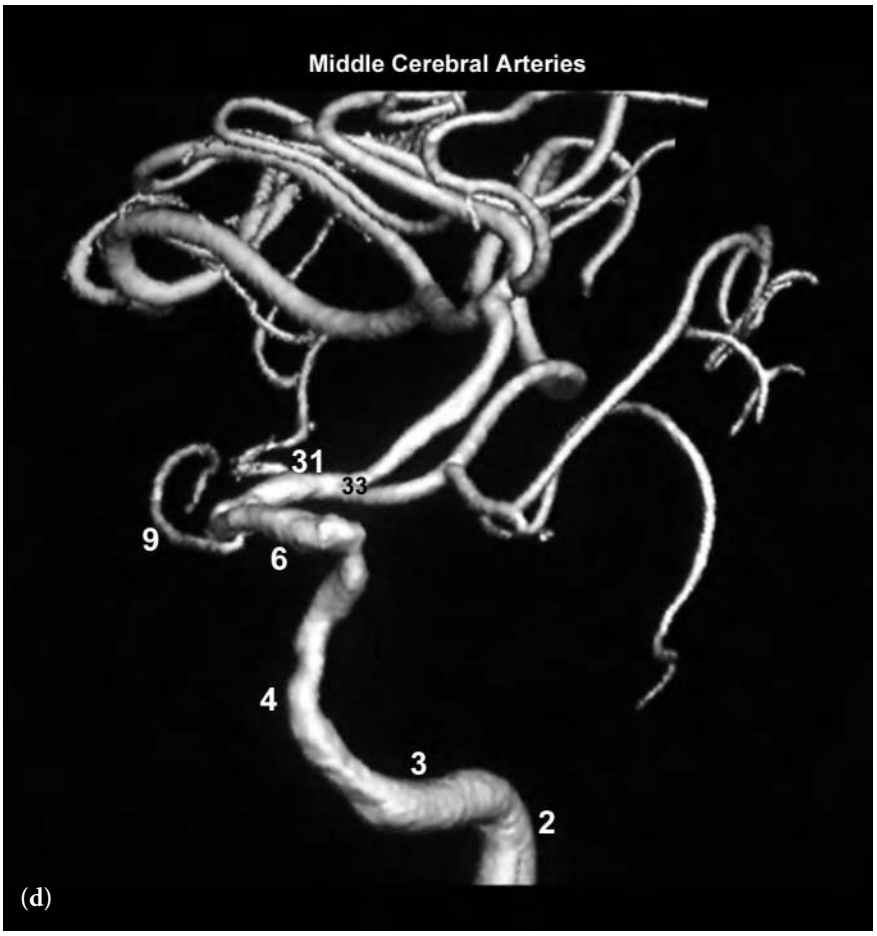

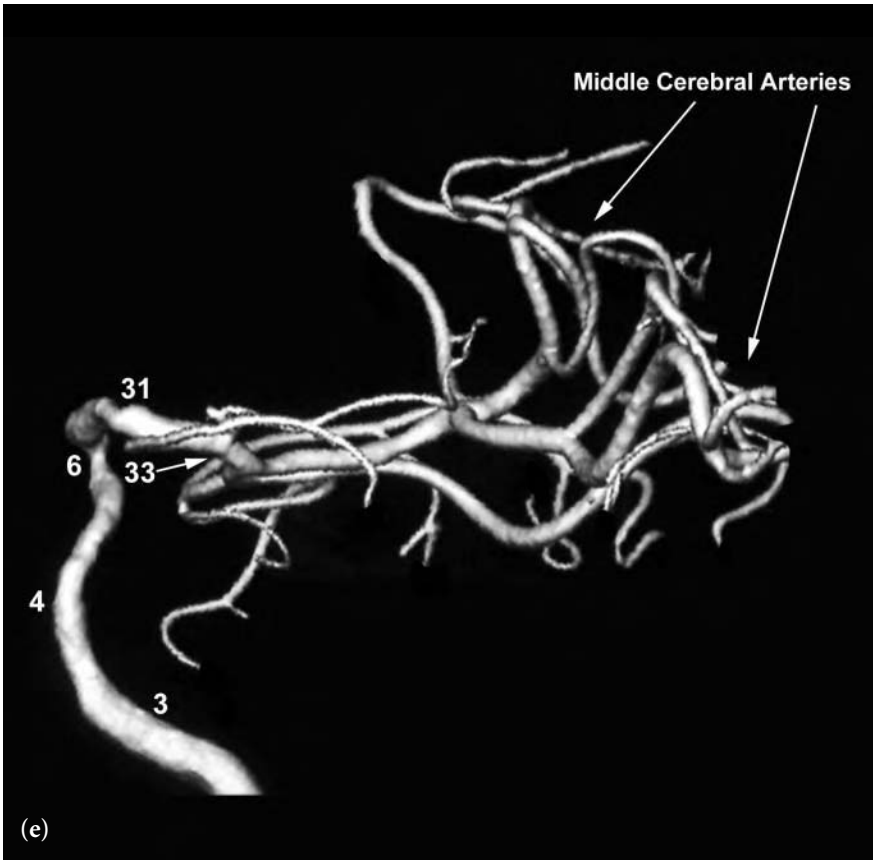

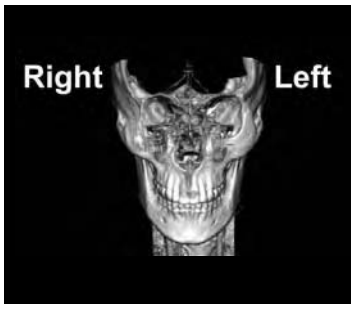

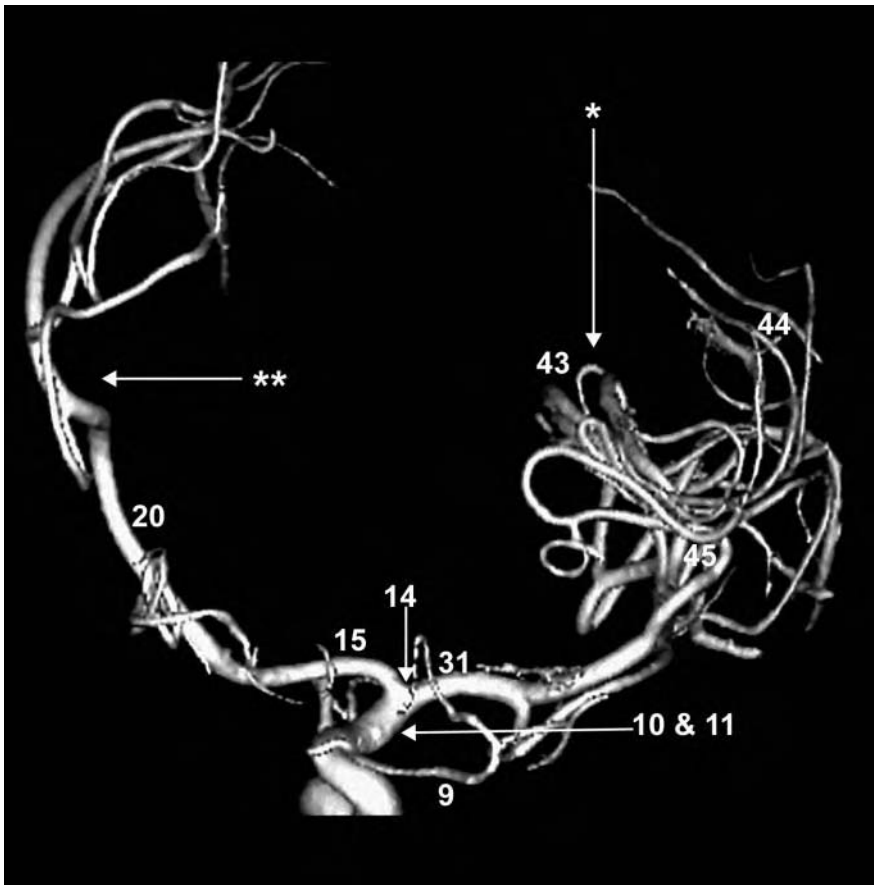

Fig. 5.31 A 3D frontal view following left internal carotid injection. This image shows the result of mass effect on the anterior and middle cerebral arteries. (*) indicates the inferior displacement of the sylvian point and sylvian (insular) branches (45) of the middle cerebral artery. (**) indicates a distal-type shift of the anterior cerebral artery complex to the right. These changes were secondary to a hypovascular mass in the left parietal lobe.

FIGURE KEY

9 ophthalmic artery
10 & 11 proximal and distal supraclinoid segments internal carotid artery
14 internal carotid artery bifurcation
15 A1 segment of anterior cerebral artery
20 proximal A2 segment anterior cerebral artery
31 M1 segment of middle cerebral artery
43 sylvian point
44 opercular branches of middle cerebral artery
45 sylvian (insular) branches of middle cerebral artery

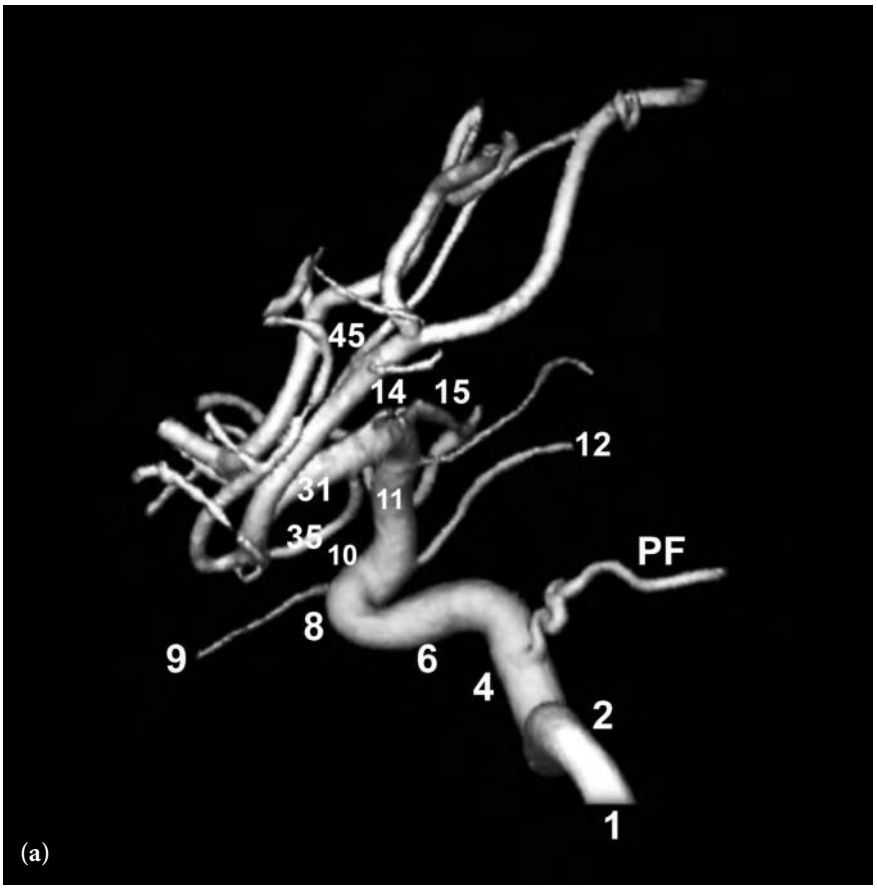

Fig. 5.32 (a–c) 3D lateral (*a*), 3D right anterior oblique (RAO) (*b*), and 3D superior to inferior (*c*) views following left internal carotid artery injection. These images show an anomalous vessel between the presellar (4) segment of the intracranial internal carotid artery and the cerebellar hemisphere on the same side (left) and represents an unusual but nonpathologic communication.

FIGURE KEY

1 internal carotid artery – cervical segment
2 internal carotid artery – vertical petrous segment
3 internal carotid artery – horizontal petrous segment
4 presellar (Fischer C5) segment internal carotid artery
6 horizontal (Fischer C4) intracavernous internal carotid artery
8 anterior genu (Fischer C3) intracavernous internal carotid artery
9 ophthalmic artery
10 & 11 proximal and distal supraclinoid segments internal carotid artery
12 posterior communicating artery
14 internal carotid artery bifurcation
15 A1 segment of anterior cerebral artery
31 M1 segment of middle cerebral artery
33 bifurcation/trifurcation of middle cerebral artery
35 orbitofrontal branch of middle cerebral artery
45 sylvian (insular) branches of middle cerebral artery
PF anomalous vessel between presellar segment (4) internal carotid artery and the ipsilateral cerebellum.

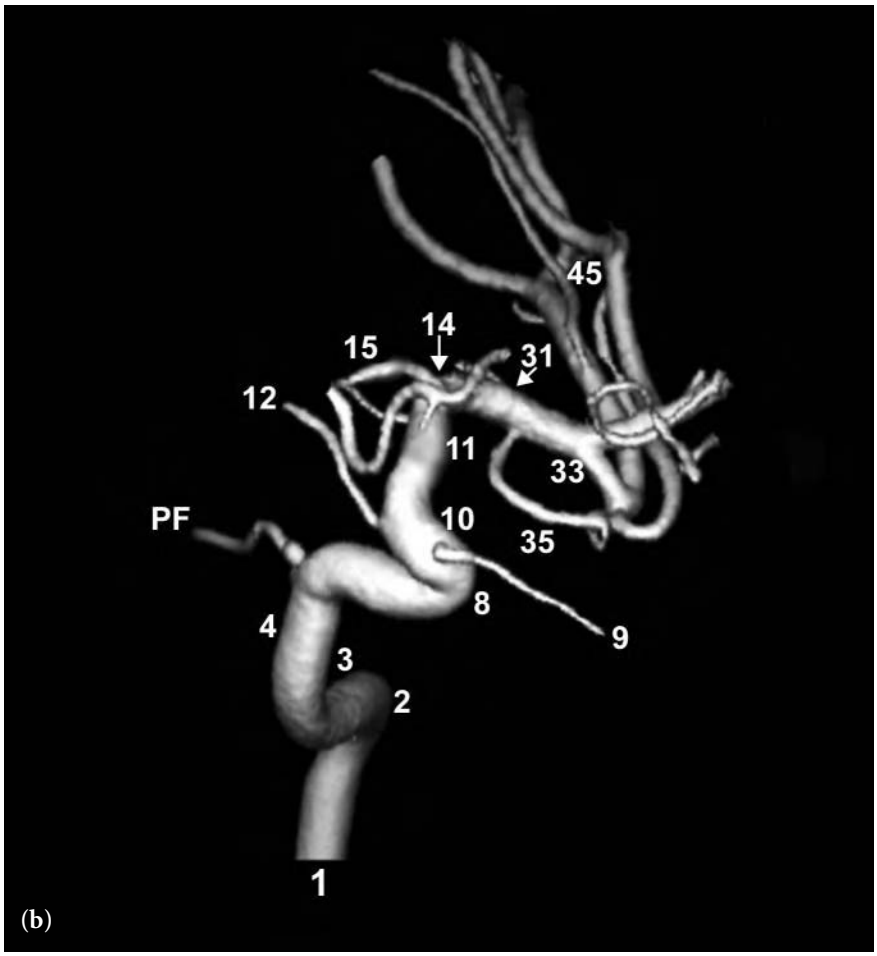
45
14
15
31
12
11
33
PF
10
35
8
9
4
3
2
1
(b)

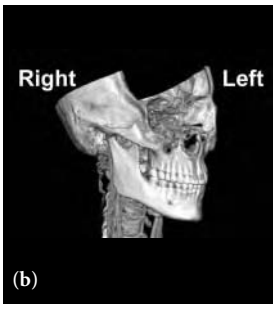
Right
Left
(b)

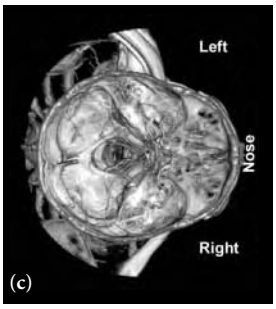
Left
Nose
Right
(c)

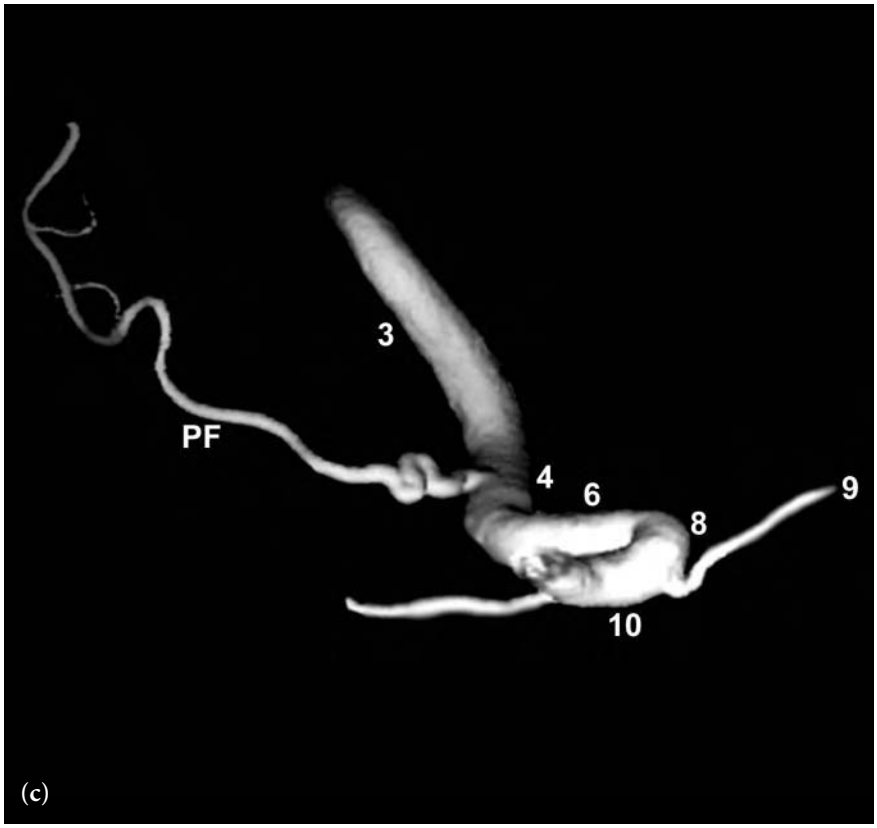
3
PF
4
6
8
9
10
(c)

CHAPTER SIX

INTRACRANIAL VERTEBRAL-BASILAR CIRCULATION (POSTERIOR CIRCULATION)

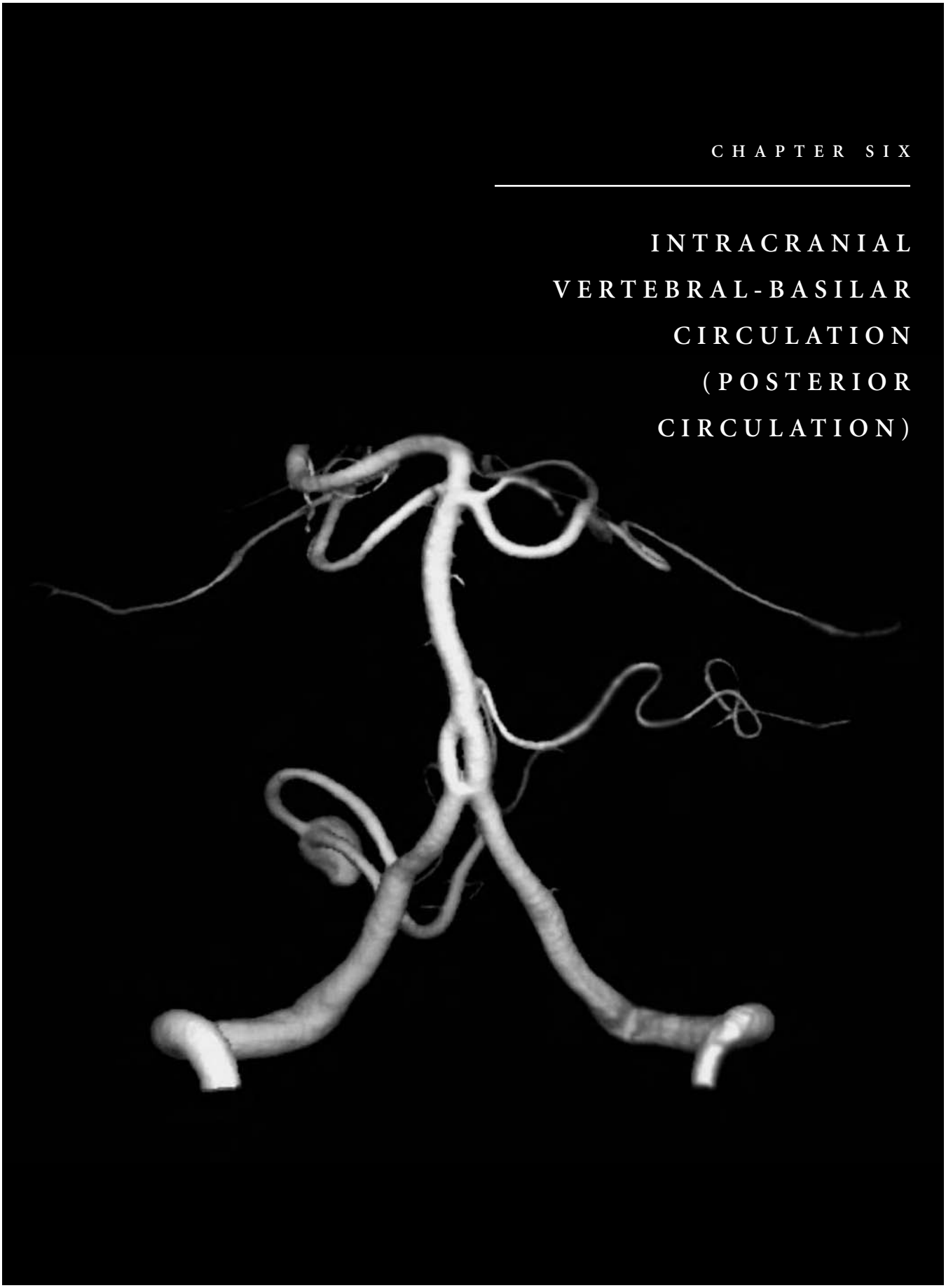

After passing through the foramen magnum the vertebral artery gives rise to numerous branches before uniting with the opposite vertebral artery at the vertebral-basilar junction. Multiple small perforating arteries arise from the distal vertebral artery which supplies the lateral regions of the medulla. The posterior inferior cerebellar artery (PICA) usually arises from the distal vertebral artery 1-2 cm below the vertebral-basilar junction. These arteries are often asymmetric and their size can vary. There is a reciprocal relationship between the size of the PICA and that of the ipsilateral anterior inferior cerebellar artery (AICA) which arises from the basilar artery. When the AICA is large, the ipsilateral PICA is often small or sometimes can be absent. In this situation a large medial branch of the AICA supplies the PICA vascular territory. The PICA divides into branches supplying the ipsilateral cerebellar tonsil, inferior vermis, and the inferior cerebellar hemisphere. Small perforators from the proximal PICA can supply the lateral and posterior medulla. The anterior spinal artery usually arises from the distal 1 cm of the vertebral artery (1). This vessel often unites with the anterior spinal artery branch from the contralateral vertebral artery to form the main anterior spinal artery. The posterior meningeal artery which supplies the falx cerebelli arises from the distal vertebral artery near the foramen magnum. This vessel courses both posteriorally and superiorally.

The vertebral arteries unite to form the basilar artery ventral to the superior medulla/inferior pons. The basilar artery typically runs in the midline but can have a tortuous course. Branches of the basilar artery include paired anterior inferior cerebellar arteries (AICA), small pontine perforator branches, paired superior cerebellar arteries (SCA), and paired posterior cerebral arteries (PCA).

The anterior inferior cerebellar artery (AICA) typically arises from the proximal (inferior) two-thirds of the basilar artery. As discussed above, the AICA has a reciprocal relationship with the ipsilateral posterior inferior cerebellar artery (PICA). The AICA runs laterally, posteriorly, and then

inferiorly around the pons. It continues to traverse the cerebellopontine angle cistern to lie anterior and medial to the facial and acoustic nerves. The AICA often loops into and out of the internal auditory canal (referred to as the "meatal loop") which is often seen at angiography. The meatal loop gives rise to a small branch supplying the eighth cranial nerve (vestibular cochlear nerve) called the acoustic branch (internal auditory artery)(2). The AICA then courses laterally to the terminal branches. It then supplies the anterior and inferior cerebellum.

Median and paramedian pontine perforators arise from the basilar artery to supply the medulla and the pons. They can normally be seen only on magnified 2D angiography with selective vertebral injections. Only their most proximal portions are usually seen on three-dimensional rotational angiography (3DRA).

The superior cerebellar artery (SCA) typically arises just proximal (inferior) to the posterior cerebral artery (PCA) from the distal (upper or superior) basilar artery. Both superior cerebellar arteries are almost always present (3). They may appear duplicated (which is seen in some of the atlas images). The SCA runs posterolaterally in the perimesencephalic cistern encircling the brainstem at the junction of the pons and the midbrain encompassing the anterior (or pontine) and ambient (or lateromesencephalic) segments. The SCA then courses into the quadrigeminal cistern for the quadrigeminal segment. The two main terminal branches of the superior cerebellar artery are the vermian and hemispheric branches that supply the superior surface of the cerebellum and cerebellar vermis as well as supply the superolateral aspect of the cerebellar hemispheres, superior cerebellar peduncle, a portion of the middle cerebellar peduncle, and the dentate nucleus (4).

The posterior cerebral artery (PCA) typically originates from the superior basilar artery (basilar tip) at the superior anterior aspect of the pons. The three segments of the PCA are the P1, the P2, and the P3 segments. The P1 segment, also termed the peduncular (or precommunicating) segment, unites the basilar tip to the posterior communicating artery (PCoA) insertion. The P2 segment, also know as the ambient segment, lies in the crural cistern (a portion of the ambient cistern) and runs from the posterior communicating artery insertion around the cerebral peduncle to the posterior aspect of the midbrain. The crural cistern is the portion of the ambient cis-

tern located between the uncus of the temporal lobe and the cerebral peduncle. The P3 segment, also known as the quadrigeminal segment, runs within the lateral aspect of the quadrigeminal cistern curving around the brainstem approaching the opposite P3 segment and then extending posteriorly under the splenium of the corpus callosum. The posterior cerebral artery supplies portions of the temporal, parietal, and occipital lobes as well as the thalamus, midbrain, choroids, and ependyma of the third and lateral ventricles. In 20% of people there is a "fetal" or direct origin of the PCA from the ipsilateral internal carotid artery. In this situation the ipsilateral P1 segment is hypoplastic (small) or absent. Other variations include the duplication of the P1 segment, origin of the superior cerebellar artery from the P1 segment, and common origins of the superior cerebellar artery and P1 segment (5).

Branches of the PCA include perforators to the thalamus and midbrain, ventricular branches to the choroid and ependyma, and cortical branches to the temporal and occipital lobes.

From the P1 segment of the PCA arise the posterior thalamoperforators. The anterior thalamoperforators arise from the posterior communicating artery. The anterior thalamoperferators supply the thalamic nuclei, posterior optic chiasm, proximal optic radiations, posterior hypothalamus, and some of the cerebral peduncle. The posterior thalamoperferators supply the thalamus, subthalamus, as well as nuclei and tracts of the upper midbrain.

From the P2 segment, or less typically the P1 segment of the posterior cerebral artery (PCA), comes the medial posterior choroidal arteries that consists of a single or several small vessels. These vessels run posteriorly and superiorly around the pineal gland and then course anteriorly in the roof of the third ventricle terminating as a sharp curve with terminal vessels ascending into the foramen of Monroe. These vessels take on the appearance of a reverse number "3" on a lateral angiogram. In addition to supplying the choroid and ependyma of the third and lateral ventricles, the medial posterior choroidal arteries supply portions of the thalamus and the pineal gland (6).

The lateral posterior choroidal arteries, a grouping of a single or several small vessels, usually arise from the P2 segment of the posterior cerebral artery (PCA). These vessels course laterally through the choroid fissure and then superiorly in the atrium (trigone) of the lateral ventricle, coursing further posteriorly around the pulvinar of the thalamus. The

lateral posterior choroidal arteries supply the choroid plexus and ependyma of the temporal horn and atrium of the lateral ventricle, portions of the cerebral peduncle, posterior commisure, lateral geniculate body, thalamus, fornix, and caudate (7).

Also arising from the P2 segment of the posterior cerebral artery are a grouping of vessels called the inferior temporal arteries. These arteries provide a cortical supply to the inferior temporal lobe. The posterior temporal branch of the posterior cerebral artery is typically the largest and most commonly seen vessel of the inferior temporal arteries. It courses posteriorly with terminal branches supplying the inferior and medial portions of the posterior temporal lobes. Other less constant temporal lobe branches may arise from the posterior cerebral artery (PCA).

The P3 segment of the posterior cerebral artery runs from the posterior portion of the quadrigeminal plate cistern towards the calcarine fissure giving off the parieto-occipital branch of the posterior cerebral artery, the calcarine branch of the posterior cerebral artery, and the posterior pericallosal (splenial) arteries.

The parieto-occipital branch of the posterior cerebral artery is the largest and most superior of the P3 branches. It arises in the ambient cistern and courses posteriorly into the parietal occipital sulcus to supply the cuneus, precuneus, and superior occipital gyrus. It may also supply the precentral region and superior parietal lobule as well as the visual cortex. (8).

The calcarine branch of the posterior cerebral artery generally arises from the distal posterior cerebral artery and appears just inferior to the parieto-occipital branch. The calcarine branch of the posterior cerebral artery runs into the calcarine sulcus. It supplies portions of the visual cortex, cuneus, and lingual gyrus (9).

With angiography, using a frontal projection, the differentiation of the course of the parieto-occipital branch from the calcarine branch can be made by noting that it is typical that the proximal aspect of the calcarine branch lies laterally to the proximal parieto-occipital artery but courses distally medial to the parieto-occipital artery. The parieto-occipital artery tends to deviate laterally while coursing posteriorly.

The posterior pericallosal arteries, also know as the splenial arteries, are a grouping of small vessels usually originating from the posterior cerebral artery that can arise from the parieto-occipital artery. They initially course

posteriorly and then sweep anteriorly and superiorly about the splenium of the corpus callosum to join with the pericallosal branch of the anterior cerebral artery. These branches can significantly enlarge and provide collateral blood flow to the anterior cerebral artery (pericallosal branch) in cases of severe stenosis or occlusion of the anterior cerebral artery.

REFERENCES

1. Stephens, R.B., and D.L. Stilwell. 1969. Arteries and Veins of the Human Brain, Springfield, Ill: Charles C Thomas, pp. 71, 73.
2. Takahashi, M. 1974. *The anterior inferior cerebellar artery*. In Radiology of the Skull and Brain: Angiography Volume 2. T.H. Newton and D.G. Potts, editors. St. Louis, Mo: C.V. Mosby Company, p. 1801.
3. Huber, P. 1982. *Krayenbuhl/Yasargil Cerebral Angiography*. New York: Thieme Medical Publishers, p. 158.
4. Rael, J. and L. Casey. 2000. Cerebral angiography. In Neuroimaging. W.W. Orrison, editor. Philadelpia: W. B. Saunders, p. 241.
5. Rael and Casey, p. 234.
6. Rothman S.L.G., W.E. Allen, III, and J.F. Simeone. 1976. The medial posterior choroidal artery as an indicator of masses at the foramen of Monro. *Neuroradiology*. 11:123–129.
7. Stephens and Stilwell, pp. 96–99.
8. Rael and Casey, p. 236.
9. Stephens and Stillwell, pp. 96–99.

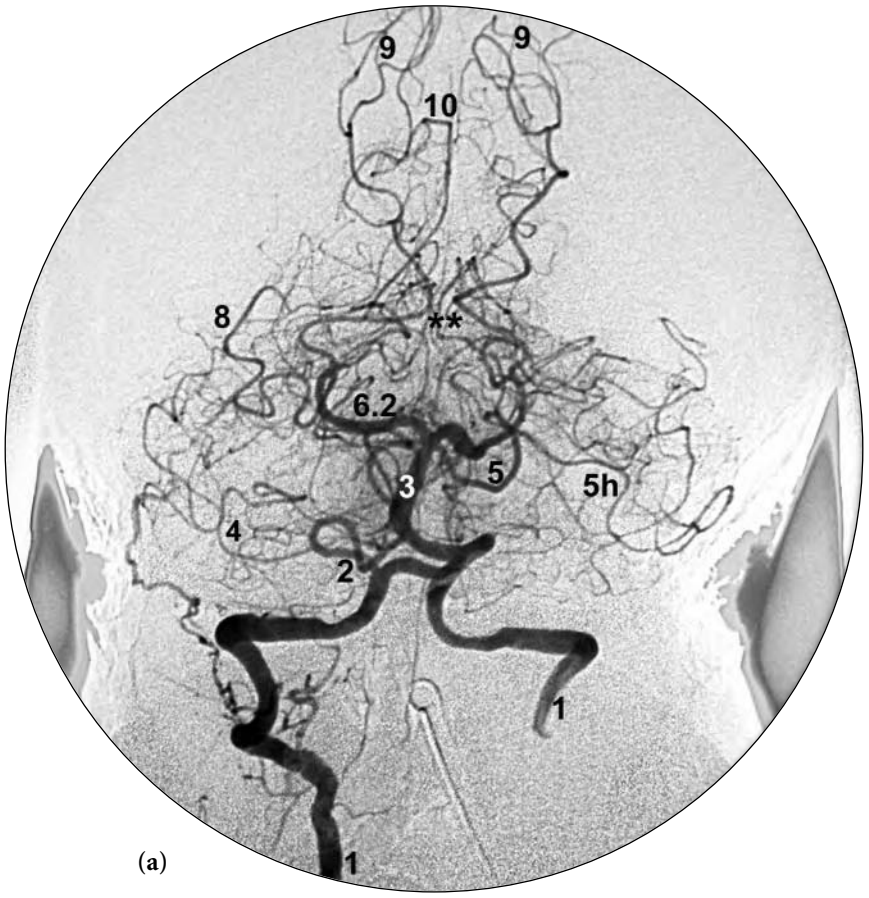

Fig. 6.1 (a–c) 2D frontal (*a*), lateral early arterial phase (*b*), and lateral late arterial phase (*c*) views following right vertebral artery injection. An intracranial view is shown. These images show normal intracranial vertebral basilar circulation.

FIGURE KEY

1 vertebral artery
2 posterior inferior cerebellar artery (PICA)
2v vermian branch of PICA
2h hemispheric branch of PICA
3 basilar artery
4 anterior inferior cerebellar artery (AICA)
5 superior cerebellar artery (SCA)
5h hemispheric branch of SCA
6 posterior cerebral artery (PCA)
6.2 P2 segment of posterior cerebral artery
7 posterior communicating artery
8 posterior temporal branch of PCA
9 parieto-occipital branch of PCA
10 calcarine branch of PCA
11 anterior thalamoperforators
12 posterior thalamoperforators
13m medial posterior choroidal arteries
13L lateral posterior choroidal arteries
14 vertebral-basilar junction
15 splenial branch (posterior pericallosal artery) of PCA
17 anterior spinal artery
** region of quadrigeminal plate cistern

(b)

(c)

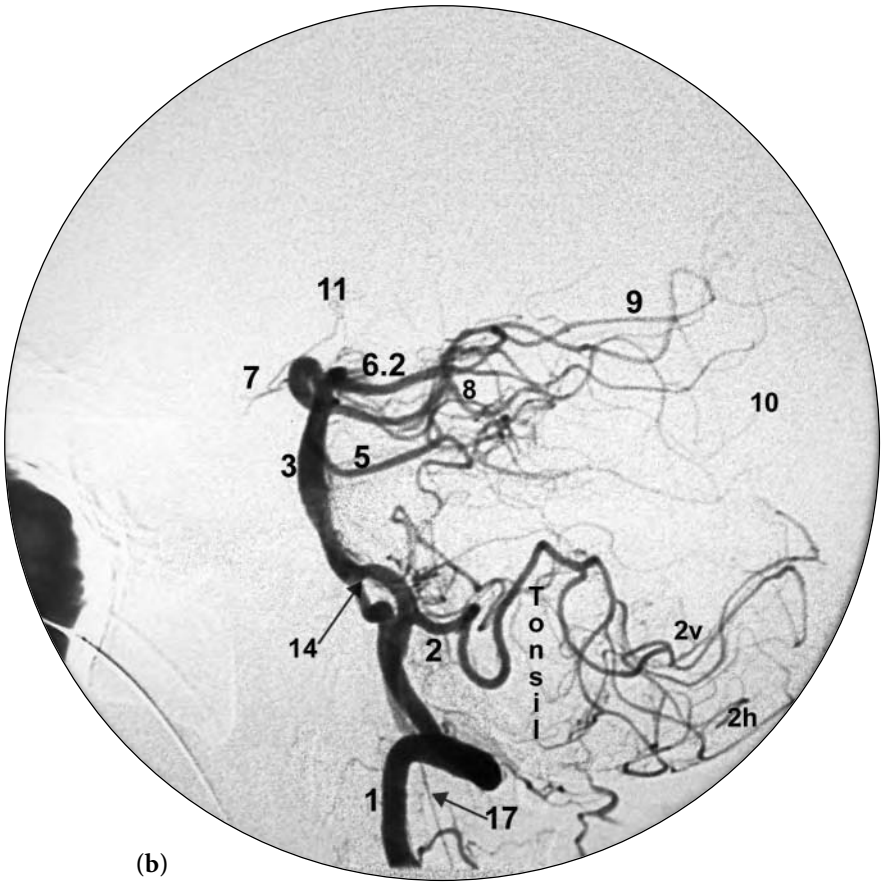
11
9
7
6.2
8
10
3
5
Tonsil
14
2
2v
2h
1
17

(**b**)

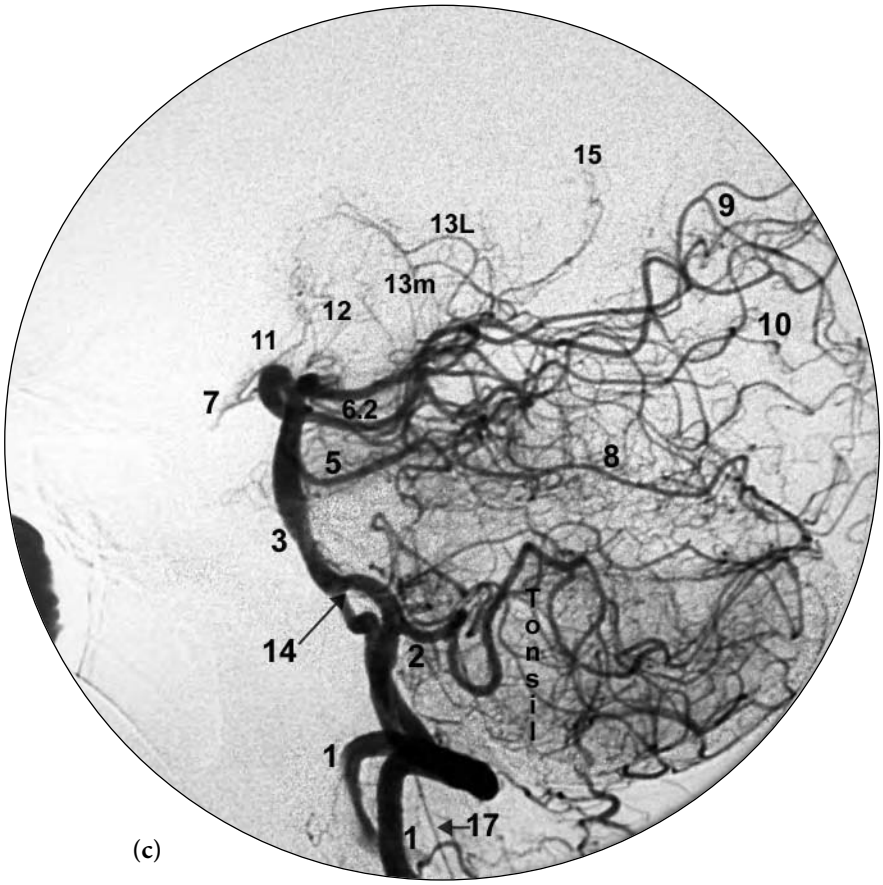
15
13L
9
13m
12
10
11
7
6.2
5
8
3
Tonsil
14
2
1
1
17

(**c**)

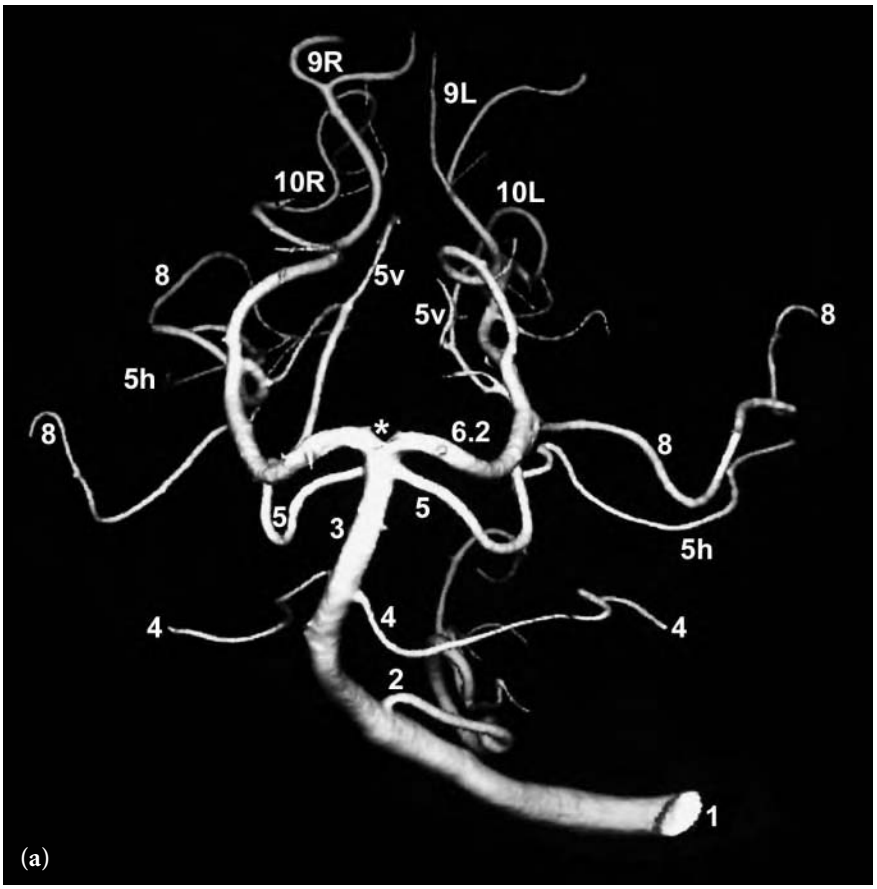

Fig. 6.2 (a–e) 3D frontal (*a*), right anterior oblique (*b*), posterior (*c*), left posterior oblique (*d*), and right posterior oblique (*e*) views following left vertebral artery injection. These views demonstrate normal vascular anatomy of intracranial vertebral basilar circulation.

FIGURE KEY

1 vertebral artery
2 posterior inferior cerebellar artery (PICA)
3 basilar artery
4 anterior inferior cerebellar artery (AICA)
5 superior cerebellar artery
5v vermian branch of superior cerebellar artery
5h hemispheric branch of superior cerebellar artery
6.1 P1 segment of posterior cerebral artery (PCA)
6.2 P2 segment of posterior cerebral artery (PCA)
7 posterior communicating artery
8 posterior temporal branch of PCA
9 parieto-occipital branch of PCA
10 calcarine branch of PCA
16 pontine perforating artery
* tip of basilar artery

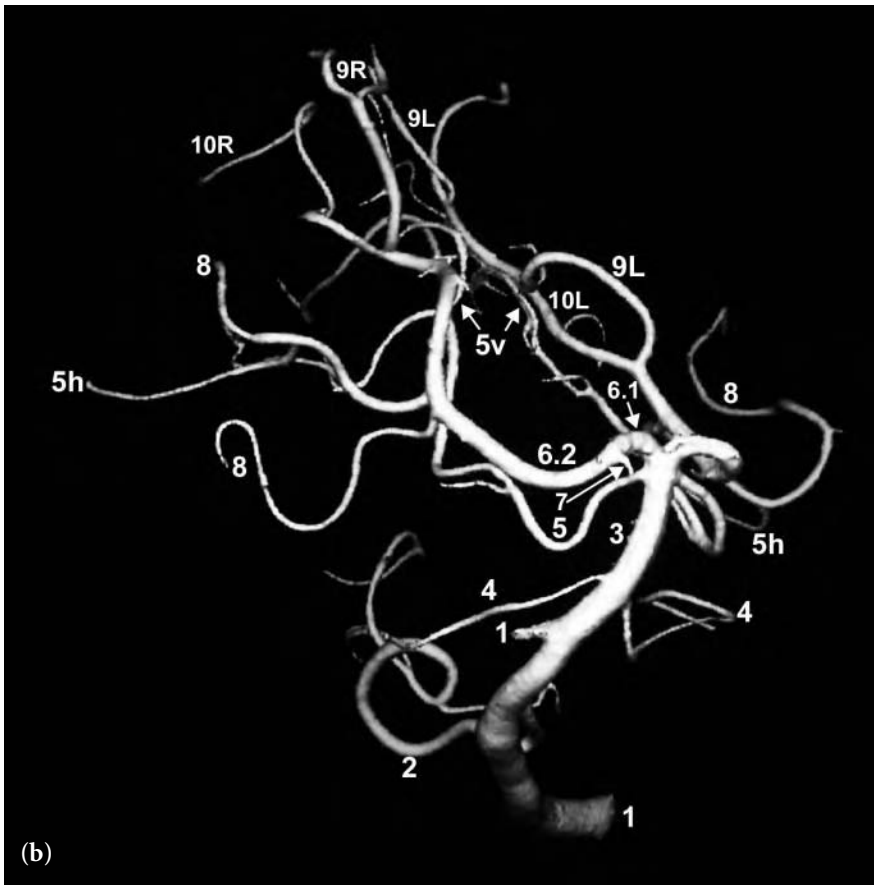
9R
9L
10R
8
9L
10L
5v
5h
6.1
8
8
6.2
7
5
3
5h
4
1
4
2
1
(b)

(b)

(c)

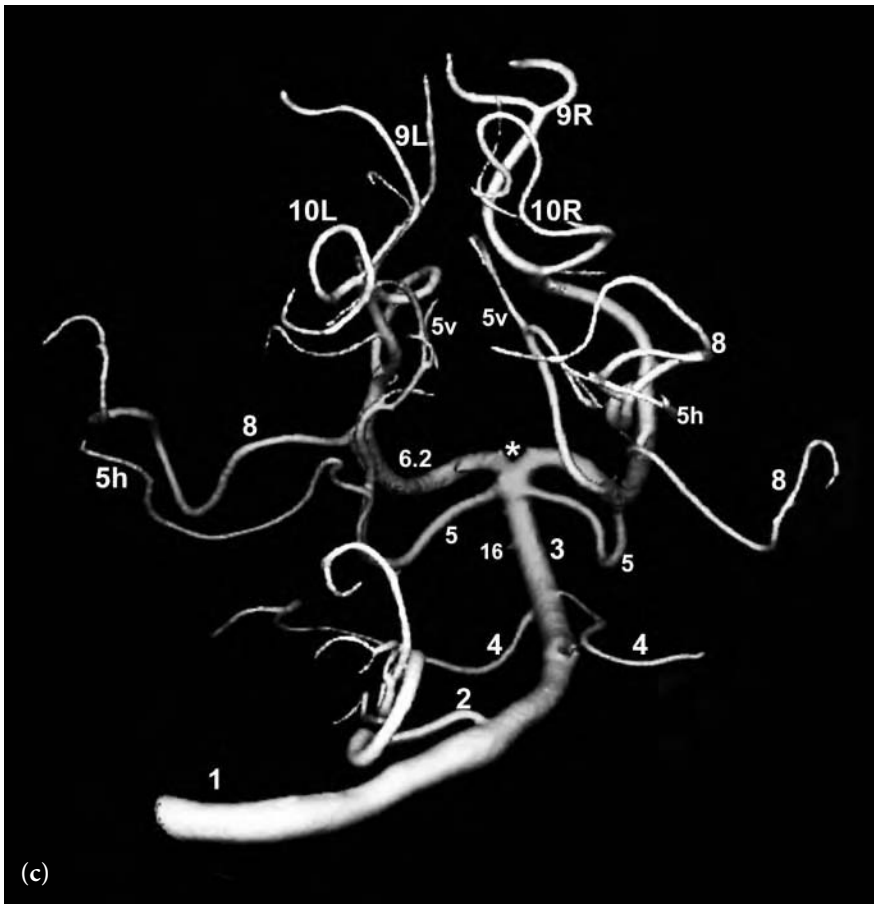
9L
9R
10L
10R
5v
5v
8
5h
8
5h
6.2
*
8
5
16
3
5
4
4
2
1
(c)

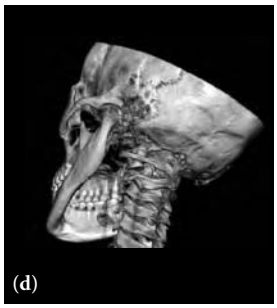

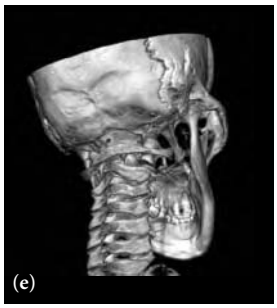

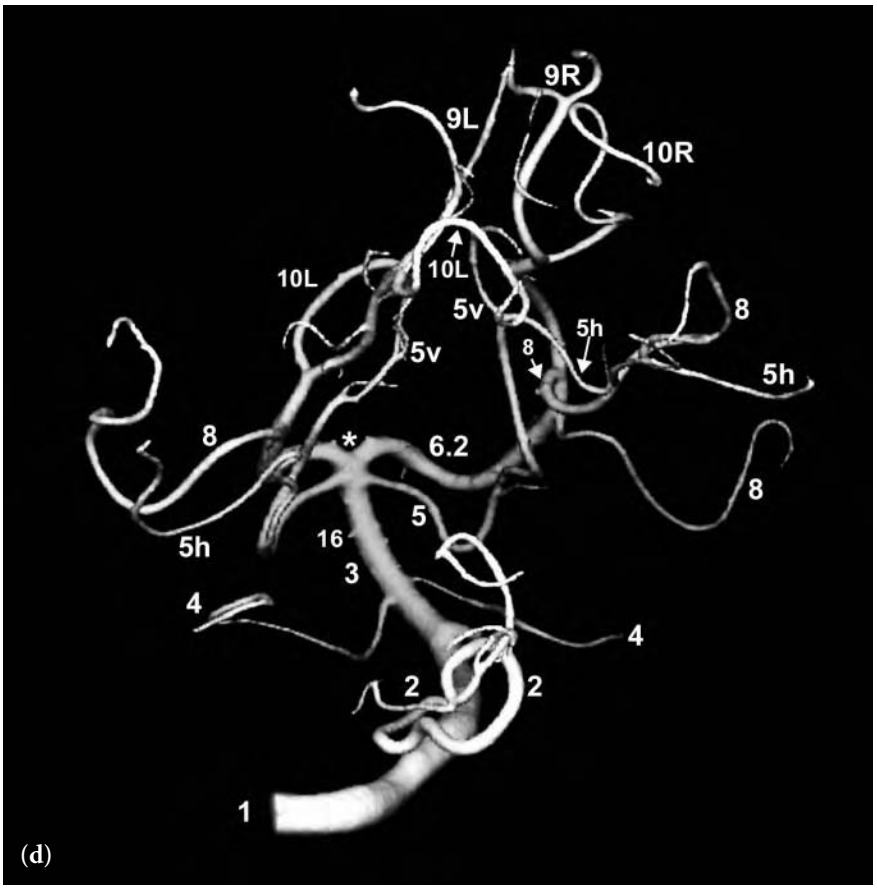

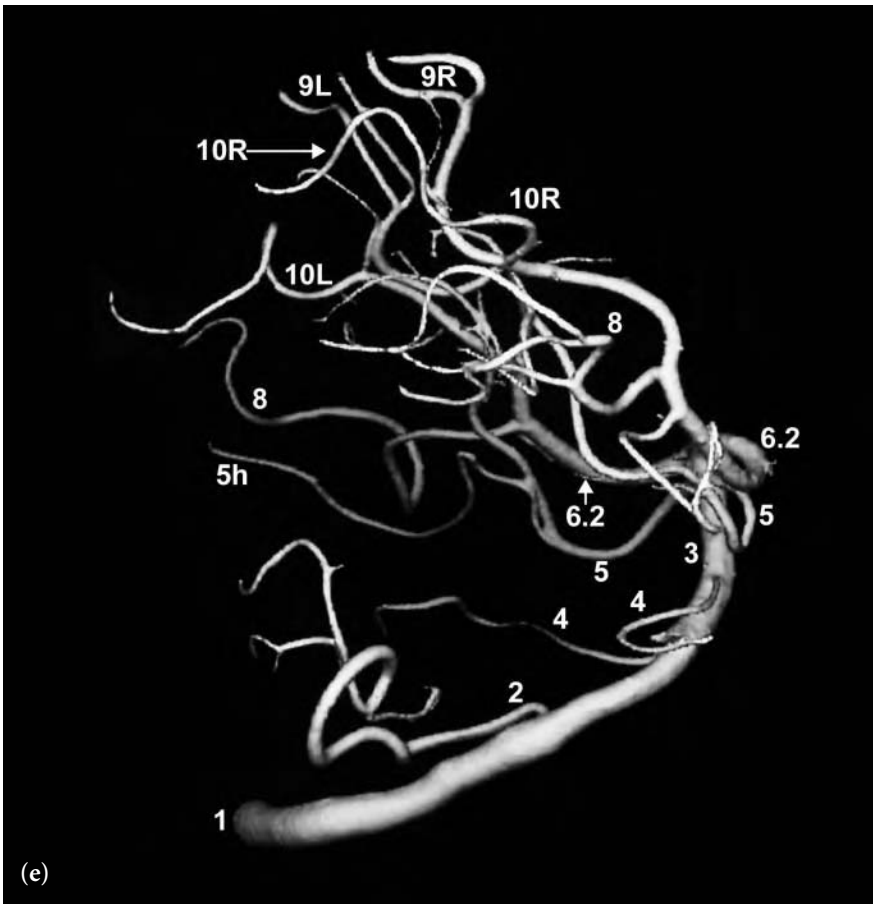

Fig. 6.2 (continued)

FIGURE KEY

1 vertebral artery
2 posterior inferior cerebellar artery (PICA)
3 basilar artery
4 anterior inferior cerebellar artery (AICA)
5 superior cerebellar artery
5v vermian branch of superior cerebellar artery
5h hemispheric branch of superior cerebellar artery
6.1 P1 segment of posterior cerebral artery (PCA)
6.2 P2 segment of posterior cerebral artery (PCA)
7 posterior communicating artery
8 posterior temporal branch of PCA
9 parieto-occipital branch of PCA
10 calcarine branch of PCA
16 pontine perforating artery
* tip of basilar artery

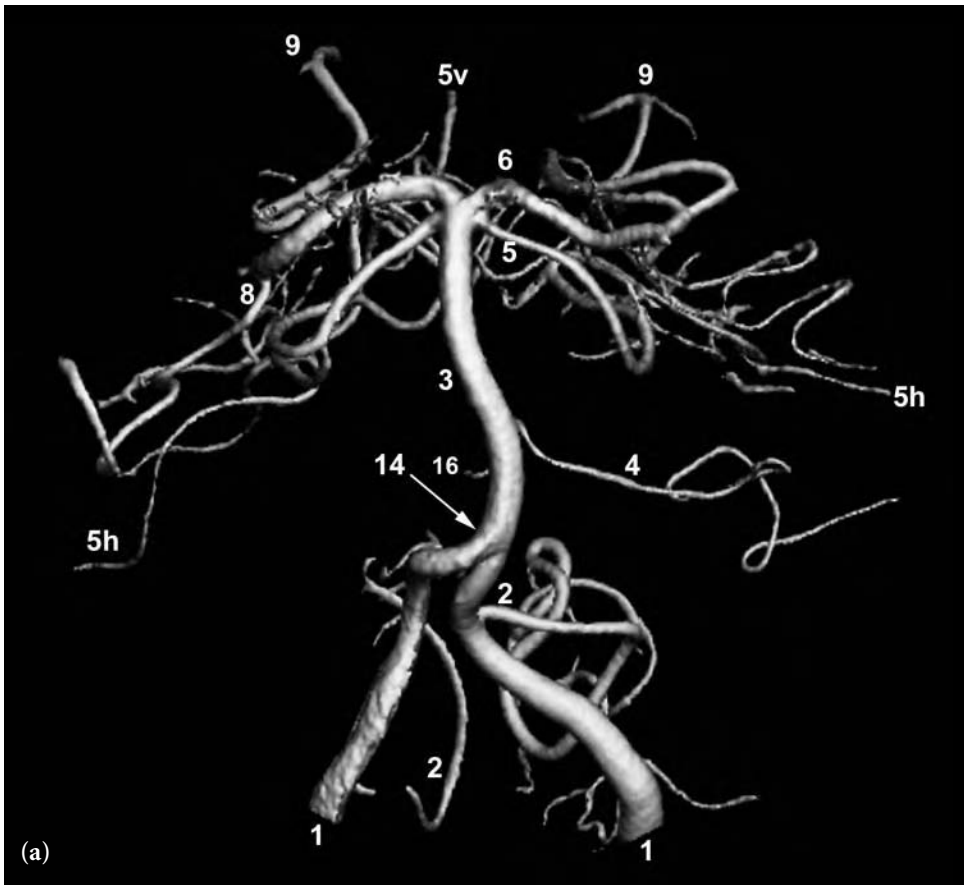

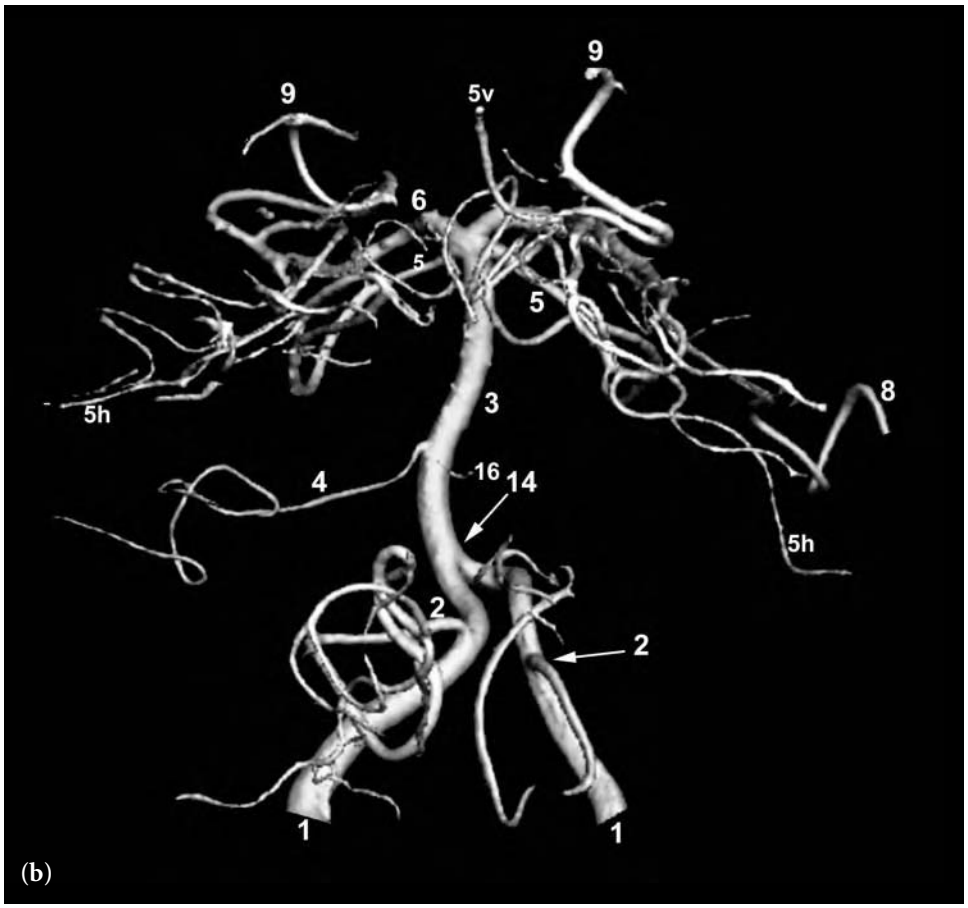

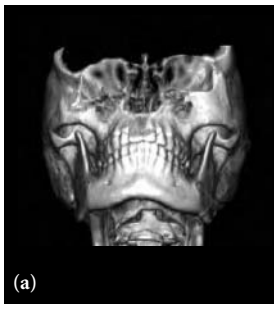

Fig. 6.3 (a,b) 3D frontal (*a*) and posterior (*b*) views of intracranial vertebral basilar circulation following vertebral artery injection. These images show normal vascular anatomy.

FIGURE KEY

1 vertebral artery
2 posterior inferior cerebellar artery (PICA)
3 basilar artery
4 anterior inferior cerebellar artery (AICA)
5 superior cerebellar artery (SCA)
5h hemispheric branch of SCA
5v vermian branch of SCA posterior cerebral artery (PCA)
8 posterior temporal branch of PCA
9 parieto-occipital branch of PCA
14 vertebral basilar junction
16 pontine perforating artery

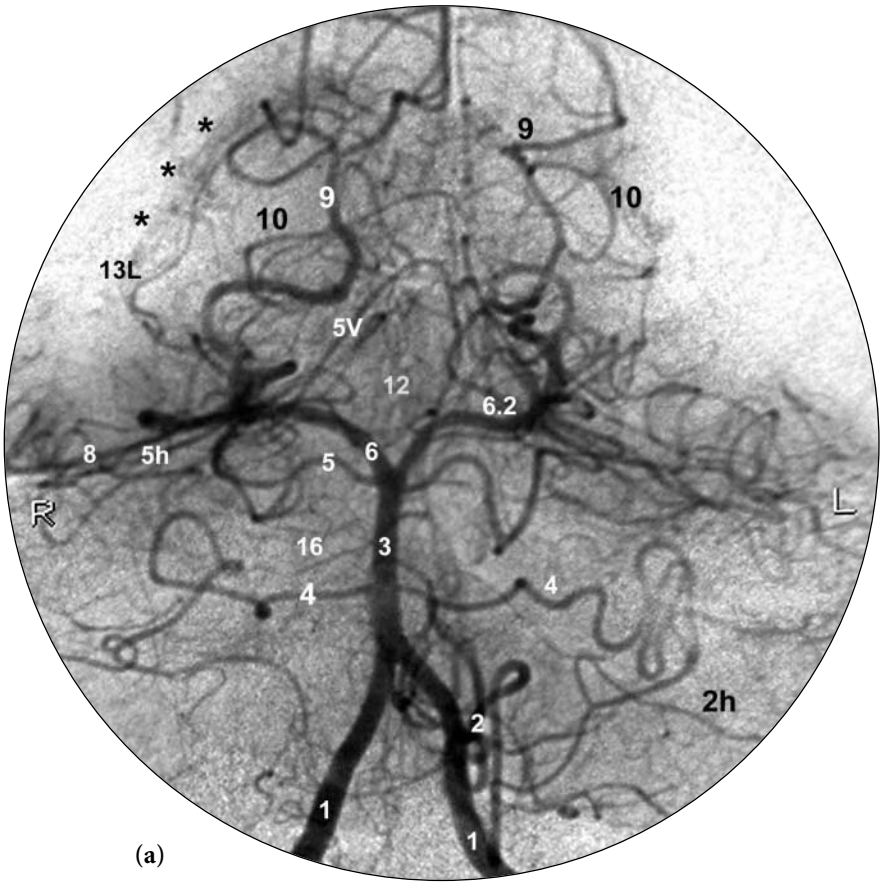

Fig. 6.4 (a,b) 2D frontal (*a*) and 3D frontal (*b*) views following vertebral artery injection. These two images show normal intracranial vertebral basilar circulation. Note the blush (*) of the choroid plexus in figure (*a*).

FIGURE KEY

1 vertebral artery
2 posterior inferior cerebellar artery (PICA)
2v vermian branch of PICA
2h hemispheric branch of PICA
3 basilar artery
4 anterior inferior cerebellar artery (AICA)
5 superior cerebellar artery (SCA)
5h hemispheric branch of SCA
5v vermian branch of SCA
6 posterior cerebral artery (PCA)
6.2 P2 segment of PCA
8 posterior temporal branch of PCA
9 parieto-occipital branch of PCA
10 calcarine branch of PCA
12 posterior thalamoperforating arteries
13L lateral posterior choroidal artery
16 pontine perforating artery
* blush of choroids plexus

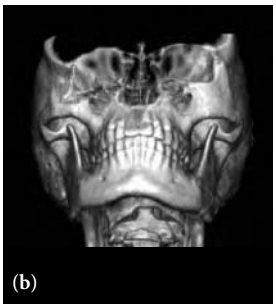
(b)

9
9
10
10
13L
5V
12
8
6.2
5h
6
5
5h
16
3
2v
4
2
2h
1
(b)

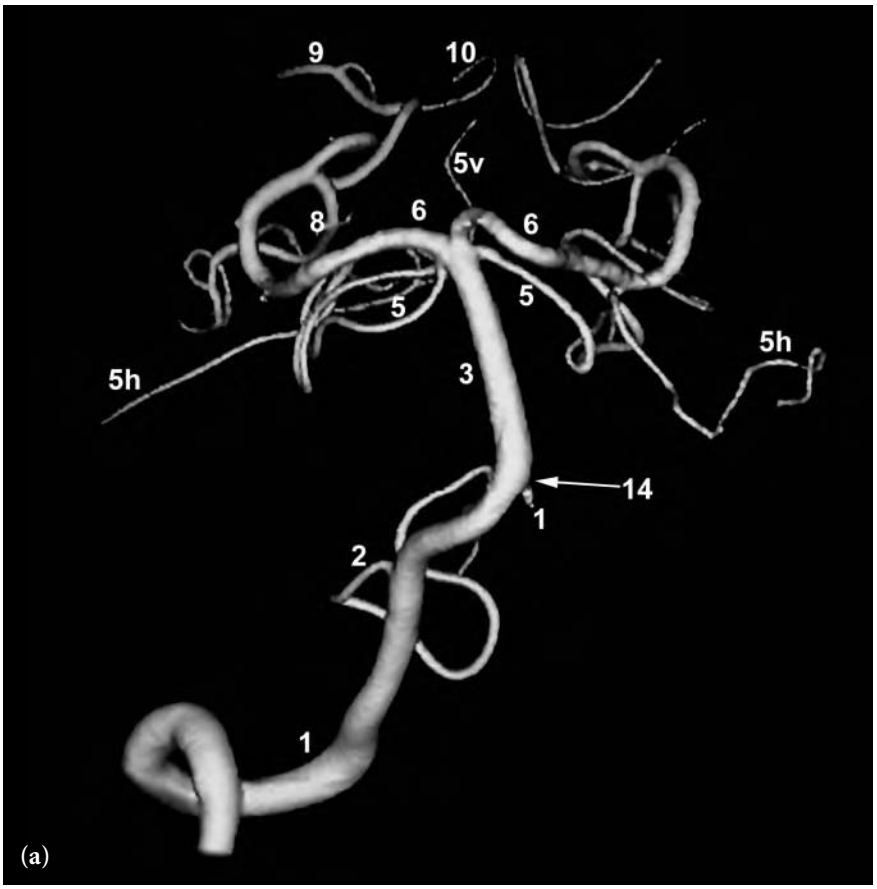

Fig. 6.5 (a–c) 3D frontal (*a*), right anterior oblique (*b*), and complex angle from below and from the left (*c*) views following right vertebral artery injection. These views show normal intracranial vertebral basilar circulation. Note the duplication of the right superior cerebellar artery. This is a normal variant.

FIGURE KEY

1 vertebral artery
2 posterior inferior cerebellar artery (PICA)
3 basilar artery
4 anterior inferior cerebellar artery (AICA)
5 superior cerebellar artery (SCA)
5h hemispheric branch of SCA
5v vermian branch of SCA
6 posterior cerebral artery (PCA)
6.1 P1 segment of PCA
6.2 P2 segment of PCA
8 posterior temporal branch of PCA
9 parieto-occipital branch of PCA
10 calcarine branch of PCA
14 vertebral basilar junction

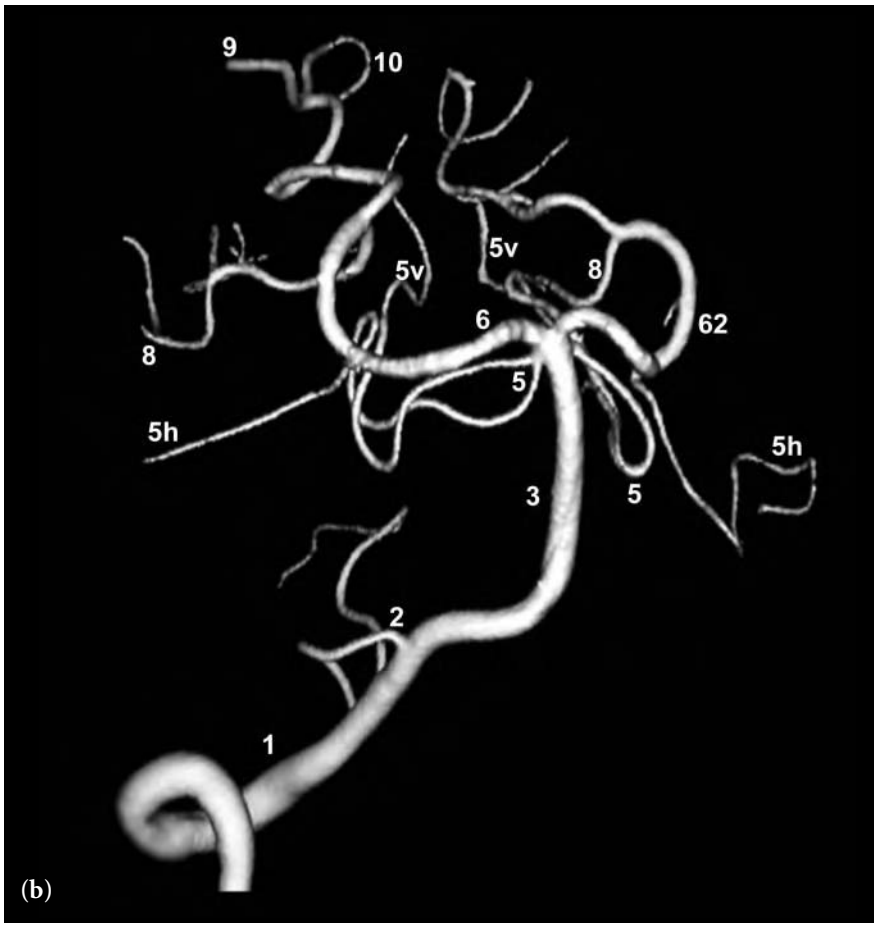
9
10
5v
5v
8
6
62
8
5
5h
5h
3
5
2
1
(b)

(b)

(c)

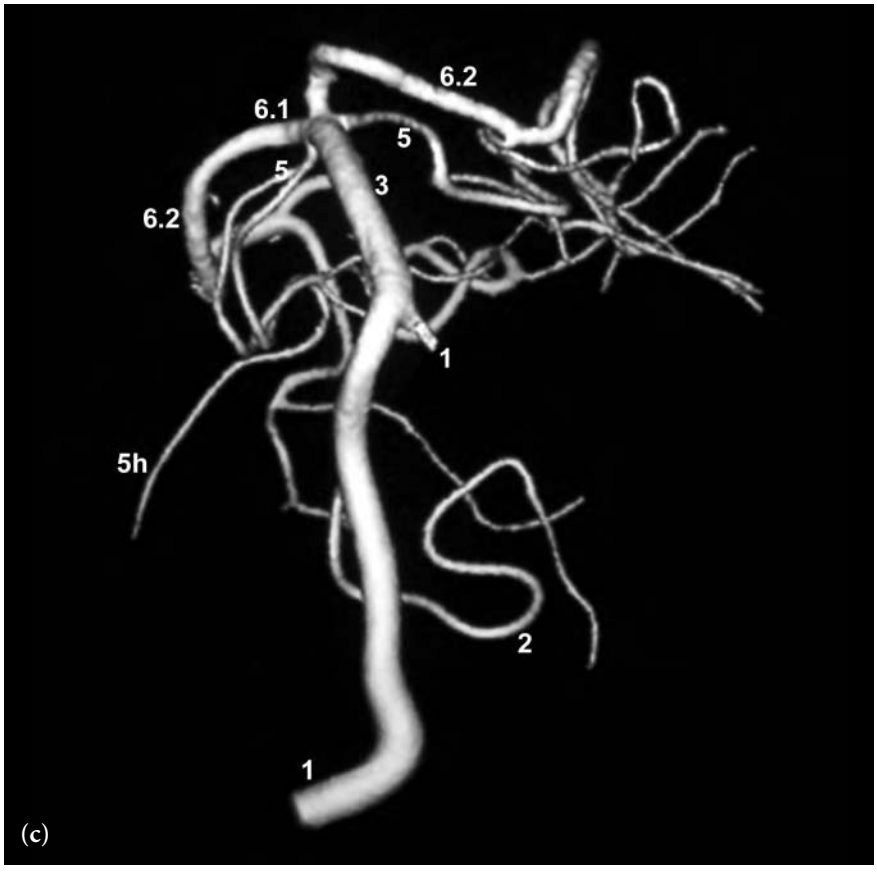
6.2
6.1
5
5
3
6.2
1
5h
2
1
(c)

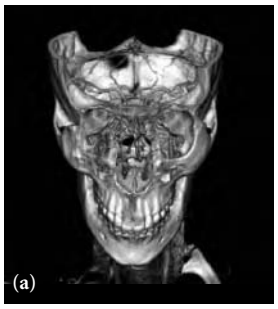

Fig. 6.6 (a–c) Frontal 2D (*a*), frontal 3D (*b*), and 2D lateral (*c*) views following left vertebral artery injection. This angiogram was obtained after GDC coiling of an aneurysm arising at the origin of the right AICA. The coil mass (**) has been subtracted from the image. No residual filling of the aneurysm is seen. This patient has a fetal/direct origin of the right PCA from the supraclinoid internal carotid artery. This allows for an unobstructed view of the right superior cerebellar artery branches. The different appearance of the branches in (*a*) versus (*b*) is related to the angle of the frontal projection which foreshortens the PCA and SCA branches on the frontal 3D image (*b*). These images show a common variant where a medial branch of the AICA supplies a part or all of the PICA territory. This is called an AICA-PICA.

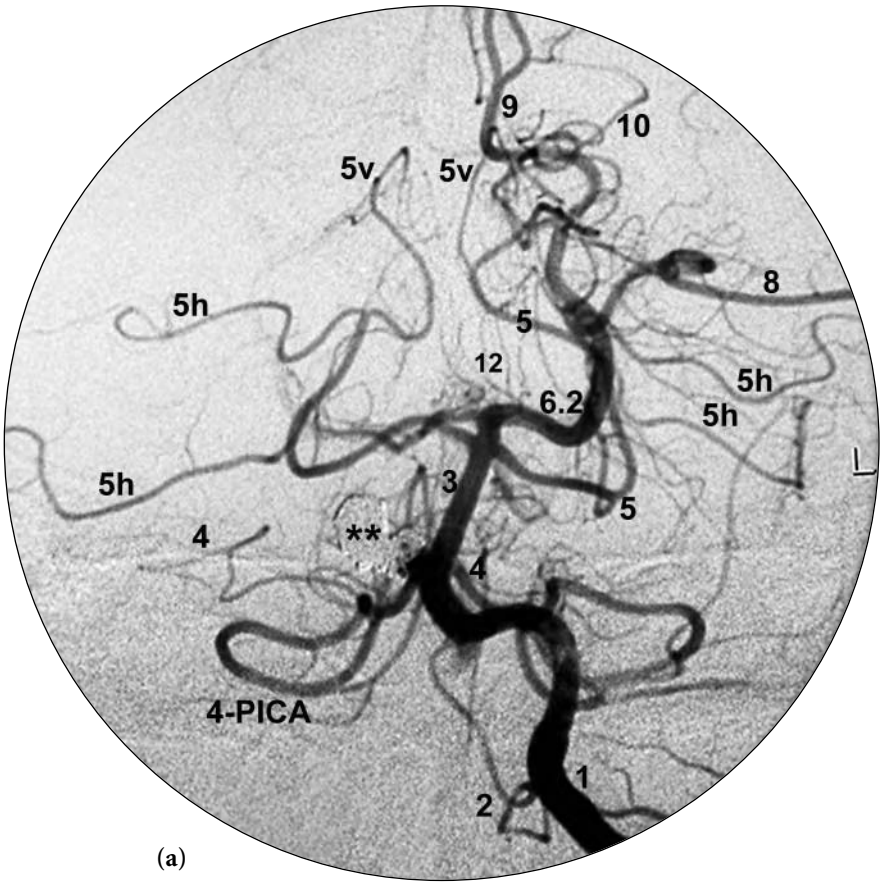

(a)

FIGURE KEY

1 vertebral artery
2 posterior inferior cerebellar artery (PICA)
2v vermian branch of PICA
2h hemispheric branch of PICA
4 anterior inferior cerebellar artery (AICA)
4-PICA AICA/PICA
5 superior cerebellar artery (SCA)
5h hemispheric branch of SCA
5v vermian branch of SCA
6.2 P2 segment of posterior cerebral artery (PCA)
7 posterior communicating artery
8 posterior temporal branch of PCA
9 parieto-occipital branch of PCA
10 calcarine branch of PCA
11 anterior thalamoperforating arteries
12 posterior thalamoperforating arteries
14 vertebral basilar junction
** GDC coil mass which has been subtracted on the 2D images.
Post choroidals medial and lateral posterior choroidal arteries

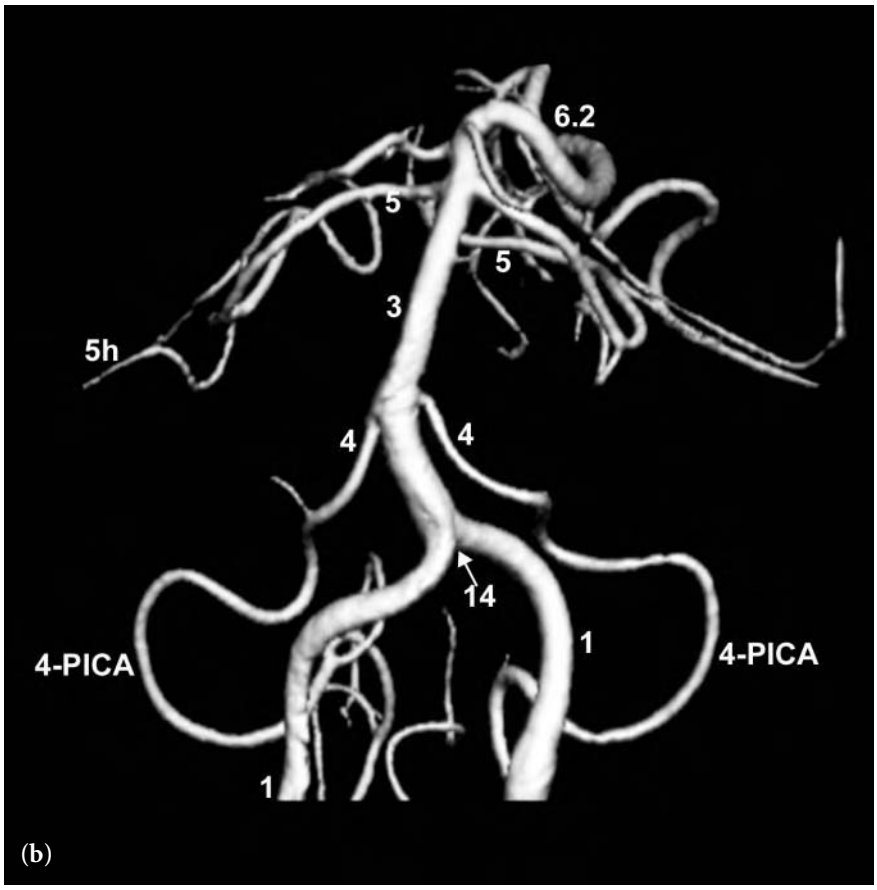
6.2
5
5
3
5h
4
4
14
1
4-PICA
4-PICA
1
(b)

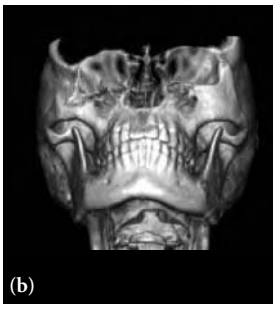
(b)

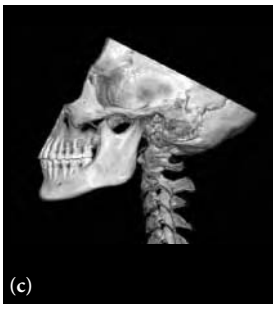
(c)

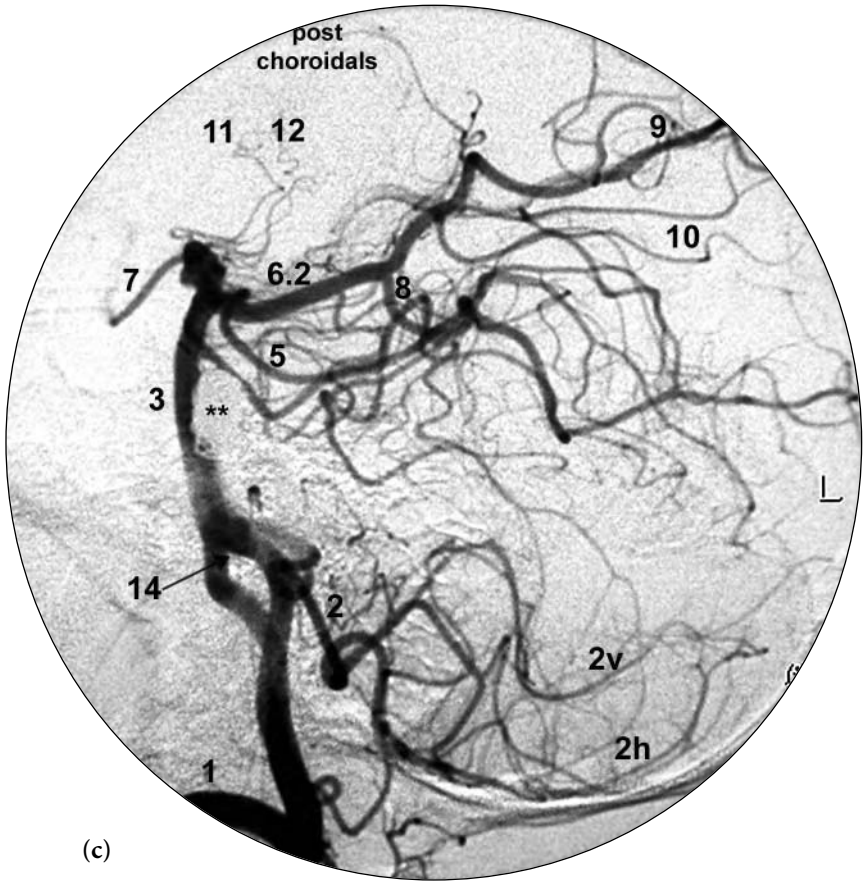
post
choroidals
11
12
9
10
7
6.2
8
5
3
**
14
2
2v
2h
1
(c)

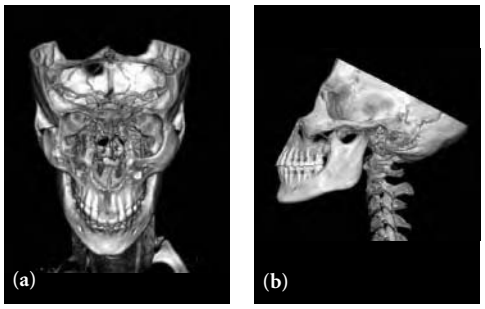

Fig. 6.7 (a,b) 2D frontal (*a*) and lateral (*b*) views following right vertebral artery injection show the intracranial vertebral basilar circulation in a patient with an arterial-venous malformation (AVM) in the right occipital lobe. This AVM is supplied by enlarged right calcarine (10) and parieto-occipital (9) branches of the right PCA. This demonstrates the enlargement of these two branches of the PCA due to the AVM and allows for easy identification. A perinidal aneurysm is indicated by (**).

FIGURE KEY

1 vertebral artery
2 posterior inferior cerebellar artery (PICA)
3 basilar artery
4 anterior inferior cerebellar artery (4)
5 superior cerebellar artery (SCA)
5v vermian branch of SCA
5h hemispheric branch of SCA
6.1 P1 segment of posterior cerebral artery (PCA)
6.2 P2 segment of posterior cerebral artery (PCA)
7 posterior communicating artery
8 posterior temporal branch of PCA
9 parieto-occipital branch of PCA
10 calcarine branch of PCA
11 anterior thalamoperforating arteries
12 posterior thalamoperforating arteries
13m medial posterior choroidal arteries
13L lateral posterior choroidal arteries
15 splenial branch (posterior pericallosal artery) of PCA
** perinidal aneurysm

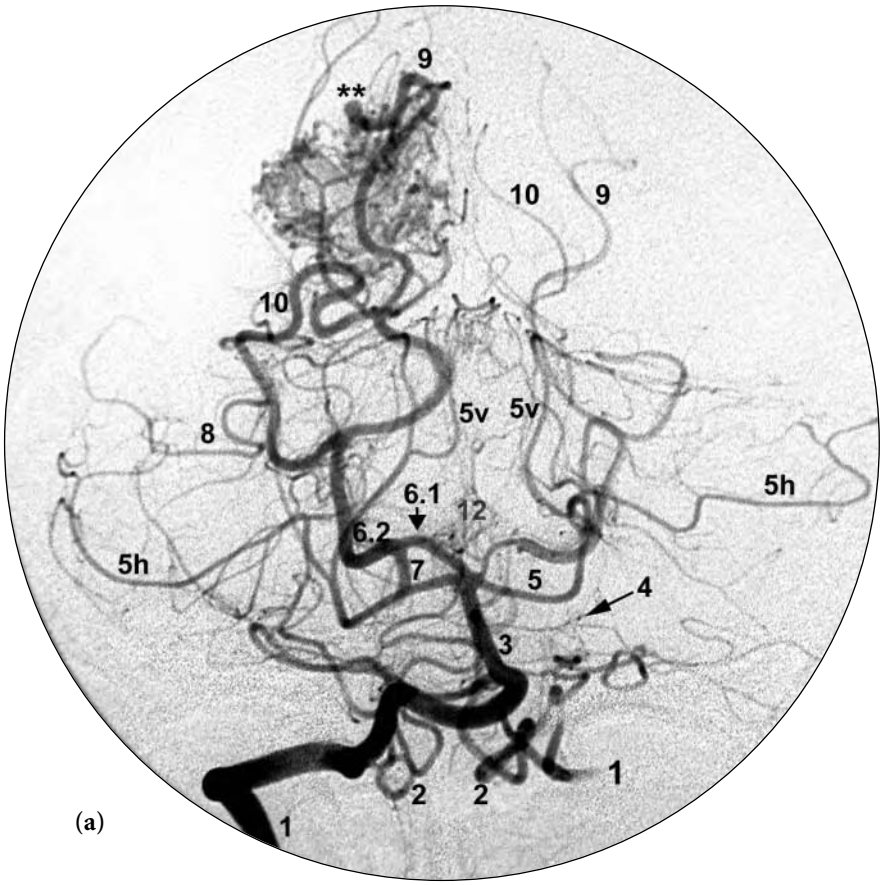

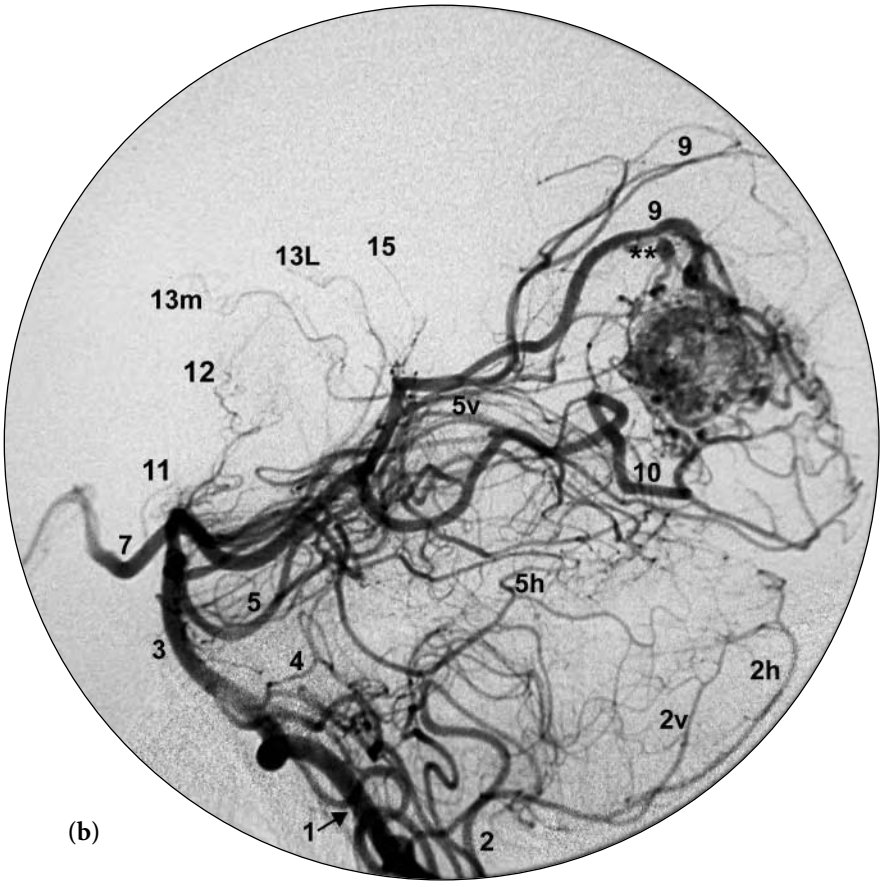

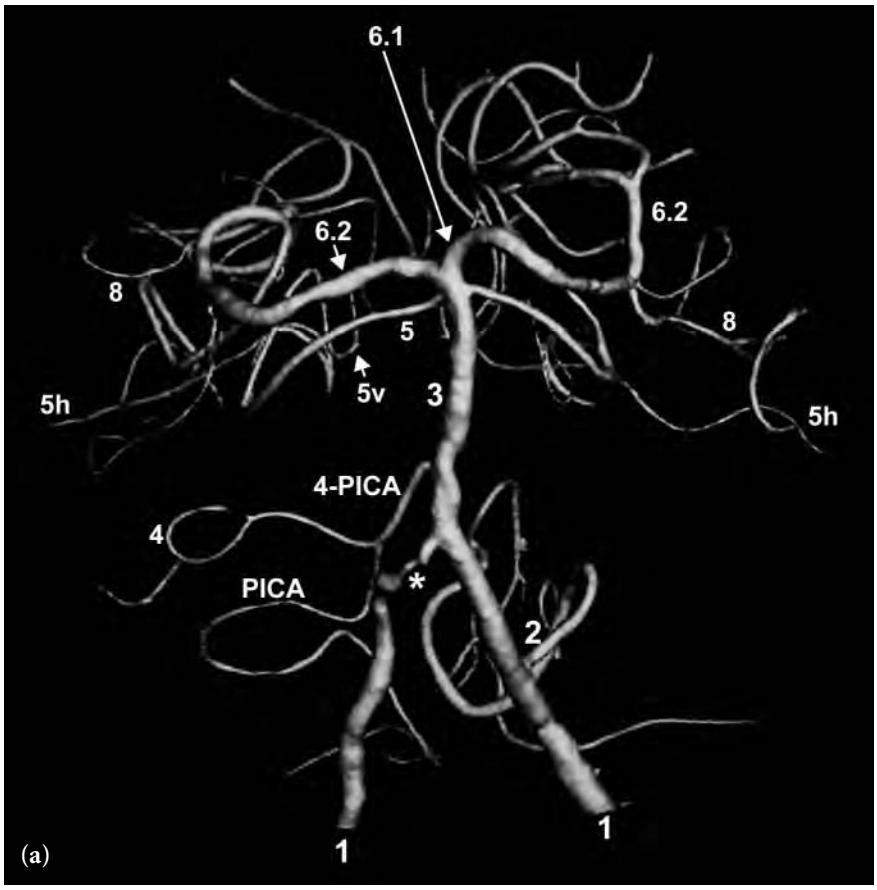

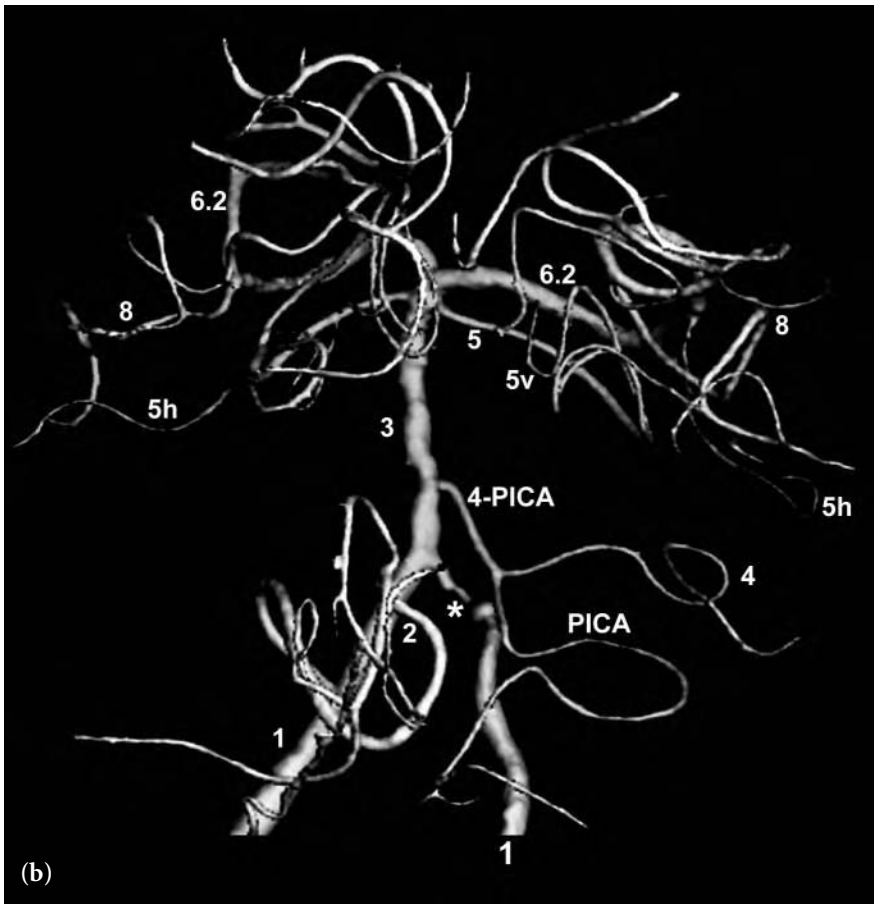

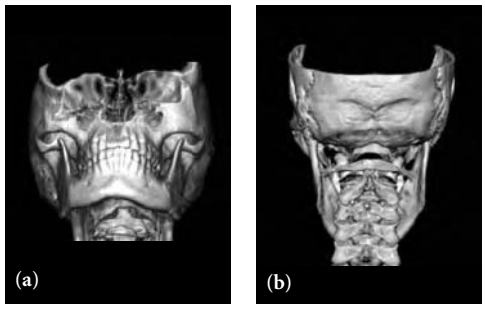

Fig. 6.8 (a,b) 3D frontal (*a*) and posterior (*b*) views following left vertebral artery injection. These views show intracranial vertebral basilar circulation in a patient with severe atherosclerotic vascular disease. Note the multifocal areas of vessel irregularity and narrowing (stenoses) and the severe narrowing of the distal right vertebral artery (*). This is a good demonstration of a right AICA-PICA where a medial branch of AICA supplies all or a portion of the PICA territory.

FIGURE KEY

1 vertebral artery
2 posterior inferior cerebellar artery (PICA)
3 basilar artery
4 anterior inferior cerebellar artery (AICA)
4 – PICA AICA-PICA
5 superior cerebellar artery (SCA)
5h hemispheric branch of SCA
5v vermian branch of SCA
6.1 P1 segment of posterior cerebral artery (PCA)
6.2 P2 segment of posterior cerebral artery (PCA)
8 posterior temporal branch of PCA
* severe stenosis (narrowing) distal right vertebral artery

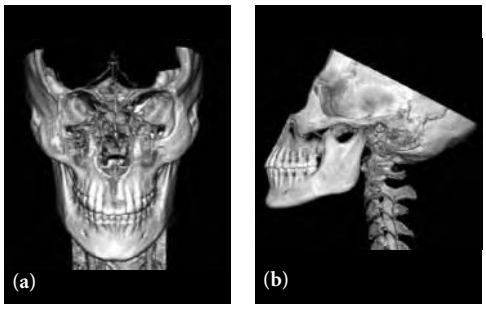

Fig. 6.9 (a,b) 3D frontal (*a*) and lateral (*b*) views following left vertebral artery injection. These images show the intracranial vertebral basilar circulation in a patient with severe atherosclerotic vascular disease. Note the moderately severe stenosis of the midbasilar artery in addition to a generalized vessel irregularity.

FIGURE KEY

1 vertebral artery
2 posterior inferior cerebellar artery (PICA)
3 basilar artery
4 anterior inferior cerebellar artery (AICA)
5 superior cerebellar artery (SCA)
5v vermian branch of SCA
5h hemispheric branch of SCA
6.1 P1 segment of posterior cerebral artery (PCA)
6.2 P2 segment of posterior cerebral artery (PCA)
8 posterior temporal branch of PCA
9 parieto-occipital branch of PCA
10 calcarine branch of PCA

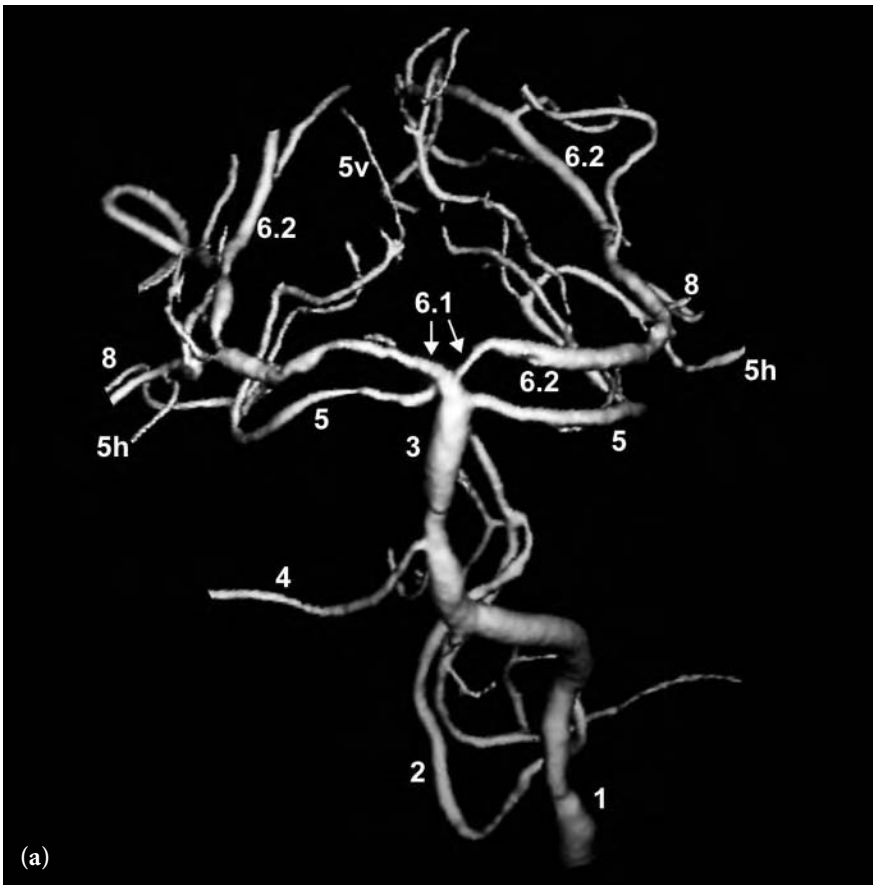

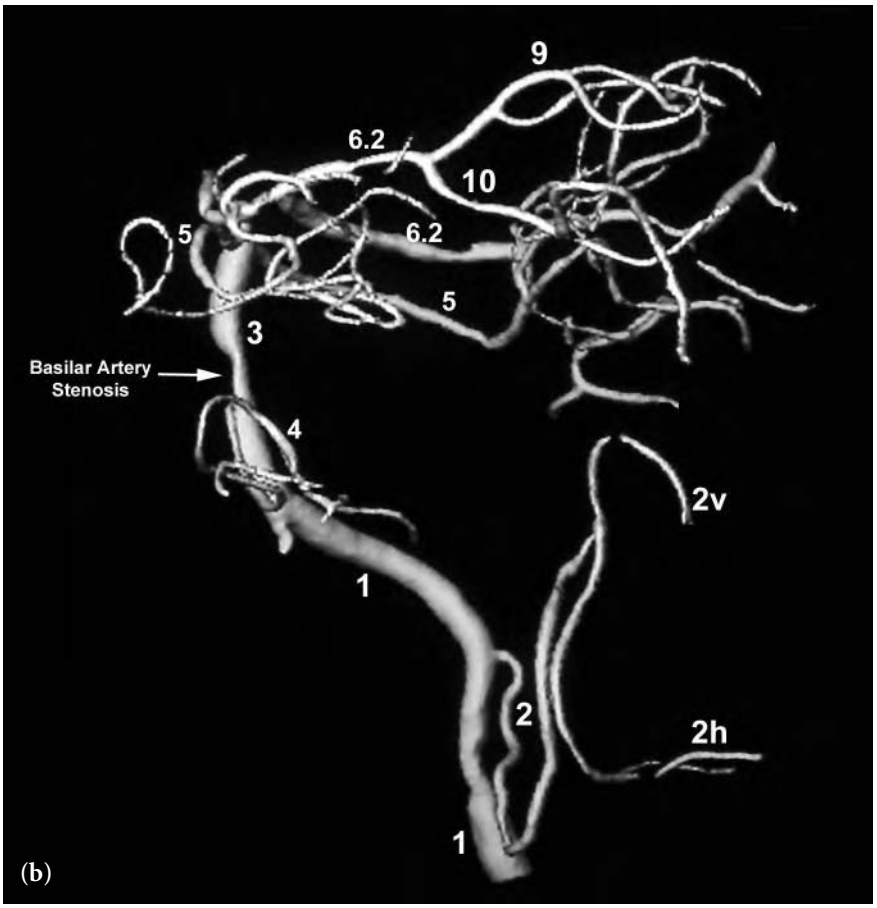

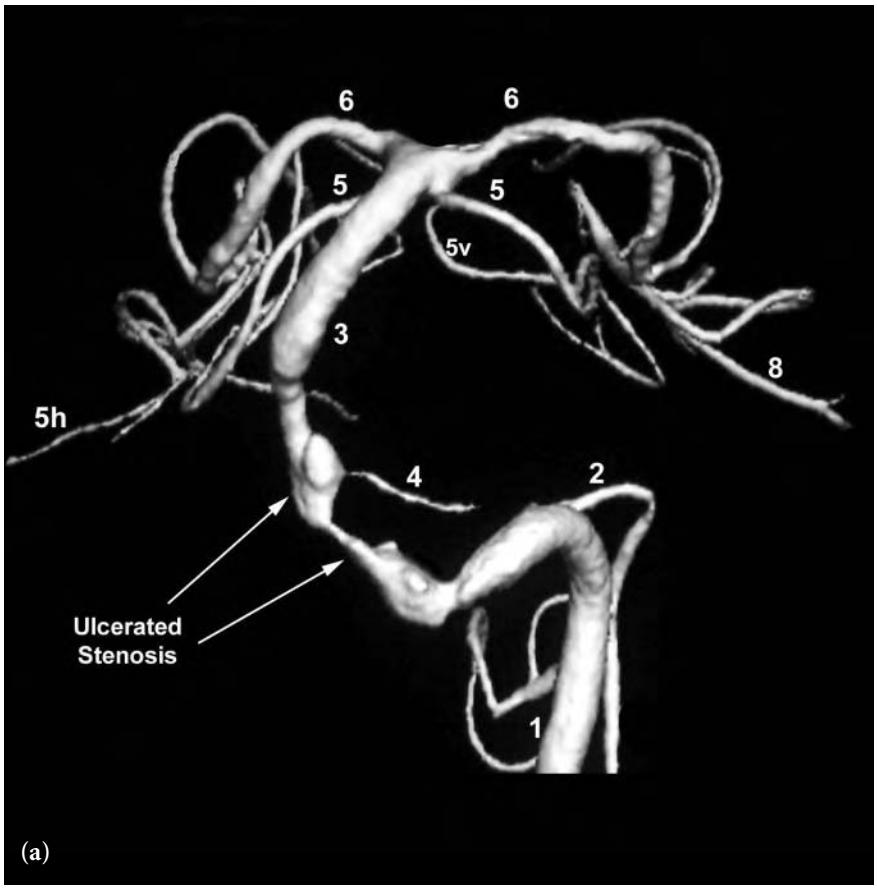

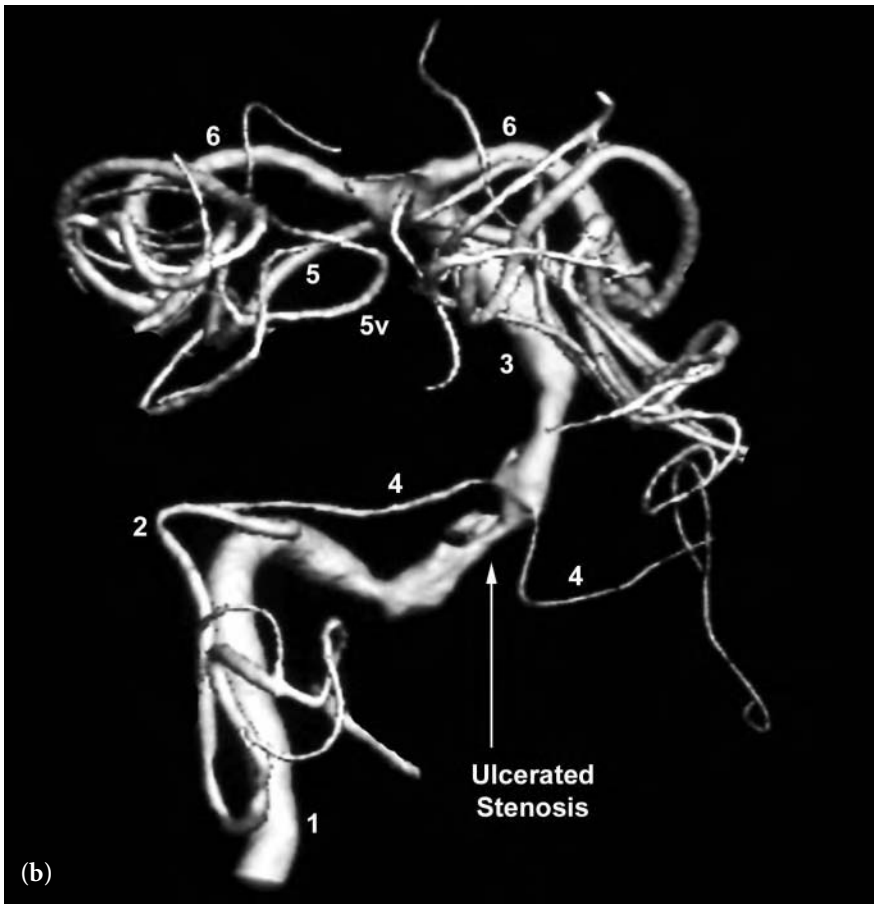

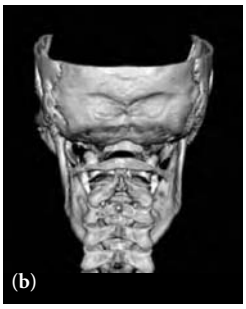

Fig. 6.10 (a–e) 3D frontal (*a*), posterior (*b*), and superior (*c*) pre-stent views and 2D frontal (*d*) and 3D frontal (*e*) post-stent views following left vertebral artery injections. The intracranial view of the vertebral basilar circulation is of a patient with severe atherosclerotic vascular disease with severe ulcerated plaque of the mid- to lower-basilar artery with high-grade stenosis. Note the endoluminal impression of the stent on the basilar artery in view (e).

FIGURE KEY

1 vertebral artery
2 posterior inferior cerebellar artery (PICA)
2v vermian branch of PICA
3 basilar artery
4 anterior inferior cerebellar artery (AICA)
5 superior cerebellar artery (SCA)
5h hemispheric branch of SCA
5v vermian branch of SCA
6 posterior cerebral artery (PCA)
8 posterior temporal branch of PCA
9 parieto-occipital branch of PCA
10 calcarine branch of PCA
* stented segment of basilar artery

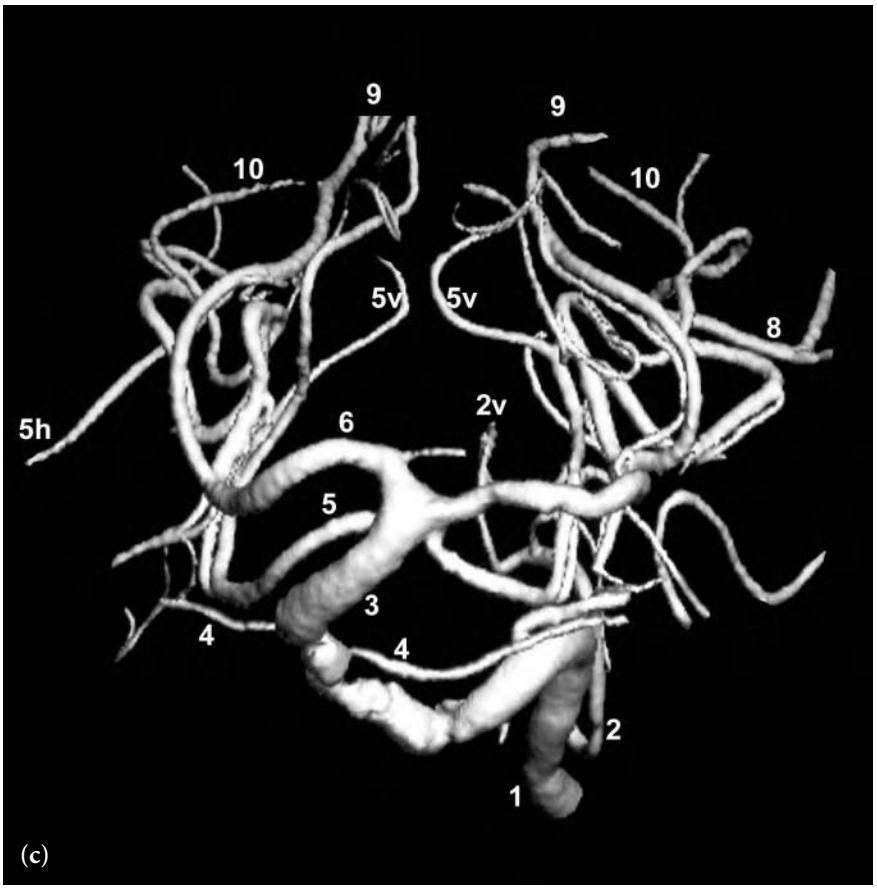

Fig. 6.10 (continued)

FIGURE KEY

1 vertebral artery
2 posterior inferior cerebellar artery (PICA)
2v vermian branch of PICA
3 basilar artery
4 anterior inferior cerebellar artery (AICA)
5 superior cerebellar artery (SCA)
5h hemispheric branch of SCA
5v vermian branch of SCA
6 posterior cerebral artery (PCA)
8 posterior temporal branch of PCA
9 parieto-occipital branch of PCA
10 calcarine branch of PCA
* stented segment of basilar artery

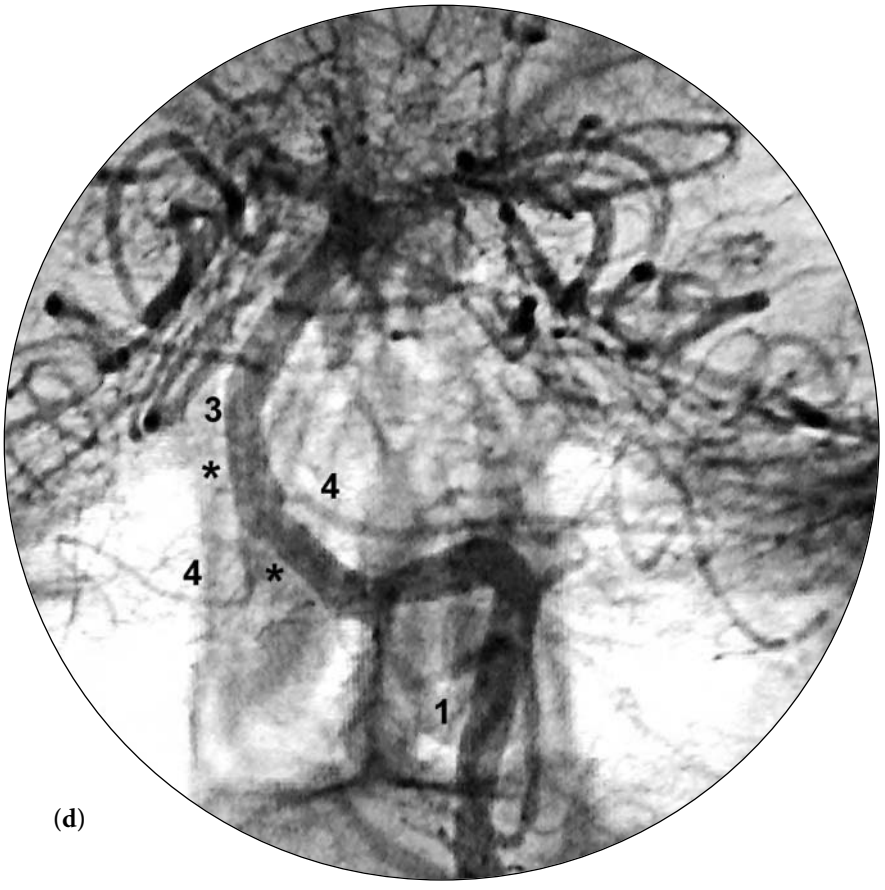

(d)

(e)

6
6
5
3
*
4
4
*
1
(e)

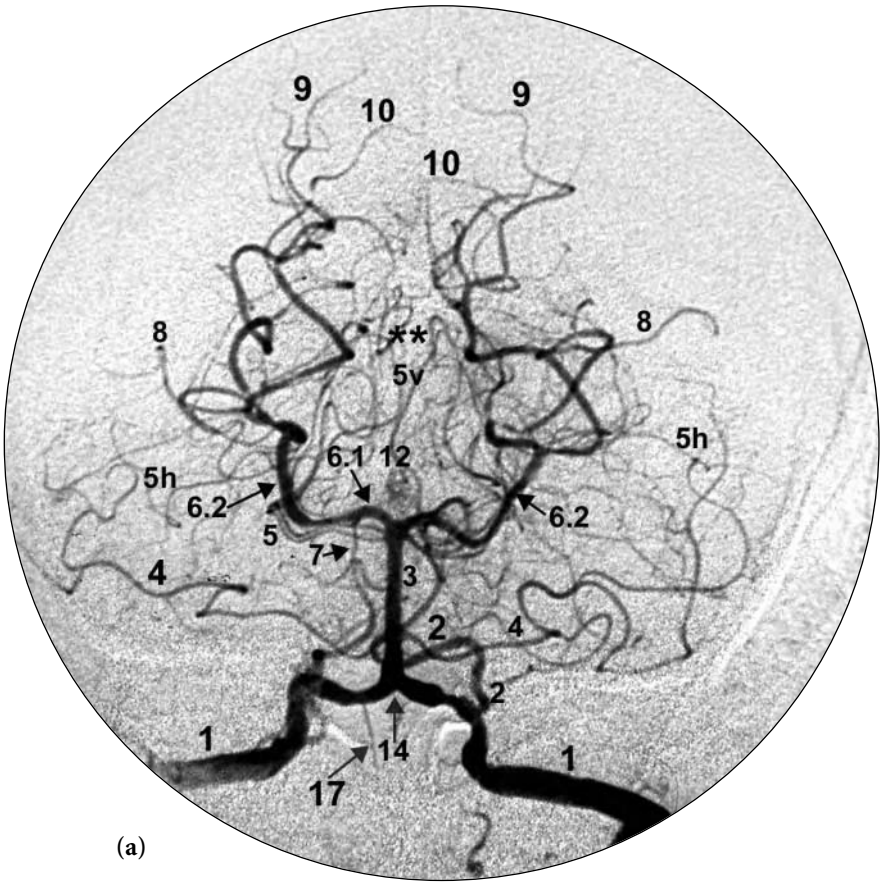

Fig. 6.11 (a–c) 2D frontal (*a*), lateral early arterial (*b*), and lateral late arterial phase (*c*) views following left vertebral artery injection. The intracranial view of the vertebral basilar circulation is of a patient with vasculitis. The vasculitis is illustrated by the multifocal areas of stenosis (narrowing). The vascular branching pattern shows a typical appearance of vertebral basilar circulation.

FIGURE KEY

1 vertebral artery
2 posterior inferior cerebellar artery (PICA)
2v vermian branch of PICA
2h hemispheric branch of PICA
3 basilar artery
4 anterior inferior cerebellar artery (AICA)
5 superior cerebellar artery (SCA)
5v vermian branch of SCA
5h hemispheric branch of SCA
6.1 P1 segment of posterior cerebral artery (PCA)
6.2 P2 segment of posterior cerebral artery (PCA)
7 posterior communicating artery
8 posterior temporal branch of PCA
9 parieto-occipital branch of PCA
10 calcarine branch of PCA
11 anterior thalamoperforating arteries
12 posterior thalamoperforating arteries
13m medial posterior choroidal artery
13L lateral posterior choroidal artery
14 vertebral basilar junction
15 splenial branch (posterior pericallosal artery) of PCA
** region of quadrigeminal plate cistern
17 anterior spinal artery

(b,c)

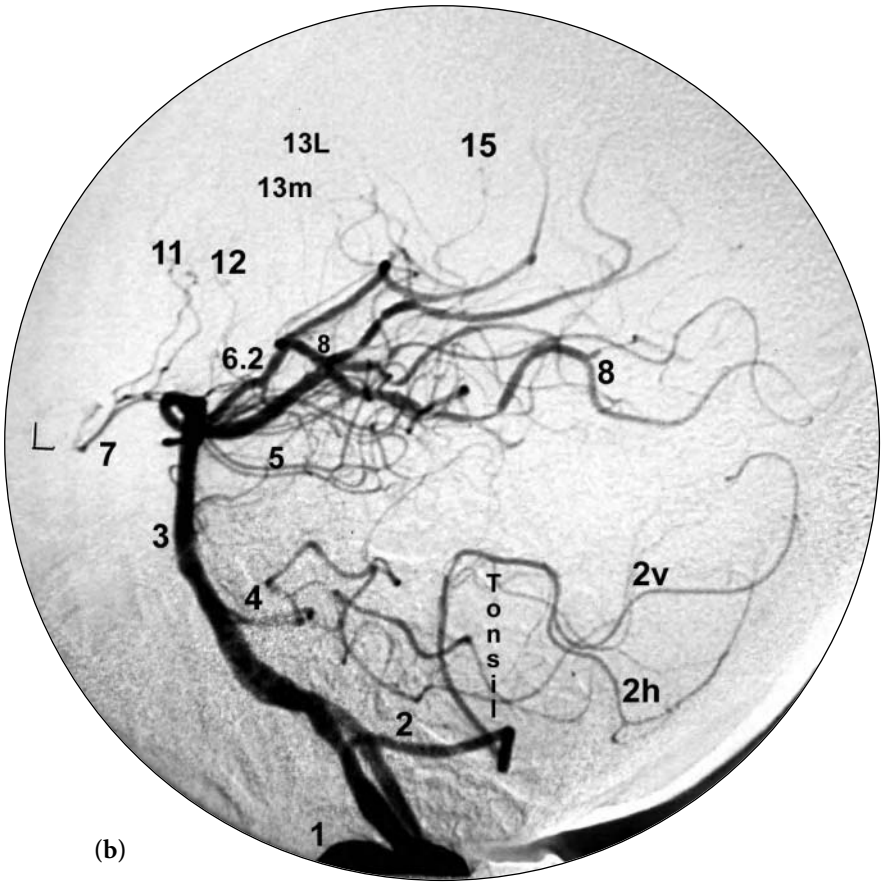
13L
15
13m
11
12
6.2
8
8
L
7
5
3
4
Tonsil
2v
2h
2
1

(b)

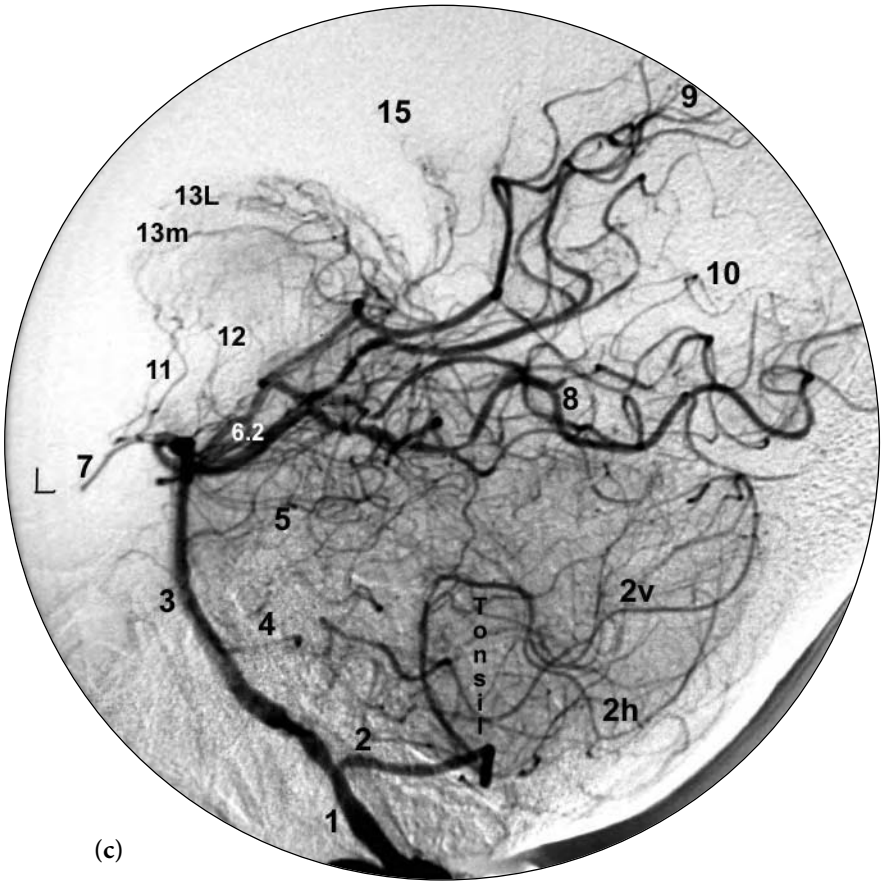
15
9
13L
13m
10
12
11
8
6.2
L
7
5
3
4
Tonsil
2v
2h
2
1

(c)

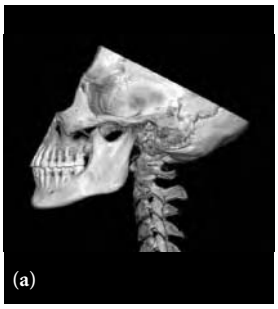

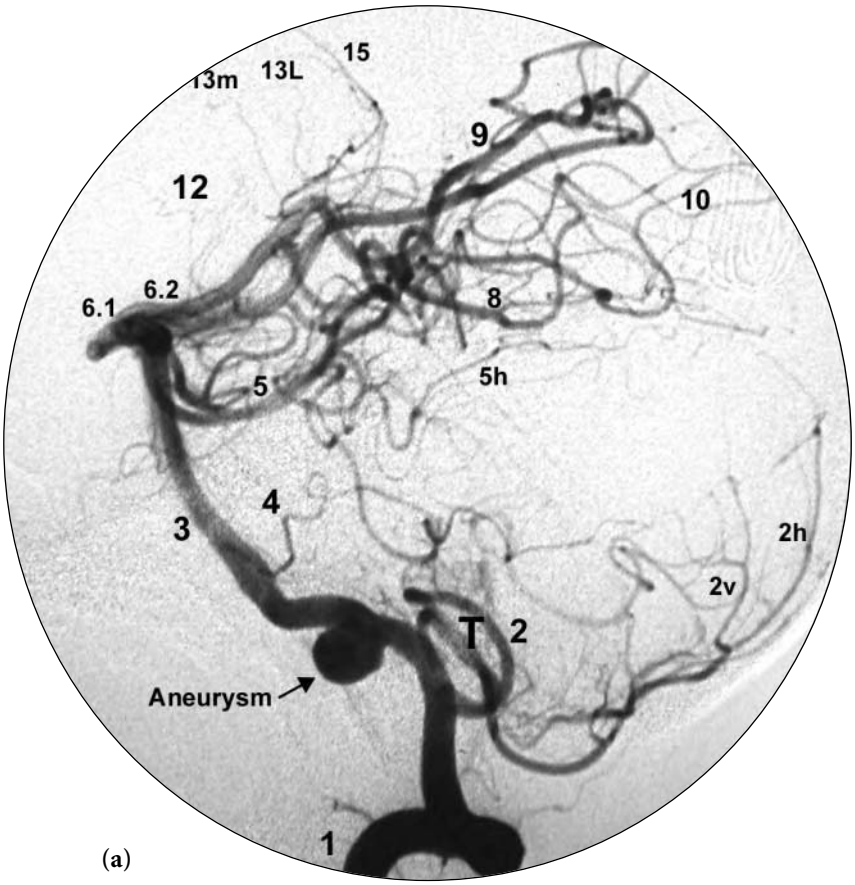

Fig. 6.12 (a–c) 2D lateral (*a*), 3D frontal (*b*), and 3D lateral (*c*) views following vertebral artery injection. Intracranial vertebral basilar circulation is seen with a moderate-size aneurysm arising from the distal vertebral artery near the origin of the PICA.

FIGURE KEY

1 vertebral artery
2 posterior inferior cerebellar artery (PICA)
2v vermian branch of PICA
2h hemispheric branch of PICA
3 basilar artery
4 anterior inferior cerebellar artery (AICA)
5 superior cerebellar artery (SCA)
5h hemispheric branch of SCA
6 posterior cerebral artery (PCA)
6.1 P1 segment of PCA
6.2 P2 segment of PCA
8 posterior temporal branch of PCA
9 parieto-occipital branch of PCA
10 calcarine branch of PCA
12 posterior thalamoperforating arteries
13m medial posterior choroidal arteries
13L lateral posterior choroidal arteries
15 splenial branch (posterior pericallosal artery) branch of PCA

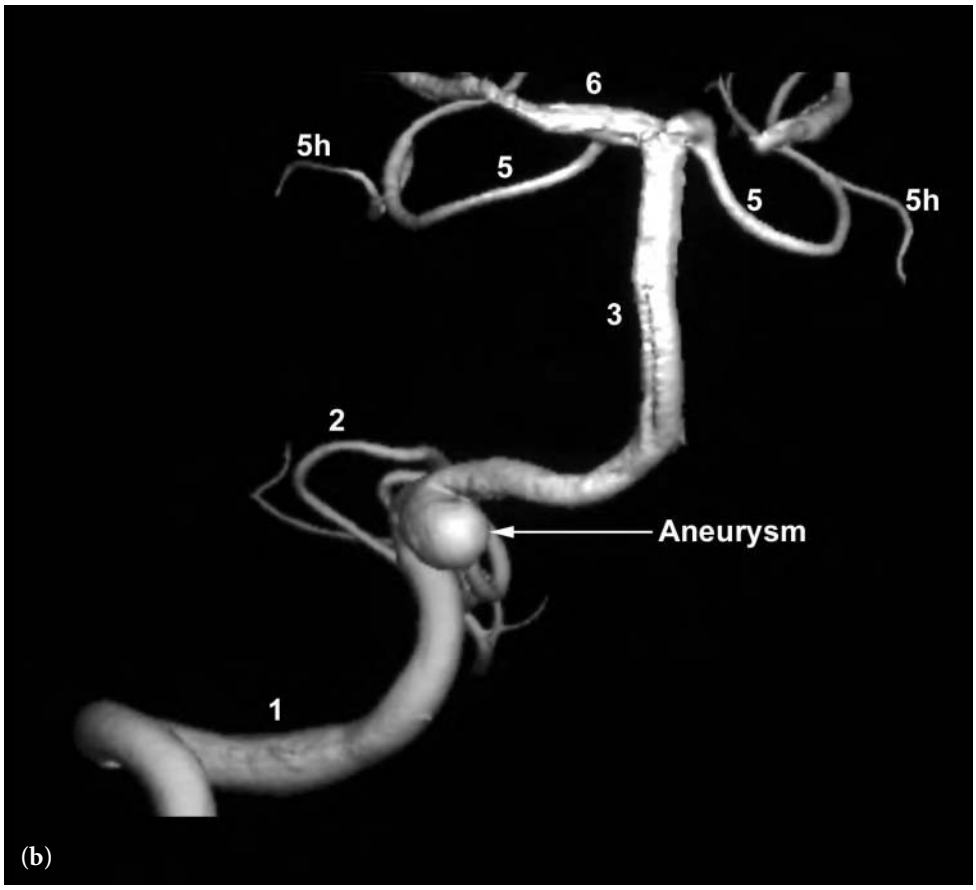
6
5h
5
5
5h
3
2
Aneurysm
1
(b)

(b)

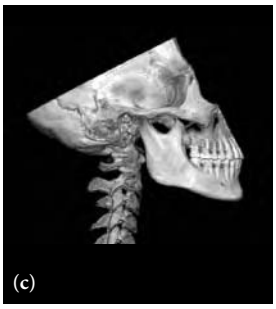
(c)

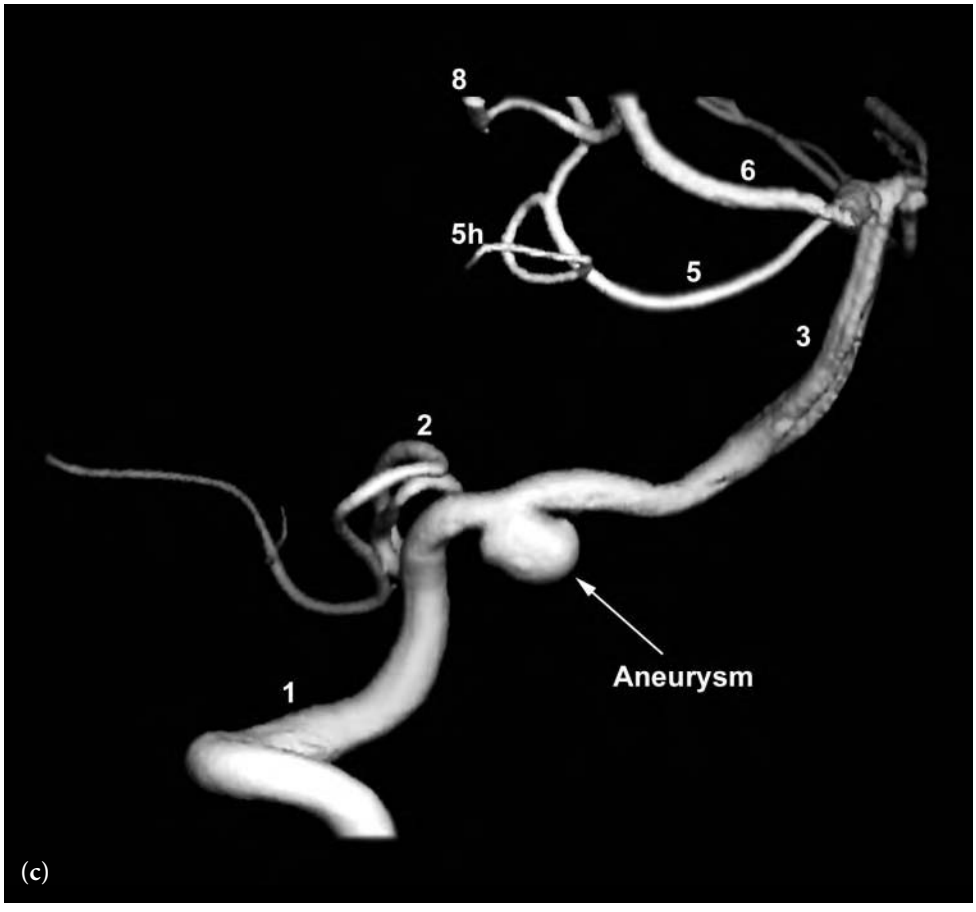
8
6
5h
5
3
2
Aneurysm
1
(c)

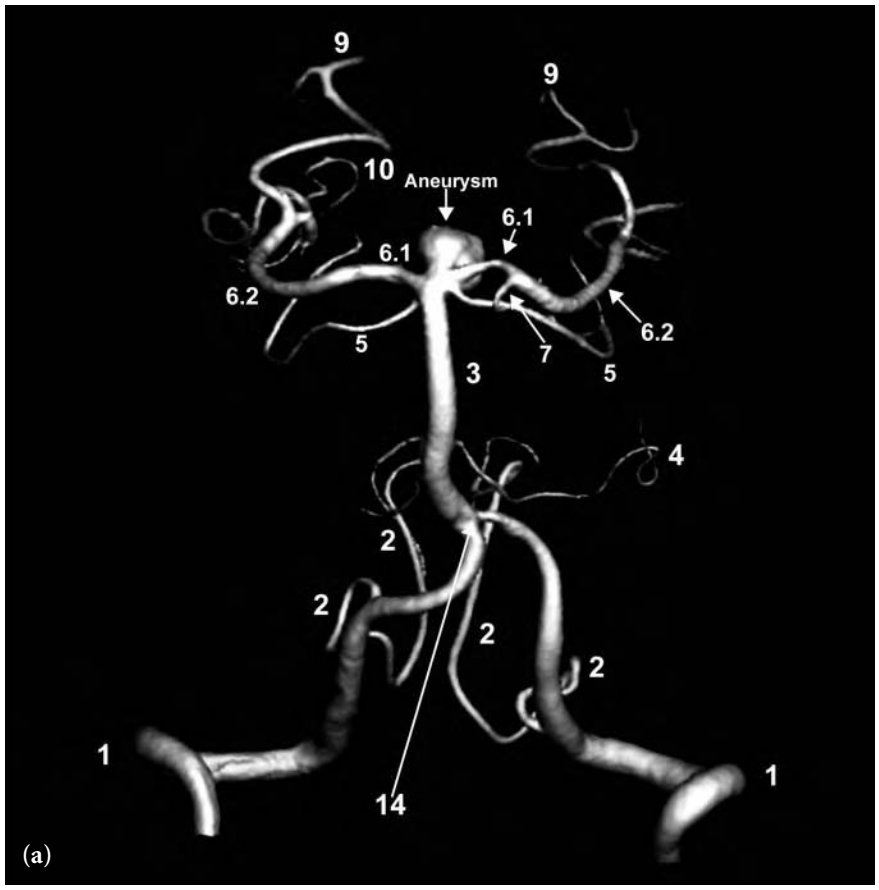

Fig. 6.13 (a–j) This series of 3D images of the intracranial vertebral basilar circulation demonstrate a lobulated aneurysm arising from the tip of the basilar artery projecting posteriorly into the interpeduncular cistern. This case also illustrates normal vertebral basilar circulation. The different projections in this series of images are good examples of the course and relationship of the vessels to each other.

PROJECTION KEY

a frontal view
b left anterior oblique view
c posterior view
d left posterior oblique view
e right posterior oblique view with inferior to superior angulation
f near lateral view with inferior to superior angulation
g inferior to superior right anterior oblique view
h inferior to superior left anterior oblique view
i superior to inferior view
j superior to inferior left anterior oblique

FIGURE KEY

1 vertebral artery
2 posterior inferior cerebellar artery
3 basilar artery
4 anterior inferior cerebellar artery
5 superior cerebellar artery
6.1 P1 segment of posterior cerebral artery (PCA)
6.2 P2 segment of posterior cerebral artery (PCA)
7 posterior communicating artery
9 parieto-occipital branch of PCA
10 calcarine branch of PCA
14 vertebral basilar junction

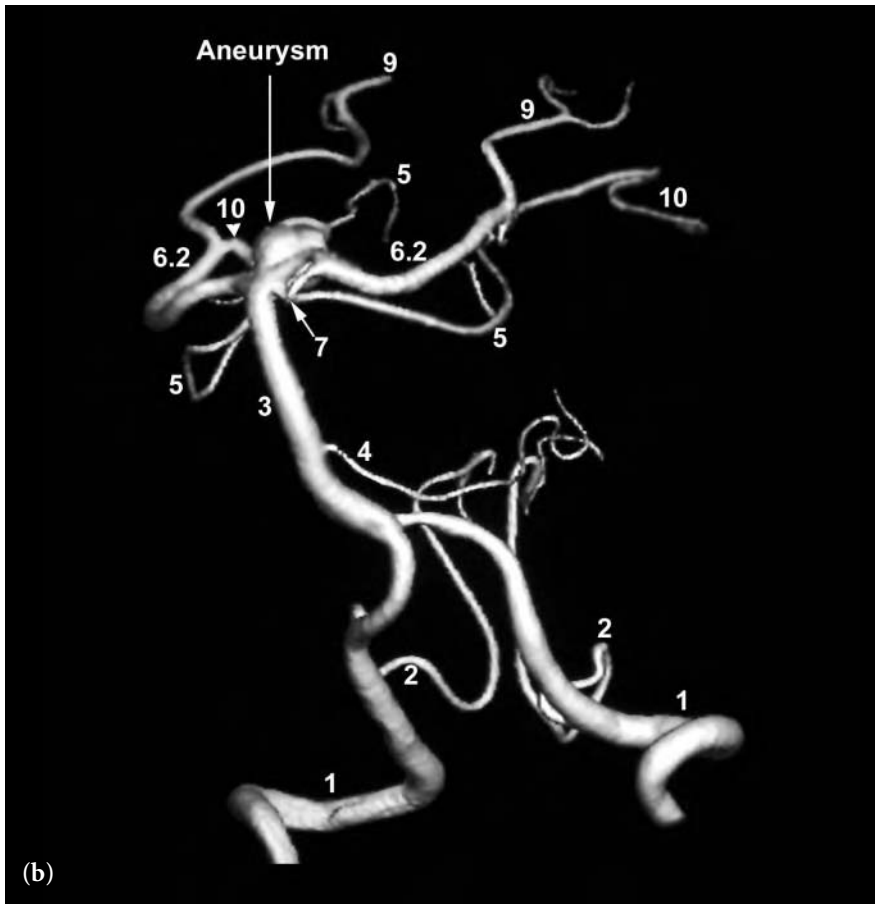

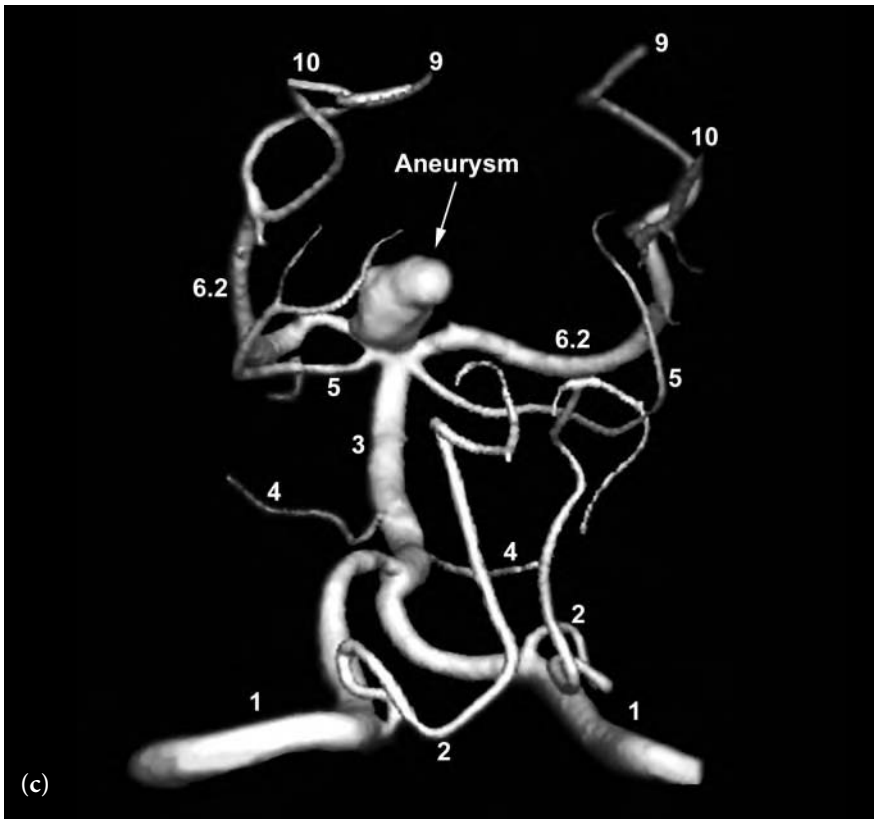
10
9
9
10
Aneurysm
6.2
6.2
5
5
3
4
4
2
1
1
2
(c)

(c)

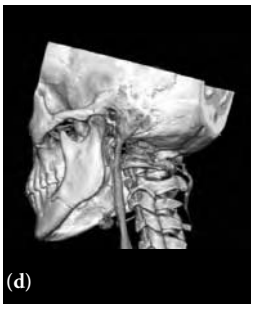
(d)

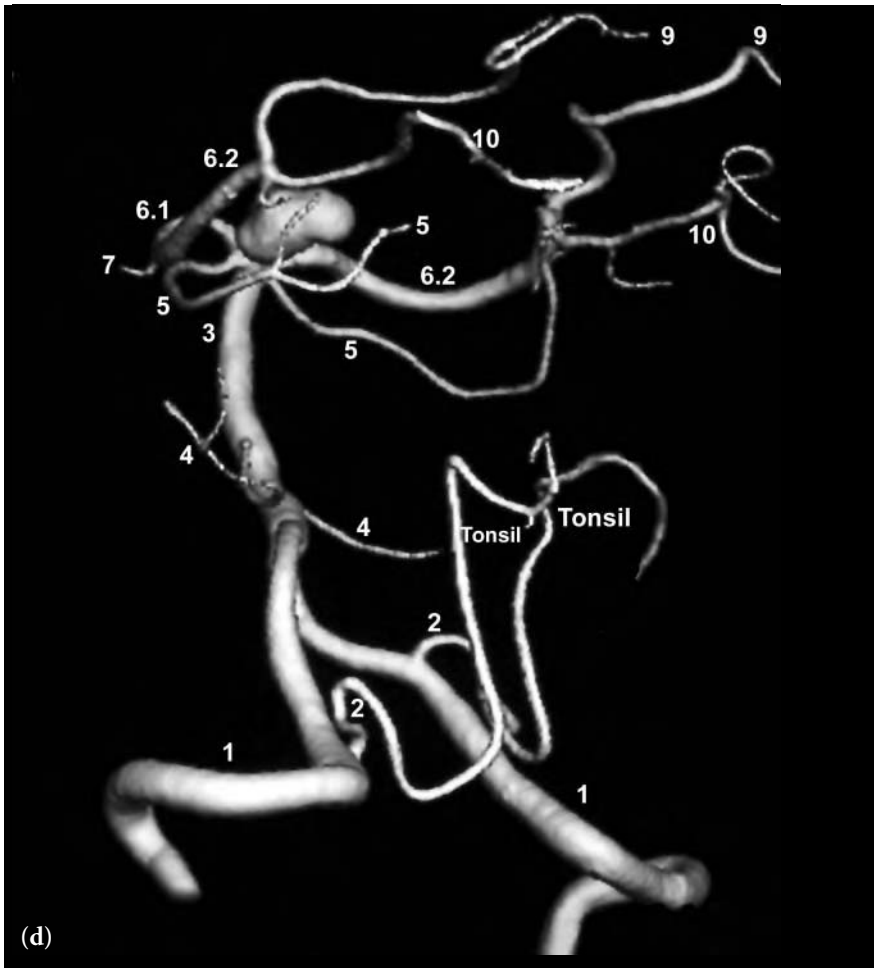
9
9
10
6.2
6.1
5
10
7
6.2
5
3
5
4
4
Tonsil
Tonsil
2
2
1
1
(d)

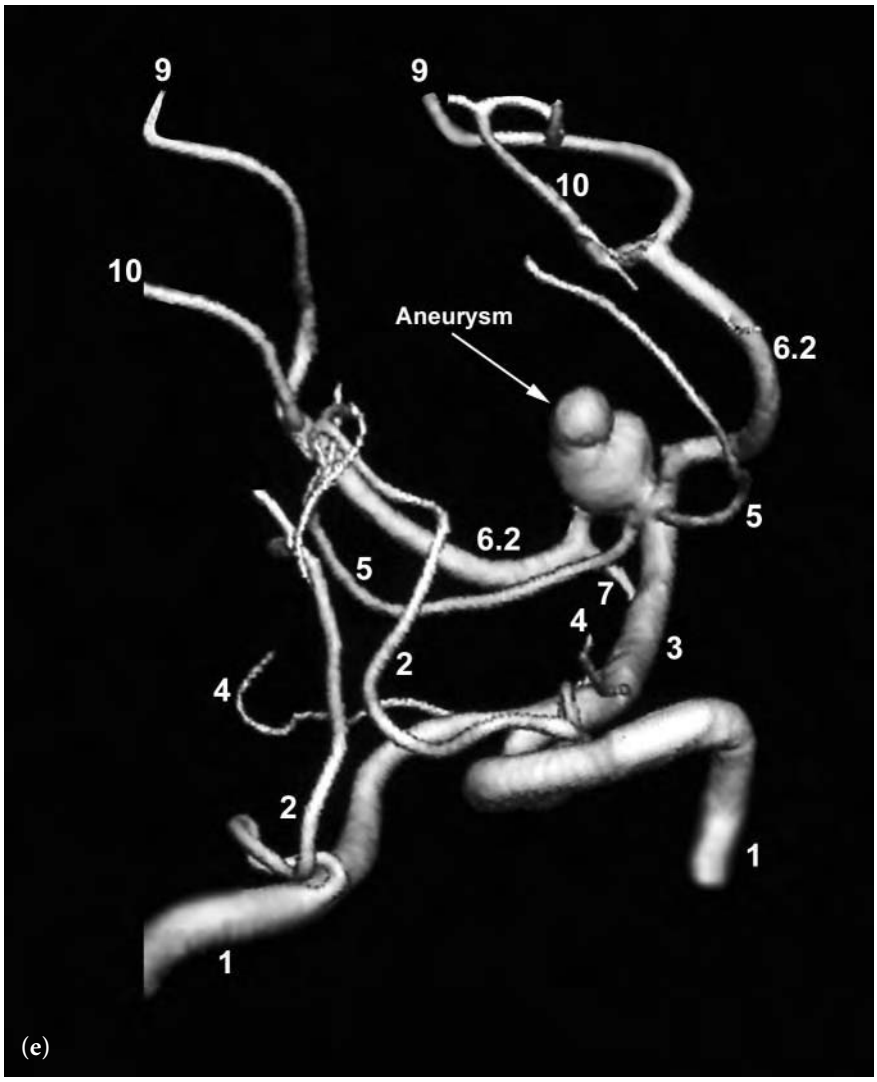

Fig. 6.13 (continued)

PROJECTION KEY

a frontal view
b left anterior oblique view
c posterior view
d left posterior oblique view
e right posterior oblique view with inferior to superior angulation
f near lateral view with inferior to superior angulation
g inferior to superior right anterior oblique view
h inferior to superior left anterior oblique view
i superior to inferior view
j superior to inferior left anterior oblique

FIGURE KEY

1 vertebral artery
2 posterior inferior cerebellar artery
3 basilar artery
4 anterior inferior cerebellar artery
5 superior cerebellar artery
6.1 P1 segment of posterior cerebral artery (PCA)
6.2 P2 segment of posterior cerebral artery (PCA)
7 posterior communicating artery
9 parieto-occipital branch of PCA
10 calcarine branch of PCA
14 vertebral basilar junction

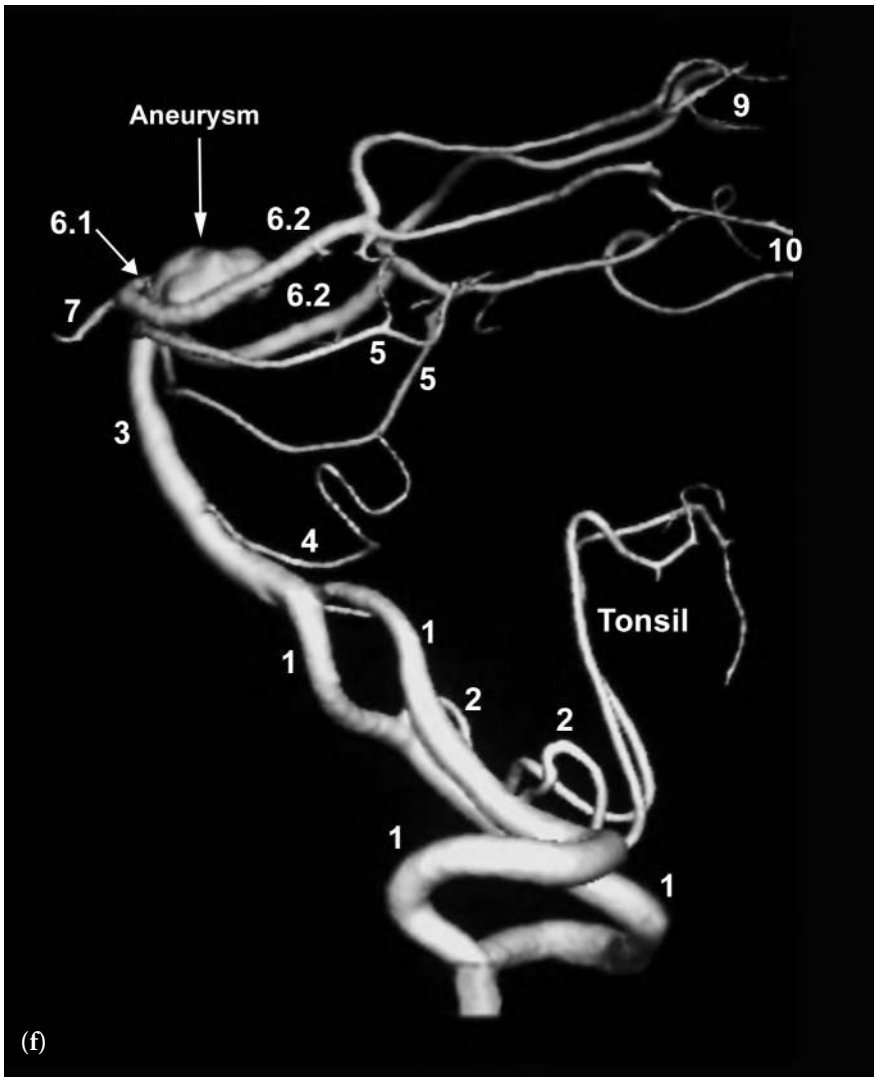
Aneurysm
9
6.1
6.2
10
7
6.2
5
5
3
4
Tonsil
1
1
2
2
1
1
(f)

(f)

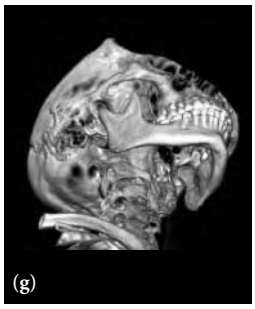

Fig. 6.13 (continued)

PROJECTION KEY

a frontal view
b left anterior oblique view
c posterior view
d left posterior oblique view
e right posterior oblique view with inferior to superior angulation
f near lateral view with inferior to superior angulation
g inferior to superior right anterior oblique view
h inferior to superior left anterior oblique view
i superior to inferior view
j superior to inferior left anterior oblique

FIGURE KEY

1 vertebral artery
2 posterior inferior cerebellar artery
3 basilar artery
4 anterior inferior cerebellar artery
5 superior cerebellar artery
6.1 P1 segment of posterior cerebral artery (PCA)
6.2 P2 segment of posterior cerebral artery (PCA)
7 posterior communicating artery
9 parieto-occipital branch of PCA
10 calcarine branch of PCA
14 vertebral basilar junction

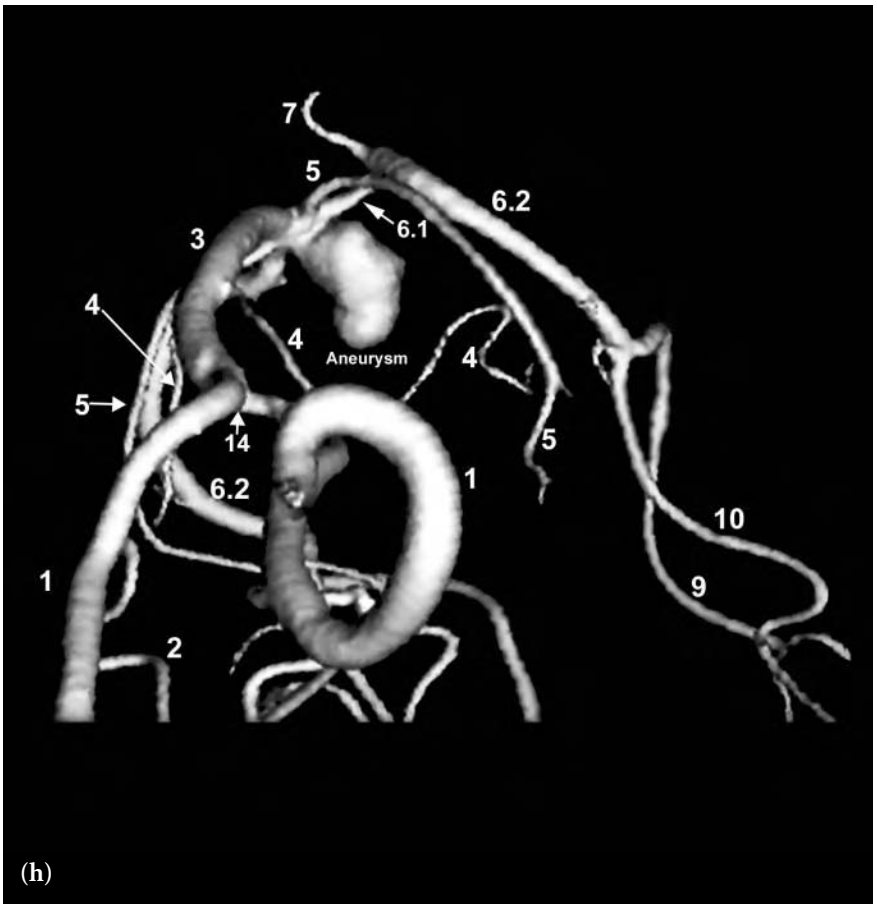

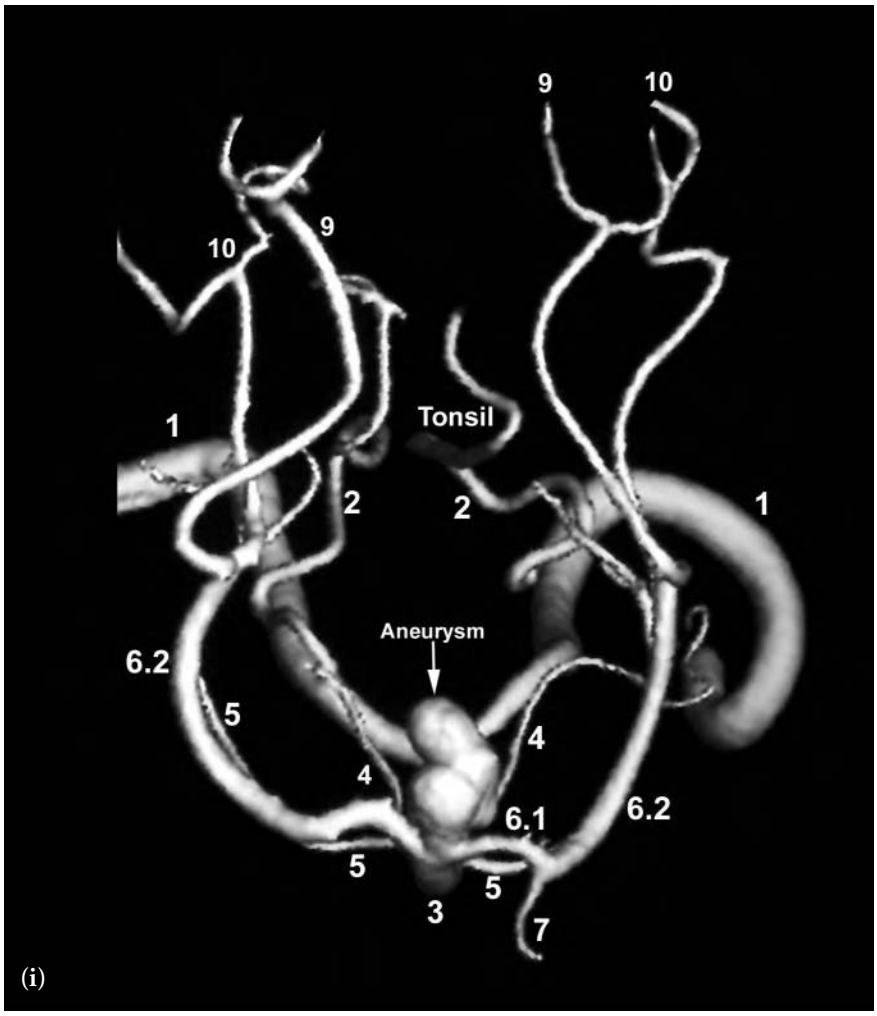
9
10
9
10
1
Tonsil
2
2
1
Aneurysm
6.2
5
4
4
6.1
6.2
5
5
3
7
(i)

(i)

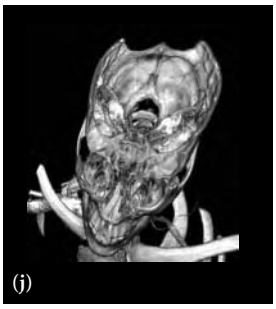
(j)

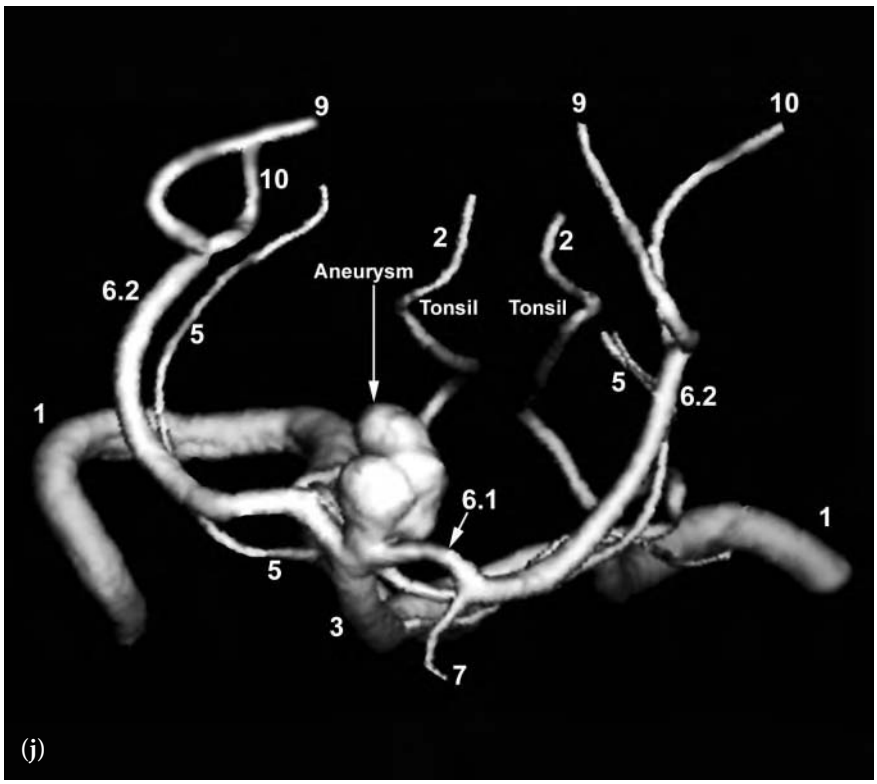
9
9
10
10
2
2
Aneurysm
6.2
Tonsil
Tonsil
5
5
6.2
1
6.1
1
5
3
7
(j)

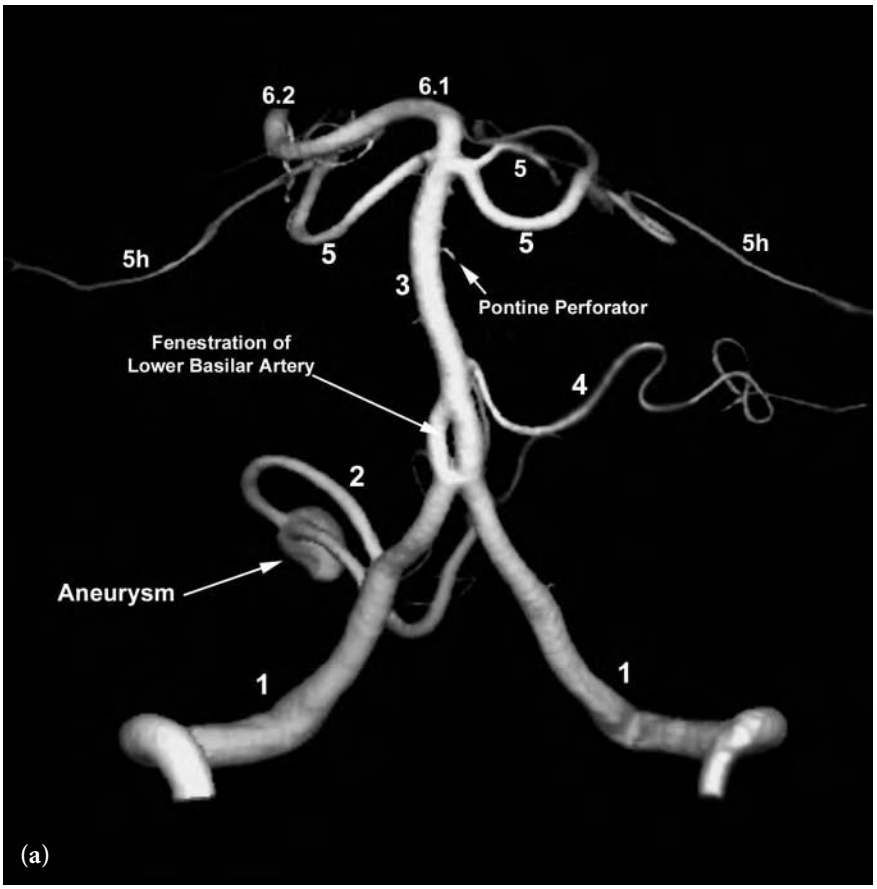

Fig. 6.14 (a–c) 3D frontal (*a*), shallow right anterior oblique (*b*), and steeper right anterior oblique (*c*) views following vertebral artery injection. These images show an aneurysm arising from the distal right PICA. Aneurysms more typically arise near the vertebral artery. These images also show normal vascular anatomy with the absence of visualization of the left posterior cerebral artery. This is secondary to a direct/fetal origin from the supraclinoid segment of the ipsilateral internal carotid artery.

FIGURE KEY

1 vertebral artery
2 posterior inferior cerebellar artery (PICA)
3 basilar artery
4 anterior inferior cerebellar artery (AICA)
5 superior cerebellar artery (SCA)
5v vermian branch of SCA
5h hemispheric branch of SCA
6 posterior cerebral artery (PCA)
6.1 P1 segment of PCA
6.2 P2 segment of PCA
14 vertebral basilar junction

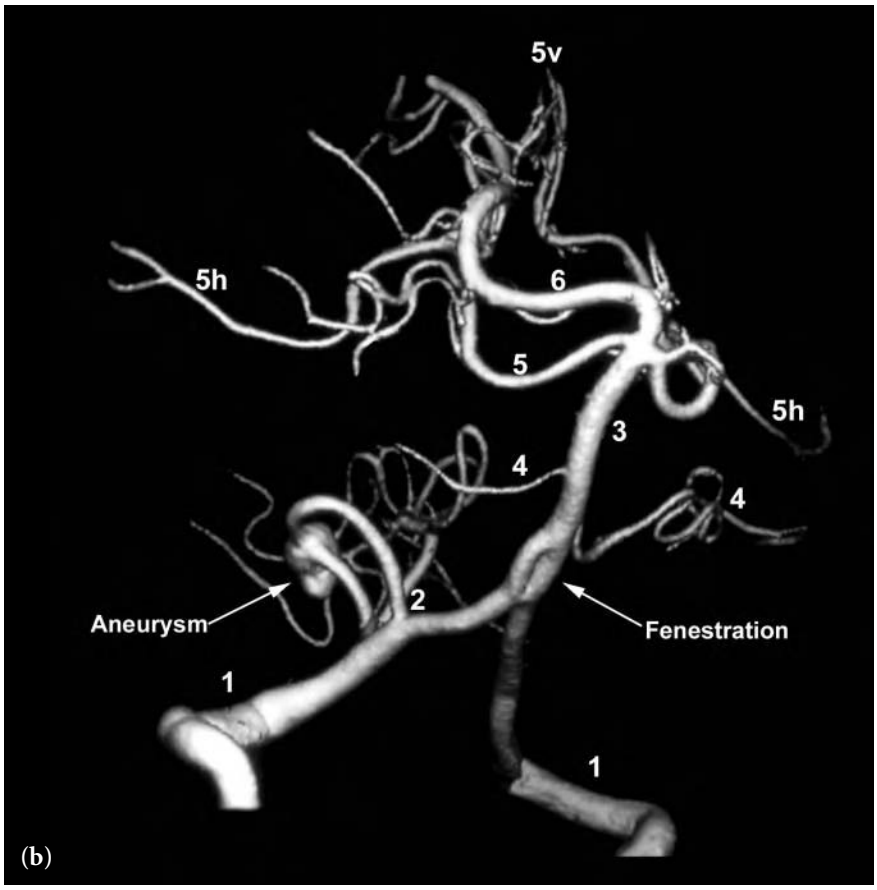
5v
5h
6
5
5h
3
4
4
Aneurysm
2
Fenestration
1
1
(b)

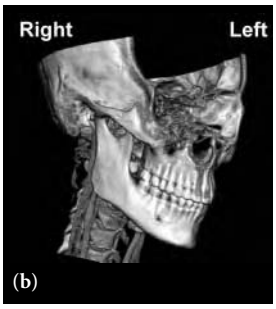
Right
Left
(b)

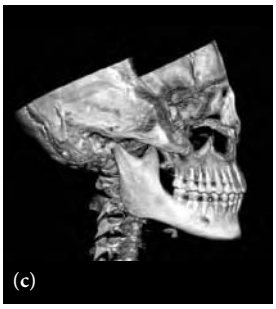
(c)

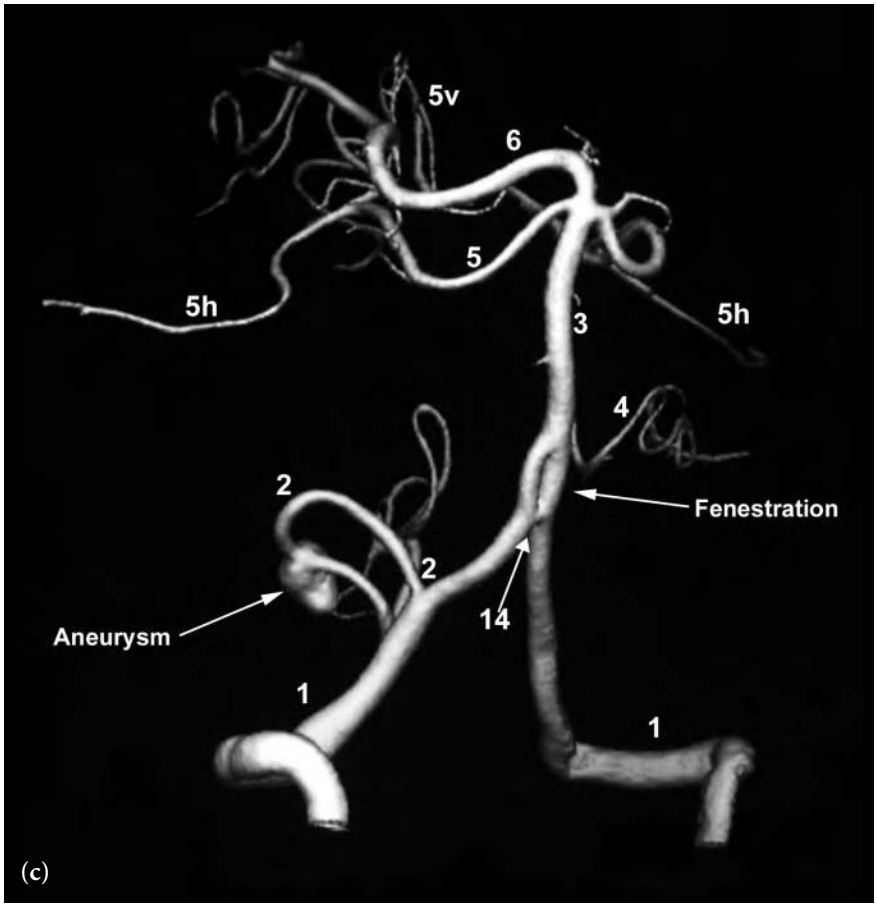
5v
6
5
5h
5h
3
4
2
Fenestration
2
14
Aneurysm
1
1
(c)

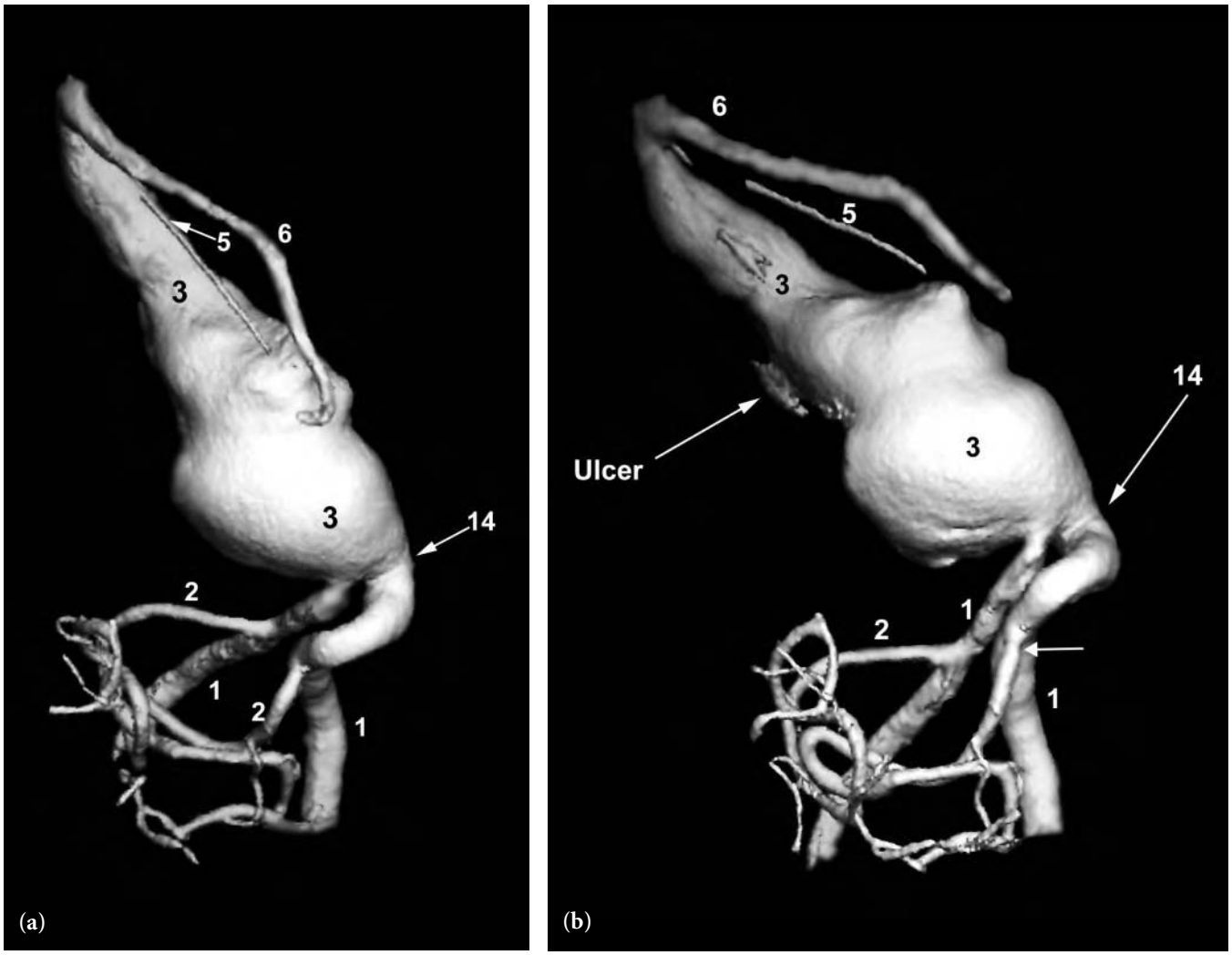

Fig. 6.15 (a–c) 3D posterior views of intracranial vertebral basilar circulation following a vertebral artery injection. These three different projections demonstrate a giant fusiform aneurysm of the basilar artery with a large ulcerative plaque seen on two of the views.

FIGURE KEY

1 vertebral artery
2 posterior inferior cerebellar artery (PICA)
3 basilar artery
5 superior cerebellar artery (SCA)
6 posterior cerebral artery (PCA)
14 vertebral basilar junction

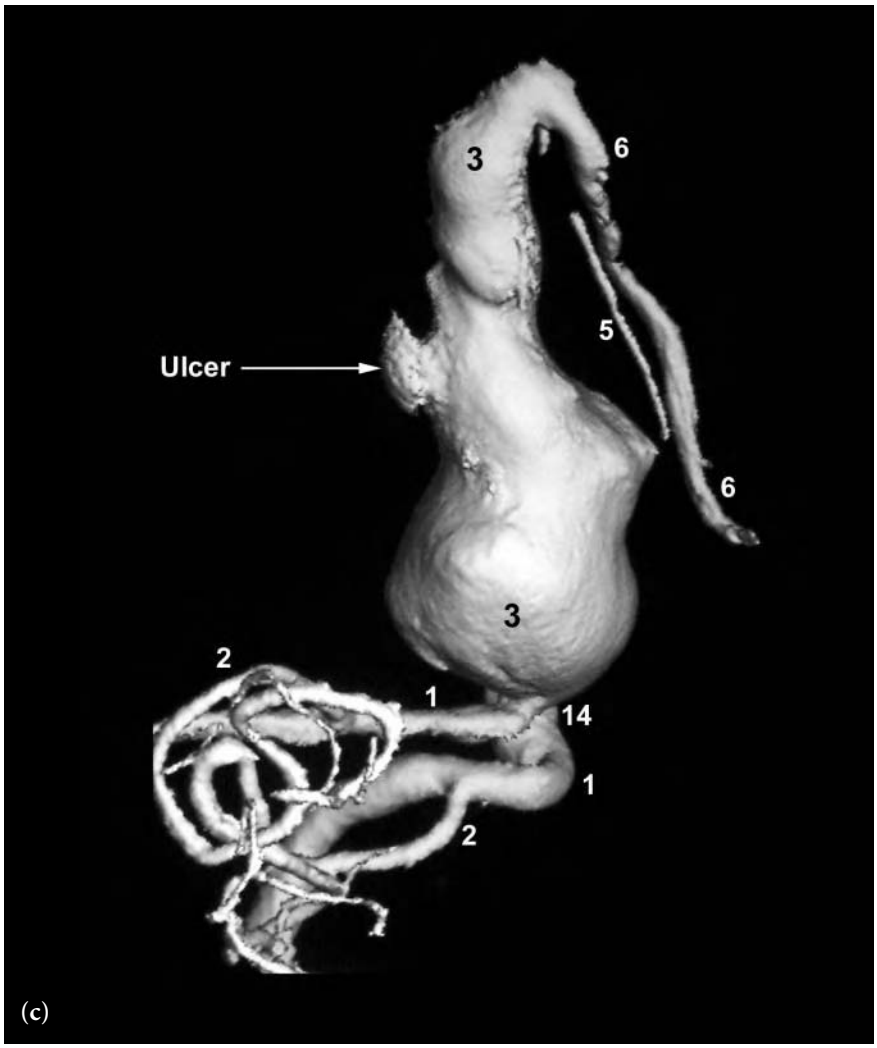
3
6
5
Ulcer
6
3
2
1
14
1
2
(c)

Fig. 6.16 (a–n) This series of both 2D and 3D images of the vertebral basilar circulation following vertebral artery injections clearly illustrates the morphologic makeup of a typical high-flow arterial-venous malformation (AVM) of the brain. These lesions generally consist of three main elements. The first element is the arterial feeder(s) to the malformation which in this case are posterior temporal artery branches of the posterior cerebral artery. The second element of an AVM is the nidus. The third element consists of draining vein(s). Some of the 2D images have been chosen to match some of the 3D views for a side by side comparison. These comparisons are *d* and *e*, *f* and *g*, and *k* and *l*. Images *m* and *n* were obtained after embolization with glue, particles, and coils and show no evidence of residual arterial venous shunting.

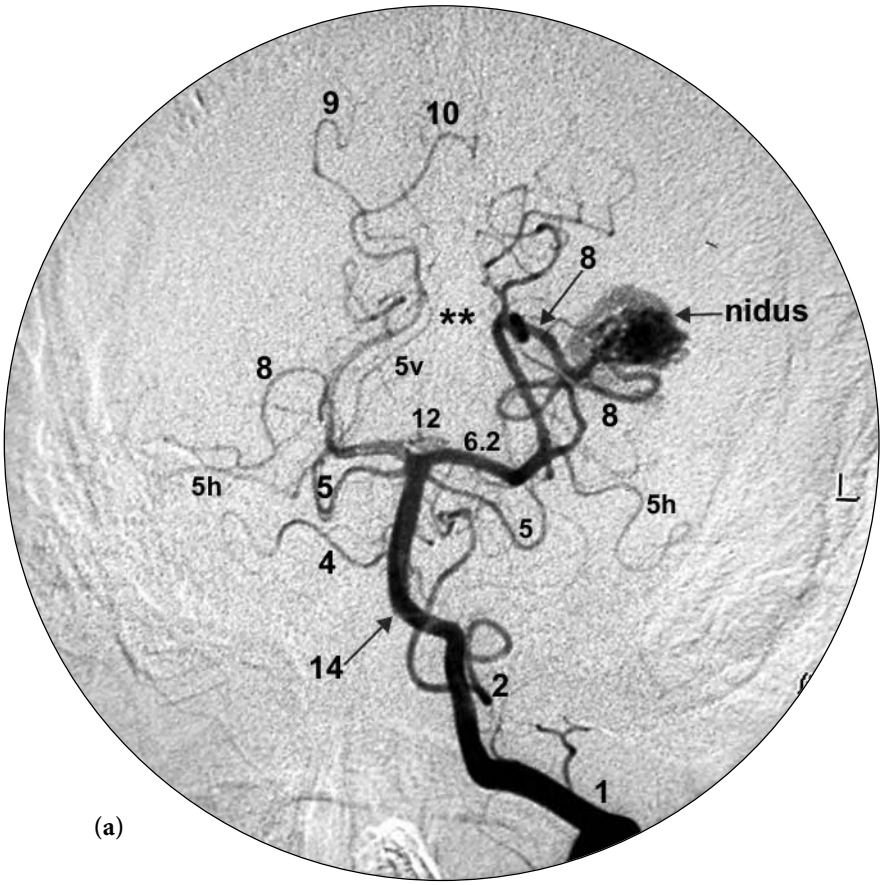

PROJECTION KEY

a 2D frontal early arterial phase
b 2D frontal late arterial phase
c 2D lateral early arterial phase
d 2D lateral late arterial phase
e 3D lateral arterial phase
f 2D lateral coned down magnified view arterial phase
g 3D lateral coned down magnified view arterial phase
h 3D left posterior oblique view arterial phase
i 3D posterior view, superior to inferior arterial phase
j 3D left anterior oblique, superior to inferior arterial phase
k 2D posterior view arterial phase to match L
L 3D posterior view arterial phase to match k
m 2D frontal view early arterial phase following embolization shows closure of the AVM.
n 2D frontal view late arterial phase after embolization shows no evidence of arterial-venous shunting.

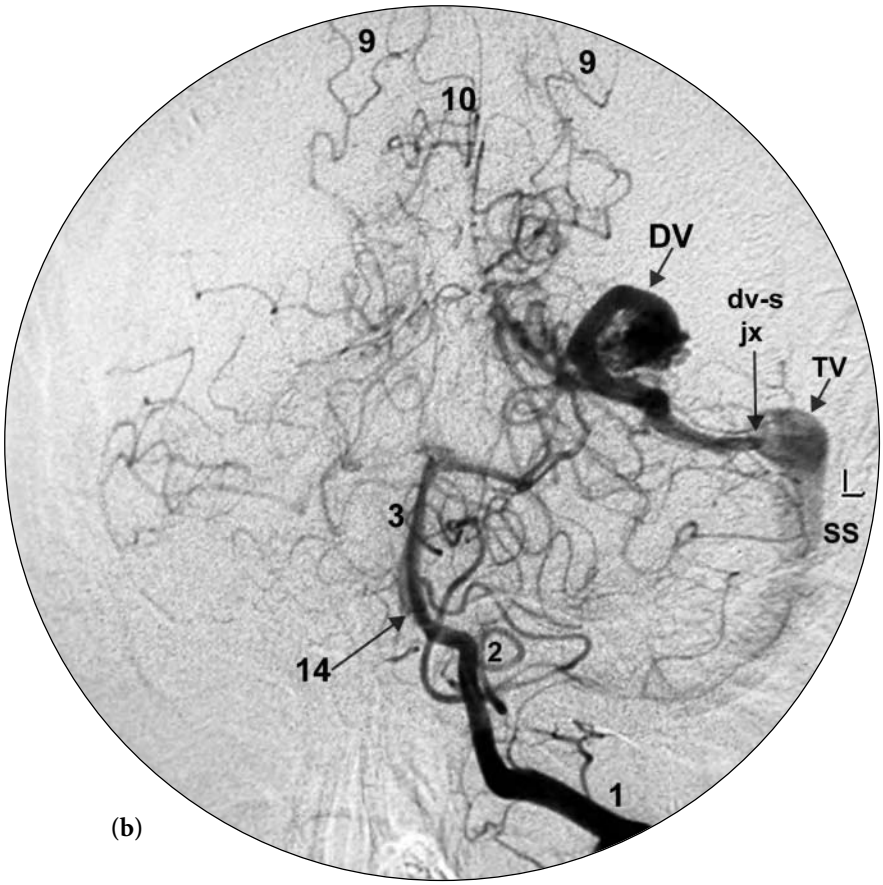

FIGURE KEY

1 vertebral artery
2 posterior inferior cerebellar artery (PICA)
3 basilar artery
4 anterior inferior cerebellar artery (AICA)
5 superior cerebellar artery (SCA)
5v vermian branch of SCA
5h hemispheric branch of SCA
6 posterior cerebral artery (PCA)
6.2 P2 segment PCA
7 posterior communicating artery
8 posterior temporal branches of PCA
9 parieto-occipital branch of PCA
10 calcarine branch of PCA
11 anterior thalamoperforating arteries
12 posterior thalamoperforating arteries
13m medial posterior choroidal arteries
13L lateral posterior choroidal arteries
14 vertebral basilar junction
15 splenial branch (posterior pericallosal artery) branch of PCA
** region of quadrigeminal plate cistern
DV main draining vein of AVM
dv-s AVM draining vein – dural sinus junction
TV transverse sinus
SS sigmoid sinus

Fig. 6.16 (continued)

PROJECTION KEY

a 2D frontal early arterial phase
b 2D frontal late arterial phase
c 2D lateral early arterial phase
d 2D lateral late arterial phase
e 3D lateral arterial phase
f 2D lateral coned down magnified view arterial phase
g 3D lateral coned down magnified view arterial phase
h 3D left posterior oblique view arterial phase
i 3D posterior view, superior to inferior arterial phase
j 3D left anterior oblique, superior to inferior arterial phase
k 2D posterior view arterial phase to match L
L 3D posterior view arterial phase to match k
m 2D frontal view early arterial phase following embolization shows closure of the AVM.
n 2D frontal view late arterial phase after embolization shows no evidence of arterial-venous shunting.

FIGURE KEY

1 vertebral artery
2 posterior inferior cerebellar artery (PICA)
3 basilar artery
4 anterior inferior cerebellar artery (AICA)
5 superior cerebellar artery (SCA)
5v vermian branch of SCA
5h hemispheric branch of SCA
6 posterior cerebral artery (PCA)
6.2 P2 segment PCA
7 posterior communicating artery
8 posterior temporal branches of PCA
9 parieto-occipital branch of PCA
10 calcarine branch of PCA
11 anterior thalamoperforating arteries
12 posterior thalamoperforating arteries
13m medial posterior choroidal arteries
13L lateral posterior choroidal arteries
14 vertebral basilar junction
15 splenial branch (posterior pericallosal artery) branch of PCA
** region of quadrigeminal plate cistern
DV main draining vein of AVM
dv-s AVM draining vein – dural sinus junction
TV transverse sinus
SS sigmoid sinus

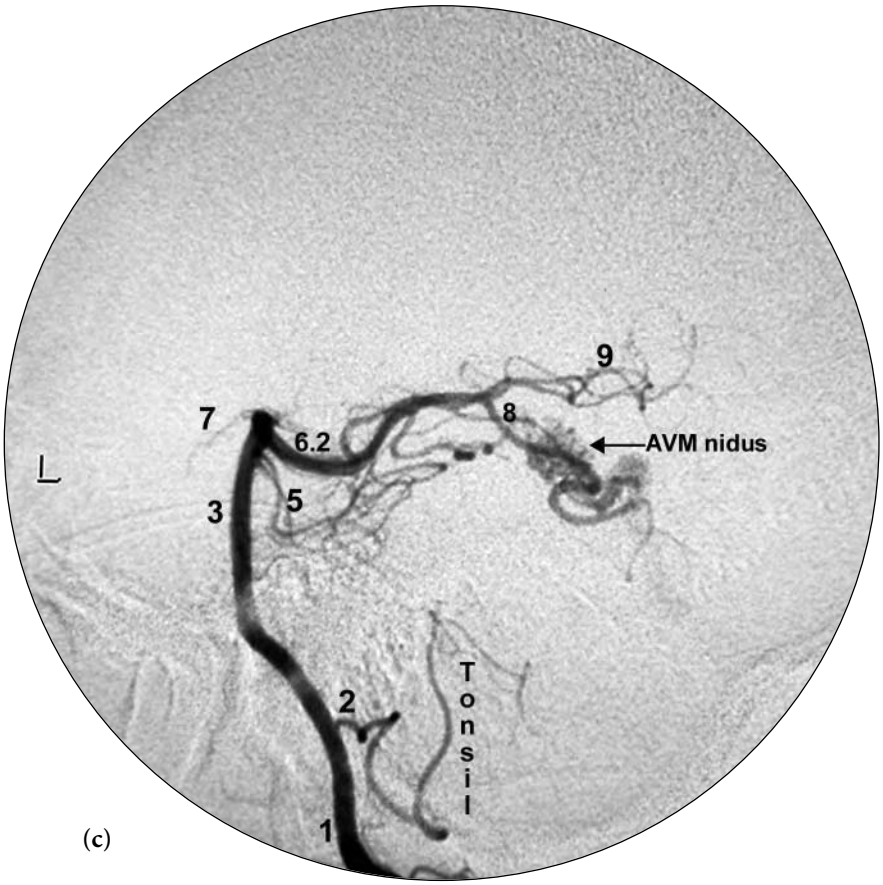

(c)

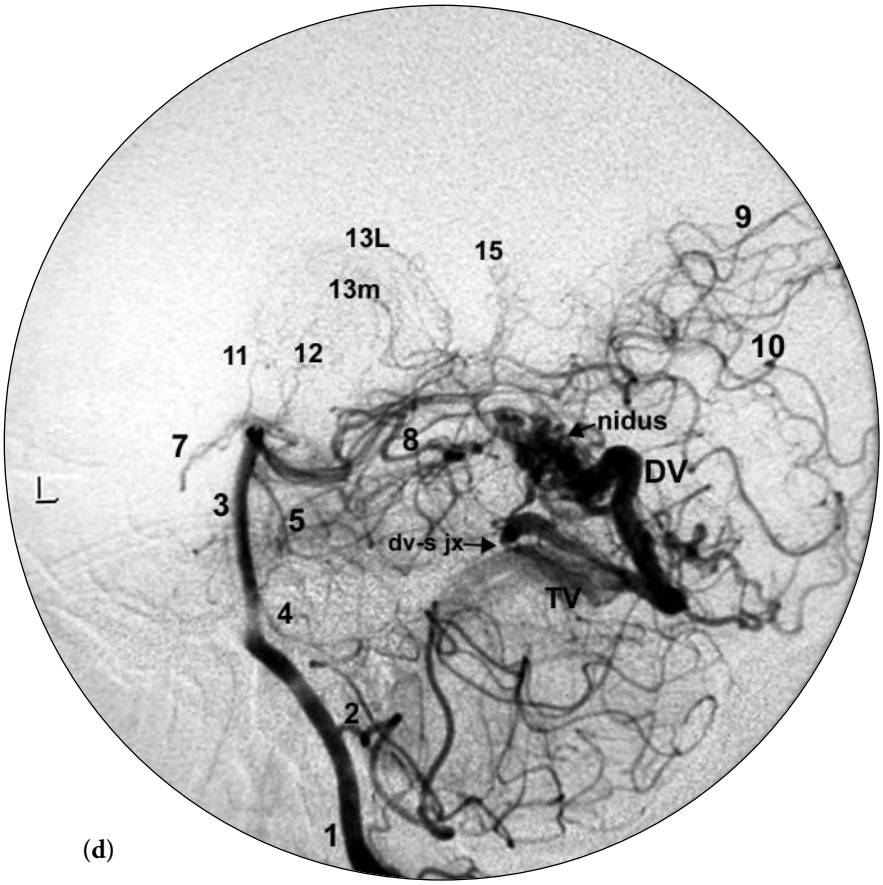

(d)

(e)

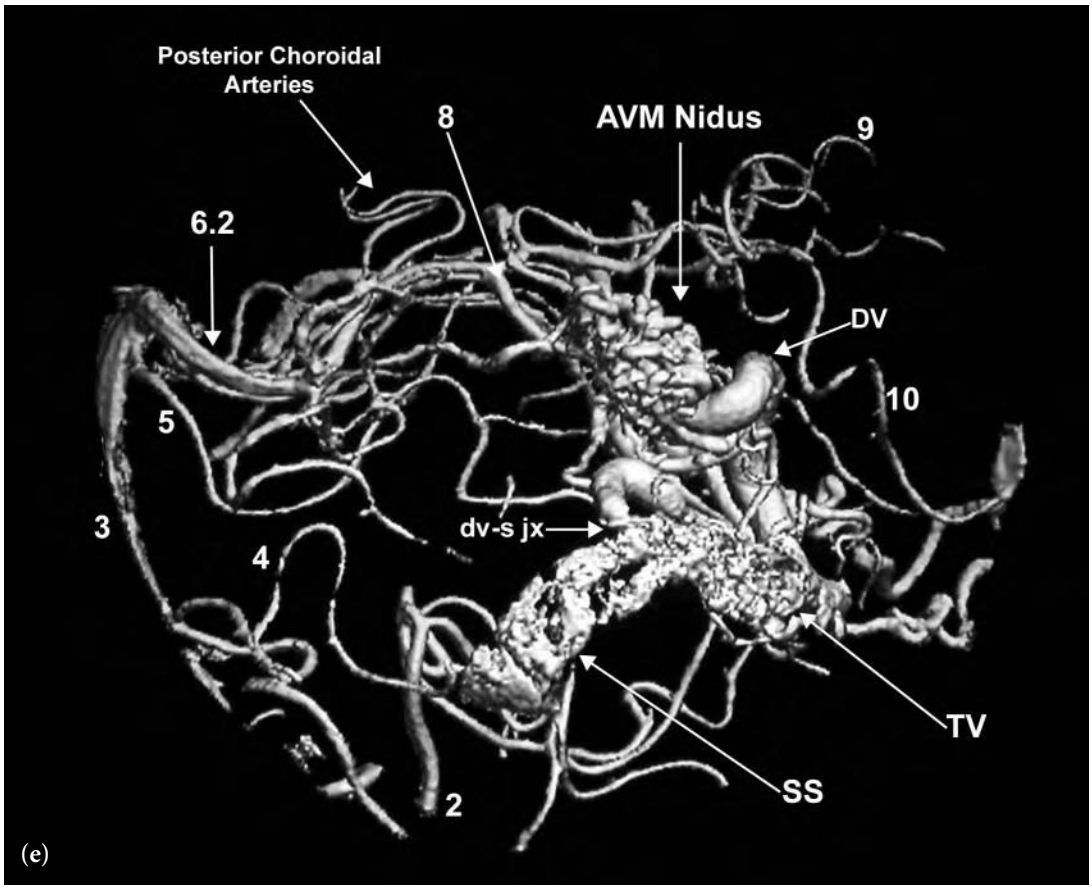
Posterior Choroidal Arteries
8
AVM Nidus
9
6.2
DV
10
5
3
dv-s jx
4
TV
SS
2
(e)

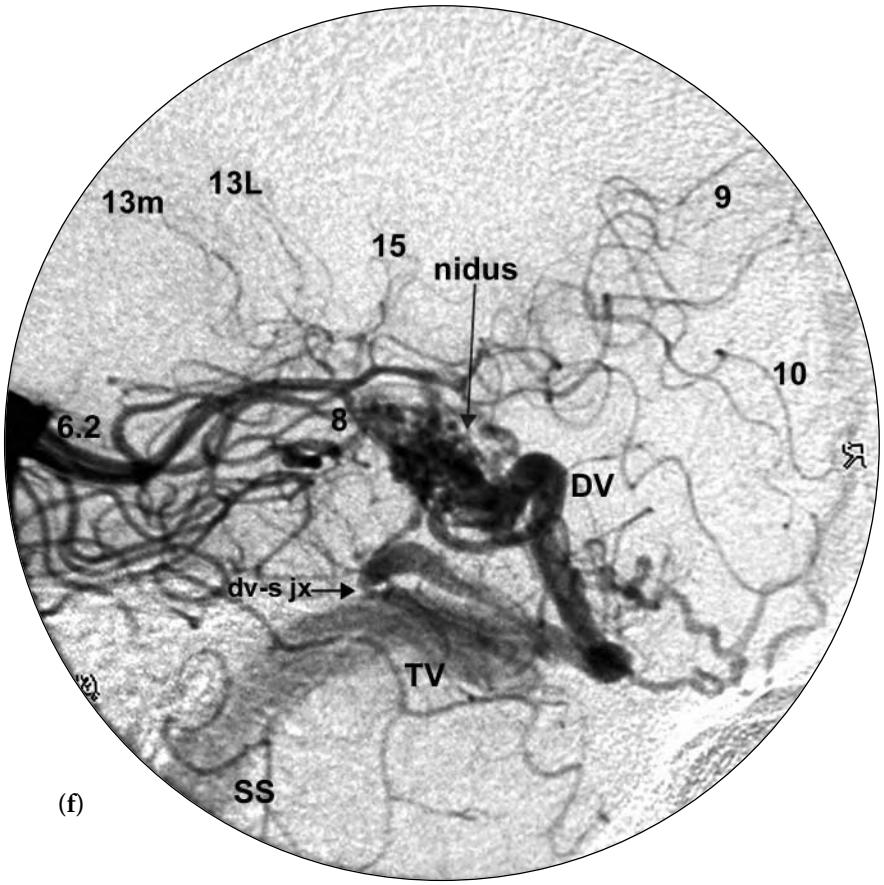

Fig. 6.16 (continued)

PROJECTION KEY

a 2D frontal early arterial phase
b 2D frontal late arterial phase
c 2D lateral early arterial phase
d 2D lateral late arterial phase
e 3D lateral arterial phase
f 2D lateral coned down magnified view arterial phase
g 3D lateral coned down magnified view arterial phase
h 3D left posterior oblique view arterial phase
i 3D posterior view, superior to inferior arterial phase
j 3D left anterior oblique, superior to inferior arterial phase
k 2D posterior view arterial phase to match L
L 3D posterior view arterial phase to match k
m 2D frontal view early arterial phase following embolization shows closure of the AVM.
n 2D frontal view late arterial phase after embolization shows no evidence of arterial-venous shunting.

FIGURE KEY

1 vertebral artery
2 posterior inferior cerebellar artery (PICA)
3 basilar artery
4 anterior inferior cerebellar artery (AICA)
5 superior cerebellar artery (SCA)
5v vermian branch of SCA
5h hemispheric branch of SCA
6 posterior cerebral artery (PCA)
6.2 P2 segment PCA
7 posterior communicating artery
8 posterior temporal branches of PCA
9 parieto-occipital branch of PCA
10 calcarine branch of PCA
11 anterior thalamoperforating arteries
12 posterior thalamoperforating arteries
13m medial posterior choroidal arteries
13L lateral posterior choroidal arteries
14 vertebral basilar junction
15 splenial branch (posterior pericallosal artery) branch of PCA
** region of quadrigeminal plate cistern
DV main draining vein of AVM
dv-s AVM draining vein – dural sinus junction
TV transverse sinus
SS sigmoid sinus

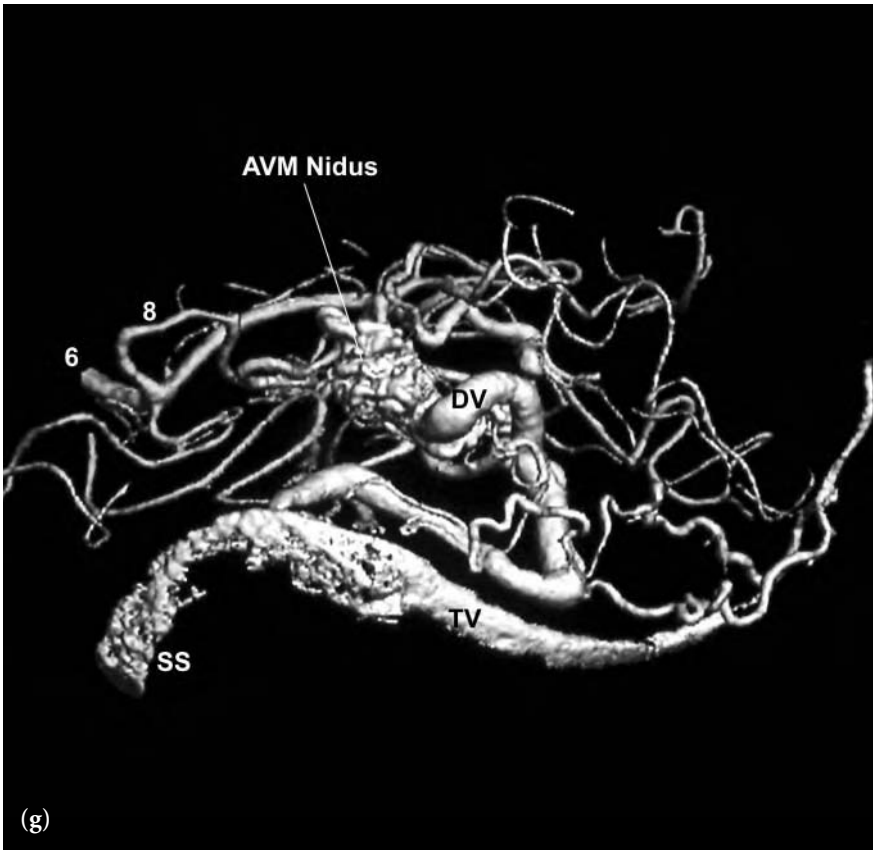

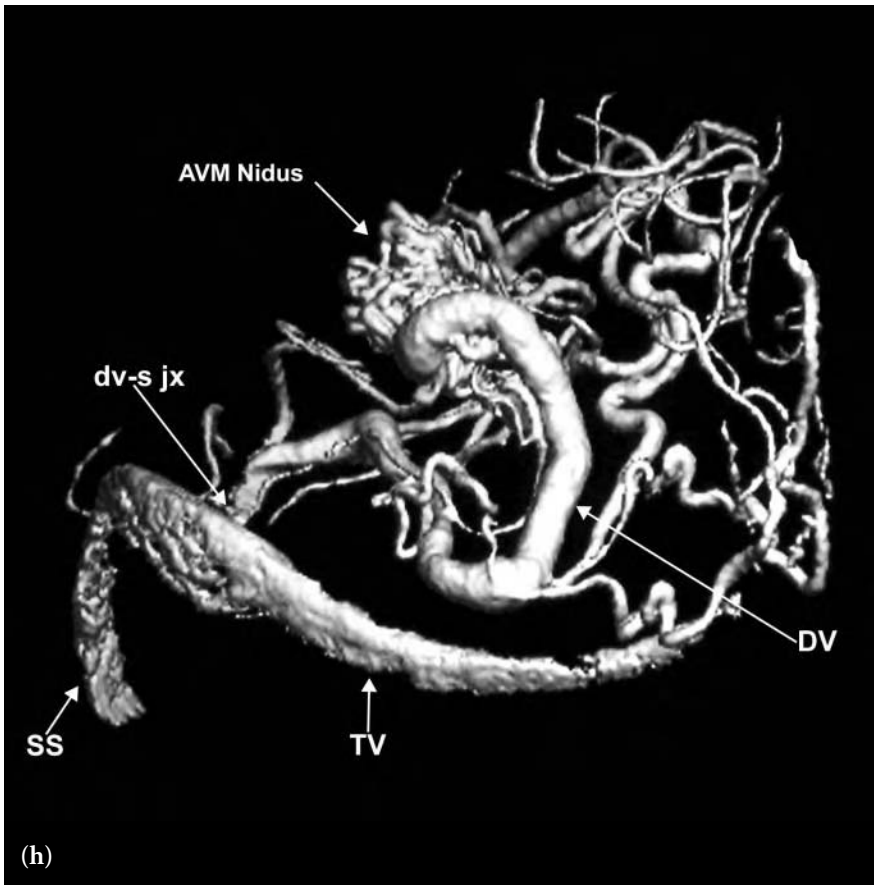
AVM Nidus
dv-s jx
DV
SS
TV
(h)

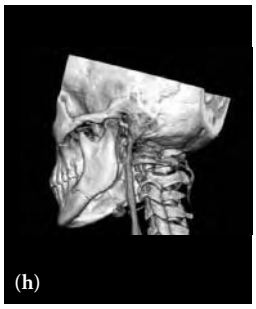
(h)

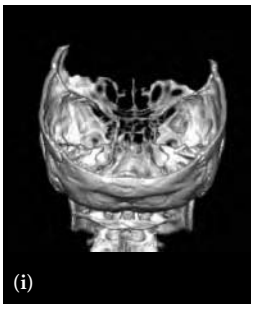
(i)

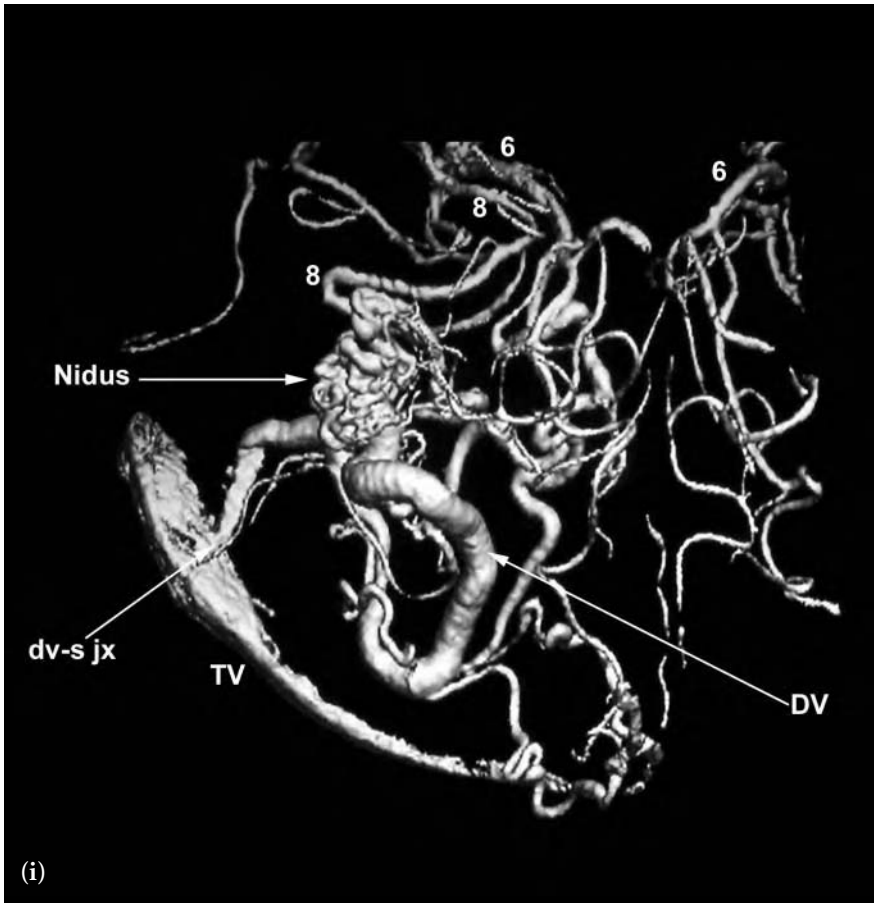
6
6
8
8
Nidus
dv-s jx
TV
DV
(i)

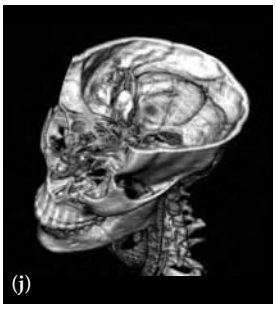

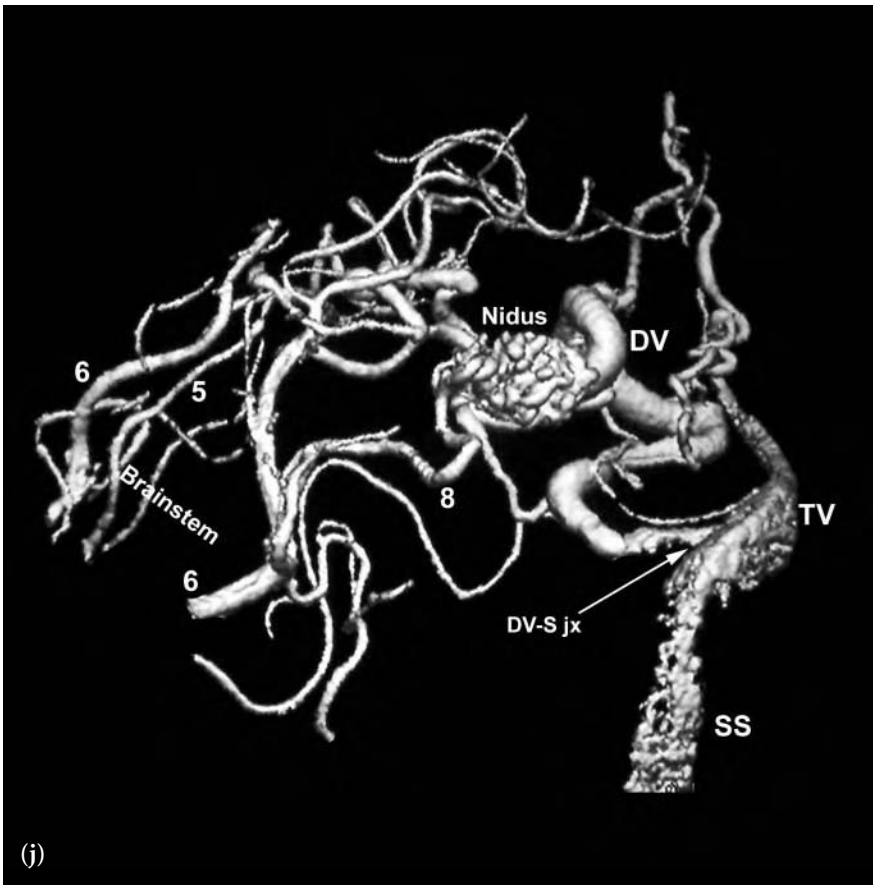

Fig. 6.16 (continued)

PROJECTION KEY

a 2D frontal early arterial phase
b 2D frontal late arterial phase
c 2D lateral early arterial phase
d 2D lateral late arterial phase
e 3D lateral arterial phase
f 2D lateral coned down magnified view arterial phase
g 3D lateral coned down magnified view arterial phase
h 3D left posterior oblique view arterial phase
i 3D posterior view, superior to inferior arterial phase
j 3D left anterior oblique, superior to inferior arterial phase
k 2D posterior view arterial phase to match L
L 3D posterior view arterial phase to match k
m 2D frontal view early arterial phase following embolization shows closure of the AVM.
n 2D frontal view late arterial phase after embolization shows no evidence of arterial-venous shunting.

FIGURE KEY

1 vertebral artery
2 posterior inferior cerebellar artery (PICA)
3 basilar artery
4 anterior inferior cerebellar artery (AICA)
5 superior cerebellar artery (SCA)
5v vermian branch of SCA
5h hemispheric branch of SCA
6 posterior cerebral artery (PCA)
6.2 P2 segment PCA
7 posterior communicating artery
8 posterior temporal branches of PCA
9 parieto-occipital branch of PCA
10 calcarine branch of PCA
11 anterior thalamoperforating arteries
12 posterior thalamoperforating arteries
13m medial posterior choroidal arteries
13L lateral posterior choroidal arteries
14 vertebral basilar junction
15 splenial branch (posterior pericallosal artery) branch of PCA
** region of quadrigeminal plate cistern
DV main draining vein of AVM
dv-s AVM draining vein – dural sinus junction
TV transverse sinus
SS sigmoid sinus

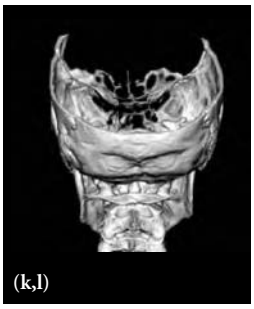
(k,l)

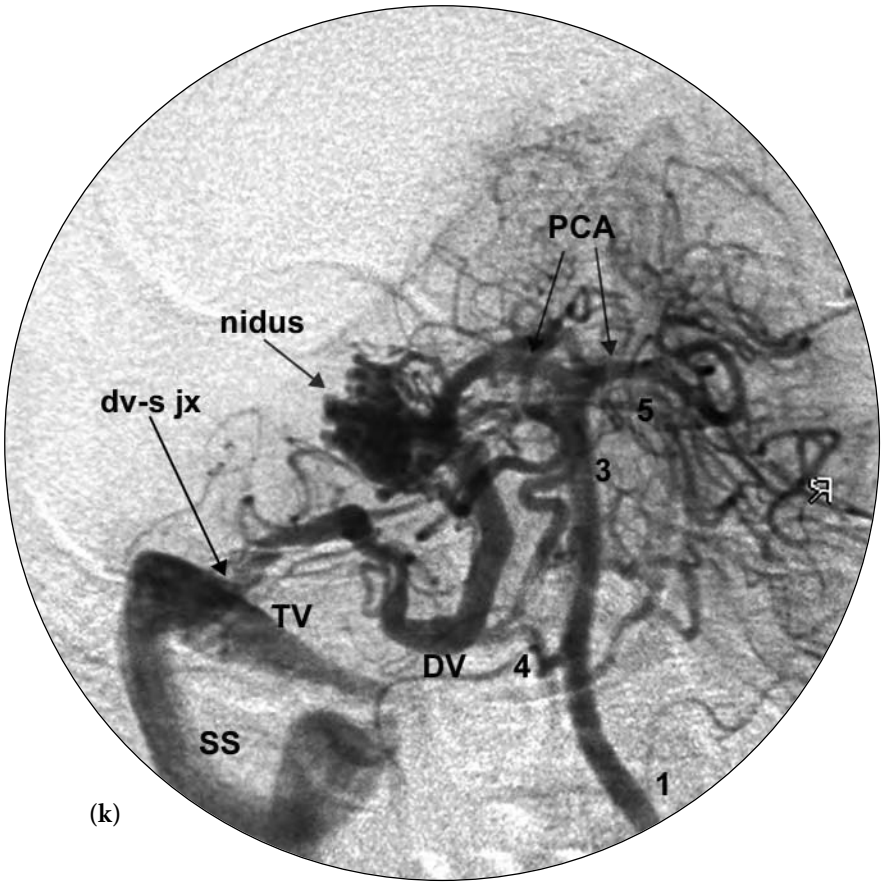
PCA
nidus
dv-s jx
5
3
TV
DV
4
SS
1
(k)

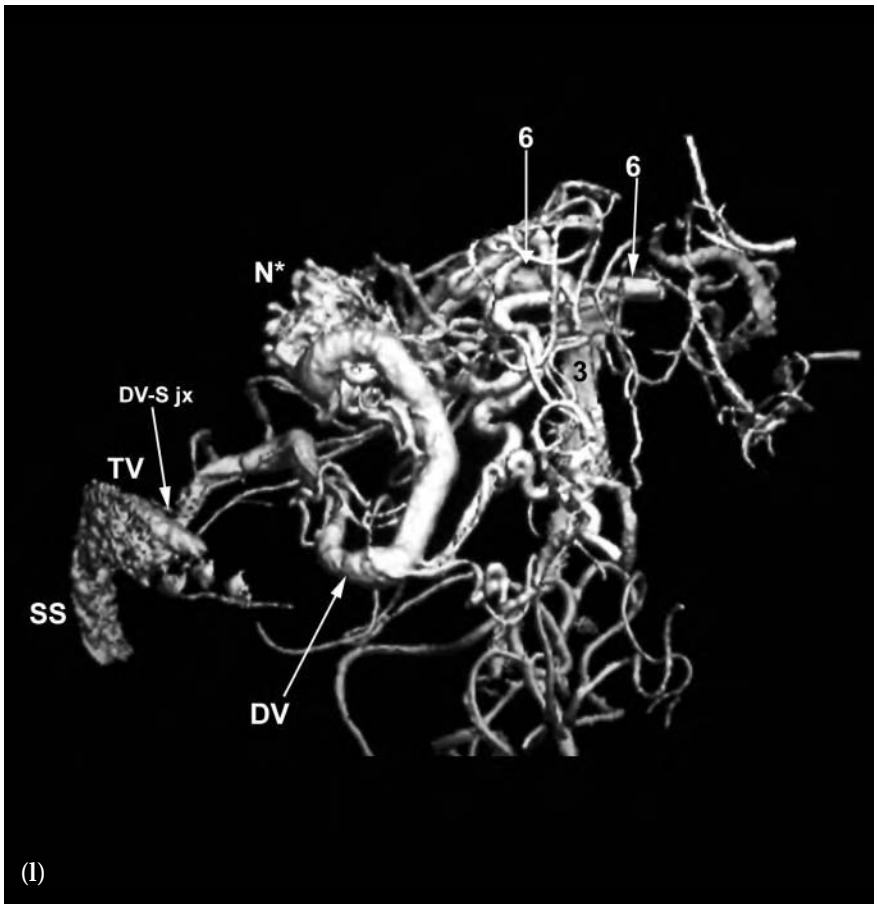
6
6
N*
3
DV-S jx
TV
SS
DV
(l)

Fig. 6.16 (continued)

PROJECTION KEY

a 2D frontal early arterial phase
b 2D frontal late arterial phase
c 2D lateral early arterial phase
d 2D lateral late arterial phase
e 3D lateral arterial phase
f 2D lateral coned down magnified view arterial phase
g 3D lateral coned down magnified view arterial phase
h 3D left posterior oblique view arterial phase
i 3D posterior view, superior to inferior arterial phase
j 3D left anterior oblique, superior to inferior arterial phase
k 2D posterior view arterial phase to match L
L 3D posterior view arterial phase to match k
m 2D frontal view early arterial phase following embolization shows closure of the AVM.
n 2D frontal view late arterial phase after embolization shows no evidence of arterial-venous shunting.

FIGURE KEY

1 vertebral artery
2 posterior inferior cerebellar artery (PICA)
3 basilar artery
4 anterior inferior cerebellar artery (AICA)
5 superior cerebellar artery (SCA)
5v vermian branch of SCA
5h hemispheric branch of SCA
6 posterior cerebral artery (PCA)
6.2 P2 segment PCA
7 posterior communicating artery
8 posterior temporal branches of PCA
9 parieto-occipital branch of PCA
10 calcarine branch of PCA
11 anterior thalamoperforating arteries
12 posterior thalamoperforating arteries
13m medial posterior choroidal arteries
13L lateral posterior choroidal arteries
14 vertebral basilar junction
15 splenial branch (posterior pericallosal artery) branch of PCA
** region of quadrigeminal plate cistern
DV main draining vein of AVM
dv-s AVM draining vein – dural sinus junction
TV transverse sinus
SS sigmoid sinus

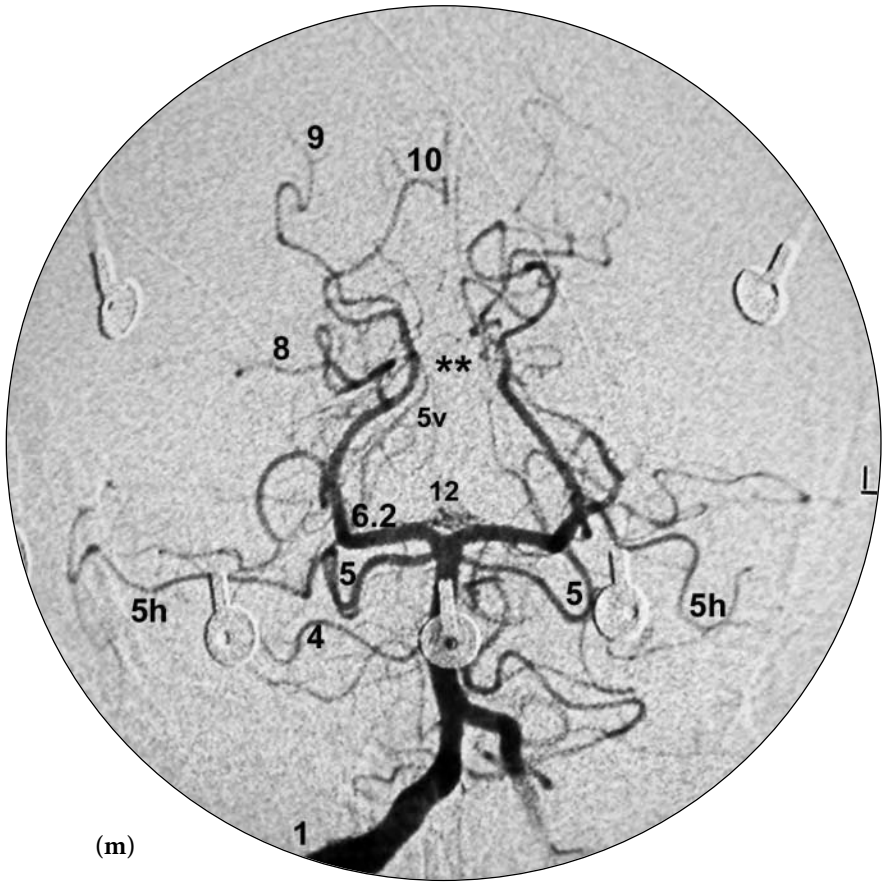

(m)

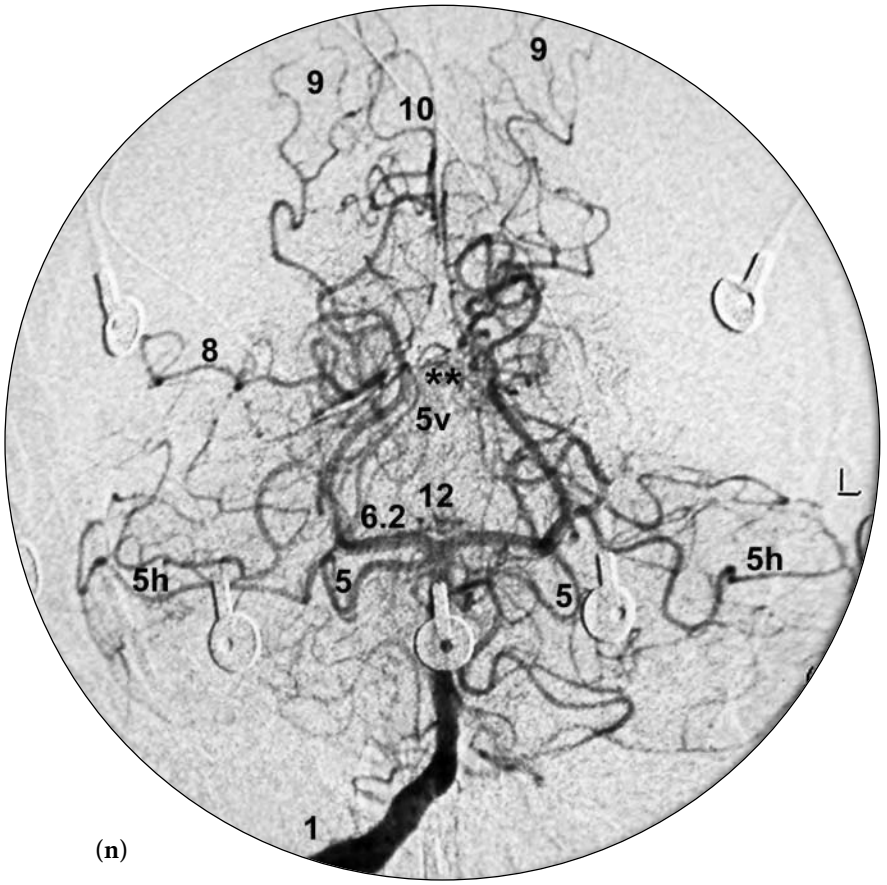

(n)

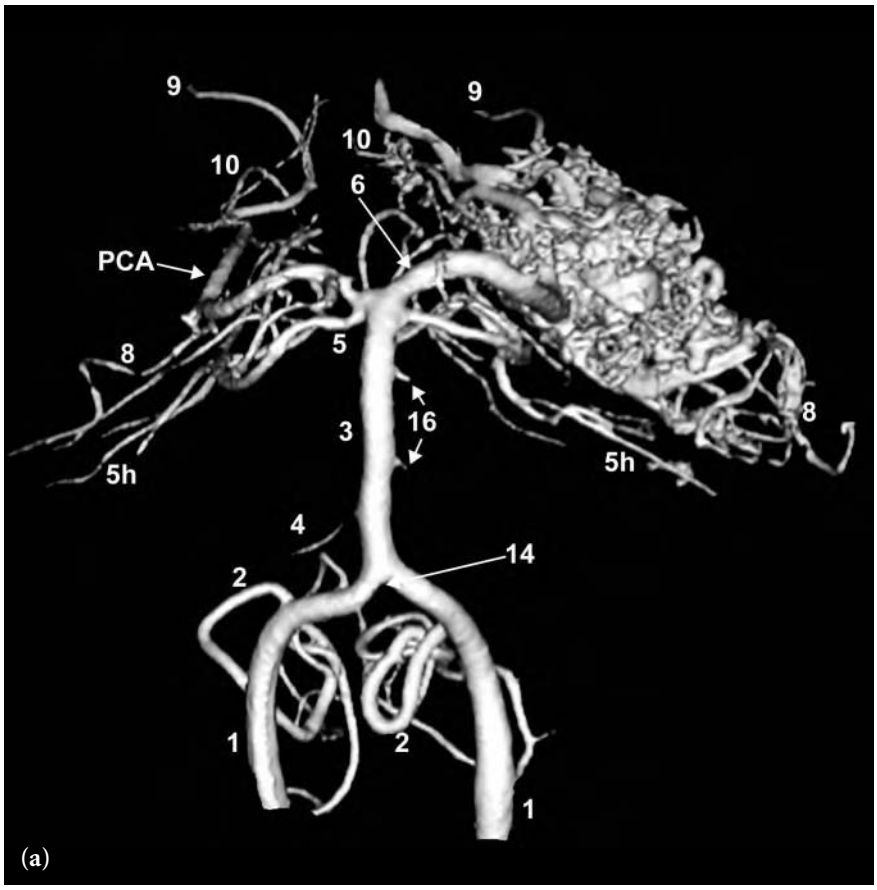

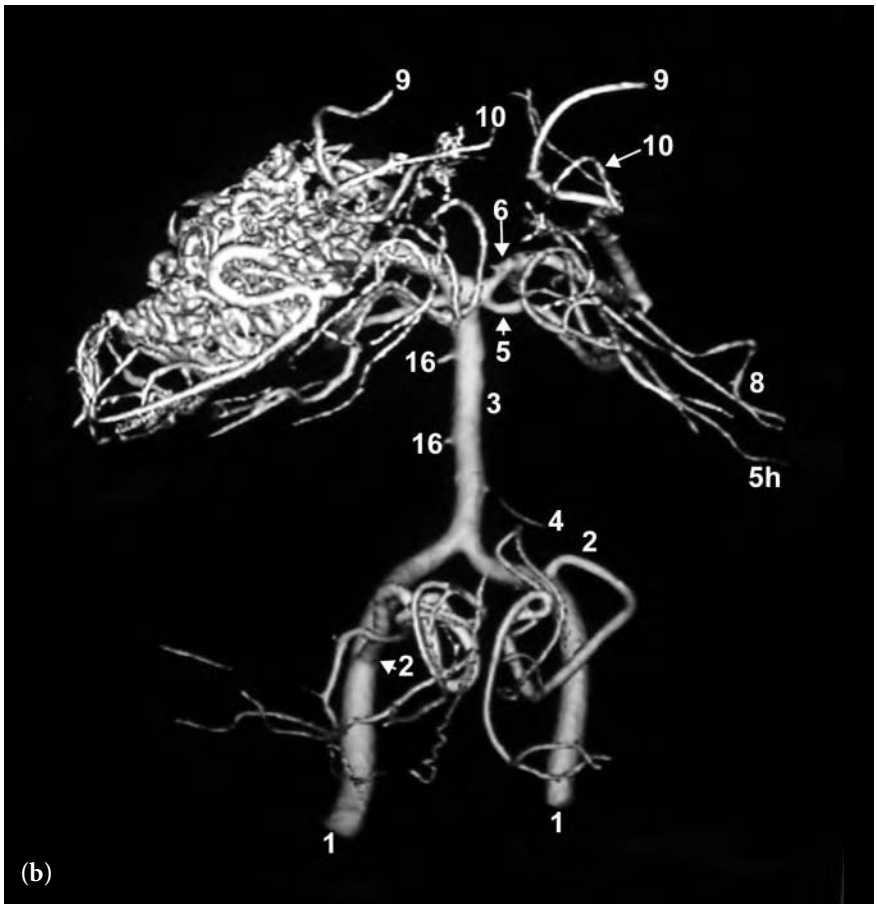

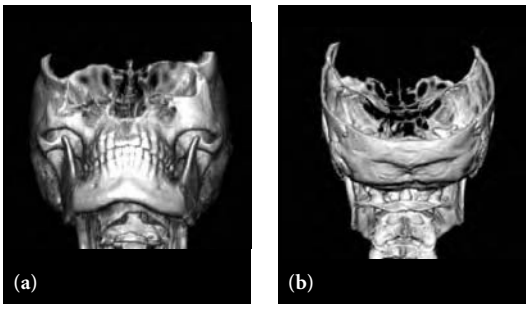

Fig. 6.17 (a–f) 3D frontal (*a*), posterior (*b*), left lateral (*c*), right lateral (*d*), superior to inferior (*e*), and inferior to superior (*f*) views following vertebral artery injection. These intracranial views demonstrate a large arterial-venous malformation (AVM) in the left temporal lobe. The vascular anatomy is otherwise normal.

FIGURE KEY

1 vertebral artery
2 posterior inferior cerebellar artery (PICA)
3 basilar artery
4 anterior inferior cerebellar artery (AICA)
5 superior cerebellar artery
5h hemispheric branch of SCA
6 posterior cerebral artery (PCA)
6.1 P1 segment of PCA
6.2 P2 segment of PCA
7 posterior communicating artery
8 posterior temporal branch of PCA
9 parieto-occipital branch of PCA
10 calcarine branch of PCA
11 anterior thalamoperforating artery
14 vertebral basilar junction
16 pontine perforating artery

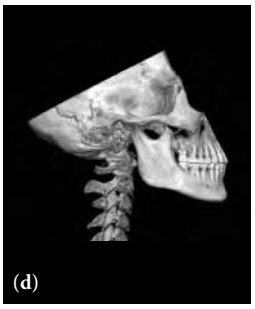

Fig. 6.17 (continued)

FIGURE KEY

1 vertebral artery
2 posterior inferior cerebellar artery (PICA)
3 basilar artery
4 anterior inferior cerebellar artery (AICA)
5 superior cerebellar artery
5h hemispheric branch of SCA
6 posterior cerebral artery (PCA)
6.1 P1 segment of PCA
6.2 P2 segment of PCA
7 posterior communicating artery
8 posterior temporal branch of PCA
9 parieto-occipital branch of PCA
10 calcarine branch of PCA
11 anterior thalamoperforating artery
14 vertebral basilar junction
16 pontine perforating artery

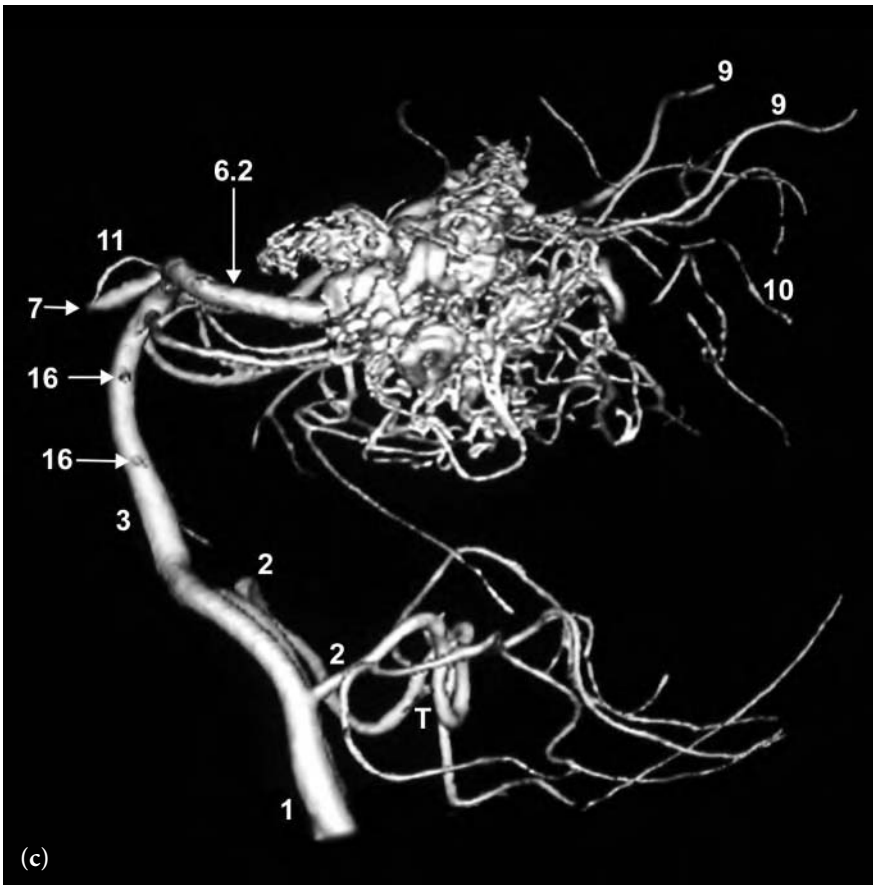

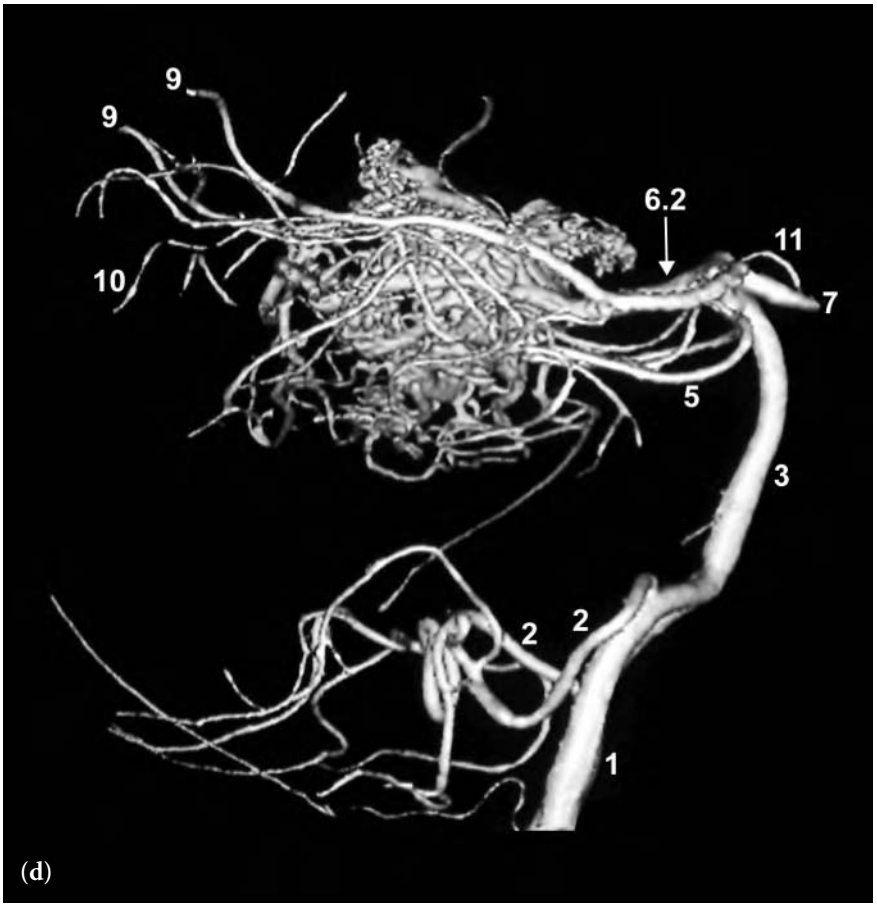

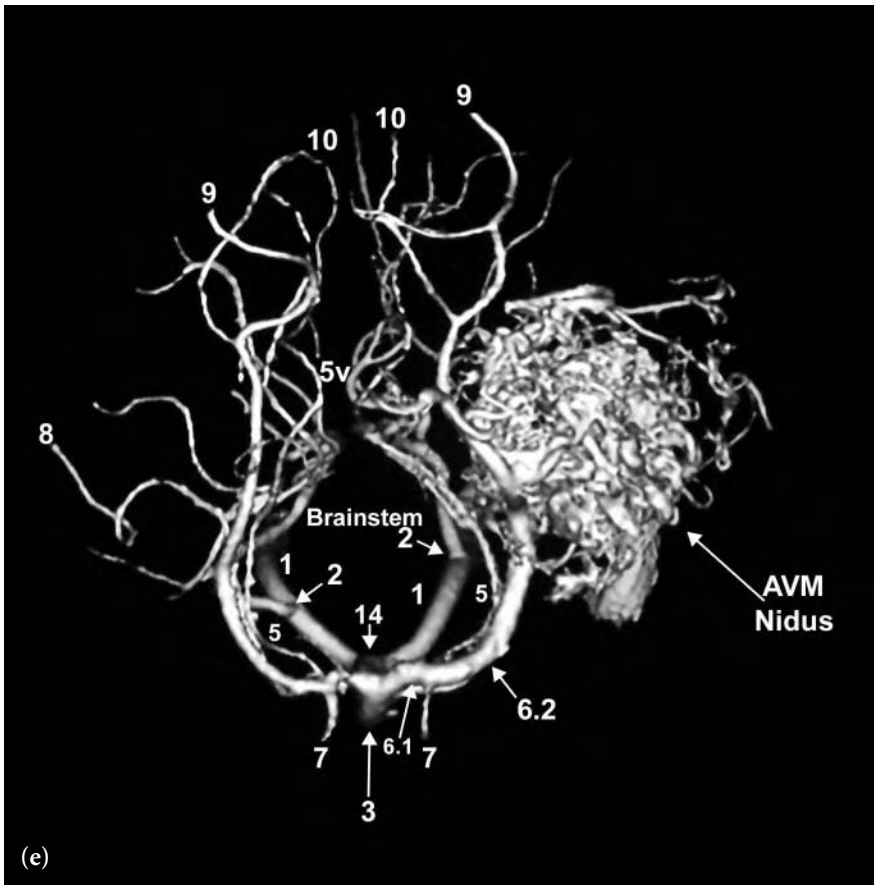
9
10
10
9
5v
8
Brainstem
2
1
2
1
5
14
5
AVM
Nidus
6.2
7
6.1
7
3
(e)

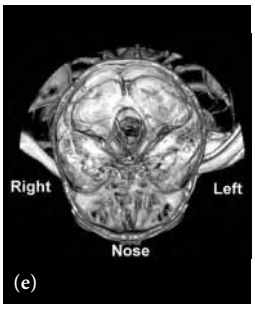
Right
Left
Nose
(e)

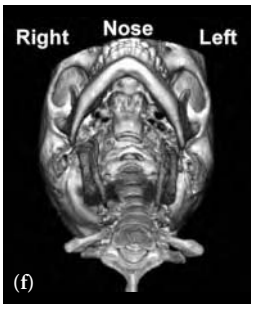
Right
Nose
Left
(f)

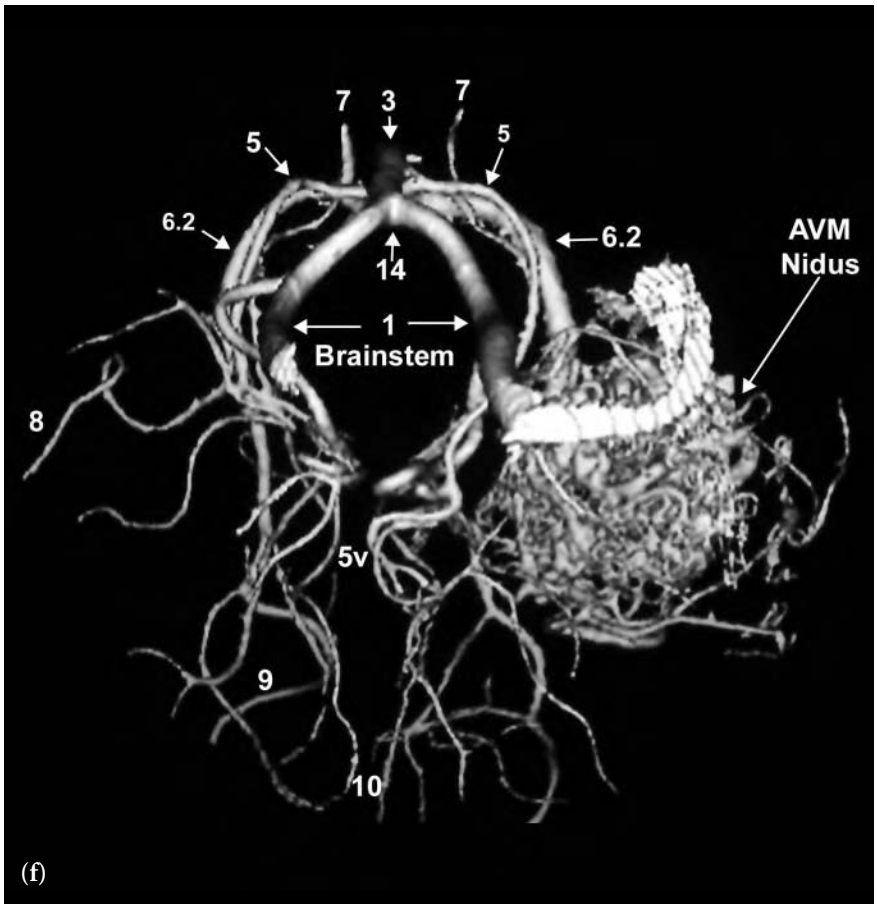
7
3
7
5
5
6.2
6.2
AVM
Nidus
14
1
Brainstem
8
5v
9
10
(f)

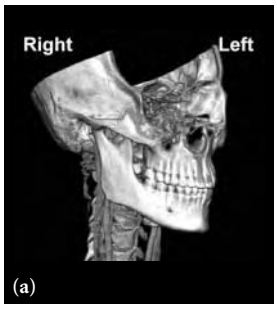

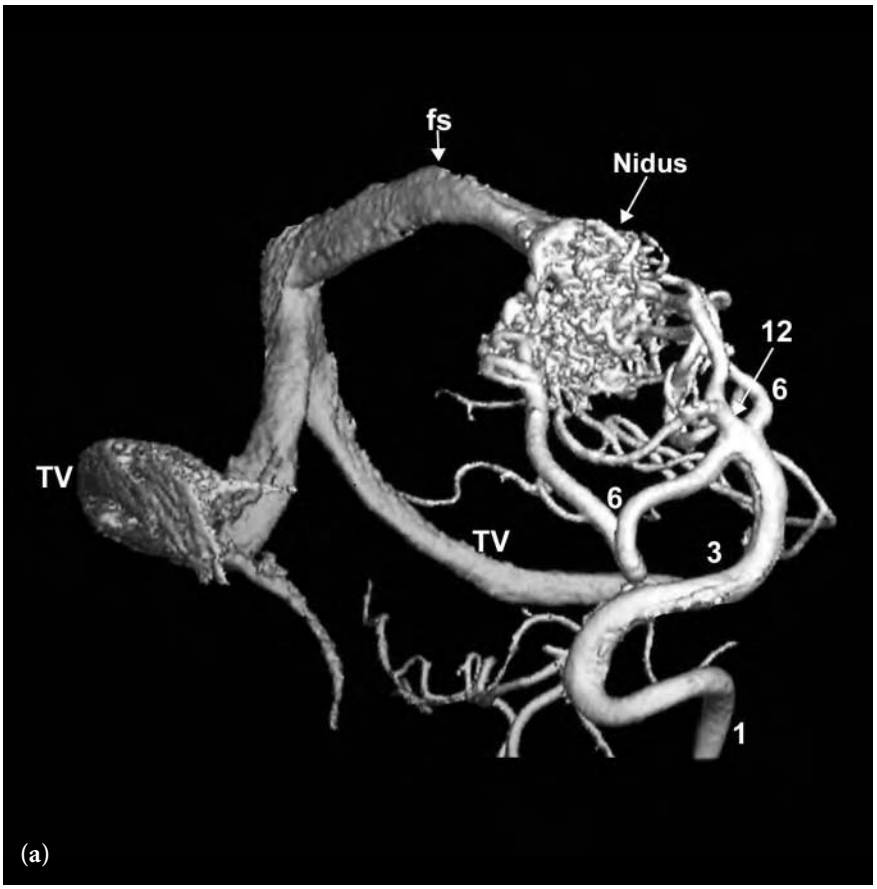

Fig. 6.18 (a–e) 3D right anterior oblique (*a*), steep right anterior oblique (*b*), frontal (*c*), right posterior oblique (*d*), and superior to inferior (*e*) views of intracranial vertebral basilar circulation following vertebral artery injection. These images demonstrate a high-flow arterial-venous malformation supplied by posterior thalamoperforaters and from other branches of the posterior cerebral artery. The nidus is in the region of the expected vein of Galen. The main venous drainage is through the falcine sinus which is an embryologic sinus that normally regresses. This unusual AVM has features of both a vein of Galen malformation and a true parenchymal AVM. Note the two perinidal aneurysms (*) on the venous side of the AVM nidus, at the nidus-falcine sinus junction.

FIGURE KEY

1 vertebral artery
3 basilar artery
5 superior cerebellar artery (SCA)
6 posterior cerebral artery (PCA)
12 posterior thalamoperforating arteries
fs falcine sinus
TV transverse sinus
* perinidal (venous side) aneurysms

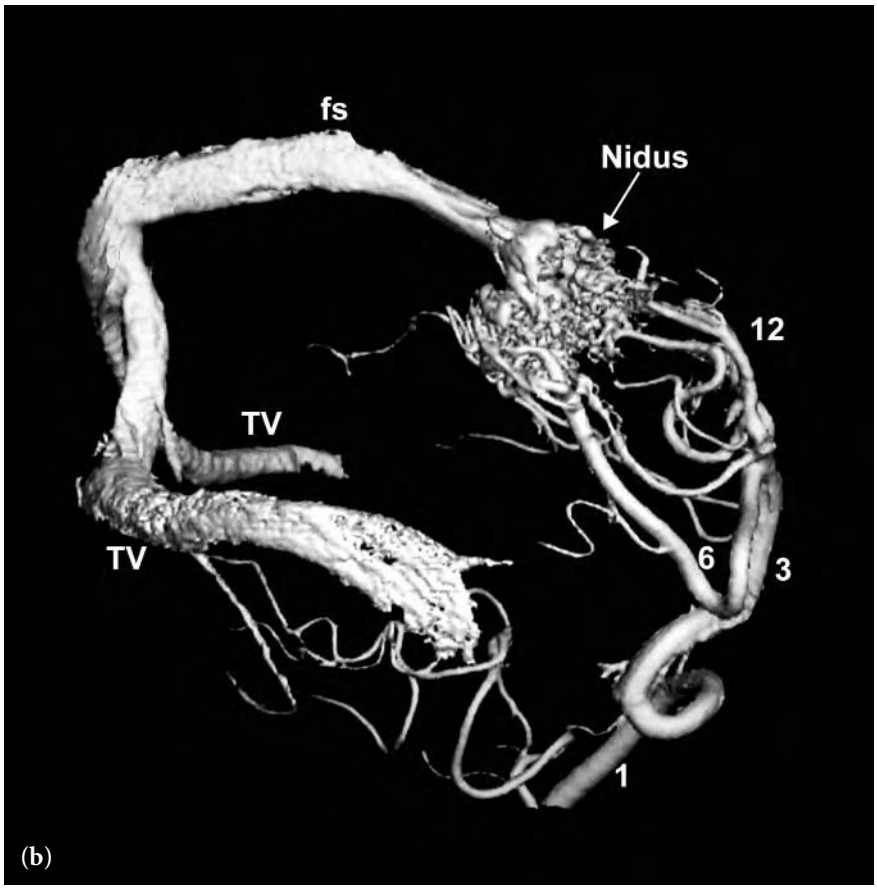
fs
Nidus
12
TV
TV
6
3
1
(b)

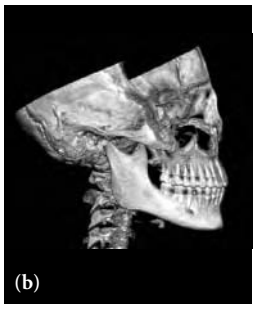
(b)

(c)

12
TV
TV
5
3
6
1
(c)

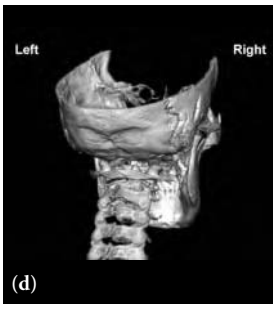

Fig. 6.18 (continued)

FIGURE KEY

1 vertebral artery
3 basilar artery
5 superior cerebellar artery (SCA)
6 posterior cerebral artery (PCA)
12 posterior thalamoperforating arteries
fs falcine sinus
TV transverse sinus
* perinidal (venous side) aneurysms

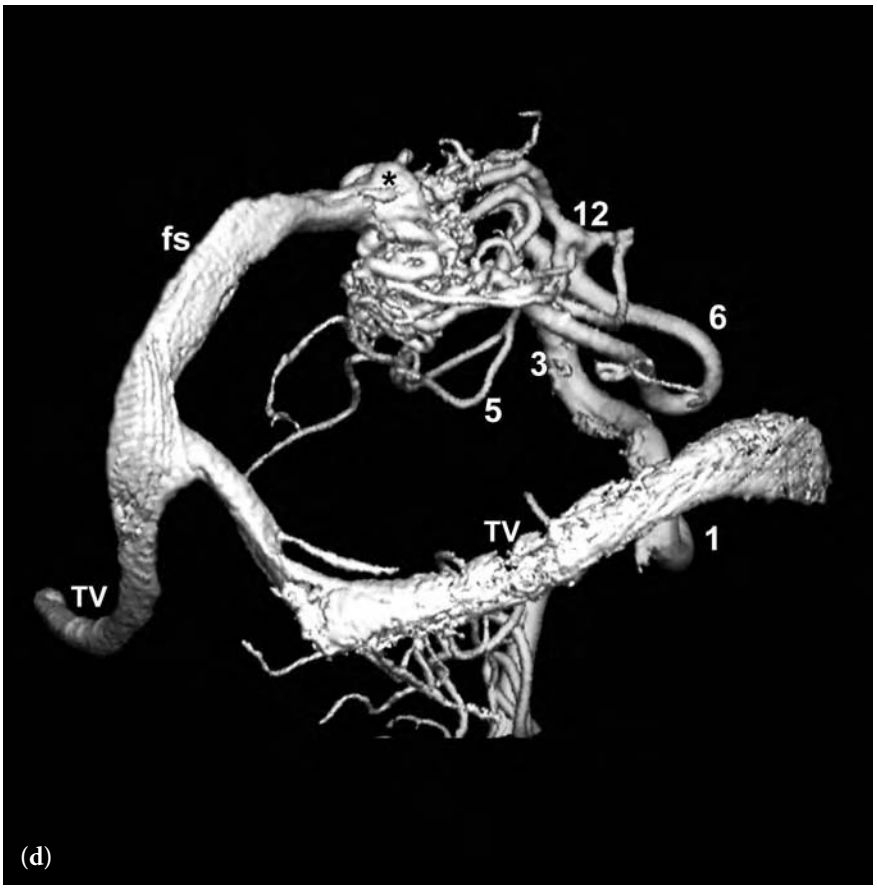

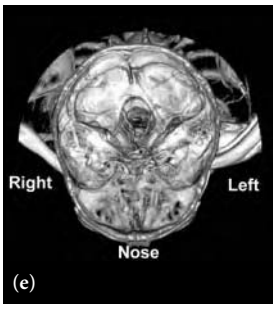
Right
Left
Nose
(e)

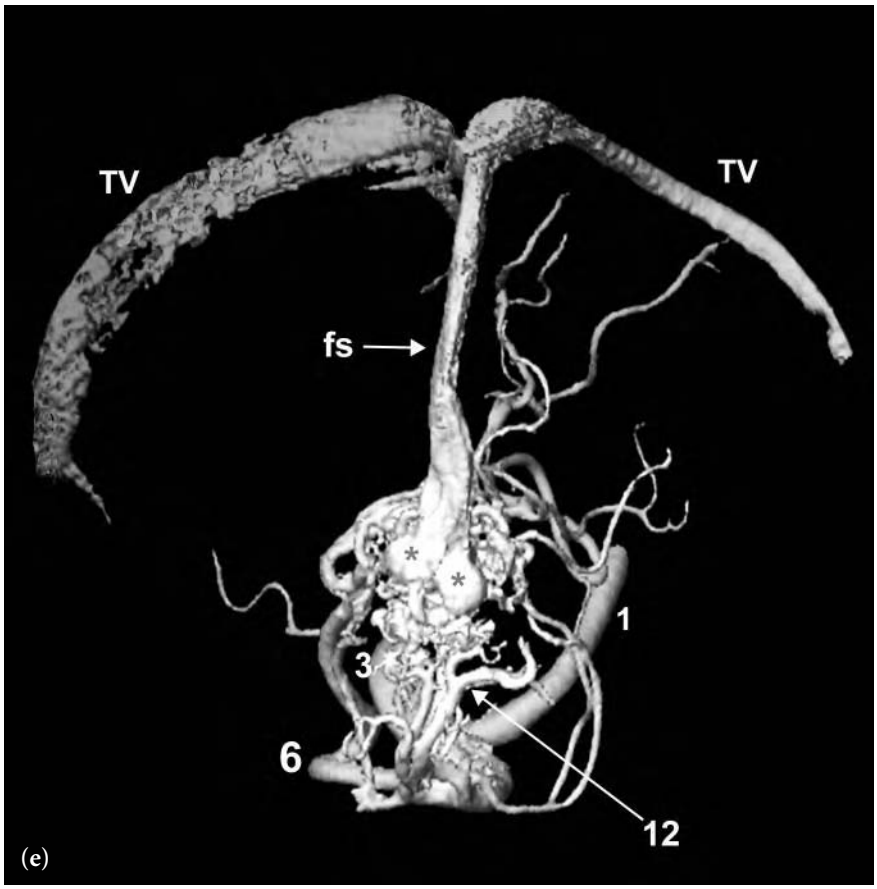
TV
TV
fs
*
*
1
3
6
12
(e)

CHAPTER SEVEN

INTRACRANIAL VENOUS SYSTEM

The venous drainage of the brain and meninges can be divided into the diploic veins, meningeal veins, dural sinuses, as well as the superficial and deep cerebral veins.

The diploic veins are small irregular endothelial-lined channels coursing between the inner and outer tables of the skull. These communicate with the extracranial venous system, the meningeal veins, and the dural sinuses. They are rarely seen using angiography unless enlarged, as in the case of an arterial-venous malformation (AVM).

Emissary veins are conduits between the extracranial scalp veins and the diploic and intracranial venous systems. These veins are valveless and therefore can transmit infection from the extracranial to the intracranial compartment.

The meningeal veins are epidural veins that lie within the dura draining the falx cerebri, the tentorium, and the cranial dura. They run in shallow grooves on the inner table of the skull to communicate with the dural sinuses or traverse extracranially to the pterygoid plexus in the deep face or vertebral plexus around the cervical spine.

The dural sinuses are venous channels lined by endothelium that are formed by opposing layers of dura. They are valveless, trabeculated, and provide the major drainage pathway for the cranial cavity. The major dural sinuses include the superior sagittal sinus, inferior sagittal sinus, straight sinus, occipital sinus, transverse sinuses, petrosal sinuses, sigmoid sinuses, sphenoparietal sinuses, and cavernous sinuses.

The superior sagittal sinus drains the superficial cerebral veins from the medial and lateral surfaces of the cerebral hemispheres and run anteriorly to posteriorly in the midline in a shallow groove along the inner table from the foramen cecum of the crista galli to the torcular Herophili. The torcular Herophili is the confluence of the superior sagittal sinus, the straight sinus, the occipital sinus, and the transverse sinuses. There are many configurations in the appearance of the torcular Herophili which at times may be

duplicated or fenestrated. The anterior portion of the superior sagittal sinus may be congenitally absent. In this case, the superior sagittal sinus is formed by several large cerebral veins overlying the frontal convexity.

The inferior sagittal sinus travels along the inferior free edge of the falx cerebri in an anterior to posterior direction draining into the straight sinus along with the great cerebral vein of Galen. The inferior sagittal sinus drains the anterior portion of the corpus callosum, the medial aspect of the cerebral hemispheres, and the falx cerebri.

The straight sinus runs from the junction of the falx cerebri and the tentorium to the torcular Herophili in a midline superior-anterior to inferior-posterior course. The straight sinus may be duplicated in 7%–15% of the cases (1). The straight sinus is the main conduit transmitting venous blood from the deep venous system towards the more superficial dural sinuses.

The occipital sinus is typically the smallest of the dural sinuses, originating at the posterior margin of the foramen magnum and draining superiorly to the torcular Herophili. It can communicate with the internal jugular vein or with the vertebral venous plexus. The marginal sinus runs along the lateral margins of the foramen magnum and communicates with the occipital sinus along the posterior margin of the foramen magnum. The marginal sinus communicates anteriorly with the basilar venous plexus on the superior surface of the clivus. The marginal sinus also communicates with the internal jugular veins and the jugular bulbs laterally via small venous connections (2).

The paired transverse sinuses begin at the torcular Herophili and run anterolaterally to become the sigmoid sinuses when turning inferiorly and medially at the posterior aspect of the petrous temporal bones. The transverse sinuses run in a groove along the inner table of the calvarium and are enveloped within the peripheral edge of the tentorium. In addition to draining the superior sagittal sinus and the straight sinus from the torcula, the transverse sinuses also drain the supratentorial veins from the temporal and occipital lobes as well as the cerebellar veins and the superior petrosal sinuses. In 25% of the cases, the transverse sinuses are unequal in size (3). An atretic segment may be seen in 5% of the cases (4). In most people the superior sagittal sinus drains preferentially into the right transverse sinus, while the deep venous system through the straight sinus drains preferentially into the left transverse sinus.

The superior petrosal sinus extends from the posterior aspect of the cavernous sinus at the petrous apex to the sigmoid sinus along a dural attachment of the tentorium to the petrous temporal bone. It provides venous drainage from the pons, upper medulla, cerebellum, and middle ear (5).

The inferior petrosal sinus runs inferiorly along the petro-occipital fissure from the posterior aspect of the cavernous sinus (near the petrous apex). It traverses the pars nervosa compartment of the jugular foramen before emptying into the jugular bulb in the pars vascularis compartment. The paired inferior petrosal sinuses are interconnected with the basilar venous plexus of the clivus and the intercavernous sinus (or circular sinus) to communicate with the cavernous, superior petrosal, marginal, and occipital sinuses.

The sphenoparietal sinus drains the superficial middle cerebral vein running along the greater sphenoid wing to the cavernous sinus. The sphenoparietal sinus often anastomoses with the basal vein of Rosenthal.

The paired cavernous sinuses are irregularly paired venous spaces that lie on either side of the sphenoid bone in the central skull base region. They lie on either side of the sella turcica, which houses the pituitary gland. The cavernous sinuses represent a complex interconnection of the intracranial and extracranial venous structures. Anteriorly the cavernous sinuses communicate with the superior and inferior ophthalmic veins as well as the sphenoparietal sinus. Laterally and inferiorly the cavernous sinuses communicate with the pterygoid plexus of the deep face through the foramen ovale. The cavernous sinuses are interconnected medially by the intercavernous sinuses (or circular sinuses) which run in the diaphragma sellae along the roof of the sella turcia. The cavernous sinus communicates posteriorly with the transverse sinus via the superior petrosal sinus and the internal jugular veins via the inferior petrosal sinuses. Contained within the cavernous sinus are the cavernous portions of the internal carotid arteries and the abducens nerve (CN VI). Portions of the occulomotor nerve (CN III), the trochlear nerve (CN IV), and the first and second divisions of the trigeminal nerve (V1 and V2) lie between dural leaves of the lateral cavernous sinus wall. The abducens nerve lies in close proximity to the lateral aspect of the horizontal intracavernous segment of the internal carotid artery. Patients may present with isolated sixth nerve palsy (inability to abduct the eye) in cases of aneurysms of the horizontal intracavernous internal carotid artery.

The superficial cerebral veins run along the surface of the brain draining cortical gray matter and portions of white matter. There is a good deal of variability in the course, size, and number of these veins. In general, the superficial cerebral veins have a spoke-like pattern converging inferiorly towards the sylvian fissure and superiorly towards the superior sagittal sinus. Typically, the superficial cerebral veins drain inferiorly through the "sylvian" or superficial middle cerebral vein, posteriorally and laterally through the anastomotic vein of Labbé, or superiorly through the anastomotic vein of Trolard or other unnamed superiorly directed superficial veins.

The superficial middle cerebral vein drains the opercular areas adjacent to the sylvian fissure coursing anteriorly and inferiorly around the temporal lobe tip to drain into the cavernous or sphenoparietal sinus. The superficial middle cerebral vein communicates with the deep cerebral system through the uncal, insular, and basal veins as well as communicating with other superficial veins and dural sinuses.

Dominant superiorly and inferiorly directed superficial veins drain into the superior sagittal sinus and the distal transverse sinus, respectively. The largest superiorly directed vein is called the anastomotic vein of Trolard. The anastomotic vein of Labbé represents the largest inferiorly and posteriorly directed superficial anastomotic vein coursing laterally over the surface of the temporal lobe and draining the temporal lobe which typically drains posteriorly into the distal transverse sinus. This is an important source of venous outlet for the temporal lobe. Care is taken during endovascular or operative procedures to ensure its integrity unless there are mitigating circumstances necessitating its sacrifice. If a normal vein of Labbé is disconnected, it can result in venous infarction of the temporal lobe. However, if the vein of Labbé is arterialized from a dural fistula or other etiology it can generally be sacrificed without troublesome consequences.

The deep supratentorial cerebral veins drain the hemispheric white matter, basal ganglia, corpus callosum, pineal area, midbrain, portions of the limbic system, and the thalamus centrally via medullary veins into the subependymal veins coursing along the medial walls of the lateral ventricles. Numerous small deep medullary veins originate 1 to 2 cm below the cortical grey matter (6) and course through deep cerebral white matter in a perpendicular direction to converge into larger tributaries that drain into the internal cerebral vein and the great cerebral vein of Galen. These tributaries are

divided into medial and lateral draining subependymal veins. In general, medullary veins are not visualized on routine 2D or 3D angiography. They may be seen on 2D angiography in situations where they are enlarged or more prominent as a result of increased blood flow.

The medial subependymal veins consist of the anterior septal veins, the posterior septal veins, and the common atrial veins. The anterior septal vein drains the convergence of medullary veins of the anterior frontal lobe and then travels posteriorly along the septum pellucidum and under the fornix to join the thalamostriate vein and the choroidal vein.

The lateral subependymal veins consist of the thalamostriate, anterior caudate, and direct lateral veins. Formed from the union of the anterior caudate vein and the terminal vein, the thalamostriate vein is the largest of the lateral subependymal veins. The thalamostriate vein drains the posterior frontal and anterior parietal lobes, caudate nucleus, and the internal capsule. The thalamostriate vein is usually a major supplier of venous blood to the internal cerebral veins. The direct lateral vein runs along the lateral wall of the atrium to receive drainage from the posterior temporal and parietal lobes typically course medially over the thalamus to join the internal cerebral vein. The inferior ventricular vein generally begins in the posterior aspect of the body of the lateral ventricle. It runs inferiorly along the anterior wall of the atrium of the lateral ventricle and then anteriorly along the roof of the temporal horn before turning medially. The inferior ventricular vein drains into the basal vein of Rosenthal after penetrating the choroidal fissure.

The internal cerebral veins are paired, originating at the junction of the anterior septal vein and the thalamostriate vein. The internal cerebral veins then course posteriorly in the roof of the third ventricle between the leaves of the velum interpositum. Receiving numerous small tributaries along their course and initially running side by side, the internal cerebral veins deviate from the midline at the pineal recess and proceed along the superolateral surface of the pineal body to converge at the level of the inferior splenium of the corpus callosum to form the great cerebral vein of Galen. Just before the convergence of the internal cerebral veins, the basal veins of Rosenthal join their ipsilateral internal cerebral veins.

The venous angle is defined as the junction of the thalamostriate vein with the internal cerebral vein and is typically located at the foramen of

Monro. A false venous angle is determined by the absence of the anteriorly, slightly ascending segment of the internal cerebral vein, the absence of the frontally convex curve seen in the thalamostriate vein where it joins the internal cerebral vein, and the increased length of the anterior and longitudinal caudate veins (7).

The basal vein of Rosenthal begins in the supra-sellar cistern, medial to the uncus. It receives venous flow from the olfactory veins, insular veins, the deep middle cerebral vein, and the inferior striate veins. As it runs posteriorly, the basal vein of Rosenthal extends from the supra-sellar cistern (medial to the uncus) into the crural cistern, lateral to the cerebral peduncle. The crural cistern lies between the uncus and the cerebral peduncle. It subsequently drains into the ipsilateral internal cerebral vein or great cerebral vein of Galen. It rarely directly enters the straight sinus (8). The basal vein of Rosenthal provides venous drainage to the orbital surface of the frontal lobe, insula, medial temporal lobe, hypothalamus, striatum, thalamus, and midbrain. On frontal projection, the basal vein of Rosenthal has the appearance of a "leg of a frog lying on its back with its toes pointing anterolaterally". The "knee of the frog's leg" represents its lateral aspect as it courses around the cerebral peduncles. The "ankle" represents the more anterior aspect of the basal vein where it lies medial to the uncus of the temporal lobe (9).

The great cerebral vein of Galen is a single "U" shaped vessel that runs under and then posterior to the splenium of the corpus callosum. It joins with the inferior sagittal sinus to form the straight sinus at the apex of the tentorial incisura. The vein of Galen receives tributaries from the inferior sagittal sinus, pericallosal veins, internal occipital veins, the posterior fossa veins, and occasionally the basal vein of Rosenthal.

The infratentorial venous system is discussed in three groups: the superior or Galenic draining group, the anterior or petrosal draining group, and the posterior or tentorial draining group.

The superior group of posterior fossa veins includes the precentral cerebellar vein, the superior vermian vein, the posterior and lateral mesencephalic veins, and the anterior pontomesencephalic veins. The precentral cerebellar vein is formed by brachial veins medially coursing over the brachium pontis. The precentral vein then runs in the fissure between the lingual and the central lobule of the vermis to terminate in the vein of Galen.

The superior vermian vein typically originates near the declive of the vermis coursing anteriorly and superiorly over the superior culmen. It then arcs slightly inferiorly just anterior to the vermis and finally runs superiorly to terminate in the vein of Galen. The posterior mesencephalic veins are paired veins arising from the lateral aspects of the respective cerebral peduncles from peduncular veins to then traverse around the brainstem within the ambient cistern, to then empty into the vein of Galen. The lateral mesencephalic vein runs superiorly and longitudinaly along the mesencephalon to join the brachial vein and the posterior mesencephalic vein. The position of the lateral mesencephalic vein marks the junction of the tegmentum and the cerebral peduncle (10). The anterior pontomesencephalic vein or plexus of veins runs longitudinaly and superiorly along the surface of the pons and mesencephalon. This vein outlines the ventral surface of the brainstem. It is a more accurate indicator of the position of the ventral brainstem than the position of the basilar artery, which can be tortuous, coursing laterally away from the ventral aspect of the brainstem. The anterior pontomesencephalic vein or plexus of veins typically curve into the interpeduncular fossa, demarcating the cerebral peduncles' undersurface and then drains into the basal vein of Rosenthal or the posterior mesencephalic vein.

The anterior or petrosal group of draining veins includes the petrosal trunk (petrosal vein) and the brachial veins to provide venous drainage for portions of the cerebellum, pons, and medulla. The petrosal trunk (petrosal vein) originates in the cerebellopontine angle cistern. It is a short vessel that receives many small venous tributaries from the pons, cerebellar hemispheres, brain stem, and the fourth ventricle. The petrosal trunk (petrosal vein) runs anteriorly and laterally below the fifth cranial nerve (trigeminal nerve) to drain into the superior petrosal sinus just above the porus acousticus. The brachial veins are paired venous vessels that typically empty into the precentral cerebellar vein or may extend laterally over the brachium pontis to drain into the petrosal vein. The brachial veins are best visualized on the frontal projection as an inverted "V".

The posterior draining group includes the inferior vermian veins and the inferior hemispheric veins. The inferior vermian veins are paired vessels that are paramedian in location originating at or near the pyramidal lobule by numerous small tributaries from the cerebellar tonsils. The inferior vermian veins run posteriorly and superiorly along the inferior vermian

surface, receiving numerous small tributaries to terminate in venous sinuses within the tentorium, the straight sinus, or the transverse sinus adjacent to the torcular Herophili. The inferior hemispheric veins provide venous drainage for the posterior inferior cerebellar hemispheres and drain into the inferior vermian veins or into a transverse sinus.

Angiographic analysis of the posterior fossa veins is challenging because of the large number of venous structures, the small compartment in which they reside, and the numerous variations of what is considered normal which can exist.

REFERENCES

1. Browder, J., H.A.Kaplan, and A.J. Krieger. 1976. Anatomic features of the straight sinus and its tributaries. *J. Neurosurg.* 44:55–61.
2. Tubbs, R. K. Ammar, and P. Liechty et al. 2006. The marginal sinus. *J. Neursosurg.* 2006:104:429–431.
3. Osborn, A. 1980. *Introduction to Cerebral Angiography*. Philadelphia: Harper & Row, p. 333.
4. Kaplan H.A., A. Browder, and J. Browder. 1973. Narrow and atretic transverse dural sinuses: Clinical significance. *Ann. Otol. Rhinol. Laryngol.* 82:351–354.
5. Osborn, pp. 329–333.
6. Osborn, p. 335.
7. Huber, P. 1982. *Krayenenbuhl/Yasargil Cerebral Angiography*. New York: Thieme Medical Publishers, pp. 195–198.
8. Huber, p. 200.
9. Huang, Y.P. and B.S. Wolf. 1974. *The basal cerebral vein and its tributaries.* In Radiology of the Skull and Brain: Angiography Volume 2. T.H. Newton and D.G. Potts, editors. St. Louis, Mo: CV Mosby Company, pp. 2111–2154.
10. Osborn, p. 395.

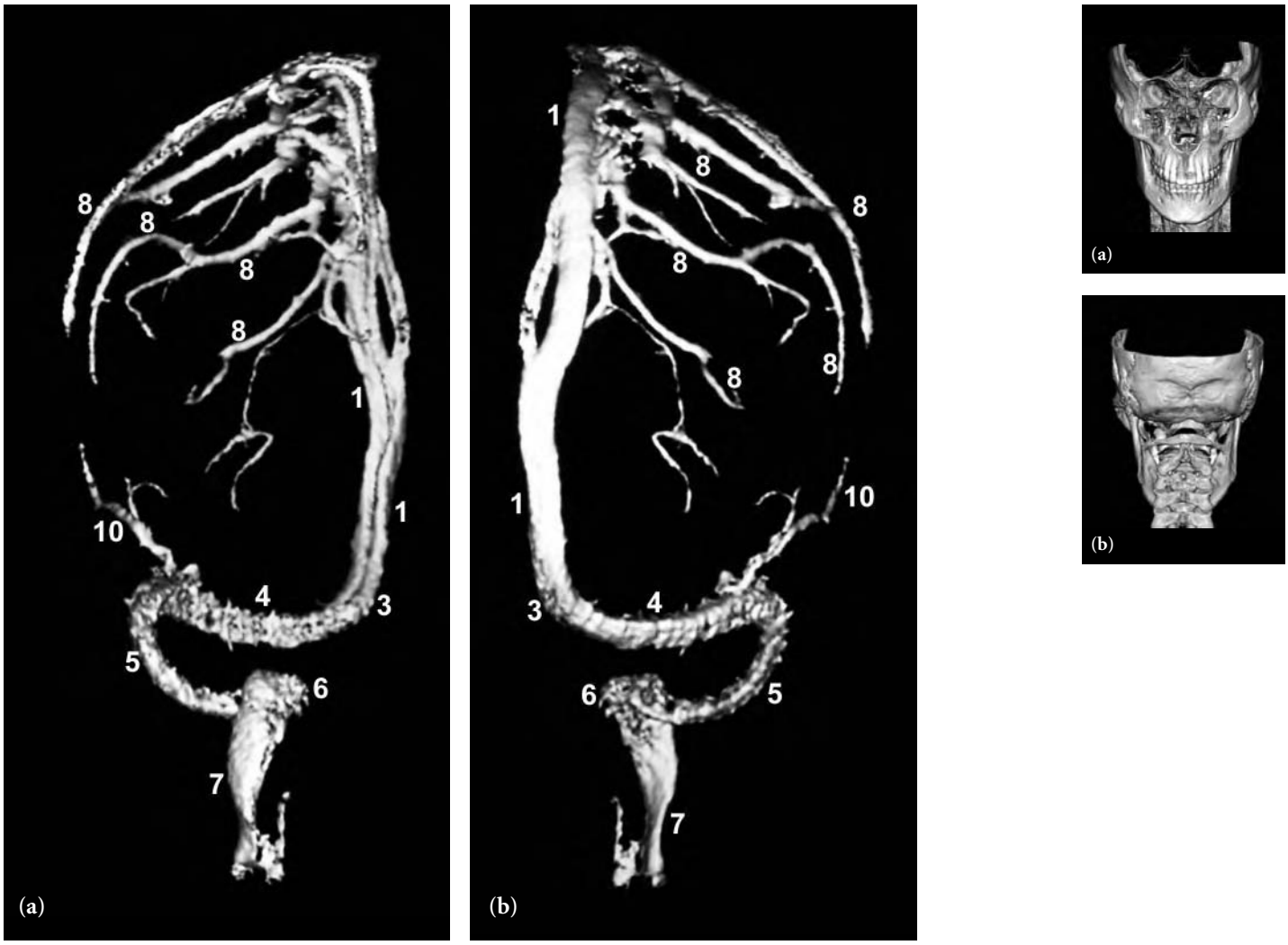

Fig. 7.1 (a–c) 3D frontal (*a*), posterior (*b*), and left lateral (*c*) views of the venous phase of circulation of the superficial intracranial veins following right carotid artery injection. None of the deep venous system is visualized due to the post-processing technique.

FIGURE KEY

1 superior sagittal sinus
3 torcular herophili
4 transverse sinus
5 sigmoid sinus
6 jugular bulb
7 internal jugular vein
8 superficial cortical vein
10 vein of Labbé

Fig. 7.1 (continued)

FIGURE KEY

1 superior sagittal sinus
3 torcular herophili
4 transverse sinus
5 sigmoid sinus
6 jugular bulb
7 internal jugular vein
8 superficial cortical vein
10 vein of Labbé

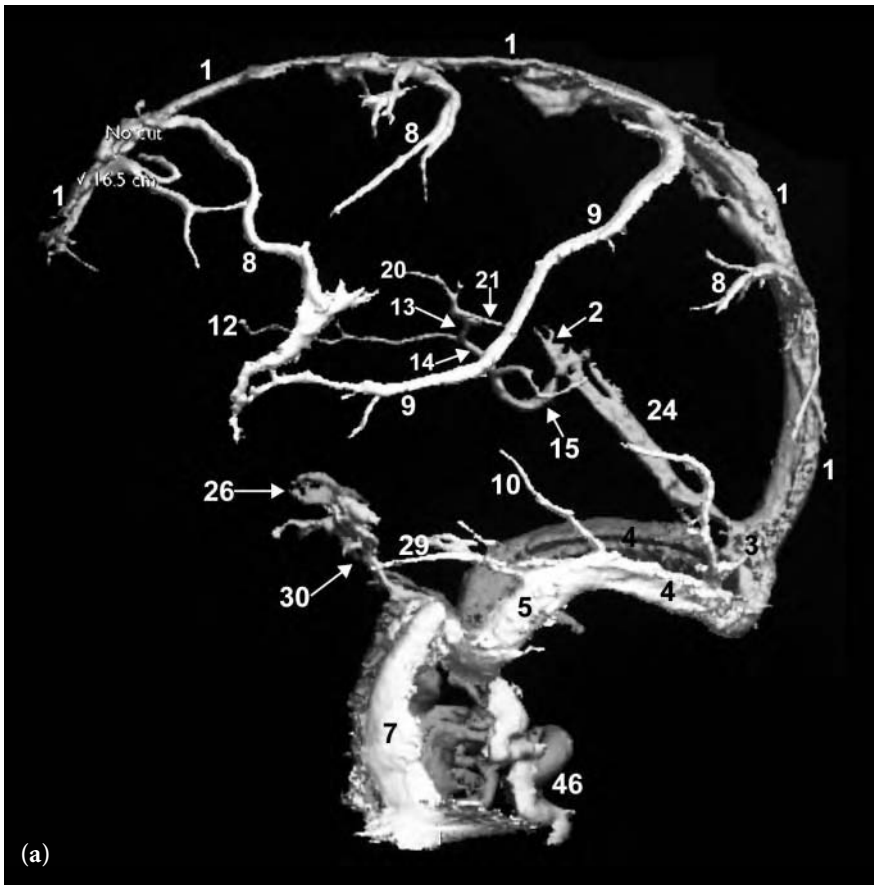

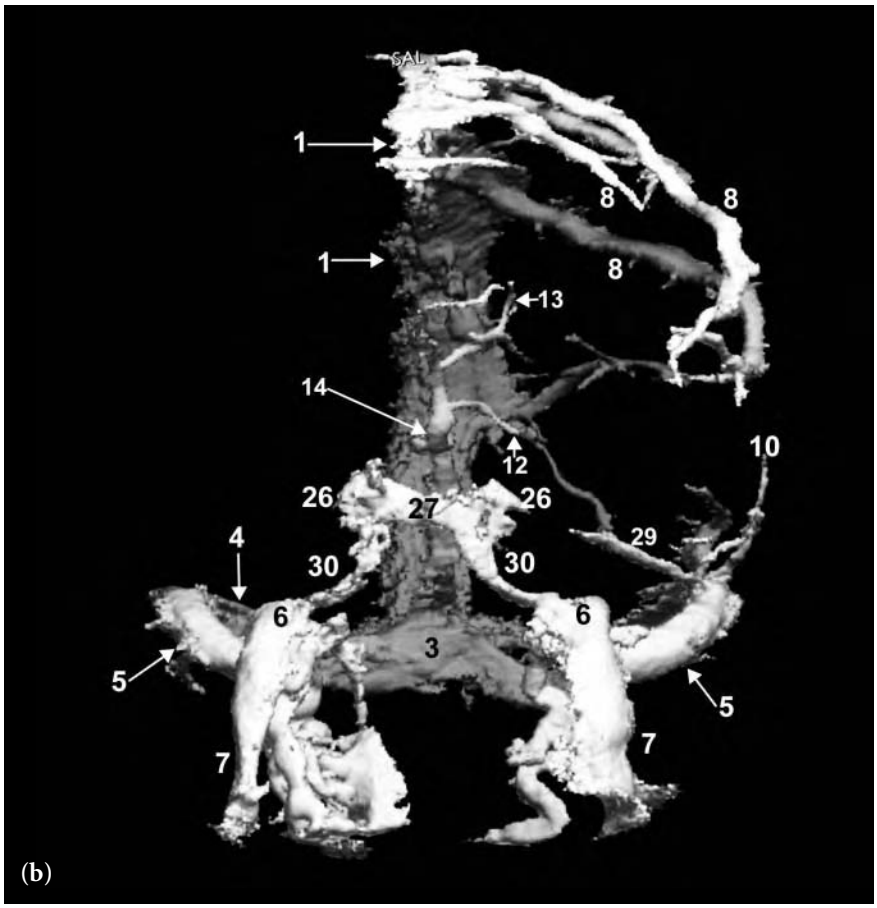

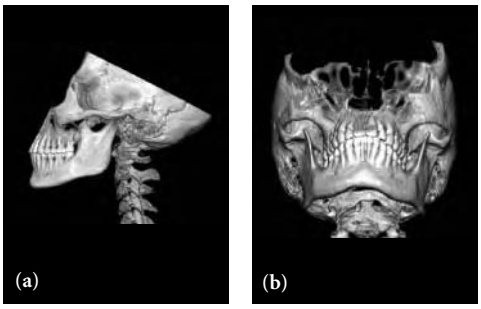

Fig. 7.2 (a,b) 3D right lateral (*a*) and frontal (*b*) views of the venous phase of circulation following left carotid artery injection. These views show a normal appearance of the superficial and deep venous systems.

FIGURE KEY

1 superior sagittal sinus
2 inferior sagittal sinus
3 torcular herophili
4 transverse sinus
5 sigmoid sinus
6 jugular bulb
7 internal jugular veins
8 superficial cortical veins
9 vein of Trolard
10 vein of Labbé
12 septal vein
13 thalamostriate vein
14 internal cerebral vein
15 great cerebral vein of Galen
16 basal vein of Rosenthal
20 anterior caudate vein
21 terminal vein
24 straight sinus
26 cavernous sinus
27 intercavernous sinus
29 superior petrosal sinus
30 inferior petrosal sinus

Fig. 7.3 (a–f) 2D frontal views of the venous phase of circulation following carotid artery injection in multiple patients. These series of frontal views demonstrate the marked variability of the intracranial venous anatomy. No two patients demonstrate the same morphologic appearance. This wide variability in the venous anatomy is to be expected.

FIGURE KEY

1 superior sagittal sinus
3 torcular herophili
4 transverse sinus
5 sigmoid sinus
6 jugular bulb
7 internal jugular vein
8 superficial cortical veins
9 vein of Trolard
10 vein of Labbé
11 superficial middle cerebral vein
12 septal vein
13 thalamostriate vein
14 internal cerebral vein
16 basal vein of Rosenthal
24 straight sinus
25 sphenoparietal sinus
26 cavernous sinus
27 intercavernous sinus
29 superior petrosal sinus
30 inferior petrosal sinus
31 occipital sinus
56 insular vein
57 deep middle cerebral vein
uncus uncus of temporal lobe
ped cerebral peduncle

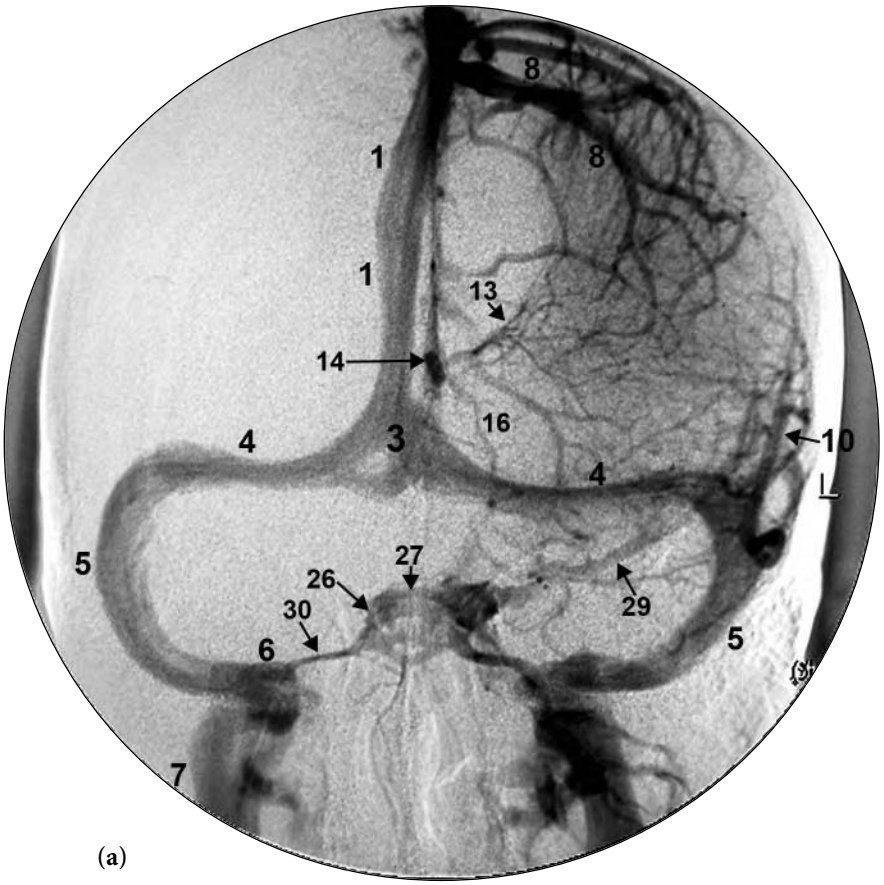

(a)

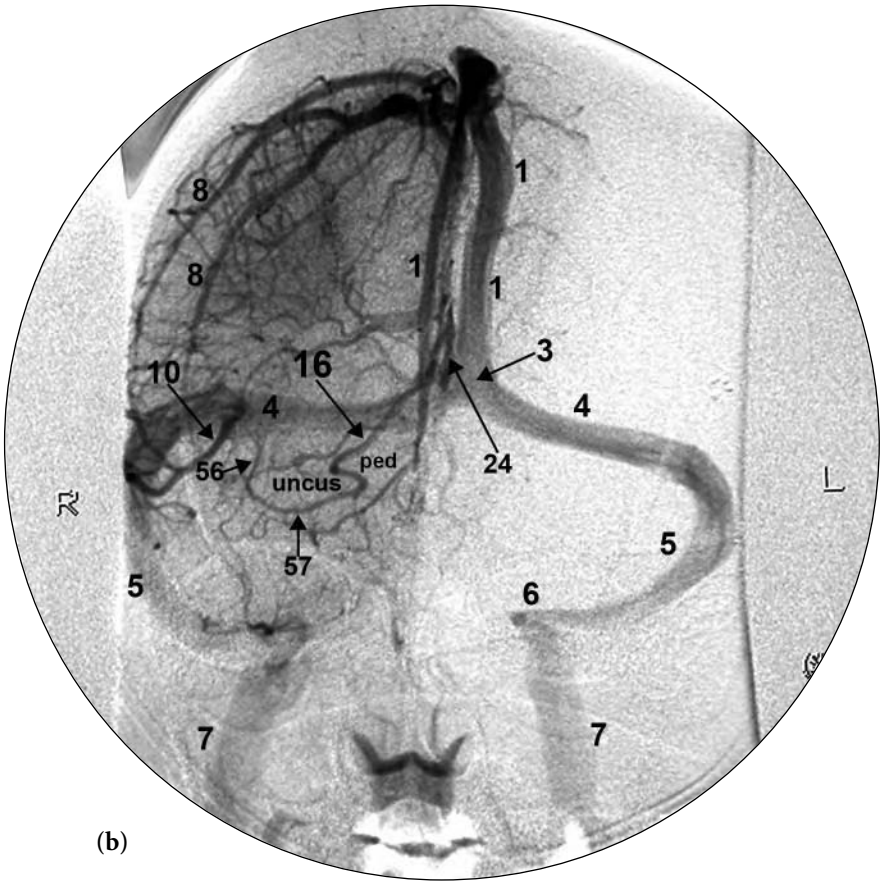

(b)

(c,d)

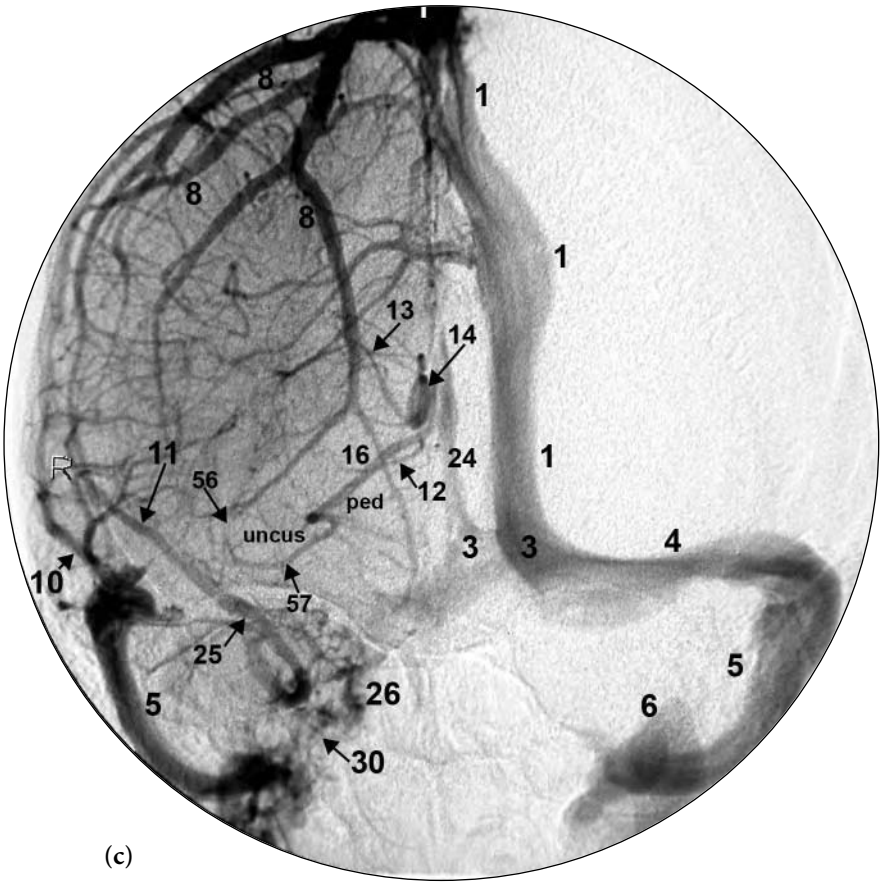
R
8
8
8
1
1
1
13
14
11
56
16
24
12
ped
uncus
3
3
4
10
57
25
5
5
26
6
30

(c)

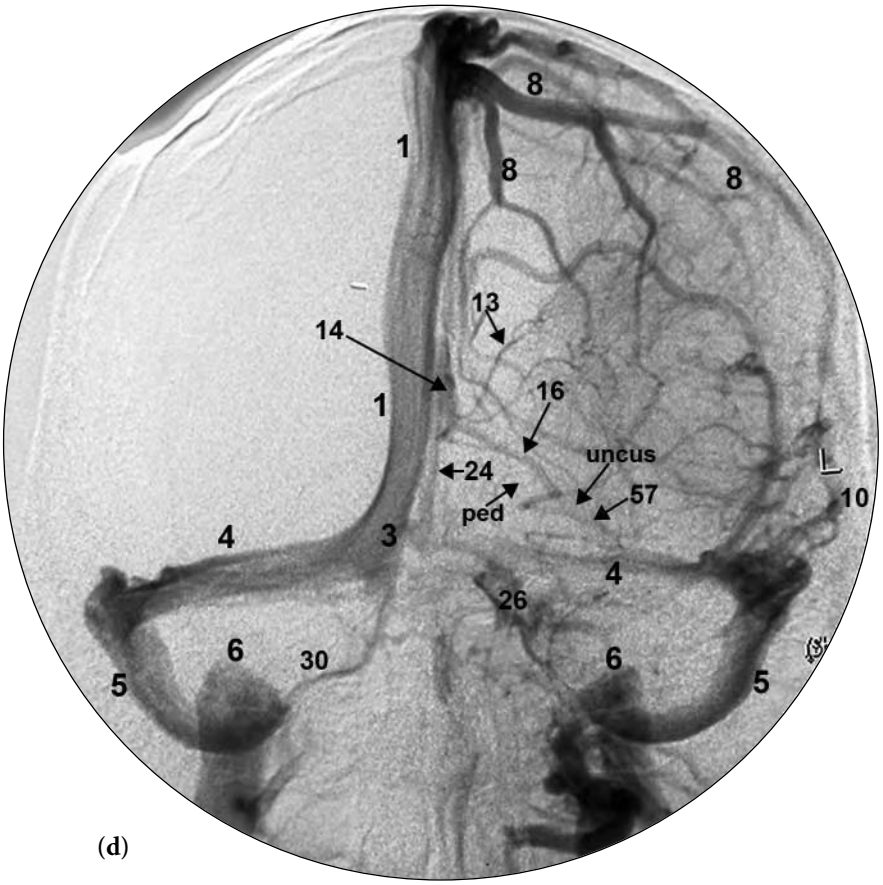
8
1
8
8
13
14
16
1
uncus
L
24
57
10
ped
4
3
4
26
6
30
6
5
5

(d)

Fig. 7.3 (continued)

FIGURE KEY

1 superior sagittal sinus
3 torcular herophili
4 transverse sinus
5 sigmoid sinus
6 jugular bulb
7 internal jugular vein
8 superficial cortical veins
9 vein of Trolard
10 vein of Labbé
11 superficial middle cerebral vein
12 septal vein
13 thalamostriate vein
14 internal cerebral vein
16 basal vein of Rosenthal
24 straight sinus
25 sphenoparietal sinus
26 cavernous sinus
27 intercavernous sinus
29 superior petrosal sinus
30 inferior petrosal sinus
31 occipital sinus
56 insular vein
57 deep middle cerebral vein
uncus uncus of temporal lobe
ped cerebral peduncle

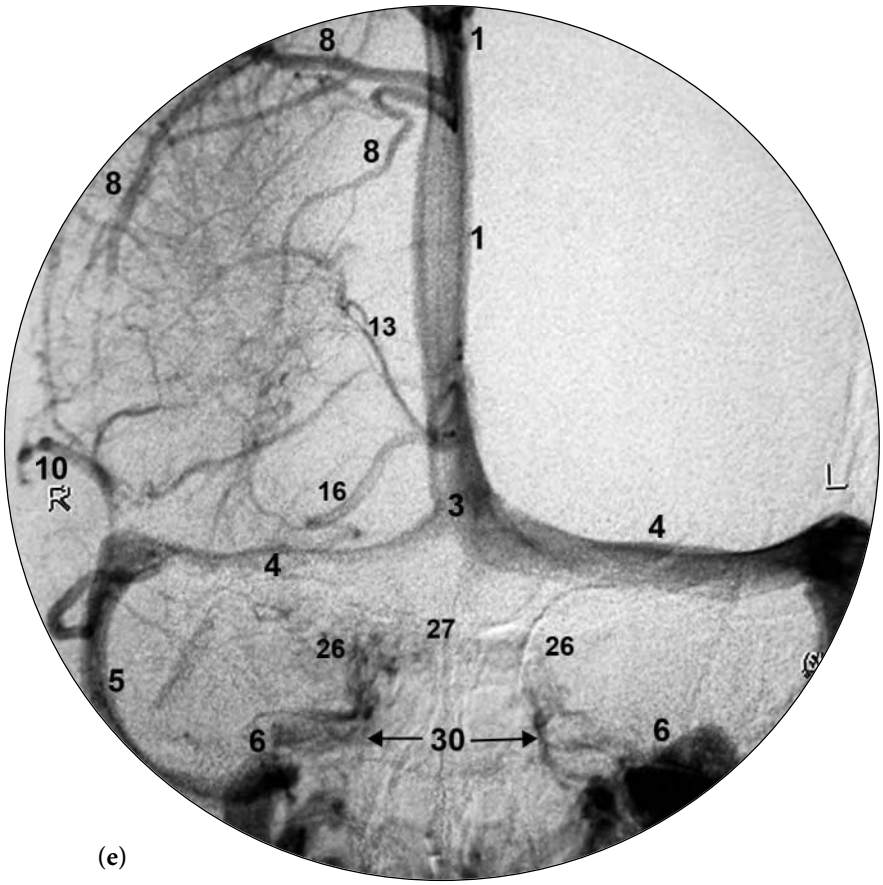

(e)

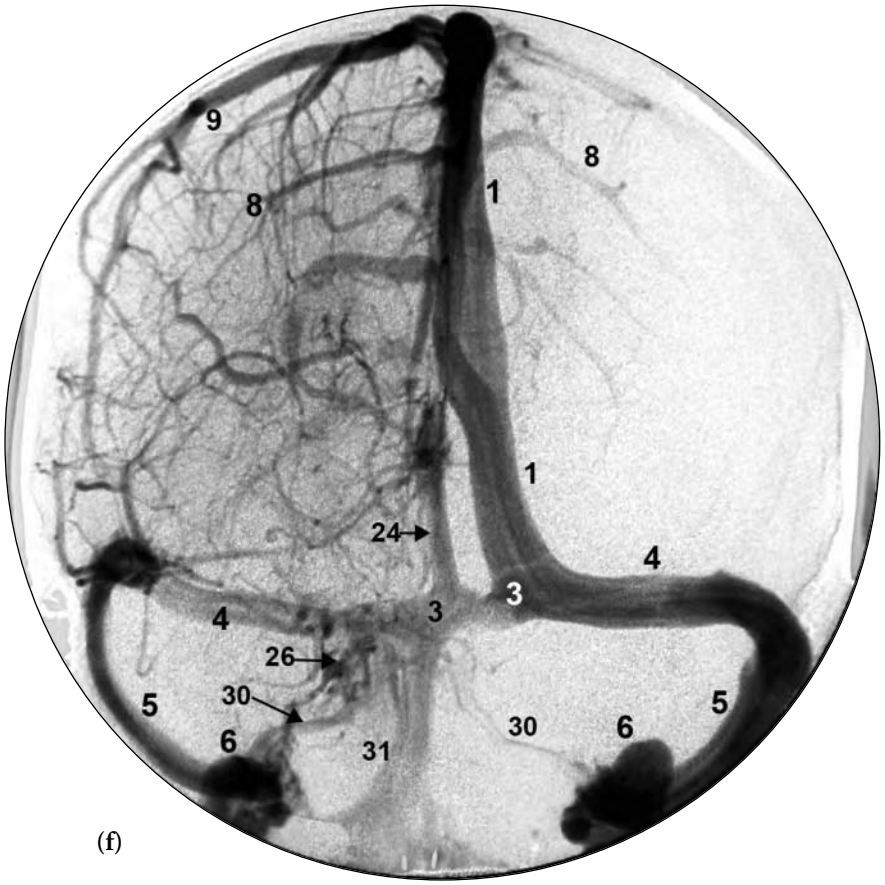

(f)

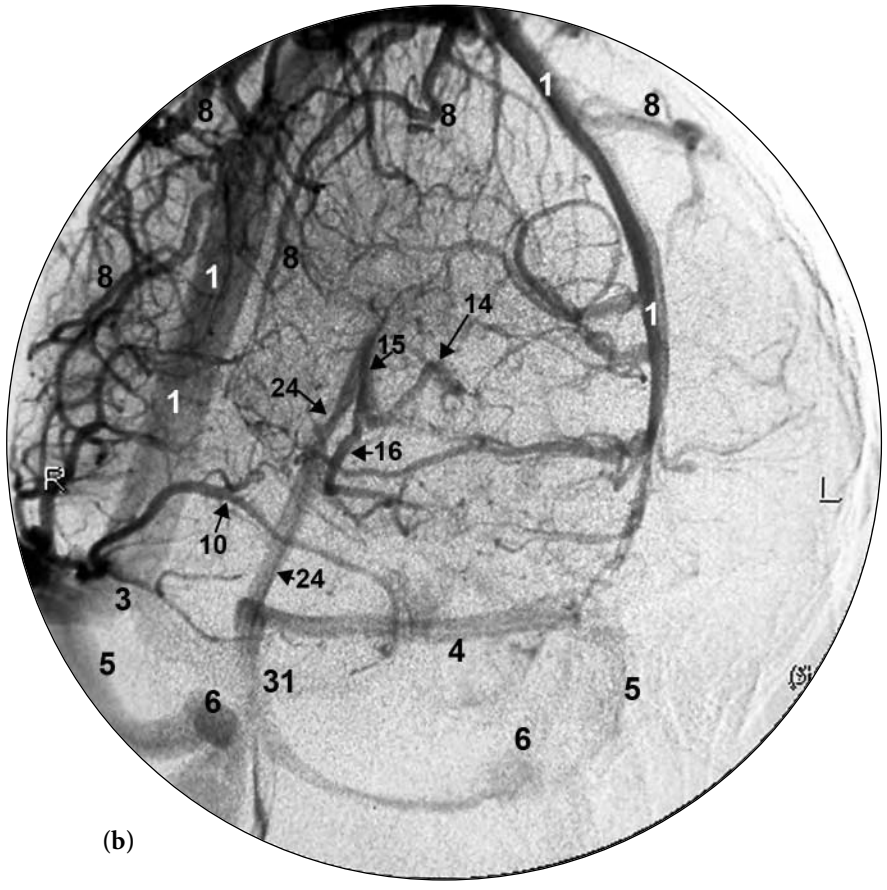

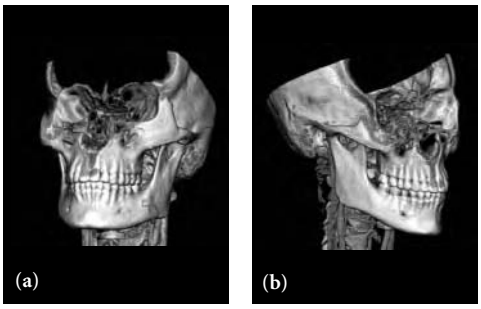

Fig. 7.4 (a,b) 2D frontal view with a shallow oblique of the head to the right (*a*) and a frontal view oblique of the head to the left (*b*) (venous phase) following carotid artery injections in two different patients. The rotation of the head allows for a better visualization of some of the venous anatomy which appears overlapped on a straight frontal view without any rotation.

FIGURE KEY

1 superior sagittal sinus
3 torcular herophili
4 transverse sinus
5 sigmoid sinus
6 jugular bulb
8 superficial cortical veins
10 vein of Labbé
14 internal cerebral vein
15 great cerebral vein of Galen
16 basal vein of Rosenthal
24 straight sinus
31 occipital sinus

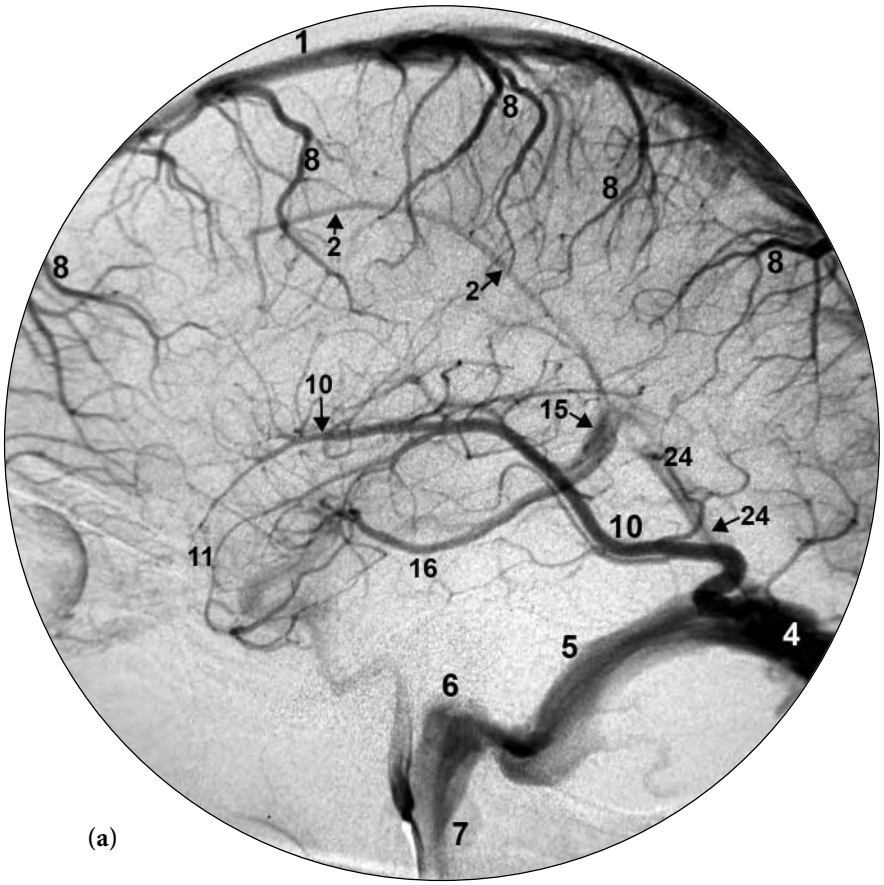

Fig. 7.5 (a–o) 2D lateral views of venous phase circulation following carotid artery injections in multiple patients. These images show the marked variability in the intracranial venous anatomy which is normal and to be expected. This series of images shows the normal variability in the size of the veins of Trolard and Labbé as well as showing the wide but normal differences in the appearance of the deep venous system. Note the variation in the appearance of the deep venous system that results in the "true" and "false" venous angles in images *c-f*, *h*, *i*, *k-m*. Note the absence of vascular structures just below the superior sagittal sinus in image *n*. This is secondary to a severe developmental hypoplasia of the A1 segment of the anterior cerebral artery on the injected side. This vascular territory would be visualized when the opposite carotid artery is injected. During the venous circulation phase, with time you normally visualize the deep venous system to a better advantage after the normal washout of the superficial veins. This is demonstrated in the views in figures *b*, *c*, *g*, *h*, *j*, and *k*.

FIGURE KEY

1 superior sagittal sinus
2 inferior sagittal sinus
3 torcular herophili
4 transverse sinus
5 sigmoid sinus
6 jugular bulb
7 internal jugular vein
8 superficial cortical vein
9 vein of Trolard
10 vein of Labbé
11 superficial middle cerebral vein
12 septal vein
13 thalamostriate vein
14 internal cerebral vein
15 great cerebral vein of Galen
16 basal vein of Rosenthal
17 inferior ventricular vein
18 medial atrial vein
20 anterior caudate vein
21 terminal vein
22 direct lateral vein
24 straight sinus
25 sphenoparietal sinus
26 cavernous sinus
28 clival venous plexus
29 superior petrosal sinus
30 inferior petrosal sinus
46 suboccipital veins
47 pterygoid venous plexus
48 true venous angle
51 superior ophthalmic vein
53 sphenopetrosal vein
55 false venous angle

(b,c)

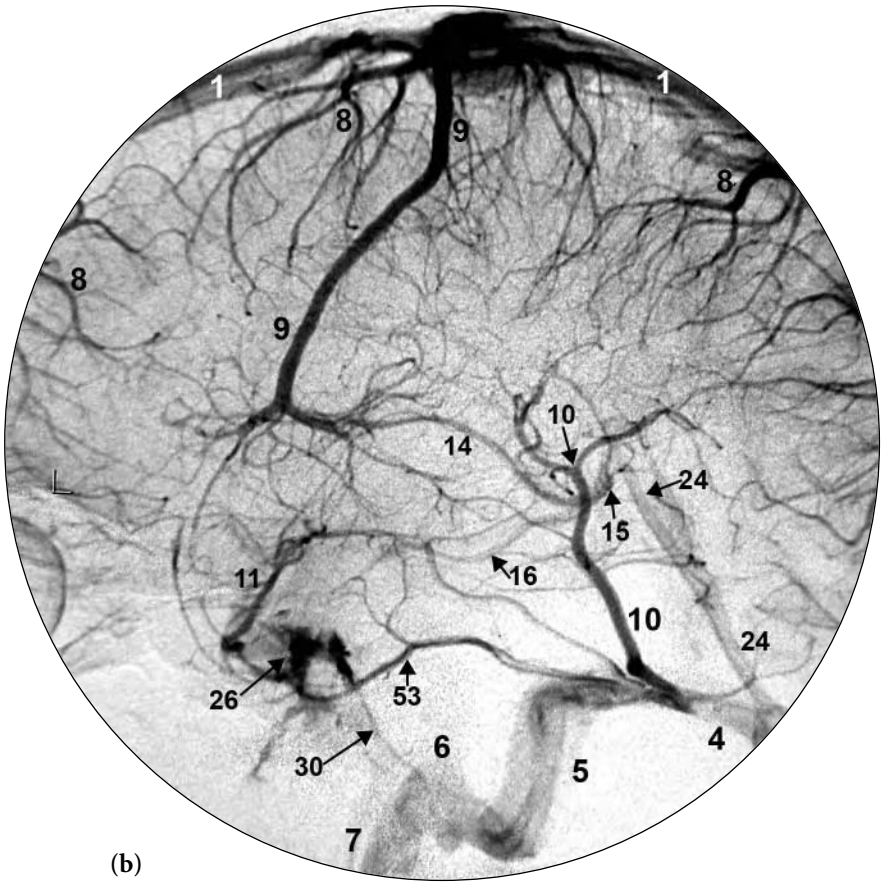
1
1
8
9
8
8
9
10
14
24
15
16
11
10
24
26
53
30
6
5
4
7

(**b**)

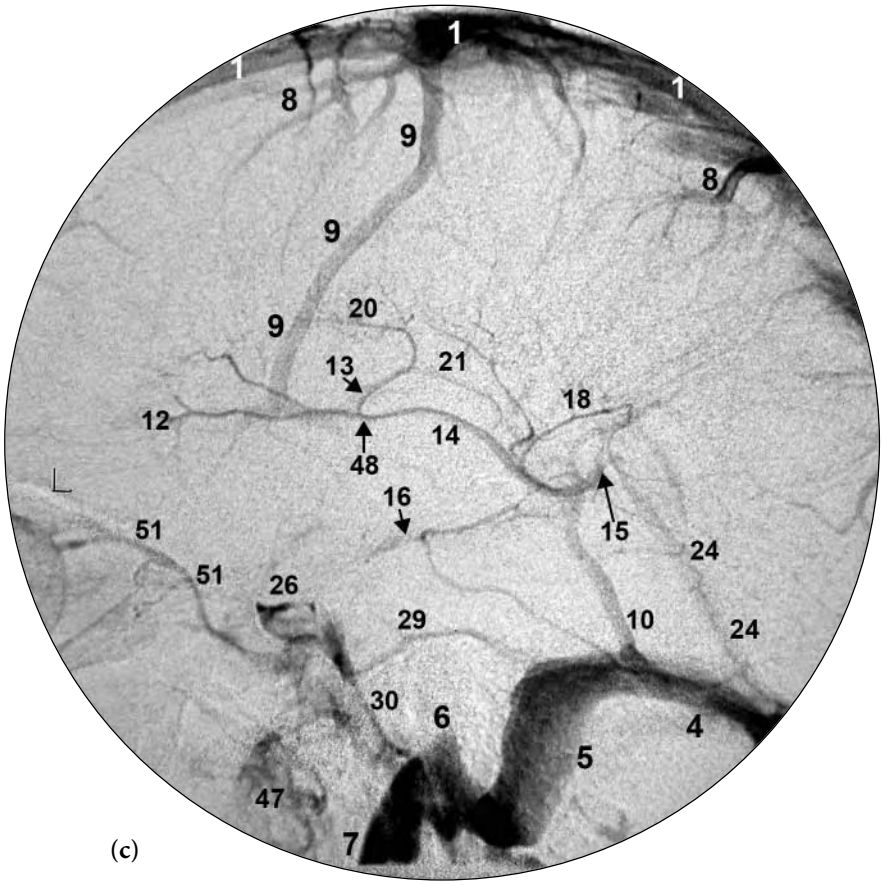
1
1
8
1
9
8
9
20
9
13
21
18
12
14
48
16
15
51
24
51
26
29
10
24
30
6
4
5
47
7

(**c**)

Fig. 7.5 (continued)

FIGURE KEY

1 superior sagittal sinus
2 inferior sagittal sinus
3 torcular herophili
4 transverse sinus
5 sigmoid sinus
6 jugular bulb
7 internal jugular vein
8 superficial cortical vein
9 vein of Trolard
10 vein of Labbé
11 superficial middle cerebral vein
12 septal vein
13 thalamostriate vein
14 internal cerebral vein
15 great cerebral vein of Galen
16 basal vein of Rosenthal
17 inferior ventricular vein
18 medial atrial vein
20 anterior caudate vein
21 terminal vein
22 direct lateral vein
24 straight sinus
25 sphenoparietal sinus
26 cavernous sinus
28 clival venous plexus
29 superior petrosal sinus
30 inferior petrosal sinus
46 suboccipital veins
47 pterygoid venous plexus
48 true venous angle
51 superior ophthalmic vein
53 sphenopetrosal vein
55 false venous angle

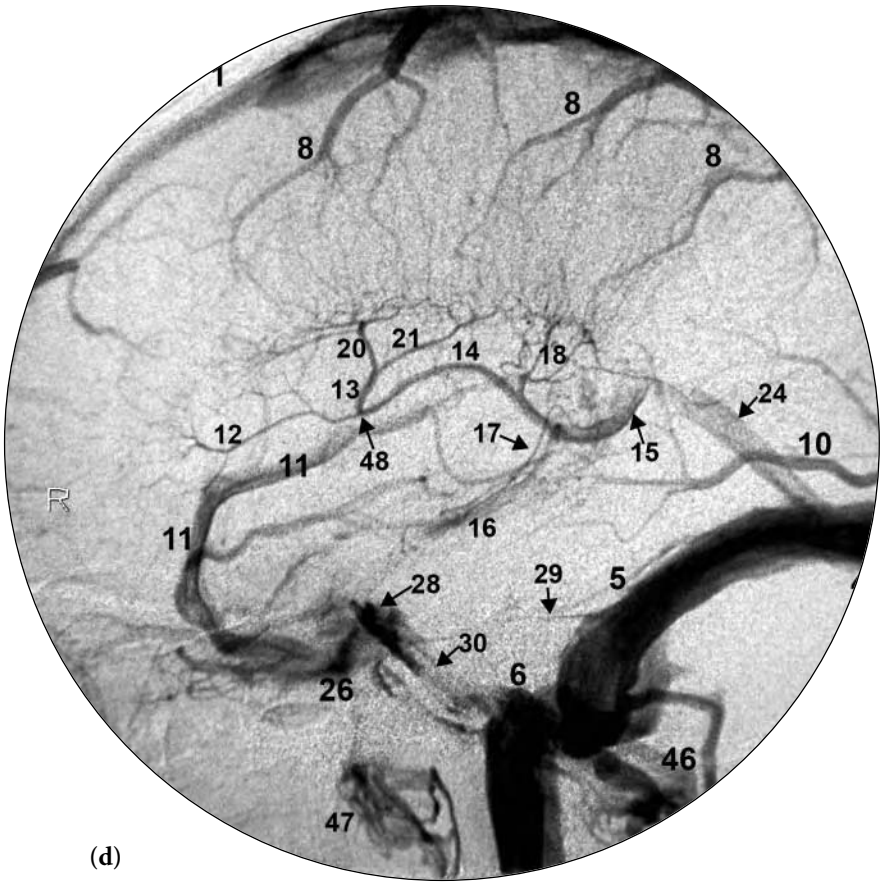

(d)

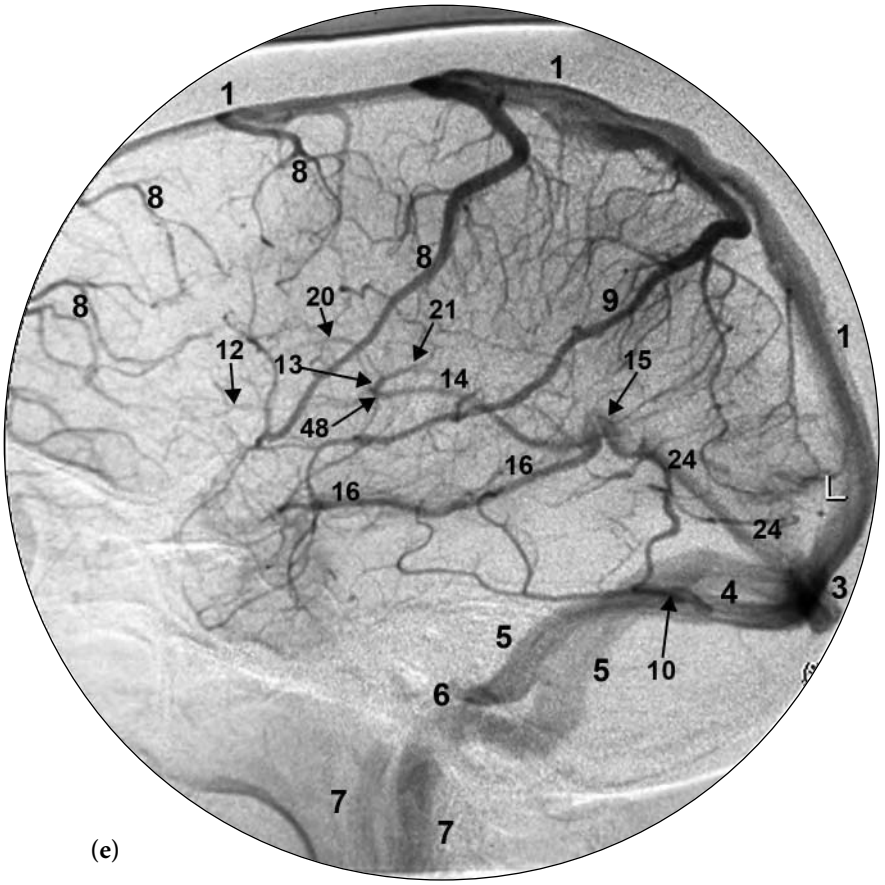

(e)

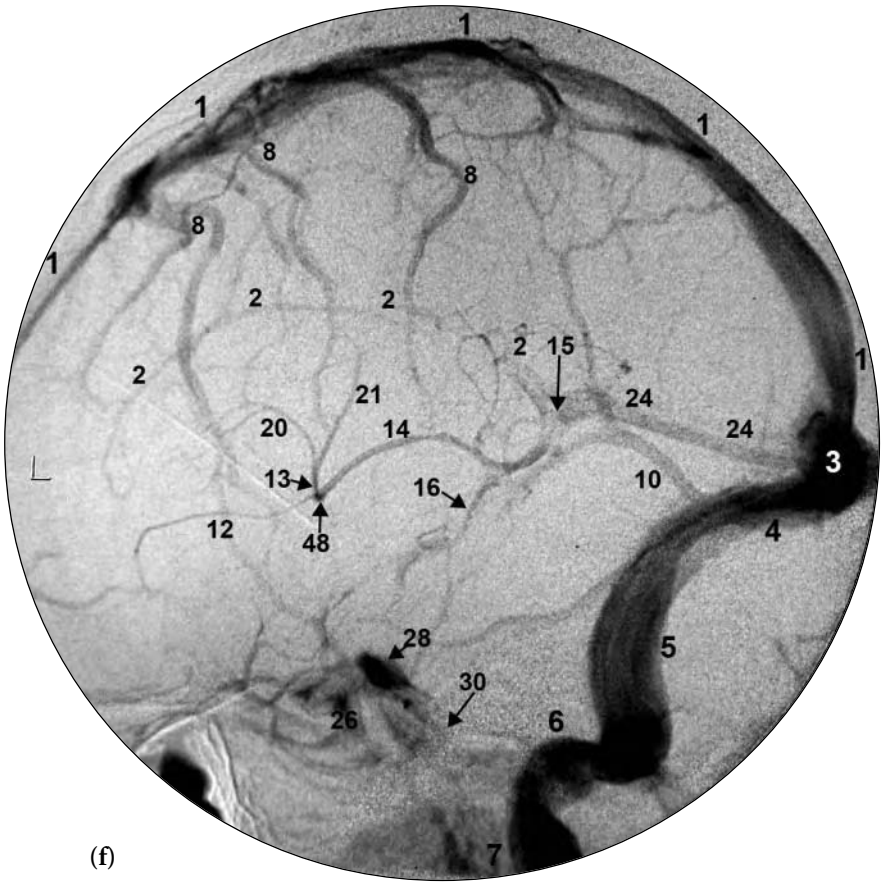

(f)

Fig. 7.5 (continued)

FIGURE KEY

1 superior sagittal sinus
2 inferior sagittal sinus
3 torcular herophili
4 transverse sinus
5 sigmoid sinus
6 jugular bulb
7 internal jugular vein
8 superficial cortical vein
9 vein of Trolard
10 vein of Labbé
11 superficial middle cerebral vein
12 septal vein
13 thalamostriate vein
14 internal cerebral vein
15 great cerebral vein of Galen
16 basal vein of Rosenthal
17 inferior ventricular vein
18 medial atrial vein
20 anterior caudate vein
21 terminal vein
22 direct lateral vein
24 straight sinus
25 sphenoparietal sinus
26 cavernous sinus
28 clival venous plexus
29 superior petrosal sinus
30 inferior petrosal sinus
46 suboccipital veins
47 pterygoid venous plexus
48 true venous angle
51 superior ophthalmic vein
53 sphenopetrosal vein
55 false venous angle

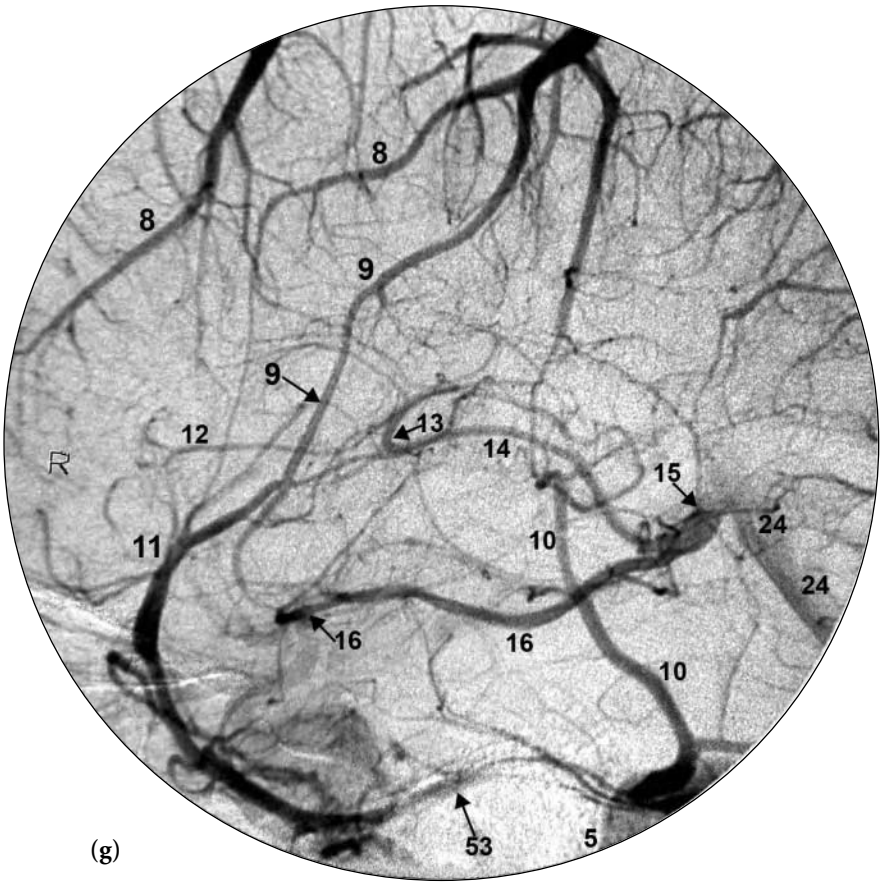

(**g**)

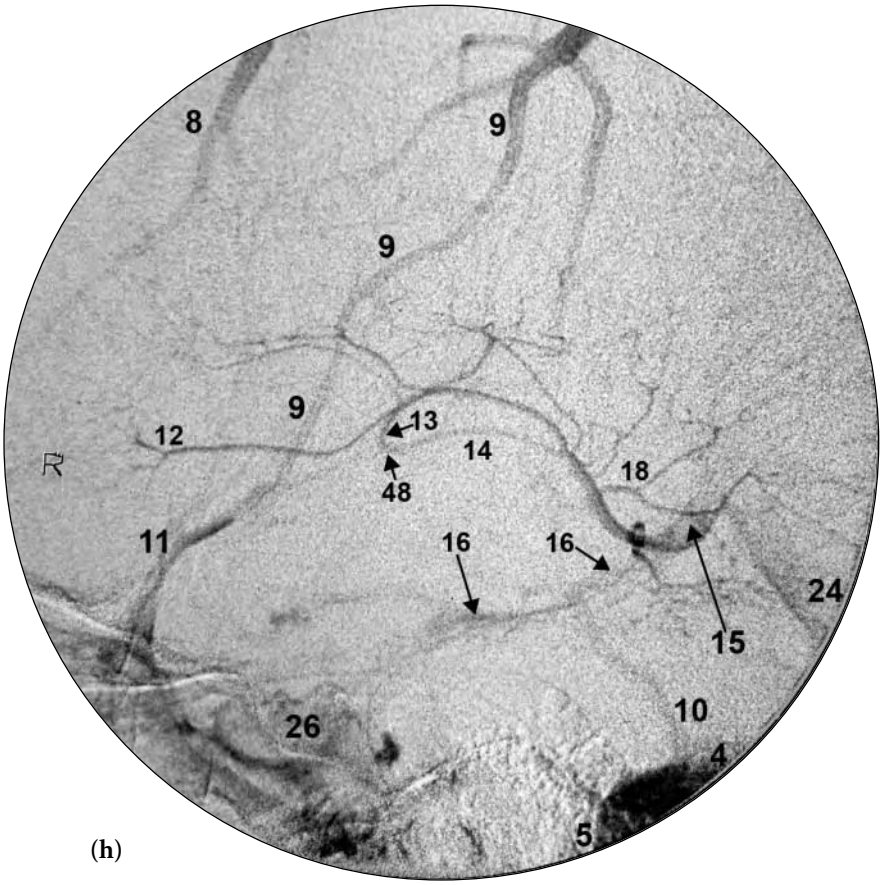

(**h**)

(i)

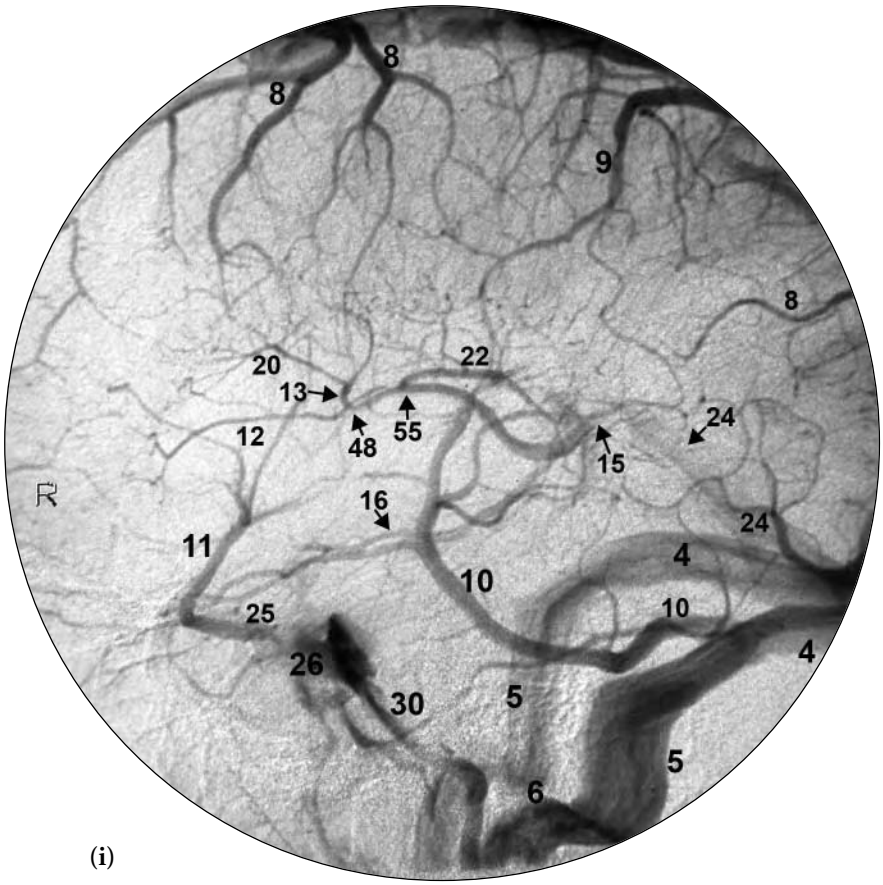

(i)

Fig. 7.5 (continued)

FIGURE KEY

1 superior sagittal sinus
2 inferior sagittal sinus
3 torcular herophili
4 transverse sinus
5 sigmoid sinus
6 jugular bulb
7 internal jugular vein
8 superficial cortical vein
9 vein of Trolard
10 vein of Labbé
11 superficial middle cerebral vein
12 septal vein
13 thalamostriate vein
14 internal cerebral vein
15 great cerebral vein of Galen
16 basal vein of Rosenthal
17 inferior ventricular vein
18 medial atrial vein
20 anterior caudate vein
21 terminal vein
22 direct lateral vein
24 straight sinus
25 sphenoparietal sinus
26 cavernous sinus
28 clival venous plexus
29 superior petrosal sinus
30 inferior petrosal sinus
46 suboccipital veins
47 pterygoid venous plexus
48 true venous angle
51 superior ophthalmic vein
53 sphenopetrosal vein
55 false venous angle

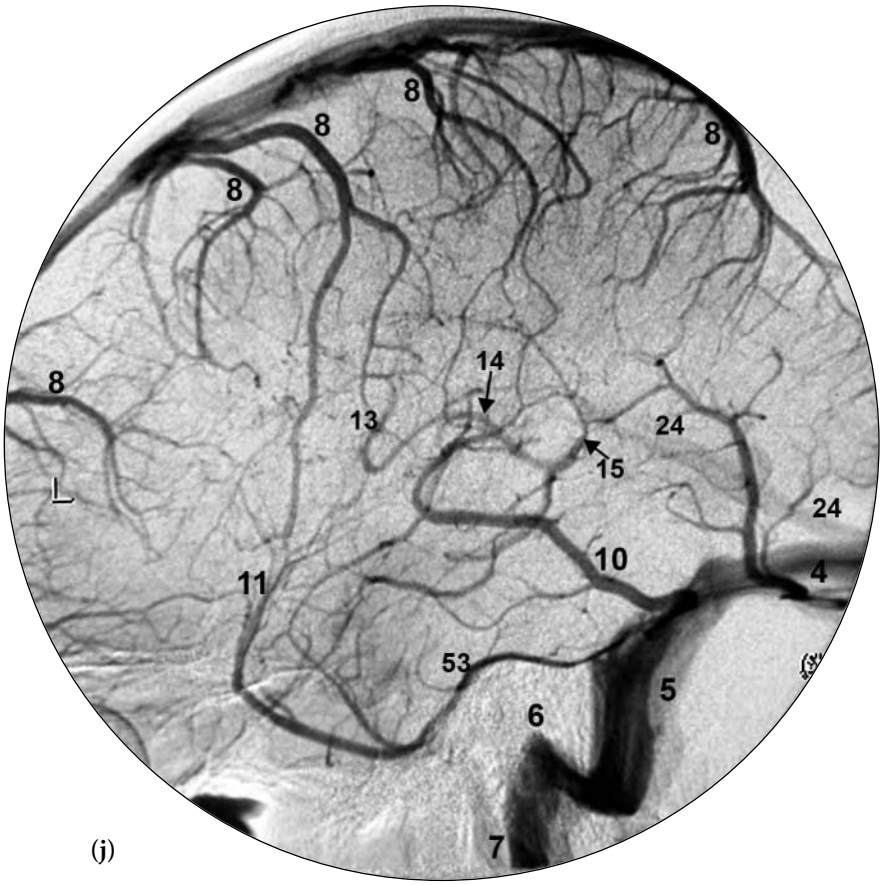

(j)

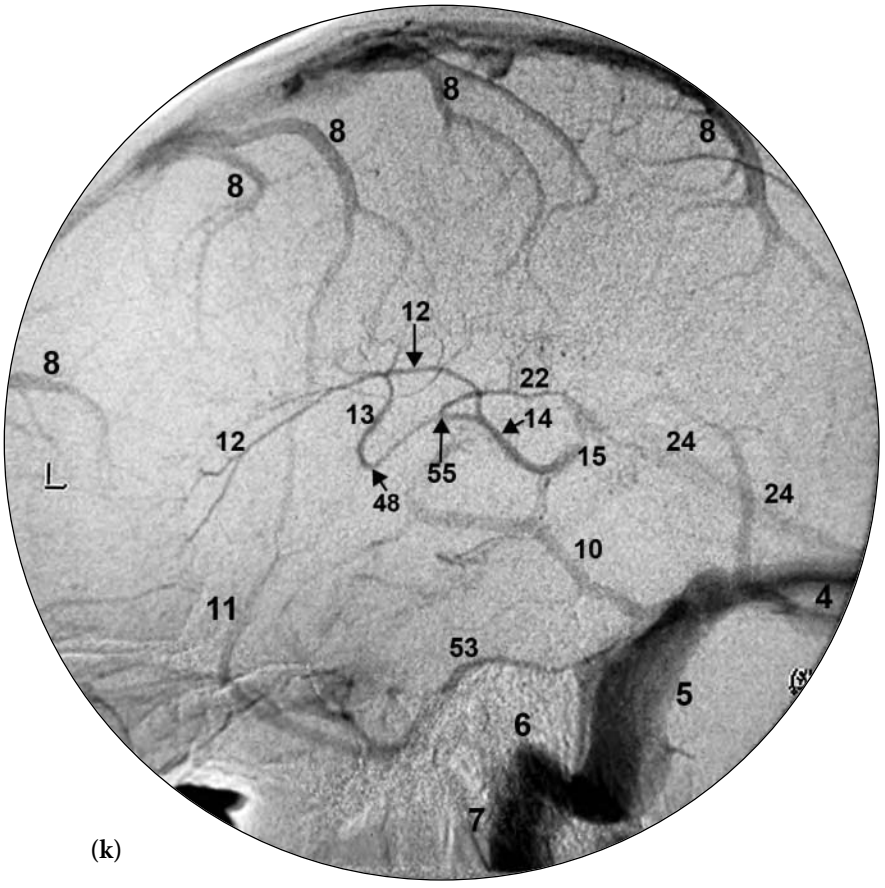

(k)

(l,m)

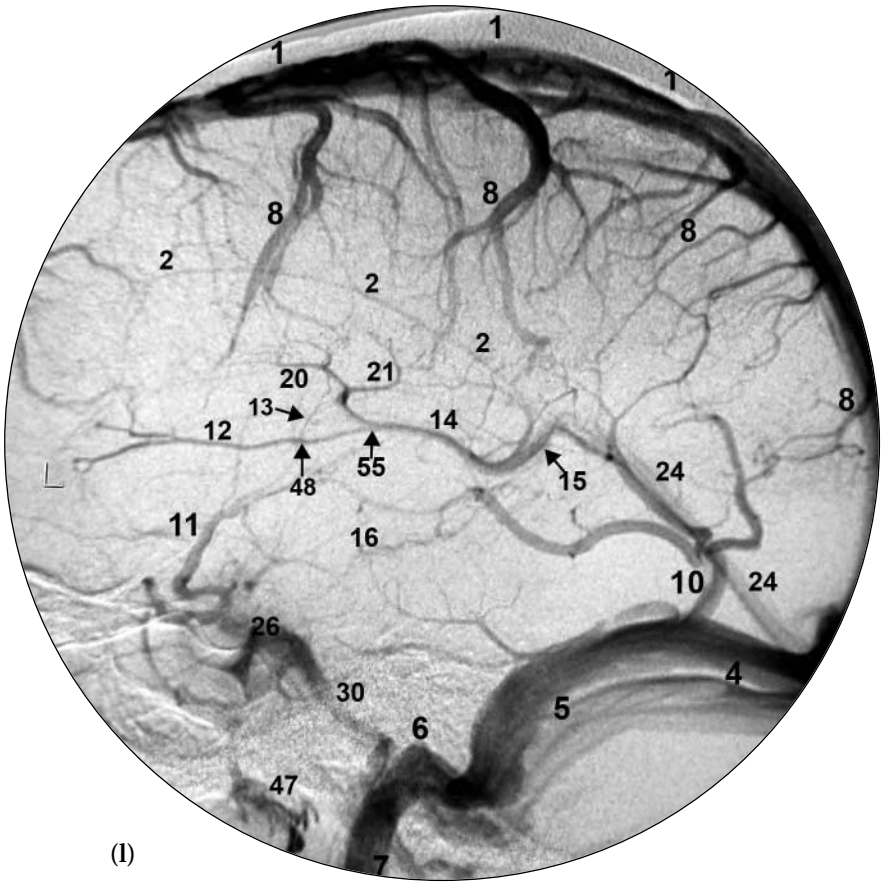
1
1
1
8
8
8
2
2
2
20
21
13
12
14
55
48
15
24
8
11
16
10
24
26
4
30
5
6
47
7

(l)

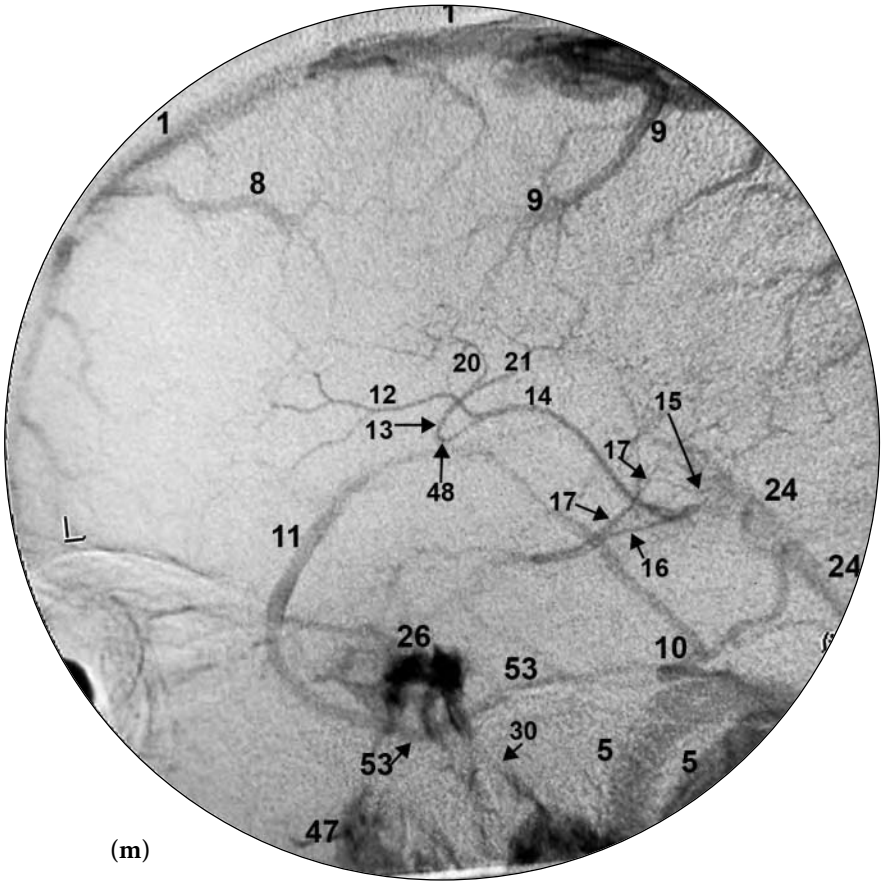
1
1
9
8
9
20
21
12
14
15
13
17
48
24
17
11
16
24
26
10
53
30
5
5
53
47

(m)

Fig. 7.5 (continued)

FIGURE KEY

1 superior sagittal sinus
2 inferior sagittal sinus
3 torcular herophili
4 transverse sinus
5 sigmoid sinus
6 jugular bulb
7 internal jugular vein
8 superficial cortical vein
9 vein of Trolard
10 vein of Labbé
11 superficial middle cerebral vein
12 septal vein
13 thalamostriate vein
14 internal cerebral vein
15 great cerebral vein of Galen
16 basal vein of Rosenthal
17 inferior ventricular vein
18 medial atrial vein
20 anterior caudate vein
21 terminal vein
22 direct lateral vein
24 straight sinus
25 sphenoparietal sinus
26 cavernous sinus
28 clival venous plexus
29 superior petrosal sinus
30 inferior petrosal sinus
46 suboccipital veins
47 pterygoid venous plexus
48 true venous angle
51 superior ophthalmic vein
53 sphenopetrosal vein
55 false venous angle

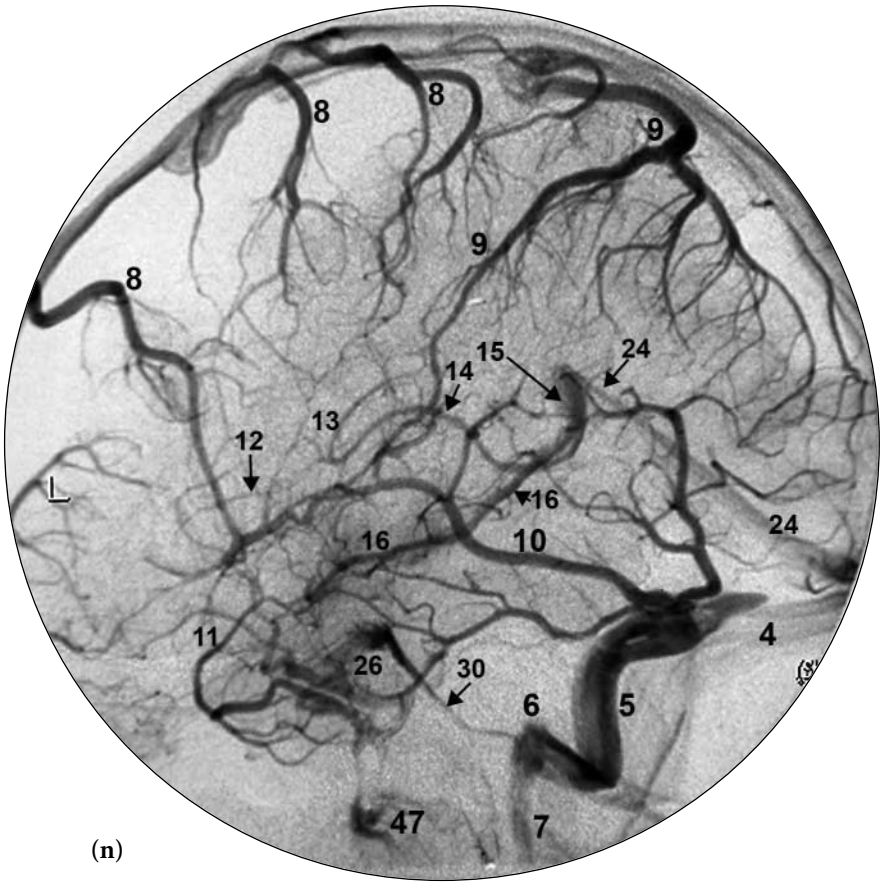

(**n**)

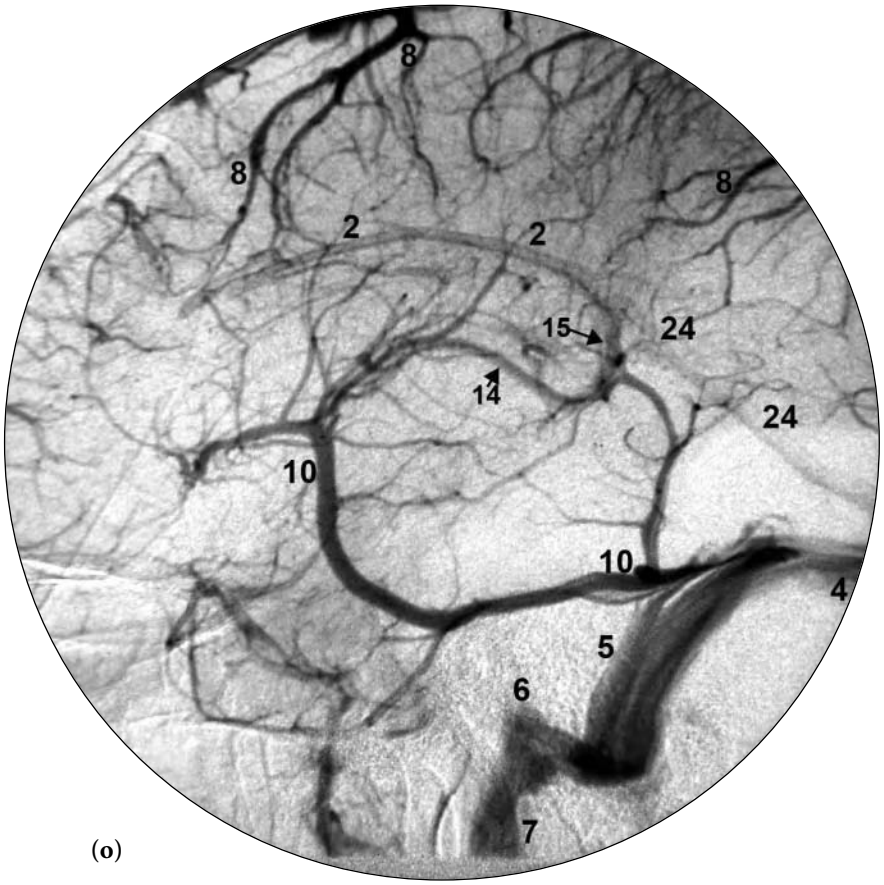

(**o**)

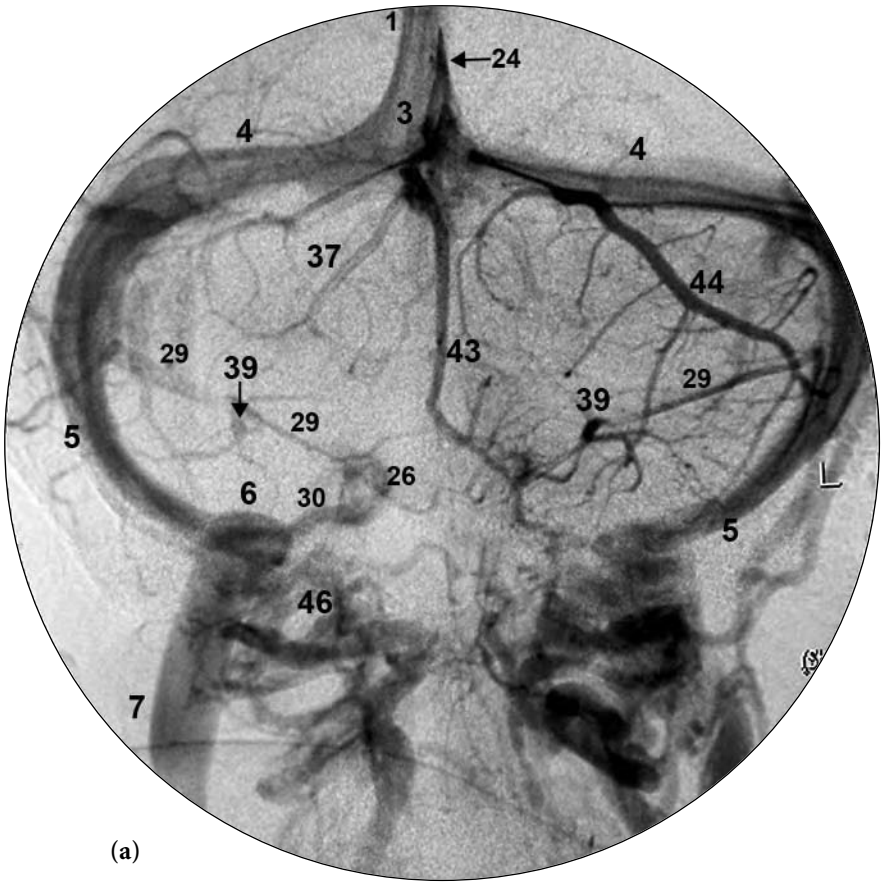

(a)

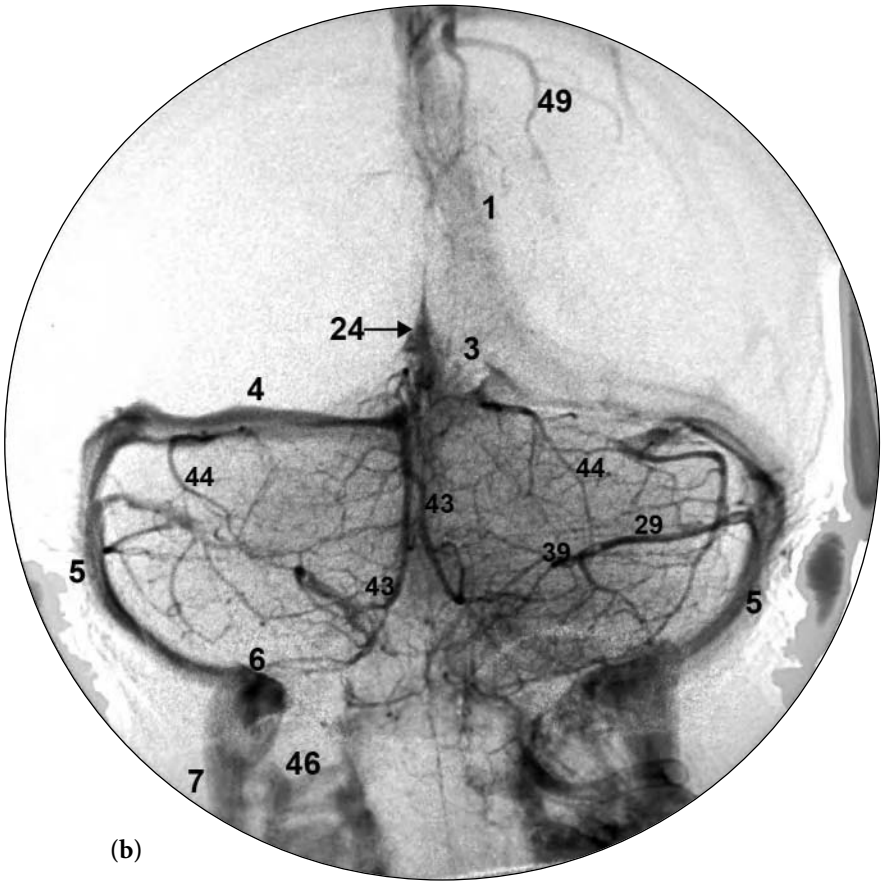

(b)

Fig. 7.6 (a-f) 2D frontal views of the venous phase of circulation following vertebral artery injections in multiple patients. This series of images shows the marked variability of the venous anatomy in the posterior fossa. This normal variability is complicated secondary to the large number of venous structures in a small compartment (the posterior fossa).

FIGURE KEY

1 superior sagittal sinus
3 torcular herophili
4 transverse sinus
5 sigmoid sinus
6 jugular bulb
7 internal jugular vein
26 cavernous sinus
27 intercavernous sinus
29 superior petrosal sinus
30 inferior petrosal sinus
35 anterior pontomesencephalic vein
37 posterior mesencephalic vein
39 petrosal vein
41 precentral cerebellar vein
43 inferior vermian vein
44 cerebellar hemispheric vein
45 brachial vein
46 suboccipital veins
49 parietal veins
50 occipital veins

Fig. 7.6 (continued)

FIGURE KEY

1 superior sagittal sinus
3 torcular herophili
4 transverse sinus
5 sigmoid sinus
6 jugular bulb
7 internal jugular vein
26 cavernous sinus
27 intercavernous sinus
29 superior petrosal sinus
30 inferior petrosal sinus
35 anterior pontomesencephalic vein
37 posterior mesencephalic vein
39 petrosal vein
41 precentral cerebellar vein
43 inferior vermian vein
44 cerebellar hemispheric vein
45 brachial vein
46 suboccipital veins
49 parietal veins
50 occipital veins

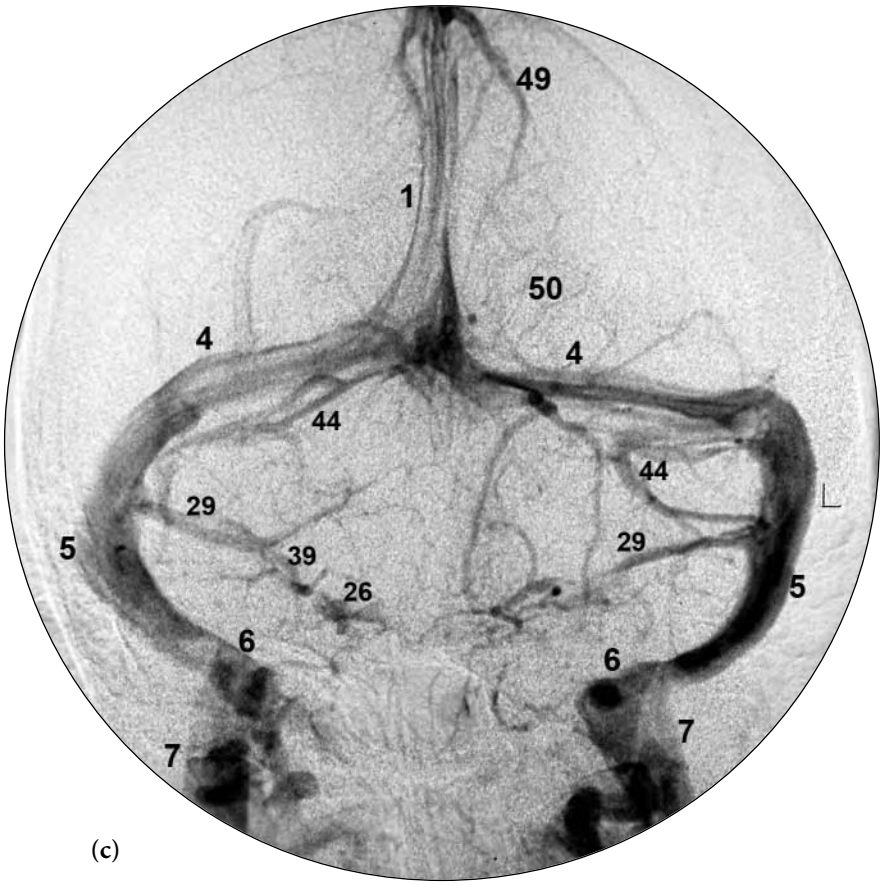

(**c**)

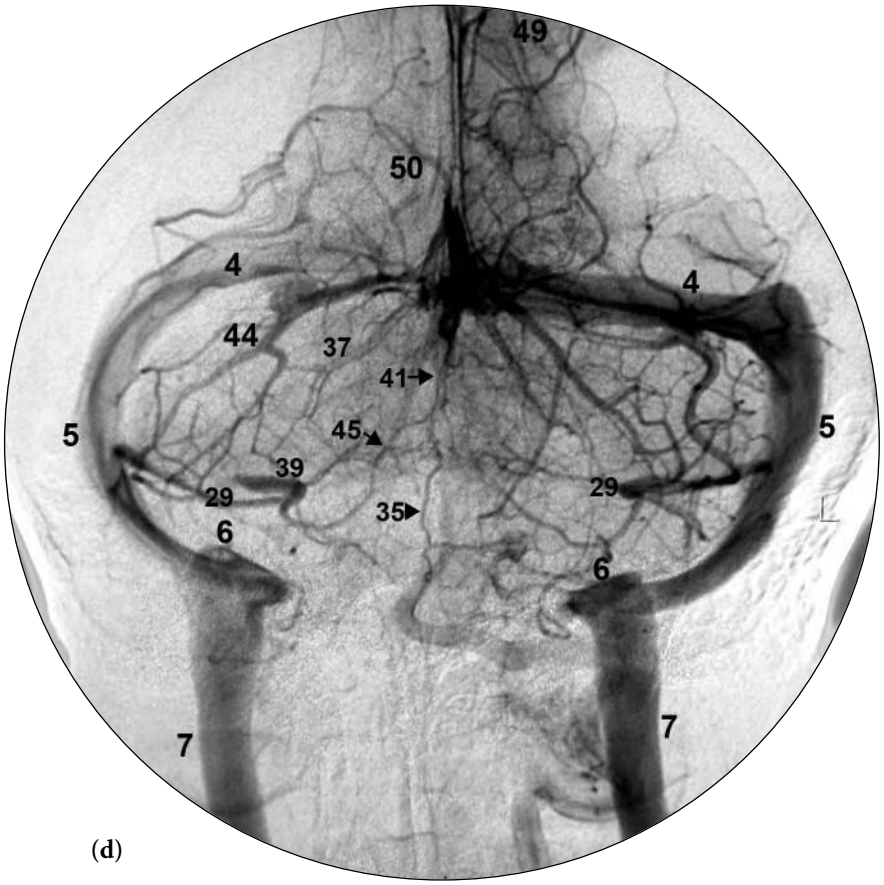

(**d**)

(e,f)

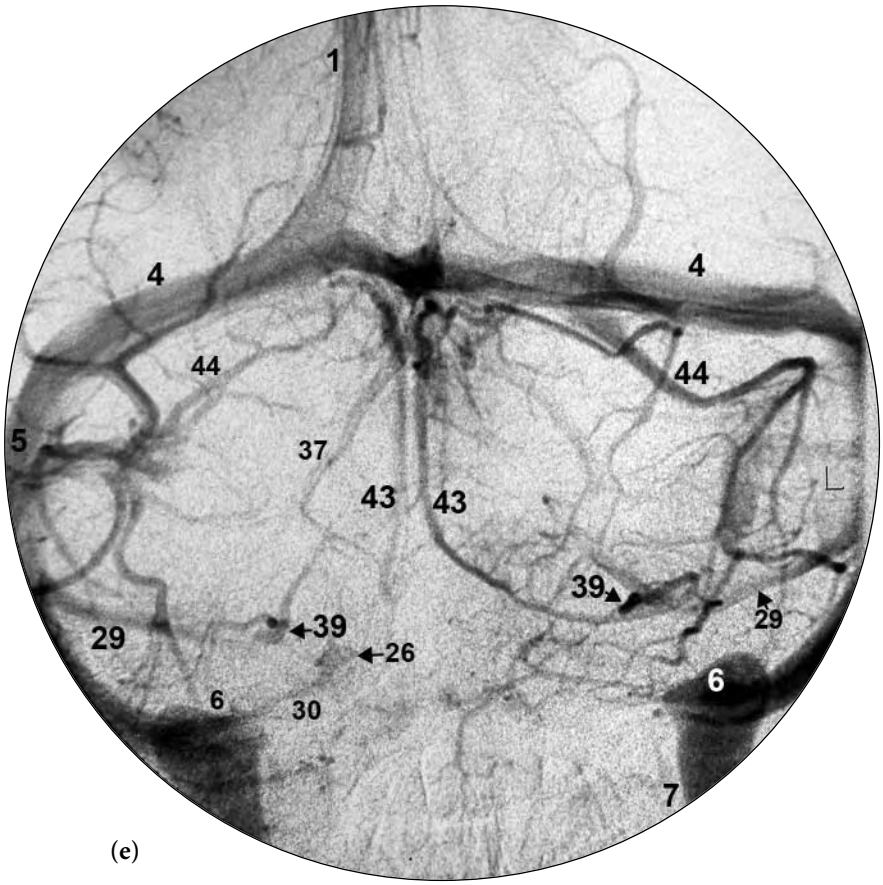
1
4
4
44
44
5
37
43
43
39
29
39
29
26
6
6
30
7

(e)

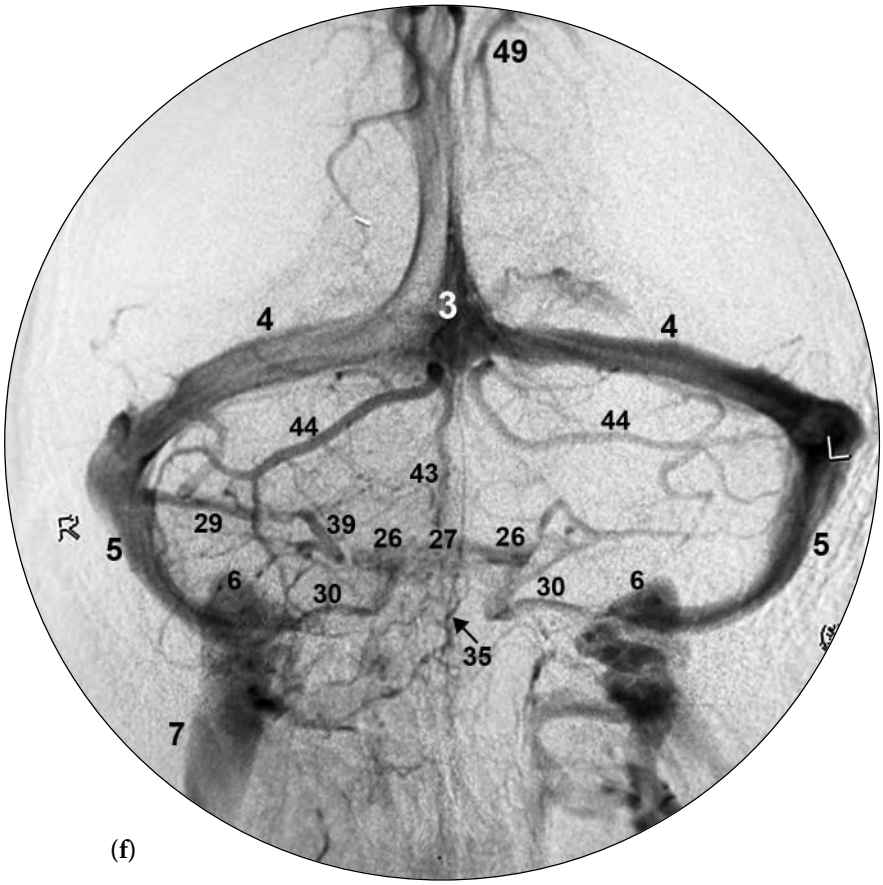
49
4
3
4
44
44
43
29
39
26
27
26
5
5
6
30
30
6
35
7

(f)

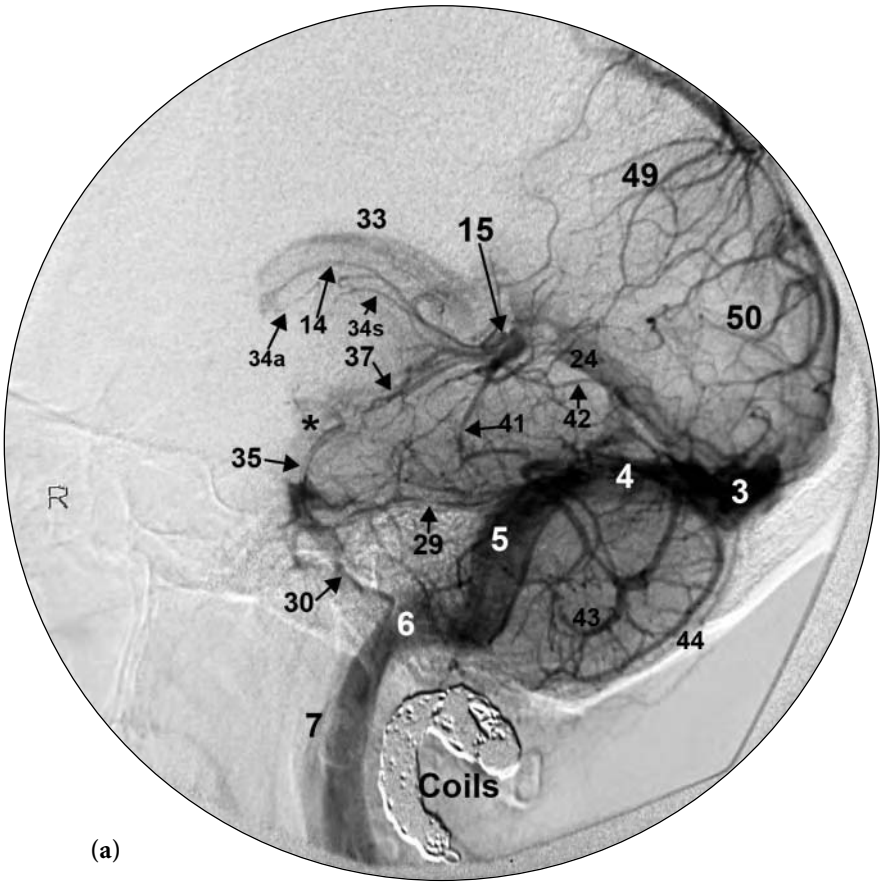

(**a**)

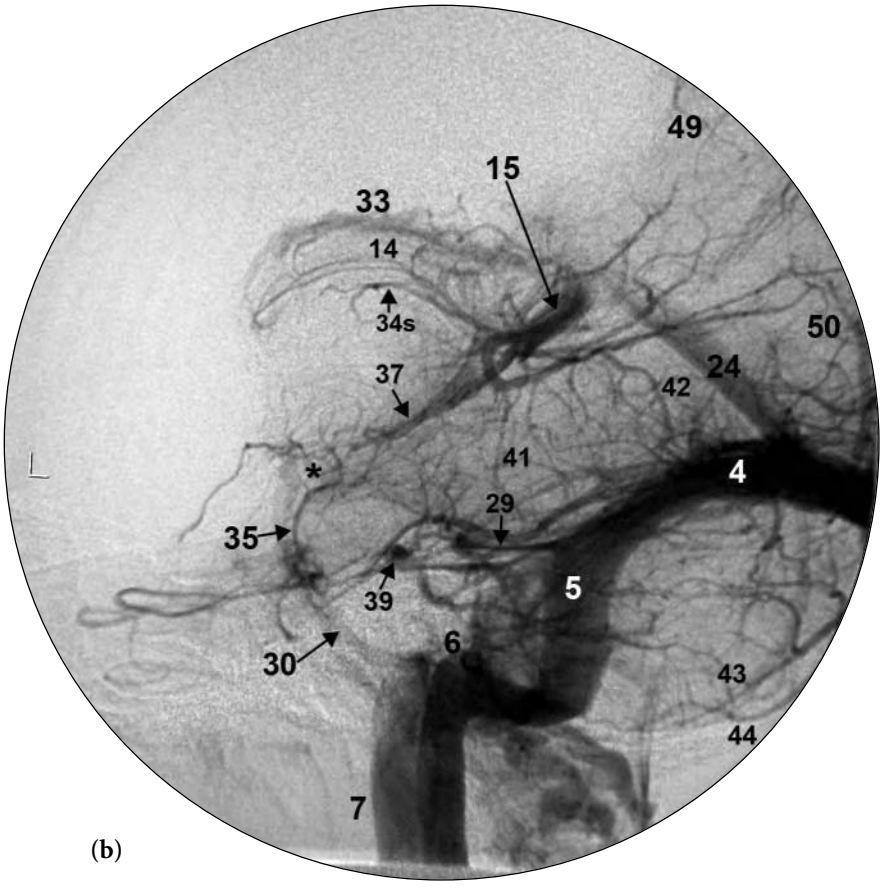

(**b**)

Fig. 7.7 (a–d) 2D lateral views of the venous phase of circulation following vertebral artery injections in multiple patients. Note the outline of the anterior surface of the brainstem by the anterior pontomesencephalic vein. The interpeduncular cistern (*) is visible anteriorly (to your left) to the upper aspect of the anterior pontomesencephalic vein. In view *a* the coils were placed in order to close a large vertebral artery-venous fistula. This postembolization angiogram shows the complete obliteration of the fistula.

FIGURE KEY

3 torcular herophili
4 transverse sinus
5 sigmoid sinus
6 jugular bulb
7 internal jugular vein
10 vein of Labbé
14 internal cerebral vein
15 great cerebral vein of Galen
16 basal vein of Rosenthal
24 straight sinus
26 cavernous sinus
29 superior petrosal sinus
30 inferior petrosal sinus
33 superior choroid vein
34s superior thalamic vein
34a anterior thalamic vein
35 anterior pontomesencephalic vein
37 posterior mesencephalic vein
39 petrosal vein
40 lateral mesencephalic vein
41 precentral cerebellar vein
42 superior vermian vein
43 inferior vermian vein
44 cerebellar hemispheric vein
49 parietal veins
50 occipital veins
* interpeduncular cistern

(c,d)

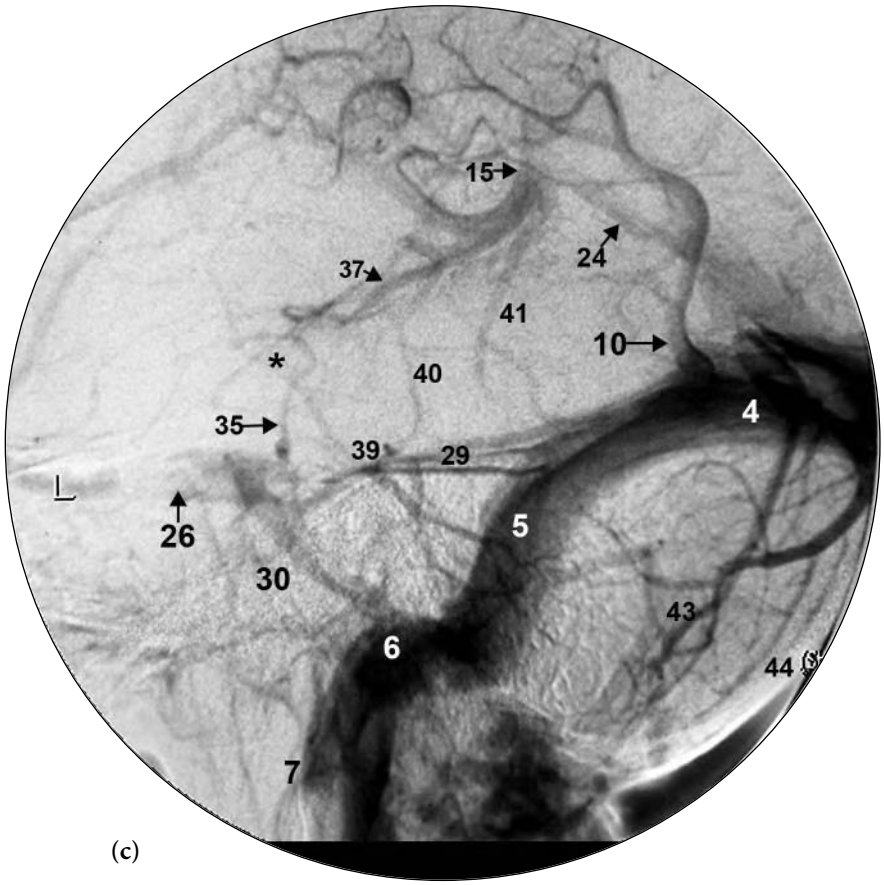
15
24
37
41
10
*
40
4
35
39
29
L
26
5
30
43
6
44
7

(c)

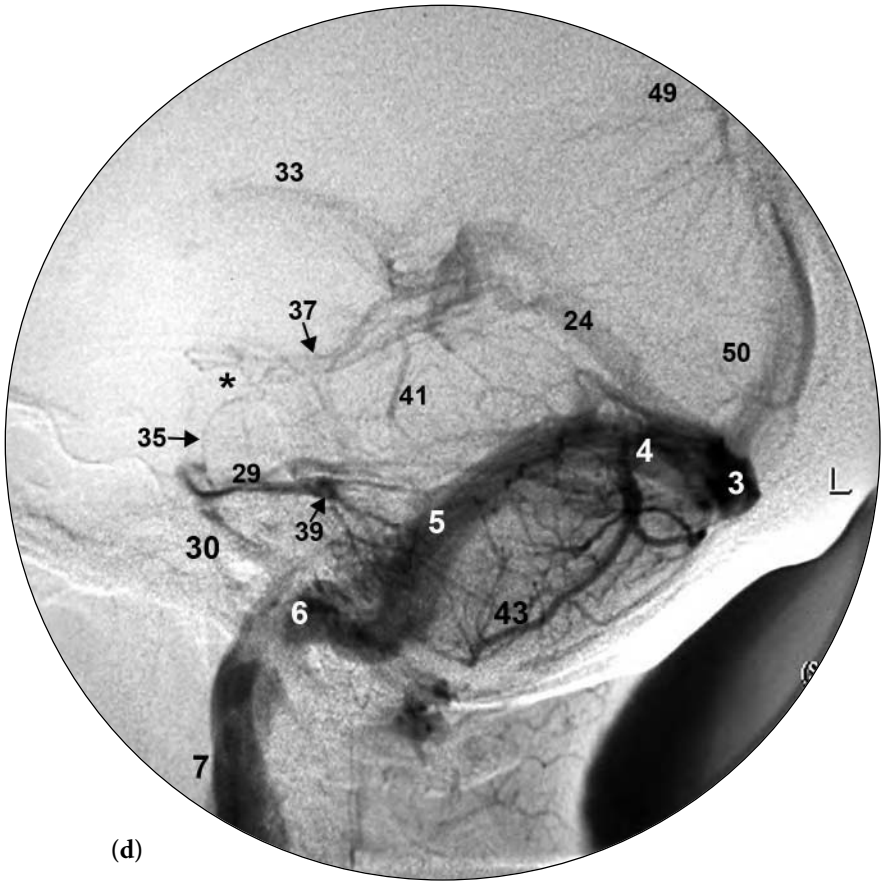
49
33
37
24
50
*
41
35
4
29
3
L
39
5
30
6
43
7

(d)

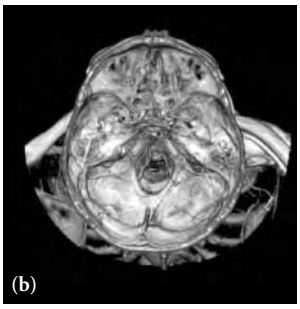

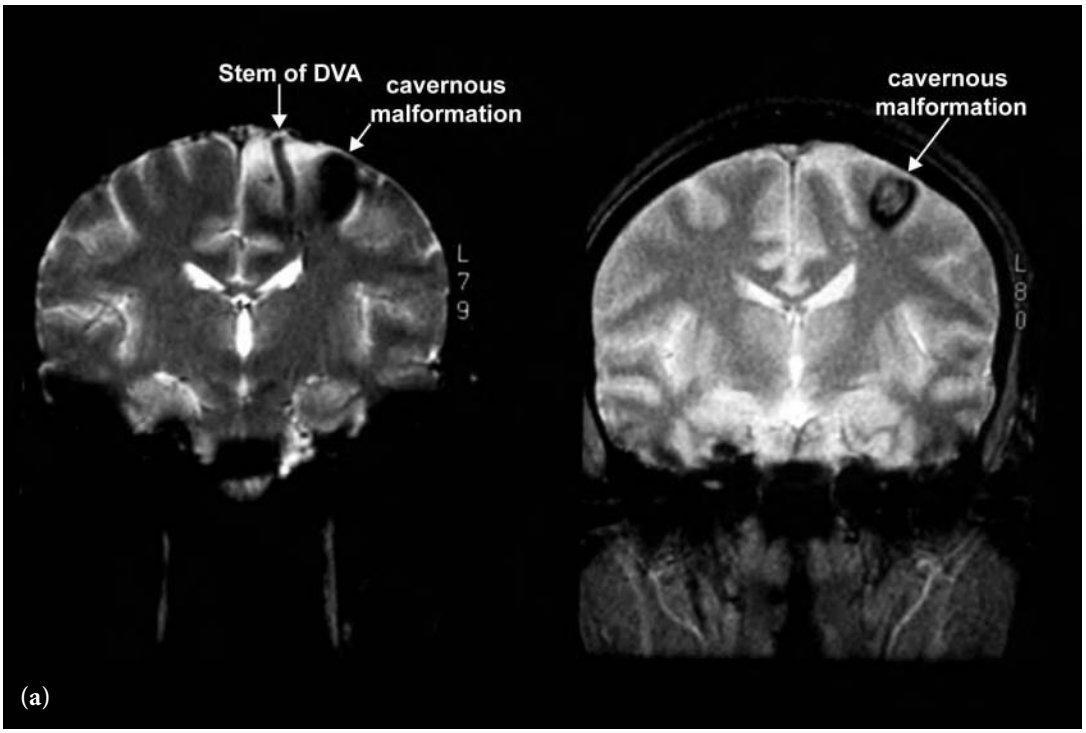

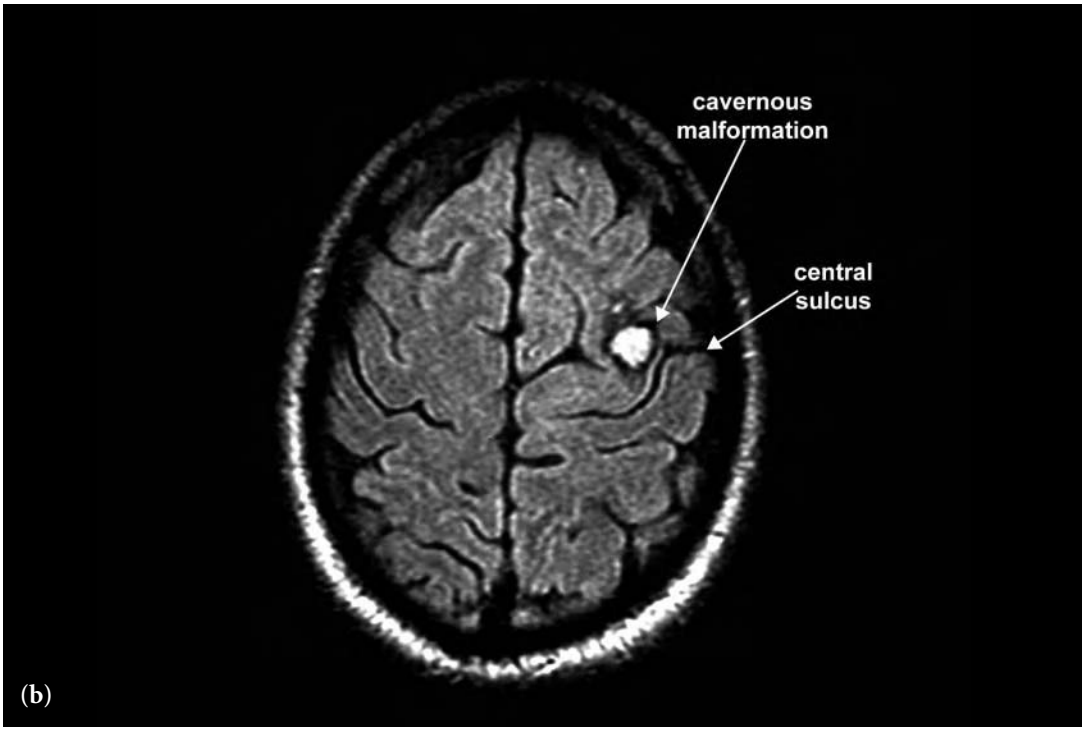

Fig. 7.8 (a,b) Coronal gradient echo T2-weighted MRI images of the brain (*a*) show a region of previous hemorrhage with an appearance consistent with a cavernous malformation. The image on your left shows the stem of a large developmental venous anomaly (DVA) that is in close proximity to the cavernous malformation. An axial FLAIR (fluid attenuated inversion recovery) sequence shows the cavernous malformation in the region of the left precentral gyrus (motor strip) (*b*). This patient presented with right-sided focal motor seizures.

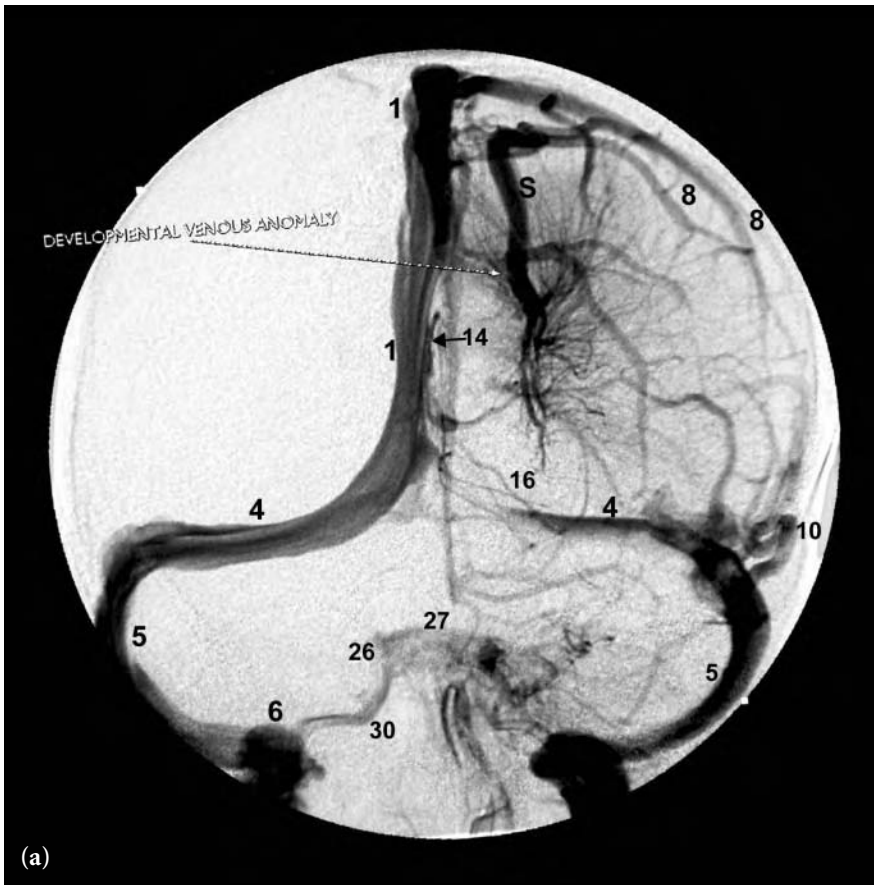

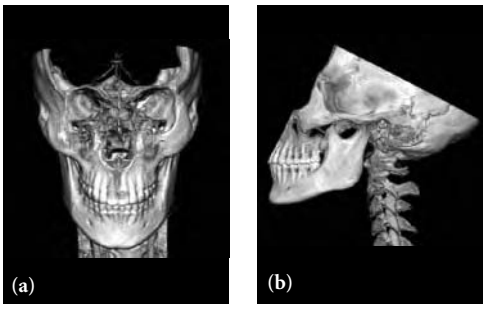

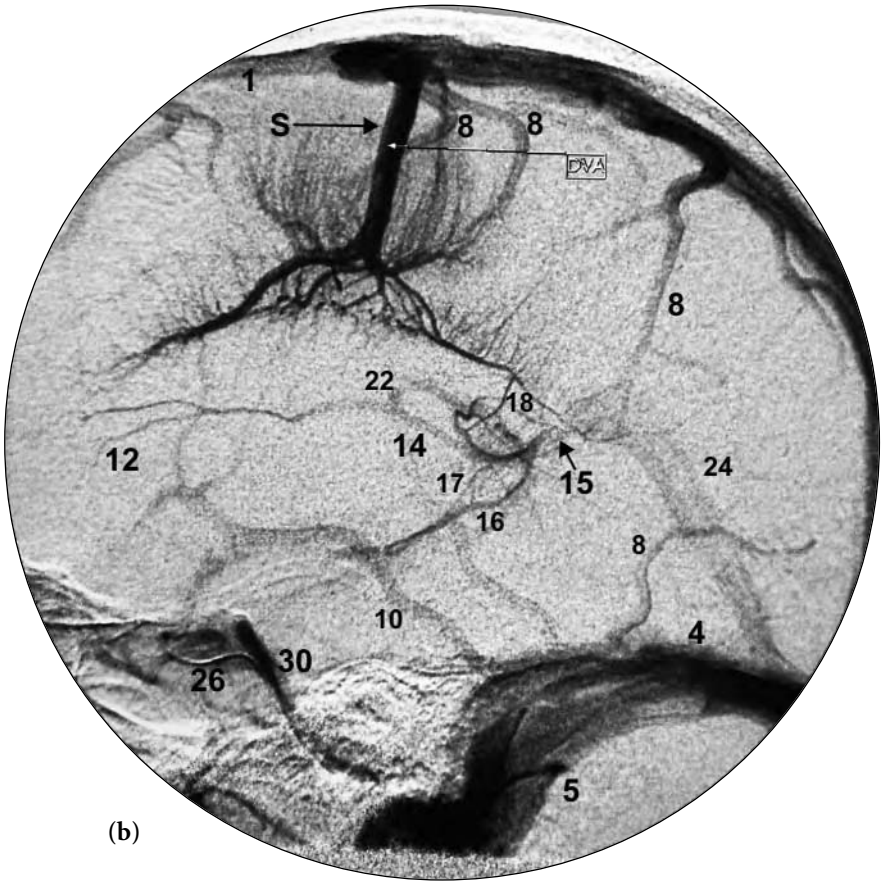

Fig. 7.9 (a,b) 2D frontal (*a*) and lateral (*b*) venous phase circulation images following left carotid artery injection. There is a very large developmental venous anomaly (DVA) draining superiorly via a large stem (S) into the superior sagittal sinus. This is the same patient that appears in Figures 7.8 *a* and *b*.

FIGURE KEY

1 superior sagittal sinus
4 transverse sinus
5 sigmoid sinus
6 jugular bulb
7 internal jugular vein
8 superficial cortical vein
10 vein of Labbé
12 septal vein
14 internal cerebral vein
15 great cerebral vein of Galen
16 basal vein of Rosenthal
17 inferior ventricular vein
18 medial atrial vein
22 direct lateral vein
26 cavernous sinus
27 intercavernous sinus
30 inferior petrosal sinus

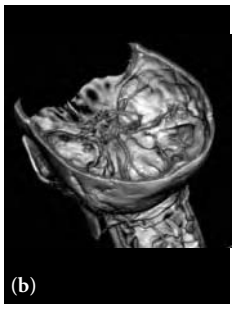

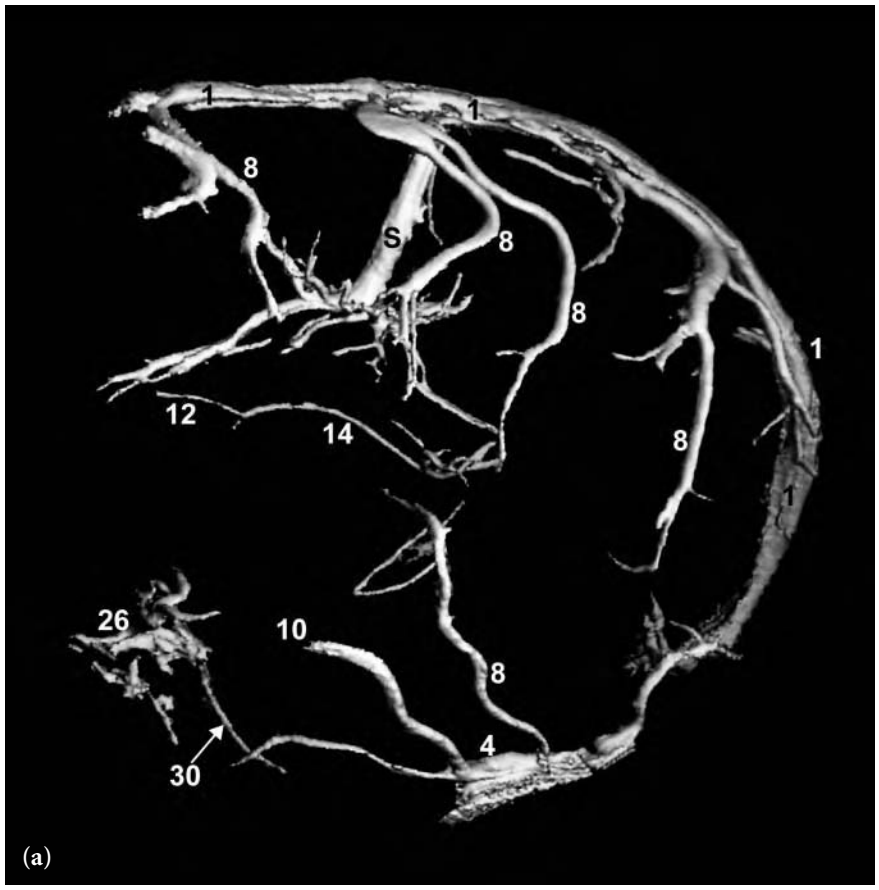

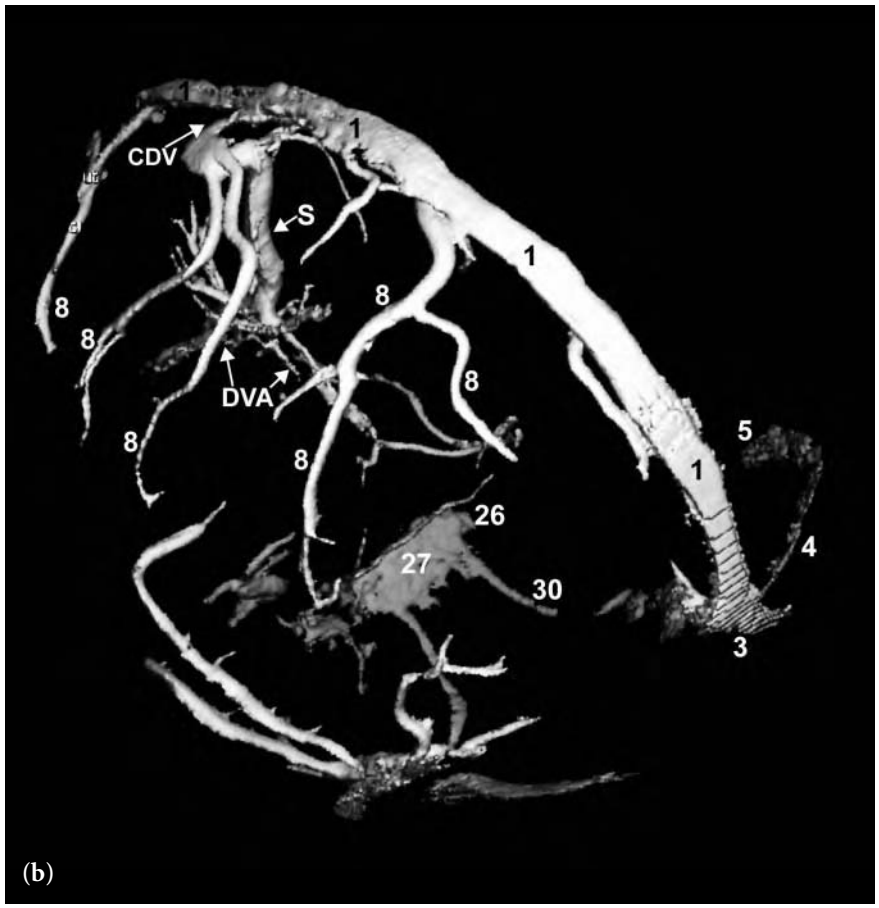

Fig. 7.10 (a–g) 3D left lateral (*a*), left posterior oblique with angulation (*b*), segmented left lateral (*c*), segmented right lateral view with angulation (*d*), and complex angle views (*e-g*) of venous phase circulation following left carotid artery injection. This is the same patient that appears in Figures 7.8 and 7.9. These images confirm the appearance of a large developmental venous anomaly (DVA). The ability to visualize the path of drainage into the superior sagittal sinus with multiple complex angles utilizing the 3D technique helps show the large DVA draining through a vein (CDV). This is also the pathway of venous drainage for two prominent superficial cortical veins. The cavernous malformation adjacent to the DVA may have resulted from venous congestion of the DVA.

FIGURE KEY

1 superior sagittal sinus
3 torcular herophili
4 transverse sinus
5 sigmoid sinus
8 superficial cortical veins
10 vein of Labbé
12 septal vein
14 internal cerebral vein
26 cavernous sinus
27 intercavernous sinus
30 inferior petrosal sinus
CDV common draining vein of DVA and 2 superficial cortical veins
S venous stem of the developmental venous anomaly
DVA developmental venous anomaly

1
1
8
8
8
S
(c)

(c)

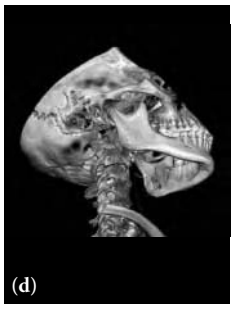
(d)

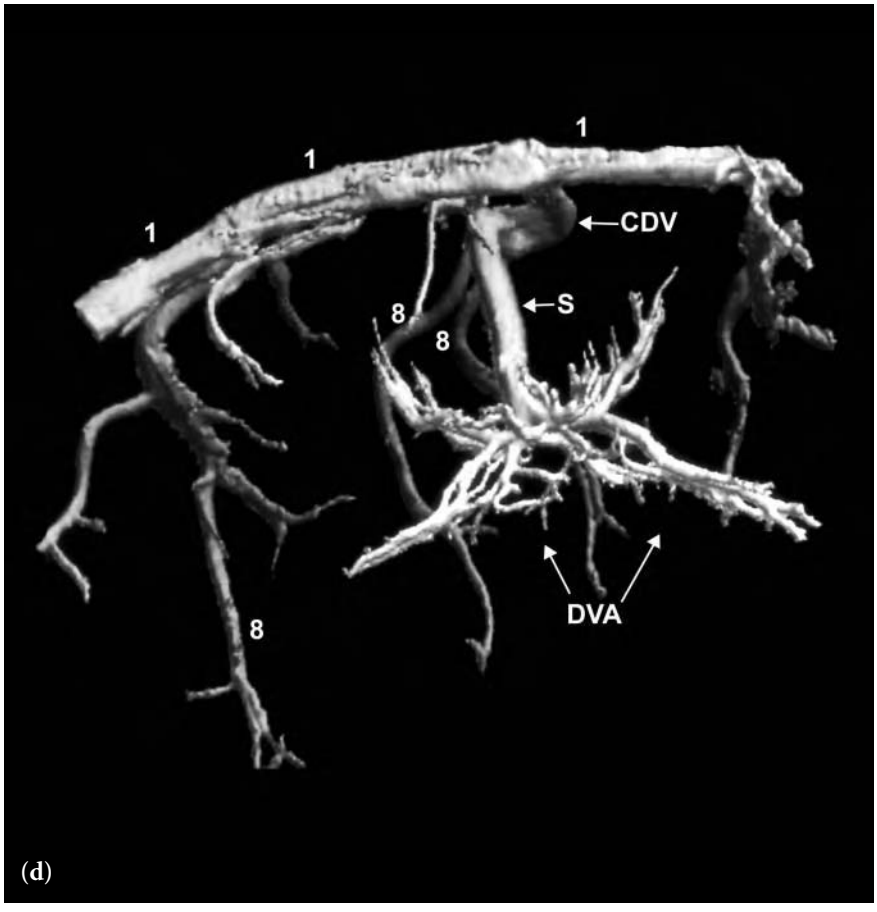
1
1
1
CDV
S
8
8
8
DVA
(d)

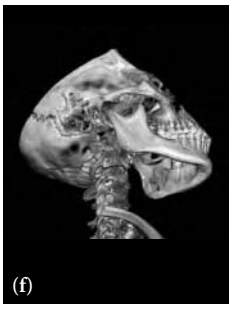

Fig. 7.10 (continued)

FIGURE KEY

1 superior sagittal sinus
3 torcular herophili
4 transverse sinus
5 sigmoid sinus
8 superficial cortical veins
10 vein of Labbé
12 septal vein
14 internal cerebral vein
26 cavernous sinus
27 intercavernous sinus
30 inferior petrosal sinus
CDV common draining vein of DVA and 2 superficial cortical veins
S venous stem of the developmental venous anomaly
DVA developmental venous anomaly

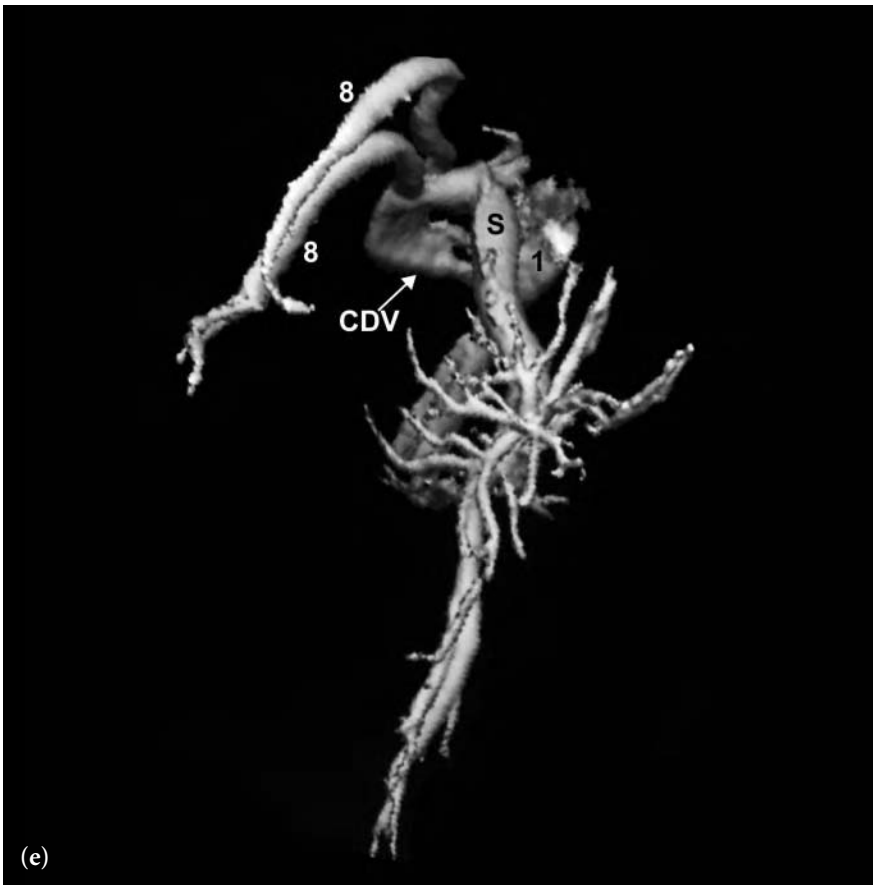

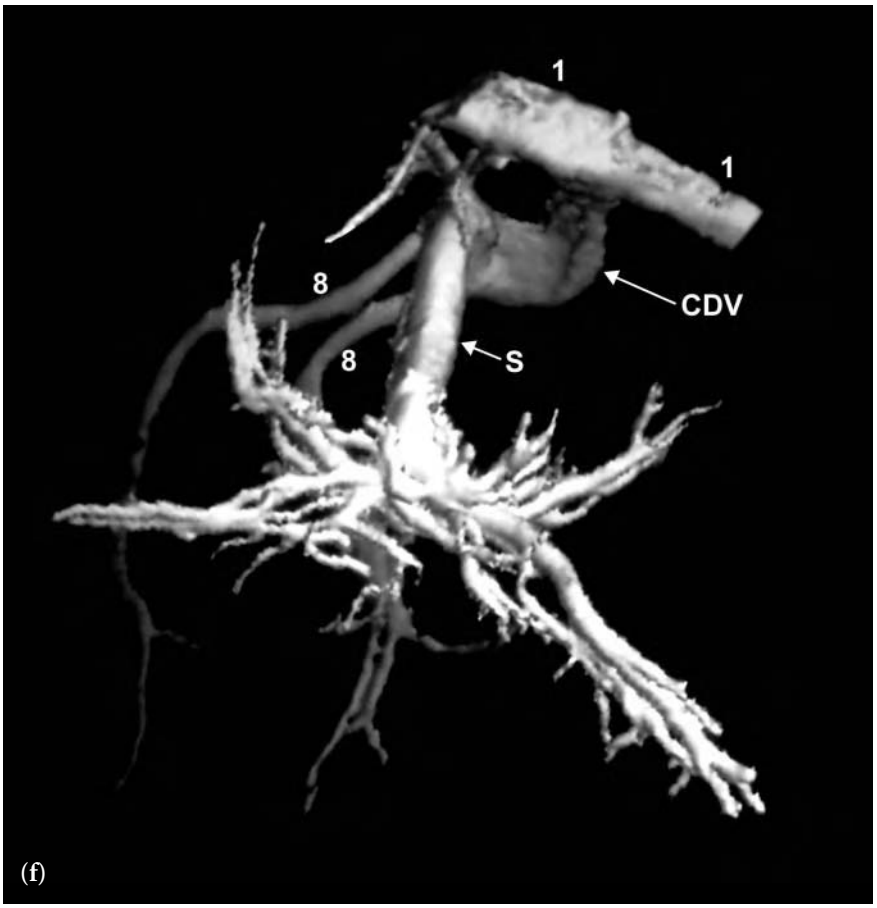

(g)

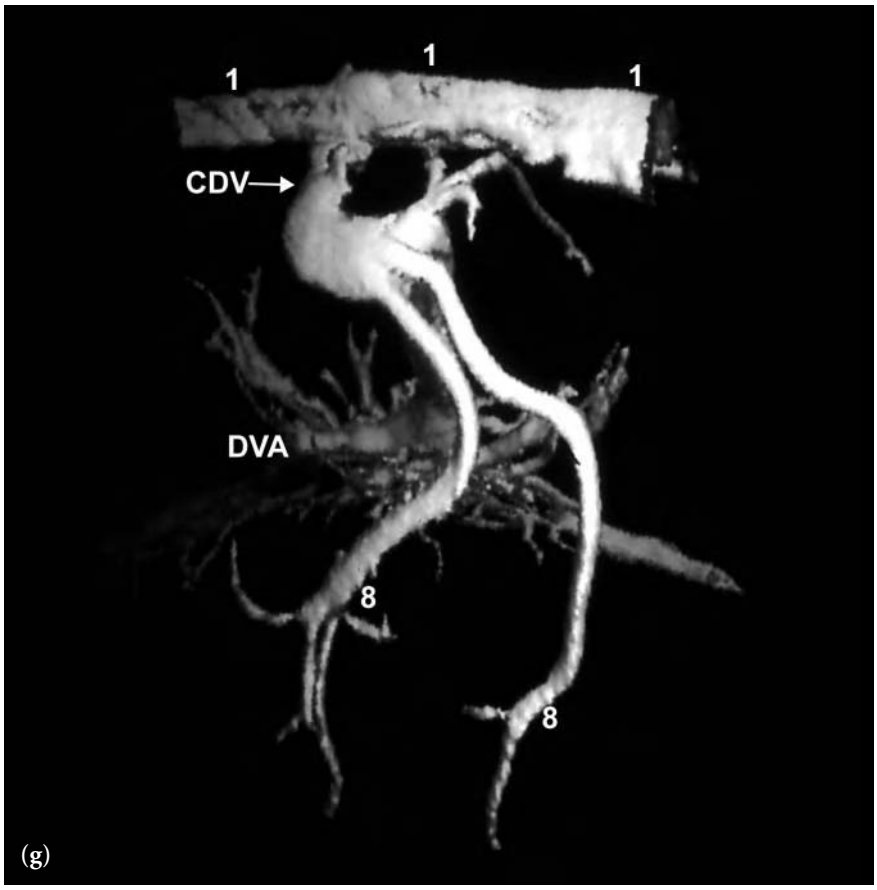
1
1
1
CDV
DVA
8
8
(g)

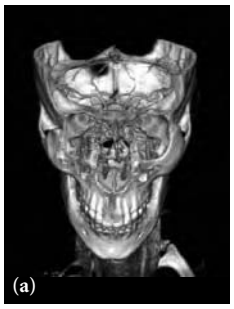

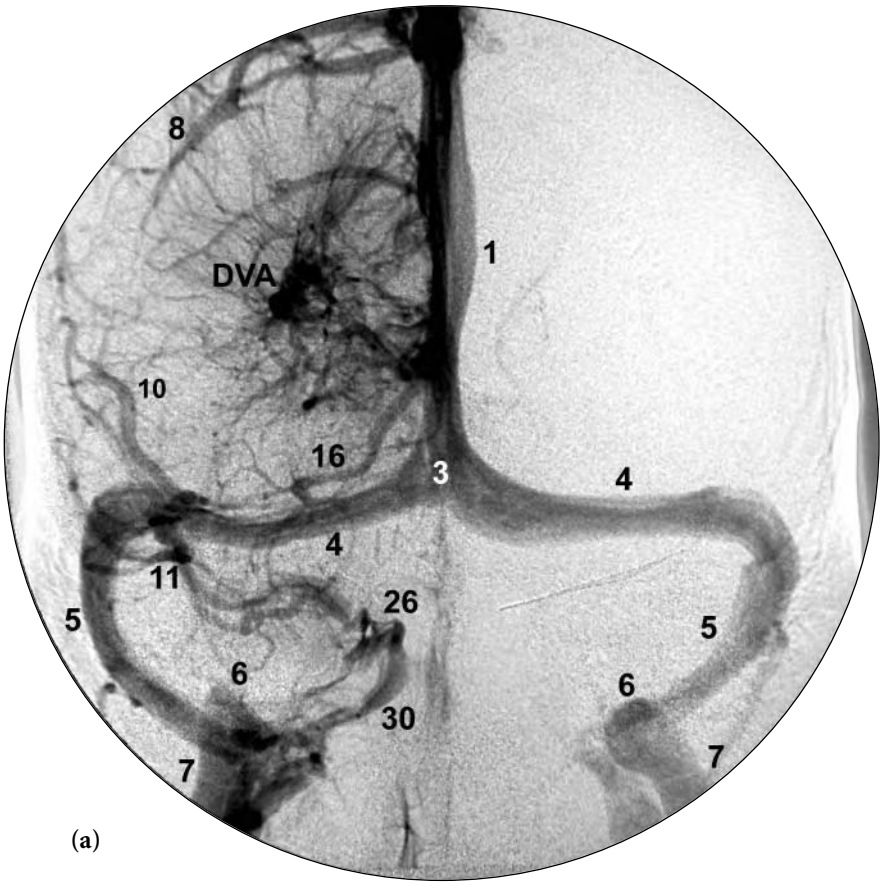

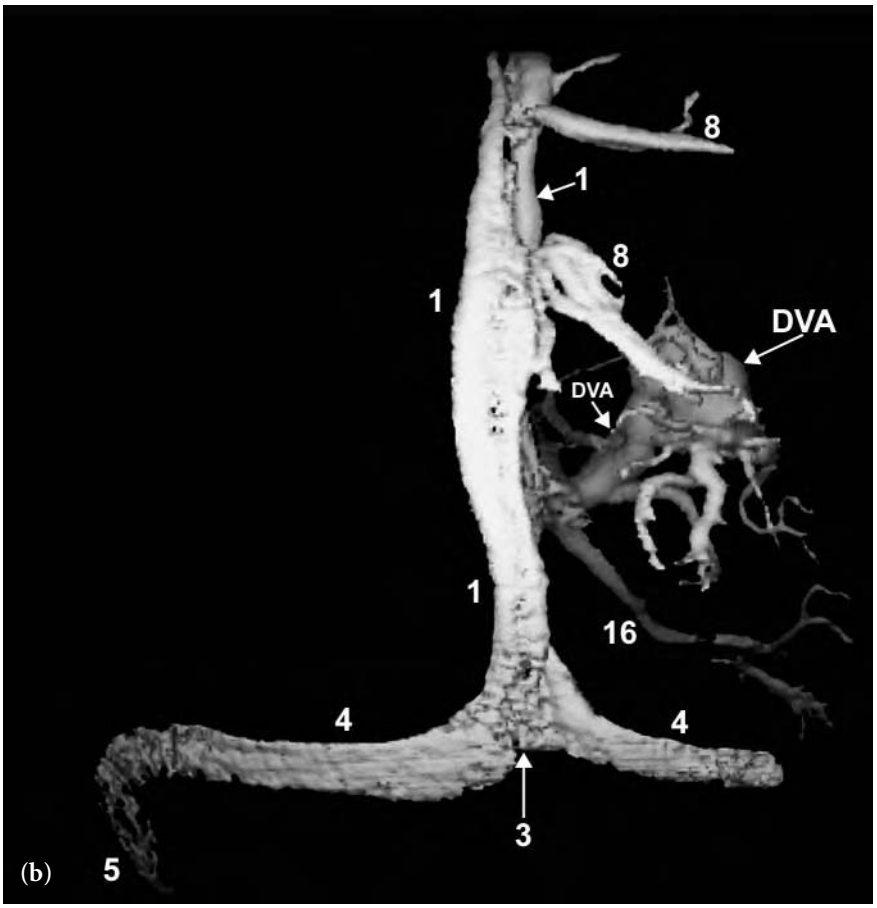

Fig. 7.11 (a–g) 2D frontal view (*a*), 3D posterior (*b*), 2D lateral (*c*), 3D right lateral (*d*), 3D left lateral (*e*), 3D right posterior oblique (*f*), and 3D inferior to superior (*g*) views of the venous phase of circulation following right carotid artery injections. This series of images shows a large developmental venous anomaly involving the medial atrial vein which drains into the great cerebral vein of Galen (15).

FIGURE KEY

1 superior sagittal sinus
3 torcular herophili
4 transverse sinus
5 sigmoid sinus
6 jugular bulb
7 internal jugular vein
8 superficial cortical vein
10 vein of Labbé
11 superficial middle cerebral vein
12 septal vein
13 thalamostriate vein
14 internal cerebral vein
15 great cerebral vein of Galen
16 basal vein of Rosenthal
20 anterior caudate vein
24 straight sinus
26 cavernous sinus
29 superior petrosal sinus
30 inferior petrosal sinus
46 suboccipital veins
47 pterygoid venous plexus
DVA developmental venous anomaly
S venous stem of the draining developmental venous anomaly

(c,d)

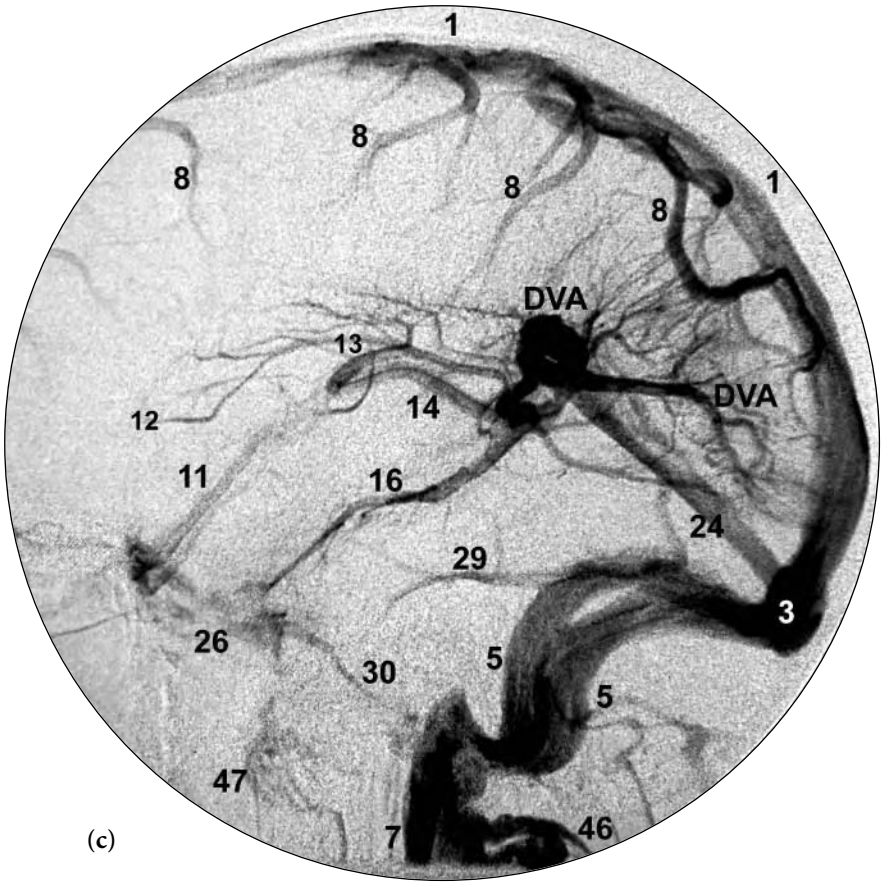
1
8
8
8
8
1
DVA
13
DVA
12
14
11
16
24
29
3
26
30
5
5
47
7
46
(c)

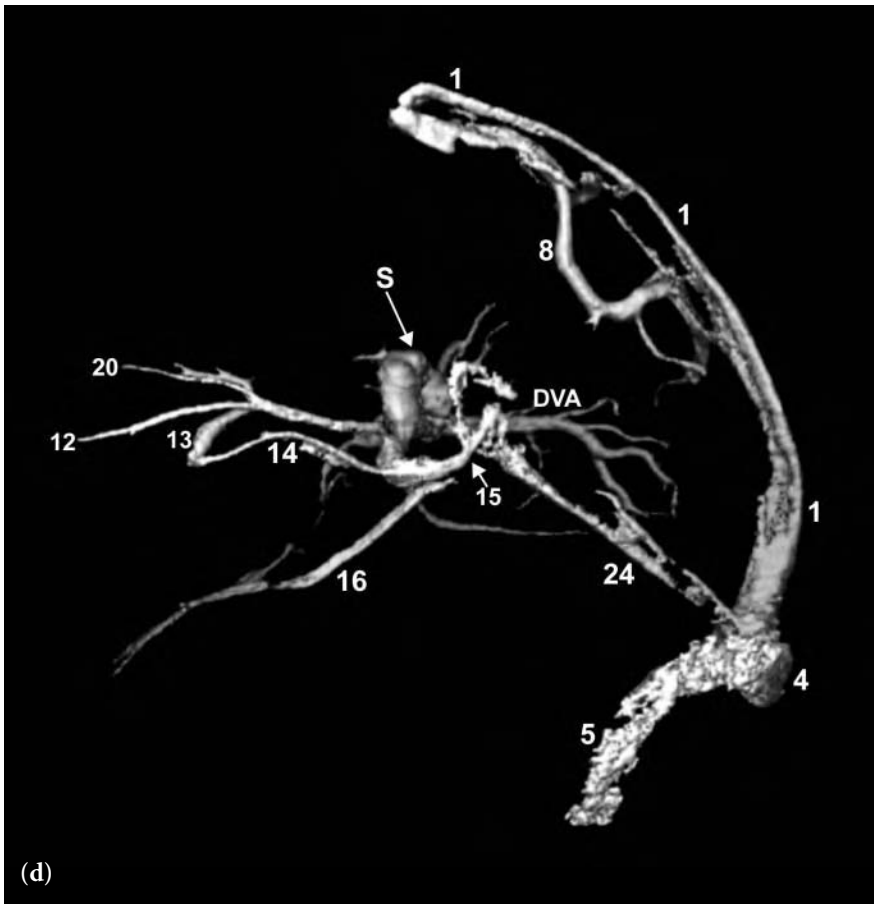
1
1
8
S
20
DVA
12
13
14
15
1
16
24
4
5
(d)

Fig. 7.11 (continued)

FIGURE KEY

1 superior sagittal sinus
3 torcular herophili
4 transverse sinus
5 sigmoid sinus
6 jugular bulb
7 internal jugular vein
8 superficial cortical vein
10 vein of Labbé
11 superficial middle cerebral vein
12 septal vein
13 thalamostriate vein
14 internal cerebral vein
15 great cerebral vein of Galen
16 basal vein of Rosenthal
20 anterior caudate vein
24 straight sinus
26 cavernous sinus
29 superior petrosal sinus
30 inferior petrosal sinus
47 pterygoid venous plexus
DVA developmental venous anomaly
S venous stem of the draining developmental venous anomaly

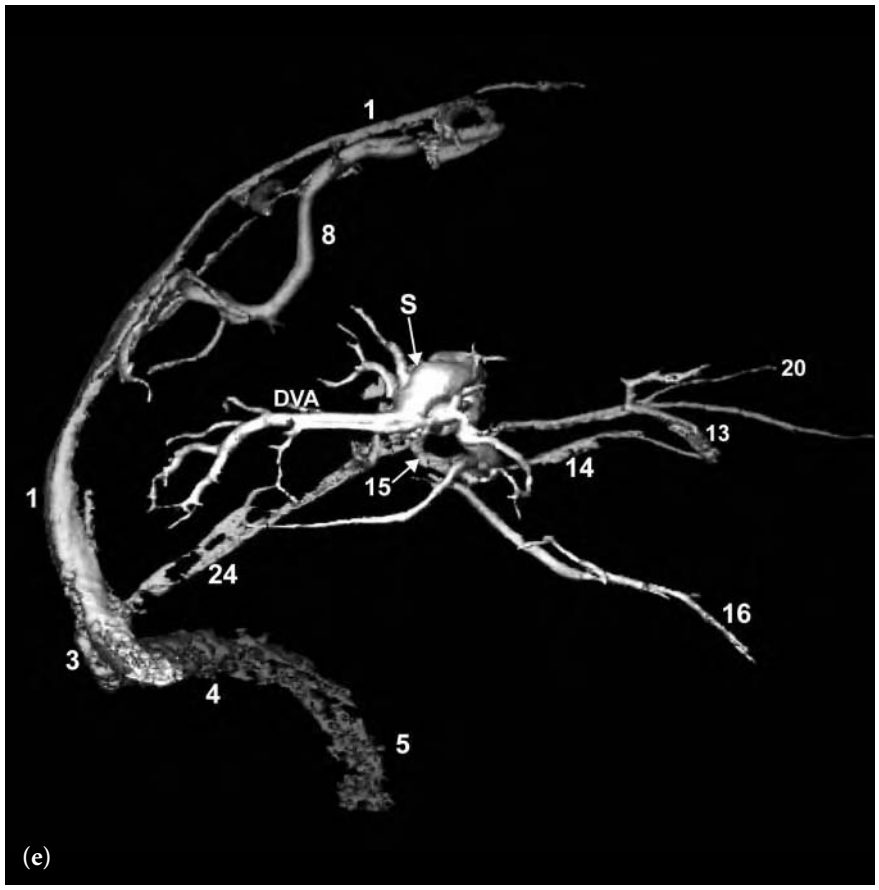

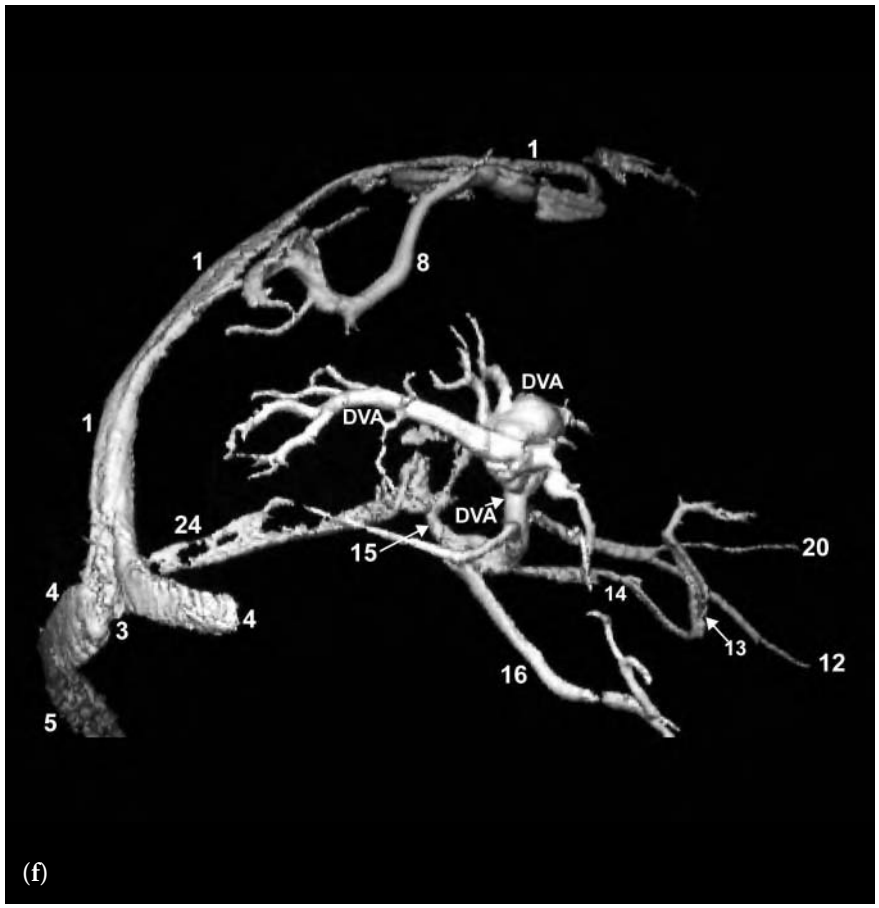

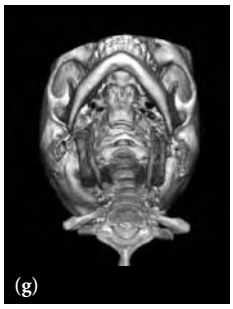
(g)

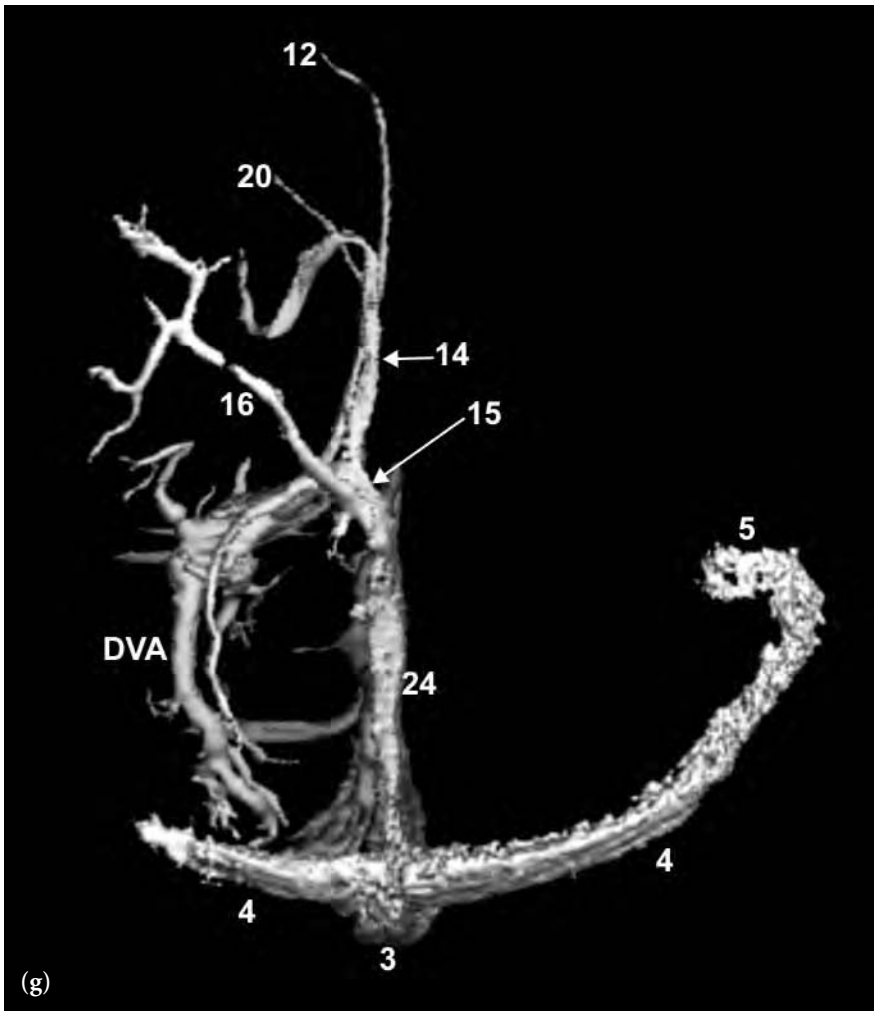
12
20
14
16
15
5
DVA
24
4
4
3
(g)

CHAPTER EIGHT

CIRCLE OF WILLIS

No atlas of neurovascular anatomy would be complete without a description of the circle of Willis. The circle of Willis is known to almost everyone who has an interest in or who has studied the intracranial vascular system. The circle of Willis is a polygonal-shaped collection of arteries at the base of the brain that provides a pathway of communication between the anterior (carotid) and the posterior (vertebral-basilar) circulations. Images demonstrating the components of the circle of Willis are seen throughout this text. This collection of arteries is especially important in providing a pathway for collateral circulation in cases of intracranial vascular occlusions. Unfortunately a complete circle of Willis is present in only approximately 18% of the population (1). The "classical" circle of Willis includes both internal carotid arteries, both A1 anterior cerebral artery segments, both posterior communicating arteries, both P1 posterior cerebral artery segments, and the anterior communicating artery. In most cases one or multiple portions of the circle of Willis are developmentally/congenitally hypoplastic or absent. Common congenital variations include hypoplasia or absence of the A1 anterior cerebral artery segment (25%), hypoplasia or absence of a posterior communicating artery (32%), or hypoplasia or absence of the P1 posterior cerebral artery segment with fetal/direct origin from the ipsilateral supraclinoid segment of the internal carotid artery (15–22%). Additionally, the anterior communicating artery may be fenestrated or absent (9%). An incomplete circle of Willis is the norm rather than the exception and often results in the isolation of a vascular territory. This can have serious implications due to the limiting of collateral flow in cases of vascular occlusive disease (2).

The circle of Willis gives rise to many small branch vessels including the lenticulostriate arteries from the A1 anterior cerebral artery and the anterior thalamoperforating branches that arise from the posterior communicating arteries. The lenticulostriate arteries supply the superior sur-

faces of the optic nerves and chiasm, anterior hypothalamus, septum pellucidum and medial anterior commissure, pillars of the fornix, and the anterior inferior striatum. The anterior thalamoperforating branches supply the posterior portion of the optic chiasm, optic tract, posterior hypothalamus, a portion of the cerebral peduncles, the mammillary bodies, and the thalamic nuclei (3). Some of these small basal perforating vessels can be seen on high-resolution (1024 x 1024 matrix) two-dimensional digital subtraction angiography (2D DSA), especially if a magnification technique is used. They are not typically visualized on three-dimensional rotational angiography (3DRA) unless they are pathologically enlarged.

Aneurysms are a frequent pathology of the circle of Willis with 90% of all intracranial aneurysms arising near the origin of the vessels forming the circle of Willis. Thirty to thirty-five percent of the aneurysms arise near the anterior communicating artery and 30–35% arise in close proximity to the origin of the posterior communicating artery (4).

It is common practice to assess the integrity of the circle of Willis during angiographic procedures for a variety of clinical indications. During the procedure if it is unclear whether the anterior communicating artery provides cross-filling from one side to the other, maneuvers can be utilized to provoke visualization of this important segment of the circle of Willis. During the initial bolus of contrast, external compression of the neck overlying the carotid artery on the side opposite the carotid artery being injected can enhance the ability to see if the anterior communicating artery is functionally present. Compression of the neck results in a transient decrease in arterial blood pressure on the side being compressed. If the anterior communicating artery is functionally present then contrast injected on the opposite side would opacify the anterior communicating artery and variable degrees of the intracranial carotid (anterior) circulation. In a similar fashion, during angiography it is possible to assess the integrity of the posterior communicating artery by compressing one side of the neck overlying the carotid artery during the initial few seconds of selective vertebral artery injection. If the posterior communicating artery is functionally present on the side being compressed you will opacify this vessel via contrast traveling through the basilar artery into the P1 segment of the posterior cerebral artery and

then through the posterior communicating artery. This maneuver can also be of value in the assessment of carotid cavernous sinus fistulas. The morphologic detail of the fistulous connection can often be better evaluated by this technique as opposed to the injection of contrast into the carotid artery on the side of the arterial-venous fistula from below. The latter often results in the flooding of contrast through the high-flow arterial-venous communication which often obscures adequate assessment of the fistulous site.

REFERENCES

1. Rael, J. and L. Casey. 2000. *Cerebral angiography*. In Neuroimaging. W.W. Orrison, editor. Philadelphia: W. B. Saunders, p. 222.
2. Osborn, A. 1980. *Introduction to Cerebral Angiography*. Philadelphia: Harper & Row, Publishers, p. 146.
3. Stephens, R.B. and D.L. Stilwell.1969. *Arteries and Veins of the Human Brain*. Springfield, Ill: Charles C Thomas, p.13.
4. Castillo, M. 1989. *Aneurysms*. In Neuroradiology Companion: Methods, Guidelines, and Imaging Fundamentals, Second Edition. Philadelphia: Lippincott-Raven, pp. 87–94.

INDEX

A

Accessory meningeal artery, 17, 18, 52–55, 66, 69
AICA-PICA, 178–179, 181
Anatomy, normal. *See* Normal neurovascular anatomy
Aneurysm
  anterior communicating artery, 130–133
  at C2-C3 vertebral level, 85
  cervical vasculature, 79, 85
  circle of Willis, 262
  distal right PICA, 196–197
  distal vertebral artery near origin of PICA, 188–189
  fibromuscular dysplasia with, 79
  fusiform basilar artery, 198–199
  internal carotid artery bifurcation, 124–129
  internal carotid artery ophthalmic artery origin, 113, 116
  intracavernous segment internal carotid artery, 112
  large posterior communicating artery/fetal posterior cerebral artery, 120
  left middle cerebral artery bifurcation/trifucation, 136–137, 145–149
  lobulated, 117–119, 190–195
  middle cerebral artery bifurcation, 138–142
  perinidal, 180, 212–215
  right middle cerebral artery bifurcation, 143–144
  supraclinoid internal carotid artery, 121
Angular artery, 97, 101–105, 124, 127–129, 145–149
Anomalous vessel from intracranial internal carotid artery, 134, 158–159
Anterior caudate vein, 26, 229, 234–242, 254–257
Anterior cerebral artery
  A1-A2 junction of, 20–21, 100, 112, 114–115, 117–119, 121, 127–129, 132–149
  A1 segment of, 19–22, 99–100, 102–103, 106–112, 114–159
  anterior internal frontal branch of, 19, 98, 101, 103
  callosomarginal branch of, 19, 21–22, 98–101, 103, 106–107, 116, 132–135, 140–149, 152–156
  frontopolar branch of, 19, 98, 101, 103, 113–119, 124–129, 138–139, 143–156
  inferior internal parietal branch of, 19, 98, 103
  middle internal frontal branch of, 19, 98, 101, 103
  orbitofrontal branch of, 19, 98, 101, 103, 110–116, 124–129, 132–133, 136–151, 154–156
  paracentral lobule artery branch of, 19, 98, 101, 103
  pericallosal branch of, 19, 21–22, 98–100, 102, 106–107, 116, 124–129, 132–135, 140–153
  posterior internal frontal branch of, 19, 98, 101, 103
  proximal A2 segment of, 19, 21, 99–100, 102–119, 106–107, 121–157
  superior internal parietal branch of, 19, 98, 101, 103
Anterior choroidal artery, 19–22, 98, 102, 104–111, 113, 116, 122–127 130–131, 134–151
Anterior communicating artery, 20–22, 127–135, 138–139, 154–156

Anterior inferior cerebellar artery, 19–24, 163–164, 168–197, 200–211
Anterior intercavernous sinus, 25
Anterior medullary vein, 28
Anterior pontomesencephalic vein, 28–29, 243–247
Anterior spinal artery, 19–24, 58, 168–169, 186–187
  radiculomedullary feeder to, 58, 86
Anterior thalamic vein, 28, 246–247
Anterior thalamoperforating arteries, 19–20, 168–169, 178–180, 186–187, 200–211
Anterior tympanic artery, 16–17
Aortic arch, 31–40
  anatomy of, 33–34
  factors limiting 3DRA imaging, 34
  great vessel imaging, 39
  normal anatomical imaging, 36–37
  normal variation in branching, 40
  proximal vertebral artery visualization, 38
Arterial-venous fistula, 66–69
Arterial-venous malformation
  of the brain, 200–208
  draining vein of, 152–153, 200–208
  left temporal lobe, 209–211
  nidus of, 212–215
  right occipital lobe, 180
  right sylvian fissure, 150–151
Artery of the foramen rotundum, 62
Ascending pharyngeal artery, 15, 49, 55, 59–61, 64–65, 73, 75
Ascending thoracic aorta, 15, 36–40
Atherosclerotic irregularity, 77–78, 100–101, 154–156
Atherosclerotic plaque, 70, –73, 76
Atherosclerotic vascular disease, 181–185

B

Balloon-expandable stent, 81
Basal vein of Rosenthal, 26–28, 224, 229–242, 246–247, 249, 254–257
Basilar artery, 19–20, 22–24, 85–86, 168–197, 200–215
  stented segment of, 183–185
Brachial vein, 29, 243–245
Brain, oblique view of, 20
Buccal muscular branches, 16–18, 52–54

C

C1 segment of vertebral artery, 84–86
C2 segment of vertebral artery, 84–86
Callosomarginal artery, 92
Carotid body tumor, 74–75
Carotid bulb, 49, 50–51, 64–65
Carotid circulation, 43–46
Carotid siphon, 100–101, 148
Cavernous malformation, 248
Cavernous sinus, 25–27, 66, 90, 229–232, 234–247, 249–257
Cerebellar hemispheric vein, 29–30, 243–247
Cerebral hemisphere, medial view of, 19
Cerebral veins, frontal view of, 27
Cervical vasculature, 43–86
  aneurysm associated with fibromuscular dysplasia, 79
  arterial-venous fistula, 66–69
  atherosclerotic plaque, 70–73, 76
  balloon expandable stent, 81
  carotid body tumor, 74–75
  carotid circulation, 43–46
  complete occlusion of internal carotid artery, 62
  developmental duplication of vertebral artery, 86
  dissection of upper cervical segment of vertebral artery, 85
  elongation and tortuosity of cervical segment of left vertebral artery, 82
  external carotid artery branches, 63
  fibromuscular dysplasia, 64–65, 79, 83–84
  high grade stenosis, 59–61, 80–81

hypervascular mass, 74–75
meningolacrimal artery, 63
normal appearance
cervical vertebral artery, 56–57
common carotid artery bifurcation region, 49–51
external carotid artery branches, 52–55
origin and lower cervical segment of left vertebral artery, 58
ophthalmic artery, 63
tortuosity of cervical segment of internal carotid artery, 77–78
ulceration, 70–73, 76
vertebral arteries, 46–47
Cervical vertebral artery, normal appearance of, 56–57
Choroid plexus, blush of, 174–175
Circle of Willis, 261–263
anatomy of, 261–262
assessing integrity of, 262–263
Clival venous plexus, 25, 234–242
Common carotid artery, 16–18, 43, 49–51, 59–61, 64–65, 70–73, 75–76, 79

D

Deep auricular artery, 16–17
Deep middle cerebral vein, 230–232
Deep temporal artery, 16–18, 52–55, 62–63, 66, 74
Descending thoracic aorta, 15, 36–40
Developmental duplication of cervical vertebral artery, 86
Developmental venous anomaly, 248–249, 254–257
Diploic veins, 219
Direct lateral vein, 234–242, 249
Distal internal maxillary artery, 16, 67
posterior directed branches of, 54
Distal middle cerebral artery branches, 96
Distal supraclinoid segment, 90
Dural sinuses, 27, 219

E

Early venous drainage of sylvian AVM, 150–153
Endovascular occlusion of MCA aneurysm, 141
External carotid artery, 15–18, 43, 49–55, 59–61, 64–65, 70–73, 75–76, 79
branches of, 63, 67, 77–78

F

Facial artery, 16–18, 49–55, 59–61, 64–65, 70, 73–75
Falcine sinus, 212–215
False venous angle, 234–242
Fenestration of basilar artery, 196–197
Fibromuscular dysplasia, 64–65, 79, 83–84
First cervical vertebrae, 56–57
FLAIR (fluid attenuated inversion recovery), 248
Focal motor seizures and DVA, 248
Foramen rotundum artery, 18, 66, 69
Foramen spinosum, 16–17, 52–55, 66
Fusiform aneurysm of basilar artery, 198–199

G

GDC coil mass, 178–179
Great cerebral vein of Galen, 26–29, 224, 229, 233–242, 246–247, 249, 254–257
Greater palatine artery, 16, 18, 52–55, 62–63, 66

H

Hypertension, 39, 77
Hypoplasia of vertebral artery, 47, 104–105, 154

I

Inferior alveolar artery, 16–18, 52–55
Inferior petrosal sinus, 26–27, 29, 221, 229–232, 234–242, 243–247, 249–257
Inferior retrotonsillar vein, 30
Inferior sagittal sinus, 26–27, 220, 229, 234–242
Inferior ventricular vein, 234–242, 249

Inferior vermian vein, 28, 30, 243–245
Inferolateral trunk, 19, 22, 62, 95
Infindibular widening, 108
Infraorbital artery, 16, 18, 52–55, 62–63
Innominate artery, 15–16, 36–40
Insular vein, 230–232
Intercavernous sinus, 27, 229–232, 243–245, 249–253
Internal carotid artery, 15–18, 49–51, 59–61, 64–65, 70–73, 75–79
  anterior genu (Fischer C3) intracavernous segment, 19, 95, 97–98 100–101, 103–105, 108–111, 113–131, 134–151, 158–159
  bifurcation, 19, 21–22, 91, 99–100, 102–103, 106–112, 114–119, 121–123, 130–149, 154–159
  cervical segment, 19, 21, 91, 95–97, 99–101, 103–107, 110–111, 113– 115, 127–129, 132–133, 138–139, 143–144, 152–153, 158–159
  distal supraclinoid segment, 95–96, 98–120, 122–123, 127–151, 154–159
  horizontal (Fischer C4) intracavernous segment, 19, 22, 95– 98, 101–102, 104–111, 113–120, 125–133, 136–142, 145–151, 154–156, 158–159
  horizontal petrous segment, 19, 21, 95–97, 99–113, 116–119, 121–137, 140–156, 158–159
  occlusion of, 62
  presellar segment (Fischer C5), 19, 21, 95–137, 140–156, 158–159
  proximal supraclinoid segment, 95–96, 98–115, 117–120, 122–123, 127–151, 154–159
  supraclinoid segment of, 19–21, 23–24, 124–126
  vertical petrous segment, 19, 21, 95–97, 99, 100–111, 113–119, 122–159
Internal cerebral vein, 26–27, 29, 223, 229–242, 246–247, 249–257
Internal jugular vein, 26–29, 227–232, 234–247, 249, 254–257
Internal maxillary artery, 15–18, 43–45, 49, 52–55, 59–66, 69, 74, 76
  arterial feeders from, 67– 68
Interpeduncular cistern, 246–247
Intracranial carotid artery circulation
  anatomy of, 89–93
  aneurysm
    anterior communicating artery, 130–131, 132–133
    internal carotid artery bifurcation, 124–126
    intracavernous segment of internal carotid artery, 112
    large internal carotid artery bifurcation, 127–129
    large posterior communicating artery/fetal posterior cerebral artery, 120
    left middle cerebral artery bifurcation/trifurcation, 136–137, 140–142, 145–149
    microcatheter and coils within, 141
    middle cerebral artery bifurcation, 138–139
    with multiple lobulations, 117–119
    ophthalmic artery origin, 113–116
    posterior wall of supraclinoid segment, 122–123
    right middle cerebral artery bifurcation, 143–144
    three separate aneurysms, 121
  anomalous vessels, 134, 158–159
  anterior cerebral artery territory, 98
  arterial-venous malformation
    in left temporal lobe, 152–153
    in right sylvian fissure, 150–151

atherosclerotic irregularity, 100–101
distal middle cerebral artery branches, 96
internal carotid artery circulation, 99
marked overlap of middle and anterior branches, 102
mass effect on anterior and middle cerebral arteries, 157
normal carotid circulation, 106–111
proximal middle cerebral artery branches, 95
separation of anterior and middle cerebral artery branches, 103
severe atherosclerotic irregularity, 154–156
severe developmental hypoplasia, 104–105
sylvian triangle, 97
Intracranial venous system
cavernous malformation, 248
developmental venous anomaly, 248–257
interpeduncular cistern, 246–247
normal appearance of superficial and deep venous systems, 229
rotation of head and venous anatomy visualization, 233
superficial intracranial veins, 227–228
variability in anatomy, 230–232, 234–245
Intracranial vertebral-basilar circulation
AICA-PICA, 178–179, 181
aneurysm
arising from distal right PICA, 196–197
distal vertebral artery, 188–189
GDC coiling of, 178–179
giant fusiform with ulcerative plaque, 198–199
lobulated, 190–195
perinidal, 180, 212–215
arterial-venous malformation of brain, 200–208
left temporal lobe, 209–211
posterior cerebral artery, 212–215
right occipital lobe, 180
atherosclerotic vascular disease, 181–185
duplication of right superior cerebellar artery, 176–177
general anatomy of, 163–167
normal circulation, 174–175, 176–177
normal vascular anatomy, 168–173
severe stenosis, 181–185
vasculitis, 186–187

J

Jugular bulb, 25–29, 227–247, 249, 254–257

L

Lateral lenticulostriate arteries, 21, 99, 104–107, 113, 124–129, 132–135, 140–151
trunk of, 104–105, 108–109
Lateral mesencephalic vein, 28–29, 246–247
Lateral posterior choroidal arteries, 19–20, 23–24, 165–166, 168–169, 174–175, 178–180, 186–189, 200–208
Lateral subependymal veins, 223
Left carotid artery
normal 2D appearance of bifurcation region, 49
normal 3D appearance of bifurcation region, 50–51
Left common carotid artery, 15, 36–40
Left costocervical trunk, 15, 16, 58, 80
Left internal mammary artery, 15–16, 36–38, 40, 58, 80–81
Left subclavian artery, 15–16, 36–40, 58, 80, 81
Left thyrocervical trunk, 15, 16, 36–37, 58, 81
Left vertebral artery, 15–16, 36–40, 58, 80, 81
developmental duplication of, 86
elongation and tortuosity of, 82
high grade stenosis, 80
normal appearance of origin and lower cervical segment of, 58

Lingual artery, 15–18, 49–55, 59–61, 64–65, 70, 73–76
Lingual-facial artery trunk, 55, 71, 72

M

Marginal sinus, 25
Masseteric muscular branches, 16–18, 52–55
Medial atrial vein, 234–242, 249
Medial lenticulostriate arteries, 21, 98, 136, 150–151
Medial posterior choroidal arteries, 168–169, 178–180, 186–189, 200–208
Medial posterior choroidal artery, 19, 23, 24
Medial subependymal veins, 223
Meningeal veins, 219
Meningohypophyseal artery, 89
Meningohypophyseal trunk, 19, 22, 99, 114–115, 120, 124–126
Middle cerebral artery, 92–93
  anterior parietal branch of, 97
  anterior temporal lobe branches of, 20–22, 102, 106–109, 122–133, 140–142, 145–149, 152–156
  bifurcation/trifurcation of, 20–22, 99–100, 102, 104–107, 110–119, 121–156, 158–159
  central rolandic branches of, 97
  M1 segment of, 20–22, 99–100, 103–112, 114–131, 134–151, 154–159
  middle temporal branches of, 97, 101, 102
  opercular branches of, 20–21, 97, 99–102, 104–111, 124–126, 132–133, 143–149, 152–153, 157
  operculofrontal branches of, 97, 103
  orbitofrontal branch of, 20, 22, 97, 99, 102, 104–109, 112, 114–116, 127–129, 136–149, 158–159
  parietal branch of, 101–105
  posterior parietal branch of, 97
  posterior temporal branches of, 97, 101, 102
  pre-central branches of, 97
  sylvian (insular) branches of, 20–24, 99–100, 102–112, 114–115, 117–119, 122–137, 140–142, 143–159
  temporo-occipital branch of, 102
Middle meningeal artery, 16–18, 44, 52–55, 59–63, 66, 69, 74
  cavernous branch of, 62
  frontal branch of, 17
  meningolacrimal branch of, 63
  parietal branch of, 17
Muscular branches, 52–54, 56–57, 66

N

Nidus, 200, 202–207, 211–213
Normal neurovascular anatomy
  frontal view of anterior (carotid) intracranial circulation, 21
  frontal view of head, neck, upper chest, 16
  frontal view of major cerebral veins and dural sinuses, 27
  lateral view of face, 17–18
  lateral view of posterior circulation, 23–24
  lateral view of posterior fossa veins, 28
  left anterior oblique view, 15
  medial view of right cerebral hemisphere, 19
  near lateral view supratentorial superficial and deep venous systems, 26
  oblique view of brain, 20
  posterior fossa veins seen from above, 29
  posterior fossa veins seen from dorsal aspect looking anteriorly, 30
  top down view of skull base, 22, 25

O

Occipital artery, 15, 49–55, 59–65, 70–72, 74, 76–79
Occipital sinus, 25–26, 28, 220, 230–233
Occipital veins, 243–247

Occlusion of internal carotid artery, 62
Ophthalmic artery, 19, 21– 22, 90, 95, 97–100, 102–111, 113–120, 122–131, 134–153, 157–159

P

Paired cavernous sinuses, 221
Parietal veins, 243–247
Pericallosal artery, 91–92
Perimesencephalic veins, 67–69
Petrosal vein, 28, 29, 67, 68, 243–247
Pharyngeal artery, 18
Pontine perforating artery, 19–20, 22–24, 170–175, 209–211
Posterior auricular artery, 15, 49–55, 59–61, 64–65, 76
Posterior cerebral artery, 136–137, 164–166, 168–169, 174–176, 183–185, 188–189, 196–215
  anterior temporal branches of, 19
  calcarine branch of, 23–24, 168–172, 174–180, 182–195, 200–211, 1920
  fetal origin of, 120
  mid-temporal branches of, 19–20
  P1 segment of, 19–20, 22–24, 170–172, 176–177, 180–182, 186–197, 209–211
  P2 segment of, 19–20, 22–24, 168–172, 174–182, 186–197, 200–211
  parieto-occipital branch of, 19–20, 22–24, 168–180, 183–195, 200–211
  posterior temporal branch of, 19–20, 20, 22–24, 23, 24, 168–169, 168–195, 170–172, 173, 176–177, 178–179, 180, 181, 182, 183–185, 200–211
  splenial branch of, 168–169, 180, 186–187, 188–189, 200–208
Posterior choroidals, 178–179
Posterior circulation, lateral view of, 23–24
Posterior communicating artery, 19–20, 22–24, 77, 98, 102, 106–109, 113, 120–121, 124–129, 134–142, 145–149, 158–159, 164, 168–172, 178–180, 186–187, 190–195, 200–211
  infundibular widening at, 150–151
  origin of, 130–131
  stump of, 112
Posterior draining group of posterior fossa veins, 225–226
Posterior fossa veins
  lateral view of, 28
  seen from above, 29
  seen from dorsal aspect looking anteriorly, 30
Posterior inferior cerebellar artery, 19–20, 22–24, 56, 84, 163, 168–211
  hemispheric branch of, 168–169, 174–175, 178–179, 186–189
  vermian branch of, 24, 168–169, 174–175, 178–179, 186–189
Posterior intercavernous sinus, 25
Posterior mesencephalic vein, 30, 243–247
Posterior pericallosal artery, 19, 23, 24, 166–167, 180, 186–189, 200–208
Posterior pericallosal vein, 26
Posterior superior alveolar artery, 16, 18, 52–55, 66
Posterior thalamoperforating arteries, 19–20, 20, 168–169, 174–175, 178–180, 186–189, 200–208, 212–215
Precentral cerebellar vein, 28–30, 243–247
Proximal meningohypophyseal trunk, 108–109
Proximal middle cerebral artery branches, 95
Proximal supraclinoid segment, 90
Pterygoid canal artery, 18, 66
Pterygoid venous plexus, 234–242, 254–257
Pterygovaginal artery, 18

Q

Quadrigeminal plate cistern, 168–169, 186–187, 200–208

R

Radiculomedullary branches of vertebral arteries, 47
Radiculomedullary feeder, 56, 86
Recurrent artery of Heubner, 21, 102, 106–107, 145
Right common carotid artery, 36–38, 40
  stump of, 15
Right costocervical trunk, 15
Right internal mammary artery, 15, 36–37, 40
Right subclavian artery, 15–16, 36–40
Right thyrocervical trunk, 15–16
Right vertebral artery, 15, 36–37, 39, 40

S

Second cervical vertebrae, 56, 57
Septal vein, 26–27, 229–232, 234–242, 249–257
Sigmoid sinus, 25–29, 200–208, 227–247, 249–257
Skull base, top down view of, 22, 25
Sphenopalatine artery, 16, 18, 52–55, 62–63, 66
  lateral nasal branches of, 52–55
  septal branches of, 52–55
Sphenopalatine loop, 69
Sphenoparietal sinus, 25, 27, 221, 230–232, 234–242
Sphenopetrosal vein, 234–242
Splenial artery, 19, 23, 24
Stenosis, 59–61, 80– 81, 84, 181, 183–185
Straight sinus, 25, 27–28, 30, 220, 229–242, 246–247, 254–257
Suboccipital veins, 234–242, 243–245, 254
Superficial cerebral veins, 222
Superficial cortical vein, 26–27, 66, 222, 227–242, 249–257
Superficial middle cerebral vein, 25–27, 66, 222, 230–232, 234–242, 254–257
Superficial temporal artery, 15, 43, 49, 52–55, 62–66, 74, 76
Superior cerebellar artery, 19–20, 23–24, 164, 168–215
  hemispheric branch of, 23, 168–189, 196–197, 200–211
  vermian branch of, 24, 170–187, 196–197, 200–208
Superior choroid vein, 28, 246–247
Superior draining group of posterior fossa veins, 224–225
Superior hypophyseal artery, 90
Superior ophthalmic vein, 25, 66, 234–242
Superior petrosal sinus, 25–27, 29, 221, 229–232, 234–247, 254–257
Superior sagittal sinus, 25–27, 29, 219, 227–245, 249–257
Superior thalamic vein, 28, 246–247
Superior thyroid artery, 15–18, 49–51, 55, 59–61, 64–65, 70–73, 75–76
Superior vermian vein, 28, 246–247
Supraclinoid segment of intracranial internal carotid artery, 90
Surgical clipping, 116, 151
Sylvian point, 21, 93, 95, 97, 99–100, 106–111, 124–135, 140–144, 150–157
Sylvian triangle, 97
Sylvian vein, 150–151

T

Temporal lobe, uncus of, 230–232
Terminal vein, 26, 229, 234–242
Thalamostriate vein, 26–27, 229–232, 234–242, 254–257
Three-dimensional rotational angiography (3DRA)
  advantages of, 1–3
  for carotid artery disease in the neck, 45–46
  delay times, 9
  injection of contrast, 8–9
  limitations of, 3

reconstruction algorithms, 9–10
techniques of, 7–10
Tonsil, 191, 193, 195
Torcular herophili, 25–29, 227–247, 249–257
Transverse facial artery, 15, 52–54
Transverse pontine vein, 28–29
Transverse sinus, 25–29, 220, 227–247, 249–257
True venous angle, 26, 234–242

U

Ulcerated plaque, 70, 72–73, 76, 183–185, 198–199
Uncus of temporal lobe, 230–232
Upper cervical segment dissection of vertebral artery, 85

V

Vasculitis, 186–187
Vein of Galen, 67– 68
Vein of Labbé, 25, 27, 227–232, 234–242, 246–247, 249–257
Vein of Trolard, 229–232, 234–242
Venous angle, 223–224
Vertebral artery, 19–20, 22–24, 46–47, 56–57, 82–86, 168–215
Vertebral-basilar junction, 19–20, 22–24, 168–169, 173, 176–179, 186–187, 190–211
Vidian artery, 18, 66